

University of Huddersfield Repository

Hollis, Zoe

Investigation of the Function and Evolution of Vitamin K Epoxide Reductases

Original Citation

Hollis, Zoe (2020) Investigation of the Function and Evolution of Vitamin K Epoxide Reductases. Doctoral thesis, University of Huddersfield.

This version is available at http://eprints.hud.ac.uk/id/eprint/35219/

The University Repository is a digital collection of the research output of the University, available on Open Access. Copyright and Moral Rights for the items on this site are retained by the individual author and/or other copyright owners. Users may access full items free of charge; copies of full text items generally can be reproduced, displayed or performed and given to third parties in any format or medium for personal research or study, educational or not-for-profit purposes without prior permission or charge, provided:

- The authors, title and full bibliographic details is credited in any copy;
- A hyperlink and/or URL is included for the original metadata page; and
- The content is not changed in any way.

For more information, including our policy and submission procedure, please contact the Repository Team at: E.mailbox@hud.ac.uk.

http://eprints.hud.ac.uk/



Investigation of the Function and Evolution of Vitamin K Epoxide Reductases

Zoe Hollis

Doctor of Philosophy

January 2020

A thesis submitted to the University of Huddersfield in partial fulfilment of the requirements for the degree of Doctor of Philosophy.

Copyright Statement

The following notes on copyright and the ownership of intellectual property rights must be included as written below:

i. The author of this thesis (including any appendices and/ or schedules to this thesis) owns any copyright in it (the "Copyright") and s/he has given The University of Huddersfield the right to use such Copyright for any administrative, promotional, educational and/or teaching purposes.

ii. Copies of this thesis, either in full or in extracts, may be made only in accordance with the regulations of the University Library. Details of these regulations may be obtained from the Librarian. This page must form part of any such copies made.

iii. iii. The ownership of any patents, designs, trademarks and any and all other intellectual property rights except for the Copyright (the "Intellectual Property Rights") and any reproductions of copyright works, for example graphs and tables ("Reproductions"), which may be described in this thesis, may not be owned by the author and may be owned by third parties. Such Intellectual Property Rights and Reproductions cannot and must not be made available for use without permission of the owner(s) of the relevant Intellectual Property Rights and/or Reproductions.

Acknowledgments

Throughout the entirety of this project, there are many people I would like to express my sincerest gratitude. Firstly, I would like to give special thanks to my supervisor, Dr. Dougie Clarke. I am ever grateful for this opportunity and for your guidance and help throughout this project. I would also like to thank the technical support staff for their support in the laboratory.

I would also like to thank my wonderful friends from Girl Street and also from Sheffield for their huge support and helping me through all the stressful times. I would like to give special thanks to Miss Sophie Glossop, who is one of my dearest friends and has gotten me through all the hard times right up until the very end.

To my amazing family, I would like to thank you for everything you do for me and believing in me throughout this project and always. With a special huge thank you to my Mom and Dad, my little sister Emma, and my Uncle Melvyn and Auntie Ann and the rest of my family for their endless support and encouragement throughout this project, especially throughout the writing of this thesis. Finally, a big thank you to Ryan for your love, patience and understanding throughout this project.

Abstract

Vitamin K epoxide reductase complex subunit 1 (VKORC1) is an important enzyme in the vitamin K cycle, and the target of anticoagulant rodenticides. Polymorphisms identified in VKORC1 in *Rattus norvegicus* (brown rat) can cause anticoagulant resistance. Previous studies have shown several anticoagulant resistance polymorphisms that are found in the UK in brown rats, but the results are mainly derived from laboratory rat samples or frozen tissue samples collected between 1990-2000. The current status of anticoagulant rodenticide resistance in wild brown rat populations in the UK is therefore largely unknown. At present there has been no study of genetic resistance in Swedish rodents. In this study DNA sequencing of the VKORC1 gene of brown rats was done to assess the frequency and distribution of anticoagulant resistance polymorphisms in wild brown rats in the UK and Sweden. DNA sequencing revealed that 69% of brown rats in the UK and 14% of Swedish brown rats contained a known anticoagulant resistance polymorphism (p.L120Q, p.L128Q, p.Y139C, p.Y139S) . As well as these known polymorphisms a novel p.R40G polymorphism was identified in UK and Swedish *Rattus norvegicus* samples. A baculovirus expression system was used to express the p.R40G VKORC1 variant and wild type rat VKORC1 to compare the effect of five anticoagulant rodenticides (warfarin, bromadiolone, brodifacoum, difenacoum and flocoumafen) using a high pressure liquid chromatography assay to produce dose-response curves, which IC_{50} values were derived. It was found that the novel p.R40G VKORC1 variant is resistant to warfarin but sensitive to the other rodenticides tested. This is also the first study in which the effects of flocoumafen were tested against wild type brown rat VKORC1 and variants *in vitro*.

With the diverse anticoagulant resistance polymorphisms found in the UK and Sweden in this study, it was of interest to observe if there was a relationship between resistance polymorphisms and mitochondrial D loop haplotypes. DNA sequencing of the mitochondrial D-loop of brown rats were completed to identify the current population structure of UK and Swedish wild brown rats. This revealed that certain resistance polymorphisms are associated with mitochondrial D-loop haplotypes.

As a result of anticoagulant resistance in *Rattus norvegicus* there has been an increased usage of more potent second generation anticoagulant rodenticides to control populations of these pests. This has in turn resulted in an increased reports of non-target poisoning in animals belonging to all vertebrate classes. At present there is little known about the effects of anticoagulant rodenticides on many of these animals, including humans. Multiple sequence alignments were used as a prediction tool to determine the potential structure, functions and susceptibility to anticoagulant rodenticides throughout vertebrate VKORC1 sequences by comparing them with known resistance polymorphisms in human and rat VKORC1s. Four representative VKORC1 sequences (*Rattus norvegicus* - brown rat*, Homo sapiens* - human*, Bos taurus* - cow and *Python bivittatus* - python) were chosen for heterologous expression in the baculovirus expression system. The human, cow and brown rat VKORC1 variant were compared to test the effect of five anticoagulant rodenticides (warfarin, bromadiolone, brodifacoum, difenacoum and flocoumafen) using a high pressure liquid chromatography assay to produce dose-response curves, which IC_{50} values were derived. The results showed that the brown rat VKORC1 was more sensitive to warfarin compared to the human and cow VKORC1, but against the other four anticoagulant rodenticides the opposite was shown. The results showed a difference in potency for the anticoagulant rodenticides depending on the species tested.

The general overall phylogeny of the VKOR family of enzymes has been well characterized in terms of phylogenetic trees and relationships of VKORs. With respect to amino acid sequence comparisons these studies have however only used a relatively small number of vertebrate VKORC1 and VKORC1L1 sequences to assess the structural, functional and evolutionary relationships between VKORs in different species and between the two enzymes. In this study multiple sequence alignments were used to determine the structural, functional and evolutionary relationships between the 135 vertebrate VKORC1 sequences and 164 VKORC1L1 sequences. It can be predicted that all vertebrate VKORC1 and VKORC1L1 enzymes have the ability to bind both vitamin K and vitamin K epoxide and also have the ability to bind warfarin. It can also be predicted that some vertebrate VKORC1 sequences may have a natural resistance or sensitivity to anticoagulant rodenticides.

Table of Contents

Copyright Statement ***2***

Acknowledgments ***3***

Abstract ***4***

List of Abbreviations ***13***

List of Figures ***15***

List of Tables ***19***

Chapter 1: Introduction ***22***

1.0 About This Chapter **22**

1.1 Rodents as Pests **22**

1.2 Pest Management **28**

1.3 Discovery of Anticoagulants **28**

1.3.1 Discovery of Dicoumarol 28

1.3.2 Synthesis and use of warfarin as an anticoagulant 29

1.4 First Generation Anticoagulant Rodenticides **30**

1.5 First Report of Anticoagulant Resistance **31**

1.6 Second Generation Anticoagulant Rodenticides **32**

1.7 Determining the Cause of Anticoagulant Resistance **36**

1.8 Discovery that Vitamin K is Essential for Coagulation **36**

1.8.1 Discovery of Vitamin K 36

1.8.2 Function of Vitamin K 38

1.8.3 Discovery of Phylloquinone Oxide 38

1.9 Vitamin K Cycle **40**

1.10 VKORC1 involvement in disulfide bond formation **42**

1.11 Chromosome Mapping of Warfarin Resistance Locus and Discovery of VKORC1 Gene **44**

1.11.1 Chromosome Mapping of Warfarin Resistance Locus 44

1.11.2 Discovery of the VKORC1 gene 45

1.12 Structure and Topology of VKORC1 ..... **46**

1.13 Important Amino Acids in VKORC1 ..... **50**

1.13.1 Active site cysteines in VKORC1 50

1.13.2 Amino Acids involved in Stabilising Helix-helix Interactions in VKORC1 50
1.13.3 Amino Acids Involved in Substrate Binding in VKORC1 52
1.13.4 Amino Acids Involved in Warfarin binding in VKORC1 52
1.13.5 Amino Acids that are proposed to act as ER Retention signals in VKOR 53

1.14 Vitamin K Epoxide Reductase Complex Subunit 1 Like-1 (VKORC1L1) 53

1.15 Evolution of the VKOR family of enzymes and their relationship with related proteins 54

1.15.1 Phylogeny of the VKOR family 54
1.15.2 Evolutionary relationship between DsbB and VKORC1 56

1.16 Molecular Basis of Anticoagulant Resistance 59

1.16.1 Anticoagulant Resistance of *Rattus norvegicus* in the UK 59
1.16.2 Anticoagulant Resistance of *Rattus norvegicus* in Europe, Asia and North America 61
1.16.3 Anticoagulant Resistance found in other rodents 63
1.16.4 Anticoagulant Resistance found in humans 65
1.16.5 Other Mechanisms for Resistance to Anticoagulants 67
1.16.6 Phylogeography of Resistant Polymorphisms in *Rattus norvegicus* 67

1.17 Biochemical Characterisation of VKORC1 and VKORC1L1 68

1.17.1 Heterologous Expression of VKORC1 68
1.17.2 Kinetic analysis of VKORC1 70
1.17.3 Biochemical Characterisation of VKORC1 Polymorphisms associated with anticoagulant resistance 71
1.17.4 Characterisation of VKORC1 and VKORC1L1 77
1.17.5 Effect of Anticoagulants Rodenticides on Non-target Species 81

1.18 Non-target Poisoning 83

1.18.1 Effects of Anticoagulants on the Environment 84
1.18.2 Non-target Poisoning of Humans 85
1.18.3 Non-target Poisoning of Birds 88
1.18.4 Non-target Poisoning of Mammals 92
1.18.5 Non-target Poisoning of Other Vertebrates 94
1.18.6 Non-target Poisoning of Invertebrates 95

1.19 Aims of the Project 95

Chapter 2: Materials and Methods 96

2.0.1 Materials 96
2.0.2 Bacterial Strains 96
2.0.3 Insect Cell Culture Cell Line 96
2.0.4 Animal Samples 96

2.0.5 Plasmid Constructs....96

2.1 DNA Analysis....97

2.1.1 DNA Extraction....97

2.1.2 Polymerase Chain Reaction (PCR)....97

2.1.2.1 Exon 1 PCR Programme....98

2.1.2.2 Exon 2 PCR Programme....98

2.1.2.3 Exon 3 PCR Programme....98

2.1.2.4 Mitochondrial D Loop PCR Programme....99

2.1.3 Agarose Gel Electrophoresis....99

2.1.4 PCR Purification....99

2.2 Growth Medium for *E. coli* Strains....100

2.2.1 Luria Broth (LB) Media....100

2.2.2 NYZ^{+} Broth - *E. coli* XL10-Gold....100

2.2.2 LB Agar (LB Plates)....100

2.2.3 Selectable and Visible Markers....100

2.2.4 Storage of *E. coli* – Glycerol Stocks....101

2.3 Preparation of Competent *E. coli* Cells Using Calcium Chloride....101

2.3.1 Freezing Competent Cells....102

2.4 Transformation of Recombinant Plasmids into *E. coli* Strains....102

2.5 Plasmid Miniprep....102

2.6 Ligation Independent Cloning (LIC) of Gene of Interest into a Desired Plasmid....104

2.6.1 PCR Primers for LIC....105

2.6.2 PCR of VKORC1 from the pET32a Vector....105

2.6.3 *DpnI* treatment of PCR Product....106

2.6.4 T4 Polymerase Treatment of Purified PCR Products....107

2.6.5 Vector Digestion of pFB-LIC-Bse plasmid with *BseRI*....107

2.6.6 T4 Polymerase Treatment of Purified Digested Vector....107

2.6.7 Ligation of T4 Treated PCR Product and T4 Treated Digested Plasmid....108

2.6.8 Colony PCR of Ligated VKORC1 insert and pFB-LIC-Bse Vector....108

2.7 Site Directed Mutagenesis of VKORC1 Constructs....110

2.7.1 Mutant Strand Synthesis Reaction....110

2.7.2 *DpnI* Digestion of the Amplification Products....111

2.7.3 Transformation into XL10-Gold Ultracompetent Cells....111

2.8 Generating the Recombinant Bacmid....112

2.8.1 Transforming the VKORC1-pFB-LIC-Bse construct into *DH10 Bac*....113

2.8.2 Verifying the Phenotype 113
2.8.3 Isolating the Recombinant Bacmid DNA 113
2.8.4 Analysing the Isolated Recombinant Bacmid DNA using PCR 115

2.9 *Spodoptera frugiperda* (*Sf9*) Insect Cell Culture 115

2.9.1 Adherent Sf9 Cell Culture – General Maintenance 115
2.9.2 Suspension Culture of *Sf9* - General Maintenance 117

2.10 Transfection of Virus into the *Sf9* Cells and Viral Amplification 118

2.10.1 Production of P0 Virus and Transfection into *Sf9* Cells 119
2.10.2 Isolating P1 Viral Stock 119
2.10.3 Amplifying Viral Stock 119

2.11 Organic Synthesis of Vitamin K 2,3-Epoxide 121

2.12 Quantification of Vitamin K_1 and Vitamin K 2,3-Epoxide by Spectrophotometric Analysis 121

2.13 Mass Spectrometry of Vitamin K_1 and Vitamin K 2,3-Epoxide 122

2.14 Calibration Standards for Vitamin K_1 and Vitamin K 2,3-epoxide 122

2.15 Microsome Preparation 123

2.15.1 Preparation of Rat Liver Microsomes 123
2.15.2 Preparation of *Sf9* Cell Microsomes 123

2.16 BCA Assay for Protein Determination 123

2.17 HPLC VKORC1 Assay 124

2.17.1 VKORC1 *in vitro* Assay - General 124
2.17.2 VKORC1 Time Course Experiments 125
2.17.3 VKORC1 K_m Determination 126
2.17.4 VKORC1 *in vitro* Assay – IC_{50} Determination 126
2.17.5 High Pressure Liquid Chromatography (HPLC) Analysis 126

2.18 Bioinformatic Analysis 127

2.18.1 Sanger Sequence Analysis 127
2.18.2 Mitochondrial Network Mapping 127
2.18.3 VKOR Multiple Sequence Alignments 127
2.18.4 Secondary Structure Prediction 128
2.18.5 3D Protein Modelling 128

Chapter 3: Frequency and Distribution of Anticoagulant Rodenticide Resistance in the UK and Sweden 129

3.0 About this Chapter 129

3.1 Genetic Analysis to determine the frequency and distribution of anticoagulant resistance in UK and Swedish wild brown rats 131

3.1.1 VKORC1 Exon 1 variants in UK and Swedish rats 131

3.1.2 VKORC1 Exon 2 variants in UK and Swedish rats 132

3.1.3 VKORC1 Exon 3 135

3.2 Mitochondrial DNA Analysis of the UK and Sweden wild brown rats 144

3.2.1 D-loop haplotypes found in UK and Sweden brown rats 144

3.2.2 D-loop haplotypes found in UK and Swedish brown rats and the relationship to known anticoagulant resistance polymorphisms 151

3.3 Computational Analysis of the Novel p.R40G Polymorphism found in the UK and Sweden wild brown rats 153

3.3.1 Multiple Sequence Alignment of Vertebrate VKORC1 to assess the evolutionary conservation of R40 position 153

3.3.2 Membrane topology and tertiary prediction modelling of the wild type brown rat VKORC1 and the p.R40G mutant 153

3.4 Expression of Recombinant VKORC1 Enzymes for Functional Analysis of the Novel p.R40G VKORC1 Polymorphisms 156

3.5 Organic Synthesis of VKE 159

3.6 Biochemical Characterisation of VKORC1 160

3.6.1 Characterisation of VKORC1 in Rat liver Microsomes 160

3.6.2 Testing of Recombinant VKORC1 Constructs for Active Protein 162

3.7 Investigation of Enzyme Kinetics of Recombinant VKORC1s 163

3.8 Effect of Anticoagulant Rodenticides on wild type and variant rat VKORC1s 164

3.9 Dose-response Curves for Wild Type Rat VKORC1 and the p.R40G VKORC1 Mutant for Five Anticoagulant Rodenticides 168

Chapter 4: Computational analysis of VKORC1 and VKORC1L1 to assess structure, function and evolutionary relationships 174

4.0 About this Chapter 174

4.1 Computational Comparison of Vertebrate VKORC1 Amino Acid Sequences 175

4.2 Analysis of VKORC1 Amino Acid Sequences in Mammals 188

4.3 Analysis of VKORC1 Amino Acid Sequences in Non-Mammals 190

4.4 Percentage Identity Comparison of Vertebrate VKORC1 191

4.5 Comparison of the vertebrate VKORC1 sequences.....192
4.5.1 Comparison of vertebrate VKORC1 sequences using an MSA.....192
4.5.2 Consensus sequences for vertebrate VKORC1.....195
4.5.3 Using the Consensus sequences to assess functional constraint across vertebrate VKORC1 195
4.6 Comparison of representative vertebrate VKORC1 sequences using Membrane topology and tertiary prediction modelling 203
4.7 Analysis of the previously reported roles of amino acids between the vertebrate classes for VKORC1 207
4.7.1 Analysis of Amino acids important in the structure and function of human and rat VKORC1 in other vertebrates 207
4.7.2 Amino Acids Involved in Warfarin Binding in human and rat VKORC1 in other vertebrate VKORC1s 212
4.7.3 Amino Acids that Cause Anticoagulant Resistance in human and rat VKORC1 in other vertebrates 214
4.8 Assessment of the conserved residues in VKORC1 between vertebrate classes 223
4.9 Computational Comparison of Vertebrate VKORC1L1 Amino Acid Sequences.....227
4.10 Analysis of VKORC1L1 Amino Acid Sequences in Mammals 238
4.11 Analysis of VKORC1L1 Amino Acid Sequences in Non-Mammals.....239
4.12 Percentage Identity Comparison of Vertebrate VKORC1L1 240
4.13 Comparison of the vertebrate VKORC1L1 sequences 240
4.13.1 Comparison of vertebrate VKORC1L1 sequences using an MSA 240
4.13.2 Consensus sequences for vertebrate VKORC1L1.....243
4.13.3 Using the Consensus sequences to assess functional constraint across vertebrate VKORC1L1....245
4.14 Comparison of representative vertebrate VKORC1L1 using membrane topology and tertiary prediction modelling.....251
4.15 Analysis of the roles of amino acids between the vertebrate classes for VKORC1L1.....254
4.15.1 Amino Acids Involved in Warfarin binding of human VKORC1L1 in other vertebrates 254
4.15.2 Amino Acids Described as Conserved in VKORC1L1 255
4.16 Assessment of the conserved residues in VKORC1L1 between vertebrate classes.....259
4.17 Analysis of the sequences between VKORC1 and VKORC1L1 vertebrates.....263
4.17.1 Analysis of the Percentage Identity for the vertebrate classes for VKORC1 and VKORC1L1 263
4.17.2 Analysis of the roles of amino acids in the VKOR family.....264

4.17.3. Analysis of site-specific VKOR enzyme differences 267
4.17.4 Assessment of the conserved residues in VKOR between vertebrate classes 269
4.18 Heterologous Expression of VKORC1 Constructs 272
4.19 Structural Modelling of Chosen VKORC1 Constructs 276
4.20 Expression of Recombinant VKORC1 Constructs 278
4.21 Enzyme Kinetics of Recombinant VKORC1 Constructs 281
4.22 Effect of anticoagulant rodenticides on VKORC1 285
Chapter 5: General Discussion and Future Work 292
5.0 About this Chapter 292
5.1 Anticoagulant Resistance in Rattus norvegicus in the UK and Sweden 292
5.2 Mitochondrial D loop analysis and the relationship of anticoagulant resistance polymorphisms. 296
5.3 Prediction of the susceptibility of vertebrate VKORC1s to anticoagulant rodenticides 297
5.4 Computational Analysis of VKORC1 and VKORC1L1 to assess the structural, functional and evolutionary relationships 301
5.4 Future Work 302
References 304
Appendix 1: Review of Literature for Non-targeted anticoagulant rodenticide poisoning in Non-raptor birds 324
Appendix 2: Review of Literature for Non-targeted anticoagulant rodenticide poisoning in raptor birds 331
Appendix 3: Review of Literature for Non-targeted anticoagulant rodenticide poisoning in mammals 339
Appendix 4: Review of Literature for Non-targeted anticoagulant rodenticide poisoning in other vertebrates 345
Appendix 5: Review of Literature for Non-targeted anticoagulant rodenticide poisoning in invertebrates 346
Appendix 6: VKORC1 and VKORC1L1 Accession Numbers 347
Appendix 7: DNA Sequences of Novel D-loop Haplotypes found in the UK and Sweden .. 353
Appendix 8: Key for Amino Acid Colours According to Physiochemical Properties 356
Appendix 9: Mass Spectra of Vitamin K epoxide and Vitamin K 357
Appendix 10: Phylogenetic Tree of Vertebrates 358

List of Abbreviations

Amplification Refractory Mutation System	ARMS
Base Pairs	bp
Bicinchoninic acid	BCA
Bovine Serum Albumin	BSA
Central Science Laboratory	CSL
Disulfide Bond Formation Protein B	DsbB
Dithiothreitol	DTT
Endoplasmic Reticulum	ER
Endoplasmic reticulum oxidoreductin 1	ERo1
Escherichia coli	*E. coli*
Familial Multiple Coagulation Factor Deficiency	FMFD
First Generation Anticoagulant Rodenticides	FGARs
Fluorescence Protease Protection	FPP
γ-glutamyl carboxylase	GGCX
Gene of Interest	GOI
Green Fluorescence Protein	GFP
half maximal inhibitory concentration	IC_{50}
High Pressure Liquid Chromatography	HPLC
Human coagulation factor IX	FIX
Human Embryonic Kidney-293 Cells	HEK-293
Isopropyl β-D-1-thiogalactopyranoside	IPTG
Lethal Dosage 50	LD_{50}
Ligation Independent Cloning	LIC
Millions of Years Ago	Mya
Mitochondrial DNA	mtDNA
Myosin Light Chain Locus	Myl2
National Centre of Biotechnology Information	NCBI

Oxidised Glutathione	GSSG
Oxidised Protein Disulfide-Isomerase	PDI^{ox}
Peroxidoreductin IV	PRDX4
Polyethylene Glycol	PEG
Polymerase Chain Reaction	PCR
Protein Disulfide-Isomerase	PDI
Redox-sensitive GTP	roGTP
Recombinant VKORC1	rVKORC1
Reduced Protein Disulfide-Isomerase	PDI^{red}
Restriction Fragment Length Polymorphisms	RFLP
Second Generation Anticoagulant Rodenticides	SGARs
Single Nucleotide Polymorphisms	SNPs
Spodoptera frugiperda insect cells	*Sf9*
Transmembrane	TM
Ultraviolet	UV
United Kingdom	UK
Vitamin K_1	VK_1
Vitamin K_2	VK_2
Vitamin K_3	VK_3
Vitamin K Dependent	VKD
Vitamin K 2,3-epoxide	K>O
Vitamin K Hydroquinone	KH_2
Vitamin K Epoxide Reductase	VKOR
Vitamin K Epoxide Reductase Complex Subunit 1	VKORC1
Vitamin K Epoxide Reductase Complex Subunit 1 Like-1	VKORC1L1
Vitamin K Clotting Factor Deficiency Type 2	VKCFD2
Volume per Volume	v/v
Waste Water Treatment Plants	WWTP
Weight per Volume	w/v

List of Figures

29: **Figure 1:** Chemical structure of dicoumarol.

30: **Figure 2:** Chemical structure of warfarin.

31: **Figure 3:** Chemical structures of 4-hydroxycoumarin and indandione first generation anticoagulants.

33: **Figure 4:** Chemical structures of second generation anticoagulants.

37: **Figure 5:** Structures of Vitamin K derivatives.

39: **Figure 6:** Proposed mechanism of vitamin K by Willingham and Matschiner (1974).

40: **Figure 7:** Vitamin K cycle with the blood coagulation pathway and the effect of warfarin.

41: **Figure 8:** Proposed the chemical model for the mechanism of VKORC1 in the conversion of vitamin K epoxide to vitamin K determined by Silverman (1981).

44: **Figure 9:** Proposed pathway of VKORC1 in the ER redox homeostasis pathway.

49: **Figure 10:** Topology diagrams of the proposed 3 TM and 4TM model of human VKORC1.

54: **Figure 11:** Topological diagram of VKORC1L1.

57: **Figure 12:** Topological diagrams of DsbB and VKORC1 highlighting the structural relationship between the two proteins.

58: **Figure 13:** An evolutionary model of the VKOR family and its proposed relationship to DsbB.

73: **Figure 14:** Percentage activity of VKORC1 variants found in *Rattus norvegicus* and *Mus musculus* at a warfarin concentration of 60 μM.

74: **Figure 15:** Inhibition values (K_i) of rVKORC1 variants found in *Rattus norvegicus* for various FGARs and SGARs.

76: **Figure 16:** IC_{50} values of human VKORC1 for different oral anticoagulants.

77: **Figure 17:** K_i values of human and rat VKORC1 and VKORC1L1 for warfarin.

78: **Figure 18:** K_i values of human VKORC1 and VKORC1L1 for different oral anticoagulant and second generation anticoagulant rodenticides.

79: **Figure 19:** IC_{50} values of human VKORC1 and VKORC1L1 for different oral anticoagulant and anticoagulant rodenticides.

82: **Figure 20:** K_i values of domesticated animal and bird species VKORC1 for warfarin.

90: **Figure 21:** Reports of the incidence of exposure or mortality of non-target non-raptor birds by anticoagulant rodenticides in different countries throughout the world.

91: **Figure 22:** Reports of the incidence of exposure or mortality of non-target raptor birds by anticoagulant rodenticides in different countries throughout the world.

93: **Figure 23:** Reports of the incidence of exposure or mortality of non-target mammals by anticoagulant rodenticides in different countries throughout the world.

104: **Figure 24:** Workflow of ligation independent cloning of VKORC1 into the pFB-LIC-Bse Vector.

112: **Figure 25:** Schematic diagram of generating the recombinant bacmid.

118: **Figure 26:** Schematic diagram showing the transfection of baculovirus with VKORC1 cDNAs into the *Sf9* system.

121: **Figure 27:** Flow diagram of the synthesis of vitamin K epoxide.

122: **Figure 28:** Vitamin K epoxide and vitamin K calibration standards.

125: **Figure 29:** Time course of 0, 5, 10, 15 and 20 minutes of vitamin K production of VKORC1 expressed in *Sf9* insect cells at 50 μM of vitamin K epoxide.
131: **Figure 30:** Sequencing electropherogram of the CL20 sample of the previously unreported p.R40G polymorphism found in exon 1.
133: **Figure 31:** Sequencing electropherogram of the p.I82I polymorphism found in exon 2.
134: **Figure 32:** Sequencing electropherogram of the p.S79P polymorphism found in exon 2.
135: **Figure 33:** Sequencing electropherogram of the p.V66L polymorphism found in exon 2.
137: **Figure 34:** Sequencing electropherogram of the p.L120Q, p.L128Q, p.Y139C and p.Y139S polymorphisms found in exon 3 in the UK brown rat samples.
138: **Figure 35:** Map of the UK highlighting the geographical distribution and proportion of anticoagulant resistant polymorphisms found in each county surveyed.
143: **Figure 36:** Map of Sweden highlighting the geographical distribution and proportion of anticoagulant resistant polymorphisms found in each county surveyed.
145: **Figure 37:** Median joining network of D-loop haplotypes found in brown rats in the UK in this study.
146: **Figure 38:** Median joining network of D-loop haplotypes found in brown rats in the Sweden in this study.
149: **Figure 39:** Median joining network of D-loop haplotypes found in brown rats in the UK in this study.
150: **Figure 40:** Median joining network of D-loop haplotypes found in brown rats in the Sweden in this study.
152: **Figure 41:** Median joining network of D-loop haplotypes found in brown rats in (a) UK and (b) Sweden and the relationship of anticoagulant resistance polymorphisms.
154: **Figure 42:** Multiple sequence alignment of representative vertebrate VKORC1 sequences.
155: **Figure 43:** TMHMM prediction graph and 3D model prediction using SWISS Model and Chimera for wild type brown rat VKORC1 and p.R40G mutant.
157: **Figure 44:** DNA sequencing electrophoretograms of rat VKORC1 with the novel p.R40G polymorphism after site directed mutagenesis.
158: **Figure 45:** Cell micrograph of *Sf9* cells before transfection and 72 hours after transfection with P1 virus to produce P2 virus.
159: **Figure 46:** HPLC chromatograms for synthesised vitamin K epoxide and vitamin K at a volume of 20 μl at 10 μM for both compounds at 246 nm detection wavelength.
160: **Figure 47:** UV spectrum of vitamin K and synthesized vitamin K epoxide both with a concentration of 10 μM.
161: **Figure 48:** HPLC chromatograms of the VKOR assay with 2 mg of rat liver microsomes after 30 minutes with control reactions using 100 μM of vitamin K epoxide (K>O).
162: **Figure 49:** HPLC chromatograms showing the vitamin K production from untransfected *Sf9* cells, recombinant rat VKORC1 and p.L120Q and p.R40G variants expressed in *Sf9* insect cells at 0 and 30 minute incubations at 50 μM of vitamin K epoxide.
163: **Figure 50:** Kinetic analysis of wild type rat VKORC1 and rat VKORC1 with p.R40G polymorphism expressed in *Sf9* cells.
165: **Figure 51**: Example HPLC chromatograms showing the vitamin K production from recombinant rat VKORC1 and p.L120Q and p.R40G variants expressed in *Sf9* insect cells using 10 μM of vitamin K epoxide substrate for 15 minutes with no inhibitor, 1 μM of warfarin and 1 μM bromadiolone
167: **Figure 52:** Normalised VKORC1 activity at different concentrations of warfarin and bromadiolone for wild type rat VKORC1 and rat VKORC1 with p.L120Q and p.R40G polymorphisms expressed in *Sf9* cells.
170: **Figure 53:** Comparison of anticoagulant dose-response curves for the wildtype rat VKORC1 and rat VKORC1 with p.R40G polymorphism expressed in *Sf9* cells.
178: **Figure 54:** Multiple sequence alignment of Mammalian Rodentia and Lagomorpha VKORC1.
179: **Figure 55:** Multiple sequence alignment of Mammalian Primate, Dermoptera and Scandentia VKORC1.
180: **Figure 56:** Multiple sequence alignment of Mammalian Cetartiodactyla VKORC1.

181: **Figure 57:** Multiple sequence alignment of Mammalian Carnivora VKORC1.

182: **Figure 58:** Multiple sequence alignment of Perissodactyla VKORC1.

182: **Figure 59:** Multiple sequence alignment of Mammalian Chiroptera VKORC1.

183: **Figure 60:** Multiple sequence alignment of Mammalian Cingulata, Afrosoricida, Macroscelidea, Tublidentata and Proboscidea VKORC1.

183: **Figure 61:** Multiple sequence alignment of Mammalian Eulipotyphia VKORC1.

184: **Figure 62:** Multiple sequence alignment of Mammalian Marsupials and Monotreme VKORC1.

185: **Figure 63:** Multiple sequence alignment of Bird Galliformes and Passeriformes VKORC1.

185: **Figure 64:** Multiple sequence alignment of Reptile Serpents, Iguania and Testundines VKORC1.

186: **Figure 65:** Multiple sequence alignment of Amphibian Anura VKORC1.

187: **Figure 66:** Multiple sequence alignment of Fish Cichlida, Cypriodontiformes, Tetraodontiformes Beloniformes and Pomcentridae VKORC1.

194: **Figure 67:** Multiple sequence alignment of representative vertebrate VKORC1 sequences.

197: **Figure 68:** Multiple sequence alignment of VKORC1 consensus sequences for each class within the vertebrate subphylum with the four transmembrane domains highlighted.

198: **Figure 69:** Multiple sequence alignment of the mammalian VKORC1 consensus sequence with the amino acid differences shown under the unconserved positions

199: **Figure 70:** Multiple sequence alignment of the bird VKORC1 consensus sequence with the amino acid differences shown under the unconserved positions.

200: **Figure 71:** Multiple sequence alignment of the reptilian VKORC1 consensus sequence with the amino acid differences shown under the unconserved positions.

201: **Figure 72:** Multiple sequence alignment of the amphibian VKORC1 consensus sequence with the amino acid differences shown under the unconserved positions.

202: **Figure 73:** Multiple sequence alignment of the fish VKORC1 consensus sequences with the amino acid differences shown under the unconserved positions.

204: **Figure 74:** Membrane topology and tertiary structure prediction models for representative mammalian VKORC1 species; human, cow, wombat and duck-billed platypus. Each panel shows a TMHMM prediction graph and 3D model prediction using SWISS-Model and Chimera for a front and top view of the VKORC1 sequence with the transmembrane domains highlighted.

205: **Figure 75:** Membrane topology and tertiary structure prediction models for representative non-mammalian VKORC1 species; chicken, python, western clawed frog and Nile tilapia. Each panel shows a TMHMM prediction graph and 3D model prediction using SWISS-Model and Chimera for a front and top view of the VKORC1 sequence with the transmembrane domains highlighted.

224: **Figure 76:** Topology diagram of VKORC1 with the conserved residues throughout vertebrate VKORC1 sequences highlighted.

229: **Figure 77:** Multiple sequence alignment of Mammalian Rodentia and Lagomorpha VKORC1L1.

230: **Figure 78:** Multiple sequence alignment of Mammalian Primate VKORC1L1 sequences.

231: **Figure 79:** Multiple sequence alignment of Mammalian Cetartiodactyla and Perissodactyla VKORC1L1.

232: **Figure 80:** Multiple sequence alignment of Mammalian Carnivora VKORC1L1.

233: **Figure 81:** Multiple sequence alignment of Mammalian Chiroptera VKORC1L1.

233: **Figure 82:** Multiple sequence alignment of Mammalian Marsupials and Monotreme VKORC1L1.

234: **Figure 83:** Multiple sequence alignment of Bird VKORC1L1 sequences

235: **Figure 84:** Multiple sequence alignment of Reptile VKORC1L1.

235: **Figure 85:** Multiple sequence alignment of Amphibian VKORC1L1 sequences.

236: **Figure 86:** Multiple sequence alignment of Fish VKORC1L1 sequences.

237: **Figure 87:** Multiple sequence alignment of Fish VKORC1L1 sequences.

238: **Figure 88:** Multiple sequence alignment of Fish VKORC1L1 sequences.

242: **Figure 89:** Multiple sequence alignment of representative vertebrate VKORC1L1 sequences.

244: **Figure 90:** Multiple sequence alignment of VKORC1L1 consensus sequences for each class within the vertebrate subphylum with the four transmembrane domains highlighted.

246: **Figure 91:** Multiple sequence alignment of the mammalian VKORC1L1 consensus sequence with the amino acid differences shown under the unconserved positions.

247: **Figure 92:** Multiple sequence alignment of the bird VKORC1L1 consensus sequence with the amino acid differences shown under the unconserved positions.

248: **Figure 93:** Multiple sequence alignment of the reptilian VKORC1L1 consensus sequence with the amino acid differences shown under the unconserved positions.

249: **Figure 94:** Multiple sequence alignment of the amphibian VKORC1L1 consensus sequence with the amino acid differences shown under the unconserved positions.

250: **Figure 95:** Multiple sequence alignment of the fish VKORC1L1 consensus sequences with the amino acid differences shown under the unconserved positions.

252: **Figure 96:** Membrane topology and tertiary structure prediction models for representative mammalian VKORC1L1 species; human, cow, wombat and duck-billed platypus. Each panel shows a TMHMM prediction graph and 3D model prediction using SWISS-Model and Chimera for a front and top view of the VKORC1 sequence with the transmembrane domains highlighted.

253: **Figure 97:** Membrane topology and tertiary structure prediction models for representative non-mammalian VKORC1L1 species; chicken, python, western clawed frog and Nile tilapia. Each panel shows a TMHMM prediction graph and 3D model prediction using SWISS-Model and Chimera for a front and top view of the VKORC1L1 sequence with the transmembrane domains highlighted.

270: **Figure 98:** Multiple sequence alignment of VKOR consensus sequences for each class within the vertebrate subphylum with the four transmembrane domains highlighted

274: **Figure 99:** Multiple sequence alignment of the four chosen VKORC1 sequences, brown rat, human, cow and python with the four transmembrane domains highlighted.

275: **Figure 100:** Multiple sequence alignment of representative vertebrate VKORC1 sequences.

277: **Figure 101:** Structural modelling diagrams of rat, human, cow and python VKORC1 based on the VKORC1 structure defined by (Li *et al.,* 2010).

278: **Figure 102:** Structural diagrams of rat, human, cow and python VKORC1 from above, based on the VKORC1 structure defined by *Li et al.* (2010).

280: **Figure 103:** HPLC chromatograms showing the vitamin K production from recombinant rat, human, cow and python VKORC1 expressed in *Sf9* insect cells at 0 and 30 minute incubations at 50 μM VKE.

281: **Figure 104:** Kinetic analysis of rat, human and cow VKORC1 expressed in *Sf9* cells.

286: **Figure 105:** Comparison of anticoagulant dose-response curves for the rat, human and cow VKORC1 expressed in *Sf9* cells.

List of Tables

23: **Table 1:** List of the top 15 rodent pest species in the world.

25: **Table 2:** Diseases caused in humans by zoonotic viruses that may be transmitted by rodents.

26: **Table 3:** Diseases caused in humans by zoonotic bacteria that may be transmitted by rodents.

27: **Table 4:** Diseases caused in humans by zoonotic parasites that may be transmitted by rodents.

32: **Table 5:** Resistance factors of anticoagulant rodenticides.

35: **Table 6:** Acute toxicity of FGAR and SGARs in different species.

51: **Table 7:** Amino acid positions with a previously reported role in structure, function, and substrate or anticoagulant binding.

60: **Table 8:** Anticoagulant resistant polymorphisms found in the VKORC1 gene in *Rattus norvegicus* in different countries.

61: **Table 9:** Geographical areas in the UK where compound heterozygotes are found in the VKORC1 gene in *Rattus norvegicus* samples.

62: **Table 10:** Anticoagulant resistant polymorphisms found in the VKORC1 gene in *Rattus norvegicus* in different countries.

64: **Table 11:** Anticoagulant resistant polymorphisms found in the VKORC1 gene in other rodent species in different countries.

66: **Table 12:** Anticoagulant resistant polymorphisms found in VKORC1 in *Homo sapiens*.

71: **Table 13:** Kinetic properties of VKORC1 in different animals with vitamin K epoxide substrate.

80: **Table 14:** Comparison of published VKOR assay methods by Matagrin *et al.* (2016) and Czogalla *et al.* (2018) for inhibition values by anticoagulants for VKORC1 and VKORC1L1.

97: **Table 15:** The volume and concentration of PCR reagents required to produce a PCR master mix.

98: **Table 16:** Forward and reverse primer sequences for exons 1, 2 and 3 of the VKORC1 gene.

101: **Table 17:** Selective markers used to identify and select for *E. coli* strains and transformed vectors.

105: **Table 18:** PCR Primers with specific upstream and downstream sequences used to amplify VKORC1 from the pET32a plasmid.

106: **Table 19:** Volume and concentration of PCR reagents required for a one sample master mix.

107: **Table 20:** Volumes of reagents required for T4 polymerase treatment of purified PCR product.

108: **Table 21:** Volumes of reagents required for T4 polymerase treatment of purified PCR product.

109: **Table 22:** Volume and concentration of PCR reagents required for a one sample master mix.

110: **Table 23:** PCR Primers with specific upstream and downstream sequences used to amplify VKORC1 from the pFB-LIC-Bse plasmid for site directed mutagenesis.

110: **Table 24:** Volume and concentration of PCR reagents required for a one sample master mix.

115: **Table 25:** Volume and concentration of PCR reagents required for a one sample master mix.

124: **Table 26:** Volumes of BSA and Ultrapure water required to make up the BSA calibration standards.

127: **Table 27:** HPLC conditions for analysis of VKORC1 reactions.

132: **Table 28:** Novel p.R40G polymorphism found in the VKORC1 gene in *Rattus norvegicus* in the UK and Sweden.

133: **Table 29:** Overview of the polymorphisms found in exon 2 in brown rat samples for all the geographical areas surveyed in the UK and Sweden.
136: **Table 30:** Overview of the polymorphisms found in exon 3 in brown rat samples for all the geographical areas surveyed in the UK.
141: **Table 31:** Overview of the polymorphisms found in exon 3 in brown rat samples for all the geographical areas surveyed in Sweden.
148: **Table 32:** Haplotypes identified for counties surveyed by this study and Haniza *et al.* (2015).
163: **Table 33:** K_m and V_{max} values derived from Michaelis-Menten graphs of wild type rat VKORC1 and rat VKORC1 with p.R40G polymorphism expressed in *Sf9* cells.
168: **Table 34:** 2 way ANOVA results showing the P values and significance of each anticoagulant and polymorphism for each concentration.
171: **Table 35:** IC_{50} values derived from dose-response curves of different anticoagulants for wild type rat VKORC1 and rat VKORC1 with p.R40G polymorphism expressed in *Sf9* cells.
188: **Table 36:** Number of VKORC1 sequences found in each taxonomic order for Mammals with the sequence identity within the specific order and the evolutionary timespan between the different species.
190: **Table 37:** Number of VKORC1 sequences found in each taxonomic class for non-mammals with the sequence identity within each class.
192: **Table 38:** Percentage identity between the five different classes of vertebrate VKORC1.
208: **Table 39:** Amino acid positions with a previously reported role in the stability of VKORC1 with the percentage of amino acids found at each position for each vertebrate class.
209: **Table 40:** VKORC1 amino acid positions with a previously reported role of naphthoquinone head binding of vitamin K and vitamin K epoxide with the percentage of amino acids found at each position for each vertebrate class.
210: **Table 41:** VKORC1 amino acid positions with a previously reported role of isoprenoid chain binding of vitamin K and vitamin K epoxide with the percentage of amino acids found at each position for each vertebrate class.
213: **Table 42:** VKORC1 amino acid positions with a previously reported role of warfarin binding of vitamin K and vitamin K epoxide with the percentage of amino acids found at each position for each vertebrate class.
217: **Table 43:** Anticoagulant resistance polymorphisms in *Rattus norvegicus* with the percentage of amino acids found at each position for each vertebrate class.
218/219: **Table 44:** Anticoagulant resistance polymorphisms in *Homo sapiens* with the percentage of amino acids found at each position for each vertebrate class.
220: **Table 45:** Anticoagulant resistance polymorphisms in *Mus musculus* with the percentage of amino acids found at each position for each vertebrate class.
222: **Table 46:** *Mus spretus* phenotype shown with the wild type house mouse and an assessment of the percentage of amino acids found at each position for each vertebrate class.
225: **Table 47:** Conserved amino acid positions in all vertebrate VKORC1 sequences that have a previously identified role.
226: **Table 48:** Conserved amino acid positions in all vertebrate VKORC1 sequences with proposed role in VKORC1.
239: **Table 49:** Number of VKORC1L1 sequences found in each taxonomic order for Mammals with the sequence identity within the specific order and the evolutionary timespan between the different species.
239: **Table 50:** Number of VKORC1L1 sequences found in each taxonomic class for non-mammals with the sequence identity within each class.
240: **Table 51:** Percentage identity between the five different classes of vertebrate VKORC1L1.
256: **Table 52:** Amino acid positions with a previously reported role in warfarin binding of VKORC1L1 with the percentage of amino acids found at each position for each vertebrate class.
258: **Table 53:** Amino acid positions with a previously reported role of conservation of amino acid positions in VKORC1L1 with the percentage of amino acids found at each position for each vertebrate class.

260: **Table 54:** Conserved amino acid positions in all vertebrate VKORC1L1 sequences that have a previously identified role.

260: **Table 55:** Conserved amino acid positions in all vertebrate VKORC1L1 sequences found at the N or C terminal in VKORC1L1 found in this study.

261: **Table 56:** Conserved amino acid positions with a potential involvement in helix-helix interactions and substrate binding in all vertebrate VKORC1L1 sequences found in this study.

262: **Table 57:** Conserved amino acid positions with a potential involvement in the structure and interactions of linking loops in all vertebrate VKORC1L1 sequences found in this study.

263: **Table 58:** Percentage identity between the five different classes of vertebrate VKORC1 compared to vertebrate VKORC1L1.

265: **Table 59:** Amino acid positions with a previously reported role by Bevans *et al.* (2015) of conserved amino acid positions TM domains leading to helix-helix interactions in VKOR with the percentage of amino acids found at each position for each vertebrate class.

266: **Table 60:** Amino acid positions with a previously reported role by Bevans *et al.* (2015) of substrate interactions in VKOR with the percentage of amino acids found at each position for each vertebrate class.

267: **Table 61:** Amino acid positions identified by Schwarz *et al.* (2009) that are fish VKORC1-specific and VKORC1L1-specific.

268: **Table 62:** Comparison of amino acid positions identified by Schwarz *et al.* (2009) that are fish VKORC1-specific and VKORC1L1-specific in all vertebrate classes.

271: **Table 63:** Conserved amino acid positions between VKORC1 and VKORC1L1 throughout all classes of vertebrates.

281: **Table 64:** K_m and V_{max} values derived from Michaelis-Menten graphs of rat, human and cow VKORC1 expressed in *Sf9* cells.

284: **Table 65:** Comparison of published kinetic VKORC1 data with vitamin K epoxide substrate with the current study.

287: **Table 66:** IC_{50} values derived from dose-response curves of different anticoagulants for rat, humans and cow VKORC1 expressed in *Sf9* cells.

287: **Table 67:** 2 way ANOVA results showing the P values and significance of each anticoagulant compared to each VKORC1 construct.

289: **Table 68:** Comparison of published warfarin inhibition data for VKORC1 with the data from the current study.

290: **Table 69:** Comparison of published second generation anticoagulant rodenticide inhibition data for the current study.

Chapter 1: Introduction

1.0 About This Chapter

This chapter will highlight the reasons as to why rodents are seen as pests and how the discovery of anticoagulants was used to control populations of rodent pests. The chapter will also explore the consequences of the uses of anticoagulants with the discovery of anticoagulant resistance in humans, rats and mice and the effects of non-target poisoning. There will also be a focus on the enzymes VKORC1 and VKORC1L1 regarding the structure, function and evolution and the interaction with anticoagulants.

1.1 Rodents as Pests

In the class of Mammalia, Rodentia is the largest order, containing over 2000 species (Carleton and Musser, 2005). With their worldwide distribution, rodents are found on every continent except for Antarctica (Meerberg *et al.*, 2009). Due to the worldwide distribution and the vast number of rodent species it is inevitable, however, that some rodent species are seen as pests to humans as they are detriments to several aspects of human 'existence'. Capizzi *et al.* (2014) described the top 15 rodent pests that have the largest impact in agriculture, ecosystems, forestry and public health. These are summarized in Table 1 (Capizzi *et al.*, 2014).

Of the top 15 rodent pests in the world, the rat species (e.g. *Rattus norvegicus, Mastomys natalensis, Rattus argentiventer*) and the house mouse (*Mus musculus*) are most commonly associated with the destruction of agricultural crops (Stenseth *et al.,* 2003). Pests such as the beaver, gopher and prairie dogs have huge impacts on ecosystems (Capizzi *et al.,* 2014). The mountain beaver is responsible for major deforestation in the Pacific Northwest (Dolbeer *et al.,* 1994). *Rattus rattus* and *Rattus norvegicus* are amongst the rodent pests that are a public health issue due to their commensal relationship with humans (Feng and Himsworth, 2014).

Common Name	Scientific Name
Black Rat	*Rattus rattus*
Brown Rat	*Rattus norvegicus*
House Mouse	*Mus musculus*
Polynesian Rat	*Rattus exulans*
Grey Squirrel	*Sciurus carolinesis*
California Ground Squirrel	*Spermophilus beecheyi*
African Rat	*Mastomys natalensis*
Ricefield Rat	*Rattus argentiventer*
Lesser Bandicoot Rat	*Bandicota bengalensis*
Gophers	*Thomomys spp.*
Coypu	*Myocastor coypus*
Small Vesper Mouse	*Calomys laucha*
Mountain Beaver	*Aplodontia rufa*
Great Bandicoot Rat	*Bandicota indica*
Black-tailed Prairie Dog	*Cynomys ludovicianus*

Table 1: List of the top 15 rodent pest species in the world. (Capizzi *et al.,* 2014).

Rodents are responsible for huge losses in arable agriculture due to damage to crops and food storages. This can cause depletion of food supplies which is especially significant in developing countries where food supplies are in high demand (Lund, 2015). Rodents are responsible for loses to cereals, vegetables, maize, rice, root crops, cacao and nuts (Stenseth *et al.,* 2003). In Asia, 5% of the production of rice harvests are lost due to rodents, which is the equivalent of enough rice to feed 180 million people for a year (Singleton, 2003). There is a large economic impact on the loss of food by rodent pests. In 1982, it was reported that commensal rodents caused an economic loss of US$30 billion worldwide (Almeida *et al.,* 2013). Tanzania alone lost $40 million to food crop destruction due to rodent pests (Leirs, 2003). Additionally, rodents can contaminate stored food by the presence of shed rodent hairs, urination and defecation (Lund, 2015; Witmer *et al.*, 2014).

As rodents typically live in close contact with humans, rodents pose a risk to human health with the spread of zoonotic diseases. There are around 60 diseases that can be transmitted by rodents to humans (Meerburg *et al.,* 2009). Human disease can be caused by the transmission of viruses, bacteria or parasites by rodents (Tables 2-4). Rodents can transmit

disease to humans directly or indirectly (Meerburg *et al.,* 2009). Direct contact can occur by rat bites; by contact with infected animals, particularly dead animals and by contact with water or food contaminated with rat urine or faeces. One zoonotic disease which has raised recent awareness due to a high-profile death of a British Olympic rower is Leptospirosis which is commonly known as Weil's disease (Forbes *et al.,* 2012). This disease can cause a variety of symptoms from haemorrhages to renal failure and can be caused by direct contact with rodents (Table 3). Indirect transmission can also occur via livestock contact with rodents when undercooked meat from these animals is consumed by humans (Meerburg *et al.*, 2009). There are 18 diseases that are caused by flea, tick and mites bites that are transmitted via rodents (Tables 2-4). One of the most famous diseases that was transmitted through fleas carried by rodents was the plague (Table 2). Plague is caused by a bacterium called *Yersinia pestis*, which is a highly infectious and deadly disease. In the 14th century, the second and most deadly pandemic claimed the lives of over a quarter of the European population with a reported 100,000 deaths in London alone (Miller, 1940).

In addition to carrying diseases that affect human health both native and invasive rodent species can also have impacts on ecosystems. Damage to trees by small rodents can have significant impacts in forestry, especially to local habitats (Singleton *et al.,* 2010). Rodents can cause damage to tree bark and stems and *Apodemus* (wood mouse) species are known to cause damage to tree roots (Singleton *et al.,* 2010). The introduction of invasive rodent species such as rats can have detrimental effects on ecosystems and can cause endangering or causing extinction of native animals such as Monarchs in French Polynesia (Witmer *et al.,* 2014; Thibault and Meyer, 2001). Rodents have a high reproduction rate and introduction into an ecosystem where there are few or no predators allows the rodents to thrive causing significant impacts on the ecosystem (Witmer *et al.,* 2014).

Disease	Transmission to Humans	Symptoms	References
Hantavirus (Bunyaviridae)	Rat bites, inhalation of viral particles, direct contact of rodent droppings/urine	Fever, headaches, dizziness, vomiting, diarrhoea, shortness of breath, respiratory compromise – 30-40% fatal	Shipley *et al.,* 2018
Haemorrhagic Fever (Bunyaviridae)	Rodent bites	Capillary leakage, haemorrhage manifestations	Zhang *et al.,* 2010
Borna Disease (Bornaviridae)	Contact with rodent saliva, urine and faeces	Fever, neurological impairment	Kinnunen *et al.,* 2013
Omsk Haemorrhagic Fever (Flaviviridae)	Contact with Infected animals and ticks	Fever, headache, myalgia, dehydration, haemorrhaging	Shah *et al.,* 2018
Kyasanur Forest Disease (Flaviviridae)	Tick bites	Haemorrhagic fever	Soloman and Mallewa, 2001; Hoogstraal, 1966
Tick- borne Encephalitis (Flaviviridae)	Tick bites	Acute central nervous system disease resulting in death	Randolph *et al.,* 1999
Lymphocytic Choriomeningitis (Arenaviridae)	Breathing air contaminated with rodent faeces	Flu-like symptoms, meningitis, encephalitis	Childs *et al.,* 1991; Childs *et al.,* 1992
Lassa Fever (Arenaviridae)	Breathing air contaminated with rodent faeces, direct contact with rodent urine/faeces, consumption of food contaminated by infected rodents, bite wounds, close contact with other infected humans	Fever, weakness, malaise, severe headaches, throat ache, persistent vomiting and diarrhoea	Meersberg *et al.,* 2009
North American Arenaviruses (Arenaviridae)	Inhalation of aerosolised rodent urine	Fever, malaise, anorexia, myalgia, sore throat, haemorrhagic fever	Enserink, 2000
Venezuelan Equine Encephalitis (Togaviridae)	Mosquito bites	Acute encephalitis, neurological problems	Aguilar *et al.,* 2004
Cowpox (Poxviridae)	Direct contact with infected rodents	Painful haemorrhagic pustules, edema, erythema	Wolfs *et al.,* 2002

Table 2: Diseases caused in humans by zoonotic viruses that may be transmitted by rodents.

Disease	Transmission of Humans	Symptoms	Reference
Leptospirosis (*Leptospira* spp.)	Consumption of food or water contaminated by rodents, contact through skin/mucus membranes with contaminated soil or water, handling dead infected rodents	Aseptic meningitis, lymphadenopathy, jaundice, renal failure, haemorrhages	Bharti *et al.,* 2003; Plank and Dean, 2000
Lyme Disease (*Borrelia burgdorferi*)	Tick bites	Erythema chronicum migrans, rash, nervous system, heart, eye and joint problems	Voordouw *et al.,* 2015
Tickborne Relapsing Fever (*Borrelia* spp.)	Infected tick bites	Periodic fevers	Dworkin *et al.,* 2008
Scrub Typhus (*Rickettsiaceae*)	Infected mite bites	Fever, headache, cough, muscle pain, gastrointestinal problems, haemorrhages	Demma *et al.,* 2006
Murine Typhus (*Rickettsia typi)*	Infected flea bites	Headache, fever, nausea, body aches, body rashes	Basra *et al.,* 2012
Sylvatic Epidemic Typhus (*Rickettsia prowazekii)*	Body lice, human-human contact	Fever, myalgia, severe headache, rash	Gillespie *et al.,* 2008
Queensland Tick Typhus (*Rickettsia australis*)	Tick bites	Fever, myalgia, severe headache, rash	Dehhaghi *et al.,* 2019
Rickettsialpox (*Rickettsia akari*)	Mite bites	Chills, fever, malaise, headache followed by papulovesicular cutaneous eruption	Comer *et al,* 2001; Heymann, 1996
Bartonella Illnesses (*Bartonella* spp)	Bites from fleas and lice	Endocarditis, cardiac disease, febrile illness	Breitsonwerdt and Kordick, 2000; Iralu *et al,* 2006; Welc-faleciak *et al,* 2008
Human Granulocytic Anaplasmosis (*Anaplasma phagocytophilum*)	Bites from infected ticks	Headaches, high fever, chills, myalgias, respiratory failures	Levin *et al.*, 2002; Fritz and Glaser, 1998
Q-fever (*Coxiella burnetii)*	Inhalation of contaminated dust, contact with contaminated animal products and birthing products	Atypical pneumonia, hepatitis, fever, jaundice, endocarditis	Maurin and Raoult, 1999
Tularemia (*Francisella tularensis*)	Direct contact with infected animal carcasses, consumption of contaminated food and water, bite from an infected animal	Ulcerglandular tularemia	Freidl *et al.,* 2005
Plague (*Yersinia pestis)*	Bites from fleas carried by rodents	Chills followed by high temperature, headache, backache, restlessness, rapid pulse, bubo, central nervous system manifestations, fatal	Perry and Fetherston, 1997; Hoffman, 1980
Rat-bite Fever (*Streptobacillus moniliformis*)	Consumption of contaminated water, milk or food that has contact with rats	Pharyngitis and pronounced vomiting	Elliot, 2007

Table 3: Diseases caused in humans by zoonotic bacteria that may be transmitted by rodents.

Disease	Transmission to Humans	Symptoms	Reference
Toxoplasmosis (*Toxoplasma gondii)*	Uncooked foods	Flu-like symptoms, damage to vital organs, blurred vision	Halonen and Weiss, 2013
Babesiosis (*Babesia* spp.)	Tick bites	Asymptomatic or cause mild non-specific illness	Vannier *et al.,* 2014
Cryptosporidiosis (*Cryptosporidium*)	Contact with contaminated human or animal faeces	Watery diarrhoea, stomach cramps, dehydration, nausea, vomiting, fever, weight loss	Leitch and He, 2011
Chagas Disease (*Trypanosoma cruzi*)	Blood-sucking assassin triatomines	Severe neurological problems in children, after 20 years – cardiomyopathy, peripheral nervous system damage	Buocaglia and Di Noia, 2003
Leishmaniasis (*Leishman* spp.)	Bite from an infected sand-fly	Chronic skin ulcers, erosive mucosal disease	Hepburn, 2000
Giardiasis (*Giardia lamblia*)	Consumption of contaminated food and water, swimming in contaminated water	Loss of appetite, diarrhoea, lethargy, fever, stomach problems, projectile vomiting, bloating, flatulence	Adam, 1999
Taeniasis (*Taenia*)	Inadequately cooked food	Tapeworms	Okello and Thomas, 2017
Echinococcosis (*Echinococcus* spp.)	Consumption of contaminated food stuffs, handling infected animals	Parasitic tumours in the liver	Basset *et al.,* 1998
Schistosomiasis (*Schistomes*)	Swimming in water infested with snails	Embolic egg granulomas, hypertension, squamous cell carcinoma, calcification	Mostafa *et al.,* 1999
Human Fasciolosis (*Fasciola hepatica*)	Consumption of raw watercress where sheep and cattle are reared	Fever, malaise, abdominal pain, eosinophilia, hepatomegaly	
Brachylmeiosis (*Trematoda* spp.)	Consumption of infected snails	Abdominal pain and diarrhoea	Spratt, 2005
Alarviosis (*Trematoda* spp.)	Humans can be a host to the parasite	Fatal	Shoop, 1994; Fernandes *et al.,* 1976
Echinostomiosis (*Echinostomatidae* spp.)	Ingestion of raw/undercooked mollusks, fish crustaceans and amphibians	Abdominal pain, vomiting, diarrhoea, weight loss, nausea, anorexia	Zhoel *et al.,* 2008
Trichinosis (*Trichinella* spp.)	Consuming inadequately cooked meat	Nausea, heartburn, dyspepsia, diarrhoea	Schmitt *et al.,* 1978
Capillariasis (*Capillaria hepatica*)	Injection of infected soil	Hepatic capillariasis	Cwiklinski *et al.,* 2016
Angiostrongyliasis (*Angiostrongylus cantonensis*)	Ingesting tissues of raw or undercooked infected hosts, contaminated salad leaves	Fatal consequences	Spratt, 2005
Toxoscariasis (*Toxocara canis)*	Ingestion of nematode eggs, handling infected animals	Visceral larva migrans	Despommier, 2003
Baylisascariosis (*Baylisascaris* procyonis)	Accidental ingestion of nematode eggs from racoon latrines (soil, vegetables) contaminated with faeces	Fatal neural larva migrans, ocular larva migrans	Gavin, 2005
Amoebic Dysentery (*Entamoeba histolytica*)	Contaminated food and water	Fulminating dysentery, diarrhoea, weight loss, fatigue, abdominal pain, amebomas	Marie and Petri, 2013

Table 4: Diseases caused in humans by zoonotic parasites that may be transmitted by rodents.

1.2 Pest Management

Due to the ecological impacts of rodents on agriculture and environments as well as public health concerns, pest control measures are used to manage populations of rodents (Tobin and Fall, 2006). Management of rodent pests typically involves removing the animal that is causing the damage, usually by killing it (Smith and Meyer, 2015). There are a number of pest control methods that can be employed to control populations of rodents. The most common pest control measures include; anticoagulant rodenticides, non-anticoagulant rodenticides, mechanical traps, fertility treatments, hunting and the use of predators (Capizzi *et al.,* 2014; Hygnstrom and Virchow, 1992). Of these, the most effective and most widely used are anticoagulant rodenticides.

Before anticoagulant rodenticides were introduced, more toxic, single feed compounds were used (Hadler and Buckle, 1992). These compounds had an immediate effect on the rodents upon consumption of the bait. The sudden onset of symptoms deterred rodents from consuming more bait (Hadler and Buckle, 1992). Pre-baiting with non-toxic bait was required to combat this 'bait shyness', which was seen as very time consuming (Hyngstrom and Virchow, 1992). These compounds had no specificity to animals and high doses were required and sub-lethal doses could have long-lasting effects in animals leading to non-target poisoning either by primary or secondary poisoning (Berny *et al.,* 2014; Hadler and Buckle, 1992).

1.3 Discovery of Anticoagulants

1.3.1 Discovery of Dicoumarol

Anticoagulants were discovered at the beginning of the 1900s. During the Great Depression, sweet clover was a common food source used to feed cattle in the USA. There were many reports in the 1920s of previously healthy cattle dying suddenly of internal bleeding (Roderick, 1931). Due to financial hardship farmers could not afford to provide fresh sweet clover to feed their cattle and often mouldy sweet clover was used to feed livestock. Studies showed that the bleeding of the cattle was due to the ingestion of mouldy sweet clover (Roderick, 1931). In the 1940s, work by Karl Link and colleagues isolated the compound that caused the internal bleeding in cattle (Campbell *et al.,* 1940; Campbell and Link, 1941; Stahmann *et al.,*

1941). This compound was 3,3'-methylene-bis[4-hydroxycoumarin], which was named dicoumarol (Stahmann *et al.,* 1941) (Figure 1).

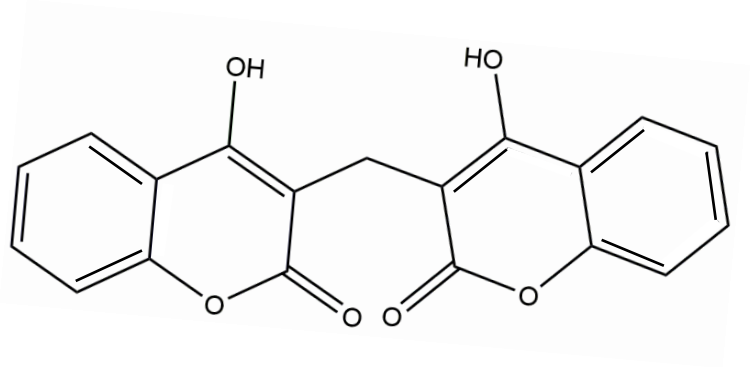


Figure 1: Chemical structure of dicoumarol. (Created by Author using ChemDraw v18, adapted from Helgeland, 1980)

1.3.2 Synthesis and use of warfarin as an anticoagulant

After the discovery of dicoumarol, Link and colleagues began to synthesise many derivatives of the 4-hydroxycoumarin compound (Strahmann *et al.,* 1943; Sullivan *et al.,* 1943; Huebner *et al.,* 1943; Strahmann *et al.,* 1944; Ikawa *et al.,* 1944; Huebner *et al.,* 1944). One key derivative, 3-α-(acetonylbenzyl)-4-hydroxycoumarin, which was later named warfarin after the Wisconsin Alumini Research Foundation (Figure 2), was found to be a more potent and more water-soluble derivative and was first introduced as a rodenticide in 1948 to control populations of rodents (West *et al.,* 1961). Warfarin is an effective rodenticide due to its properties as an odorless and colourless substance with a delayed onset in animals (King and Tran, 2015). The new method of using anticoagulants as rodenticides allowed a higher mortality rate of the animals within two weeks of baiting (Pelz *et al.,* 2005), giving a more efficient way of treating populations of rodents.

In the mid-1950s warfarin was introduced as an oral anticoagulant in humans to treat arterial and venous thromboembolic events (Wardrop and Keeling, 2008). The first human to be treated with warfarin as an oral drug was President Eisenhower (Helgeland, 1980). Although, warfarin was introduced as a rodenticide and a human drug, the mechanism of action of warfarin was not fully understood until the 1970s (See Section 1.8).

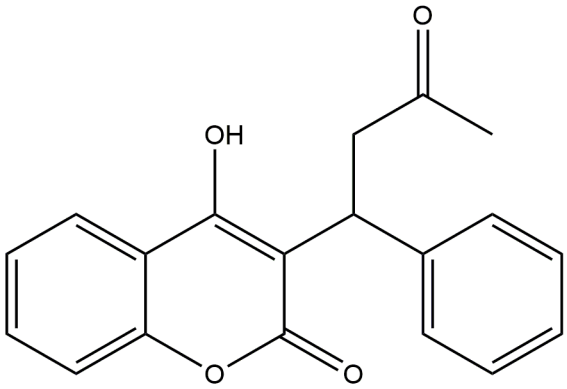


Figure 2: Chemical structure of warfarin. (Created by Author using ChemDraw v18, adapted from Helgeland, 1980)

1.4 First Generation Anticoagulant Rodenticides

Following the synthesis of warfarin, other commercial anticoagulant rodenticides were synthesised during the 1950s. These are known as 'first generation anticoagulant rodenticides' (FGARs) (Hadler and Buckle, 1992). FGARs were derived from indandiones or 4-hydroxycoumarins (Hadler and Buckle, 1992) (Figure 3). Coumachlor, coumafuryl and coumatetralyl were amongst the first derivatives of 4-hydroxycoumarins to be developed commercially (Hadler and Buckle, 1992). Diphacinone and chlorophacinone were derived from indandiones (Bentley, 1972). Pindone another indandione was first developed as an insecticide and then later used as a rodenticide (Hadler and Buckle, 1992).

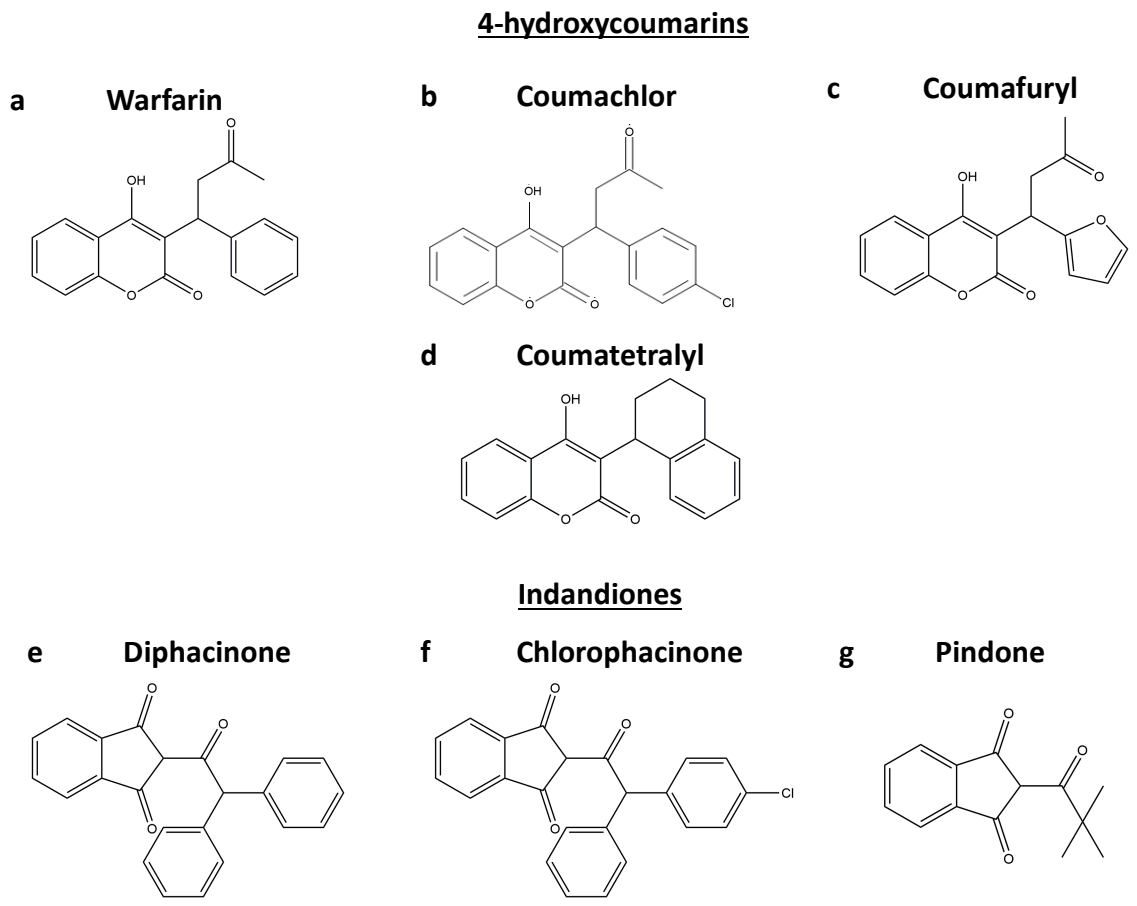


Figure 3: Chemical structures of 4-hydroxycoumarin and indandione first generation anticoagulants. (Created by Author using ChemDraw v18, based on Vudathala *et al.,* 2010). **a** Warfarin. **b** Coumachlor. **c** Coumafuryl. **d** Coumatetralyl. **e** Diphacinone. **f** Chlorophacinone. **g** Pindone.

1.5 First Report of Anticoagulant Resistance

Around 10 years after the introduction of anticoagulants as rodenticides, the first incidence of anticoagulant resistance was reported. In 1958, a Scottish farm with a large infestation of brown rats (*Rattus norvegicus*) was treated with both warfarin and diphacinone (Boyle, 1960). Although there was evidence of bait consumption by the rats the warfarin and diphacinone had little effect on the population size (Boyle, 1960). 28 rats caught from the farm were tested using feeding tests over a 5 day period with both warfarin and diphacinone compared with wild type 'control' rats (Boyle, 1960). These tests showed a low mortality rate in the rats found on the farm compared to the control rats, suggesting resistance to these anticoagulant rodenticides (Boyle, 1960). Resistance in mice were reported later in 1961 (Dodsworth, 1961). This anticoagulant rodenticide resistance is defined as the loss of efficiency of rodenticides in

practical conditions, after proper application (Meersburg *et al.,* 2014) and is further explored in Section 1.16.

1.6 Second Generation Anticoagulant Rodenticides

During the 1970s, whilst the mechanism of anticoagulant resistance was being studied, there were other more potent anticoagulant rodenticides synthesisied. These more potent compounds are known as 'second generation anticoagulant rodenticides' (SGARs). The first major development of a more potent anticoagulant rodenticide was difenacoum, a derivative of a 4-hydroxycoumarin (Hadler and Shadbolt, 1975). This was the first new anticoagulant rodenticide that could target a wide range of rodents and was also active against anticoagulant resistant rats (Bull, 1976). Hadler and Shadbolt (1975) synthesised compounds based on the 4-hydroxycoumarin structure and compared the activity of the new compound in wild-type and resistance rats. The ratio of prothrombin effective dose at 50% (ED_{50}) for resistant and normal rats was represented as a resistance factor (Hadler and Shadbolt, 1975). It allowed a comparison of the measure of potential activity against resistant rats (Dubock and Kaukeinen, 1978). Resistance factors of different anticoagulants are given in Table 5. The closer the values are to 1 the more effective the anticoagulant rodenticide is to resistant rats (Dubock and Kaukeinen, 1978).

Compound	Prothrombin Time (mg/kg)		Resistance Factor
	Wistar Rats	Resistant Rats	
Diphacinone	0.22	50	227
Chlorophacinone	0.22	>20	>90
Coumatetralyl	0.30	4.4	14
Warfarin (S-)	0.30	>50	>166
Difenacoum	0.17	0.32	1.9

Table 5: Resistance factors of anticoagulant rodenticides. (Adapted from Hadler and Shadbolt, 1975)

Resistance factors indicate that diphacinone is the weakest anticoagulant rodenticide against resistant rats (Table 5). Other FGARs, warfarin and chlorophacinone, have resistance factors above 90 suggesting a lower activity against resistant rats. On the other hand, coumatetralyl has a resistance factor of 14 which is at least 6-fold lower than the other FGARs. The newly

synthesised SGAR compound difenacoum was very effective against resistant rats in comparison to FGARs (Table 5). Following the synthesis of difenacoum, other anticoagulants were developed including; brodifacoum, bromadiolone and later in the 1980s, difethialone and flocoumafen (Figure 4).

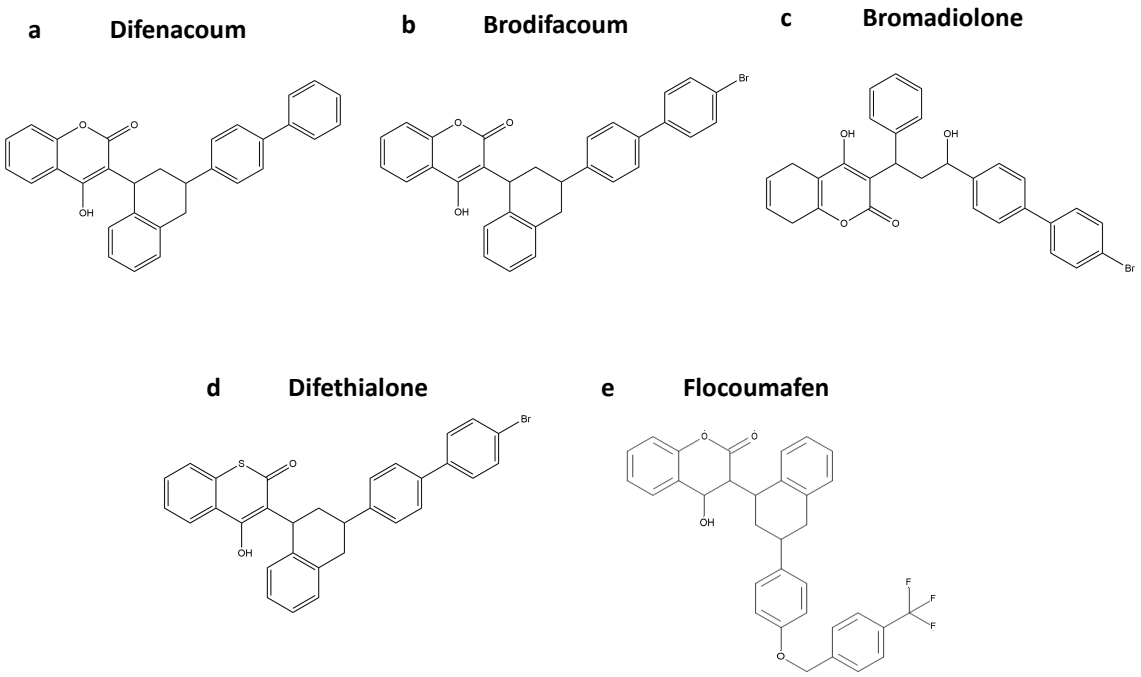


Figure 4: Chemical structures of second generation anticoagulants. (Created by Author using ChemDraw v18, adapted from Hodroge *et al.,* 2011). **a** Difenacoum. **b** Brodifacoum. **c** Bromadiolone. **d** Difethialone. **e** Flocoumafen.

Brodifacoum, a similar compound structurally to difenacoum, was the next anticoagulant to be introduced but as a 'single-feed' rodenticide, meaning that the continuous feeding on bait was not necessary unlike other anticoagulants (Dubock and Kaukeinen, 1978). Brodifacoum, like difenacoum, can kill anticoagulant resistant rats effectively and has a resistance factor of 1.3 (Dubock and Kaukeinen, 1978). It is also effective at very low concentrations of bait (Dubock and Kaukeinen, 1978).

Another anticoagulant rodenticide developed in the mid 1970s was a compound called bromadiolone. Bromadiolone is a potent anticoagulant (Meehan, 1978). Another compound difethialone has a structure based on a 4-hydroxycoumarin, however, a chemical modification replacing the oxygen by a sulphur in the 1'hydroxy-4 coumarin allows this compound to be

the first of a new chemical family of hydroxy-4 benzothiopyranones (Lechevin and Poche, 1988). This new anticoagulant was shown to be an effect rodenticide against both wild-type and resistant rodents (Lechevin and Poche, 1988). Flocoumafen was developed in the 1980s and produced as loose grain bait, small pellets and wax blocks for the treatment of populations of rats and mice (Lund, 1988). It is a derivative of a 4-hydroxycoumarin and has a resistance factor of 0.8-1.0 (Lund 1988). Although these compounds were effective against anticoagulant resistant rats when first introduced, there are reports of anticoagulant resistance against these SGARs (Greaves *et al.,* 1982; Gill *et al.,* 1994; Pelz *et al.,* 2005).

The acute oral toxicity of first- and second-generation anticoagulant rodenticides in target and non-target species are shown in Table 6. There were 8 species used to assess the oral toxicity of the anticoagulant rodenticides (Table 6). Oral toxicity is measured using the lethal dosage 50 (LD_{50}). LD_{50} estimates the concentration of a compound that is expected to be lethal to 50% of the animals tested when an oral dose is directly administered (Erickson and Urban, 2004). Of these species there are seven mammals and one bird (chicken). Of the mammals, four are catagorised under the glire clade (rat, mouse, guinea pig and rabbit), two are part of the carnivora order (dog and cat) and one is part of the even-toed ungulate order (pig). Only 3 out of the 8 species have oral toxicity values for all 8 anticoagulant rodenticides (Table 6). The glires are more sensitive in general to anticoagulant rodenticides in comparison to the non-glire organisms with exceptions. For example, flocoumafen has a greater effect in the dog in comparison to the rat with a 3-fold difference between the lowest LD_{50} values. The chicken appears to be the most resistant to anticoagulant rodenticides compared to the other species except when subjected to difenacoum. Warfarin has the least effect on all the species compared to the other anticoagulant rodenticides tested.

Compound	LD_{50} (mg/kg)							
	Rat	**Mouse**	**Guinea Pig**	**Rabbit**	**Dog**	**Cat**	**Pig**	**Chicken**
Warfarin	1-58[a,g]	374[a]	182[a]	~800[a]	200-300[a]	48-320[b]	200-1000[b]	>1000[a]
Diphacinone	1.75[c]	141-340[c]	-	35[c]	0.88-15[c]	5-15[c]	-	-
Chlorophacinone	0.8-5.0[c]	1-6[c]	-	-	50-100[c]	-	-	-
Bromadiolone	1.13[c]	1.75[c]	-	1[c]	8.1-10[c]	>25[c]	-	-
Brodifacoum	1.35[b]	0.2[b]	2.7[c]	5.8[b]	25-250[b]	1000[b]	1000[b]	200-2000[b]
Difenacoum	1.8-3.5[d]	0.8[d]	50[d]	2[d]	50[d]	100[d]	80-100[d]	50[e]
Difethialone	0.29-0.51[c]	0.47[c]	-	-	4-11.8[c]	>16[c]	2-3[c]	-
Flocoumafen	0.25-0.56[f]	0.79-2.4[f]	>10[f]	0.7[f]	0.075-0.25[f]	-	70[f]	50-100[e]

Table 6: Acute toxicity of FGAR and SGARs in different species. LD_{50} values obtained from (a) Hagen and Radomski, 1953; (b) Dubock and Kaukeinen, 1978; (c) Erickson and Urban, 2004; (d) Bull, 1976; (e) Rattner *et al.,* 2018; (f) Lund, 1988, (g) Papworth, 1958.

1.7 Determining the Cause of Anticoagulant Resistance

Determining the cause of anticoagulant resistance was important to understand the mechanism of resistance, as well as the mechanism of action of warfarin. It was postulated that resistance could be caused by the change in uptake, rate of metabolism or excretion of the anticoagulant and might be explained by a genetic factor (Bell and Matschiner, 1972). Using backcrossing experiments with a laboratory rat strain (Sprague-Dawley) and known resistant rats resulted in inbred resistant laboratory rats with the behavior and characteristics of the Sprague-Dawley rats but hosting the resistance gene trait. This proved a genetic basis for anticoagulant resistance (Pool *et al.,* 1968). Through these backcrossing experiments in rats, anticoagulant resistance was also shown to be a dominant gene trait (O'Reilly *et al.,* 1968). Studies proposed that a mutation could be responsible for anticoagulant resistance (Bell and Matschiner, 1972). However, it was not understood in which gene the resistance mutation was found until over thirty years later (Section 1.11.2).

1.8 Discovery that Vitamin K is Essential for Coagulation

1.8.1 Discovery of Vitamin K

Linked to the studies on anticoagulants was the discovery of vitamin K, a fat-soluble vitamin which was discovered in the early 1930s by Dam and Schønheyder, whilst studying sterol metabolism in chicks (Dam and Schønheyder, 1934). It was observed that the chicks fed with an artificial diet developed a disease that resembled scurvy (Dam and Schønheyder, 1934). The chicks suffered from symptoms such as; increased haemorrhaging, insufficient growth, anaemia and changes in the mucus membrane of the gizzard (Dam and Schønheyder, 1934). The lack of anti-haemorrhagic factors in the diet of the chicks was found to be the cause of this disease (Dam, 1935). The investigation of the anti-haemorrhagic factors led to the discovery of a fat-soluble factor called vitamin K, named after the German word for coagulation, *koagulation*. Vitamins are defined as an organic compound that is required for metabolism, growth and reproduction (National Research Council Committee on Diet and Health, 1989). Doisy *et al.* (1940) isolated vitamin K from dried alfalfa leaves and purified fish meal. The compounds isolated were named vitamin K_1 (VK_1) and vitamin K_2 (VK_2) (Doisy *et al*., 1940). Doisy *et al.* (1940) deduced that vitamin K compounds are part of an organic group of

1,4-naphthoquinones (Doisy *et al*., 1940) and all vitamin K derivatives had a 2-methyl-1,4-naphthoquinone basic structure (Figure 5).

VK_1, also referred to as phylloquinone (Figure 5a), is mainly synthesised by green plants and is the main source of the vitamin in the diet (Suttie and Booth, 2011). Bacteria that contain the mechanisms for vitamin K synthesis are responsible for producing VK_2, known as menaquinone (Figure 5b) (Shearer and Newman, 2008). There are many forms of menaquinone grouped under the name VK_2 (Walther *et al*., 2013). Menaquinones share the same 2-methyl-1,4-naphthoquinone structure but differ in isoprenoid side chain length (Walther *et al*., 2013). A third vitamin K 'type' is vitamin K_3 (VK_3) also known as menadione which has the 2-methyl-1,4-naphthaquione ring without any isoprenoid side chains (Figure 5c) (Walther *et al*., 2013).

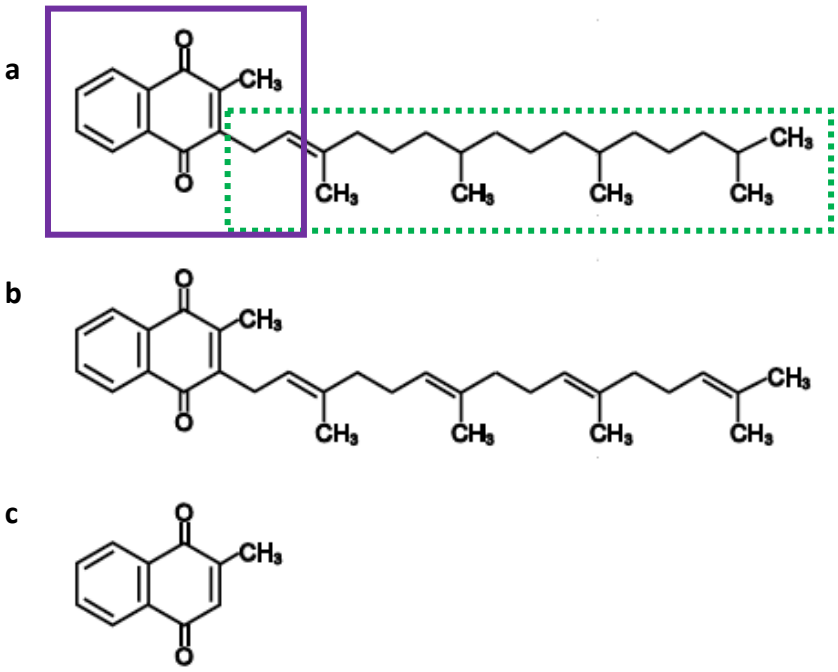


Figure 5: Structures of Vitamin K derivatives. a Vitamin K_1 (Phylloquinone; VK_1). **b** Vitamin K_2 (Menaquinone; VK_2). **c** Vitamin K_3 (Menadione; VK_3). Purple box denotes naphthoquinone head. Green dotted box denotes isoprenoid chain. (Created by Author using ChemDraw v18, adapted from Shearer and Newman, 2008).

1.8.2 Function of Vitamin K

The function of vitamin K was not fully understood after its discovery, but it was accepted that vitamin K regulated the rate of synthesis of prothrombin and other vitamin K dependent blood clotting factors (VII, IX and X) (Shah and Suttie, 1971). However, it was hypothesized that vitamin K acts to initiate the synthesis of prothrombin or acts as a mediator to convert an undefined precursor protein to the biologically active form of the blood coagulation factor prothrombin (Shah and Suttie, 1971) that is part of the blood coagulation cascade (Pozzi and Di Cera, 2014). Shah and Suttie (1971) showed that the after administration of vitamin K to vitamin K-deficient rats a precursor is converted to biologically active prothrombin (Shah and Suttie, 1971). Vitamin K appears to alter the precursor protein by adding a non-carbohydrate prosthetic group (Nelsestuen and Suttie, 1972). Later, Nelsestuen and Suttie (1973) isolated the peptide containing the vitamin K-dependent part of prothrombin (Nelsestuen and Suttie, 1973). The identified peptide contains a large excess of carboxyl groups on glutamic acid residues (Nelsestuen *et al.*, 1974). It was therefore shown that vitamin K is essential for the addition of carboxyl groups on vitamin K dependent (VKD) proteins (Nelsestuen *et al.*, 1974).

1.8.3 Discovery of Phylloquinone Oxide

The link between vitamin K and anticoagulant resistance led to studies on the metabolism of vitamin K in the livers of animals administered anticoagulant rodenticides (Drummond and Wilson, 1968). Drummond and Wilson (1968), whilst studying resistance in rats from Shropshire, identified an involvement of vitamin K in the mechanism of resistance to anticoagulants (Drummond and Wilson, 1968). Matschiner *et al.* (1970) studied the metabolism of radioactively labelled vitamin K in warfarin treated rats and found an accumulation of a metabolite. The compound was isolated and was more hydrophilic than vitamin K. The compound was called phylloquinone oxide (later known as vitamin K epoxide) (Matschiner *et al.,* 1970). Generally, anticoagulants were hypothesized to compete against vitamin K in an unknown active site (Bell *et al.,* 1972). However, this accumulation of phylloquinone oxide suggests a different mode of action of anticoagulants. Bell and Matschiner (1972) suggested the oxide were converted to vitamin K and this reaction was inhibited by warfarin (Bell and Matschiner, 1972).

With the knowledge that vitamin K was involved in the activation of prothrombin and that phylloquinone oxide is converted to vitamin K by an enzyme called vitamin K epoxide reductase (Matschiner *et al.,* 1974) and the reaction inhibited by warfarin, Willingham and Matschiner (1974) studied the relationship between prothrombin and the conversion of vitamin K epoxide to vitamin K in control and warfarin resistant rats (Willingham and Matschiner, 1974). Experiments with vitamin K-deficient rats and warfarin-resistant rats given vitamin K intravenously, showed a decrease in vitamin K epoxide accumulation and an increase in prothrombin production (Willingham and Matschiner, 1974). When warfarin was given to the vitamin K-deficient rats there was an increase in the accumulation of vitamin K epoxide and a decrease in prothrombin production, whereas in the warfarin resistant rats there was no change in either the epoxide accumulation or prothrombin production (Willingham and Matschiner, 1974). Based on this Willingham and Matschiner (1974) proposed a scheme for the mechanism of vitamin K (Figure 6) (Willingham and Matschiner, 1974).

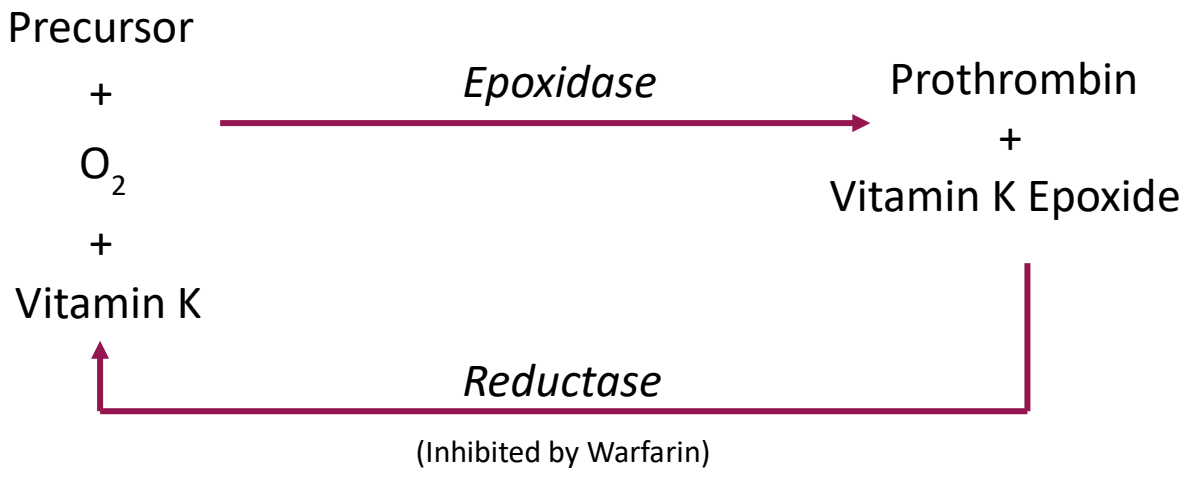


Figure 6: Proposed mechanism of vitamin K by Willingham and Matschiner (1974). (Created by Author, Based on Willingham and Matschiner, 1974).

1.9 Vitamin K Cycle

Later studies identified the enzyme responsible for the post-translational modifications of vitamin K dependent proteins such as prothrombin (Esmon *et al.,* 1975). The enzyme was γ-glutamyl carboxylase (GGCX) (Wu *et al.,* 1991). GGCX is responsible for the addition of carboxyl groups onto glutamic acid residues to form γ-carboxyglutamic acid (Stafford, 2005). GGCX uses another metabolite of vitamin K called vitamin K hydroquinone as a cofactor along with molecular oxygen to activate VKD proteins such as those in the blood coagulation cascade and as a by-product vitamin K epoxide is produced (Stafford, 2005). Vitamin K epoxide is then converted to vitamin K by vitamin K epoxide reductase complex subunit 1. This process is known as the vitamin K cycle (Figure 7).

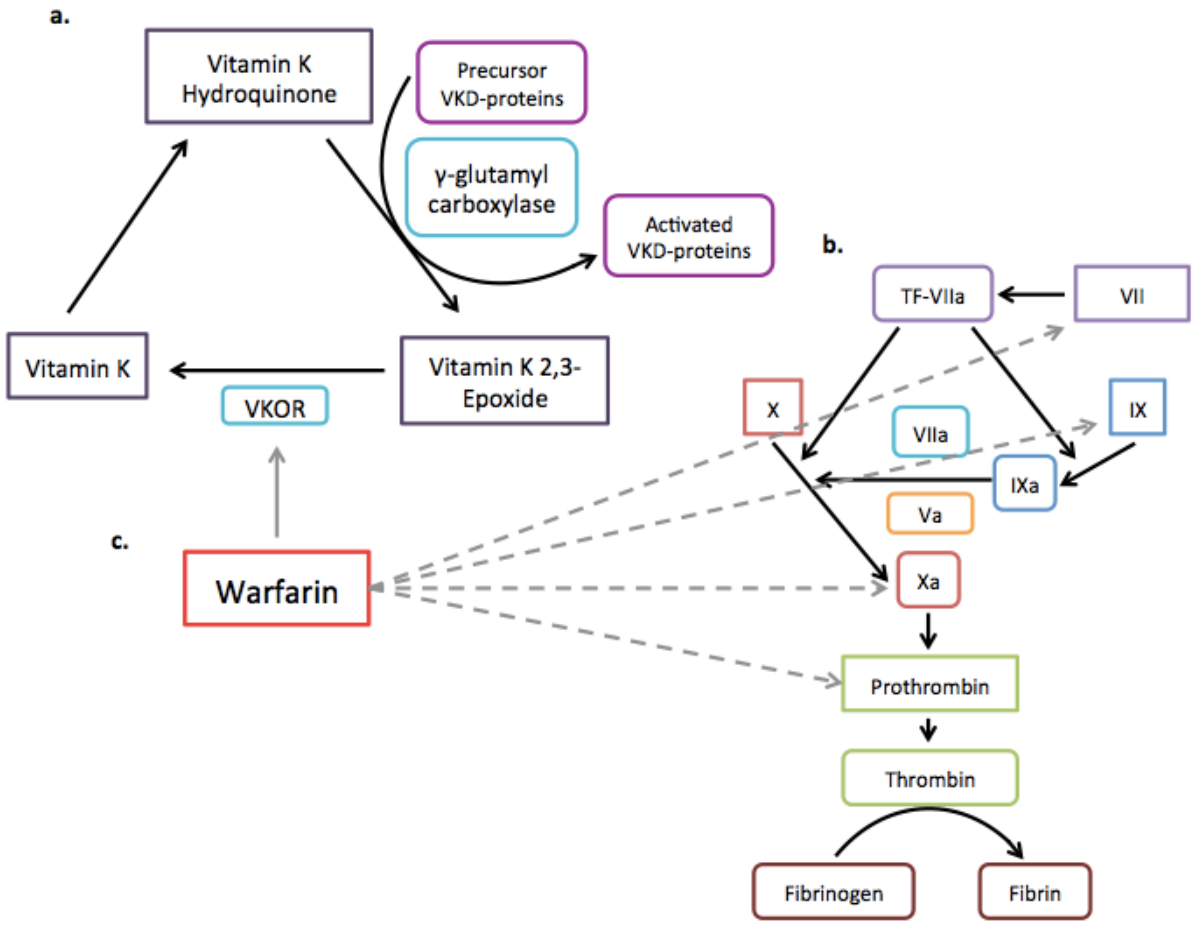


Figure 7: Vitamin K cycle with the blood coagulation pathway and the effect of warfarin. a Vitamin K cycle showing the activation of the VKD proteins. **b** Blood coagulation cascade. **c** Warfarin targets VKORC1 and inhibits VKOR activity. The grey-dotted arrows show the blood factor proteins that will not be activated by carboxylation reactions due to the inhibition of VKOR by warfarin, causing internal haemorrhaging (Created by Author, based on Helgeland, 1980).

Silverman (1981) proposed the chemical model for the mechanism of VKORC1 in the conversion of vitamin K epoxide to vitamin K (Figure 8).

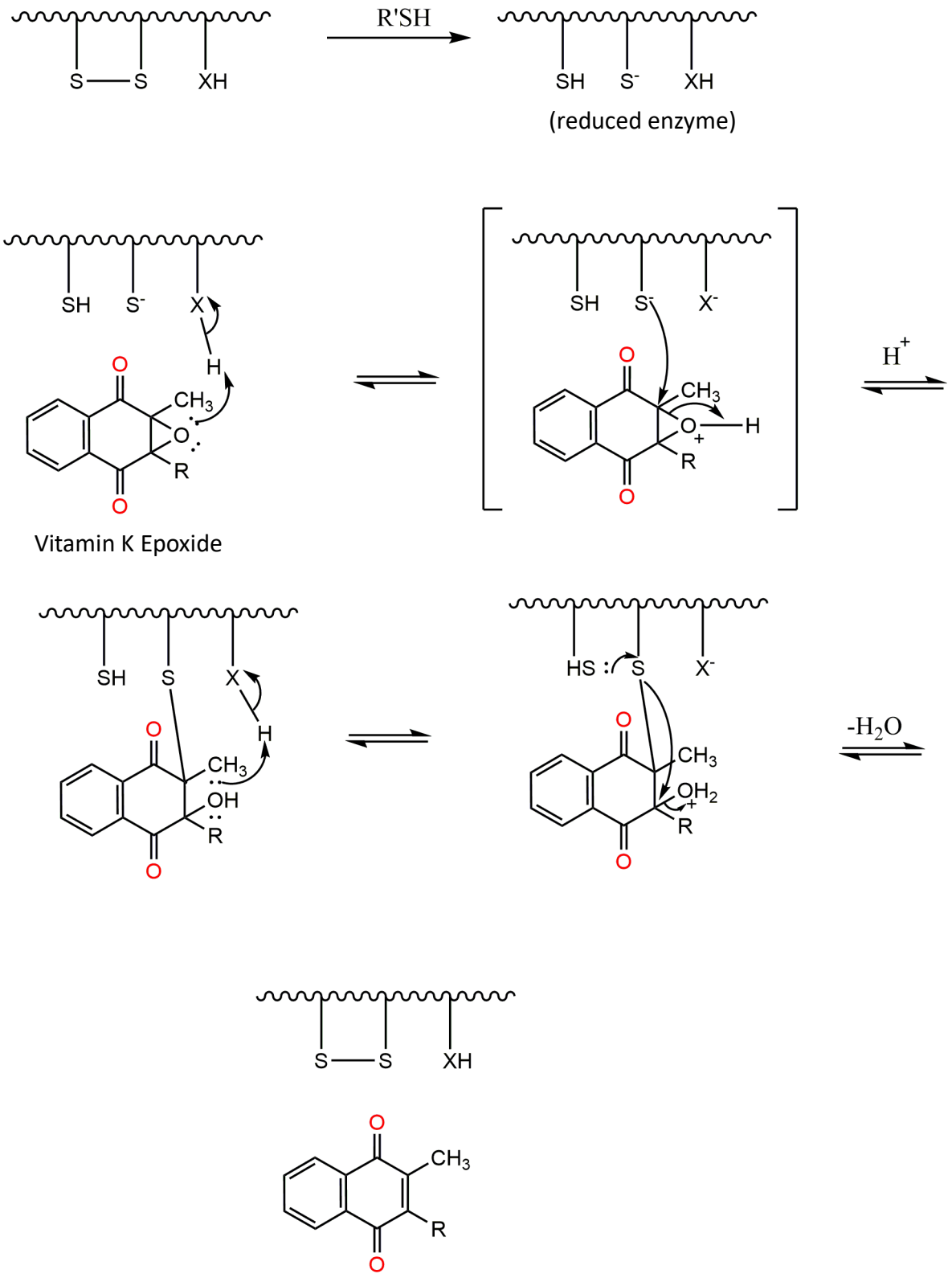


Figure 8: Proposed chemical model for the mechanism of VKORC1 in the conversion of vitamin K epoxide to vitamin K determined by Silverman (1981). (Created by Author using ChemDraw v18)

1.10 VKORC1 involvement in disulfide bond formation

The use of a reducing agent, dithiothreitol (DTT), in the *in vitro* microsomal VKORC1 assay showed an increased effect on vitamin K carboxylation (Mack *et al.,* 1976). Mack *et al.* (1976) suggested that VKORC1 system required a -SH group. Studies by Whitlon *et al.* (1978) showed that VKORC1 reactions in microsomal preparations require DTT in order to sustain activity and suggested that there is a physiological reducing agent required in which DTT replaces *in vitro*. Silverman and Nandi (1988) replaced DTT with either reduced lipoic acid or reduced thioredoxin in rat and cow microsome *in vitro* assays. From these experiments it was proposed that reduced thioredoxin could be a possible physiological reductant for VKORC1.

Further studies by Soute *et al.* (1992) used protein disulfide-isomerase (PDI), an enzyme responsible for catalyzing disulfide bond formation of polypeptide chains that enter into the endoplasmic reticulum lumen, to replace DTT in the *in vitro* VKORC1 assay. They showed that PDI and thioredoxin is superior to DTT in the reduction of the vitamin K cycle and suggest PDI and thioredoxin could be candidates for physiological co-factors for the vitamin K cycle (Soute *et al.,* 1992). Studies by Wajih *et al.* (2007) proposed that PDI provides the electrons for the reduction of the CXXC motif centre of VKORC1. Immunoprecipitation results showed PDI-VKORC1 complexes formed (Wajih *et al.,* 2007). Wajih *et al.* (2007) proposed that the vitamin K cycle and γ-carboxylation is linked to protein synthesis and dithiol-dependent oxidative protein folding in the ER after showing that PDI and VKORC1 can form a complex.

Schulman *et al.* (2010) screened for redox partners that interact with VKORC1. They found that VKORC1 prefers to form covalent bonds with membrane anchored Trx-proteins with weaker interactions with TMX4 and ERp18 protein. These interactions in mammalian VKORC1 imitate the interactions seen in bacteria with bacterial VKORC1 and its Trx-like redox partners. Schulman *et al.* (2010) suggest that VKORC1 likely interacts with the transmembrane (TM) portion of TMX and TMX4. Both TMX and TMX4 have a CPXC active site motif and the proline residue is important in the formation of mixed disulfide bonds formed with VKORC1. The study hypothesised that VKORC1 has a general role in disulfide bridge formation of newly synthesised proteins.

Rutkevich and Williams (2012) used a knockdown approach to determine the contributions of known and potential candidates of ER redox homeostasis and disulfide bond formation. They showed that known oxidant enzymes; Ero1 and PRDX4 and the potential candidate VKORC1 are important for redox homeostasis and disulfide bond formation. Although Ero1 is the predominant pathway for generation of disulfide bonds in the ER, knockdown of Ero1 shows that other oxidative pathways act to maintain the ER redox homeostasis. Knockdown of PRDX4 in the presence of Ero1 caused a delayed recovery in ER redox homeostasis. To assess VKORC1 as a potential candidate for ER redox homeostasis and disulfide bond formation, VKORC1 was knocked down with Ero1 and resulted in the same delayed response seen with the PRDX4 knockdown (Rutkevich and Williams, 2012). Importantly, when both Ero1 and PRDX4 were depleted, VKORC1 was able to maintain oxidative folding and secretion of the protein albumin as well as a delayed recovery of redox homeostasis in the ER after a redox challenge. A deletion of all three oxidative enzymes, Ero1, PRDX4 and VKORC1 resulted in death to the cells, suggesting that there are no other pathways involved in ER redox homeostasis. The proposed pathway of VKORC1 in the ER redox homeostasis pathway and the formation of oxidative disulfide bonds is shown in Figure 9. The oxidant enzymes Ero1, PRDX4 and VKORC1 accept electrons from the PDI family. This in turn converts reduced PDI (PDI^{red}) to the oxidised form (PDI^{ox}) (Rutkevich and Williams, 2012). Disulfide bond formation in folding proteins or the oxidization of glutathione to oxidised glutathione (GSSG) is catalysed by PDI^{ox} (Figure 9).

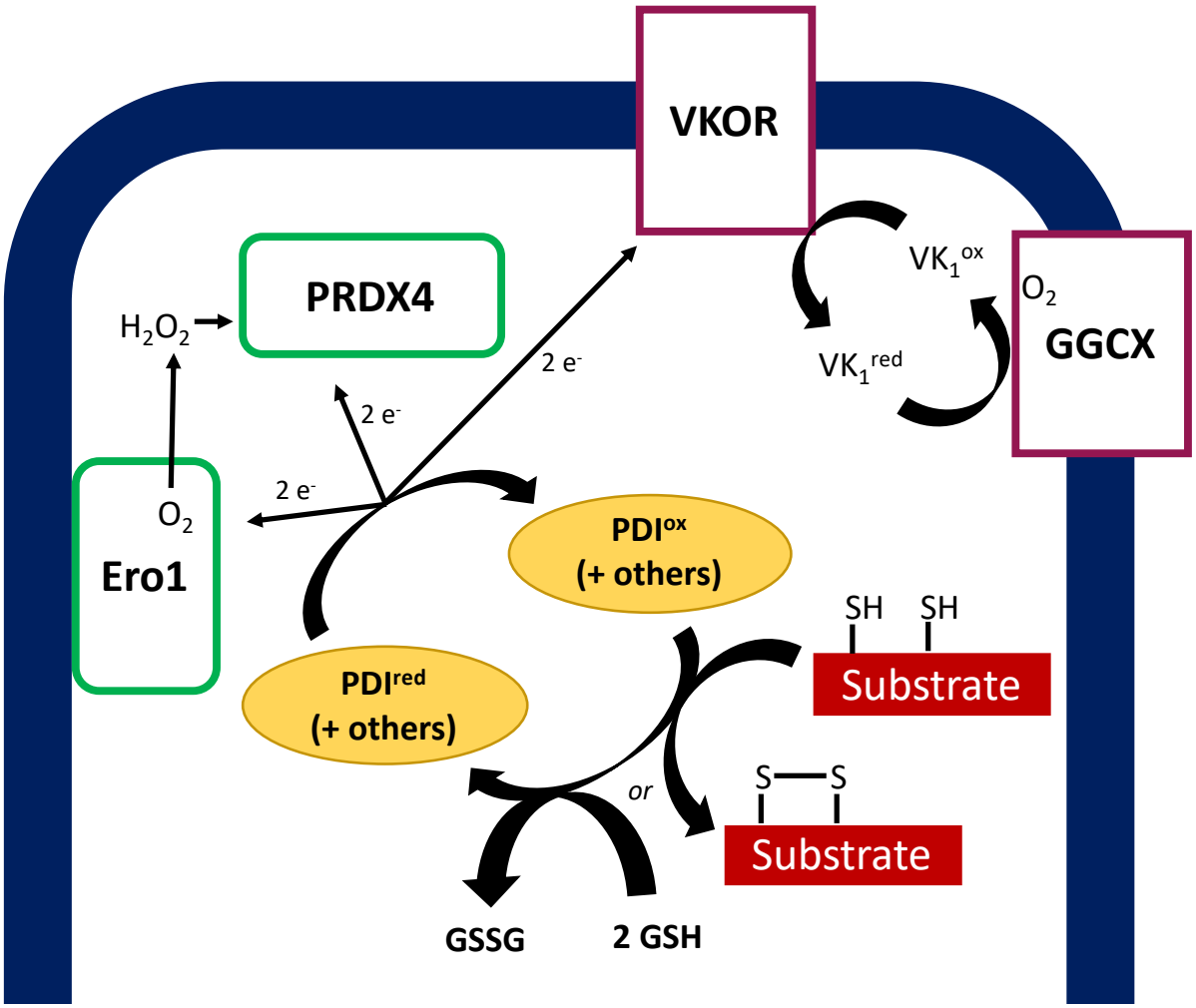


Figure 9: Proposed pathway of VKORC1 in the ER redox homeostasis pathway. (Created by Author, based on Rutkevich and Williams, 2012). Abbreviations: VKOR, vitamin K epoxide reductase; GGCX, γ-glutamyl carboxylase; VK_1^{ox}, oxidised vitamin K; VK_1^{red}, reduced vitamin K; Ero1, endoplasmic reticulum oxidoreductin 1; PRDX4, peroxidoreductin IV; PDI^{ox}, oxidised protein disulfide isomerases; PDI^{red}, reduced protein disulfide isomerases; GSH, glutathione; GSSG, oxidised glutathione.

1.11 Chromosome Mapping of Warfarin Resistance Locus and Discovery of VKORC1 Gene

1.11.1 Chromosome Mapping of Warfarin Resistance Locus

Greaves and Ayres (1969) determined the approximate linkage position of the resistance gene locus, *Rw*, by identifying the linkage between coat colour and resistance to warfarin in *Rattus norvegicus*. They determined that the *Rw* locus was on chromosome 1. Comparative mapping by Yamada *et al.* (1994) placed the *Rw* locus close to *Myl2* (myosin light chain locus) identified

by *D1Arb18*. Studies by Kohn and Pelz (1999) measured resistance by segregating backcross populations of resistant *Rattus norvegicus* to identify a microsatellite that co-segregates with resistance. They placed the *Rw* locus on the q arm of chromosome at a ≈ 6 cM about *D1Arb18* between microsatellite markers *D1Mit13* and *D1Rat130*. Although there is no link between warfarin resistance and *Myl2*, it is used as an anchor to map the *Rw* locus (Kohn and Pelz, 1999). Kohn and Pelz (1999) suggest that resistance to warfarin, bromadiolone and other anticoagulant rodenticides is due to the same gene. Kohn and Pelz (2000) used ortholog mapping to determine the position of the warfarin resistance locus between rat, human and mouse. The *Rw* locus was placed between 60-63 cM on chromosome 7 in mouse. The position in humans was narrowed down to three positions; 10q25.3-q26, 12q23-q24.3 and 16p13.1-p11.

Fregin *et al.* (2002) mapped the locus for familial multiple coagulation factor deficiency (FMFD), which is an autosomal recessive rare bleeding disorder. Biochemical studies elucidated that the FMFD is a result of a defect in the enzyme VKORC1 (Oldenburg *et al.,* 2000). Resistance to warfarin in rats and mice appears to be linked to the same gene that causes human FMFD. Fregin *et al.* (2002) suggests that an alteration in one part of the gene could cause anticoagulant resistance, whereas a different alteration in the same gene could cause FMFD. Previous studies highlight the *Rw* locus in rats on chromosome 1 and syntenic region in mice on chromosome 7 (Kohn and Pelz, 2000). Homology mapping between the mouse and human chromosomes narrowed down the human FMFD locus to chromosome 16. A genome wide analysis performed by Fregin *et al.* (2002) mapped the FMFD to chromosome 16 between markers D16S3131 on 16p12 and D166S419 on 16q21.

1.11.2 Discovery of the VKORC1 gene

In 2004 the gene for human and rat VKORC1 was discovered independently by two groups using two different approaches to identify the VKORC1 gene (Rost *et al.,* 2004; Li *et al.,* 2004). Rost *et al.* (2004) noted that the gene regions around the localisation of vitamin K clotting factor deficiency type 2 (VKCFD2) in humans was orthologous to the region of warfarin resistance localisation in rats (Rost *et al.,* 2004) and proposed that VKCFD2 and warfarin resistance could be caused by different mutations in the same gene. Mutation screening was

conducted in humans with two VKCFD2 index patients and three unrelated warfarin resistant patients by directly sequencing genomic DNA. A gene with missense mutations and unknown function was identified.

Li *et al.* (2004) used the chromosome localisation to search for the VKORC1 gene by analysing 190 predicted coding sequences using BLASTX database searching (Li *et al.,* 2004). Genes of known function were eliminated, and the remaining 52 candidates were subjected to transmembrane (TM) prediction programmes, as VKORC1 appeared to be a transmembrane protein (Carlisle and Suttie, 1980). Thirteen candidate genes were identified, and siRNA knockdown was used to identify the one that encoded VKORC1 activity (Li *et al.,* 2004).

Both groups identified a gene at position 16p11.2 in humans and position 1q37 in rats comprising of three exons encoding for a protein of 163 amino acids with a molecular weight of 18 kDa (Rost *et al.,* 2004; Li *et al.,* 2004).

1.12 Structure and Topology of VKORC1

Upon discovery of the gene, Rost *et al*. (2004) and Li *et al.* (2004) used prediction software to determine the number of TM domains VKORC1 contained and both stated either a one or three TM model depending on the prediction software used (Rost *et al.,* 2004; Li *et al.,* 2004). However, a study by Goodstadt and Ponting (2004) predicted a four TM domain model for VKORC1 using multiple sequence alignments and a prediction software (Goodstadt and Ponting, 2004). In 2010, the structure of VKORC1 in the bacterial homologue *Synechococcus sp.* was determined by x-ray crystallisation (Li *et al.,* 2010). The VKORC1 homologue contained 5 TM domains. TM 1-4 are homologous with mammalian VKORC1 with the fifth TM domain associated only with the bacterial homologue.

Following the structural elucidation of the bacterial homologue of VKORC1, Tie *et al.* (2012) predicted that human VKORC1 contains 3 TM domains using cell culture and biochemical techniques (Figure 10a). Fluorescence protease protection (FPP) assays were used to determine the position of the N and C terminus of VKORC1 in cytoplasm and the ER lumen. Green fluorescent protein (GFP) was fused to either the N or C terminal of VKORC1 and

expressed in Human Embryonic Kidney-293 mammalian cells (HEK-293). After plasma membranes were disrupted with digitonin, trypsin was added to the cells which targets sites for digestion (Lorenz *et al.,* 2006) on the modified human VKORC1 to determine the location of the N and C terminals. If the GFP is fused to the N-terminus of VKORC1 it is protected by the trypsin digestion, whereas when GFP is fused to the C-terminus it is susceptible to protease digestion (Tie *et al.,* 2012). The study also determined the positioning of the loop cysteines. This was done with the selective modification of the loop cysteines by a membrane-impermeable polyethylene glycol (PEG) maleimide which increases the molecular mass of VKORC1 if the cysteines are present in the cytoplasm. In the 3 TM model the four cysteines are predicted to be in the cytoplasm and VKORC1 was shown to increase in molecular mass after treatment. Therefore, both results suggest a 3 TM model for VKORC1. Previously Schulman *et al.* (2010) used the same technique to determine the position of the loop cysteines to confirm the TM prediction model by using a membrane-impermeable cysteine modification reagent. However, the results obtained predicted a 4 TM model for VKORC1 (Schulman *et al.,* 2010) (Figure 10b). The difference in conclusions could be due to the interpretation of the results, Schulman *et al.* (2010) shows one band for the increase of VKORC1 size with PEG modification and uses the intensity of the bands as a measure of the degree of modification, whereas, Tie *et al.* (2012) suggest that multiple modifications of cysteines would result in multiple bands of different sizes depending on the degree of PEG modification (Tie *et al.,* 2012).

With conflicting data, a study by Wu *et al.* (2014) compared the stability of the three TM and the four TM topologies computationally. They concluded that the three TM topology was more stable and produced a more reasonable arrangement of the Tyr139 position, required for warfarin binding, in comparison to the four TM topology (Wu *et al.,* 2014). To explain the differences seen in membrane topology by different groups, Müller *et al*. (2014) suggested that the difference in TM domains could be tissue-specific or as part of the VKORC1 reaction mechanism and the TM domains could shift between three and four TM domains (Müller *et al.,* 2014).

In 2016, Cao *et al.* (2016) used redox-sensitive GTP (roGTP) fused to the N and C terminals of human VKORC1 to detect different redox environments within the ER and the cytosol. This technique uses live cells to eliminate any artifacts created by cell permeablisation. If both N and C terminals are present in the cytoplasm, roGTP will be fully reduced but only partially reduced if only the C terminus is present in the cytoplasm in accordance with the 3 TM model of VKORC1. The results showed a fully reduced roGTP suggesting a 4 TM model for VKORC1. To determine the position of the loop region, glycosylation sites were introduced into VKORC1 (Cao *et al.,* 2016). The presence of N-glycosylation on VKORC1 confirmed that the loop region was positioned within the ER lumen, where the introduced sites were exposed to glycosylation machinery within the ER. Therefore, this suggests a 4 TM model for VKORC1.

One major difference between the 3 TM model and the 4 TM model of VKORC1 is the orientation of TM1. Sinhadri *et al.* (2017) noted that the 4 TM model contradicts the "positive inside rule" (Sinhadri *et al.,* 2017), which controls the orientation of a TM domain within a membrane and the rule suggests that the positively charged residues face into the cytoplasm (von Heijne, 1989). By mutating critical amino acids in the disputed TM regions, it shows that the proposed TM2 in the 4 TM model does not function as an authentic TM helix which supports the 3 TM model (Sinhadri *et al.,* 2017). Also, TMHMM computational prediction showed 3 TM domains for human VKORC1 (Sinhadri *et al.,* 2017).

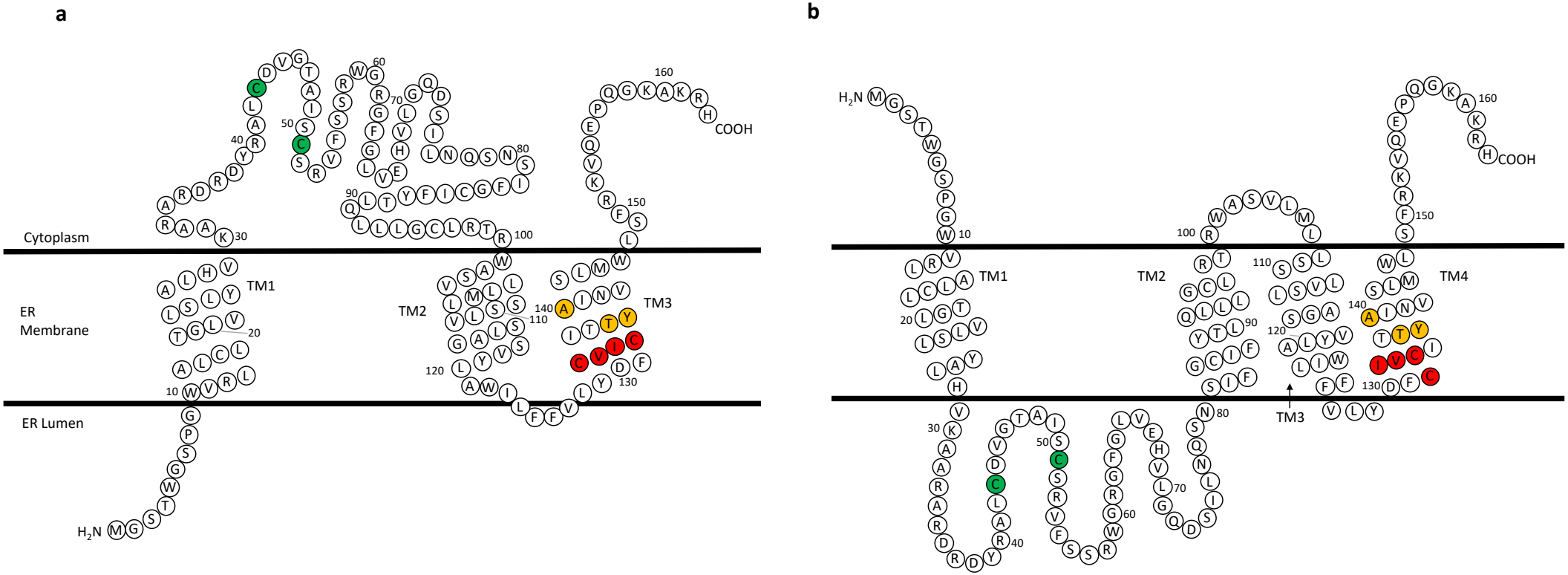


Figure 10: Topology diagrams of the proposed 3 TM and 4TM model of human VKORC1. a 3 TM VKORC1 model. **b** 4 TM VKORC1 model. (Created by Author, based on structures by Tie *et al.* 2012 and Bevans *et al.,* 2015). Red denotes active site domain. Green denotes conserved cysteines. Yellow denotes the proposed warfarin binding domain.

1.13 Important Amino Acids in VKORC1

Analysis of the amino acid sequence of VKORC1 allows for a deeper understanding of important amino acids that are related to structure and function. Table 7 shows the amino acid positions which have a reported role in VKORC1.

1.13.1 Active site cysteines in VKORC1

There are two main cysteines which form part of the active site of VKORC1 these are C132 and C135 along with two other conserved cysteines C43 and C51 (Table 7). These cysteines were identified after the identification of the gene for VKORC1. Goodstadt and Ponting (2004) aligned homologous sequences from diverse species of vertebrates, invertebrates, plants, bacteria and archaea (Goodstadt and Ponting, 2004). Highly conserved residues including C43, C51, C132 and C135 were identified and these residues were hypothesized to be part of the catalytic active site. VKORC1 contains a $C_{132}xxC_{135}$ motif, which is characteristic of the redox family of enzymes (Fomenko and Gladyshev, 2003). Rost *et al.* (2005) used site directed mutagenesis to confirm whether these residues identified by Goodstadt and Ponting (2004) are important in the mechanism of human VKORC1. The four conserved residues C43, C51, C132, and C135 when substituted with other amino acids showed a loss in activity suggesting a key role in the structure and function of VKORC1, which is consistent with previous studies (Wajih *et al.,* 2005). The function of the two cysteines, C43 and C51 is controversial, due to the two opposing topological models of VKORC1.

1.13.2 Amino Acids involved in Stabilising Helix-helix Interactions in VKORC1

There are many amino acids in VKORC1 which are important to the structure of VKORC1 (Table 7). Bevans *et al.* (2015) suggested that specific amino acids in VKORC1 have potential roles helix-helix interactions in the 4TM model of VKORC1 (Table 7). These include: C16, G19, S23, A26 (on TM1); S81, G84 (on TM2); S117, L124 (on TM3); and T138 (on TM4). Another study by Wu *et al.* (2018) suggest that position L15 and L128 are essential for TM1 and TM3 respectively to maintain a stable VKORC1 structure and positions L22 and L105 help to hold TM1 and TM2 together in the 3TM model (Table 7).

Position	Previously Reported Role in VKORC1	Reference
R12	Resist warfarin access	Wu *et al.* (2018)
L15	Maintain a stable VKOR structure	Wu *et al.* (2018)
C16	Conserved in TM1 - Putative helix-helix contacts	Bevans *et al.* (2015)
G19	Conserved in TM1 - Putative helix-helix contacts	Bevans *et al.* (2015)
L22	Helps to hold TM1 and TM2 in VKORC1 together	Wu *et al.* (2018)
S23	Conserved in TM1 - Putative helix-helix contacts	Bevans *et al.* (2015)
Y25	Interact with Y139 to stabilise warfarin binding	Wu *et al.* (2018)
A26	Interact with Y139 to stabilise warfarin binding. Conserved in TM1 - Putative helix-helix contacts	Wu *et al.* (2018), Bevans *et al.* (2015)
K30	Naphthoquinone head binding – VKE and VK	Czogalla *et al.* (2017)
R33	Charge stabilization in warfarin binding	Czogalla *et al.* (2017)
R40	Charge stabilization in warfarin binding	Czogalla *et al.* (2017)
C43	Involved in active site – conserved cysteine	Goodstadt and Ponting, (2004); Rost *et al.* (2005)
D44	Involved in substrate reduction/binding/specificity	Bevans *et al.* (2015)
C51	Involved in active site – conserved cysteine	Goodstadt and Ponting, (2004) Rost *et al.* (2005)
R53	Charge stabilization in warfarin binding	Czogalla *et al.* (2017)
F55	Aromatic stacking – warfarin binding. Naphthoquinone head binding – VKE and VK.	Czogalla *et al.* (2017)
W59	Naphthoquinone head binding – VKE and VK. Warfarin binding.	Wu *et al.* (2018) Czogalla *et al.* (2017)
F63	Warfarin binding.	Wu *et al.* (2018)
Q78	Naphthoquinone head binding – VK.	Czogalla *et al.* (2017)
N80	Naphthoquinone head binding – VK. Involved in substrate reduction/binding/specificity	Bevans *et al.* (2015) Czogalla *et al.* (2017)
S81	Conserved in TM2 - Putative helix-helix contacts	Bevans *et al.* (2015)
G84	Steric hinderance. Conserved in TM2 - Putative helix-helix contacts Involved in substrate reduction/binding/specificity.	Bevans *et al.* (2015) Czogalla *et al.* (2017)
F87	Isoprenoid chain binding	Czogalla *et al.* (2017)
Y88	Isoprenoid chain binding Involved in substrate reduction/binding/specificity.	Bevans *et al.* (2015) Czogalla *et al.* (2017)
L90	Isoprenoid chain binding	Czogalla *et al.* (2017)
G95	Involved in substrate reduction/binding/specificity.	Bevans *et al.* (2015)
L105	Helps to hold TM1 and TM2 in VKORC1 together	Wu *et al.* (2018)
V112	Isoprenoid chain binding	Czogalla *et al.* (2017)
S113	Isoprenoid chain binding	Czogalla *et al.* (2017)
G116	Steric hinderance	Czogalla *et al.* (2017)
S117	Conserved in TM3 - Putative helix-helix contacts	Bevans *et al.* (2015)
L120	Naphthoquinone head binding – VKE and VK. Involved in substrate reduction/binding/specificity	Bevans *et al.* (2015) Czogalla *et al.* (2017)
I123	Naphthoquinone head binding – VK.	Czogalla *et al.* (2017)
L124	Naphthoquinone head binding – VK. Conserved in TM3 - Putative helix-helix contacts	Bevans *et al.* (2015) Czogalla *et al.* (2017)
F125	Resist warfarin access.	Wu *et al.* (2018)
L128	Naphthoquinone head binding – VKE and VK. Involved in substrate reduction/binding/specificity. Maintain stable VKORC1 structure.	Wu *et al.* (2018) Bevans *et al.* (2015) Czogalla *et al.* (2017)
C132	Active site cysteine.	Goodstadt and Ponting, (2004); Rost *et al.* (2005)
V134	Strong hydrophobic interactions	Czogalla *et al.* (2017)
C135	Active site cysteine.	Goodstadt and Ponting, (2004); Rost *et al.* (2005)
T138	Conserved in TM4 - Putative helix-helix contacts	Bevans *et al.* (2015)
Y139	Warfarin binding site.	Rost *et al.* (2005); Wu *et al.* (2018)

Table 7: Amino acid positions with a previously reported role in structure, function, and substrate or anticoagulant binding.

1.13.3 Amino Acids Involved in Substrate Binding in VKORC1

There are many amino acids identified that are responsible for substrate binding. Bevans *et al.* (2015) proposed that D44, N80, Y88, G95, L120 and L128 are involved in substrate binding, reduction or specificity (Table 7). A study by Czogalla *et al.* (2017) used 3D modelling and molecular docking of vitamin K epoxide and vitamin K to identify the positions used for substrate binding. K30, F55, W59, L120 and L128 are required for the binding of the naphthoquinone head of both vitamin K epoxide and vitamin K. Positions Q78, N80, I123 and L124 also play a role in naphthoquinone head binding of vitamin K. Positions F87, Y88, L90, V112 and S113 are required for the isoprenoid chain binding for both vitamin K epoxide and vitamin K.

1.13.4 Amino Acids Involved in Warfarin binding in VKORC1

With the discovery of the VKORC1 gene, mutation screening by Rost *et al.* (2004) showed that missense mutations at Y139 in human and rat resulted in warfarin resistance. In order to assess the importance of this tyrosine for warfarin binding, Rost *et al.* (2005) performed site-directed mutagenesis and suggested that Y139 was part of a warfarin binding motif, TYA. Mutation screening by Pelz *et al.* (2005) suggested tyrosine-139 as a mutation hotspot, in a hydrophobic motif TYA. This motif is found in other enzymes such as NAD(P)H:quinone reductase which is sensitive to the related coumarin dicoumarol (Myszeka and Swenson, 1991). A recent study by Wu *et al.* (2018) used molecular dynamics to show warfarin binding to the 3TM model of human VKORC1. They showed that warfarin interacted with the tyrosine at position 139 in the proposed warfarin binding site with T-shaped stacking interactions. They also showed that other amino acids such as Y25 and A26 were involved in warfarin binding. Another amino acid that they identified as important in their simulations was F55. They also showed that this phenylalanine was important in both vitamin K substrate binding as well as warfarin binding. These results are consistent with Czogalla *et al.* (2017) as they showed using both computational and biochemical methods that as well as a major binding residue for substrate, F55 has a role in aromatic stacking interactions with the conjugated rings of warfarin. Positions W59 and F63 were also recently identified by Wu *et al.* (2018) as they are both found on the same face of an α-helix and these residues contribute to warfarin binding but have no involvement in vitamin K binding.

Additionally, Czogalla *et al.* (2017) showed that F55 was involved in both substrate binding and warfarin stacking. They also showed that some arginine residues R33, R40 and R53 in VKORC1 have charge stabilisation properties upon the binding of anionic warfarin using 3D modelling predictions, mutagenesis and functional studies (Table 7).

1.13.5 Amino Acids that are proposed to act as ER Retention signals in VKOR

ER retention signals are required for a protein to be directed to and retained in the specific organelle it resides in (Jackson *et al.,* 1990). These ER retention signals have been identified in VKORC1 proteins. Rost *et al.* (2004) showed that the six VKORC1 sequences they assessed had a Lys-Lys-X-X or Lys-X-Lys-X-X motif at the positions -5 and -3 from the C-terminus of VKORC1. Another study by Czogalla *et al.* (2014) showed that human VKORC1 also contains a di-arginine motif at positions R98 and R100 that are likely for localisation and retention in the ER membrane.

1.14 Vitamin K Epoxide Reductase Complex Subunit 1 Like-1 (VKORC1L1)

Vitamin K epoxide reductase complex subunit 1 like-1 (VKORC1L1) is paralogous enzyme to VKORC1 and was simultaneously discovered in 2004 by Rost *et al*. (2004) whilst carrying out tBLASTn searches against VKORC1 sequences. The searches showed a protein with 50% identity to VKORC1 (Rost *et al.,* 2004) named VKORC1L1 localised to chromosome 7 in humans (Robertson, 2004).

The function of VKORC1L1 was studied by Westhofen *et al.* (2011). This study showed that VKORC1L1 had a role in driving vitamin K-mediated intracellular antioxidation pathways. VKORC1L1 expression was upregulated when hydrogen peroxide was applied to cultured cells to induce oxidative stress. VKORC1L1 appears to support the conversion of vitamin K to vitamin K hydroquinone. Westhofen *et al.* (2011) hypothesized VKORC1L1 transfers reducing equivalents generated by products of oxidative protein folding to VK mediated intracellular pathways.

Westhofen *et al.* (2011) used sequence alignments of VKORC1 and VKORC1L1 sequences and the bacterial homologue recently crystallised by Li *et al.* (2010) to predict the structure of VKORC1L1. They predicted a 4 TM structure (Figure 11).

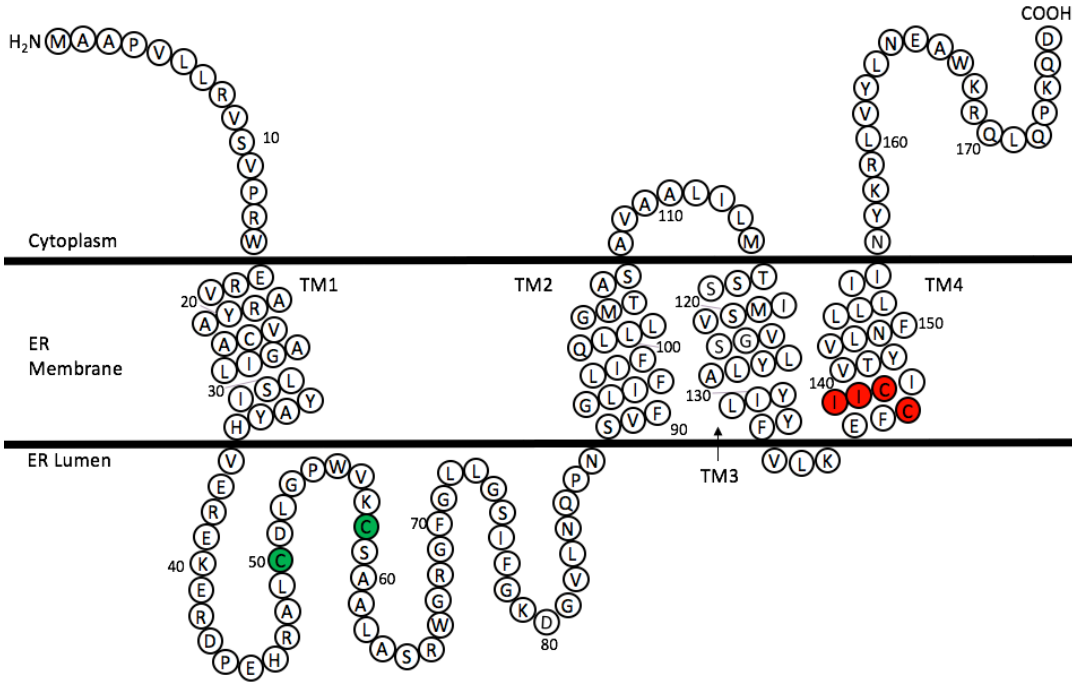


Figure 11: Topological diagram of VKORC1L1. Green denotes the conserved cysteines. Red denotes the active site. (Created by Author, based on Westhofen *et al.,* 2011).

Hammed *et al.* (2013) identified the differences in expression in different extrahepatic tissues between VKORC1 and VKORC1L1. VKORC1L1 was found to be expressed more in the brain and in the testis compared to other extrahepatic tissues whereas, VKORC1 was shown to be highly expressed in the liver compared to other tissues where expression was much lower (Hammed *et al.,* 2013).

1.15 Evolution of the VKOR family of enzymes and their relationship with related proteins

1.15.1 Phylogeny of the VKOR family

The phylogeny of the VKOR family of enzymes has been well characterised (Rost *et al.,* 2004; Goodstadt and Ponting, 2004; Robertson, 2004; Wan *et al.,* 2014; Bevans *et al.,* 2015). With the discovery of the VKORC1 gene, Rost *et al.* (2004) identified VKORC1 homologues for human, rat, mouse, frog (*Xenopus laevis*), fish (*Fugu rubripes*), and mosquito using TBLASTN database searches. Paralogous VKORC1L1 sequences were also found for human, rat, mouse

and fish. The searches showed no evidence of a VKORC1 or VKORC1L1 sequence for *Drosophila* species suggesting that the VKOR family evolved after the carboxylase family of enzymes that *Drosophila* have a known homologue (Li *et al.,* 2000).

A study by Goodstadt and Ponting (2004) used PSI-BLAST to identify 37 homologs of the VKOR family of enzymes. These included; archaea, eubacteria, plants, invertebrates and vertebrates. They noted that plant and prokaryote VKORC1 have a C-terminal thioredoxin-like domain, which have the potential to shuttle electrons for the catalytic activity of VKOR (Goodstadt and Ponting, 2004). Unlike, Rost *et al.* (2004) a *Drosophila* sequence for VKOR was identified by Goodstadt and Ponting (2004).

Phylogenetic analysis of the VKOR family of enzymes by Robertson (2004) revealed that vertebrates contain two VKOR enzymes; VKORC1 and VKORC1L1, whereas members of invertebrates, basal deuterostomes, protists and plants contain only one VKOR. No VKOR enzymes were detected in fungi. Robertson (2004) concluded that vertebrate VKORC1 and VKORC1L1 was the result of a gene duplication event after the divergence of vertebrates form non-chordates.

A study by Wan *et al.* (2014) constructed a phylogenetic tree consisting of 41 species including, plants algae, photosynthetic bacteria and vertebrates. Their results revealed vertebrates, monocot and dicot plants separated into three main clades. The cyanobacteria, mosses and green algae formed a weak clade. Wan *et al.* (2014) identified a VKOR homolog in the tomato plant and showed that all plant homologs contain a C-terminal thioredoxin-like domain with four conserved cysteines, which is consistent with the findings of Goodstadt and Ponting (2004). Plant VKOR homologs also contain a N-terminal signal peptide which transits the protein to the inner thylakoid membrane (Wan *et al.,* 2014).

Bevans *et al.* (2015) reconstructed a comprehensive phylogeny for the VKOR family of enzymes. This included 327 species of the major phyla of the Kingdoms of Life. Five principle clades were identified. Non-photosynthetic prokaryotes resided in Clade 1 and included archaea, eubacteria, actinobacteria, acidiobacteria, crenarchaeota, proteobacteria and

spirochetes. Vertebrate VKORC1 and VKORC1L1 paralogs segregated into two separate clades, Clade 2 and 3 respectively. Clade 4 included primitive single-celled animals and invertebrates comprising of amoebozoans, choanoflagellates and lower metazoans through to invertebrates. Clade 5 included photosynthetic prokaryotes and plants.

1.15.2 Evolutionary relationship between DsbB and VKORC1

Bevans *et al.* (2015) proposed an evolutionary relationship between VKORC1 and Disulfide Bond Formation Protein B (DsbB) (Bevans *et al.*, 2015). In prokaryotes, VKOR homologs and DsbB are responsible for oxidative protein folding and disulfide bond formation. The study showed that the structural elements of VKORC1 and DsbB were related due to circular permutation (Figure 12). The circular permutation occurs between the four helical domains of DsbB and VKORC1 (Figure 12). Bevans *et al.* (2015) suggest that the two enzymes arose from a gene duplication/deletion event, which resulted in the change in orientation of the transmembrane domains in VKORC1 compared to DsbB. DsbB has a structure of N-**ABCD**-C, whereas VKORC1 has a structure of N-**CDAB**-C (Figure 12).

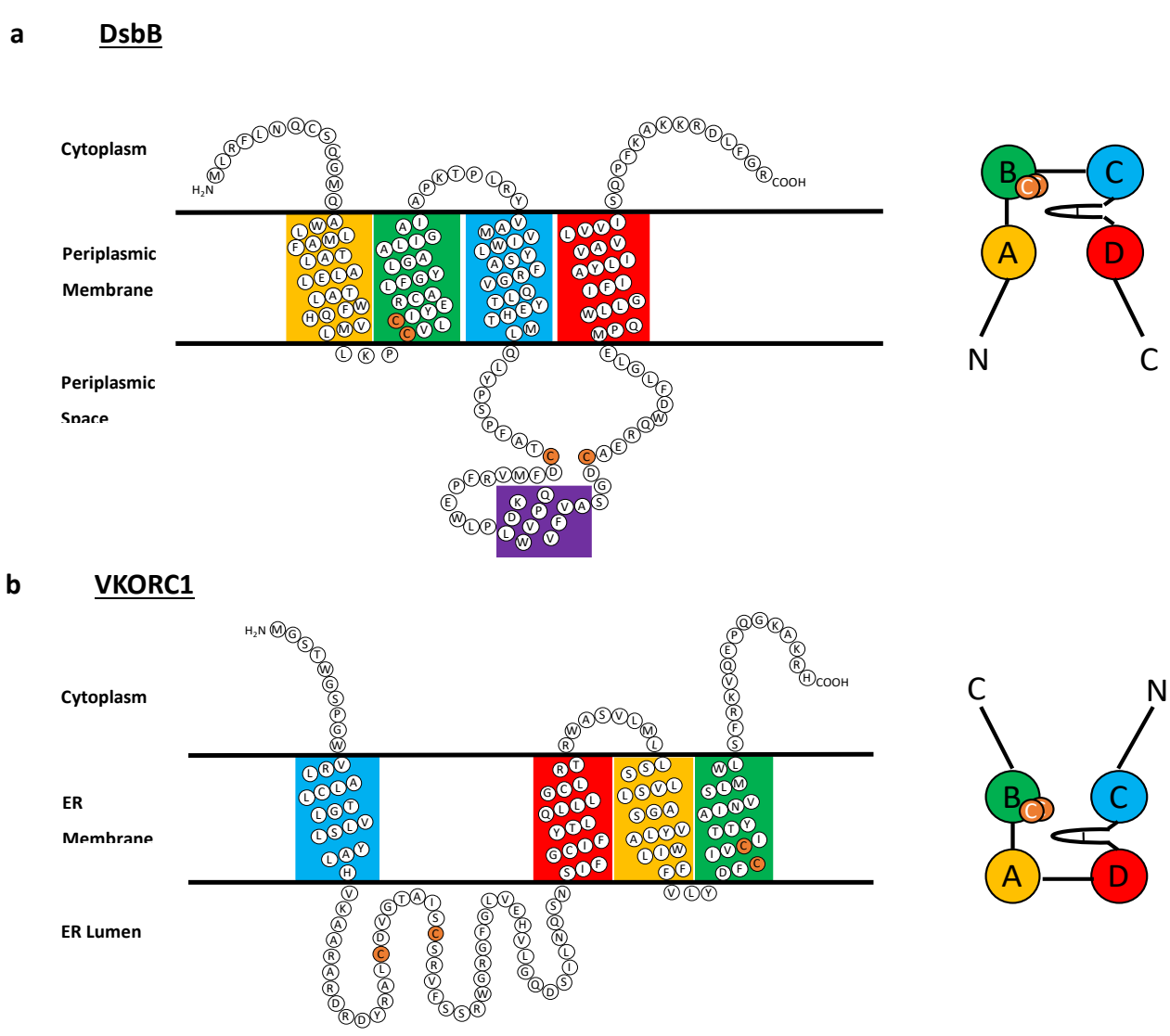


Figure 12: Topological diagrams of DsbB and VKORC1 highlighting the structural relationship between the two proteins. (Created by Author, based on Bevans *et al.,* 2015).

During this study, Bevans *et al.* (2015) proposed an evolutionary model for VKOR family enzymes (Figure 13).

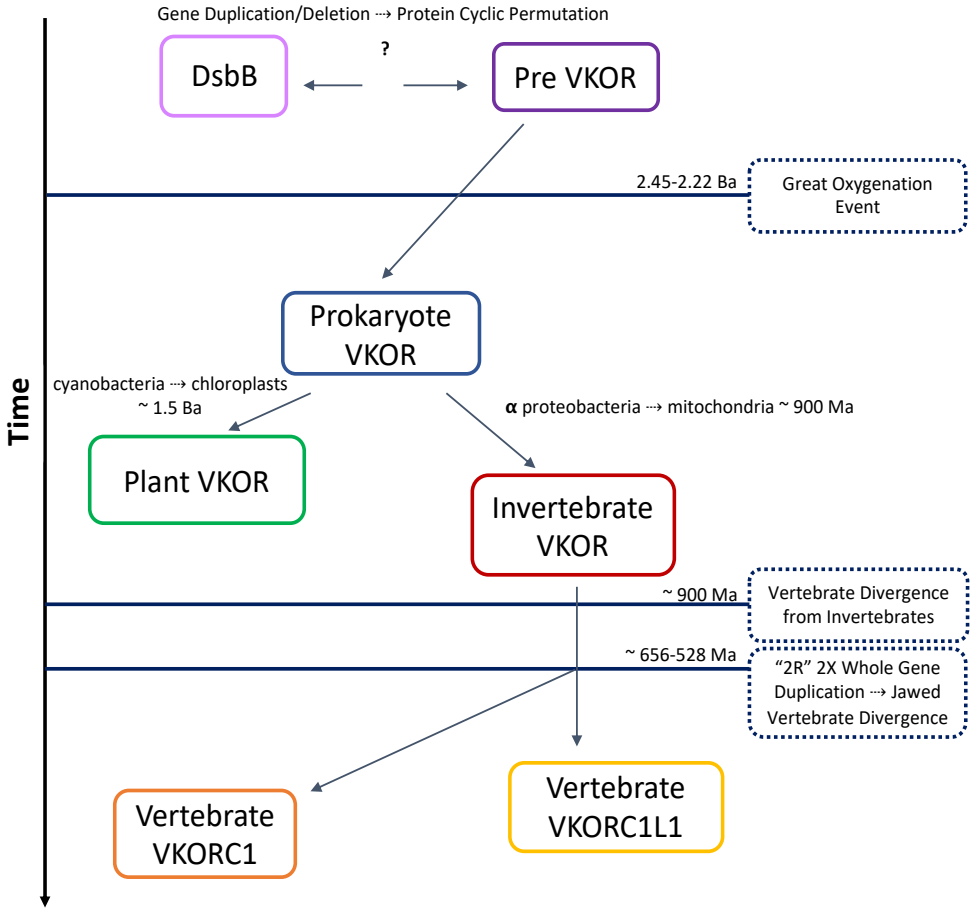


Figure 13: An evolutionary model of the VKOR family and its proposed relationship to DsbB. (Created by Author, adapted from Bevans *et al.*, 2015). Ba denotes billions of years ago. Ma denotes millions of years ago.

Bevans *et al.* (2015) proposed that VKORC1 and DsbB are evolutionary divergent members of a single lipidic quinone:disulfide oxidoreductase superfamily (LQOR superfamily) due to their structural relationship by circular permutation. This homology likely arose from a gene duplication/deletion event before the evolution of eukaryotes. The CDAB structure of DsbB likely arose from a duplication of a tandem repeat of the ABCD structure – ABCDABCD. The flanking paired helices were likely deleted revealing final structure of DsbB - ~~AB~~**CDAB**~~CD~~. It is likely that the catalysis of de-epoxidation arose after the great oxygenation event in the evolution of prokaryotic VKOR. In separate evolutionary events, prokaryotic VKORC1 appears to evolve in two separate events that correlate with the evolution of chloroplasts and mitochondria to form plant VKOR and invertebrate VKOR, respectively. It is proposed that the vitamin K cycle arose in invertebrates. After the divergence of vertebrates from invertebrates ~ 900 millions of years ago (Mya) and the two rounds of whole genome duplication ~500-600

Mya, it is proposed that VKORC1 and VKORC1L1 arose by a gene duplication event resulting in neofunctionalisation (Bevans *et al.,* 2015).

1.16 Molecular Basis of Anticoagulant Resistance

Following the identification of the VKORC1 gene in 2004 (Rost *et al.,* 2004; Li *et al.,* 2004) single nucleotide polymorphisms (SNP) were identified in VKORC1 in brown rats (Section 1.16.1 and 1.16.2), mice (Section 1.16.3) and humans (Section 1.16.4) (e.g. Rost *et al.,* 2004; Pelz *et al.,* 2005).

1.16.1 Anticoagulant Resistance of *Rattus norvegicus* in the UK

The first anticoagulant resistance polymorphism, p.Y139C, was identified in the brown rat by Rost *et al.* (2004). Following on from Rost *et al.* (2004) a study by Pelz *et al.* (2005) identified six different anticoagulant resistant polymorphisms in brown rat samples in the UK and Europe. However, brown rat samples used to determine VKORC1 polymorphisms in the UK were derived from a small sample size of laboratory rat strains from the Central Science Laboratory (CSL) in York and Reading University or were frozen samples collected between the years 1990-2000. Likewise, a low number of samples were used to determine the anticoagulant resistance polymorphisms in UK brown rats in a study by Rost *et al.* (2009) were frozen and collected between 1994 and 1996 (Rost *et al*., 2009). A study by Prescott *et al.* (2011) identified a p.Y139F polymorphism on one farm in Kent collected during 2009. Although there were 15 samples which was greater than other studies (e.g. Pelz *et al.,* 2005), all samples were collected from one farm and were only representative of one population of brown rats. A more recent study by Haniza *et al.* (2015) screened brown rat tissue samples obtained from frozen samples collected between the years 1990-2000 from the CSL, York with some samples from Leicestershire, Cambridge and Yorkshire collected between 2004 and 2005, to identify polymorphisms found within the 'hotspots' proposed by Pelz *et al.* (2005). The distribution of anticoagulant resistance polymorphisms in the UK is unique as it contains all five well known polymorphisms associated with resistance (p.L120Q, p.L128Q and p.Y139C/S/F), as well as three other polymorphisms that have a resistance phenotype (Table 8). Interestingly, there were a number of reports of compound heterozygotes found in the VKORC1 gene in *Rattus norvegicus* samples sampled by Haniza *et al.* (2015) (Table 9).

Although these studies give an indication about the resistance polymorphisms found in the UK, it does not give a good representation of the current UK anticoagulant resistance status in brown rats.

Geographical Area		N° of Specimens	Codon	WT	Mut	AA WT	AA Mut	Ref
England	Hampshire	2	120	CTC	CAG	Leu	Gln	1
		1	139	TAT	TGT	Tyr	Cys	4
		1	120	CTC	CAG	Leu	Gln	4
	Berkshire (Reading)	2	120	CTC	CAG	Leu	Gln	1
	Berkshire (CSL) – Lab strain	2	120	CTC	CAG	Leu	Gln	1
	Berkshire	16	139	TAT	TGT	Tyr	Cys	4
		1	120	CTC	CAG	Leu	Gln	4
	Cambridge/Essex	16	63	TTT	TGT*	Phe	Cys	2
		1	26	GCA	ACA*	Ala	Thr	2
		13	139	TAT	TGT	Tyr	Cys	4
	Norfolk	2	139	TAT	TGT	Tyr	Cys	2
	Gloucestershire	1	139	TAT	TGT	Tyr	Cys	2
		2	139	TAT	TGT	Tyr	Cys	4
	Lincolnshire	2	139	TAT	TGT	Tyr	Cys	2
	Shropshire	2	139	TAT	TCT	Tyr	Ser	2
	Lancashire	2	128	CTG	CAG	Leu	Gln	2
	Nottinghamshire	2	33	CGC	CCC*	Arg	Pro	2
	Kent	10	139	TAT	TTT	Tyr	Phe	3
		4	139	TAT	TGT	Tyr	Cys	4
	Yorkshire (wild)	3	139	TAT	TGT	Tyr	Cys	1
		1	128	CTG	CAG	Leu	Gln	1
	North Yorkshire	8	139	TAT	TGT	Tyr	Cys	4
		1	120	CTC	CAG	Leu	Gln	4
	Dorset	4	139	TAT	TGT	Tyr	Cys	4
	Greater London	2	139	TAT	TGT	Tyr	Cys	4
	Leicestershire	16	139	TAT	TGT	Tyr	Cys	4
	Oxfordshire	7	139	TAT	TGT	Tyr	Cys	4
Scotland	(CSL) – Lab strain	2	128	CTG	CAG	Leu	Gln	1
Wales	(CSL) – Lab strain	2	139	TAT	TCT	Tyr	Ser	1

Table 8: Anticoagulant resistant polymorphisms found in the VKORC1 gene in *Rattus norvegicus* in different countries. * denotes a predicted codon change (not stated in literature). CSL denotes samples from the Central Science Laboratory, York. (Adapted from (1) Pelz *et al.,* 2005; (2) Rost *et al.,* 2009; (3) Prescott *et al.,* 2011; (4) Haniza *et al.,* 2015.

Geographical Area	N° of Specimens	Compound Heterozygote Polymorphisms
Berkshire	5	p.Y139C/p.L120Q
Gloucestershire	1	p.Y139C/p.L120Q
Hampshire	4	p.Y139C/p.L120Q
	1	p.Y139C/p.L120Q/p.Y139S
North Yorkshire	2	p.Y139C/p.Y139S
Oxfordshire	1	p.Y139C/p.L120Q

Table 9: Geographical areas in the UK where compound heterozygotes are found in the VKORC1 gene in *Rattus norvegicus* samples. (Haniza *et al.,* 2015)

1.16.2 Anticoagulant Resistance of *Rattus norvegicus* in Europe, Asia and North America

There are 11 other countries that have reported anticoagulant rodenticide resistance in brown rats (Table 10). Reports in North America and Asia show that anticoagulant resistance in *Rattus norvegicus* is established in these areas (Table 10). However, anticoagulant resistance is more prevalent in Europe with 9 countries reporting resistance. The distribution of anticoagulant resistance polymorphisms in Europe contains all five well known polymorphisms associated with resistance (p.L120Q, p.L128Q and p.Y139C/S/F), as well as six other polymorphisms that have a resistance phenotype (Table 10).

Geographical Area		N° of Specimens	Codon	WT	Mut	AA WT	AA Mut	Ref
Europe								
France		81	139	TAT	TTT	Tyr	Phe	1,3
		1	128	CTG	TCA	Leu	Ser	3
		1	103	TCT	TAT	Ser	Tyr	3
		1	155	GAA	AAA	Glu	Lys	3
		1	139	TAT	TGT	Tyr	Cys	3
		4	128	CTG	CAG	Leu	Gln	3
		1	35	CGC	CCC	Arg	Pro	1,3
		7	120	CTG	CAG	Leu	Gln	3
Belgium		26	120	CTG	CAG	Leu	Gln	4
		15	139	TAT	TTT	Tyr	Phe	1,4
Hungary		10	139	TAT	TGT	Tyr	Cys	2
Denmark		43	139	TAT	TGT	Tyr	Cys	1
Netherlands		22	139	TAT	TGT	Tyr	Cys	5
		1	139	TAT	TTT	Tyr	Phe	5
Germany		286	139	TAT	TGT	Tyr	Cys	1
		2	56	TCC	CCC	Ser	Pro	1
		N/A	26	GCA	ACA*	Ala	Thr	9
		N/A	79	TCC	TTC*	Ser	Phe	9
		N/A	139	TAT	TGT	Tyr	Cys	9
Italy		6	123	ATC	ACC*	Ile	Ser	6
North America								
USA	Chicago	14	35	CGC	CCC*	Arg	Pro	2
Asia								
Japan		6	35	CGC	CCC*	Arg	Pro	7
Korea	Seoul	7	139	TAT	TTT	Tyr	Phe	2
China		N/A	140	GCC	ACC*	Ala	Thr	8

Table 10: Anticoagulant resistant polymorphisms found in the VKORC1 gene in *Rattus norvegicus* in different countries. * denotes a predicted codon change (not stated in literature). Adapted from (1) Pelz *et al.,* 2005; (2) Rost *et al.,* 2009; (3) Grandemange *et al.,* 2010; (4) Baert *et al.,* 2012; (5) Meersburg *et al.,* 2014; (6) Iacucci *et al.,* 2018; (7) Tanaka *et al.,* 2013; (8) Ma *et al.,* 2018, (9) Runge *et al.,* 2011.

1.16.3 Anticoagulant Resistance found in other rodents

There are also reports of resistance in other rodent species including; *Rattus rattus, Rattus flavipectus, Mus musculus* and *Mastomys natalensis* (Table 11). There are 8 polymorphisms found in *Mus musculus*. All reported polymorphisms for *Mus musculus* are found in Europe. Song *et al.* (2011) report four polymorphisms that confer resistance in *Mus* musculus species were introduced by adaptive introgressive hybridisation with *Mus spretus* which have a natural resistance to anticoagulants (Song *et al.,* 2011). Polymorphisms found in the two species of the genus *Rattus* are mostly found in Asia with an exception of one report of a p.Y25F polymorphism in *Rattus rattus* in Spain (Goulois *et al.,* 2016). All rodent species with reported anticoagulant resistance polymorphisms were classified as the top pests in the world (Capizzi *et al.,* 2004). Table 11 summarises anticoagulant polymorphisms found in rodents other than *Rattus norvegicus*.

Geographical Area		N° of Specimens	Codon	WT	Mut	AA WT	AA Mut	Ref
Rattus rattus								
Japan	Tokyo	44	76	CTC	CCC	Leu	Pro	1
		38	61	CGG	TGG	Arg	Trp	1
	Osaka	16	41	GCG	ACG	Ala	Thr	1
		17	41	GCG	GTG	Ala	Val	1
New Zealand		8	25	TAC	TTC*	Tyr	Phe	2
Spain		10	25	TAC	TTC*	Tyr	Phe	3
Rattus flavipectus								
China		2	139	TAT	TTT*	Tyr	Cys	4
Mus musculus								
UK	CSL	6	128	TTA	TCA	Leu	Ser	5
	Reading	4	139	TAT	TGT	Tyr	Cys	5
Ireland	Dublin	11	128	TTA	TCA	Leu	Ser	6
		11	139	TAT	TGT	Tyr	Cys	6
	Kildare	4	128	TTA	TCA	Leu	Ser	6
		2	139	TAT	TGT	Tyr	Cys	6
	Meath	5	128	TTA	TCA	Leu	Ser	6
		9	139	TAT	TGT	Tyr	Cys	6
	Tipperary	1	128	TTA	TCA	Leu	Ser	6
		1	139	TAT	TGT	Tyr	Cys	6
	Wexford	5	128	TTA	TCA	Leu	Ser	6
Germany	Berlin	12	37	GAG	GGG*	Glu	Gly	7
	Lower Saxony	1	37	GAG	GGG*	Glu	Gly	7
	Westphilia	13	58	CGG	GGG*	Arg	Gly	7
		N/A	12	CGG	TGG*	Arg	Trp	7
		N/A	26	GCA	TCA*	Ala	Ser	7
		N/A	48	GCC	ACC*	Ala	Thr	7
		N/A	61	CGG	CTG*	Arg	Leu	7
	Rhineland	17	128	TTA	TCA	Leu	Ser	7
		1	139	TAT	TGT	Tyr	Cys	6
Azores		1	139	TAT	TGT	Tyr	Cys	7
Mastomys natalensis								
Tanzania		10	108	CTG	GTG*	Leu	Val	8
		2	140	GCC	ACC*	Ala	Thr	8
		1	100	CGT	CAT*	Arg	His	8

Table 11: Anticoagulant resistant polymorphisms found in the VKORC1 gene in other rodent species in different countries. * denotes a predicted codon change (not stated in literature). CSL denotes samples from the Central Science Laboratory, York. (Adapted from (1) Tanaka *et al.,* 2012; (2) Cowan *et al.,* 2016; (3) Goulois *et al.,* 2016; (4) Huang *et al.,* 2011; (5) Pelz *et al.,* 2005; (6) Mooney *et al.,* 2018; (7) Rost *et al.,* 2009; (8) Gryseels *et al.,* 2015.

1.16.4 Anticoagulant Resistance found in humans

As well as in rodent species, there are resistance polymorphisms found in human VKORC1 (Table 12). There are 26 polymorphisms associated with anticoagulant resistance in humans. Some polymorphisms are only found in certain ethnic groups e.g. p.A26P is only found in African populations (Table 12). Polymorphisms such as p.D36Y are found in 16 different ethnic groups, which range geographically over 4 continents. There are two polymorphisms identified, p.L128R and p.Y139H, which are found in the 'hotspot' described by Pelz *et al.* (2005). In humans, there are also SNPs identified in non-coding regions of the VKORC1 gene that can cause an effect on the gene function. A SNP was identified in the promoter region of the intron at -1639G>A (Rieder *et al.,* 2005) that causes a decrease in the expression leading to an increased sensitivity to warfarin (Wang *et al.,* 2008).

Codon	WT	Mut	AA WT	AA Mut	N° of Patients	Ethnicity	Ref
26	G	C	Ala	Pro	4	African	Bodin *et al.*, 2008
26	G	A	Ala	Thr	1	Moroccan	Watzka *et al.*, 2011
27	C	G	Leu	Val	1	Bengali	Peoch *et al.*, 2009
28	C	T	His	Gln	2	German	Watzka *et al.*, 2011
29	G	T	Val	Leu	1	Lithuanian	Rost *et al.*, 2004
					1	Caucasian	Harrington *et al.*, 2011
					3	Swiss	Watzka *et al.*, 20112
34	G	C	Ala	Pro	1	-	Harrington *et al.*, 2011
36	A	G	Asp	Gly	10	Russian	Watzka *et al.*, 2011
36	G	T	Asp	Tyr	1	Afro-Italian	D'Ambrosio *et al.*, 2007
					1	Sephardic Jewish	Scott *et al.*, 2008
					53	Ashkenazi Jewish	Bodin *et al.*, 2008; Scott *et al.*, 2008
					4	German	Watzka *et al.*, 2011
					5	Afro-American	Watzka *et al.*, 2011
					21	Russian	Watzka *et al.*, 2011
					9	Turkish	Watzka *et al.*, 2011
					10	Egyptian	Shahin *et al.*, 2013
					4	Kenyan	Shahin *et al.*, 2013
					5	Sudanese	Shahin *et al.*, 2013
					5	Saudi Arabian	Shahin *et al.*, 2013
					3	Spanish	Anton *et al.*, 2013
41	G	T	Ala	Ser	1	-	Reider *et al.*, 2005
45	T	C	Val	Ala	1	German	Rost *et al.*, 2004
52	C	T	Ser	Leu	1	Dutch	Schmeits *et al.*, 2010
52	C	G	Ser	Trp	11	German	Watzka *et al.*, 2011
54	G	C	Val	Leu	3	Caucasian	Bodin *et al.*, 2008
56	C	T	Ser	Phe	12	German	Watzka *et al.*, 2011
58	A	G	Arg	Gly	3	Norwegian	Rost *et al.*, 2004
					1	Han Chinese	Wang *et al.*, 2008
59	T	C	Trp	Arg	1	Caucasian	Wilms *et al.*, 2008
					2	Dutch	Schmeits *et al.*, 2010
59	G	T	Trp	Cys	14	German	Watzka *et al.*, 2011
59	G	T	Trp	Leu	13	Iranian	Watzka *et al.*, 2011
66	T	G	Val	Gly	18	German	Watzka *et al.*, 2011
66	G	A	Val	Met	34	Afro-Caribbean	Bodin *et al.*, 2008; Wilms *et al.*, 2008
					1	Caucasian	Bodin *et al.*, 2008
					1	Caribbean	Bodin *et al.*, 2008
					15	Austrian	Watzka *et al.*, 2011
					2	Black South African	Mitchel *et al.*, 2011
71	G	C	Gly	Ala	19	German	Watzka *et al.*, 2011
77	A	G	Asn	Ser	20	German	Watzka *et al.*, 2011
77	A	T	Asn	Tyr	21	German	Watzka *et al.*, 2011
123	T	A	Ile	Asn	22	German	Watzka *et al.*, 2011
128	T	G	Leu	Arg	2	British	Rost *et al.*, 2004
					1	Caucasian	Bodin *et al.*, 2008
					1	Spanish	Anton *et al.*, 2013
139	T	C	Tyr	His	23	German	Watzka *et al.*, 2011

Table 12: Anticoagulant resistant polymorphisms found in VKORC1 in *Homo sapiens*.

1.16.5 Other Mechanisms for Resistance to Anticoagulants

Although anticoagulant resistance is associated with single nucleotide polymorphisms (SNP) in VKORC1, some studies have shown that other mechanisms could contribute to resistance to anticoagulants (Wallin *et al.,* 2001; Ishizuka *et al.,* 2007; Markussen *et al.,* 2008). One mechanism of resistance showed that a chaperone protein known as calumenin has the ability to bind to VKORC1 reducing activity (Wallin *et al.,* 2001). Wallin *et al.* (2001) hypothesized that the binding of calumenin to VKORC1 prevents anticoagulants from reaching the binding site on VKORC1. Another mechanism to explain anticoagulant resistance is the metabolism of anticoagulants by cytochrome P450 enzymes. Ishizuka *et al.* (2007) showed that there was an increase in cytochrome P450 enzyme, CYP3A2, in resistant *Rattus rattus* (Ishizuka *et al.,* 2007; Ishizuka *et al.,* 2008). A study by Markussen *et al.* (2008) also suggested that resistant *Rattus norvegicus* have an increased expression of cytochrome P450 CYP2E1, CYP2C13, CYP3A2 and CYP3A3 thereby facilitated increased detoxification of bromadiolone (Markussen *et al.,* 2008).

1.16.6 Phylogeography of Resistant Polymorphisms in *Rattus norvegicus*

Mitochondrial DNA (mtDNA) is used to study population genetics and phylogeography (Brown, 2007). Due to its maternal inheritance and the inability for recombination to occur it allows phylogenetic histories to be traced using a single lineage (Ladoukakis and Zouros, 2017). Using mtDNA sequencing it has been shown that *Rattus norvegicus* originated in Southwest China ~1.2 million years ago (Jin *et al.,* 2008; Wu and Wang, 2012). Song *et al.* (2014) mapped the phylogeography of *Rattus norvegicus* using D-loop and cytochrome b sequences and compared mitochondrial variation of rats with resistant polymorphisms such as p.Y139C. 25 D-loop haplotypes were identified and of these resistant rats were grouped in 6 haplotypes (D2, D5, D6, D7, D11 and D12) (Song *et al.,* 2014). The samples tested for VKORC1 polymorphisms were predominantly from Germany (Song *et al.,* 2014). It was hypothesized that because of the high frequency of haplotypes found in the German rats, resistance probably evolved elsewhere, for example the USA where warfarin was synthesised (Song *et al.,* 2014).

A study by Haniza *et al.* (2015) used mtDNA to identify D-loop haplotypes in populations of *Rattus norvegicus* in the UK from frozen tissue samples collected in 1990 to 2000 from UK

Government Central Science Library (CSL) in order to draw conclusions related to geographical population structure. They found 6 haplotypes differing at 10 nucleotide positions in the 187 samples tested and there was no geographical structuring to the haplotype distributions and no haplotype domination. They concluded from their results that populations of *Rattus norvegicus* were introduced simultaneously or at separate stages. There is currently only this study which comments on the population genetics of *Rattus norvegicus* in the UK.

1.17 Biochemical Characterisation of VKORC1 and VKORC1L1

1.17.1 Heterologous Expression of VKORC1

Before the discovery of the VKORC1 gene (Section 1.11.2), rat liver microsomes were used to determine the activity of VKOR in both wild type and resistant rats (MacNicoll, 1985). Since the discovery of the VKORC1 gene (Rost *et al.,* 2004; *Li et al.,* 2004) different expression systems have been used to express recombinant VKORC1 including; mammalian cell systems, baculovirus, *Pichia* and bacterial expression systems. Expression systems have been used to observe the effect of polymorphisms on the function of VKORC1 and how different anticoagulants interact with VKORC1 and to observe functional differences between VKORC1 and VKORC1L1.

Since the discovery of the VKORC1 gene (Rost *et al.,* 2004; *Li et al.,* 2004), three research groups used the baculovirus insect cell system to express VKORC1 (e.g. Li *et al.,* 2004; Jin *et al.,* 2007; Richavy *et al.,* 2011; Chu *et al.,* 2006). This expression system has many advantages in the production of biologically active proteins over yeast and bacterial systems. One benefit is that insect cells are eukaryotic cells and have the mechanisms for protein folding and post-translational modifications, which resemble the mechanisms performed in mammalian cells (Contreras-Gómez *et al.,* 2014). This expression system produces high levels of expression and late expression of potentially toxic proteins. The baculovirus system has been used with *Spodoptera frugiperda* (*Sf9*) insect cells to make several important discoveries about VKOR. Li *et al.* (2004) identified the gene for VKORC1 by expressing and measuring the activity produced. A study by Chu *et al.* (2006) used *Sf9* cells to express and purify VKORC1 to show that a single VKORC1 polypeptide is responsible for the conversion of vitamin K epoxide to

vitamin K and the conversion of vitamin K to vitamin K hydroquinone (Chu *et al.,* 2006). Both Jin *et al.* (2007) and Richavy *et al.* (2011) used insect cells to express VKORC1 in order to study the importance of the conserved cysteine residues. The advantage of using the baculovirus system is that *Sf9* insect cells have no measurable VKORC1 activity (Li *et al.,* 2004).

Four research groups used the human embryonic kidney cell line (HEK-293) to express VKORC1 (e.g. Rost *et al.,* 2004; Tie *et al.,* 2012; Fregin *et al.,* 2013; Czogalla *et al.,* 2017). Fregin *et al.* (2013) described a novel indirect cell culture assay using HEK-293 cells to characterise the properties of wild-type and variant VKORC1 against warfarin. Human coagulation factor IX (FIX) and VKORC1 was coexpressed in HEK-293 cells and the secreted FIX activity was used as a marker to report the activity of VKORC1 (Fregin *et al.,* 2013).

There are two research groups which used *Pichia pastoris* expression system (e.g Hodroge *et al.,* 2011; Hodroge *et al.,* 2012; Krettler *et al.,* 2015). Hodroge *et al.* (2011) used the yeast, *Pichia pastoris* expression system to characterise known VKORC1 polymorphisms and the resistance affect against FGARs and SGARs. To validate the *Pichia* expression system, Hodroge *et al.* (2011) compared the K_m and the K_i of liver microsomes of susceptible and p.Y139F resistant rats with the recombinant VKORC1 and recombinant VKORC1-Y139F. The data showed that the recombinant VKORC1 expressed in *Pichia* expression system had similar properties as the native enzyme in liver microsomes, which validated the system as a good model to study the consequences of VKORC1 mutations. This study also showed that VKORC1 dominates the activity in the liver because the kinetic properties between the recombinant VKORC1 and the VKOR activity in liver microsomes were similar (Hodroge *et al.,* 2011).

Current literature shows that expression of VKORC1 enzymes in *E. coli* requires modifications in order to express the active enzyme. Jaenecke *et al.* (2015) expressed human VKOR as an hexahistidine-tagged ketosteroid isomerase insoluble fusion protein in *E. coli.* In order for active enzyme to be produced the VKORC1-fusion protein was purified and chemical cleavage under denaturation conditions was undertaken. Hatahet *et al.* (2015) showed that VKORC1 could be expressed in *E. coli* by altering the membrane translocation machinery and modifying the VKORC1 enzyme. The YidC protein that is involved in translocation of

membrane proteins in *E. coli* was mutated along with modifications being made with VKORC1 including a deletion of a highly conserved 'AAR' at positions 31 to 33 and point mutation at p.G60D (Hatahet *et al.,* 2015). In this case, a β-galactosidase reporter assay was used to indirectly detect the activity of the modified VKORC1 (Hatahet *et al.,* 2015).

1.17.2 Kinetic analysis of VKORC1

There have been many studies that have determined the kinetic properties of VKORC1 in different species (Table 13). The kinetic properties of both rat and human VKORC1 have been well studied in three different expression systems. For example, there is a large range of K_m values for rat VKORC1 from 0.6 μM to 176.1 μM (e.g. Hildebrandt *et al.,* 1984; Wilson *et al.,* 2003; Wantanabe *et al.,* 2010; Hodroge *et al.,* 2011). This difference in K_m values can be due to different experimental design as well as the differences in expression system used. Table 13 summarises studies K_m on VKOR in all species that have been studied.

From Table 13, liver microsomes are the most used source of VKORC1 protein to determine the K_m. The issue with using liver microsomes is that both VKORC1 and VKORC1L1 are found in liver tissue, although it is a representative value due to VKORC1 being the predominant enzyme in liver tissue (Hammed *et al.,* 2013).

Scientific Name	Common Name	Expression System	Km (μM)	Study
Rattus norvegicus	Brown rat	Liver Microsomes	0.60 ± 0.03	Hildebrandt *et al.,* 1984
			57.7 ± 12.5	Lasseur *et al.,* 2005
			8.40 ± 0.90	Hodroge *et al.,* 2011
			4.25 ± 0.40	Wilson *et al.,* 2003
			176.1 ± 14.2	Wantanabe *et al.,* 2010
		HEK-239 cells	19.6 ± 1.6	Hammed *et al.,* 2013
		Pichia pastoris	15.9 ± 4.5	Goulois *et al.,* 2015
			7.2 ± 2.5	Matagrin *et al.,* 2013
			7.2 ± 2.5	Hodroge *et al.,* 2011
Rattus rattus	Black rat	Liver Microsomes	15.9 ± 4.5	Goulois *et al.,* 2015
Mus musculus	House mouse	Liver Microsomes	12.73 ± 0.93	Lasseur *et al.,* 2006
			4.16 ± 1.06	Wilson *et al.,* 2003
Homo sapiens	Human	Liver Microsomes	8	Wallin and Martin, 1985
			3.09	Wilson *et al.,* 2003
		HEK-239 cells	21.5 ± 4.2	Hammed *et al.,* 2013
			1.88 ± 0.13	Westhofen *et al.,* 2011
		Pichia pastoris	1.20	Krettler *et al.,* 2015
			1.24	Bevans *et al.,* 2013
			19.8	Hodroge *et al.,* 2012
			21.5 ± 4.2	Matagrin *et al.,* 2016
Bos taurus	Cow	Liver Microsomes	6.46 ± 0.77	Wilson *et al.,* 2003
Ovis aries	Sheep	Liver Microsomes	2.41 ± 0.23	Wilson *et al.,* 2003
Canis lupus familiaris	Dog	Liver Microsomes	3.60 ± 0.16	Wilson *et al.,* 2003
Equus caballus	Horse	Liver Microsomes	5.24 ± 1.65	Wilson *et al.,* 2003
Sus scrofa	Pig	Liver Microsomes	6.32 ± 0.68	Wilson *et al.,* 2003
Gallus gallus	Chicken	Liver Microsomes	165.8 ± 41.3	Wantanabe *et al.,* 2010
Struthio camelus	Ostrich	Liver Microsomes	187.5 ± 14.6	Wantanabe *et al.,* 2010

Table 13: Kinetic properties of VKORC1 in different animal with vitamin K epoxide substrate.

1.17.3 Biochemical Characterisation of VKORC1 Polymorphisms associated with anticoagulant resistance

A study by Rost *et al.* (2004) assessed the VKOR activity of HEK-293 cells transfected with wild type and mutated VKORC1 cDNA. In general, the anticoagulant resistant VKOR variants had reduced VKOR activity compared with the wild-type. The p.V29L and p.Y139C polymorphisms retained a higher activity compared to the wild-type after inhibition with >20 μM of warfarin.

Pelz *et al.* (2005) expressed eight VKORC1 variants with resistance polymorphisms reported in *Rattus norvegicus* and *Mus musculus* in HEK-293 cells to assess VKORC1 activity with increasing concentrations of warfarin. These included; p.R35P, p.S56P, p.L120Q, p.L128S, p.L128Q, p.Y139C, p.Y139F and p.Y139S. Of the three polymorphisms p.Y139F, p.Y139S and p.Y139C; p.Y139F appeared to be largely insensitive to warfarin compared to the wild-type with 87% activity, and p.Y139S and p.Y139C had an activity of 33% and 25%, respectively at 100 μM warfarin. The other polymorphisms tested (p.L120Q, p.L128Q, p.R35P, p.S56P) showed varying degrees of resistance against warfarin and VKOR activity with p.L120Q and p.L128Q with activities of 50% and 20%, respectively. Both p.R35P and p.S56P had an activity of below <5%. This study suggested that these resistance polymorphisms are the genetic basis of resistance.

A later study by the same research group (Rost *et al.*, 2009) described 18 novel and 5 previously reported polymorphisms in *Rattus norvegicus* and *Mus musculus*. VKORs with these polymorphisms were expressed in HEK-293 cells to assess the percentage inhibition of the VKORC1 variants with 60 μM of warfarin (Figure 14). The study concluded that the Y139 variants in both *Rattus norvegicus* and *Mus musculus* conferred warfarin resistance, however, the other polymorphisms tested had little or no effect on the inhibition of VKORC1 (Figure 14). Warfarin had the least effect on the p.Y139S polymorphism with activity only being reduced by ~ 30%, whereas warfarin had the most effect on the p.W59R polymorphism with an activity being reduced by ~ 90%. There are only three polymorphisms that have activity a reduction of ~ 50% these include p.Y139C, p.Y139F and p.Y139S in *Rattus norvegicus* (Figure 14). The p.Y139C polymorphism in *Mus musculus* has an activity reduction of ~ 50% and is affected the least by warfarin. Warfarin had the most effect on the p.R12W polymorphism found in the *Mus musculus* (Figure 14).

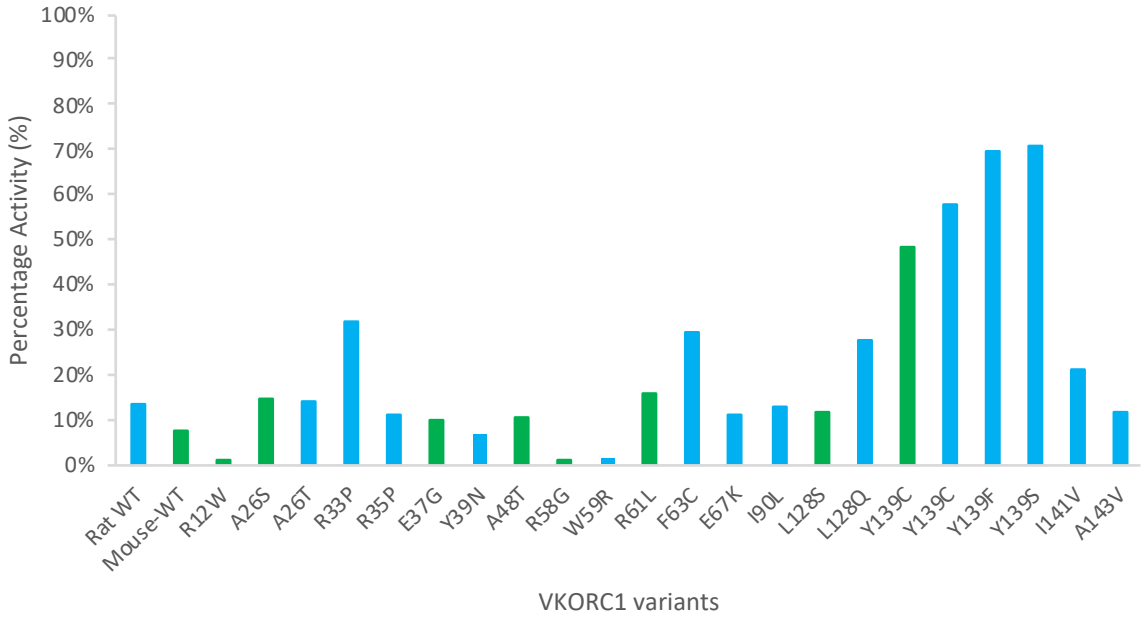


Figure 14: Percentage activity of VKORC1 variants found in *Rattus norvegicus* and *Mus musculus* at a warfarin concentration of 60 μM. Blue bars denote *Rattus norvegicus* polymorphisms. Green bars denote *Mus musculus* polymorphisms. (Adapted from table in Pelz *et al.,* 2005).

A later study by Díaz *et al.* (2010) reanalyzed the SNPs found in *Rattus norvegicus* VKORC1 by using *Rattus rattus* as an outgroup due to the implausibility of the high frequency of polymorphisms reported by Rost *et al.* (2009). Díaz *et al.* (2010) identified the novel polymorphisms reported by Rost *et al.* (2009) as interspecies differences between *Rattus norvegicus* VKORC1 and *Rattus rattus* VKORC1 due to the misidentification of species. These include; p.I90L, p.W59R, p.V112L, p.I141V and p.A143V which were actually in *Rattus rattus* VKORC1. This gives an explanation for the low activity seen for these polymorphisms when subjected to warfarin (Figure 14).

Hodroge *et al.* (2011) used *Pichia pastoris* to express and characterise major VKORC1 polymorphisms found in *Rattus norvegicus* and the resistance effect against different FGARs and SGARs. The quantitative data obtained by this group is summarized in Figure 15.

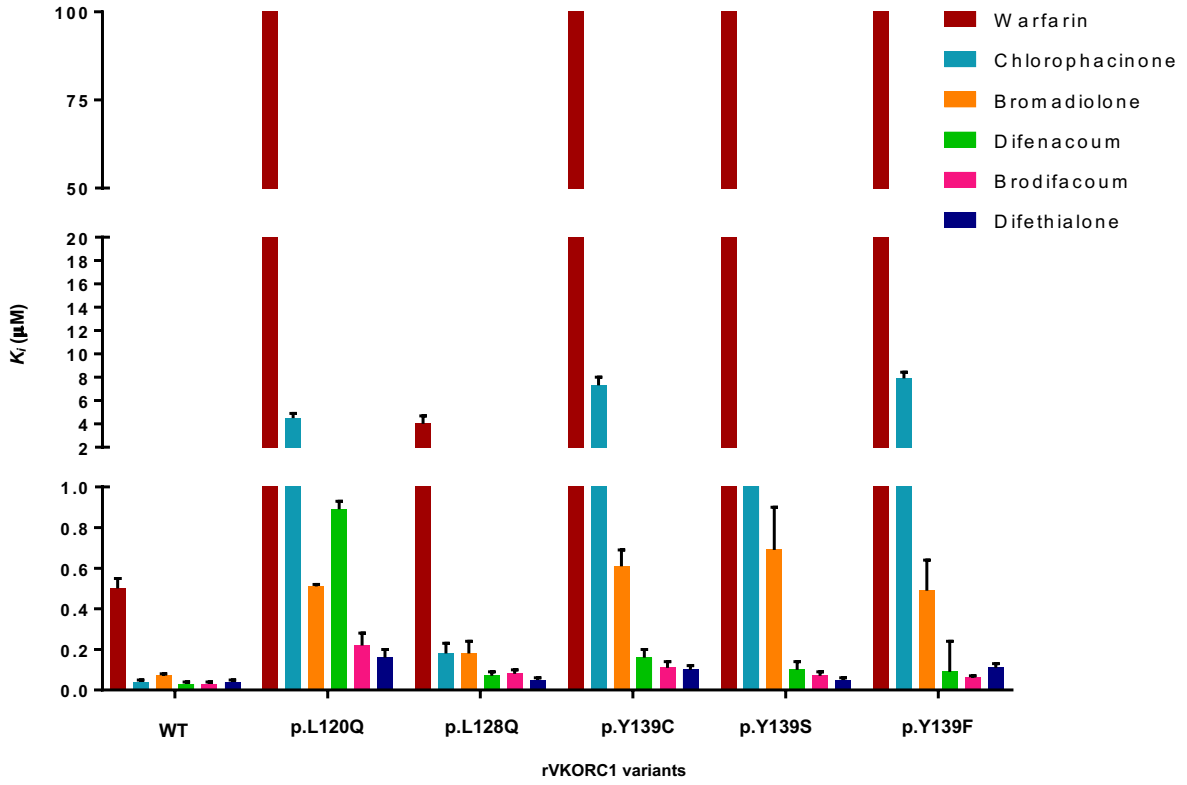


Figure 15: Inhibition values (K_i) of rVKORC1 variants found in *Rattus norvegicus* for various FGARs and SGARs. (Adapted from Hodroge *et al.,* 2011).

Hodroge *et al.* (2011) compared two FGARs, warfarin and chlorophacinone with four SGARs, bromadiolone, difenacoum, brodifacoum and difethialone. Warfarin had the greatest effect on the wild type recombinant rat VKORC1 (rVKORC1) in comparison to VKORs hosting the polymorphisms p.L120Q, p.Y139C, p.Y139F and p.Y139F in which warfarin has little effect and requires greater than 100 μM of warfarin to have an effect (Figure 15). Warfarin has some effect on the p.L128Q polymorphism and there is an 8-fold difference in K_i value of the p.L128Q polymorphism and the wild type rVKORC1. The second of the FGARs, chlorophacinone has a stronger anticoagulant effect on the wild type and the VKORC1 variants in comparison to warfarin. Of the polymorphisms and anticoagulants tested, chlorophacinone had the most effect on the p.L128Q polymorphism and the least effect on p.Y139F, followed by p.L120Q (Figure 15).

In comparison to the FGARs, all SGARs have a greater effect on the rat VKORC1 (rVKORC1) variants (Figure 15). The p.Y139F polymorphism had the least effect when inhibited by

bromadiolone with a K_i value of 0.69 μM compared to the wild type (0.07 μM). Difenacoum, brodifacoum and difethialone had the least effect on the p.L120Q variant compared to the wild type. Difethialone is the most potent inhibitor across all rVKORC1 variants with an exception of p.Y139S in which brodifacoum is the most potent (Figure 15). Overall, the p.L128Q polymorphism is the least resistant to anticoagulant rodenticides and has a weak resistance in comparison to the other polymorphisms (Figure 15).

As well as studies on rat VKOR variants, a study by Hodroge *et al.* (2012) assessed the susceptibility of human VKORC1 and its natural variants to warfarin and two other oral anticoagulants, acenocoumarol and fluindione. It was found that six polymorphisms (p.A26P, p.A41S, p.V54L, p.H68Y, p.I123N and p.Y139H) were associated with an increase in K_i which suggested an involvement in resistance phenotypes seen in patients. Polymorphisms p.A41S and p.H68Y had a selective resistance to indandione and 4-hydroxycoumarin derivatives. Other polymorphisms did not increase the K_i. Interestingly, ten polymorphisms (p.S52L, p.S52W, p.W59L, p.W59R, p.V66M, p.V66G, p.G71A, p.N77S, p.N77T and p.L128R) resulted in total loss of VKORC1 activity. This study suggests that not all naturally occurring polymorphisms are associated with resistance and there is potentially another resistance mechanism in these individuals (Hodroge *et al.,* 2012). A study by Chen *et al.* (2018) used IC_{50} to identify the inhibitory effect of different oral anticoagulants on human VKORC1 (Figure 16). Chen *et al.* (2018) showed that the efficiency of oral anticoagulants in humans from most to least was; acenocoumarol > phenprocoumon > warfarin > fluindione. The natural VKORC1 variants appeared to have a natural resistance to fluindione and warfarin, whereas with acenocoumarol and phenprocoumon there is varied inhibition causing both natural resistance and sensitivity in the different VKORC1 variants.

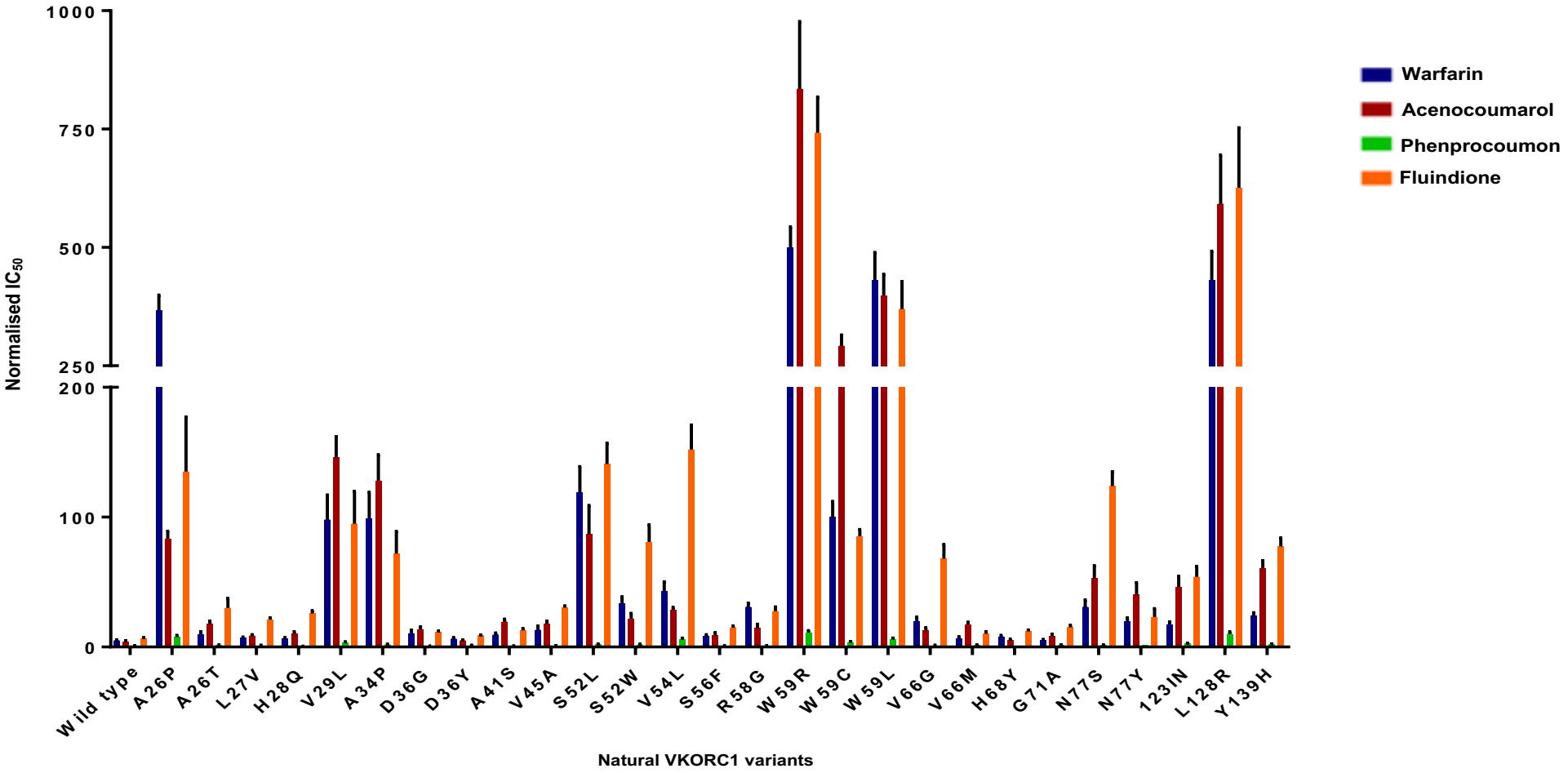


Figure 16: IC_{50} values of human VKORC1 for different oral anticoagulants. (Adapted from Chen *et al.,* 2018).

1.17.4 Characterisation of VKORC1 and VKORC1L1

Whilst the sensitivity of anticoagulants on VKORC1 has been well characterised, the effect of anticoagulants on its paralogue, VKORC1L1 has not been as well studied. Westhofen *et al.* (2011) determined the percentage inhibition of VKORC1 and VKORC1L1 with 5 μM warfarin. They showed that the percentage inhibition for VKORC1 and VKORC1L1 was 52.9% and 29.2%, respectively, suggesting that VKORC1L1 is less susceptible to warfarin compared to VKORC1. Hammed *et al.* (2013) compared the susceptibility of human and rat VKORC1 and VKORC1L1 to warfarin. Rat and human VKORC1L1 are between 30 and 50-fold more resistant to warfarin respectively, than VKORC1 (Figure 17).

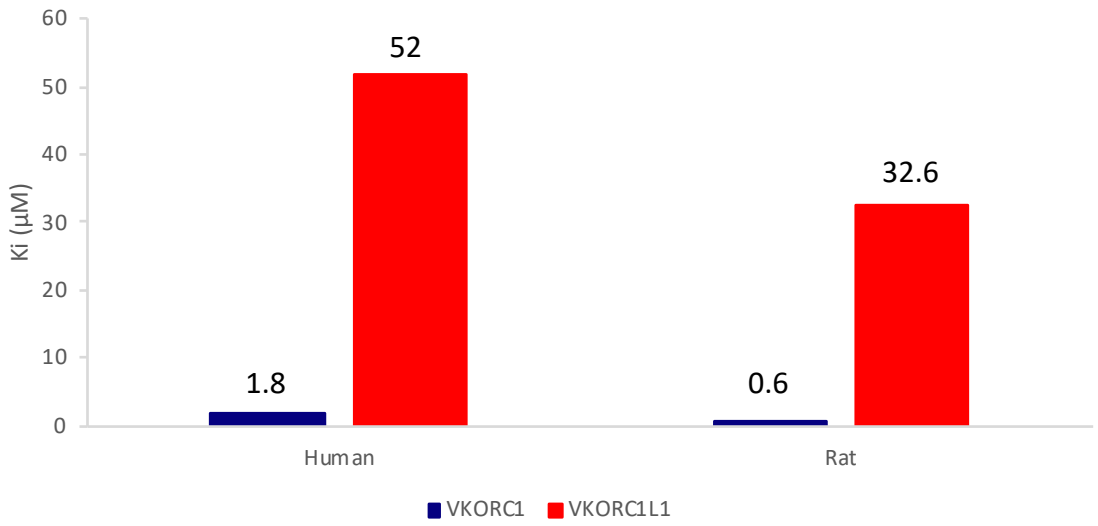


Figure 17: K_i values of human and rat VKORC1 and VKORC1L1 for warfarin. (Adapted from Hammed *et al.,* 2013).

A study by Matagrin *et al.* (2016) compared the K_i values for human VKORC1 and VKORC1L1 for oral anticoagulants and some SGARs (Figure 18).

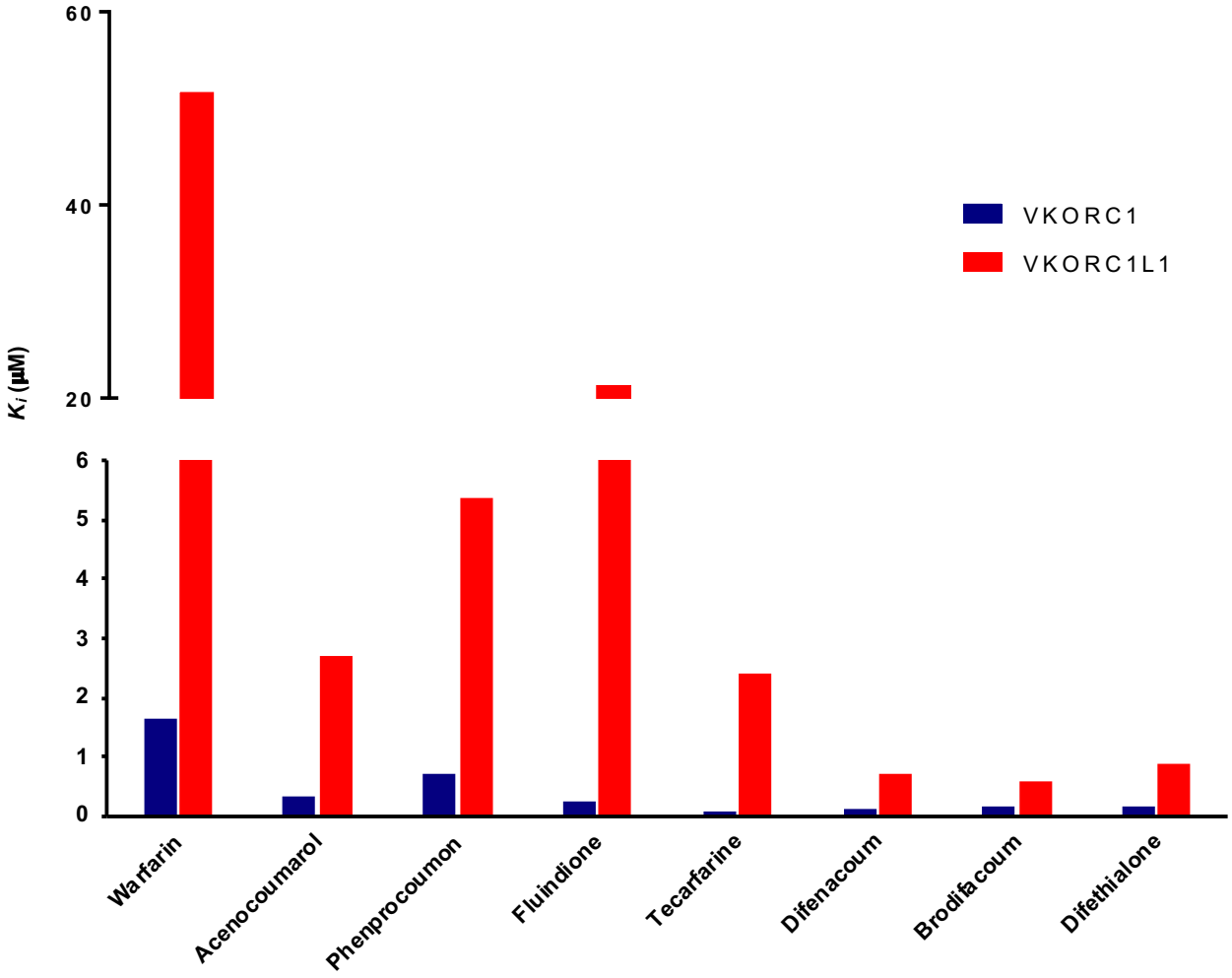


Figure 18: K_i values of human VKORC1 and VKORC1L1 for different oral anticoagulant and second generation anticoagulant rodenticides. (Adapted from Matagrin *et al.,* 2016).

All anticoagulants except for warfarin and phenprocoumon inhibited VKORC1 with a K_i lower than 0.5 µM, whereas the K_i values for VKORC1L1 were above 0.5 µM. VKORC1L1 therefore appears to have a natural resistance to inhibition by anticoagulants (Figure 18). In addition, second generation anticoagulant rodenticides appear to have the greatest effect on both VKORC1 and VKORC1L1.

A detailed study by Czogalla *et al.* (2018) compared the IC_{50} values of different anticoagulants with human VKORC1 and VKORC1L1 (Figure 19).

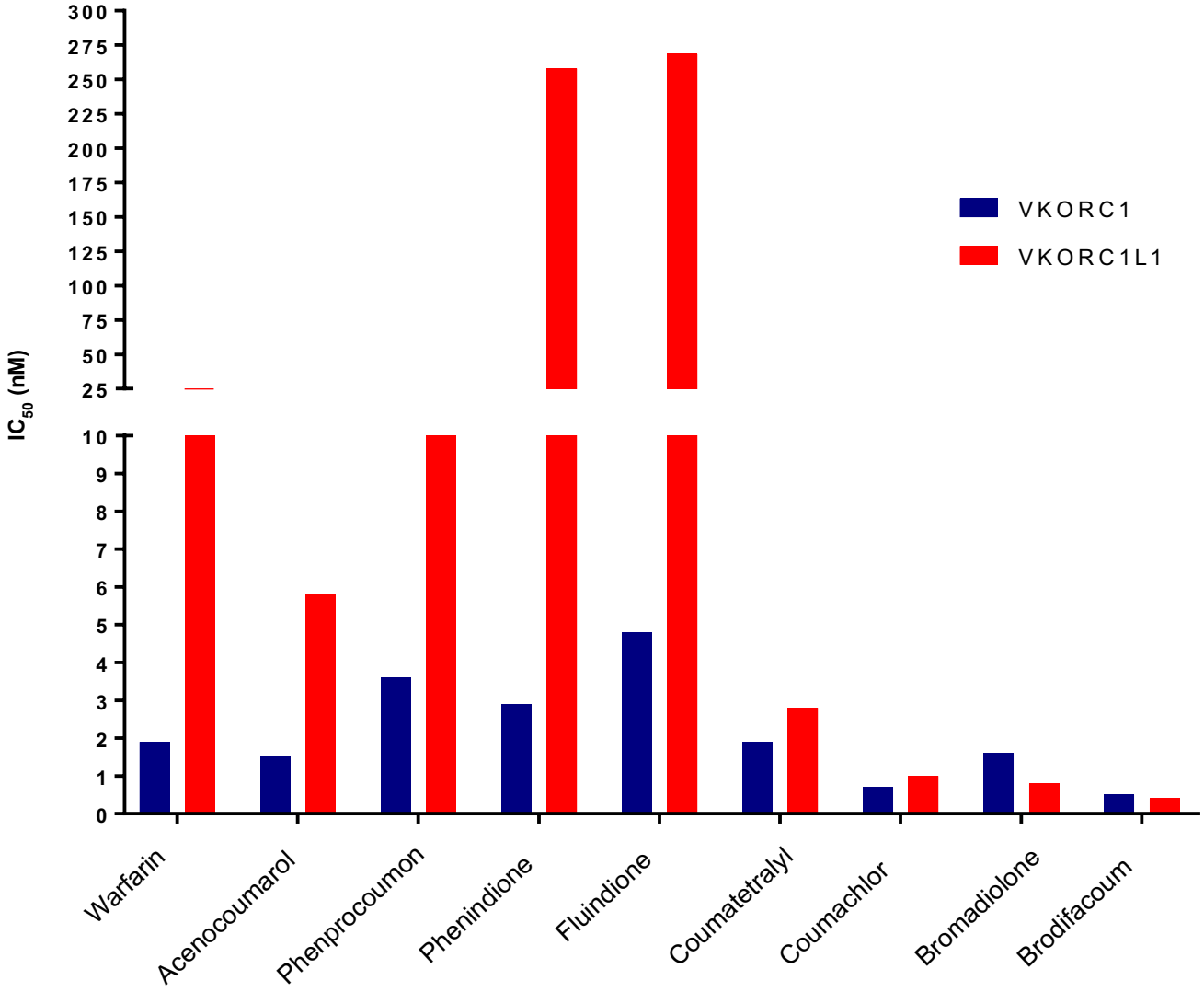


Figure 19: IC_{50} values of human VKORC1 and VKORC1L1 for different oral anticoagulant and anticoagulant rodenticides. (Adapted from Czogalla *et al.,* 2018).

The studies by Matagrin *et al.* 92016) and Czogalla *et al.* (2018) compared the susceptibility of human VKORC1 and VKORC1L1 to different anticoagulant rodenticides (Figure 18 and 19). The study by Matagrin *et al.* (2016) showed a greater difference between the anticoagulants tested between VKORC1 and VKORC1L1 than the study by Czogalla *et al.* (2018). For example, there is a 32-fold difference between VKORC1 and VKORC1L1 when inhibited by warfarin in the Matagrin *et al.,* (2013) study, compared to the study by Czogalla *et al.* (2018), which showed a 13.4 fold difference. In general, the results from Matagrin *et al.* (2013) for the susceptibility of human VKORC1 and VKORC1L1 to different anticoagulant rodenticides are

between 1.5 and 5-fold higher for all common anticoagulants tested compared to the study by Czogalla *et al.* (2018). From Figure 19, Czogalla *et al.* (2018) showed that for all anticoagulants tested, with the exception of bromadiolone and brodifacoum, human VKORC1L1 is less sensitive to anticoagulant rodenticides than human VKORC1. Whereas the study by Matagrin *et al.* (2016) showed that for all anticoagulants tested human VKORC1L1 is less sensitive to anticoagulant rodenticides than human VKORC1 (Figure 18).

Table 14 highlights the differences between the results obtained by both of these studies. The hierarchy of sensitivity to the common anticoagulants reported in the studies by Matagrin *et al.* (2016) and Czogalla *et al.* (2018) are different for VKORC1 but are very similar for VKORC1L1 (Table 14).

	Matagrin *et al.* (2016)	Czogalla *et al.* (2018)
Hierarchy of Inhibition of VKORC1 (least to most sensitive)	warfarin > phenprocoumon > acenocoumarol > fluindione > brodifacoum	fluindione > phenprocoumon > warfarin > acenocoumarol > brodifiacoum
Hierarchy of Inhibition of VKORC1L1 (least to most sensitive)	warfarin > fluindione > phenprocoumon > acenocoumarol > brodifacoum	fluindione > warfarin > phenprocoumon > acenocoumarol > brodifacoum
Expression System/Cell Line	*Pichia pastoris*	HEK 293T
Type of Measurement	Direct	Indirect
Activity Measurement	K>O conversion	Factor IX (FIX)
Type of Assay	DTT-driven HPLC	Clotting Assay
Substrate	3 to 200 μM K>O	12 μM K>O
Time of Assay	30 minutes	72 hours (3 days)
Inhibition Assay	K_i	IC_{50}

Table 14: Comparison of the hierarchy of inhibition by different anticoagulants and the VKOR assay methods used by Matagrin *et al.* (2016) and Czogalla *et al.* (2018) for VKORC1 and VKORC1L1.

The reason for the hierarchical differences between these two studies may be due to experimental design. Table 14 summarises the differences between the two assays.

Matagrin *et al.* (2016) used a direct DTT-driven HPLC assay which measured the conversion of vitamin K epoxide to vitamin K. This is the typical assay used to measure VKORC1 activity (e.g. Whitlon *et al.,* 1978; Wilson *et al.,* 2003; Wantanabe *et al.* 2010; Hodroge *et al.*, 2011; Bevans *et al.,* 2013; Louvet *et al.* 2015). Whereas, Czogalla *et al.* (2018) used an indirect cell culture-based assay that coexpressed human VKORC1 and a blood coagulation factor, Factor IX (FIX) to report warfarin inhibition. This system was first reported by Fregin *et al.* (2013). FIX is a vitamin K dependent blood coagulation factor which requires activation via GGCX in the vitamin K cycle and the activation of FIX is indirectly affected by the inhibition of anticoagulants on VKORC1 (Figure 7). The assay makes use of active FIX as a marker of VKORC1 activity and the inhibition by anticoagulants. This system involves transfection of a linear bicistronic vector which encodes both human VKORC1 and FIX into HEK-293T cells (Fregin *et al.,* 2013). After 72 hours of transfection the supernatant was collected and an ELISA was used to measure the FIX antigen levels of calibration plasma, control plasma and the cell culture supernatant samples (Fregin *et al*., 2013). FIX activities were then measured by an active partial thromboplastin time (aPTT) coagulation assay (Czogalla *et al.,* 2018), which measures how long coagulation occurs in citrated plasma (Raber, 1990). Fregin *et al.* (2013) claimed the cell culture method gives a better approximation of inhibition as it is comparable to *in vivo* patient warfarin dosage phenotypes. Whereas the method used by Matagrin *et al.* (2016), which was first described by Hodroge *et al.* (2011), used a heterologous expression system using *Pichia pastoris* to express VKORC1 and determine anticoagulant inhibition. This method was comparable to assays carried out using liver microsomes (Hodroge *et al.,* 2011).

1.17.5 Effect of Anticoagulants Rodenticides on Non-target Species

As well as the target species, rodents, anticoagulant rodenticides can have an effect on non-target animals such as birds and domesticated farm animals. Two studies have observed the inhibitory effect of warfarin on the VKOR of non-target animals using liver microsomes. Wantanabe *et al.* (2010) and Louvet *et al.* (2015) used the K_i values to compare the effects of warfarin on different non-target animal VKORC1 (Figure 20).

Comparison of K_i values for non-target animals can give an indication of the effect anticoagulant rodenticides such as warfarin have on the VKORC1 enzyme. Between the two studies, five species (cow, goat, sheep, pig and boar) belong to the even-toed ungulate order, one species (horse) belongs to the odd-toed ungulate order, one species belong to the rodent order (rat) and two species (chicken and ostrich) are birds. From the data in Figure 20, the chicken has the highest K_i value in comparison to all other species suggesting a resistance to warfarin. Indeed, feeding tests in chicken show LD_{50} values of >1000 mg/kg compared to the rat with a value of 58-328 mg/kg (Section 1.6), which shows a consistency with the data from Wantanabe *et al.* (2010) implying resistance to anticoagulants in the chicken.

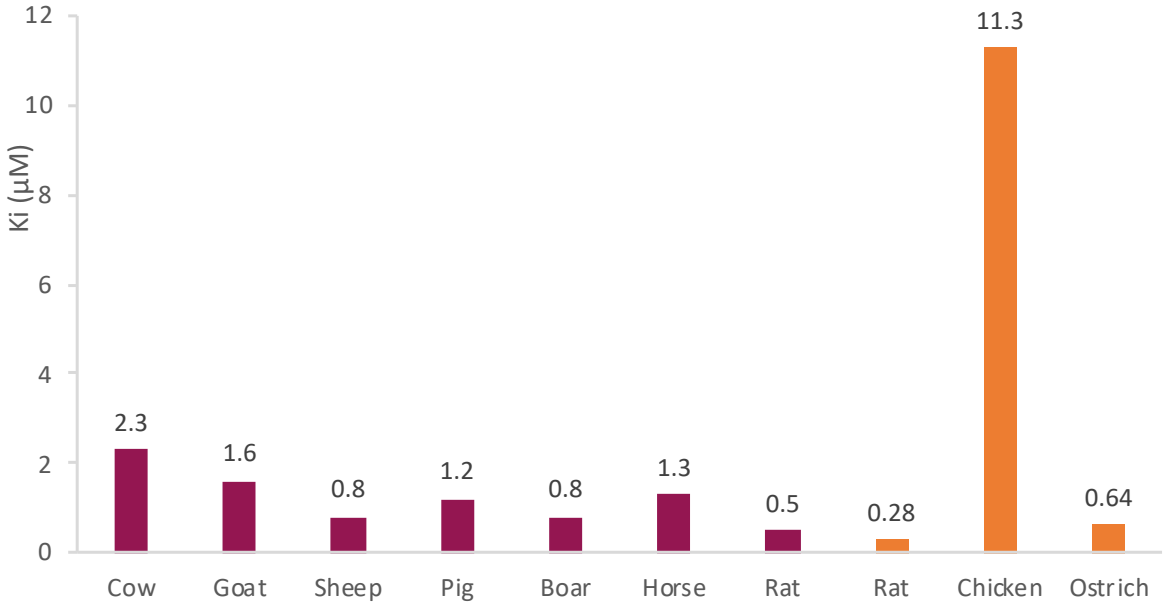


Figure 20: K_i values of domesticated animal and bird species VKORC1 for warfarin. (Adapted from Louvet *et al.,* 2015 and Wantanabe *et al.,* 2010). Pink denotes values from Louvet *et al.* (2015). Orange denotes values from Wantanabe *et al.* (2010).

The cow has the highest K_i value at 2.3 µM compared to other even-toed ungulates (sheep/pig/goat). There is a 4.6-fold difference between the cow and rat K_i values, suggesting cow is more resistant to warfarin compared to the rat. Compared to the rat K_i values all non-target mammals and birds are more resistant to warfarin (Figure 20). The concern with these studies is that the K_i values are actually for both VKORC1 and VKORC1L1 which are both found in the liver.

1.18 Non-target Poisoning

With the increased use of SGARs, there is an increased presence of the anticoagulant rodenticides in the environment (Vyas, 2017). Like non-anticoagulant rodenticides, FGARs and SGARs are not species specific and can have an impact in non-target organisms, humans and the environment (Health and Safety Executive, 2012).

There are two pathways by which non-target organisms can have contact with anticoagulant rodenticides which can contribute to or cause their death. The first pathway is called primary poisoning which is the direct consumption of bait (Health and Safety Executive, 2012). Direct consumption can occur when baits are not administered correctly, or if baits are left uncovered (Oppel *et al.,* 2016a). The second pathway is known as secondary poisoning and is a result of consumption of animals by predators that have been treated with anticoagulant rodenticides (Health and Safety Executive, 2012). There are many factors that can lead to secondary poisoning. SGARs in particular, have the ability to bioaccumulate inside an animal (Erickson and Urban, 2004). This poses a risk to predators as high concentrations of anticoagulant rodenticide can exist inside of prey animals (Sánchez-Barbudo *et al.,* 2012). This effect could be exaggerated if the predated animal (e.g. rat) is resistant to anticoagulant rodenticides. Survival of the resistant animal after ingestion of bait could also increase the activity of the animal during the day and have a higher risk of predation (Lefebvre *et al.*, 2017).

Physical symptoms are the most obvious signs of anticoagulant rodenticide poisoning. Symptoms of poisoning include; internal haemorrhaging in cadaver animals and bleeding, weakness and shortness of breath in live animals (Laakso *et al.,* 2010; Sheafor and Couto, 1999). The main site of action for anticoagulant rodenticides is the liver and accumulation of rodenticides in the liver allows for a useful postmortem tissue to test for anticoagulant rodenticide poisoning (Vudathala *et al.,* 2010). The blood of live animals also can be used to determine rodenticide levels (Vudathala *et al.,* 2010). Residue levels are compared with known LD_{50} values to determine whether doses are the cause of death for an animal (Godfrey, 1986). Animals found dead may contain anticoagulant rodenticide residues, but the cause of death may be attributed to another cause e.g. trauma, hunting or disease (Laakso *et al.,* 2010). Low levels of anticoagulant rodenticides can also cause the exposed animal to show

symptoms of weakness such as slower movements and may be at increased risk of accidents, predation or infection (Laasko *et al.,* 2010).

1.18.1 Effects of Anticoagulants on the Environment

Anticoagulant rodenticides are present in the environment due to the application of rodenticides in agriculture, urban areas, island pest eradications and in sewage systems (Gómez-Canela *et al.,* 2014). Anticoagulants (including rodenticides and human anticoagulant therapeutics) can reach sewage waters by the leeching of anticoagulant rodenticide baits or through excretion of urine by humans when administered as a drug (Gómez-Canela *et al.,* 2014). Sewage water enters waste water treatment plants (WWTP) or is released into river water. Sludge treatments in a WWTP allows for more lipophilic compounds to accumulate in the sludge and allows for the biodegradation of compounds. Other soluble compounds may be released as WWTP effluent unchanged into the environment exposing potential toxic compounds (Gómez-Canela *et al.,* 2014). Anticoagulants/drugs have been identified in the WWTP effluent but the risk to aquatic animals is low (Gómez-Canela *et al.,* 2014). However, these effluents need to be monitored to avoid a potential build up in the environment and the potential risk to non-target organisms.

Invasive rodent species introduced on island nations can have serious impacts on the native habitats (Witmer *et al.,* 2014). Rat eradication programs involve the total eradication of the entire population of rodent pests in a short period of time (Pitt *et al.,* 2015). One of the most effective means of distributing anticoagulant rodenticides on an island is by aerial broadcasting using a helicopter (Howald *et al.,* 2007). Aerial broadcasting is effective but exposed bait can have effects on the environment and non-target animals (Ogilvie *et al.,* 1997). D'Alessio *et al.* (2018) identifies the risk of leaching of three anticoagulant rodenticide compounds; diphacinone, chlophacinone and brodifacoum. These anticoagulants are most commonly used in aerial baiting (D'Alessio *et al.,* 2018). Soil samples from different Hawaii islands were used to determine the degradation rate of the anticoagulant rodenticides in the soil. Depending on the soil type, degradation values ranged from 27 to 248 days for diphacinone, 39 to 1000 days for chlorophacinone and 72 to 462 days for brodifacoum

(D'Alessio *et al.,* 2018). Despite the degradation values, it was concluded that there is a low risk of leaching in the Hawaii Islands (D'Alessio *et al.,* 2018).

There is a potential risk to oceans and water systems after aerial baiting or incidents involving anticoagulant rodenticides (Ogilvie *et al.,* 1997; Primus *et al.,* 2005). Primus *et al.* (2005) reported the detection of brodifacoum in tidal water after a spillage. The rodenticide showed significant levels 1 day after the initial incident but after 9 days very low levels of below 0.020 ppb were found. Seabed sediment was also tested for brodifacoum residues, again 1 day after the initial incident there were high levels of brodifacoum found but after 9 days low levels of 0.020 ppm and below were found (Primus *et al.,* 2005). This evidence suggests there could be an immediate risk to the aquatic environment after aerial baiting or incidents involving anticoagulant rodenticides.

1.18.2 Non-target Poisoning of Humans

Humans can be at risk of both primary and secondary poisoning of anticoagulant rodenticides. Exposure to anticoagulant rodenticides can be from accidental use, intentional use or from the misuse of these rodenticides. Unfortunately, the public have limited knowledge about the toxicity of anticoagulant rodenticides in humans and therefore misuse these anticoagulant rodenticides (Lin *et al.,* 2018).

Accidental exposure typically occurs in children with the ingestion of anticoagulant rodenticides (Chua and Friedenberg, 1998; Smolinske *et al.,* 1989). The bright colours of the bait may attract children (Yan *et al.,* 2016). Pest control operators and people responsible for providing pest control are also at risk of poisoning from anticoagulant rodenticides (Özdemir *et al.,* 2016). Özdemir *et al.* (2016) reports a 40 year old man with a hypochromic microcytic anemia consistent with chronic blood loss and unusually long prothrombin times. After blood and urine tests, high levels of a superwarfarin was found. The patient admitted exposure to anticoagulant rodenticides by not using necessary precautions whilst administering rodenticides. The repeated exposure via direct skin contact was the cause of the anticoagulant rodenticide poisoning (Özdemir *et al.,* 2016).

Compounds used as rodenticides have been used for committing suicide for over a century (Mowat, 1891). There have been many reports of intentional use of rodenticides for suicide (Chua and Freidenberg, 1998; Palmer *et al.,* 1999). Suicide by anticoagulant rodenticides may be under reported and studied as they are traditionally categorized generally under 'suicides by pesticides' (Lin *et al.,* 2018). Intentional poisoning using anticoagulant rodenticides has been also used to commit attempted murder (McCurdy, 1988).

Misuse of rodenticides can range from cases of Munchausen syndrome to use within the illegal drug industry. Munchausen syndrome is a rare factitious disorder causing pathological lying about physical or psychological symptoms to gain sympathy or attention (Prakash *et al.*, 2014). People suffering with Munchausen syndrome have been reported to use anticoagulant rodenticides to fabricate illness (Chua and Freidenberg, 1998). Chua and Freidenberg (1998) describe two patients with Munchausen syndrome. The first patient was admitted to hospital with multiple ecchymosis and hematuria. Brodifacoum was found in blood samples of the patient at a concentration of 79 ng/ml. When confronted the patient admitted taking brodifacoum (Chua and Freidenberg, 1998). The second patient was admitted to hospital due to bruising and a subungual hematoma. Brodifacoum was found in the patients' blood sample at a concentration of 310 ng/ml. After treatment with vitamin K_1 over 11 months the patient was suspected of continued consumption of brodifacoum (Chua and Freidenberg, 1998). Another example of the misuse of rodenticides is people with Munchausen syndrome by proxy (Babcock *et al.,* 1993). Munchausen syndrome by proxy is the intentional production of illness in another and is most common in parents fabricating a childs illness (Gehlawat *et al.,* 2015). This is seen as a serious form of child abuse (Gehlawat *et al.,* 2015). Babcock *et al.* (1993) describe a case of a 2 year old child who had developed bruising and had a prolonged prothrombin time after receiving multiple doses of brodifacoum added to his breakfast cereal by his mother (Babcock *et al.,* 1993).

"Lacing" of drugs with other compounds is common amongst drug abusers to prolong the effect of illicit drugs (Spahr *et al.,* 2007). Anticoagulant rodenticides have been reported as one of the compounds that are used to "lace" drugs to increase the bioavailability of the illicit drugs by blocking hepatic drug metabolism pathways which in turn enhances the euphoric

effects of the drug (Boettcher *et al.,* 2010). Brodifacoum is a common anticoagulant used in the lacing of drugs (La Rosa *et al.,* 1997; Panigrahi *et al.,* 2018). The first report of a 17 year old boy smoking marijuana mixed with brodifacoum was in 1997 (La Rosa *et al,* 1997). Spahr *et al.* (2007) reports a patient who was admitted to the hospital with severe coagulopathy, later admitting to using brodifacoum daily using six boxes in three months and concluded that if "lacing" was effective, direct ingestion would have a greater effect (Boettcher *et al.,* 2010). More recently, reports of brodifacoum use with synthetic marijuana (also known as; spice, K2) has led to severe coagulopathy in drug users (Panigrahi *et al.,* 2018).

Humans can be subjected to secondary poisoning of anticoagulant rodenticides. Secondary poisoning in humans can occur by the consumption of animals that have been subjected to anticoagulant rodenticide poisoning (Pitt *et al.,* 2011). Rodents can be problem for farmers and therefore anticoagulant rodenticides are used to control populations of rodent pests (Lund, 2015). Domestic animals such as pigs, cows, sheep and chickens have been reported with non-target poisoning from anticoagulant rodenticides (Guitart *et al.,* 2010). Care should therefore be taken to avoid consumption of these animals with potential exposure to anticoagulant rodenticides. In Hawaii, feral pigs are freely hunted and consumed as a staple food source where diphacinone is used throughout the island to control rodent pests (Pitt *et al.,* 2011). Rodenticide pellets are attractive to feral pigs and thereby pose a risk to hunters consuming contaminated pigs (Pitt *et al.,* 2011). Pitt *et al.* (2011) report on the effects of cooking pig tissue that has been exposed to diphacinone.

Any animal exposed to rodenticides that can be used for human consumption has the potential to cause secondary poisoning. In some parts of the world e.g. Cambodia, Philippines, Thailand, China and Vietnam, rodent meat is seen as a delicacy (Gruber, 2016). Consumption of rodent meat by humans may have secondary poisoning effects if the rodent meat was contaminated with anticoagulant rodenticides.

Incidents involving anticoagulant rodenticides can further transfer through the food chain for humans and other animals. In 2001, a road transport accident resulted in the release of around 20 tonnes of brodifacoum into the environment on the east coast of the South Island in New Zealand (Primus *et al.,* 2005). The area was a popular tourist spot but also a collection

point for marine invertebrates for human consumption. These included; shiny rock lobster, sea urchin and abalone (Primus *et al.,* 2005). Residues in the water began to decline after 9 days from the initial incident. However, it took 2 years and 7 months for the marine invertebrates to have brodifacoum residues suitable for human consumption (Primus *et al.,* 2005). According to the New Zealand food agency, brodifacoum levels of 0.001 ppm or below are considered acceptable for human consumption (Primus *et al.,* 2005).

The consumption of animal products may also be a cause of secondary poisoning in humans. Poultry are less susceptible to anticoagulant rodenticides compared with other animals (Erickson and Urban, 2004) however, exposure to anticoagulant rodenticides can pose a risk to humans due to the carryover of anticoagulant rodenticides inside the eggs of hens (Shimshoni *et al.,* 2013).

1.18.3 Non-target Poisoning of Birds

Birds (Aves) are regarded as the most diverse order of all the vertebrates with over 10,000 species of living birds. (Prum *et al.,* 2015). Most modern living birds are found under the infraclass, *Neognathae,* with the exception of flightless birds which are part of the *Palaeognathae* infraclass. Within *Neognathae* bird families can be subdivided into raptor and non-raptor birds. Raptors or 'birds of prey' belong to the *Falconiformes* and *Stringiformes* families (Tudge, 2000) and are predatory birds that prey on other bird species, small mammals, reptiles, insects and fish (Newton, 1979). All other families that belong to the *Neognathae* infraclass are regarded as non-raptor birds.

A literature search of the incidence of exposure or mortality to anticoagulant rodenticides in non-raptor and raptor birds was carried out and summarized in tables found in Appendix 1 and 2, respectively. A graphical representation of the reports of incidence of exposure or mortality to anticoagulant rodenticides in non-raptor and raptor birds found in Appendix 1 and 2 is shown in Figure 21 and 22, respectively. Non-target bird species poisoned due to anticoagulant rodenticides have been reported worldwide including in Europe (United Kingdom, France, Spain, Denmark and Finland), North America (United States of America and Canada), Africa (Seychelles) and Australasia (Australia, New Zealand and Mongolia) (Walker *et al.,* 2015; Berny *et al.,* 1997; Sánchez-Barbudo *et al.,* 2012; Christensen *et al.,* 2012; Koivisto

et al., 2018; Stone *et al.,* 1999; Howald *et al.,* 1999; Merton *et al.,* 2002; Lohr, 2018; Spurr *et al.,* 2005; Dolgormaa, 2004). For both non-raptor and raptor birds, the majority of reports reported mortality caused by non-target anticoagulant rodenticide poisoning which is mostly due to SGARs (Figure 21 and Figure 22). Brodifacoum is the most commonly identified anticoagulant rodenticide in non-raptor birds (Figure 21). Some studies report multiple rodenticides found within the liver of dead birds. Brodifacoum and difenacoum are the most common identified in non-raptor birds in Europe. Non-raptor birds can have a varied diet, with some birds that only eat fruits and seeds and other birds that have a diet of small mammals, insects and other birds (Vyas, 2017). This variety in diet allows the exposure to anticoagulants to be greater and increases the chances of primary and secondary poisoning (Vyas, 2017). In raptor birds, most birds reported had multiple rodenticides identified in the livers of the animals (Figure 22). In Scotland, there are reports of both exposure and mortality in red kites (Scottish Agricultural Science Agency, 2012). Brodifacoum is the most commonly identified cause of non-target poisoning in the United States whereas in the United Kingdom bromadiolone is the most common cause of death in raptor birds (Figure 22). Raptor birds, such as owls and hawks have a largely rodent-based diet and are therefore exposed to secondary poisoning via rodents that have consumed anticoagulant rodenticides. The general focus for monitoring for rodenticide exposure and effects on birds is on raptor bird species (Vyas, 2017; Lohr, 2018; Christensen *et al.,* 2012; Walker *et al.,* 2015). Whereas there are also reports of non-raptor birds subjected to non-target poisoning (Vyas, 2017).

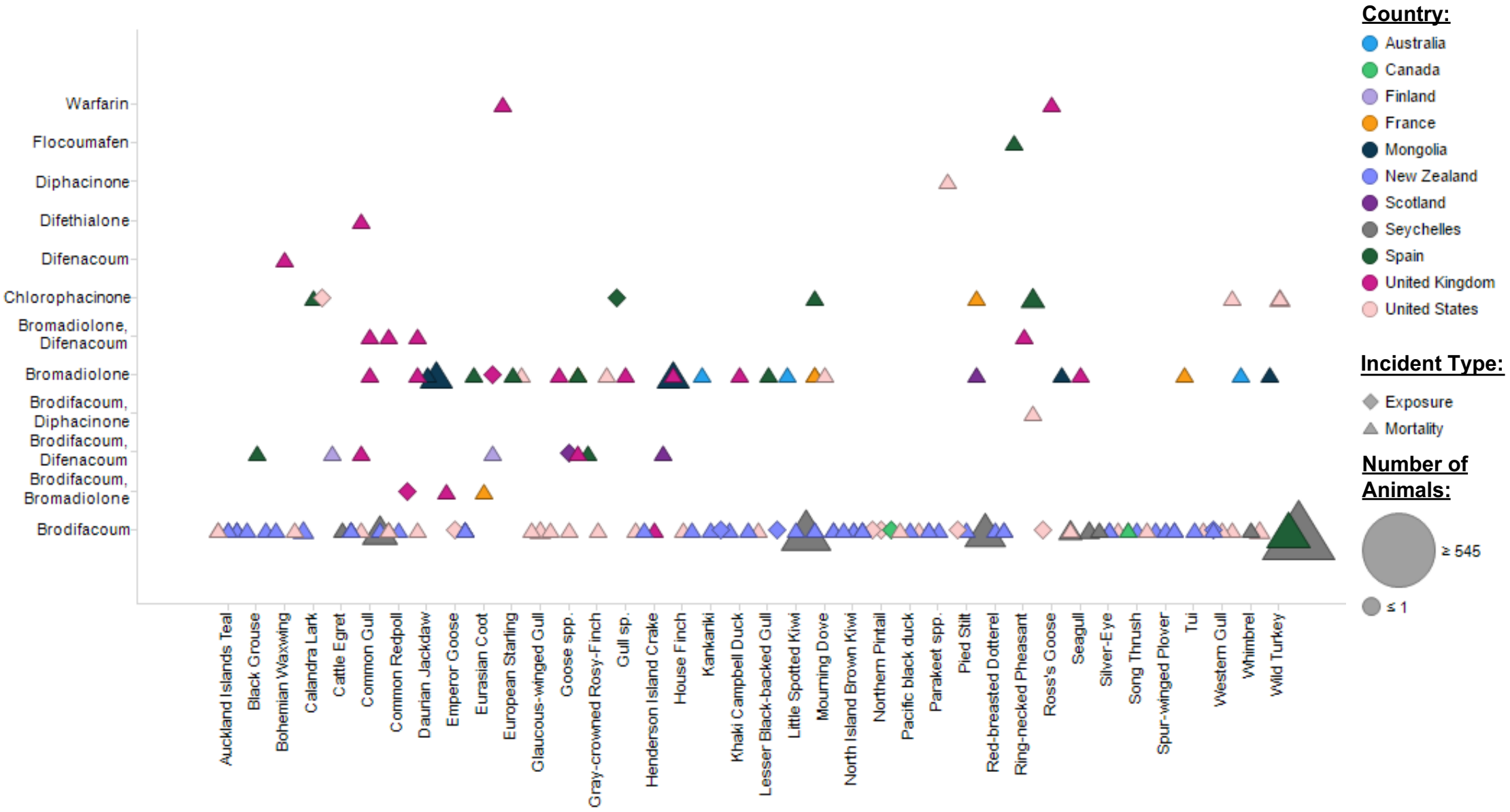


Figure 21: Reports of the incidence of exposure or mortality of non-target non-raptor birds by anticoagulant rodenticides in different countries throughout the world. (Data analysed by author using TIBCO Spotfire) Diamonds denote exposure to anticoagulant rodenticides. Triangles denote mortality by anticoagulant rodenticides. The size of the shapes is representative of the number of animals reported. Colours denote the different countries; Blue – Australia, Green – Canada, Lilac – Finland, Orange – France, Dark Blue – Mongolia, Purple – New Zealand, Dark Purple – Scotland, Grey – Seychelles, Dark Green – Spain, Pink – United Kingdom, Pale Pink – United States.

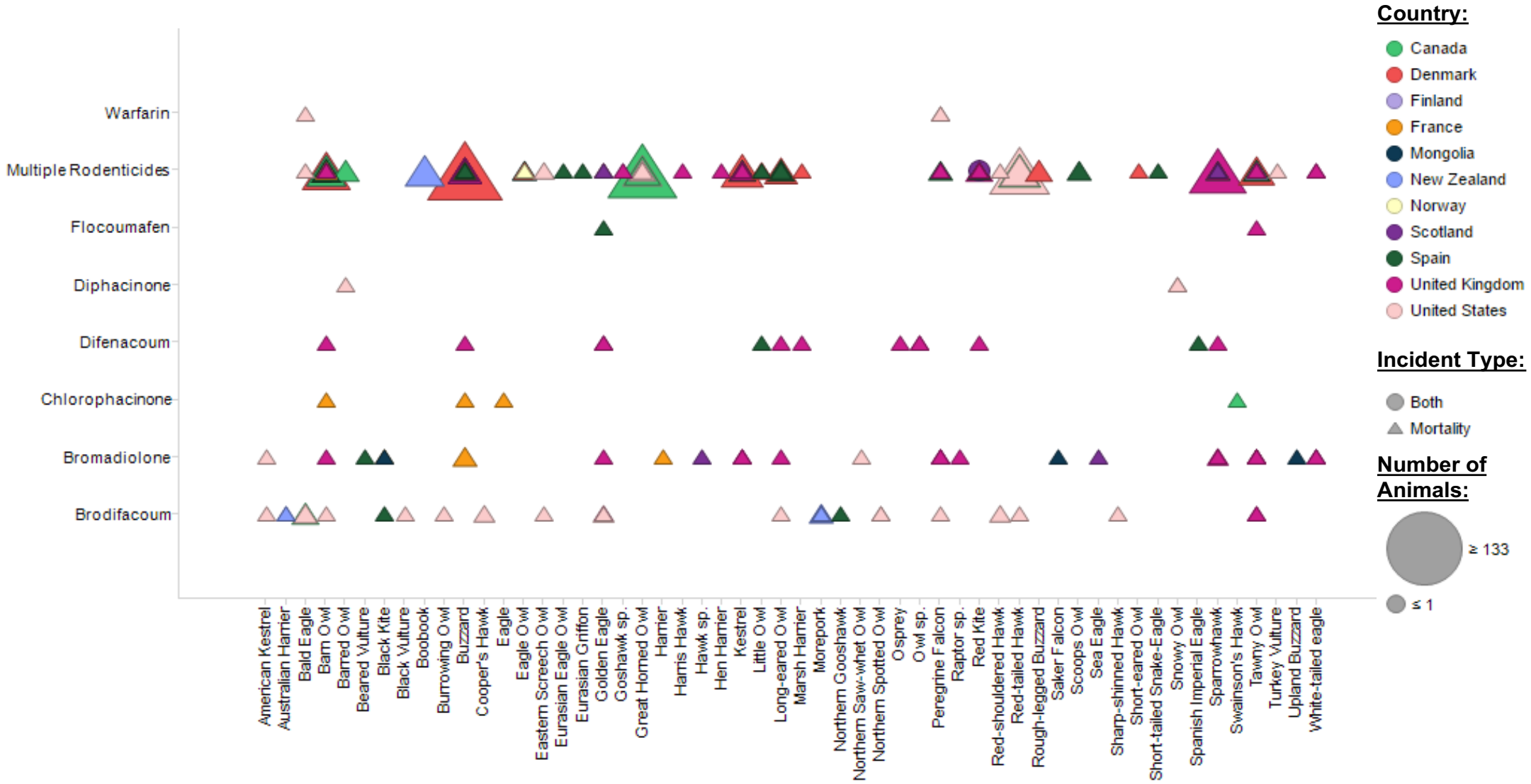


Figure 22: Reports of the incidence of exposure or mortality of non-target raptor birds by anticoagulant rodenticides in different countries throughout the world. (Data analysed by author using TIBCO Spotfire) Circles denote both exposure and mortality to anticoagulant rodenticides reported. Triangles denote mortality by anticoagulant rodenticides. The size of the shapes is representative of the number of animals reported. Colours denote the different countries; Green – Canada, Red – Denmark, Lilac – Finland, Orange – France, Dark Blue – Mongolia, Purple – New Zealand, Pale Yellow – Norway, Dark Purple – Scotland, Dark Green – Spain, Pink – United Kingdom, Pale Pink – United States.

1.18.4 Non-target Poisoning of Mammals

A literature search of the incidence of exposure or mortality to anticoagulant rodenticides in mammals was carried out and summarized in tables found in Appendix 3. A graphical representation of the reports of incidence of exposure or mortality to anticoagulant rodenticides in mammals found in Appendix 3 is shown in Figure 23. Non-target poisoning of anticoagulant rodenticides has been reported in mammals around the world including Europe (United Kingdom, France, Spain, Denmark and Finland), North America (United States of America and Canada), Africa (Seychelles) and Australasia (Australia, New Zealand and Mongolia) (Walker *et al.,* 2015; Berny *et al.,* 1997; Sánchez-Barbudo *et al.,* 2012; Christensen *et al.,* 2012; Koivisto *et al.,* 2018; Stone *et al.,* 1999; Howald *et al.,* 1999; Merton *et al.,* 2002; Lohr, 2018; Spurr *et al.,* 2005; Dolgormaa, 2004).

Non-target poisoning can affect a wide variety of mammals including both wild and domestic animals (Figure 23). Wild animals such as coyotes, mountain lions and foxes are largely at risk from secondary poisoning due to their diet of small mammals (Riley *et al.,* 2007; Erickson and Urban, 2004; Berny *et al.,* 1997). Domestic animals are also at risk from primary and secondary poisoning. Some studies have reported deaths related to anticoagulant rodenticide ingestion in pets such as dogs and cats but also in farm animals such as cows, pigs and sheep (Sánchez-Barbudo *et al.,* 2012; Koivisto *et al.,* 2018; Dolgormaa, 2004; Berny *et al.,* 1997; Taylor *et al.*, 2009). Most non-target mammals reported as cause of death by multiple rodenticides identified within the livers of the animals which may be the result of both primary and secondary poisoning in these animals (Figure 23). Bromadiolone and brodifacoum are the most common anticoagulant rodenticides identified as the cause of death in mammals. Brodifacoum is the most commonly identified cause of non-target poisoning of mammals in the United States and New Zealand. In New Zealand, there are a large number of animals reported with both exposure and mortality to diphacinone for example the New Zealand lesser short-tailed bats (Figure 23).

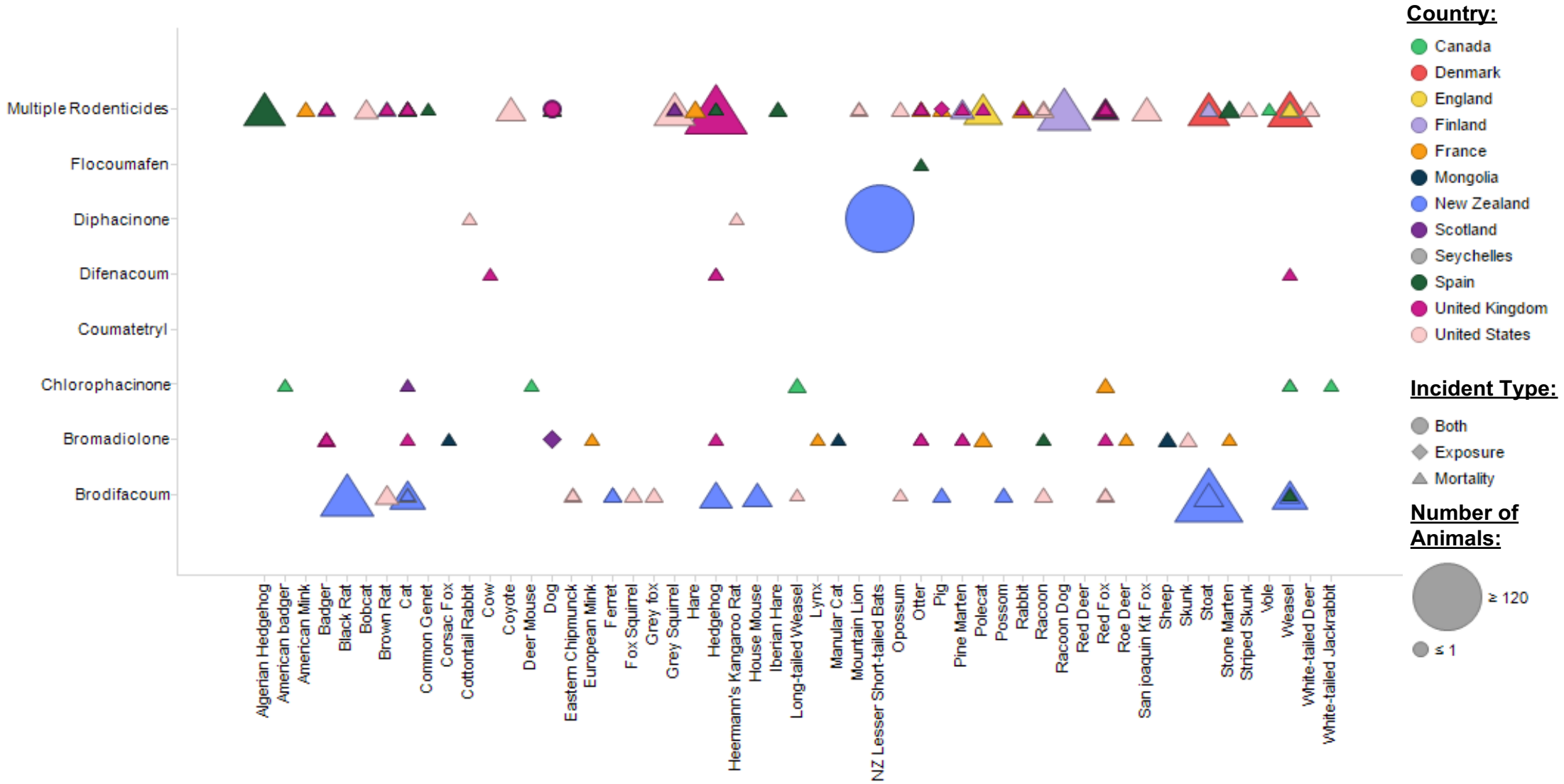


Figure 23: Reports of the incidence of exposure or mortality of non-target mammals by anticoagulant rodenticides in different countries throughout the world. (Data analysed by author using TIBCO Spotfire) Circles denote both exposure and mortality to anticoagulant rodenticides reported. Diamonds denote exposure to anticoagulant rodenticides. Triangles denote mortality by anticoagulant rodenticides. The size of the shapes is representative of the number of animals reported. Colours denote the different countries; Green – Canada, Red – Denmark, Yellow – England, Lilac – Finland, Orange – France, Dark Blue – Mongolia, Purple – New Zealand, Dark Purple – Scotland, Grey – Seychelles, Dark Green – Spain, Pink – United Kingdom, Pale Pink – United States.

1.18.5 Non-target Poisoning of Other Vertebrates

Reptiles and fish are the other vertebrate groups in which poisoning to anticoagulant rodenticides has been reported (Bettink, 2015; Sánchez-Barbudo *et al.,* 2012; Pitt *et al.,* 2015; Merton *et al.,* 2002; Rueda *et al.,* 2016). Generally, as a result of rat eradication programs on islands such as those in the Pacific, reptiles and fish are exposed to anticoagulant rodenticides (Pitt *et al.,* 2015).

Aerial baiting is usually the most effective means of dispersing anticoagulant rodenticides on islands and can cause problems to both reptiles and aquatic life. Exposed bait can be ingested by reptiles and cause primary poisoning. Although a study by Weir *et al.* (2015) showed that when a common lizard species (*Sceloporus occidentalis*) was fed 'neat' brodifacoum it was less susceptible to the rodenticide in comparison to birds and mammals and had an LD_{50} value of >1750 μg/g (Weir *et al.,* 2015). Due to the prolonged exposure of anticoagulants omnivorous lizards are at risk of both primary and secondary poisoning by anticoagulant rodenticides (Rueda *et al.,* 2016). As lizards are less susceptible to anticoagulant rodenticides, this could pose a threat to predatory bird species that ingest reptile species and thereby could contribute to secondary poisoning of birds (Rueda *et al.,* 2016).

There are 6 different reptile species reported to have been subjected to poisoning by anticoagulant rodenticides (Appendix 4). Brodifacoum is the most reported anticoagulant found in reptile species. One study reported a horseshoe whip snake with flocoumafen residues (Sánchez-Barbudo *et al.,* 2012).

Aerial baiting also has a significant drawback as the dispersal method cannot be entirely controlled where the bait lands. Therefore, bait could contaminate water ways including oceans. This exposure can therefore cause poisoning in non-target aquatic animals. Pitt *et al.* (2015) describe residues of brodifacoum found in fish species in United States including black spotted sergeant fish, mullet fish and puffer fish (Pitt *et al.,* 2015).

1.18.6 Non-target Poisoning of Invertebrates

Recent studies have shown that invertebrate species contain residues of anticoagulant rodenticides (e.g. Pitt *et al.,* 2015; Primus *et al.,* 2005). There are 15 reported invertebrates that have been subjected to non-target poisoning (Appendix 5). Invertebrates can be exposed to anticoagulant rodenticides through direct consumption or exposure to bait (Liu *et al.,* 2015). Controlling exposure of invertebrates to anticoagulant rodenticides is difficult due to the size of most invertebrates (e.g. ants, earthworms and snails), even if the bait has been administered correctly. These animals are small enough to enter bait boxes and feed on the bait. Invertebrates therefore can contribute to the secondary poisoning of birds, mammals and reptiles that feed on invertebrates.

1.19 Aims of the Project

The aims of the project are as follows:

i. To determine the current frequency and geographical distribution of VKORC1 resistance polymorphisms in wild *Rattus norvegicus* from UK and Sweden by sequencing the VKORC1 gene
ii. To identify mitochondrial genetic haplotypes in *Rattus norvegicus* from UK and Sweden and assess the relationship between these haplotypes and anticoagulant resistant populations. This will be achieved using DNA sequencing of the mitochondrial D loop sequence
iii. To determine the effects of anticoagulants on the *Rattus norvegicus* VKORs with novel polymorphisms found in aim (i) by heterologous expression of VKORC1 in insect cell system and use the VKORC1 HPLC assay for enzyme kinetic and inhibition studies.
iv. To determine the relationship between amino acid differences in evolutionary diverse VKORC1 and VKORC1L1 sequences by using multiple sequence alignments.
v. To determine the effect of anticoagulants on chosen VKORs expressed using the same heterologous expression system as used in (iii) and use the VKORC1 HPLC assay for enzyme kinetic and inhibition studies as a prediction system on their effects without the necessity for animal toxicity testing.

Chapter 2: Materials and Methods

2.0.1 Materials

All chemicals and reagents were AnalaR grade and purchased from Fisher and Sigma unless otherwise stated.

2.0.2 Bacterial Strains

The *Escherichia coli* (*E. coli*) strains used during this project were; *DH5α* provided by the University of Huddersfield and *DH10 Bac* provided by Dr. Christopher Cooper, University of Huddersfield and the *XL-10 Gold* strain was purchased from Agilent.

2.0.3 Insect Cell Culture Cell Line

The *Spodoptera frugiperda* (*Sf9*) cell line was used for insect cell culture. These were provided by Dr. Christopher Cooper, University of Huddersfield.

2.0.4 Animal Samples

Rodent tail samples were collected by pest control organisations from different geographical locations of the United Kingdom. Animals were caught by trapping and the tail tip of the dead rat was excised and sent in vials that contained 70% v/v ethanol. Once received, samples were frozen and stored at -80 °C. Rat liver was provided by Dr. Dougie Clarke, University of Huddersfield.

2.0.5 Plasmid Constructs

The VKORC1 cDNA of *Rattus norvegicus* (AY423047.1), *Homo sapiens* (BC002911.2), *Bos taurus* (AY682746.1) and *Python bivittatus* (XM_007437549.1) was synthesised and incorporated into the pET-32a vector by Dundee Cell Products.

The pFB-LIC-Bse vector was provided by Dr. Christopher Cooper, University of Huddersfield.

2.1 DNA Analysis

2.1.1 DNA Extraction

A Qiagen DNeasy Blood and Tissue Kit was used to extract the DNA from the rat tail samples. Between 0.4-0.6 cm of the rat tail was excised and placed into a microcentrifuge tube. 180 µl of Buffer ATL and 20 µl of proteinase K was added to the tissue sample. The samples were vortexed and incubated at 56 °C at 150 rpm in a shaking incubator overnight to allow lysis to occur. After incubation, samples were vortexed for 15 seconds after which, 200 µl of Buffer AL was added and mixed thoroughly by vortexing. 200 µl of 100% v/v ethanol was then added to the sample and vortexed. The mixture was pipetted into a DNeasy mini spin column placed in a 2 ml collection tube and centrifuged for 1 minute at 6000 xg. The flow-through and collection tubes were discarded and the spin column was placed into a clean 2 ml collection tube. 500 µl of Buffer AW1 was added to the samples and centrifuged for 1 minute at 6000 xg. The flow through and collection tubes were discarded and the spin column was placed into a clean 2 ml collection tube. 500 µl of Buffer AW2 was added to the tube and centrifuged for 3 minutes at 20000 xg. The flow-through and collection tubes were discarded and the spin column was placed into a clean 2 ml collection tube. The DNA was eluted with the addition of 200 µl of Buffer AE. The samples were incubated at room temperature for 1 minute and then centrifuged for 1 minute at 6000 xg. The extracted DNA was stored at -20 °C.

2.1.2 Polymerase Chain Reaction (PCR)

All reagents and DNA extracts were kept on ice. A PCR master mix for 1 sample was produced following the volumes in Table 15. The forward and reverse primers for VKORC1 exon 1, 2 and 3 and the mitochondrial D loop primers are shown in Table 16.

PCR Reagent	Volume Added to Master Mix (µl)	Concentration
Peqlab 5X Enhancer Solution P	6	-
Peqlab 10X reaction Buffer Y	3	-
Peqlab peqGOLD dNTP-Mix	0.6	10 mM
Eurofins MWG Operon Forward Primer	0.3	10 pmol/µl
Eurofins MWG Operon Reverse Primer	0.3	10 pmol/µl
Peqlab Taq-DNA-Polymerase	0.3	5 µg/µl
Autoclaved Deionised Water	16	-
Total:	26.5	-

Table 15: The volume and concentration of PCR reagents required to produce a PCR master mix.

DNA Template	Forward Primer	Reverse Primer
VKORC1 Exon 1	5'-GTGGCGGGTTCTTCCCTC-3'	5'-GACTCCAAAATCATCTGGCAACC-3'
VKORC1 Exon 2	5'-AAGAGTAGGGGACAAGGTGGC-3'	5'-GGGTCACCAAGACATGAGGTG-3'
VKORC1 Exon 3	5'-GGAGGTGTTACAGAGTTCCAGG-3'	5'-ACACTTGGGCAAGGCTCATGTG-3'
Mitochondrial D loop	5'-TCAGGACAATCAAGAAGAAGGA-3'	5'-TGAGGGTAGGCAAGTAAAGAGG-3'

Table 16: Forward and reverse primer sequences for exons 1, 2 and 3 of the VKORC1 gene. Both forward and reverse for exon 1 and 2 and reverse for exon 3, designed by Grandemange *et al.* (2010). Exon 3 forward was designed by GeneJockey Software. Mitochondrial D loop primers were designed by Song *et al.* (2014).

26.5 µl of the PCR master mix was pipetted into each 0.2 ml PCR tube. 3.5 µl of the DNA sample (~50 ng) was pipetted into the corresponding PCR tube giving a total volume of 30 µl. The tubes were centrifuged in a mini-centrifuge (VWR Mini Star Silverline Centrifuge) for 30 seconds. The tubes were then placed into the Bio-rad C1000 Touch Thermal Cycler. The following sections 2.1.2.1, 2.1.2.2, 2.1.2.3 and 2.1.2.4 describe the PCR programmes used for each exon.

2.1.2.1 Exon 1 PCR Programme

Amplification of exon 1 was achieved by using the following programme; 94 °C for 3 minutes, 10 cycles of 94 °C for 30 s, a touchdown from 63 °C to 60 °C (with 0.2 °C steps) for 30 s, and 72 °C for 1 minute, then 30 cycles of 94 °C for 30 s, 60 °C for 30s and 72 °C for 1 minute, and a final extension of 72 °C for 10 minutes (Grandemange *et al.,* 2010).

2.1.2.2 Exon 2 PCR Programme

Amplification was achieved at 94 °C for 3 minutes, 12 cycles of 94 °C for 30 s, 67 °C for 45 s and 72 °C for 1 minute, then 31 cycles of 94 °C for 30 s, 64 °C for 45 s and 72 °C for 1 minute, and a final extension of 72 °C for 10 minutes (Grandemange *et al.,* 2010).

2.1.2.3 Exon 3 PCR Programme

The PCR programme used was an initial temperature of 95 °C for 2 minutes and 30 s, followed by 40 cycles of 95 °C for 30 s, a touchdown from 65 °C (with 0.3 °C steps) to 53 °C and 72 °C for 1 minute 10 s and a final extension of 72 °C for 5 minutes.

2.1.2.4 Mitochondrial D Loop PCR Programme

The PCR programme used was an initial temperature of 94 °C for 2 minutes, followed by 30 cycles of 94 °C for 30 seconds, 56 °C for 30 seconds, and 72 °C for 1 minute and a final extension of 72 °C for 5 minutes (Song *et al.,* 2014).

2.1.3 Agarose Gel Electrophoresis

2.2% w/v agarose gels were used. The gels were made by the combination of 0.88 g of agarose and 40 ml of 0.5X TBE. This was then melted to a clear liquid. 3 µl of Peqlab peqGREEN DNA/RNA dye was added to stain the gel for visualisation of the DNA on the gel. The gels were left to set for a minimum of 20 minutes at room temperature. 5 µl of the PCR samples were mixed with 1 µl of Peqlab Blue Loading Buffer 6X and a total of 5 µl of the mixture was loaded into the wells of the agarose gel. One well contained a Peqlab peqGOLD 100 bp DNA Ladder. 1 µl of the DNA ladder was mixed with 2 µl of Peqlab Blue Loading Buffer 6X and 3 µl of autoclaved deionised water; the total volume was added to the well. The DNA was electrophoresed for 30 minutes at 200 A and 100 V. The gel was visualised using ultraviolet (UV) light (312 nm) and photographed.

2.1.4 PCR Purification

A Qiagen QIAquick PCR Purification Kit was used for PCR purification. All centrifugation steps were at 13000 rpm. 5 volumes of Buffer PB were added to 1 volume of the PCR reaction and were mixed by vortexing. The total volume from the PCR tube was pipetted into a QIAquick column in a provided 2 ml collection tube. The DNA was bound to the column by 1 minute of centrifugation. The flow-through was discarded and the spin column was placed into the same collection tube. 750 µl of Buffer PE was added to the column and centrifuged for 1 minute. The flow-through was discarded and the spin column was placed in the same collection tube. The spin column was centrifuged for 1 minute to remove residual wash buffer. The flow-through and collection tube was discarded and the spin column was placed in a clean 2 ml collection tube. The DNA was eluted by adding 50 µl of Buffer EB to the column and centrifuged for 1 minute. 15 µl of the purified DNA was placed in a microcentrifuge tube with 2 µl of primer (100 µM) used in the PCR reaction. This was then sent to Eurofins Genomics for sequencing. The remaining purified DNA stock was stored at -80 °C.

2.2 Growth Medium for *E. coli* Strains

2.2.1 Luria Broth (LB) Media

For all bacteria except for the *E.* coli DH10 Bac strain, LB media was prepared by the addition of 12.5 g of LB to 500 ml of distilled water. This was autoclaved and stored at 4 °C. To culture the *E. coli DH10 Bac* strain, LB media was prepared by the addition of 25 g of LB to 500 ml of distilled water. This was autoclaved and stored at 4 °C.

2.2.2 NYZ^+ Broth - *E. coli* XL10-Gold

For site directed mutagenesis, NYZ^+ Broth was prepared by the addition of 10 g of NZ amine (casein hydrolysate) with 5 g of yeast extract and 5 g of NaCl to 1 litre of deionized water adjusted to pH 7.5. This was autoclaved and the following filter-sterilised supplements were added; 12.5 ml of 1 M $MgCl_2$, 12.5 ml of 1 M $MgSO_4$ and 20 ml of 20% (w/v) glucose.

2.2.2 LB Agar (LB Plates)

For all bacterial strains, the LB plates were prepared by dissolving 12.5 g of LB and 10 g of agar in 500 ml of distilled water. This was autoclaved and cooled to 50 °C before pouring the plates. Selectable and visible markers were added according to the specific experiment (Section 2.2.3).

2.2.3 Selectable and Visible Markers

Selectable and visible markers were added to the bacterial LB growth media to identify and select the correct strains of *E. coli* that had been transformed with vectors containing selectable or visible markers (Table 17).

Selective Marker	Working Concentration (mg/ml)	Final Concentration (μg/ml)	Solvent used to dissolve antibiotic	Plasmid/*E.coli* cells
Ampicillin	50	50	Deionised water	pET-32a, pFB-LIC-Bse
Kanamycin	50	50	Deionised water	*E.coli* DH10 Bac
Tetracycline	5	10	100% (v/v) ethanol	*E. coli* DH10 Bac
Gentamicin	7	7	Deionised water	*E. coli* DH10 Bac
IPTG	40	40	Deionised water	*E. coli* DH10 Bac
X-gal	20	200	100% (v/v) DMSO	*E. coli* DH10 Bac
Sucrose	25% (w/v)	2.5% (w/v)	Deionised water	pFB-LIC-Bse

Table 17: Selective or visible markers used to identify and select for *E. coli* strains and transformed vectors.

2.2.4 Storage of *E. coli* – Glycerol Stocks

333 μl of 60% v/v of filter-sterilised glycerol was mixed by gentle inversion to 1 ml of overnight culture of *E. coli* (OD_{600}: 0.4-1) and stored at -80 °C.

2.3 Preparation of Competent *E. coli* Cells Using Calcium Chloride

This method was adapted from Sambrook and Russell (2001). A single bacterial colony (2-3 mm in diameter) was taken from a plate that was incubated for 16-20 hours at 37 °C and used to inoculate 5 ml of LB culture medium and was placed in a shaking incubator overnight at 37 °C at 180 rpm. 1 ml of pre-culture was added to 50 ml of LB medium and grown at 37 °C at 180 rpm in a shaking incubator to an OD_{600} of 0.4-0.6. When the *E. coli* reached the correct OD_{600}, the bacterial cells were transferred to a sterile ice cold 50 ml centrifuge tube. The cultures were cooled to 0 °C by placing on ice for 10 minutes. The cells were recovered by centrifugation at 2500 rpm for 15 minutes at 4 °C. The supernatant was decanted, and the pellets were resuspended gently in 30 ml of ice cold 80 mM $MgCl_2$ – 20 mM $CaCl_2$. The cells were centrifuged at 2500 rpm for 15 minutes at 4°C. The supernatant was decanted, and the pellets were resuspended by gently vortexing in 2 ml of ice cold 0.1 mM $CaCl_2$ for each 50 ml

of original culture. The cells were then used directly for transformation (Section 2.4) or frozen in liquid nitrogen at -80 °C (Section 2.3.1).

2.3.1 Freezing Competent Cells

This method was adapted from Sambrook and Russell (2001). 140 µl of DMSO was added to 4 ml of resuspended cells. The solution was mixed gently by swirling and stored on ice for 15 minutes. A further 140 µl of DMSO was added to each suspension and gently mixed by swirling and stored on ice. The solution was aliquoted into 200 µl volumes and flash frozen in liquid nitrogen. The aliquots were stored at -80 °C.

2.4 Transformation of Recombinant Plasmids into *E. coli* Strains

This method is adapted from Sambrook and Russell (2001). 50 ng of plasmid in 10 µl was added to 200 µl of competent *E. coli* cells and left on ice for 30 minutes. The cells were heat shocked at 42 °C in a water bath for 45 seconds and then placed immediately on ice for 2 minutes. The newly transformed cells were added to 3 ml of LB media with no antibiotics and left in the shaking incubator for 1 hour at 37 °C at 180 rpm. 100 µl of each transformation in the LB was placed onto an LB agar plate (with appropriate selectable or visible marker) and incubated overnight at 37 °C.

2.5 Plasmid Miniprep

To purify plasmid DNA the *Bioline Isolate II Plasmid Mini Kit* was used. A single colony was used to inoculate 5 ml of LB with appropriate selective markers and incubated for 16 hours to an OD_{600} of 0.4 to 0.6 in a shaking incubator at 37 °C at 180 rpm. The bacterial cells were harvested by centrifugation at 2500 rpm for 20 minutes at 4 °C. The supernatant was discarded. 250 µl of Resuspension Buffer P1 was added and used to resuspend the cell pellet. The cell pellet was completely resuspended by gentle vortexing to ensure there was no remaining cell clumps. The solution was transferred into a 1.5 ml microcentrifuge tube. 250 µl of Lysis Buffer P2 was added and mixed gently by inverting the tubes up and down 6 to 8 times. The mixture was incubated at room temperature for 5 minutes or until the lysate appeared clear. 300 µl of Neutralisation Buffer P3 was added and mixed thoroughly by

inverting the tube 6-8 times. The mixture was centrifuged for 5 minutes at 11000 xg at room temperature. This step was repeated if the supernatant was not clear. For each preparation, one ISOLATE II Plasmid Mini Spin Column was placed into a collection tube and a maximum of 750 μl of clarified sample supernatant was pipetted into the column. The column containing the sample was centrifuged for 1 minute at 11000 xg and the flow through was discarded. This was repeated with any remaining clarified sample. 500 μl of Wash Buffer PW1 which was pre-heated to 50 °C was added and the column was centrifuged for 1 minute at 11000 xg. 600 μl of Wash Buffer PW2 was added and then centrifuged for 1 minute at 11000 xg. The flow through was discarded. The column was centrifuged again for 2 minutes at 11000 xg to remove any remaining ethanol. The spin column was placed into a clean collection tube and 50 μl of Elution Buffer P was added directly onto the silica membrane on the column and incubated at room temperature for 1 minute before centrifugation at 11000 xg for 1 minute. The purified plasmid DNA was stored at -20 °C.

2.6 Ligation Independent Cloning (LIC) of Gene of Interest into a Desired Plasmid

The LIC was performed using Savitsky *et al.* (2010) following the schematic diagram in Figure 24.

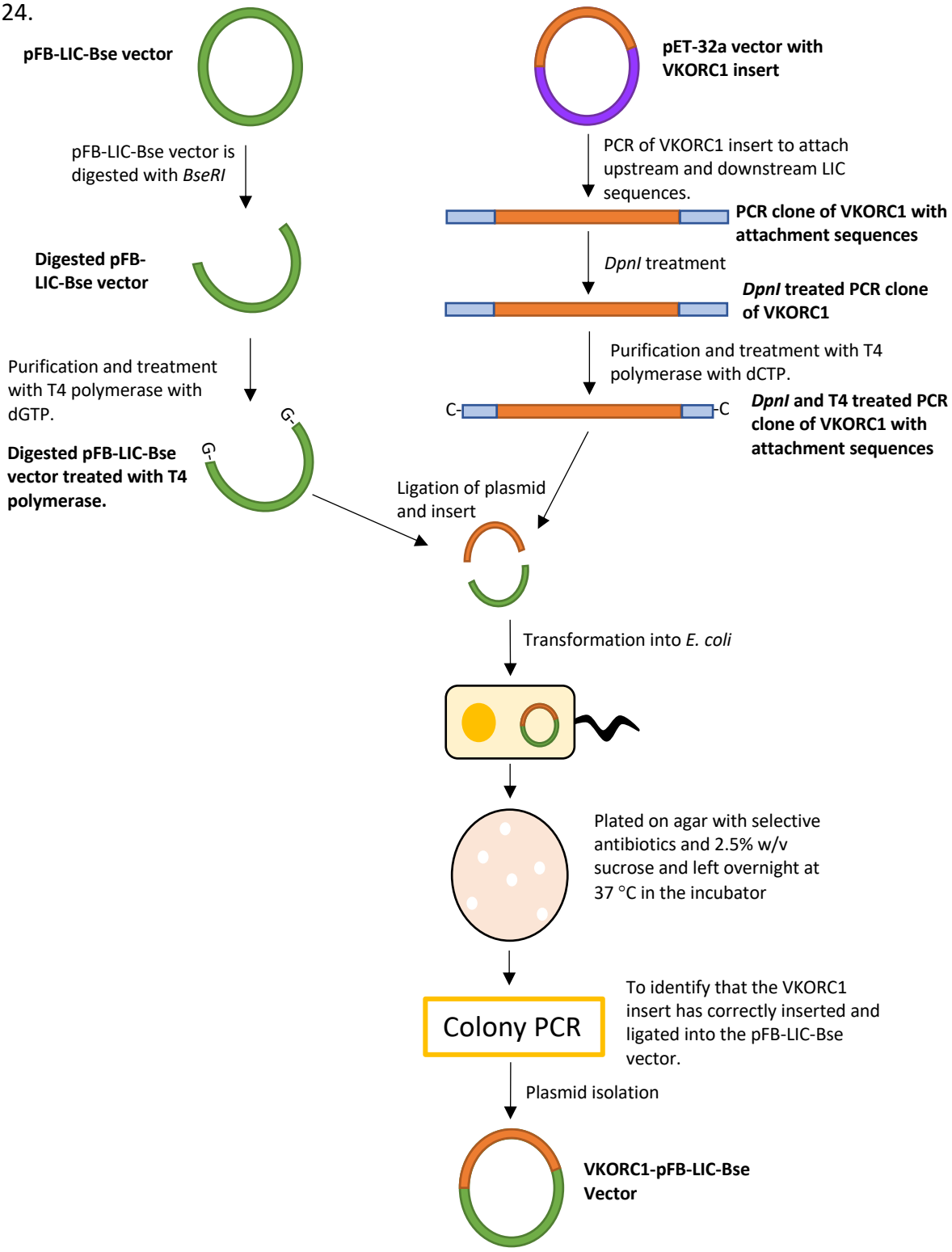


Figure 24: Workflow of ligation independent cloning of VKORC1 into the pFB-LIC-Bse Vector. (Created by Author, based on Savitsky *et al.,* 2010). Green denotes pFB-LIC-Bse vector. Orange denotes VKORC1 gene insert. Purple denotes the pET-32a vector. Blue attachment sequences allow for the cloning of the VKORC1 insert.

2.6.1 PCR Primers for LIC

PCR primers were designed for each VKORC1-pET32a construct with specific upstream and downstream primer sequences to clone the individual VKORC1 insert only without any vector sequence being added (Table 18).

Primer	Primer Sequence
LIC5'(ATG)RatN	5'-TACTTCCAATCCATGGGCACCACCTGGAGGAGC-3'
LIC3'(TERM)RatN	5'-TATCCACCTTTACTGTCAGGGCTTTTTGACCTTGTG-3'
LIC5'(ATG)Human	5'-TACTTCCAATCCATGGGCAGCACCTGGGGGAGC-3'
LIC3'(TERM)Human	5'-TATCCACCTTTACTGTCAGTGCCTCTTAGCCTTGCC-3'
LIC5'(ATG)Cow	5'-TACTTCCAATCCATGGGCGCTACCTGGCGGAGT-3'
LIC3'(TERM)Cow	5'-TATCCACCTTTACTGTCAGTGCCCCTTGACCTTGCC-3'
LIC5'(ATG)Python	5'-TACTTCCAATCCATGACGGTGCCCAGGTGGGAG-3'
LIC3'(TERM)Python	5'-TATCCACCTTTACTGTCAGTGCCTCTTGGCTTTCGT-3'

Table 18: PCR Primers with specific upstream and downstream sequences used to amplify VKORC1 from the pET-32a plasmid. Red highlighted sequence is the upstream and downstream sequence added to the PCR primers to amplify the VKORC1 construct. Black denotes the VKORC1 gene. TERM denotes the termination codon which is underlined in the primer sequence.

2.6.2 PCR of VKORC1 from the pET32a Vector

PCR was used to amplify the gene of interest (GOI), VKORC1 from the pET-32a vector. All reagents and DNA extracts were kept on ice throughout. Table 19 shows the volume of reagent and concentration required for a master mix for one sample.

PCR Reagent	Volume of reagent (µl)	Concentration
NEB Phusion HF Buffer (5x)	5	-
Peqlab peqGOLD dNTP-Mix	0.5	10 mM
NEB Phusion Polymerase	0.25	2 units/µl
Sigma Molecular Biology Water	11.75	-
Eurofins MWG Operon Forward Primer	2.5	5 µM
Eurofins MWG Operon Reverse Primer	2.5	5 µM
Extracted DNA	2.5	50 ng
Total:	25	-

Table 19: Volume and concentration of PCR reagents required for a one sample master mix.

17.5 µl of master mix was added to each PCR tube and the specific primers and VKORC1-pET32a construct was added separately. The thermocycler conditions were; 95 °C for 10 minutes, then 5 cycles of 95 °C for 30 seconds, 68 °C for 30 seconds and 72 °C for 1 minute, followed by 5 cycles of 95 °C for 30 seconds, 60 °C for 30 seconds and 72 °C for 1 minute, then 5 cycles of 95 °C for 30 seconds, 55 °C for 30 seconds and 72 °C for 1 minute, followed by 10 cycles of 95 °C for 30 seconds, 50 °C for 30 seconds and 72 °C for 1 minute with a final extension time of 10 minutes at 72 °C. 5 µl of PCR product with 1 µl of loading dye was run on a 2.2% w/v agarose gel (refer to Section 2.1.3).

2.6.3 *DpnI* treatment of PCR Product

DpnI treatment of the PCR products allows the degradation of the parent PCR template. *DpnI* targets methylated DNA and degrades this. In this case the original plasmid will be methylated and therefore will be degraded. The *DpnI* was diluted by 1 in 20 in NEB 2.1 Buffer. 1 µl of diluted *DpnI* enzyme was added 25 µl of the PCR product made in Section 2.6.2 and incubated in a thermocycler for 1 hour at 37 °C, then at 88 °C for 20 minutes to denature the *DpnI* enzyme. After treatment with *DpnI*, the PCR products were purified using the QIAquick PCR Purification Kit (Qiagen) (Section 2.1.4).

2.6.4 T4 Polymerase Treatment of Purified PCR Products

Table 20 shows the reagents and volumes required for T4 treatment of the purified PCR product.

Reagent	Volume Added (µl)
Purified PCR Product	5
Sterile Water	2.25
10X NEB Buffer 2.1	1
25 mM dCTP	0.5
100 mM DTT	0.5
NEB T4 DNA Polymerase	0.25

Table 20: Volumes of reagents required for T4 polymerase treatment of purified PCR product.

After the addition of the reagents required for T4 treatment of the purified PCR product, the PCR tube was incubated in a thermocycler for 30 minutes at 22 °C followed by 20 minutes at 75 °C.

2.6.5 Vector Digestion of pFB-LIC-Bse plasmid with *BseRI*

5 µg of plasmid was added to 10 µl of NEB Cutsmart Buffer and 3 µl of *BseRI*. The volume is adjusted to 100 µl with water. The mixture was incubated overnight at 37 °C in a heating block. 1.5 µl of *BseRI* was added and 5 µl of Cutsmart buffer and further digested for 3 hours. The digestion was checked on a 0.8% (w/v) agarose gel (refer to Section 2.1.3). The digested plasmid was purified using the QIAquick PCR Purification Kit (Qiagen) (Section 2.1.4).

2.6.6 T4 Polymerase Treatment of Purified Digested Vector

Table 21 shows the reagents and volumes required for T4 treatment of the purified *BseRI*-digested vector.

Reagent	Volume Added (μl)
Purified *BseRI*-digested Vector	50
Sterile Water	22.5
10X NEB Buffer 2.1	10
25 mM dGTP	10
100 mM DTT	5
NEB T4 DNA Polymerase	2.5

Table 21: Volumes of reagents required for T4 polymerase treatment of purified PCR product.

After the addition of the reagents required for T4 treatment of the purified PCR product, the PCR tube was incubated in a thermocycler for 30 minutes at 22 °C followed by 20 minutes at 75 °C.

2.6.7 Ligation of T4 Treated PCR Product and T4 Treated Digested Plasmid

0.02 pmol of insert DNA and 25-50 ng of digested plasmid was mixed together. The mixture was incubated for 5 minutes at 22 °C in a heating block. 1 μl of 25 mM EDTA was added and mixed gently by stirring the solution with the pipette tip. The mixture was incubated for a further 5 minutes at 22 °C in a heating block. The newly ligated plasmid and PCR product were transformed into *E. coli* DH5α strain as described in Section 2.4 and cultured on LB agar.

2.6.8 Colony PCR of Ligated VKORC1 insert and pFB-LIC-Bse Vector

To identify that the VKORC1 insert has correctly ligated with the pFB-LIC-Bse vector, one colony from the transformants on the LB agar plates was taken and used to inoculate 5 ml of LB with appropriate antibiotics and incubated overnight at 37 °C at 180 rpm in a shaking incubator. Table 22 shows the volume of reagent and concentration required for a master mix for one sample.

PCR Reagent	Volume of reagent (µl)	Concentration
Peqlab 5X Enhancer Solution P	6	-
Peqlab 10X Reaction Buffer Y	3	-
Peqlab peqGOLD dNTP-Mix	0.6	10 mM
Eurofins MWG Operon Forward Primer (FBAC1 – 5'-TATTCATACCGTCCCACCA-3')	1.5	5 µM
Eurofins MWG Operon Reverse Primer (FBAC2 – 5'-GGGAGGTTTTTTAAAGCAAGTAAA-3')	1.5	5 µM
DMSO (100%)	0.9	-
Glycerol (60%)	1.5	-
Peqlab Taq-DNA-Polymerase	0.3	5 µg/µl
Sigma Molecular Biology Water	15.3	-

Table 22: Volume and concentration of PCR reagents required for a one sample master mix.

One colony from the transformants on the LB agar plate was added to the tube. The thermocycler conditions were as follows; 94 °C for 10 minutes, then 30 cycles of 94 °C for 30 seconds, 50 °C for 30 seconds and 72 °C for 1 minute with a final 5 minutes at 72°C. 5 µl of PCR product with 1 µl of loading dye was run on a 2.2% w/v agarose gel (refer to Section 2.1.3). A DNA band of around ~700 base pairs (bp) were identified as colonies that contained the newly ligated vector.

1 ml of the pre-culture grown overnight was made into a glycerol stock (Section 2.2.4). The remaining culture was centrifuged at 2500 rpm at 4 °C for 20 minutes. The supernatant was discarded, and the pellet was frozen at -80 °C or used immediately for a plasmid miniprep assay (Section 2.5).

2.7 Site Directed Mutagenesis of VKORC1 Constructs

2.7.1 Mutant Strand Synthesis Reaction

The *Agilent QuikChange Lightning Site-Directed Mutagenesis Kit* was used to mutagenise the ligated VKORC1 pFB-LIC-Bse constructs to substitute an arginine for a glycine at position 40 and also to mutate a leucine to a glutamine at position 120. PCR primers were designed for the rat VKORC1-pFB-LIC-Bse construct which were complementary to the desired mutation (Table 23).

Primer	Primer Sequence
SDM-R40G-RatF	5'-ATGAGGATTACGGCGCGCTCTGC-3'
SDM-R40G-RatR	5'-GCAGAGCGCGCCGTAATCCTCAT-3'
SDM-L120Q-RatF	5'-GTTCTCTGTACCAGGCCTGGATCC-3'
SDM-L120Q-RatR	5'-GGATCCAGGCCTGGTACAGAGAAC-3'

Table 23: PCR Primers with specific upstream and downstream sequences used to amplify VKORC1 from the pFB-LIC-Bse plasmid for site directed mutagenesis.

The sample preparation was prepared for mutagenesis as shown in Table 24.

PCR Reagent	p.L120Q (50 ng of plasmid)		p.R40G (50 ng of plasmid)	
	Volume of reagent (µl)	Concentration	Volume of reagent (µl)	Concentration
10x Reaction Buffer	5	-	5	-
DNA Template	3.84	50 ng/µl	3.84	50 ng/µl
Forward Primer	1.5	10 pmol/µl	1.33	10 pmol/µl
Reverse Primer	1.31	10 pmol/µl	1.5	10 pmol/µl
dNTP mix	1	-	1	-
QuikSolution Reagent	1.5	-	1.5	-
Sigma Molecular Biology Water	Up to the volume of 50 µl	-	Up to the volume of 50 µl	-
QuikChange Lightening Enzyme	1	-	1	-

Table 24: Volume and concentration of PCR reagents required for a one sample master mix.

Amplification was achieved by using the following programme; 95 °C for 2 minutes, 18 cycles of 95 °C for 20 s, then 60 °C for 10 s, then 68 °C for 30 s/kb of plasmid length and 68 °C for 5 minutes.

2.7.2 *DpnI* Digestion of the Amplification Products

To digest the parental DNA, 2 μl of *DpnI* restriction enzyme was added directly to the PCR reaction tubes. The solution was pipetted up and down gently several times to mix. The reaction was briefly spun down in a microcentrifuge and immediately incubated in the thermocycler at 37 °C for 5 minutes to digest the parental DNA.

2.7.3 Transformation into XL10-Gold Ultracompetent Cells

The XL10-Gold ultracompetent cells (*Agilent*) were thawed on ice and for each sample reaction to be transformed 45 μl of the ultracompetent cells into a prechilled 15 ml centrifuge tube. 2 μl of the Agilent β-mercaptoethanol mix was added to the 45 μl of cells and swirled gently to mix. The cells were incubated on ice for 2 minutes. 2 μl of the *Dpn I*-treated DNA was added to the ultracompetent cells and swirled gently to mix and incubated for 30 minutes on ice.

The chilled tubes were then placed into a water bath at 42 °C for 30 seconds. The tubes were immediately placed onto ice for 2 minutes. 0.5 ml of preheated (42 °C) NZY^+ broth was added to each tube and incubated at 37 °C for 1 hour in a shaking incubator at 225 rpm. 100 μl of the transformation reaction was plated on agar plates containing the appropriate antibiotic for the plasmid vector. The plates were incubated at 37 °C for around 16 hours. An individual colony was taken and purified using the *Bioline Isolate II Plasmid Mini Kit* (Section 2.5). 15 μl of the purified plasmid DNA was placed in a microcentrifuge tube with 2 μl of the FBAC1 – 5'-TATTCATACCGTCCCACCA-3' primer. This was then sent to Eurofins Genomics for sequencing to determine whether the clones have the selected mutation. The remaining purified DNA stock was stored at -20 °C.

2.8 Generating the Recombinant Bacmid

The recombinant bacmid was generated according to the Bac-to-Bac Manual (Invitrogen) according to manufacturer's instructions and this is represented in Figure 25.

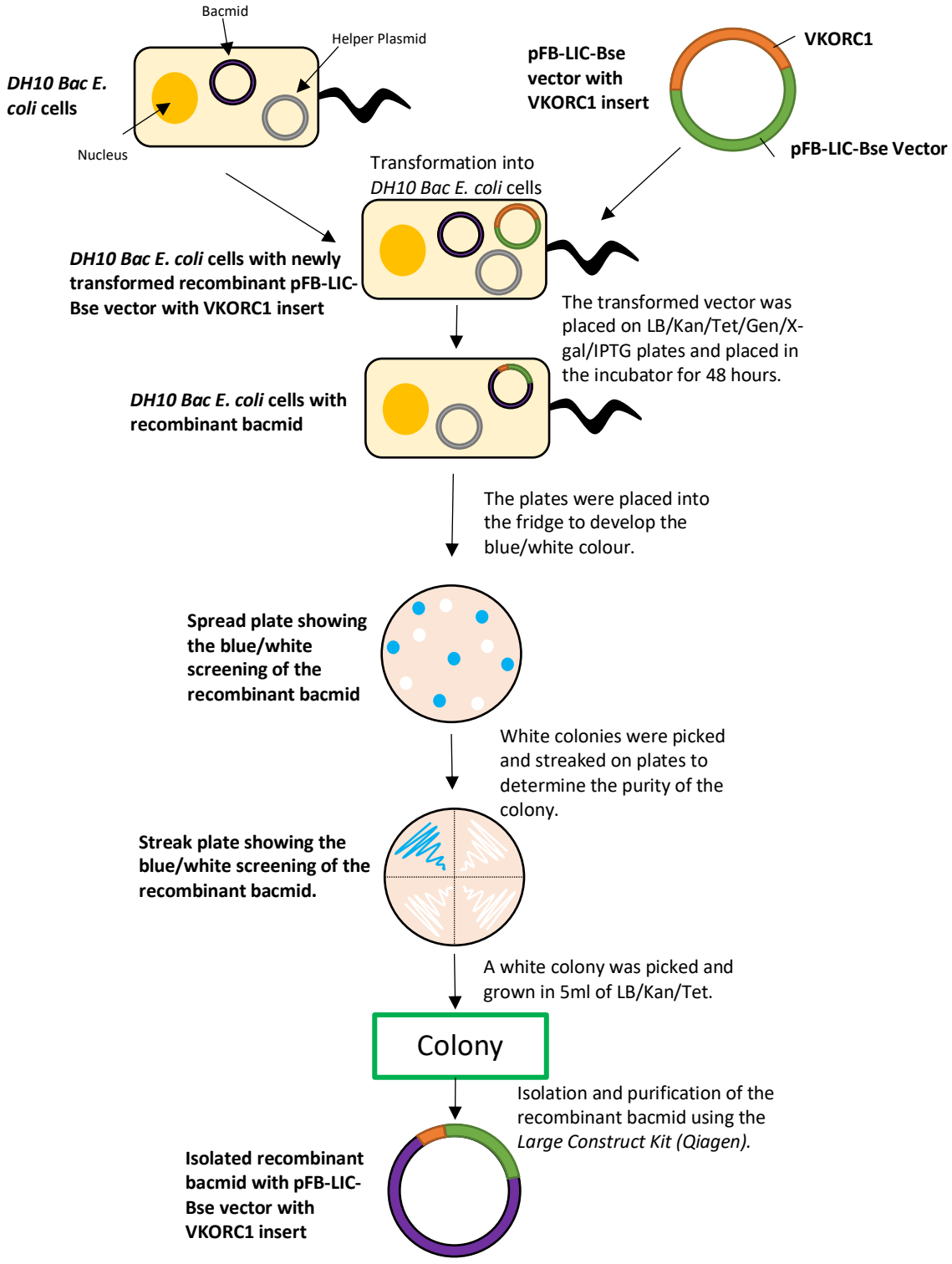


Figure 25: Schematic diagram of generating the recombinant bacmid. (Created by Author, based on Bac-to-Bac Manual (Invitrogen)). Kan denotes kanamycin. Tet denotes tetracycline. Gen denotes gentamicin.

2.8.1 Transforming the VKORC1-pFB-LIC-Bse construct into *DH10 Bac*

The method is adapted from the Bac-to-Bac manual (Invitrogen). *DH10 Bac* competent cells were made using the method described in Section 2.3. For each transformation, 100 μl of *DH10 Bac* competent cells were gently mixed and transferred into a pre-chilled, 15 ml polypropylene tube. 1 ng of recombinant plasmid was added to the cells and mixed gently. The cells were incubated for 30 minutes on ice. The cells were heat shocked for 45 seconds in a 42 °C water bath without shaking. The tubes were immediately transferred to ice and chilled for 2 minutes. 900 μl of room temperature 2X LB was added to each transformation. The tubes were placed in a shaking incubator for 4 hours at 37 °C at 220 rpm. For each transformation 10-fold serial dilutions were prepared (10^{-1}, 10^{-2} and 10^{-3}) with 2X LB. 100 μl of each dilution was placed onto a LB agar plate containing 50 μg/ml of Kanamycin, 7 μg/ml of Gentamicin, 10 μg/ml of Tetracycline, 200 μg/ml of X-gal and 20 μg/ml of IPTG. The plates were incubated for 48 hours at 37 °C. After the incubation for 48 hours, the plates were incubated at 4 °C overnight to allow the colour to develop on the plates.

2.8.2 Verifying the Phenotype

10 white colonies were picked from the incubated plates and re-streaked on LB agar plates containing 50 μg/ml of Kanamycin, 7 μg/ml of Gentamicin, 10 μg/ml of Tetracycline, 200 μg/ml of X-gal and 20 μg/ml of IPTG and incubated overnight at 37 °C to confirm the white phenotype.

2.8.3 Isolating the Recombinant Bacmid DNA

The Large Construct Kit (Qiagen) was used to isolate the recombinant bacmid DNA. A single colony from a freshly streaked selective plate was isolated and used to inoculate 5 ml of LB containing the appropriate selective antibiotics (50 μg/ml of Kanamycin, 7 μg/ml of gentamicin and 10 μg/ml of Tetracycline for the VKORC1-pFB-LIC-Bse recombinant bacmid). The culture was incubated at 37 °C at 180 rpm in a shaking incubator for 8 hours. 1 ml of the starter culture was used to inoculate 500 ml of LB medium and incubated at 37 °C at 180 rpm for 12-16 hours. The bacterial cells were harvested by centrifugation at 6000 xg for 15 minutes at 4 °C. The supernatant was discarded and all traces of the supernatant was removed by inverting the open centrifuge tubes until all of the medium had been drained. The bacterial

pellet was resuspended in 20 ml of Buffer P1. 20 ml of Buffer P2 was added and mixed gently but thoroughly by inverting 4-6 times. The tubes were then incubated at room temperature for 5 minutes. 20 ml of chilled Buffer P3 was added and mixed thoroughly but gently by inverting 4-6 times. The samples were incubated on ice for 10 minutes. The solution was centrifuged at 20000 xg for 30 minutes at 4 °C. The supernatant containing the bacmid DNA was removed and the lysate was filtered through folded filter paper that was pre-moistened with distilled water. The DNA was precipitated by adding 0.6 volumes of room temperature isopropanol to the cleared lysate. The solution was mixed and centrifuged immediately at 15000 xg for 30 minutes at 4 °C. The supernatant was carefully decanted and discarded. The DNA pellet was washed with 5 ml of room temperature 70% v/v ethanol and centrifuged at 15000 xg for 1 minutes. The supernatant was decanted and discarded without disturbing the pellet. The tube containing the DNA pellet was placed upside to remove any traces of ethanol and the pellet was left to air dry for 2 minutes. The DNA was dissolved in 9.5 ml of Buffer EX. 200 μl of ATP-dependent exonuclease and 300 μl of 100 mM ATP solution was added to the dissolved DNA. The solution was mixed gently but thoroughly and incubated in a water bath at 37 °C for 1 hour. A QIAGEN-tip 500 was equilibrated by applying 10 ml of Buffer QBT and allowed to empty by gravity flow. After incubation in the water bath for 1 hour, 10 ml of Buffer QS was added to the DNA sample and the whole sample was applied to the QIAGEN-tip and allowed to enter the resin by gravity flow. The QIAGEN-tip was washed with 2X 30 ml Buffer QC. The DNA was eluted with 15 ml of Buffer QF pre-warmed to 65 °C. The DNA was then precipitated by adding 0.7 volumes of room temperature isopropanol to the eluted DNA. The solution was mixed and centrifuged immediately at 15000 xg for 30 minutes at 4 °C. The supernatant was decanted. The DNA pellet was washed with 5 ml of room temperature 70% v/v ethanol and centrifuged at 15000 xg for 15 minutes. The supernatant was decanted without disturbing the pellet. The pellet was air dried for 5-10 minutes and re-dissolved in 300 μl of Buffer TE and left overnight to re-dissolve the DNA. The DNA was pipetted into a microcentrifuge tube and stored at 4 °C.

2.8.4 Analysing the Isolated Recombinant Bacmid DNA using PCR

Table 25 shows the volume of reagent and concentration required for a master mix for one sample.

PCR Reagent	Volume of reagent (µl)	Concentration
Peqlab 5X Enhancer Solution P	6	-
Peqlab 10X Reaction Buffer Y	3	-
Peqlab peqGOLD dNTP-Mix	0.6	10 mM
Eurofins MWG Operon Forward Primer (FBAC1 – 5'-TATTCATACCGTCCCACCA-3')	1.5	5 µM
Eurofins MWG Operon Reverse Primer (M13bac_rev – 5'-CAGGAAACAGCTATGAC-3')	1.5	5 µM
DMSO (100%)	0.9	-
Peqlab Taq-DNA-Polymerase	0.3	5 µg/µl
Sigma Molecular Biology Water	16.8	-

Table 25: Volume and concentration of PCR reagents required for a one sample master mix.

1 µl of 50 ng recombinant DNA sample was added to the tube. The thermocycler conditions were as follows; 94 °C for 5 minutes, then 30 cycles of 94 °C for 45 seconds, 50 °C for 45 seconds and 72 °C for 5 minutes with a final 7 minutes at 72°C. 5 µl of PCR product with 1 µl of loading dye was run on a 2.2% w/v agarose gel (refer to Section 2.1.3). DNA fragments of around ~1100 bp were identified as colonies that contained the newly ligated vector.

2.9 *Spodoptera frugiperda* (*Sf9*) Insect Cell Culture

2.9.1 Adherent Sf9 Cell Culture – General Maintenance

Cell cultures were started from frozen stocks of $1x10^6$ cells in a T25 flask in a total volume of 5 ml of SF-900 II serum free media (Gibco). *Sf9* insect cells were cultured in T25, T75 or T175 tissue culture flasks at 27 °C. SF-900 II serum free media supplemented with

penicillin/streptomycin (1X) (Gibco) was used to maintain the cells. The cells were passaged at ≥85-90% confluency.

2.9.1.1 Passage of Sf9 Insect Cells

The *Sf9* cells were passaged twice a week in a ratio of 1:3-1:5 with media changes every 3 days. To passage the cells in a T75 flask, the medium was removed from the insect cells. 5 ml of 1X PBS was added to cells and slowly moved over the cells to remove any dead cells and any remaining medium. The 1X PBS was removed from the cells and 10 ml of SF-900 II serum free medium supplemented with penicillin/streptomycin (1X) was added to the cells in a T75 flask. Gently moving the media across the cells was used as well as gentle tapping of the flask to dislodge the adherent cells into the medium. The cells were split into the appropriate ratio and added to new flasks with the appropriate amount of media to a total of 10 ml and placed in the incubator at 27 °C. The volumes were adjusted depending on the size of flask used.

2.9.1.2 Seeding Cells for Recombinant Expression

Cells were dislodged as in Section 2.9.1.1. The cells were counted using 10 µl of the dislodged cells onto a haemocytometer. For experiments involving a 6 well dish, $2x10^6$ cells per well were seeded in a total of 3 ml of medium per well. For experiments using a 10 cm^2 culture dish, $1x10^7$ cells per dish were seeded in a total of 10 ml of medium per well.

2.9.1.3 Producing Frozen Cell Stocks for Sf9 Cell Lines

Cells were dislodged as in Section 2.9.1.1 and counted to determine the total number of cells in the cell suspension. For each cryovial $1x10^7$ cells in 1 ml of freezing medium was required for the frozen stocks. After the cells were counted the cells were centrifuged at 100 xg for 5 minutes. The supernatant was discarded and the required volume of freezing medium (46.25% v/v of Sf-900 II medium with antibiotics, 46.25% v/v fresh Sf-900 II medium without antibiotics and 7.5% v/v of DMSO) was used to resuspend the pelleted cells. 1 ml of resuspended cells were added to each cryovial and cryopreserved at a controlled rate using a Thermofisher Cryo-freezing container. The Cryo-freezing container was placed into the -80 °C freezer overnight. The frozen stocks were then placed into a liquid nitrogen Dewar for long term storage.

2.9.1.4 Thawing Frozen Stocks of Sf9 cells

A frozen vial of the *Sf9* cells were quickly thawed in a 37 °C water bath until just before the cells completely thawed. The vial was sprayed with 70% v/v of ethanol to decontaminate. The cells were gently resuspended dropwise into 10 ml of pre-warmed Sf-900 II medium. Cell viability was assessed using a 1:1 ratio of a 10 μl of thawed cells to 10 μl of Trypan Blue stain and 10 μl of the mixture was added to a haemocytometer and counted. Stained cells are not-viable and non-stained cells are viable cells. The cells were seeded at $1.5x10^6$ viable cells in 5 ml of medium in a T25 culture flask or $4.5x10^6$ viable cells in 10 ml of media in a T75 culture flask. The flasks were rocked gently backwards and forwards and then side to side to distribute the cells evenly within the flask. The flasks were placed into an incubator at 27 °C. The cells were observed for 48-72 hours post-thaw and the media was changed every 3 days until ≥85-90% confluency was reached.

2.9.2 Suspension Culture of *Sf9* - General Maintenance

Sf9 insect cells were cultured in 250 ml and 1000 ml autoclaved conical flasks in a shaking incubator at 27 °C at 130 rpm. SF-900 II serum free medium supplemented with penicillin/streptomycin (1X) was used to maintain the cells.

2.9.2.1 Passage of Sf9 Insect Cells – Adherent to Suspension Culture

From adherent cell culture flasks, $2x10^6$ cells/ml are seeded into 50 ml of Sf-900 II medium into a 250 ml conical flask for suspension culture. The flasks were placed into a shaking incubator at 27 °C at 130 rpm. The cells were kept within a log phase of between $1x10^6$ and $8x10^6$ cells/ml and required passaging at the higher density. *Sf9* cells require passaging twice a week.

2.9.2.2 Seeding Sf9 Cells for Recombinant Protein Expression

Cells were counted and seeded at $2x10^6$ cells/ml in the appropriate conical flasks in Sf-900 II medium, for further experiments and placed into the shaking incubator at 27 °C at 130 rpm.

2.10 Transfection of Virus into the *Sf9* Cells and Viral Amplification

The schematic diagram in Figure 26 shows the transfection of virus containing the recombinant bacmid into the *Sf9* cells. The transfection was undertaken according to the instructions in the Bac-to-Bac manual (Invitrogen).

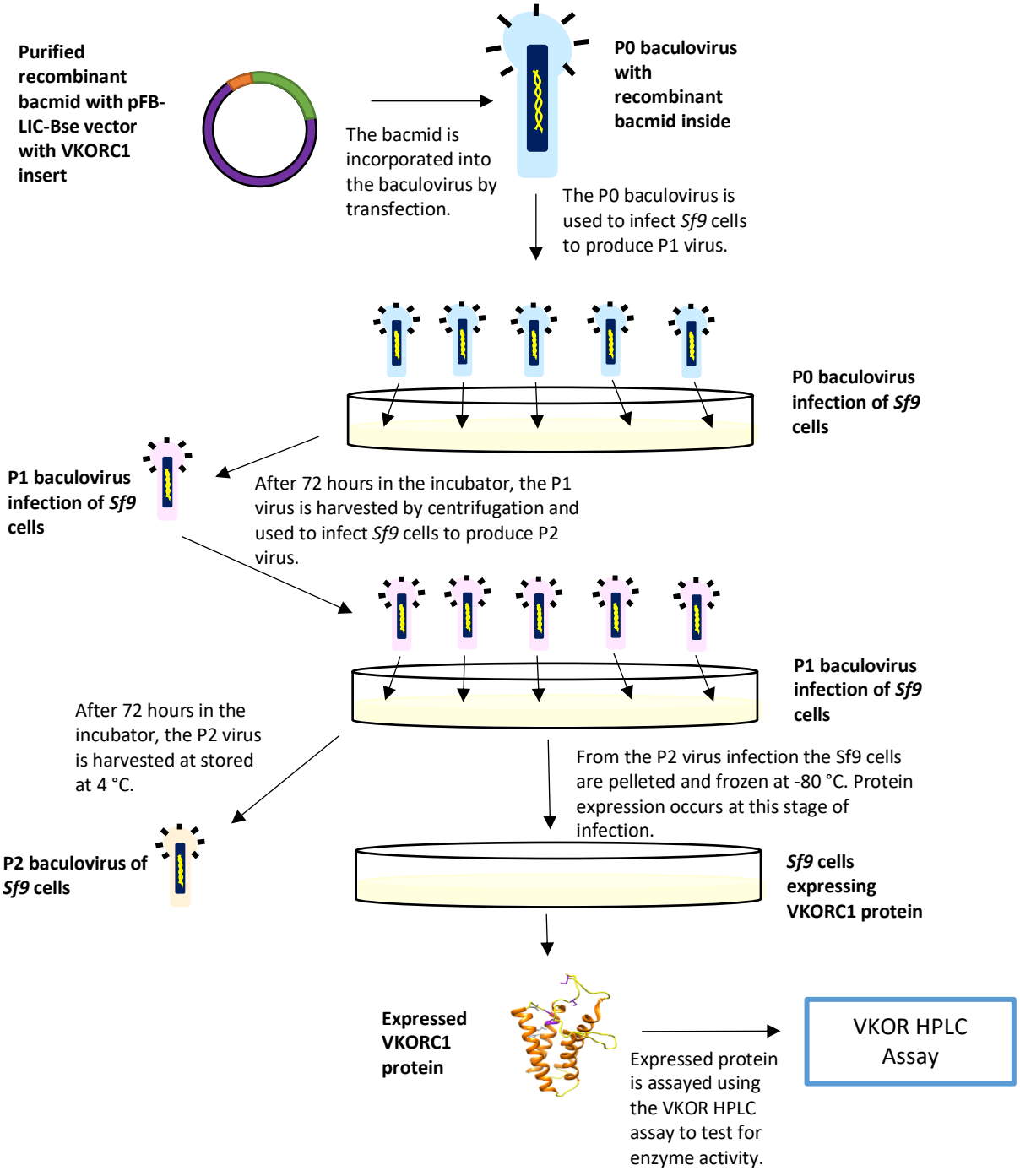


Figure 26: Schematic diagram showing the transfection of baculovirus with VKORC1 cDNAs into the *Sf9* system. (Created by Author based on the Bac-to-Bac manual (Invitrogen)).

2.10.1 Production of P0 Virus and Transfection into *Sf9* Cells

$2x10^6$ cells/well in 3 ml of media was seeded into a 6 well culture dish and left overnight to attach. For each transfection reaction a bacmid DNA:Insect GeneJuice (Novogen) reagent complex was prepared in sterile 1.5 ml microcentrifuge tubes. This was achieved by diluting 1 μg of purified bacmid DNA in 100 μl of unsupplemented Sf-900 II media. The Insect GeneJuice reagent was mixed thoroughly before use and the tube was inverted 5-10 times. 6 μl of the Insect GeneJuice was diluted in 100 μl of unsupplemented Sf-900 II media. The diluted bacmid DNA was combined with the diluted Insect GeneJuice and mixed gently and incubated for 45 minutes at room temperature. Whilst the DNA:lipid complexes were incubating the media was removed from the cells and washed with 2 ml of unsupplemented Sf-900 II media. The wash media was removed. 0.8 ml of unsupplemented Sf-900 II media was added to each tube containing the DNA:lipid complexes and mixed gently. The entire contents of the tubes containing the DNA:lipid complexes were added to each well containing cells. The cells were incubated at 27 °C for 5 hours. The DNA:lipid complexes were removed and 2 ml of complete growth media with 2% v/v FBS (Gibco) was added to the cells. The cells were incubated in the dark for 72 hours in the incubator at 27 °C. Transfected cells began to appear grainy and larger in size compared to the untransfected cells.

2.10.2 Isolating P1 Viral Stock

After 72 hours of transfection, the medium containing the virus was collected from each well and placed into sterile 15 ml centrifuge tubes. The cells were centrifuged at 1000 xg for 5 minutes to remove large debris and cells. The clarified sample was transferred into clean 15 ml centrifuge tubes and stored at 4 °C. The cells adhered to the plate at this stage are not used and therefore discarded.

2.10.3 Amplifying Viral Stock

2.10.3.1 Viral Stock Amplification in Adherent Cell Culture

The P1 viral stock was first amplified to a P2 viral stock using 6 well plates. $2x10^6$ cells/well in 3 ml of medium was seeded into a 6 well culture dish and left overnight in a 27 °C incubator to attach. The medium was removed and replaced with 3 ml of Sf-900 II medium containing 2% v/v FBS and equilibrated for 4 hours at 27 °C. 250 μl of the P1 virus was added dropwise

to each well and incubated for 72 hours in a 27 °C incubator. The P2 viral stock was isolated as described in Section 2.10.2. However, unlike Section 2.10.2 the cells can be used at this stage of infection. 2 ml of medium was added to each well and the sloughing method was used to lift the cells. The medium from each well was collected and placed into a 15 ml centrifuge tube, then centrifuged at 1000 xg for 5 minutes. The supernatant was discarded and the pellets were frozen at -80 °C.

To amplify the volume of viral stock in adherent cell culture for recombinant protein expression, 10 cm^2 culture dishes were used. $10x10^6$ cells/dish in 10 ml of medium was seeded and left overnight in a 27 °C incubator to attach. The medium was removed and replaced with 10 ml of medium containing 2% v/v FBS and equilibrated for 4 hours at 27 °C. 500 – 1000 µl of P1 viral stock (or other higher viral stock) was added to each plate and left for 72 hours at 27 °C. The amplified viral stock was isolated as described in Section 2.10.2. However, unlike Section 2.10.2 the cells can be used at this stage of infection. 5 ml of medium was added to each plate and the sloughing method was used to lift the cells. The medium from each well was collected and placed into a 15 ml centrifuge tube, then centrifuged at 1000 xg for 5 minutes. The supernatant was discarded and the pellets were frozen at -80 °C.

2.10.3.2 Viral Stock Amplification in Suspension Culture

Suspension culture was used to amplify the volume of viral stock (P2 and higher) and the number of cells for recombinant protein expression. $2x10^6$ cells were seeded into a culture volume of 50 ml or 250 ml and left overnight at 27 °C at 130 rpm in a shaking incubator. 2% v/v FBS was added to the cells and the cells were left for 4 hours at 27 °C at 130 rpm in a shaking incubator to equilibrate. 1-10 ml of viral stock was added to the cells. After infection, the cells were left for 72 hours at 27 °C at 130 rpm in a shaking incubator.

To separate the virus and the cells, the whole suspension culture was centrifuged at 1500 xg for 5 minutes. The supernatant which contain the virus was placed into 50 ml centrifuge tubes and stored at 4 °C. The pelleted cells were frozen at -80 °C.

2.11 Organic Synthesis of Vitamin K 2,3-Epoxide

The method used to synthesise vitamin K 2,3-epoxide was described by Thierry-Palmer (1984) (Figure 27) (Thierry-Palmer, 1984). All procedures were carried out in reduced light conditions due to the light sensitivity of vitamin K_1 and the product, vitamin K_1 2,3-epoxide.



Figure 27: Flow diagram of the synthesis of vitamin K epoxide.

2.12 Quantification of Vitamin K_1 and Vitamin K 2,3-Epoxide by Spectrophotometric Analysis

Determination of the concentration of vitamin K_1 and vitamin K_1 2,3-epoxide were achieved spectrophotometrically in 100% v/v ethanol. This was attained by using the extinction

coefficients of 30800 M^{-1} cm^{-1} at 266 nm for vitamin K_1 2,3-epoxide and 18900 M^{-1} cm^{-1} at 248 nm for vitamin K_1 (Wallin and Martin, 1985). 1 ml of 100% v/v ethanol was used as the blank. All samples including the blank were placed in quartz cuvettes.

2.13 Mass Spectrometry of Vitamin K_1 and Vitamin K 2,3-Epoxide

Vitamin K_1 and newly synthesised vitamin K_1 2,3-epoxide were analysed using mass spectrometry. The samples were sent to the IPOS centre, University of Huddersfield for analysis. The analysis was performed using an Agilent 6210 TOF MS instrument. Detection was achieved by using electrospray ionisation mass spectrometry (ESI-MS). Conditions were as follows: 40 psig nebuliser pressure, 350 °C gas temperature and 10 l/min drying gas flow rate. 5 µl of the sample was injected at a concentration of 100 ppm.

2.14 Calibration Standards for Vitamin K_1 and Vitamin K 2,3-epoxide

To calculate the concentration of vitamin K_1 and vitamin K_1 2,3-epoxide, calibration standards were produced and analysed using HPLC (Section 2.17.5). To calculate the concentration of vitamin K_1 and vitamin K_1 2,3-epoxide, calibration standards were produced and analysed using HPLC (Section 2.17.5). The standards for Vitamin K_1 2,3-epoxide and vitamin K were as follows; 0, 10, 25, 50, 100, 250 and 500 µM and 0, 5, 10, 25, 50 and 100 µM, respectively (Figure 28). These were prepared in 1 ml volumes diluted using 100% v/v ethanol. These were prepared in 1 ml volumes diluted using 100% v/v ethanol.

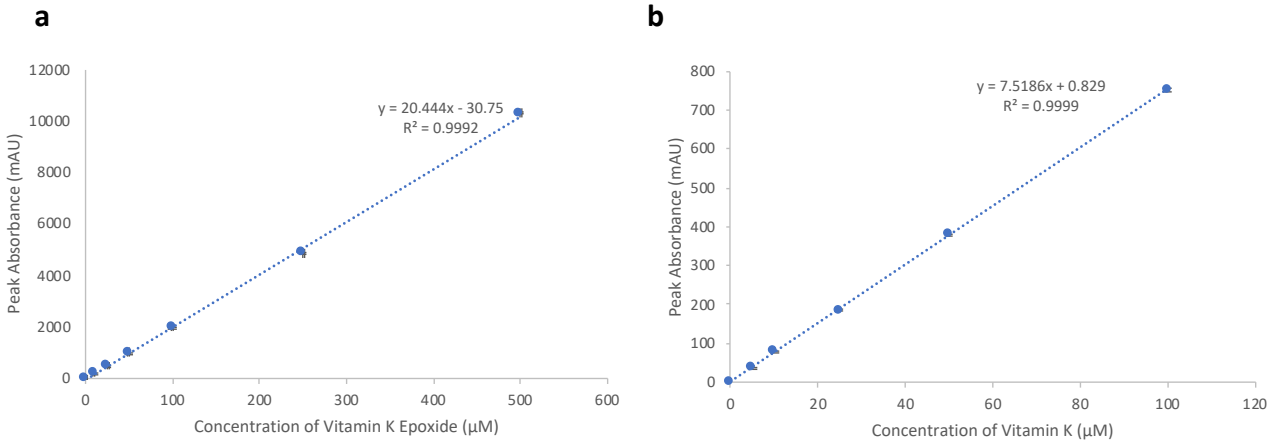


Figure 28: Vitamin K epoxide and vitamin K calibration standards. a Vitamin K epoxide calibration standards. **b** Vitamin K calibration standards. Experiments were performed in triplicate and values are shown as mean and standard deviation.

2.15 Microsome Preparation

2.15.1 Preparation of Rat Liver Microsomes

To each gram of rat liver, 4 ml of ice cold sucrose buffer (250 mM sucrose, 25 mM Tris, pH 7.4) was added on ice, and then the liver was homogenised using the Dounce homoginiser. The homogenate was centrifuged at 10000 xg for 15 minutes at 4 °C. The supernatant was then centrifuged at 100000 xg for 1 hour. The supernatant was discarded and the microsomal pellet was resuspended in 4 ml of homogenization buffer and stored at -80 °C.

2.15.2 Preparation of *Sf9* Cell Microsomes

~$2x10^6$ cells were pelleted *Sf9* cells (Section 2.10.3) were resuspended in 4 ml of homoginisation buffer (250 mM sucrose, 25 mM Tris, pH 7.4). The lysates were sonicated using a Sonics Vibra Cell sonicator for 3 minutes at 20 second bursts at 30% amplitude, followed by Dounce homogenisation. The lysates were centrifuged at 10000 xg for 15 minutes at 4 °C. The supernatant was then centrifuged at 100000 xg for 1 hour. The supernatant was discarded and the microsomal pellets were resuspended in 4 ml of homogenization buffer and stored at -80 °C.

2.16 BCA Assay for Protein Determination

The protein determination for each sample was determined using Bicinchoninic acid (BCA) assay (Smith *et al.,* 1985). To produce the volume of protein determination reagent needed for the assay, 1 part 4% w/v $CuSO_4.5H_2O$ was added to 50 parts BCA. The calibration standards were produced from a 1mg/ml stock of bovine serum albumin (BSA) and prepared in duplicate (Table 26). 15 µl of the protein standards was added to 300 µl of the protein determination reagent and mixed.

Final Protein Concentration (mg/ml)	Volume of BSA stock solution (µl)	Ultrapure Water (µl)
0	0	1000
0.2	200	800
0.4	400	600
0.6	600	400
0.8	800	200
1	1000	0

Table 26: Volumes of BSA and Ultrapure water required to make up the BSA calibration standards.

Protein samples were diluted 1:5 or 1:10 and prepared in duplicate. 15 µl of the protein samples was added to 300 µl of the protein determination reagent and mixed. The mixed protein samples and the protein standards were added to a 96 well plate and incubated at 37 °C for 30 minutes in the microplate reader. The absorbance was measured at 562 nm on the microplate reader. The protein concentration of the unknown samples was calculated using the standard curve created from the BSA calibration standard measurements.

2.17 HPLC VKORC1 Assay

HPLC VKORC1 assays to determine the amount of VK produced were carried out in triplicate, specific conditions for enzyme kinetic and inhibition experiments are highlighted in sections 2.17.3 and 2.17.4. Experiments are based on methods from Whitlon *et al.* (1978), Chu *et al.* (2006) and Hodroge *et al.* (2011) with minor modifications.

2.17.1 VKORC1 *in vitro* Assay - General

200 µl of 25 mM Tris HCl (pH 8.6), 150 mM NaCl, 20% w/v glycerol was added to a microcentrifuge tube. 0.1 – 0.5 mg of *Sf9* microsomal protein or 2 mg of rat liver microsomal protein was then added followed by 40 µl of 50 mM DTT and the water was added to make up a final volume 360 µl. The samples were then incubated at 30 °C in a heating block for 5 minutes prior to starting the reaction. The reaction was started with 40 µl of 1-50 µM vitamin K epoxide (concentration dependent on the type of assay, 50 µM for time course assays

(Section 2.17.2), between 1-35 μM for K_m (Section 2.17.3) and 10 μM for enzyme inhibition assays (Section 2.17.4)) with a total assay volume of 400 μl. The different vitamin K epoxide concentrations were produced by dilution from a 100 μM stock diluted with 100% v/v ethanol and the percentage of ethanol was consistent throughout the dilutions and in assays. The samples were then incubated at 30 °C in a heating block for 5 minutes prior to starting the reaction. The sample was vortexed immediately after vitamin K epoxide was added for 5 seconds, then placed into the 30 °C heating block for the desired amount of time. To stop the reaction 800 μl of ice cold propan-2-ol:hexane (3:2) was added. The sample was then vortexed immediately after stopping the reaction for 15 seconds and then placed onto ice. The samples were shaken at 49 min^{-1} for 2 minutes in the Turbula shaker-mixer. The samples were then centrifuged for 5 minutes at 9000 rpm. 200 μl of the hexane layer was removed, placed into a clean microcentrifuge tube and then dried down under nitrogen in a sample concentrator for 15-20 minutes. The samples were then resuspended in 100 μl of propan-2-ol and vortexed for 10 seconds before being added to the HPLC vial inserts. The samples were analysed using HPLC with an injection volume of 20 μl (Section 2.17.5).

2.17.2 VKORC1 Time Course Experiments

A time course of 0, 5, 10, 15 and 20 minutes were obtained for each VKORC1 construct. The assay was carried out following section 2.17.1. 50 μM VKE was used to start the reaction. Figure 29 shows an example of the linearity of the VKORC1 assay.

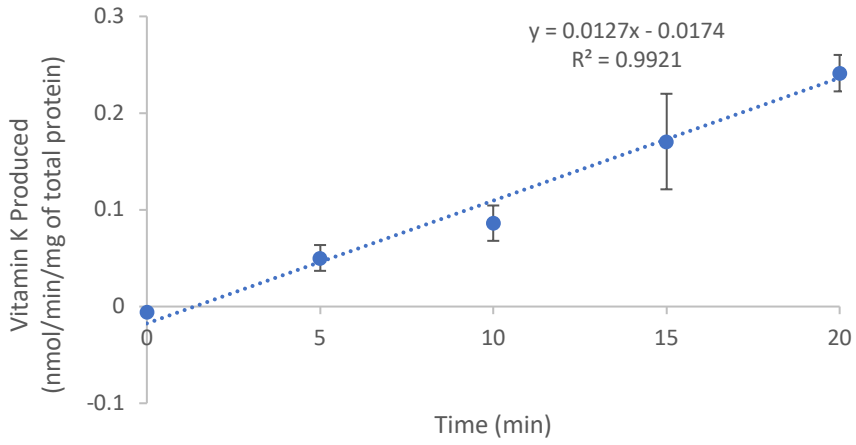


Figure 29: Time course of 0, 5, 10, 15 and 20 minutes of vitamin K production of VKORC1 expressed in *Sf9* insect cells at 50 μM of vitamin K epoxide. Experiments were performed in triplicate and values are shown as mean and standard deviation.

2.17.3 VKORC1 K_m Determination

K_m and V_{max} values were obtained with seven different concentrations of vitamin K epoxide. 0.1 mg of protein was used to determine the K_m and $V_{max.}$ The different vitamin K epoxide concentrations were produced by dilution from a 100 μM stock diluted with 100% v/v ethanol and the percentage of ethanol was consistent throughout the dilutions and in assays. These were; 0, 1, 2, 5, 10, 25 and 35 μM. Incubations were carried out for 15 minutes. Ethanol was used for 0 μM. The assay was carried out following Section 2.17.1.

2.17.4 VKORC1 *in vitro* Assay – IC_{50} Determination

For anticoagulant inhibition assays, the assay was carried out as indicated in Section 2.17.1 with the anticoagulants being added after the protein and incubated for 5 minutes before the DTT and water were added to a final volume of 360 μl, prior to 40 μl of 10 μM vitamin K epoxide to make a total volume of 400 μl. IC_{50} values were obtained with of 14 different concentrations of anticoagulant rodenticide. The anticoagulant rodenticides used were; warfarin, bromadiolone, brodifacoum, difenacoum and flocoumafen. The different anticoagulant rodenticide concentrations were produced by dilution from a 1 mM stock diluted with 100% v/v DMSO and the percentage of DMSO was consistent throughout the dilutions and in assays. These were; 0, 0.01, 0.025, 0.05, 0.1, 0.25, 0.5, 1, 2.5, 5, 10, 25, 50, 100 μM. Incubations were carried out for 15 minutes. DMSO was used for 0 μM. 0.1 – 0.5 mg of protein were used in the assays in order to ensure linearity within the assays and to account for different recombinant protein expression levels for the different VKORC1 constructs. For the inhibition assays of VKORC1 constructs the amount of microsomal protein was 0.1-0.2 mg for rat VKORC1, 0.15-0.2 mg for p.R40G variant, 0.5 mg for p.L120Q variant, 0.1-0.15 mg for human VKORC1 and 0.15-0.3 mg for cow VKORC1. The amount of protein was taken into consideration when calculating enzymatic activity.

2.17.5 High Pressure Liquid Chromatography (HPLC) Analysis

The Agilent 1260 Infinity HPLC with diode array detector and fluorescence detector was used to quantitate vitamin K production the VKORC1 catalysed reactions. The conditions used for the HPLC analysis are shown in Table 27. The retention times of vitamin K and vitamin K

epoxide were 3.2 and 2.2 minutes, respectively. Data analysis was performed using the Workstation Software LC Solutions programme.

HPLC Conditions	
Mobile Phase	HPLC Grade Methanol (100%)
Column Oven Temperature	40 °C
Flow Rate	1 ml/min
Injection Volume	Autosampler Injection: 20 µl
Detection	248 nm wavelength using Diode Array 190-800 nm
HPLC Column	Agilent Poroshell 120 EC-C18 4.6 x 50 mm
Run Time	6 minutes

Table 27: HPLC conditions for analysis of VKORC1 reactions.

2.18 Bioinformatic Analysis

2.18.1 Sanger Sequence Analysis

DNA Sanger sequencing data received form Eurofins Genomics was analysed using 4Peaks (https://nucleobytes.com/4peaks/index.html).

2.18.2 Mitochondrial Network Mapping

FASTA sequences for D-loop sequences were inputted into Text Wrangler and transferred into CLC Genomics Workbench 12.0 (https://www.qiagenbioinformatics.com/) to create multiple sequence alignments with existing *Rattus norvegicus* D loop data obtained from National Centre of Biotechnology Information (NCBI) database (https://www.ncbi.nlm.nih.gov/). NETWORK programme (https://www.fluxus-engineering.com/) was used to reconstruct phylogenetic medium joining networks.

2.18.3 VKOR Multiple Sequence Alignments

All protein sequences for creating VKORC1 and VKORC1L1 alignments were downloaded from NCBI databases (https://www.ncbi.nlm.nih.gov/) see Appendix 6 for accession numbers. Multiple sequence alignments were performed using CLC Genomics Workbench 12.0 (https://www.qiagenbioinformatics.com/).

2.18.4 Secondary Structure Prediction

VKORC1 protein sequences obtained from the NCBI database were inputted into TMHMM (http://www.cbs.dtu.dk/services/TMHMM/) to predict the secondary structure.

2.18.5 3D Protein Modelling

VKORC1 protein sequences obtained from the NCBI database were inputted into Swiss-model (https://swissmodel.expasy.org/). 3D VKORC1 models were based on the *Synechococcus sp.* VKOR 3kp9 model defined by Li *et al.* (2010). The models were inputted into UCSF Chimera 1.10.2 which was used to visualize the models (https://www.cgl.ucsf.edu/chimera/).

Chapter 3: Frequency and Distribution of Anticoagulant Rodenticide Resistance in the UK and Sweden

3.0 About this Chapter

Anticoagulant resistance in *Rattus norvegicus* (brown rats) was first reported in Scotland in 1958 (Boyle, 1960) Since this first report, there have been numerous reports of anticoagulant resistance in brown rats in the UK (Greaves and Ayres, 1973). It was only after the discovery of the VKORC1 gene that the molecular basis of resistance was determined (Section 1.16). Studies by Pelz *et al.* (2005), Rost *et al.* (2009) and Haniza *et al.* (2015) reported the VKORC1 polymorphisms in brown rats associated with anticoagulant resistance in the UK. However, the brown rat samples used to determine VKORC1 polymorphisms in the UK by these studies were either derived from laboratory rat strains from the Central Science Laboratory (CSL) in York and Reading University or were frozen samples collected between the years 1990-2005. The sample size of brown rats tested by Pelz *et al.* (2005) was 11 UK brown rats, the research group later expanded this to 28 UK animals Rost *et al.* (2009). Also, both studies by *Pelz et al.* (2005), Rost *et al.* (2009) and Haniza *et al.* (2015) did not use DNA sequencing to genotype anticoagulant resistance polymorphisms in the VKORC1 gene and used an amplification refractory mutation system (ARMS) PCR and restriction fragment length polymorphism (RFLP) to screen for known polymorphisms. to screen for polymorphisms. These previous studies were biased as they only used resistant animals and also do not account for a further two to three decades of evolutionary 'survival of the fittest' pressure due to the continued use of anticoagulant rodenticides which will result in the selection of resistant rat genotypes / phenotypes.

At the University of Huddersfield, a project was initiated in 2010 to sequence the VKORC1 gene of randomly sampled wild brown rat populations along the resistance foci within the UK. Resistance foci were determined using previous historic areas known for anticoagulant resistance (Greaves and Ayres, 1974). 60% of the VKORC1 exon sequencing was completed by the Author to complete the project, with 40% completed by Julius Nana, Ellie Pierson and Fareeha Tariq. All D loop sequencing was completed by the Author. During the project, areas

beyond the previous resistance foci were incorporated to provide a more complete status of anticoagulant resistance in wild brown rat populations in the UK. There are also no reports of anticoagulant resistance in wild populations of brown rats in the Scandinavian country, Sweden, so the University of Huddersfield Swedish project began in 2012 with the aim of sequencing the VKORC1 gene in wild brown rat populations within Sweden due to the lack of information regarding anticoagulant resistance in the country. The completion of both VKORC1 resistance polymorphism projects was a focus of this thesis and were completed along with mitochondrial D-loop analysis of the brown rat samples in the UK and Sweden. One of the focusses of this chapter will assess the frequency and distribution of anticoagulant rodenticide resistance polymorphisms in wild *Rattus norvegicus* (brown rat) populations in the UK and Sweden using genetic analysis of the VKORC1 gene. Using recombinant expression and enzyme assays previously reported anticoagulant resistant VKORC1 polymorphisms found in the brown rat reflect practical resistance in field and *in vivo*, in wild and congenic lab strains (Hodroge *et al.,* 2011). In this chapter another focus is to assess the effect of a range of rodenticides on rat VKOR variants using a baculovirus recombinant expression system and a VKOR HPLC assay (Section 2.17) with wild type and a novel polymorphism. Rodenticides to be tested include the more potent SGAR flocoumafen which has not been tested previously in an *in vitro* assay system.

With regards to the research on the phylogeography of brown rats, studies by Song *et al.* (2014) used mitochondrial DNA sequencing of rats to map mtDNA variants worldwide although no UK rat and only one Swedish rat sample were included. The study also looked at relationships of French and German rodenticide resistance rats and the mtDNA genotypes (Song *et al.,* 2014). The only study that has assessed the geographical population structure of rats in the UK was by Haniza *et al.* (2015) that used a partial mtDNA D-loop sequence of 333 bp to identify haplotypes in populations of *Rattus norvegicus* in the UK. The samples used were frozen tissue samples from the years 1990-2000 from the CSL, York, which does not provide a current population structure for wild brown rats in the UK. In this study detailed in the final part of this chapter, the D-loop sequences of 625 bp were used to determine the haplotypes of wild brown rat populations in both the UK and Sweden and to also observe the relationship between the D-loop haplotypes and anticoagulant resistance.

3.1 Genetic Analysis to determine the frequency and distribution of anticoagulant resistance in UK and Swedish wild brown rats

Between the years 2010 and 2017, 151 wild brown rat samples were collected from 21 counties throughout the UK and in 2012, 22 wild rat samples were collected from 8 counties in Sweden. DNA sequencing analysis of the VKORC1 gene took place in order to scruitinise the gene for known anticoagulant resistant polymorphisms as well as novel polymorphisms. All DNA sequences were compared to the wild type (NM_203335.2).

3.1.1 VKORC1 Exon 1 variants in UK and Swedish rats

Exon 1 of the VKORC1 gene was sequenced for wild brown rat samples in the UK and Sweden. 98% of UK samples and 94% of Swedish samples were wild type and showed no variation compared to the wild type sequence (NM_203335.2). However, two samples from Gloucestershire in the UK and one sample from Kronoberg in Sweden showed a heterozygous polymorphism at codon position 40 resulting in an arginine residue being substituted by a glycine residue. This p.R40G polymorphism is previously unreported in wild brown rat populations. Figure 30 shows an example of the DNA sequencing electropherogram of one of the Cheltenham samples with the heterozygous p.R40G polymorphism. Table 28 shows the nucleotide change and the resulting amino acid differences for the p.R40G polymorphism.

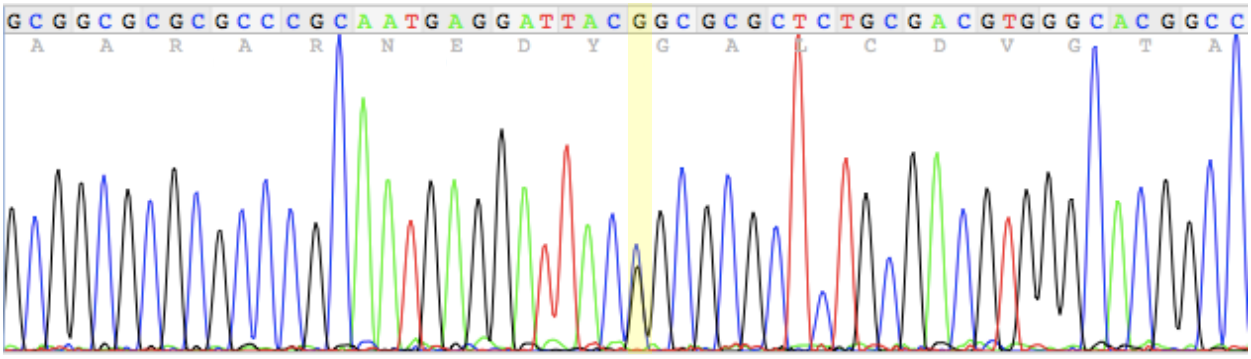


Figure 30: Sequencing electropherogram of the previously unreported p.R40G polymorphism found in exon 1. Yellow highlight denotes the position of the polymorphism.

Geographical Area		N° of Specimens	Codon	WT	Mut	AA WT	AA Mut
England	Gloucestershire	2	40	CGC	GGC	Arg	Gly
Sweden	Kronoberg	1	40	CGC	GGC	Arg	Gly

Table 28: Novel p.R40G polymorphism found in the VKORC1 gene in *Rattus norvegicus* in the UK and Sweden. WT denotes wild type. Mut denotes mutant polymorphism. AA WT denotes amino acid of the wild type sequences. AA Mut denotes amino acid of the mutant VKORC1 sequence.

The novel polymorphism identified in the two samples in Gloucestershire and the one sample from Kronoberg result in a change in amino acids from a positive arginine residue to a small, uncharged glycine residue which is a significant change in physiochemical properties of the amino acids (Figure 30 and Table 28). Previously a study by Czogalla *et al.* (2017) showed that arginine residues have a role in charge-stabilisation upon warfarin binding to VKORC1 and the replacement of arginines (R33, R40, R53) with negatively charged amino acids shifts the warfarin dose-response curves with an increase in IC_{50} values. Therefore, a change at position 40 to a small uncharged glycine may also have an impact on anticoagulant rodenticide binding to VKORC1 in the brown rat with the potential of causing anticoagulant resistance. This is investigated in Section 3.9.

3.1.2 VKORC1 Exon 2 variants in UK and Swedish rats

Table 29 shows an overview of the polymorphisms found in exon 2 in brown rat samples for all the geographical areas surveyed in the UK and Sweden that differ from the wild type sequence (NM_203335.2).

Geographical Area		N° of Specimens with SNPs	Codon	WT	Mut	AA WT	AA Mut
England	City of Bristol	5	82	ATA	ATT	Ile	Ile
		1	79	TCC	TTC	Ser	Phe
	East Riding	1	82	ATA	ATT	Ile	Ile
	Gloucestershire	5	82	ATA	ATT	Ile	Ile
	Greater Manchester	1	82	ATA	ATT	Ile	Ile
	Hampshire	3	82	ATA	ATT	Ile	Ile
	Norfolk	1	82	ATA	ATT	Ile	Ile
		1	66	GTG	TTG	Val	Leu
	Shropshire	6	82	ATA	ATT	Ile	Ile
	Sussex	1	82	ATA	ATT	Ile	Ile
	West Midlands	6	82	ATA	ATT	Ile	Ile
	West Yorkshire	6	82	ATA	ATT	Ile	Ile
Sweden	Östergötland	2	82	ATA	ATT	Ile	Ile
	Skåne	1	82	ATA	ATT	Ile	Ile
	Stockholm	1	82	ATA	ATT	Ile	Ile

Table 29: Overview of the polymorphisms found in exon 2 in brown rat samples for all the geographical areas surveyed in the UK and Sweden.

24% of UK samples and 21% of Swedish samples contained a silent p.I82I polymorphism (Table 29). Figure 31 shows the sequencing electropherograms of an example of a sample with the homozygous p.I82I polymorphism.

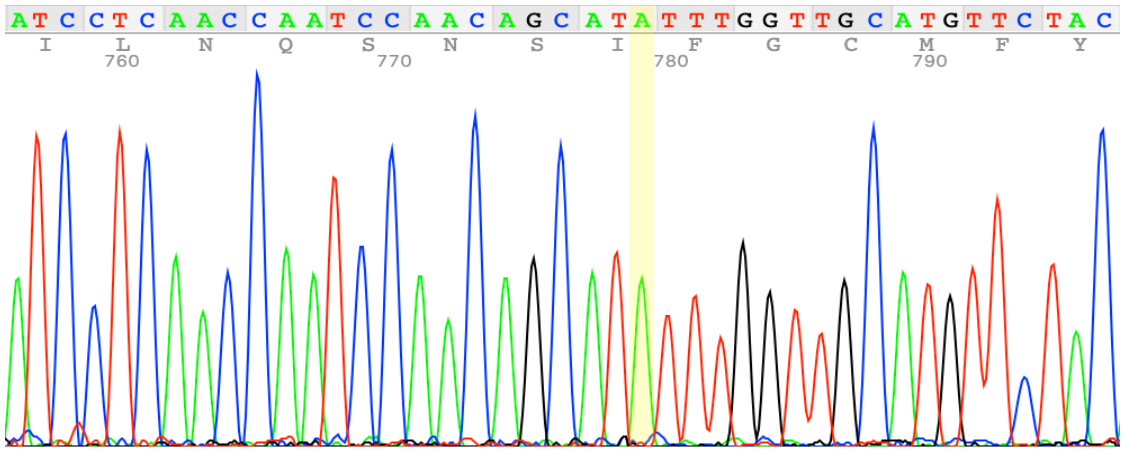


Figure 31: Sequencing electropherogram of the p.I82I polymorphism found in exon 2. Yellow highlight denotes the position of the polymorphism.

Of the 21 areas surveyed in the UK only 10 counties contained brown rats with the silent p.I82I polymorphism all found across England (Table 29). In Sweden, 3 out of 8 areas surveyed contained the p.I82I polymorphism. The silent polymorphism resulted in a codon change from an ATA to ATT. Prescott *et al.* (2011) reported the silent p.I82I polymorphism in all 10 of the

brown rat samples surveyed in Kent. It was also reported in 28% of brown rat samples in France in a study by Grandemange *et al.* (2010). The p.I82I polymorphism is not likely to have an effect on the binding of anticoagulant rodenticides. Although Prescott *et al.* (2011) suggested that a silent change in a codon may alter the efficiency of translation, thereby altering the effect of anticoagulant exposure.

Another previously reported polymorphism was found in one brown rat sample from the City of Bristol (Table 29 and Figure 32). It is a heterozygous p.S79F polymorphism with a codon change from TCC to TTC that Runge *et al.* (2011) discovered in regions of Germany specifically, Saxony-Anhalt and Berlin.

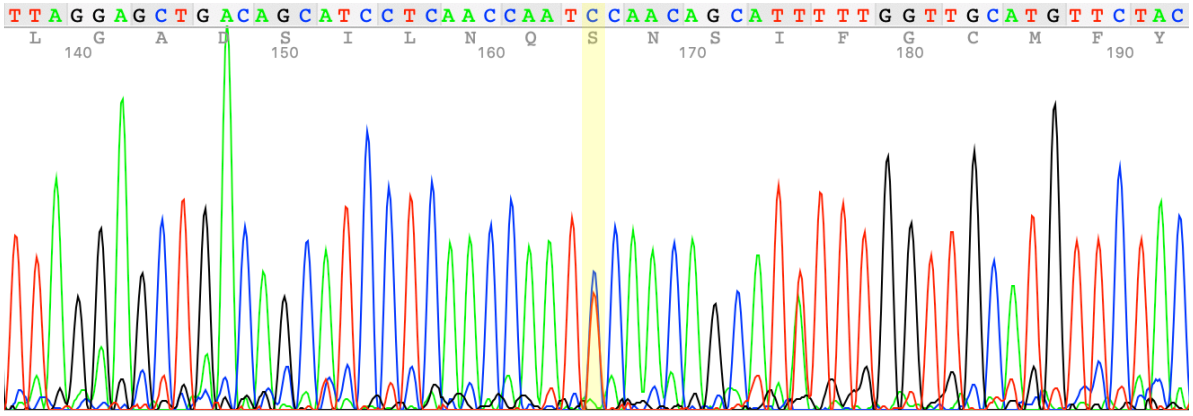


Figure 32: Sequencing electropherogram of the p.S79P polymorphism found in exon 2. Yellow highlight denotes the position of the polymorphism.

The change from a small polar serine residue to an aromatic residue phenylalanine may cause a change in the structure of VKORC1 and the affinity for anticoagulants due to the differences in physiochemical properties of the amino acids. This has not been tested *in vitro*.

A previously unreported heterozygous polymorphism was found in one brown rat sample from Norfolk (Table 29 and Figure 33). It is a change at position 66 from a valine residue to a leucine residue with a codon change of GTG to TTG.

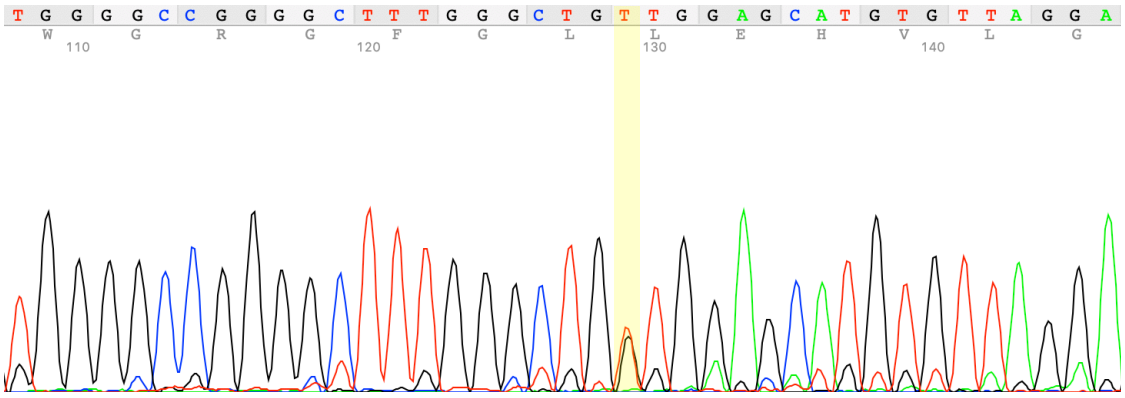


Figure 33: Sequencing electropherogram of the p.V66L polymorphism found in exon 2. Yellow highlight denotes the position of the polymorphism.

Valine and leucine are both hydrophobic amino acids and a potential change may not result in any effect on the binding of anticoagulants due to the similar physiochemical properties. Although in brown rats, a change at position 66 has not been previously reported, in humans at this position a p.V66M and p.V66G change has been reported and resulted in anticoagulant resistance (Watzka *et al.,* 2011). A study by Czogalla *et al.* (2013) used 3D modelling to assess the binding sites of warfarin in relation to human anticoagulant resistance polymorphisms. They showed that V66 does not directly bind to warfarin, but a change may cause a conformational change to the large loop in which V66 is found. Therefore, a change from a valine to a leucine at this position may not cause a difference to the large loop due to the similar physiochemical properties as there is no direct interaction with warfarin and probably would not cause anticoagulant resistance.

3.1.3 VKORC1 Exon 3

3.1.3.1 VKORC1 Exon 3 Polymorphisms in the UK

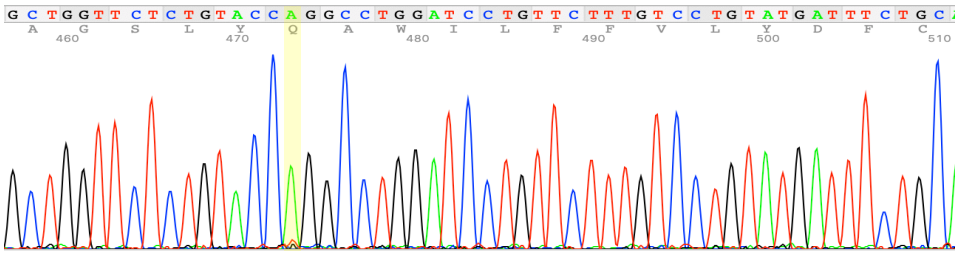
Exon 3 of the VKORC1 gene has been reported as the 'hotspot' for anticoagulant resistant polymorphisms (Pelz *et al.,* 2005). There are many reports of anticoagulant resistance in brown rats in numerous countries including the UK (e.g. Pelz *et al.,* 2005; Rost *et al.,* 2009; Grandemange *et al.,* 2010) (See Section 1.16). Within these reports there are five anticoagulant resistance polymorphisms which are prevalent in brown rat populations, these are; p.L120Q, p.L128Q, p.Y139C, p.Y139S and p.Y139F. Figure 34 shows example electropherogram of the VKORC1 polymorphisms found in exon 3. These polymorphisms are

the most studied and characterised biochemically in terms of the effect of both first and second generation anticoagulants on the VKORC1 enzyme with these polymorphisms (Hodroge *et al.,* 2011). Table 30 shows an overview of the polymorphisms found in exon 3 in brown rat samples for all the geographical areas surveyed in the UK. Figure 35 shows the geographical map of the UK with the representation of polymorphisms found in each county represented as pie charts.

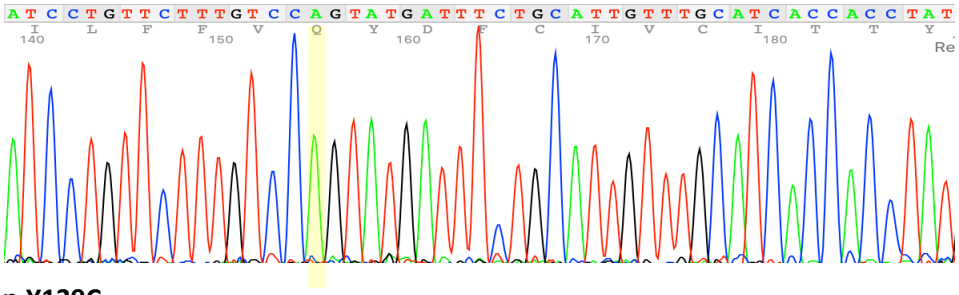
Geographical Area	N° of Specimens with SNPs	Codon	WT	Mut	AA WT	AA Mut
Aberdeenshire	5	128	CTG	CAG	Leu	Gln
Berkshire	6	120	CTG	CAG	Leu	Gln
City of Bristol	2	139	TAT	TGT	Tyr	Cys
	1	120	CTG	CAG	Leu	Gln
Dumfries and Galloway	8	128	CTG	CAG	Leu	Gln
East Riding	1	128	CTG	CAG	Leu	Gln
Edinburgh	4	128	CTG	CAG	Leu	Gln
Gloucestershire	2	120	CTG	CAG	Leu	Gln
	4	139	TAT	TGT	Tyr	Cys
Greater Manchester	0	-	-	-	-	-
Gwynedd	1	120	CTG	CAG	Leu	Gln
Hampshire	3	120	CTG	CAG	Leu	Gln
	3	139	TAT	TGT	Tyr	Cys
Lincolnshire	0	-	-	-	-	-
Norfolk	3	139	TAT	TGT	Tyr	Cys
Oxfordshire	13	120	CTG	CAG	Leu	Gln
Shropshire	4	139	TAT	TGT	Tyr	Cys
	3	139	TAT	TCT	Tyr	Ser
South Yorkshire	5	139	TAT	TGT	Tyr	Cys
Suffolk	0	-	-	-	-	-
Surrey	3	139	TAT	TGT	Tyr	Cys
Sussex	3	120	CTG	CAG	Leu	Gln
West Midlands	5	139	TAT	TGT	Tyr	Cys
West Yorkshire	2	128	CTG	CAG	Leu	Gln
	3	139	TAT	TGT	Tyr	Cys
Wiltshire	17	120	CTG	CAG	Leu	Gln

Table 30: Overview of the polymorphisms found in exon 3 in brown rat samples for all the geographical areas surveyed in the UK.

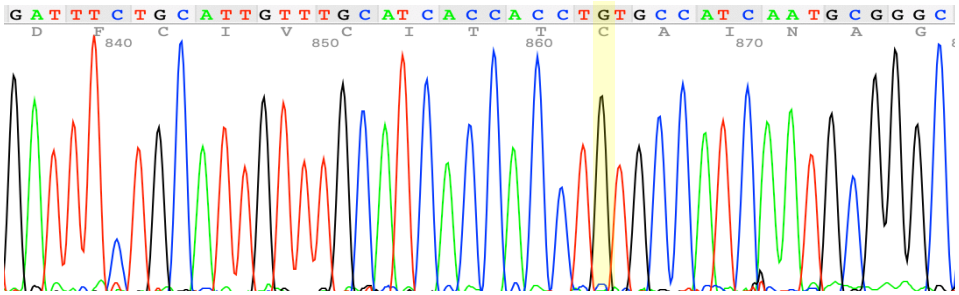
a **p.L120Q**



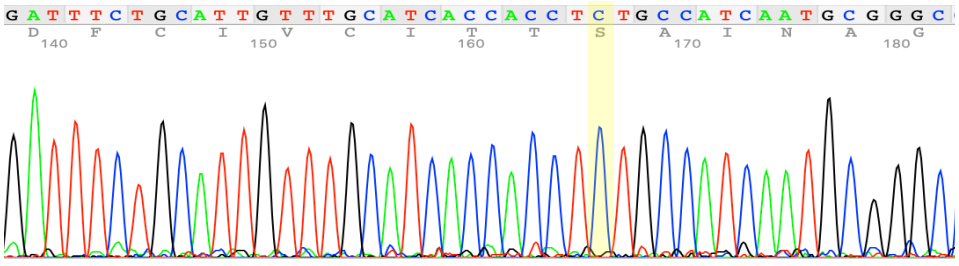
b **p.L128Q**



c **p.Y139C**



d **p.Y139S**



e **p.L120Q and p.Y139C (compound heterozygote)**

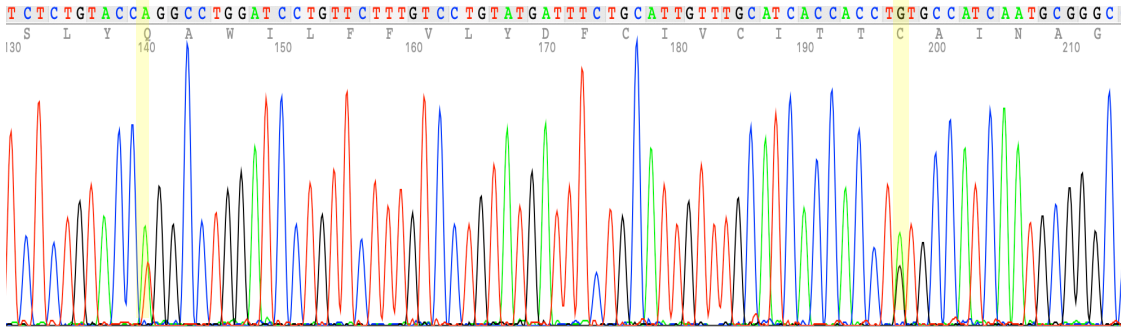


Figure 34: Sequencing electropherogram of the p.L120Q, p.L128Q, p.Y139C and p.Y139S polymorphisms found in exon 3 in the UK brown rat samples. a WN1 sample showing the homozygous p.L120Q polymorphism. **b** AB2 sample showing the homozygous p.L128Q polymorphism. **c** SF11 sample showing the p.Y139C polymorphism. **d** OS1 sample showing S polymorphism. **e** AF2 sample showing the compound heterozygote p.L120Q and p.Y139C. Yellow highlight denotes the position of the polymorphism.

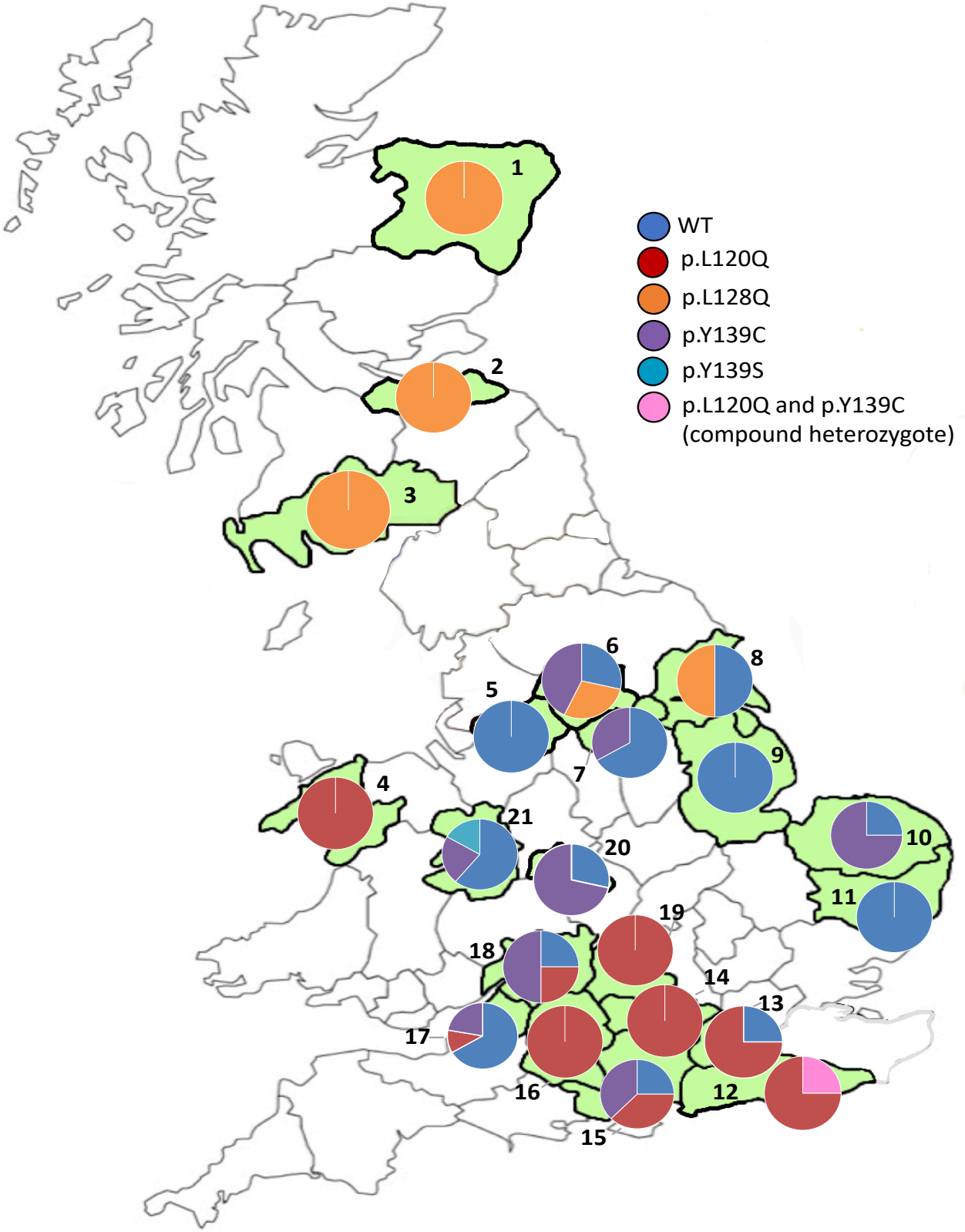


Figure 35: Map of the UK highlighting the geographical distribution and proportion of anticoagulant resistant polymorphisms found in each county surveyed. 1 Aberdeenshire, **2** Edinburgh, **3** Dumfries and Galloway, **4** Gwynedd, **5** Greater Manchester, **6** West Yorkshire, **7** South Yorkshire, **8** East Riding, **9** Lincolnshire, **10** Norfolk, **11** Suffolk, **12** Sussex, **13** Surrey, **14** Berkshire, **15** Hampshire, **16** Wiltshire, **17** City of Bristol, **18** Gloucestershire, **19** Oxfordshire, **20** West Midlands, **21** Shropshire. Blue denotes wild type (WT). Red denotes p.L120Q. Orange denotes p.L128Q. Purple denotes p.Y139C. Turquoise denotes p.Y139S. Pink denotes p.L120Q and p.Y139C compound heterozygote.

From Table 30, 69% of randomly sampled UK brown rats tested contained an anticoagulant resistant polymorphism. Four of the most common polymorphisms were found in the UK, p.L120Q, p.L128Q, p.Y139C and p.Y139S (Figure 34). The only polymorphism that was not found in the UK samples tested was the p.Y139F polymorphism that is the predominant resistance polymorphism in France (Grandemange *et al.,* 2010). This may be due to the areas surveyed in this study as the p.Y139F polymorphism has only previously identified in Kent (Prescott *et al.,* 2011).

The most common polymorphism found in the UK brown rats was the p.L120Q polymorphism with a frequency of 32% (Table 30 and Figure 35). The p.L120Q polymorphism predominately found in the South of England in 8 counties; City of Bristol, Gloucestershire, Oxfordshire, Berkshire, Hampshire, Wiltshire, Surrey and Sussex. The only exception is a sample tested from Gwynedd (Sample code GW15), which contained a p.L120Q polymorphism. This is the first report of this polymorphism in Wales. This is different to previous reports as the polymorphism usually associated with Wales is p.Y139S which is based on 2 samples of lab strain derived Welsh wild rat (Pelz *et al.* 2005). In this study, only 2% of UK brown rat samples contained the p.Y139S polymorphism and was found in samples from Shropshire, specifically Oswestry close to the Welsh border. The p.Y139C polymorphism is the most geographically widespread polymorphism in the UK and is found in 22% of UK brown rats. In 13% of brown rat samples a p.L128Q polymorphism was identified. This included all three areas surveyed in Scotland and two areas in the north of England (West Yorkshire and East Riding). These findings are consistent with geographical locations of polymorphisms in other studies (Pelz *et al.,* 2005). There were three areas tested that showed no anticoagulant resistance in brown rat populations. These were; Greater Manchester, Lincolnshire and Suffolk. In total 31% of all samples showed no anticoagulant resistance polymorphisms. These results differ from a study by Rost *et al.* (2009) which analysed two resistant brown rat samples the county Lincolnshire and found a p.Y139C polymorphism in 2 brown rat samples.

This study randomly surveyed 21 counties for anticoagulant resistance polymorphisms, 14 of which are previously unreported areas in the UK for anticoagulant resistance polymorphisms. However, 7 of the counties surveyed in this study have been previously reported by a number of studies (Pelz *et al.,* 2005; Rost *et al.,* 2009; Haniza *et al.,* 2015). A study by Pelz *et al.* (2005)

reported resistance in Berkshire (p.L120Q), Yorkshire (p.Y139C and p.L128Q) and Hampshire (p.L120Q) in brown rats (Section 1.16). The results from this study are consistent with Pelz *et al.* (2005) findings, although the samples used by Pelz *et al.* (2005) are either derived from laboratory rat strains from the Central Science Laboratory (CSL) in York and Reading University or a small number of frozen samples (n < 11) collected between the years 1990-2005. However, this study also revealed an additional polymorphism found in brown rat samples in Hampshire (Table 30 and Figure 35), this was the p.Y139C polymorphism in samples from Southampton. A study by Rost *et al.* (2009) reported resistance in Gloucestershire (p.Y139C), Lincolnshire (p.Y139C) Norfolk (p.Y139C) and Shropshire (p.Y139S) in brown rats (Section 1.16). The results from this study are consistent with Rost *et al.* (2009) findings with the exception of Lincolnshire as previously discussed. However, this study also revealed additional polymorphisms found in brown rat samples in Gloucestershire and Shropshire (Table 30 and Figure 35). Samples tested in Gloucestershire and Shropshire also contained the p.L120Q and p.Y139C polymorphism, respectively (Table 30 and Figure 35). A study by Haniza *et al.* (2015) is the most recent report of anticoagulant resistance in the UK. Of the areas surveyed by Haniza *et al.* (2015) in the UK, 4 counties were surveyed within this study, these included; Berkshire, Gloucestershire, Hampshire and Oxfordshire. Similar to previous studies, Haniza *et al.* (2015) reported a p.L120Q and a p.Y139C polymorphism in Hampshire and p.Y139C polymorphism in Gloucestershire which are consistent with the polymorphisms found in these counties within this study (Table 30 and Figure 35). However, Haniza *et al.* (2015) reports of both p.Y139C and p.L120Q polymorphisms in Berkshire and p.Y139C polymorphisms only in Oxfordshire. These results contradict the present study as 100% of samples tested in both Berkshire and Oxfordshire contain the p.L120Q polymorphism only (Table 30 and Figure 35). The study by Haniza *et al.* (2015) also reports of 14 compound heterozygotes from 184 samples including a sample with a triple polymorphism; p.L120Q/p.Y139C/p.Y139S in Hampshire. Whereas, in this study only one sample from Sussex (Sample code AF2) contained a compound heterozygote p.L120Q and p.Y139C out of 146 samples (Figure 34e). As well as the high proportion of compound heterozygotes, there appears to be a high number of p.Y139C polymorphisms occurring in all 15 of the counties surveyed by Haniza *et al.* (2015), which is not consistent with the current study (Table 30 and Figure 35).

There are limitations to the study by Haniza *et al.* (2015). Only the anticoagulant resistance hotspots were sequenced using ARMS-PCR to identify the p.Y139C polymorphism and restriction fragment length polymorphisms (RFLP) to identify p.L120Q, p.L128Q and p.L128S. By only studying the 'hotspots' rather than sequencing whole exons, additional polymorphisms may have been missed, resulting in partially biased data towards the four known polymorphisms. Also, there is an overrepresentation of the p.Y139C polymorphism and may be due to false positive results. At the beginning of the project at the University of Huddersfield, ARMS-PCR and RFLP were used to identify anticoagulant resistance polymorphisms but was found to be unreliable and produced a high volume of false positives and therefore Sanger DNA sequencing was subsequently used (D. Clarke, Personal Communication, 2019).

3.1.3.2 VKORC1 Exon 3 Polymorphisms in Sweden

There have been many reports of anticoagulant resistance in brown rat populations throughout Europe, including Germany, France, Belgium and Denmark (Grandemange *et al.,* 2010; Baert *et al.,* 2012; Pelz *et al.,* 2005) (Section 1.16). However, there a no current reports of anticoagulant resistance in Sweden. In this study, brown rat samples were sequenced from 8 areas in Sweden for exon 3 of the VKORC1 gene and compared to the wild type sequence (NM_203335.2). Table 31 shows an overview of the polymorphisms found in exon 3 in brown rat samples for all the geographical areas surveyed in Sweden.

Geographical Area	N° of Specimens with SNPs	Codon	WT	Mut	AA WT	AA Mut
Jönköping	1	139	TAT	TGT	Tyr	Cys
Östergötland	1	139	TAT	TGT	Tyr	Cys
Skåne	1	128	CTG	CAG	Leu	Gln

Table 31: Overview of the polymorphisms found in exon 3 in brown rat samples for the geographical areas surveyed in Sweden.

From Table 31, 14% of Swedish brown rats tested contained an anticoagulant resistant polymorphism and 86% of brown rats were found to be wild type and showed no polymorphisms. Two samples from the two different counties Östergöland and Jönköping (Sample codes 112 and 415) contained a p.Y139C polymorphism and one sample contained a

p.L128Q polymorphism from Skåne (Sample code 803). Figure 36 shows the geographical map of Sweden with the representation of polymorphisms found in each county represented as pie charts.

The most common polymorphism found in Swedish brown rats was the p.Y139C polymorphism with a frequency of 10% (Table 31 and Figure 36). The p.Y139C polymorphism found in Swedish samples may have been acquired due to the close proximity to countries with reported resistance with this polymorphism, such as Germany and Denmark (Pelz *et al.* 2005). The least common polymorphism found in Swedish brown rats was the p.L128Q polymorphism with a frequency of 4% (Table 31 and Figure 36). The only other countries in Europe to report the p.L128Q polymorphism are in France (Grandemange *et al.,* 2010) and Scotland (This study).

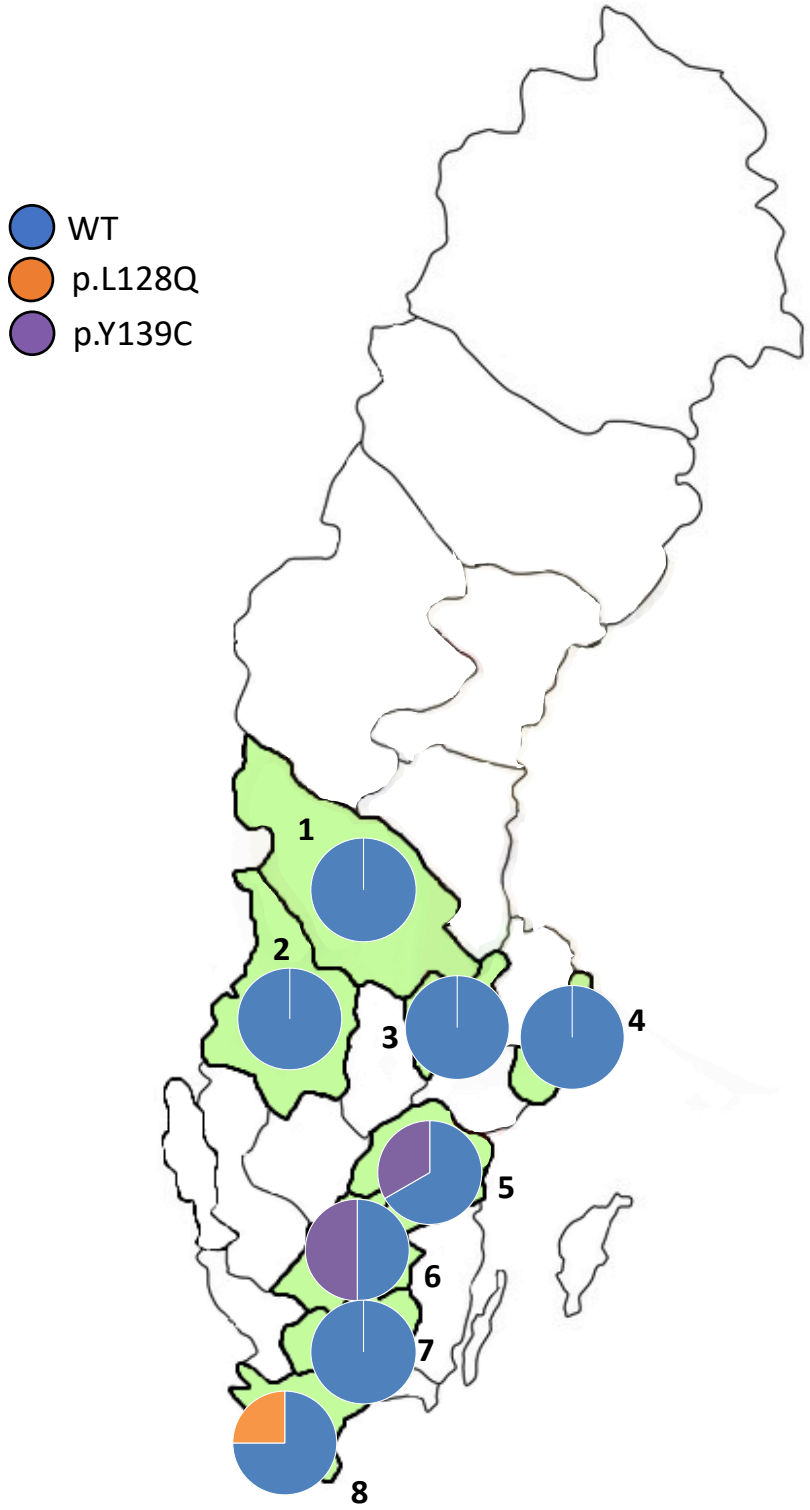


Figure 36: Map of Sweden highlighting the geographical distribution and proportion of anticoagulant resistant polymorphisms found in each county surveyed. **1** Dalarna (n=3), **2** Västergötland (n=1), **3** Västmanland (n=3), **4** Stockholm (n=2), **5** Östergöland (n=4), **6** Jönköping (n=3), **7** Kronoberg (n=2), **8** Skåne (n=4). Blue denotes wild type (WT). Orange denotes p.L128Q. Purple denotes p.Y139C.

3.2 Mitochondrial DNA Analysis of the UK and Sweden wild brown rats

To determine genetic relationships of brown rats in the UK and Sweden mtDNA D-loop sequencing haplotypes were compared to existing D-loop data by Song *et al.* (2014) and Haniza *et al.* (2015). Song *et al.* (2014) mapped the phylogeography of *Rattus norvegicus* using D-loop and cytochrome b sequences from brown rat samples from Europe excluding the UK, Asia, Africa and North America and compared mitochondrial variation of rats with resistant polymorphisms. Song *et al.* (2014) gave a comprehensive overview of D-loop haplotypes reporting 25 haplotypes and therefore these haplotypes were used to compare with the brown rat samples sequenced in this study. Haniza *et al.* (2015) used mtDNA to identify haplotypes specifically in populations of *Rattus norvegicus* in the UK in order to draw conclusions related solely to UK geographical population structure. The study by Haniza *et al.* (2015) is currently the only study to report on the haplotypes found within the UK and therefore was used to compare with the brown rat samples sequenced in this study. Also, both studies used different sequence lengths to determine D-loop haplotypes, therefore the D loop sequences from this study were compared to the haplotypes from Song *et al.* (2014) and Haniza *et al.* (2015) individually to ensure all possible haplotypes and differences in the brown rat samples from the UK and Sweden were identified. Due to the smaller D loop sequence length from the study by Haniza *et al.* (2015), the study did not reveal as many SNPs and was therefore less informative in comparison to the study by Song *et al.* (2014).

3.2.1 D-loop haplotypes found in UK and Sweden brown rats

To understand the genetic structure and phylogeography of the brown rat in the UK and Sweden, 110 out of a total of 151 UK and 16 out of a total of 22 Swedish brown rat samples were successfully sequenced for the mitochondrial D-loop sequence. Figure 37 and 38 shows the D loop haplotype median joining network (Section 2.18) for the UK and Swedish brown rat samples highlighting the haplotypes found in each county compared to haplotypes by Song *et al.* (2014). DNA sequences of novel haplotypes are found in Appendix 7.

There are three main haplotypes that are found in brown rat samples in the UK. These are D1, D5 and D12 (Figure 37). These haplotypes are found within the European clades identified by Song *et al.* (2014). The D1 haplotype has the lowest frequency within the UK with only 18% of brown rats having the D1 haplotype and is only found in six counties.

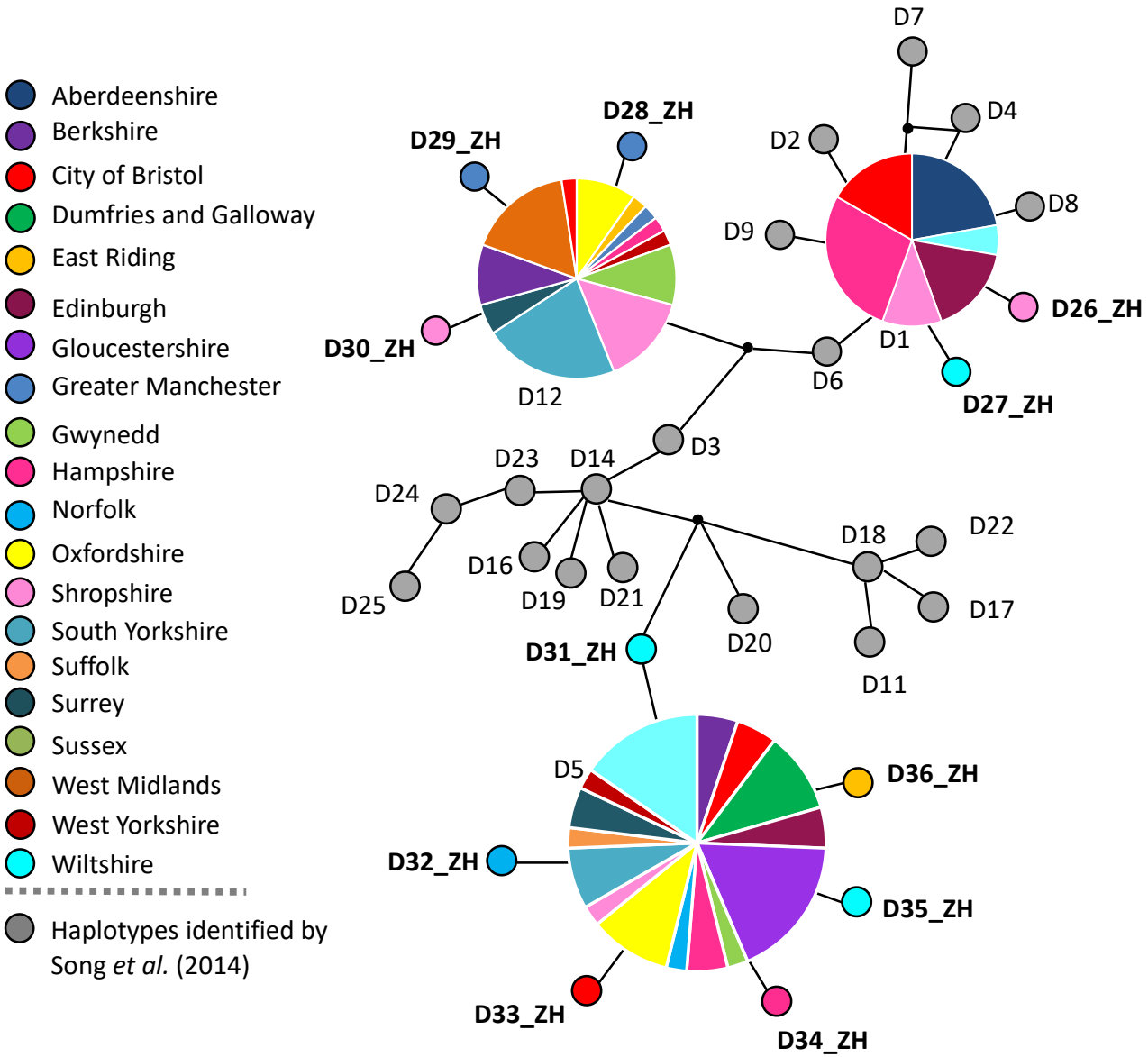


Figure 37: Median joining network of D-loop haplotypes found in brown rats in the UK in this study. Colours of pie charts indicate the county the haplotypes were identified in. Grey denotes haplotypes found by Song *et al.* (2014) but were not found in this present study. Bold DXX_ZH represents novel haplotypes found in this study where XX is the haplotype number.

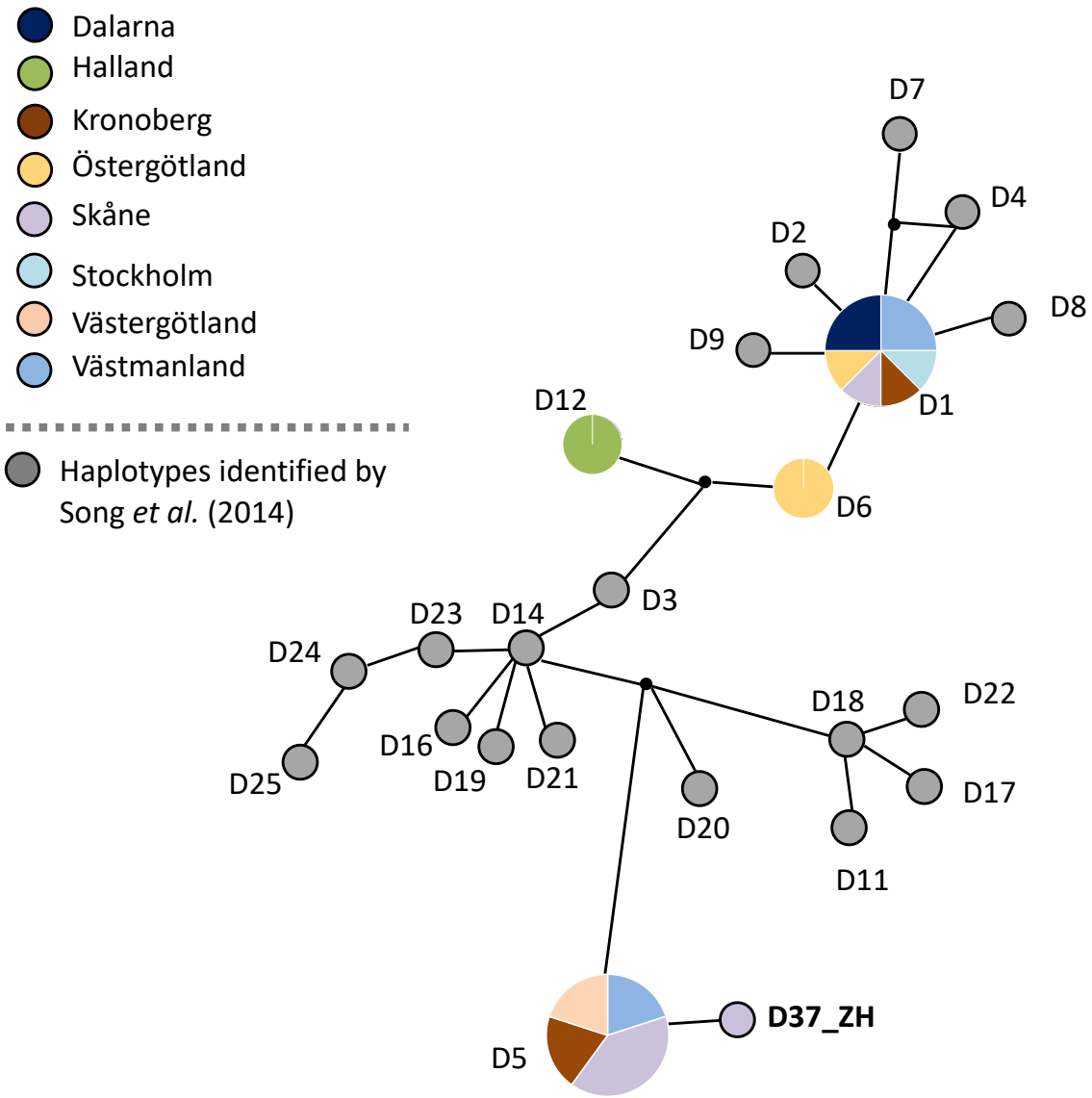


Figure 38: Median joining network of D-loop haplotypes found in brown rats in the Sweden in this study. Colours of pie charts indicate the county the haplotypes were identified in. Grey denotes haplotypes found by Song *et al.* (2014) but were not found in this present study. Bold DXX_ZH represents novel haplotypes found in this study where XX is the haplotype number.

These results are different to the findings by Song *et al.* (2014) in which D1 was identified in 52% of samples tested and found predominantly in France (n=11), Germany (112), USA (n=1) and French Polynesia (n=2). There were two novel haplotypes identified in this study which were related to the D1 haplotype. These were found in a sample from Shropshire (D26_ZH) and in a sample from Wiltshire (D27_ZH). The D5 haplotype previously identified in France, Germany, Sweden, Japan, Egypt and Society Islands (Song *et al.,* 2014) is also found in the UK and is the most widespread throughout the UK and is found in 15 counties (Figure 37). The D5 haplotype is found in 39% of UK samples. There were six novel haplotypes identified in this study which were related to the D5 haplotype. These were found in two samples from Wiltshire (D31_ZH and D35_ZH), a sample from Norfolk (D32_ZH), a sample from City of Bristol (D33_ZH), a sample from Hampshire, (D34_ZH) and a sample from East Riding (D35_ZH). The D12 haplotype is found in 41% of brown rats in the UK and is the most common haplotype found in the UK. The D12 haplotype was identified in one sample from Denmark in the study by Song *et al.* (2014). There was one novel haplotype identified in this study which is related to the D12 haplotype. This was found in a sample from Shropshire (D30_ZH).

There are four main haplotypes that are found in brown rat samples from Sweden. These are D1, D5, D6 and D12 (Figure 38). These haplotypes are found within the European clades identified by Song *et al.* (2014). The D1 haplotype was identified in 75% of brown rats from 6 areas. This is in contrast to the results for the UK, where D1 is the least frequent haplotype (Figure 37 and 38). As Sweden is part of mainland Europe, this may be a reason for the high frequency of this haplotype as the D1 haplotype is the most frequent in Europe (Song *et al.*, 2014). The D5 haplotype is found in 40% of samples in four areas and was the same as identified by Song *et al.* (2014) for the Swedish sample. There was one novel haplotype identified in this study which were related to the D5 haplotype. This was found in a sample from Skåne (D37_ZH). One sample had the D6 haplotype and another sample had the D12 haplotype.

Figure 39 and 40 shows the D loop haplotype network for the UK and Swedish brown rat samples highlighting the haplotypes found in each country compared to haplotypes by Haniza *et al.* (2015). Haniza *et al*. (2015) identified six haplotypes in UK brown rats. In the UK samples from this study, only three haplotypes were identified, RNH1, RNH2 and RNH3 and one novel

haplotype found in Wiltshire (D31_ZH). Other novel haplotypes found in Figure 39 are hidden when analysed against data by Haniza *et al.* (2015) and are identified as either RNH1, RNH2 or RNH3. This is due to the shortened mtDNA D-loop sequences used. Haniza *et al.* (2015) used a shorter nucleotide sequence of 333, whereas Song *et al.* (2014) used a nucleotide sequence of 625. This results in loss of novel haplotypes and DNA changes between brown rat samples. There were 7 counties in which were surveyed by this study and Haniza *et al.* (2015). Table 32 shows the haplotypes identified by this study and Haniza *et al.* (2015) in the 7 counties in the UK.

County	Haplotypes identified by Haniza *et al.* (2015)	Haplotypes identified in this study
Berkshire	RNH1, RNH2, RNH4, RNH6	RNH1, RNH2
Gloucestershire	RNH1, RNH2	RNH1
Hampshire	RNH1	RNH2, RNH3
Oxfordshire	RNH1, RNH2	RNH1, RNH2
Sussex	RNH1, RNH2	RNH1
Wiltshire	RNH1, RNH2, RNH5	RNH1, RNH3, D31_ZH
Yorkshire	RNH1, RNH2	RNH1, RNH2

Table 32: Haplotypes identified for counties surveyed by this study and Haniza *et al.* (2015). Red denotes haplotypes which are unique to the respective study.

In general, the haplotypes identified in this study were similar to those identified by Haniza *et al.* (2015) in the counties that overlapped between the two studies. The haplotypes identified in Oxfordshire and Yorkshire were the same, RNH1 and RNH2.

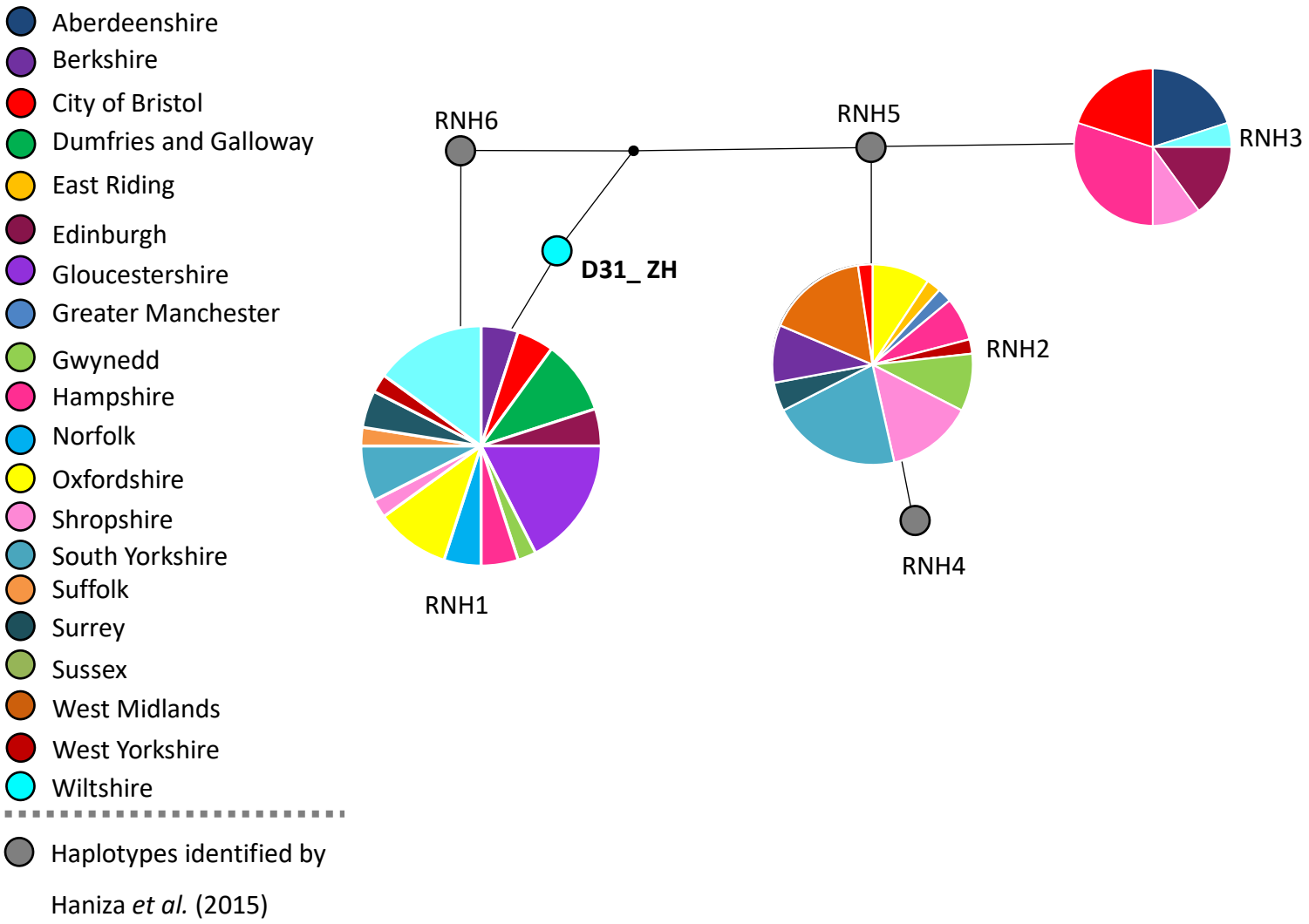


Figure 39: Median joining network of D-loop haplotypes found in brown rats in the UK in this study. Colours of pie charts indicate the county the haplotypes were identified in. Grey denotes haplotypes found by Haniza *et al.* (2015) but were not found in this present study. Bold DXX_ZH represents novel haplotypes found in this study where XX is the haplotype number.

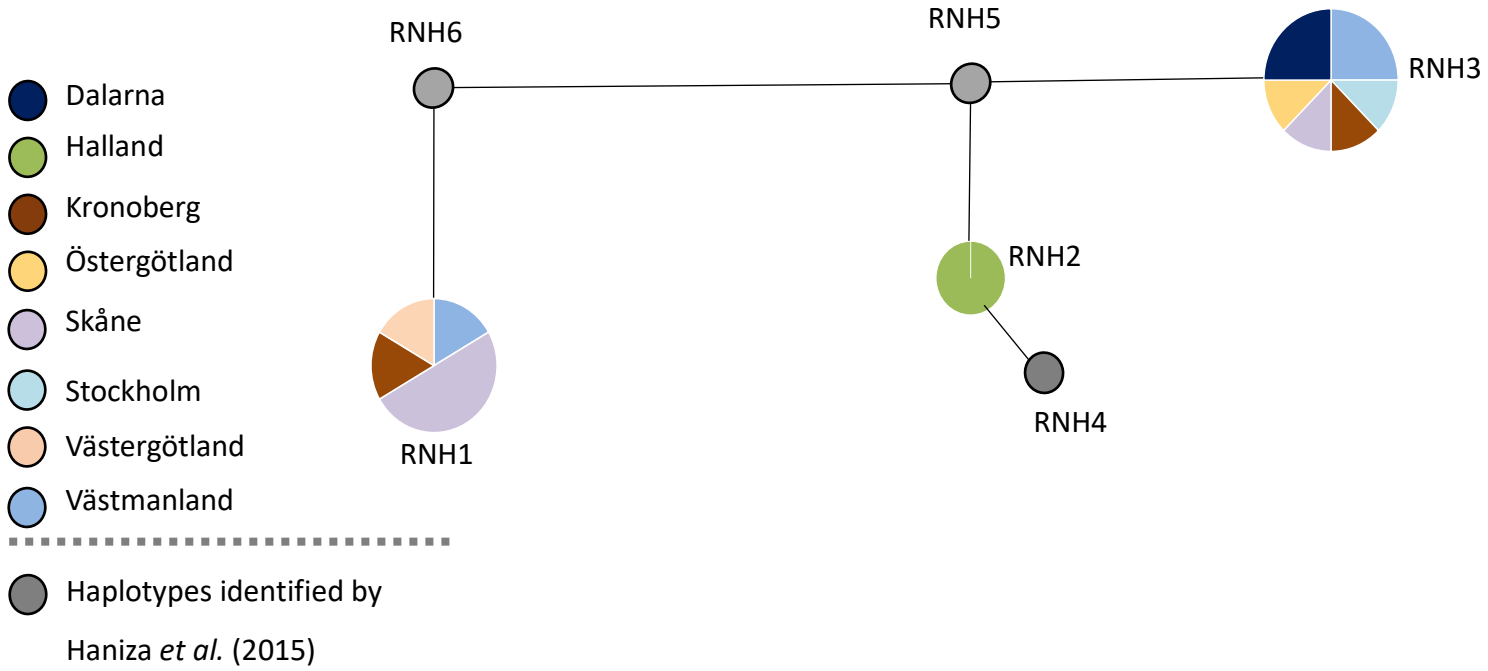


Figure 40: Median joining network of D-loop haplotypes found in brown rats in the Sweden in this study. Colours of pie charts indicate the county the haplotypes were identified in. Grey denotes haplotypes found by Haniza *et al.* (2015) but were not found in this present study. Bold DXX_ZH represents novel haplotypes found in this study where XX is the haplotype number.

However, in Hampshire Haniza *et al*. (2015) reported a RNH1 haplotype whereas in this study only a RNH2 and RNH3 haplotype was identified. In Berkshire, Haniza *et al.* (2015) identified additional haplotypes RNH4 and RNH6, whereas in this study only RNH1 and RNH2 were found.

Like the brown rats in the UK, in Sweden only three haplotypes were identified, RNH1, RNH2 and RNH3. Novel haplotypes that were found in the analysis against Song *et al.* (2014) are lost when analysed against data by Haniza *et al.* (2015) and are identified as either RNH1, RNH2 or RNH3.

3.2.2 D-loop haplotypes found in UK and Swedish brown rats and the relationship to known anticoagulant resistance polymorphisms

To determine if there is a relationship between the D-loop haplotypes and anticoagulant resistance genotypes a D-loop haplotype network was created for the UK and Swedish brown rat samples highlighting the anticoagulant resistance polymorphisms associated with the samples within haplotypes compared to haplotypes by Song *et al.* (2014) (Figure 41). The results show that certain polymorphisms appear to be associated with specific haplotypes. In the D1 haplotype, >50% of brown rats contain a p.L128Q polymorphism. ~50% of brown rat samples including those associated with the haplotype have a p.L120Q polymorphism in the D5 haplotype and ~50% of brown rat samples that are wild type are found in the D12 haplotype. The p.Y139S polymorphism is only found within the D1 haplotype. The results by Song *et al*. (2014) focused on the p.Y139C mainly on German samples and the relationship to different haplotypes. Song *et al.* (2014) showed that there was no direct correlation but noted that the majority of brown rat samples with the p.Y139C polymorphism was associated with the D1 haplotype. Contrary to the results by Song *et al.* (2014), the current study shows that the p.Y139C polymorphism was not found in any samples with the D1 haplotype but only in samples with the D5 or D12 haplotype. The only polymorphism that is found across all D loop haplotypes is the p.L120Q. The p.R40G and p.S79F polymorphisms were excluded because at the time of analysis these polymorphisms are not definite resistance polymorphisms. However, the p.R40G polymorphism in UK samples has a D5 haplotype and in the Swedish sample it has a D1 haplotype. The p.S79F polymorphism is contained within the novel D33_ZH haplotype, which is related to the D5 haplotype.

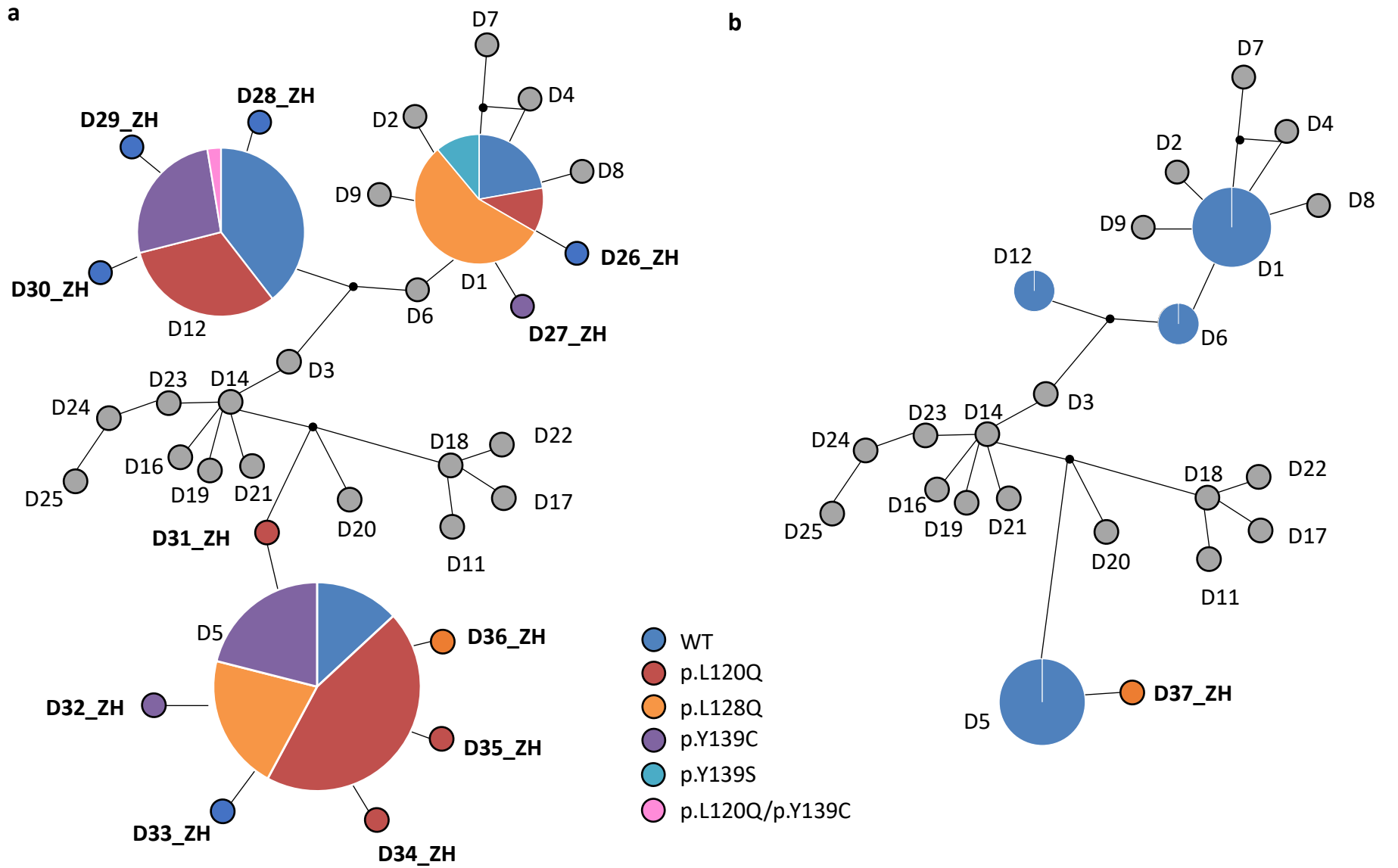


Figure 41: Median joining network of D-loop haplotypes found in brown rats in (a) UK and (b) Sweden and the relationship of anticoagulant resistance polymorphisms. Colours of pie charts indicate the anticoagulant resistant polymorphisms. Grey denotes haplotypes found by Song *et al.* (2014) but were not found in this present study. Bold DXX_ZH represents novel haplotypes found in this study where XX is the haplotype number.

3.3 Computational Analysis of the Novel p.R40G Polymorphism found in the UK and Sweden wild brown rats

3.3.1 Multiple Sequence Alignment of Vertebrate VKORC1 to assess the evolutionary conservation of R40 position

Multiple sequence alignments can be used to determine the conservation of a particular amino acid across different animals to assess the importance through evolution. In order to assess the significance of the p.R40G polymorphism discovered in this study (Section 3.1) an alignment was created to compare position 40 throughout representative VKORC1 sequences throughout vertebrates (Figure 42). The arginine at position 40 is highly conserved and only differs in amphibian VKORC1 sequences, where a threonine is found. Due to the high conservation of charged or polar residues at this position a change to a glycine may have an effect on the ability for anticoagulants to bind to VKORC1 effectively.

3.3.2 Membrane topology and tertiary prediction modelling of the wild type brown rat VKORC1 and the p.R40G mutant

Secondary and tertiary structure prediction can help to understand how polymorphisms can have an effect on the structure of a protein. Preliminary structural models were performed for wild type brown rat VKORC1 and the p.R40G mutant using TMHMM for a membrane topology prediction model. For the tertiary prediction, models were created using SWISS-Model based on the original structure of the bacterial homologue *Synechococcus sp.* VKORC1 determined by x-ray crystallisation (PDB. 3KP9) (*Li et al.,* 2010) and then Chimera was used for visualisation of the models. Figure 43 shows the prediction of the membrane topology and tertiary structures of wild type brown rat VKORC1 and the p.R40G mutant.

From the TMHMM prediction, both wild type brown rat and p.R40G mutant VKORC1 structures contained 3 TM domains and the orientation of the protein is the same, the N terminus is on the outside of the ER membrane and the C terminus is in the inside of the ER lumen, as is the large loop between TM1 and TM2 (Figure 43).

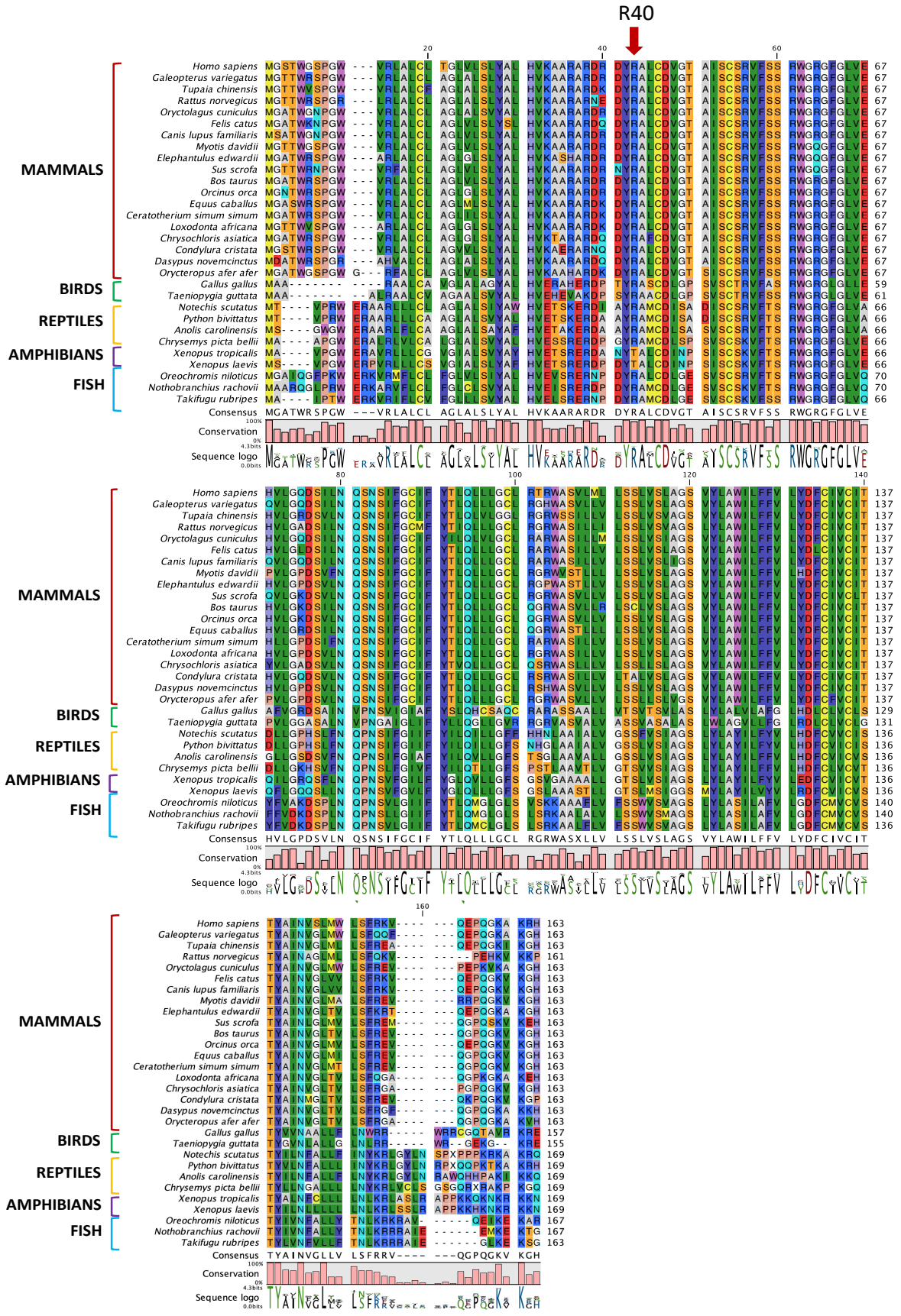


Figure 42: Multiple sequence alignment of representative vertebrate VKORC1 sequences. Red line denotes Mammalian sequences. Green line denotes bird sequences. Yellow line denotes reptile sequences. Purple line denotes amphibian sequences. Blue line denotes fish sequences. Colours of amino acids are according to physiochemical properties, refer to Appendix 8.

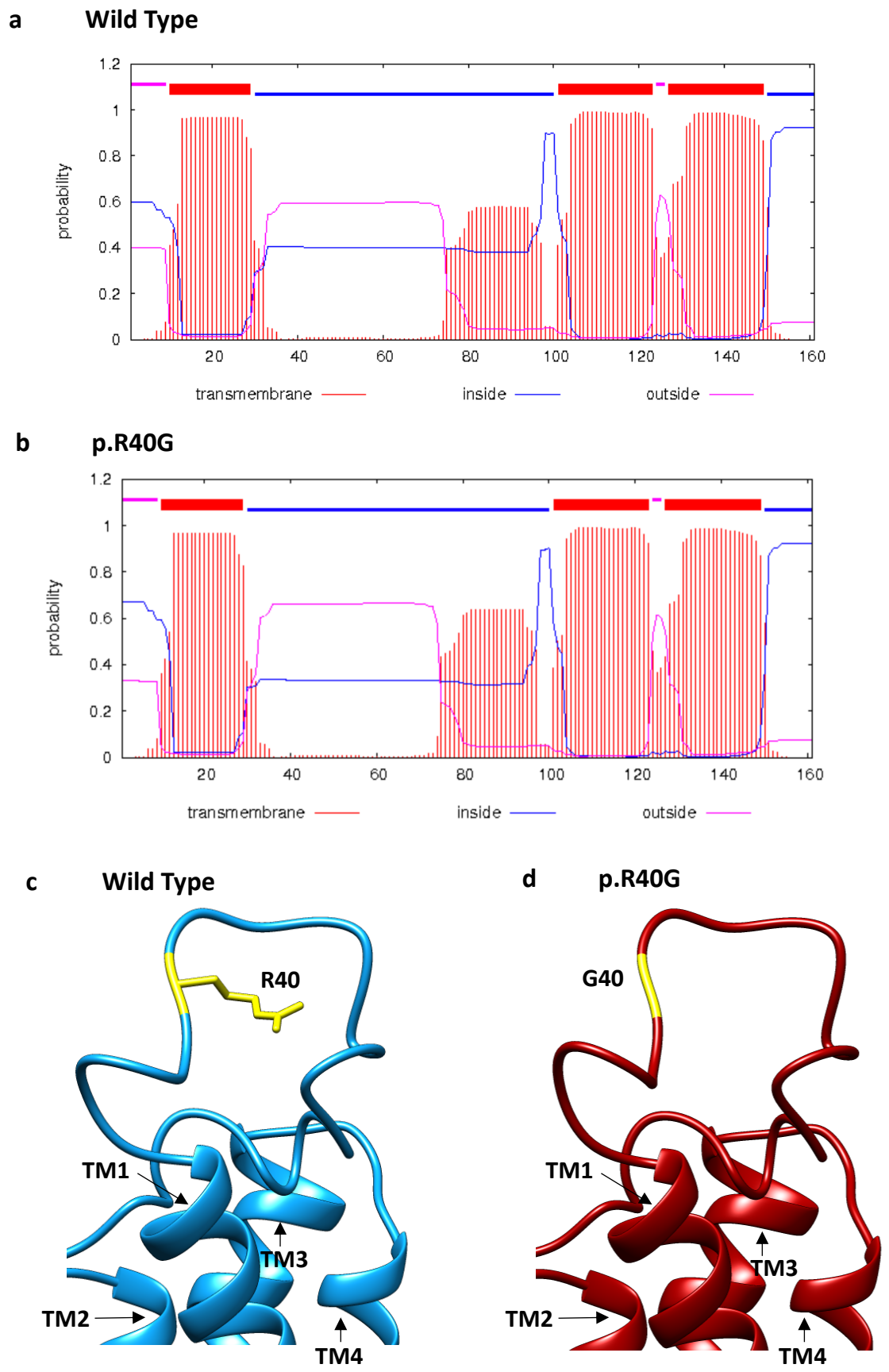


Figure 43: TMHMM prediction graph and 3D model prediction using SWISS-Model and Chimera for wild type brown rat VKORC1 and p.R40G mutant. a Wild Type brown rat VKORC1 TMHMM prediction. **b** p.R40G VKORC1 TMHMM prediction. **c** Wild Type brown rat VKORC1 3D model highlighting the arginine at position 40. **d** p.R40G VKORC1 3D model highlighting the glycine at position 40.

As the arginine at position 40 is found in the large loop and not in a transmembrane domain the results from the TMHMM prediction are as expected. There is no change in transmembrane prediction between the wild type brown rat and p.R40G mutant (Figure 43a and 43b). The TMHMM prediction models show a 4 TM domain structure for both VKORC1 sequences (Figure 43). The prediction of the models is based on the original structure of the bacterial homologue *Synechococcus sp.* VKORC1 by Li *et al.* (2010). As this is the only defined structure for any VKORC1, all models based on this structure by Li *et al.* (2010) will show a 4 TM prediction. Figure 43c and 43d show the wild type brown rat and the p.R40G mutant VKORC1 structure, respectively, highlighting the amino acid change at position 40. From the tertiary prediction it shows that a change at position 40 from an arginine to a glycine does not have an impact on the structure but may have a potential effect on the binding of anticoagulant rodenticides due to the missing positively charged side group of the arginine.

3.4 Expression of Recombinant VKORC1 Enzymes for Functional Analysis of the Novel p.R40G VKORC1 Polymorphisms

In order to biochemically characterise and assess the effect of anticoagulant rodenticides such as flocoumafen, the recombinant wild type rat VKORC1 and variant p.R40G VKORC1 constructs were created and expressed using a baculovirus expression system. A previously published resistance polymorphism, p.L120Q was chosen to be expressed as a control for comparison.

The brown rat VKORC1-pFB-LIC-Bse construct containing the wild type VKORC1 cDNA was generated following the methods by Savitsky *et al.* (2010) with modifications stated in Section 2.6. To obtain the rat VKORC1 with p.L120Q or p.R40G polymorphism, site directed mutagenesis was used to modify the rat VKORC1-pFB-LIC-Bse construct (Section 2.7). Figure 44 shows the DNA sequencing electrophoretograms of rat VKORC1 with the novel p.R40G polymorphism after site directed mutagenesis. The results show correct nucleotides were incorporated at this position. Examination of the entire VKORC1 cDNA revealed no other changes were incorporated in the mutagenized DNA sequence (data not shown).

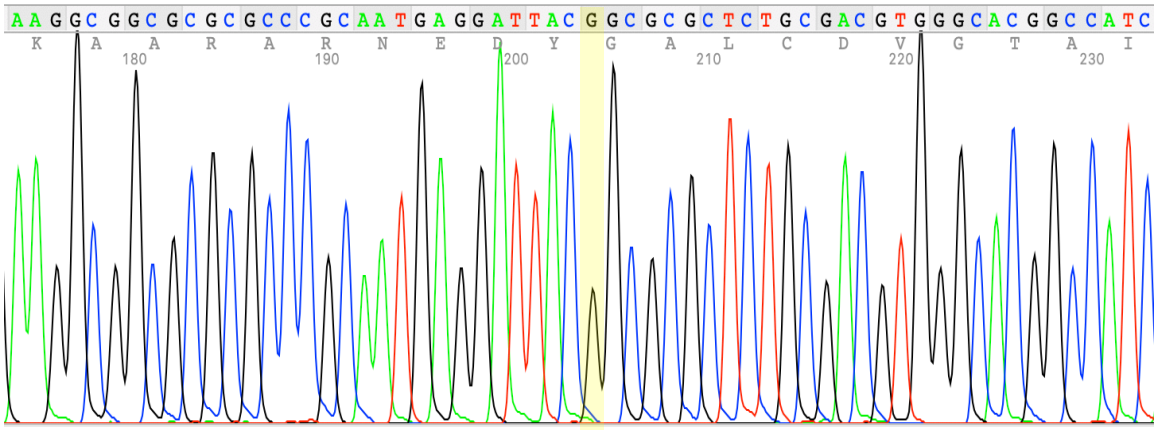


Figure 44: DNA sequencing electrophoretograms of rat VKORC1 with the novel p.R40G polymorphism after site directed mutagenesis.

The recombinant rat, p.L120Q and p.R40G VKORC1 constructs were expressed in *Sf9* cells. Figure 45 shows an example of the cell micrographs of *Sf9* cells before and after transfection for p.L120Q VKORC1 constructs compared to the untransfected controlled *Sf9* cells.

Before transfection the cells are small and round in morphology, whereas after transfection at 72 hours changes in cell density and changes in cell morphology are seen in comparison to the untransfected control (Figure 45). The untransfected control shows a high density of small cells and is around 90% confluence, whereas in the transfected p.L120Q cell images it shows less confluency and changes to the cell morphology and increase in cell size. These changes are consistent with the findings of Üstün-Aytekin *et al.* (2014) which shows an opposing relationship of a decrease in cell density with the increase of infection in *Sf9* cells and that cell density, cell size and change in morphology are a sign of infection (Üstün-Aytekin *et al.,* 2014).

After expression of all rat recombinant DNA constructs in *Sf9 cells*, microsomes were produced according to methods in Section 2.15 ready for the VKORC1 assay.

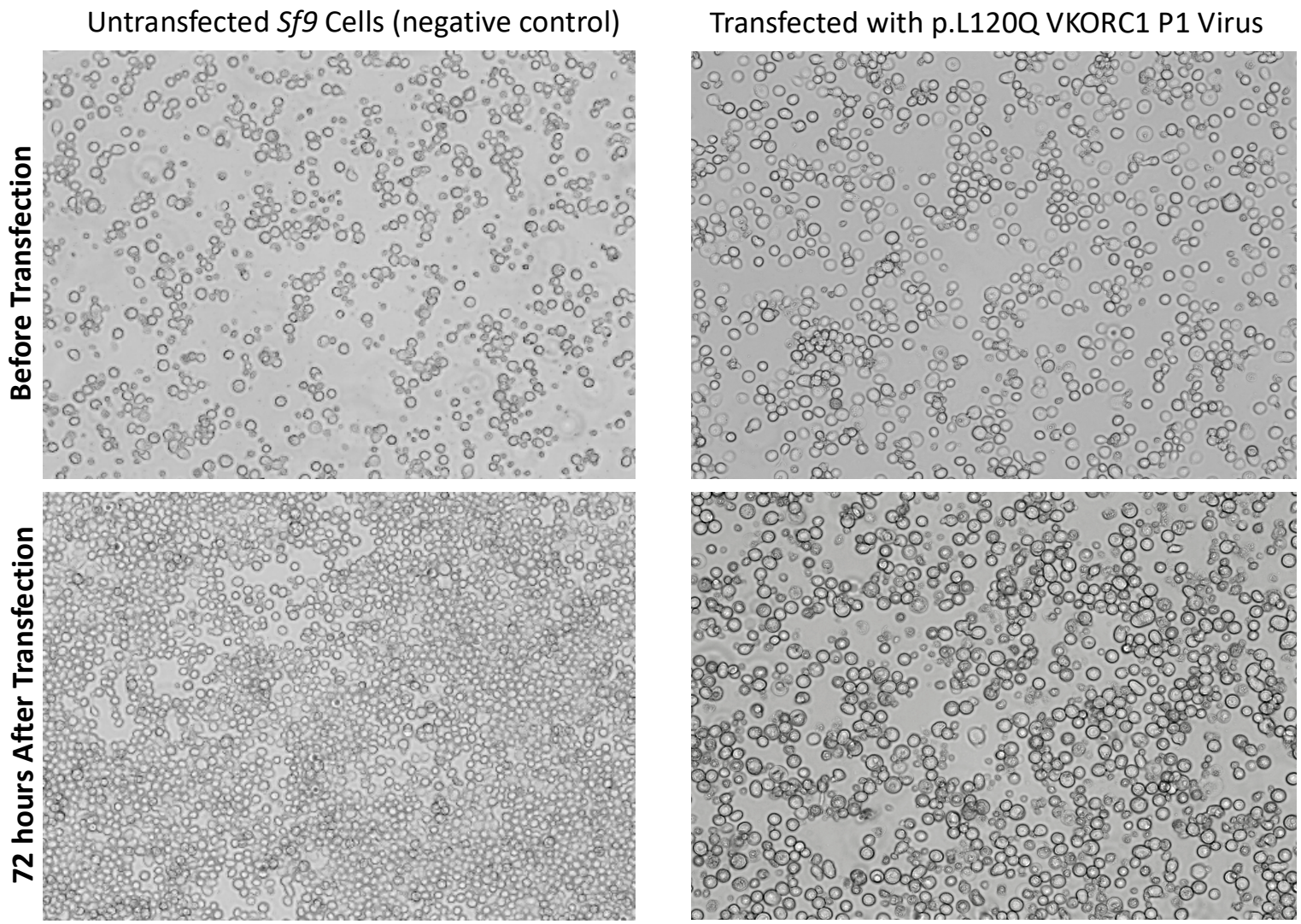


Figure 45: Cell micrograph of *Sf9* cells before transfection and 72 hours after transfection with P1 virus to produce P2 virus.

3.5 Organic Synthesis of VKE

Vitamin K epoxide was synthesised in order to produce the substrate for the VKORC1 assay using vitamin K by methods described by Thierry-Palmer (1984) (Section 2.11). To confirm the correct synthesis of vitamin K epoxide both vitamin K and the newly synthesised vitamin K epoxide were analysed using HPLC (Figure 46), HPLC UV spectra (Figure 47) and mass spectrometry (Appendix 9). The retention time for vitamin K epoxide was 2.3 minutes and vitamin K was 3.2 minutes and there was no trace of the 3.2 minute vitamin K peak in the vitamin K epoxide chromatogram. The peak separation is expected between vitamin K epoxide and vitamin K due to the difference in physiochemical characteristics.

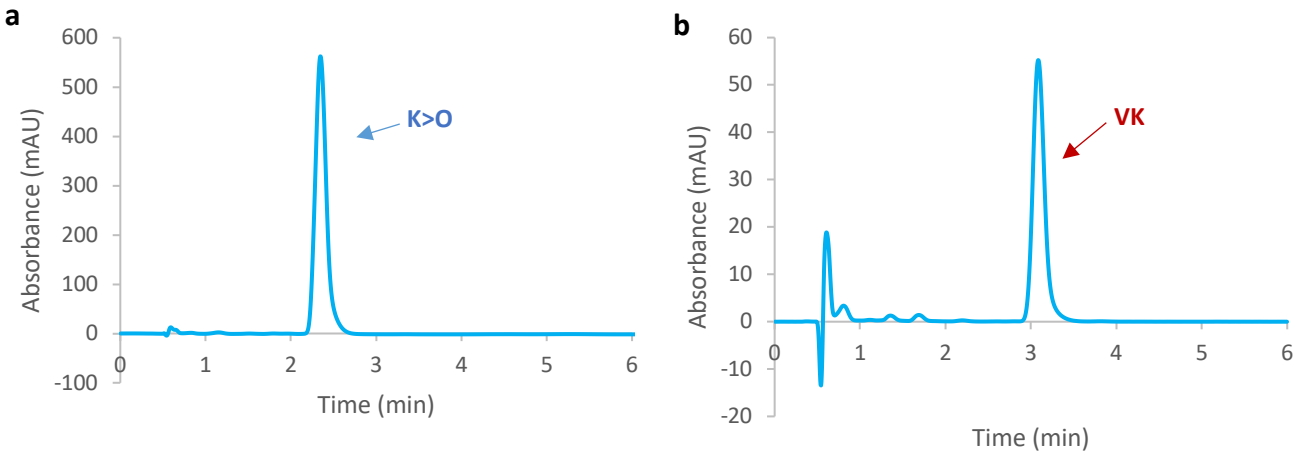


Figure 46: HPLC chromatograms for synthesised vitamin K epoxide and vitamin K at a volume of 20 µl at 10 µM for both compounds at 246 nm detection wavelength. a Synthesized vitamin K epoxide using UV detection. **b** Vitamin K using UV detection.

Individual compounds can produce a unique absorbance spectra, so this was used verify the identity of the peaks shown by HPLC analysis by comparing with published data for the compounds (Thierry-Palmer, 1984). Spectra obtained during this study was compared against reference wavelength patterns found in Matschiner *et al.* (1970) and Thierry-Palmer (1984) and was consistent with the wavelength patterns in the published literature. Vitamin K had absorbance peaks at 200, 250, 270, 280 and 330 nm and vitamin K epoxide had absorbance peaks at 230, 260 and 310 nm (Figure 47).

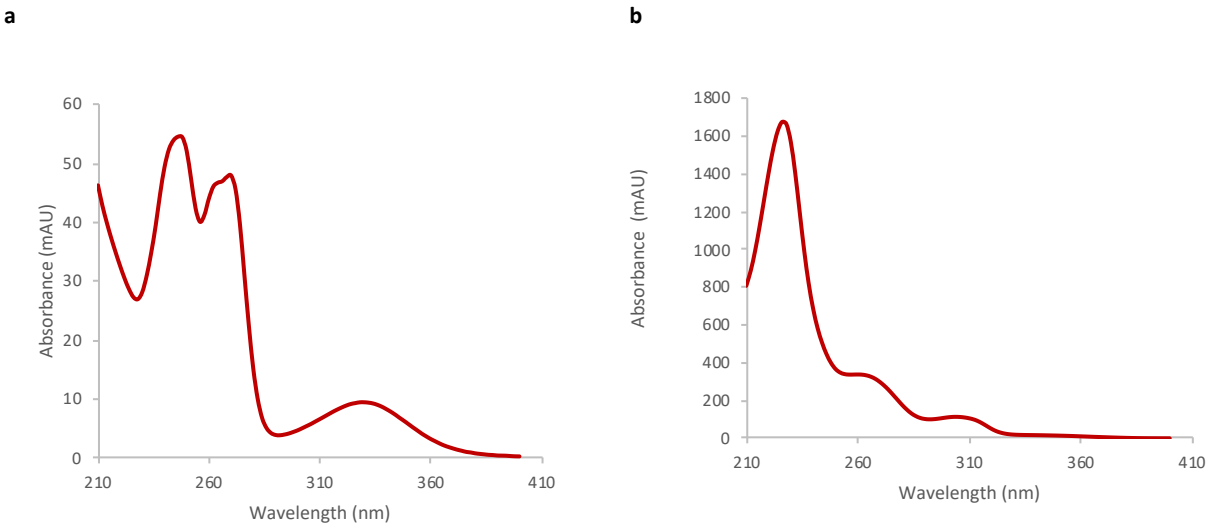


Figure 47: UV spectrum of vitamin K and synthesized vitamin K epoxide both with a concentration of 10 µM. **a** UV spectrum of vitamin K. **b** UV spectra of synthesised vitamin K epoxide.

The synthesised vitamin K epoxide and the vitamin K were also analysed using mass spectrometry (Appendix 9). From the mass spectrometry data, the vitamin K epoxide peak had a $[M+H]^+$ of 467.4 (Appendix 9), giving vitamin K epoxide a final mass of 466.4. The $[M+H]^+$ of the vitamin K peak was 451.4 (Appendix 9) and therefore the mass final of vitamin K was 450.4. These mass values are consistent with the mass spectrometry data for vitamin K and vitamin K epoxide found in Osman and Hannestad (2008). The UV spectra and the mass spectrometry data for the synthesised vitamin K epoxide therefore confirmed that vitamin K epoxide had been successfully synthesised.

3.6 Biochemical Characterisation of VKORC1

3.6.1 Characterisation of VKORC1 in Rat liver Microsomes

Rat liver microsomes were used as a control before experiments with recombinant enzymes were conducted. Activity of VKOR was assessed in rat liver microsomes following the dithiothreitol (DTT)-driven methods of Wallin and Martin (1985) (Figure 48).

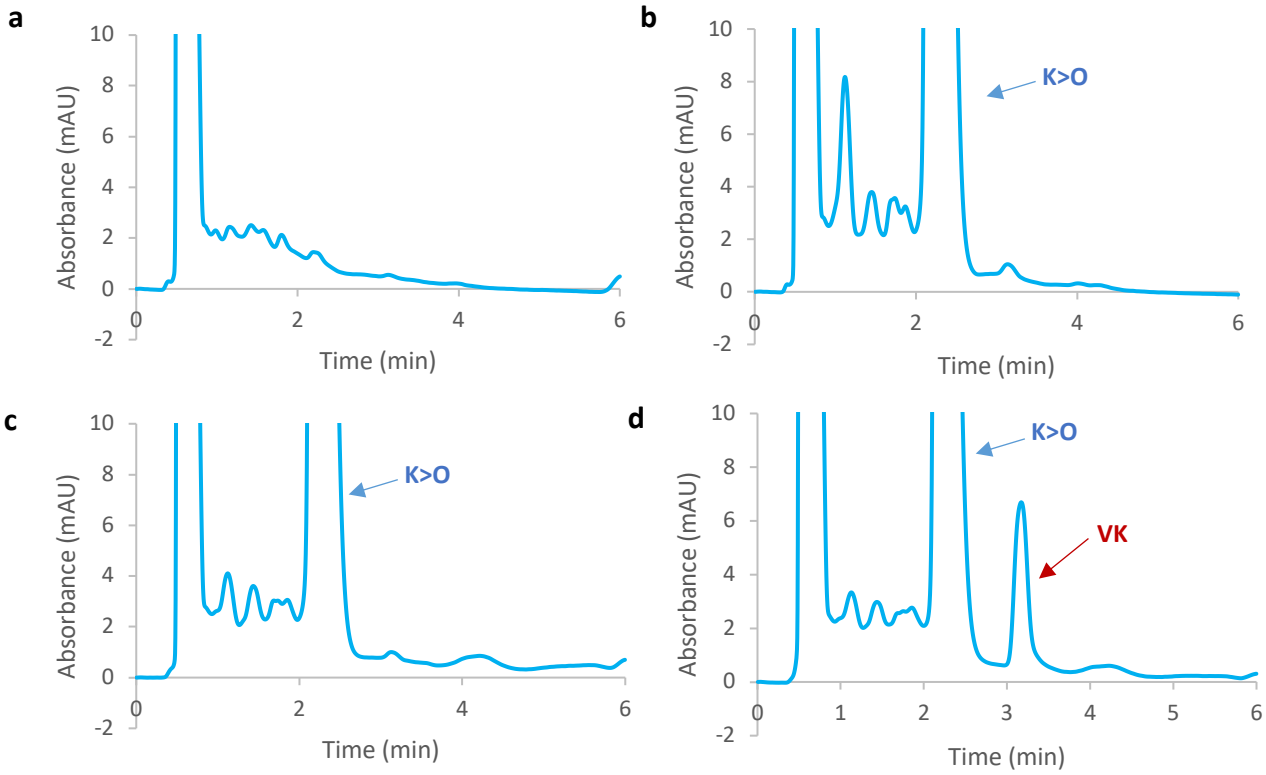


Figure 48: HPLC chromatograms of the VKOR assay with 2 mg of rat liver microsomes after 30 minutes with control reactions using 100 µM of vitamin K epoxide (K>O). a Control incubation with rat liver microsomes but without substrate, using UV detection. **b** Control incubation without rat liver microsomes added using UV detection. **c** 0 minute incubation using UV detection. **d** 30 minute incubation using UV detection.

In the control VKOR assays, there were no detectable background presence of vitamin K epoxide and vitamin K in the VKOR assay when no substrate was added to the reaction (Figure 48a). Control VKOR assays were also performed in which vitamin K epoxide substrate was added to a reaction with no rat liver microsomes added (Figure 48b). This resulted in no production of vitamin K. Figure 48c shows the chromatogram of VKOR activity at 0 minute incubation with both vitamin K epoxide substrate and rat liver microsomes with no vitamin K being formed. Figure 48d show a typical chromatogram after a 30 minute incubation with vitamin K epoxide. The chosen DTT-driven method has been used in previous studies to characterise *Rattus norvegicus* polymorphisms (Hodroge *et al.,* 2011; Lasseur *et al.,* 2005). Studies that use the baculovirus expression system also use the DTT-driven method (Chu *et al.,* 2006; Li *et al.,* 2004; Jin *et al.,* 2007) and therefore, this was the chosen method to assess recombinant rat VKORC1 and its polymorphisms.

3.6.2 Testing of Recombinant VKORC1 Constructs for Active Protein

The DTT-driven VKORC1 HPLC assay (Section 2.17) was conducted to observe the production of vitamin K by recombinant VKORC1s. HPLC chromatograms are shown at zero and 30 minutes for the untransfected *Sf9* and rat VKORC1 and rat VKORC1 mutants p.L120Q and p.R40G expressed in *Sf9* cells (Figure 49).

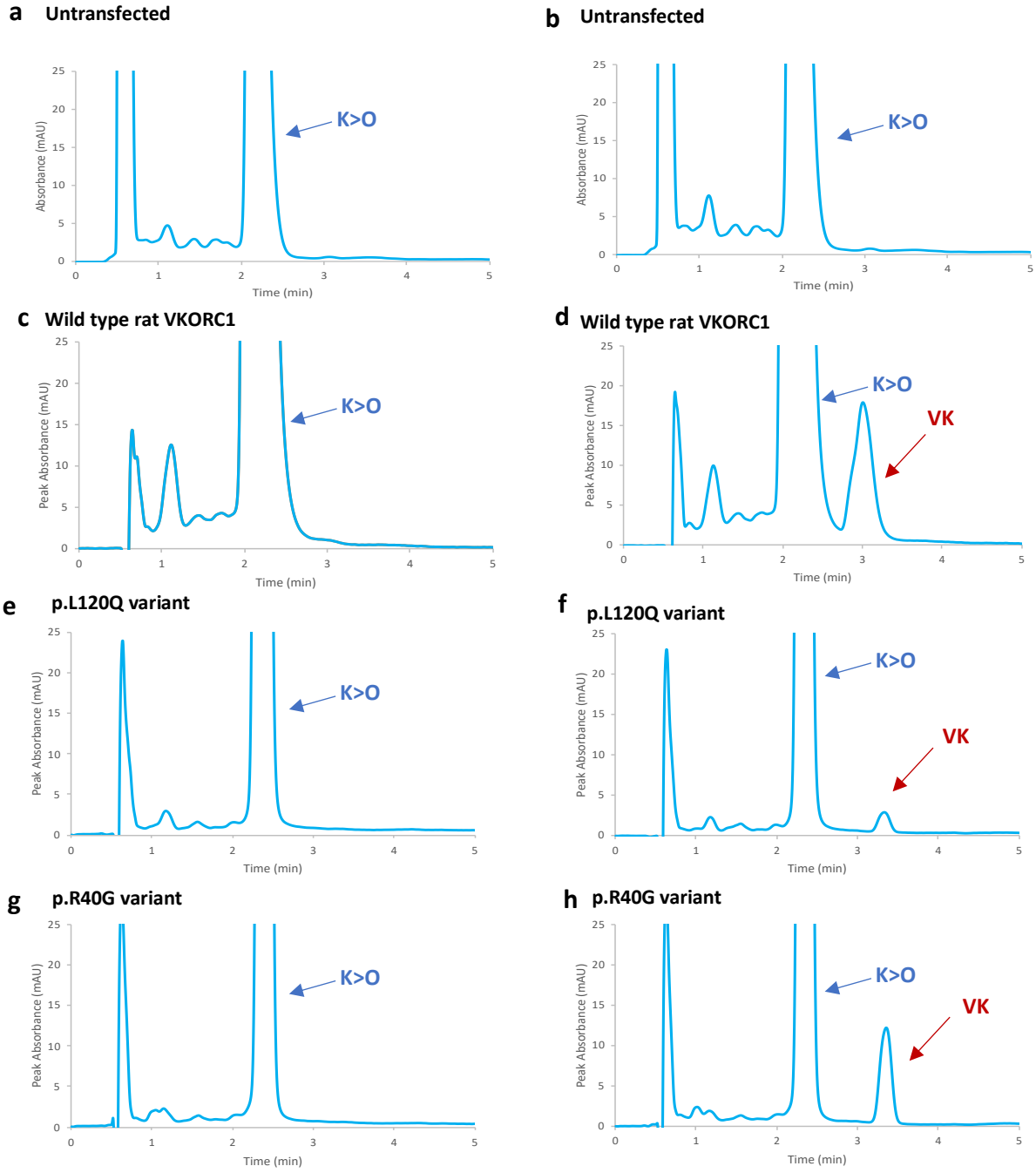


Figure 49: HPLC chromatograms showing the vitamin K production from untransfected *Sf9* cells, recombinant rat VKORC1 and p.L120Q and p.R40G variants expressed in *Sf9* insect cells at 0 and 30 minute incubations at 50 μM of vitamin K epoxide. a, c, e and g 0 minute incubations of untransfected, wild type rat, and p.L120Q and p.R40G variants respectively**. b, d, f and h** 30 minute incubations of untransfected, wild type rat and p.L120Q and p.R40G variants respectively.

Figure 49 shows that wild type rat VKORC1 and rat VKORC1 mutants p.L120Q and p.R40G were expressed in *Sf9* cells successfully and had active VKORC1 protein. The untransfected cells have no background VKORC1 activity due to no detectable vitamin K peak after 30 minutes, which is consistent with results from Li *et al.* (2004) and Chu *et al.* (2006).

3.7 Investigation of Enzyme Kinetics of Recombinant VKORC1s

To determine if the p.R40G polymorphism affected the enzyme kinetics of rat VKORC1, the affinity constant, K_m was determined for the vitamin K epoxide substrate for wild type and p.R40G mutant VKORC1 (Figure 50). The K_m and V_{max} values for rat VKORC1 and the mutant p.R40G is listed in Table 33.

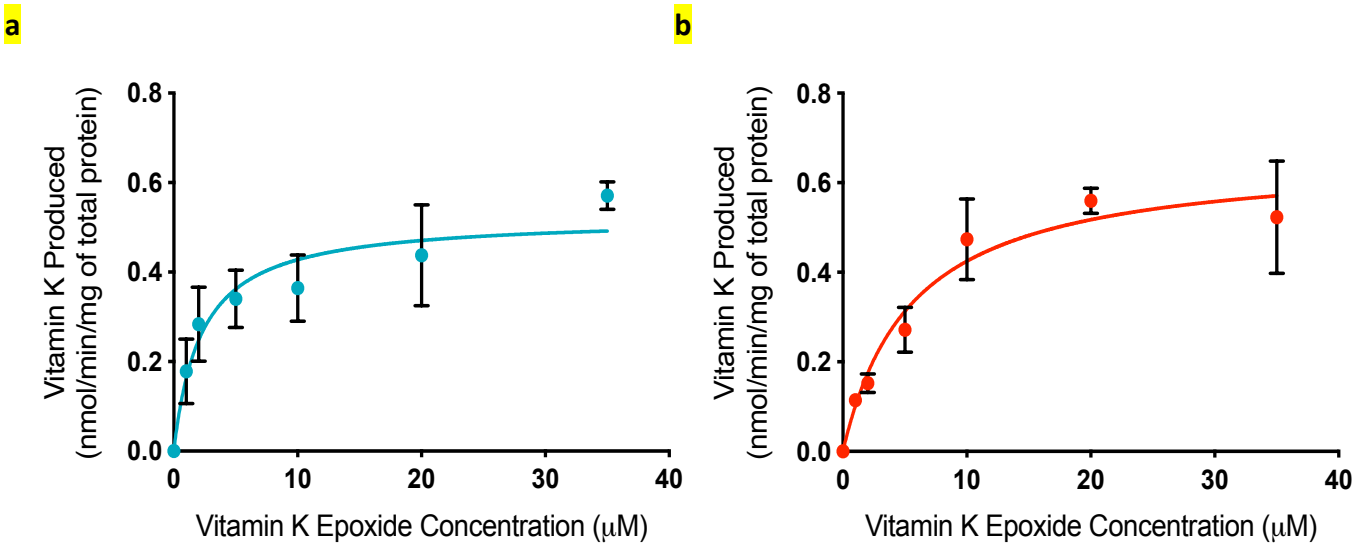


Figure 50: Kinetic analysis of wild type rat VKORC1 and rat VKORC1 with p.R40G polymorphism expressed in *Sf9* cells. Michaelis-Menten graph of **a** wild type rat VKORC1 and **b** p.R40G VKORC1 mutant rat VKORC1. Experiments were performed in triplicate and values are shown as mean and standard deviation.

	K_m (μM)	V_{max} (nmol min^{-1} mg^{-1})
WT	2.23 ± 0.67	0.52 ± 0.038
p.R40G	5.58 ± 1.36	0.66 ± 0.051

Table 33: K_m and V_{max} values derived from Michaelis-Menten graphs of wild type rat VKORC1 and rat VKORC1 with p.R40G polymorphism expressed in *Sf9* cells. Experiments were performed in triplicate and values shown as mean and standard deviation.

The graphs for the recombinant VKORC1 constructs followed Michaelis-Menten kinetics and followed a rectangular hyperbola shape (Figure 50). The wild-type rat VKORC1 has a K_m of 2.23 ± 0.67 μM (Table 33). Hodroge *et al.* (2011) previously expressed recombinant rat VKORC1 using a *Pichia pastoris* expression system and obtained a K_m value of 7.2 ± 2.5 μM (Table 33). There is a 3-fold difference between the results in this study and the results obtained by Hodroge *et al.* (2011) that may be due to the microsomal membrane composition being different in the more primitive fungi expression system they used. The wildtype rat VKORC1 has lower K_m compared to its mutant p.R40G. The K_m for the mutant p.R40G rat VKORC1 is increased by 2.5-fold. This suggests that wild type rat VKORC1 has a stronger affinity for vitamin K epoxide compared to the p.R40G mutant. The result obtained for the p.R40G VKORC1 reflect Matagrin *et al.* (2013) who obtained higher K_m values for rat VKORC1 resistance polymorphisms (p.L120Q, p.L128Q, p.Y139C, p.Y139F and p.Y139S).

3.8 Effect of Anticoagulant Rodenticides on wild type and variant rat VKORC1s

Preliminary experiments were undertaken with the first generation anticoagulant, warfarin and a second generation anticoagulant, bromadiolone to assess the effects of a range of concentrations (between 1-100 μM) of these compounds on the wild-type rat VKORC1 and mutated p.L120Q and p.R40G rat VKORC1 (Figure 52). An example of the HPLC chromatograms for 1 μM of warfarin and bromadiolone for wild type VKORC1 and p.L120Q and p.R40G variants are shown in Figure 51. Table 34 shows the statistical values from the 2-way ANOVA for the conditions tested from Figure 52.

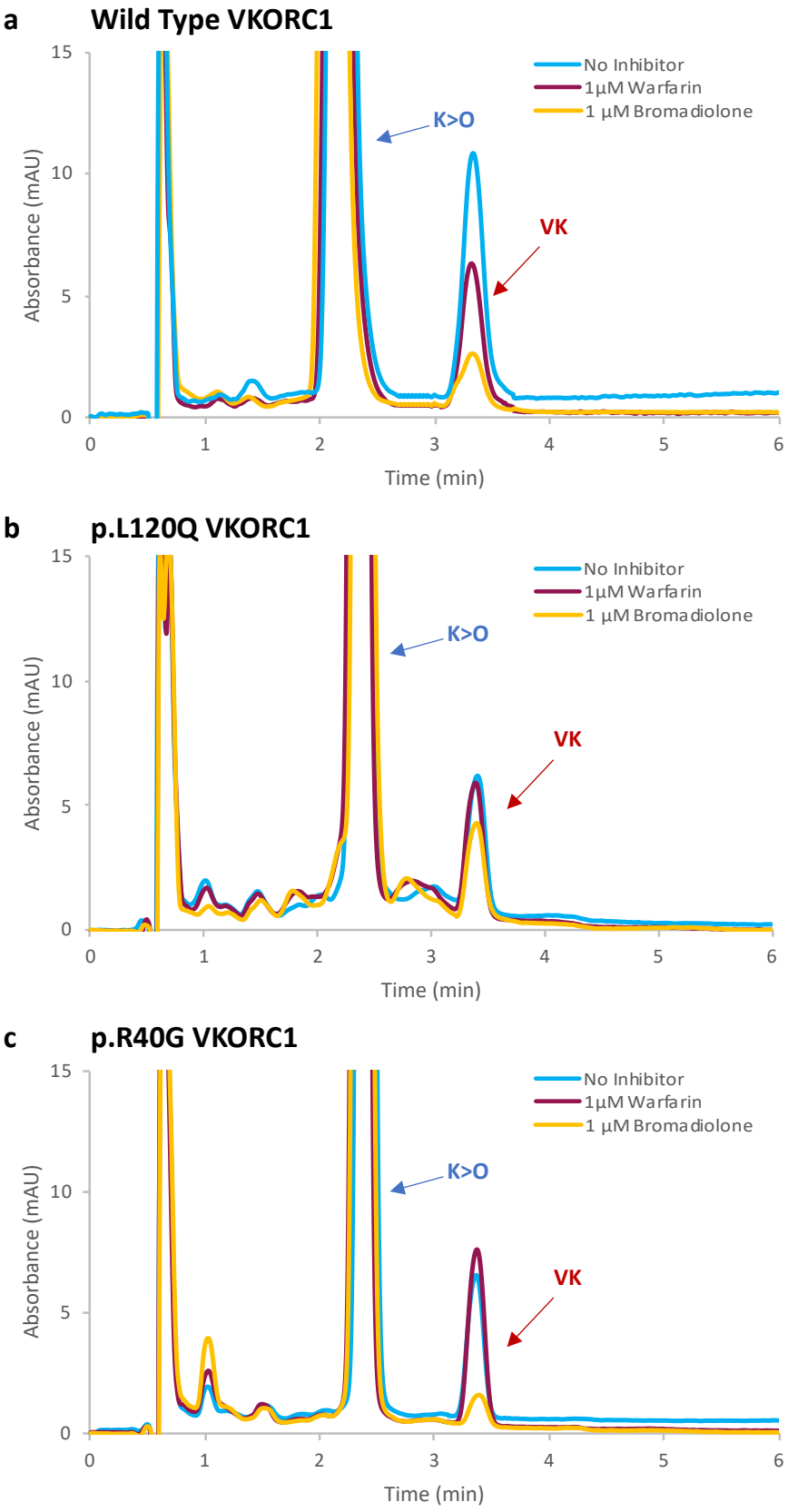


Figure 51: Example HPLC chromatograms showing the vitamin K production from recombinant rat VKORC1 and p.L120Q and p.R40G variants expressed in *Sf9* insect cells using 10 µM of vitamin K epoxide substrate for 15 minutes with no inhibitor, 1 µM of warfarin and 1 µM bromadiolone. a Rat VKORC1 inhibited with warfarin and bromadiolone. **b** p.L120Q variant inhibited with warfarin and bromadiolone. **c** p.R40G variant inhibited with warfarin and bromadiolone.

From the preliminary results, differences in activity between the wild type and mutants can be seen for both warfarin and bromadiolone over the range of concentrations tested. A significant difference can be seen between the wild-type and the p.L120Q mutant for both warfarin and bromadiolone with the inhibitors having a less effect on the activity of the p.L120Q VKORC1 over the range of concentrations in comparison to the wild type. This suggests that the p.L120Q polymorphism is relatively resistant to warfarin and bromadiolone inhibition, which is consistent with published studies by Pelz *et al.* (2005) and Hodroge *et al.* (2011). The preliminary results suggest that for the p.R40G mutant has some resistance to warfarin compared to the wild type but is more sensitive to warfarin inhibition compared to the p.L120Q mutant. Hodroge *et al.* (2011) suggests that different polymorphisms can have varying degrees of resistance. Inhibition with bromadiolone has a greater effect on all three constructs in comparison to the effect of warfarin. However, statistical tests showed that there was no statistical difference over all of the bromadiolone concentrations used for the wild type and p.R40G mutant, suggesting that the p.R40G polymorphism has little resistance effect when inhibited by bromadiolone.

This data gives an insight into the inhibition effects of first and second generation anticoagulant rodenticides on the wild type rat VKORC1, a known anticoagulant resistance mutant p.L120Q and a novel mutant p.R40G. By using a control polymorphism, it provides a comparison for novel VKORC1 polymorphisms. However, to gain a better understanding of the effects of anticoagulant rodenticides on the mutant p.R40G, more concentrations of anticoagulant rodenticides are needed to produce a dose-response curve to estimate the IC_{50}.

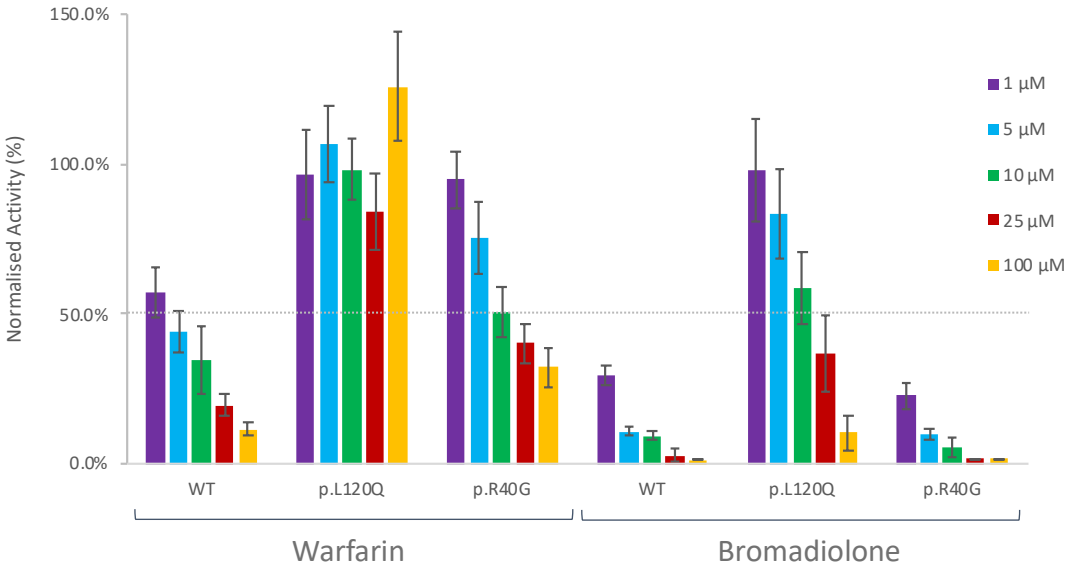


Figure 52: Normalised VKORC1 activity at different concentrations of warfarin and bromadiolone for wild type rat VKORC1 and rat VKORC1 with p.L120Q and p.R40G polymorphisms expressed in *Sf9* cells using 10 µM of vitamin K epoxide substrate for 15 minutes. Dotted line denotes the activity at 50% inhibition. Experiments were performed in triplicate and values shown as mean and standard deviation.

Variable	P value	Significant?
1 µM:		
Warfarin WT vs Warfarin p.L120Q	<0.0001	YES ****
Warfarin WT vs Warfarin p.R40G	<0.0001	YES ****
Warfarin p.L120Q vs Warfarin p.R40G	>0.9999	NO
Bromadiolone WT vs Bromadiolone p.L120Q	<0.0001	YES ****
Bromadiolone WT vs Bromadiolone p.R40G	0.9332	NO
Bromadiolone p.L120Q vs Bromadiolone p.R40G	<0.0001	YES ****
Warfarin WT vs Bromadiolone WT	0.0068	YES **
Warfarin p.L120Q vs Bromadiolone p.L120Q	>0.9999	NO
Warfarin p.R40G vs Bromadiolone p.R40G	<0.0001	YES ****
5 µM:		
Warfarin WT vs Warfarin p.L120Q	<0.0001	YES ****
Warfarin WT vs Warfarin p.R40G	0.0014	YES **
Warfarin p.L120Q vs Warfarin p.R40G	0.0014	YES **
Bromadiolone WT vs Bromadiolone p.L120Q	<0.0001	YES ****
Bromadiolone WT vs Bromadiolone p.R40G	>0.9999	NO
Bromadiolone p.L120Q vs Bromadiolone p.R40G	<0.0001	YES ****
Warfarin WT vs Bromadiolone WT	0.0006	YES ***
Warfarin p.L120Q vs Bromadiolone p.L120Q	0.0338	YES *
Warfarin p.R40G vs Bromadiolone p.R40G	<0.0001	YES ****
10 µM:		
Warfarin WT vs Warfarin p.L120Q	<0.0001	YES ****
Warfarin WT vs Warfarin p.R40G	0.2873	NO
Warfarin p.L120Q vs Warfarin p.R40G	<0.0001	YES ****

Bromadiolone WT vs Bromadiolone p.L120Q	<0.0001	YES ****
Bromadiolone WT vs Bromadiolone p.R40G	0.9958	NO
Bromadiolone p.L120Q vs Bromadiolone p.R40G	<0.0001	YES ***
Warfarin WT vs Bromadiolone WT	0.0161	YES *
Warfarin p.L120Q vs Bromadiolone p.L120Q	<0.0001	YES ****
Warfarin p.R40G vs Bromadiolone p.R40G	<0.0001	YES ****
25 μM:		
Warfarin WT vs Warfarin p.L120Q	<0.0001	YES ****
Warfarin WT vs Warfarin p.R40G	0.0725	NO
Warfarin p.L120Q vs Warfarin p.R40G	<0.0001	YES ****
Bromadiolone WT vs Bromadiolone p.L120Q	0.0005	YES ***
Bromadiolone WT vs Bromadiolone p.R40G	>0.9999	NO
Bromadiolone p.L120Q vs Bromadiolone p.R40G	0.0003	YES ***
Warfarin WT vs Bromadiolone WT	0.2556	NO
Warfarin p.L120Q vs Bromadiolone p.L120Q	<0.0001	YES ****
Warfarin p.R40G vs Bromadiolone p.R40G	<0.0001	YES ****
100 μM:		
Warfarin WT vs Warfarin p.L120Q	<0.0001	YES ****
Warfarin WT vs Warfarin p.R40G	0.0822	NO
Warfarin p.L120Q vs Warfarin p.R40G	<0.0001	YES ****
Bromadiolone WT vs Bromadiolone p.L120Q	0.8404	NO
Bromadiolone WT vs Bromadiolone p.R40G	>0.9999	NO
Bromadiolone p.L120Q vs Bromadiolone p.R40G	0.8586	NO
Warfarin WT vs Bromadiolone WT	0.7598	NO
Warfarin p.L120Q vs Bromadiolone p.L120Q	<0.0001	YES ****
Warfarin p.R40G vs Bromadiolone p.R40G	0.002	YES **

Table 34: 2 way ANOVA results showing the P values and significance of each anticoagulant and polymorphism for each concentration.

3.9 Dose-response Curves for Wild Type Rat VKORC1 and the p.R40G VKORC1 Mutant for Five Anticoagulant Rodenticides

To fully scruitinise the effect of anticoagulant rodenticides on the VKORC1 enzyme, the half maximal inhibitory concentration (IC_{50}) was used. A range of concentrations of the inhibitor were used to create a sigmoidal curve and that had a good range before and after 50% inhibition. Dose-response curves were produced for the wild type rat VKORC1 and the p.R40G mutant for five anticoagulant rodenticides; warfarin, bromadiolone, brodifacoum, difenacoum and flocoumafen (Figure 53). IC_{50} values were then derived from the dose response curves (Table 35).

Figure 53a shows a shift in the warfarin dose-response for the p.R40G mutant compared to the wild type rat curve. There is an ~6 fold difference in IC_{50} values between the wild-type and the p.R40G mutant with warfarin which shows that the p.R40G variant is warfarin resistant (Table 35).

With regards to the R40 residue, Czogalla *et al.* (2017) previously showed that positively charged arginine residues have a role in charge-stabilisation in warfarin binding and resistance and the replacement of arginines (R33, R40, R53) with negatively charged amino acids, this causes a shift in the warfarin dose-response curves. As arginines play a role in charge-stabilisation and the positive charge stabilises the anionic warfarin, the p.R40G polymorphism abolishes any charged residue at that position. This may reduce effective binding of the warfarin to VKORC1 which might be predicted to cause warfarin resistance in brown rats with the p.R40G polymorphism.

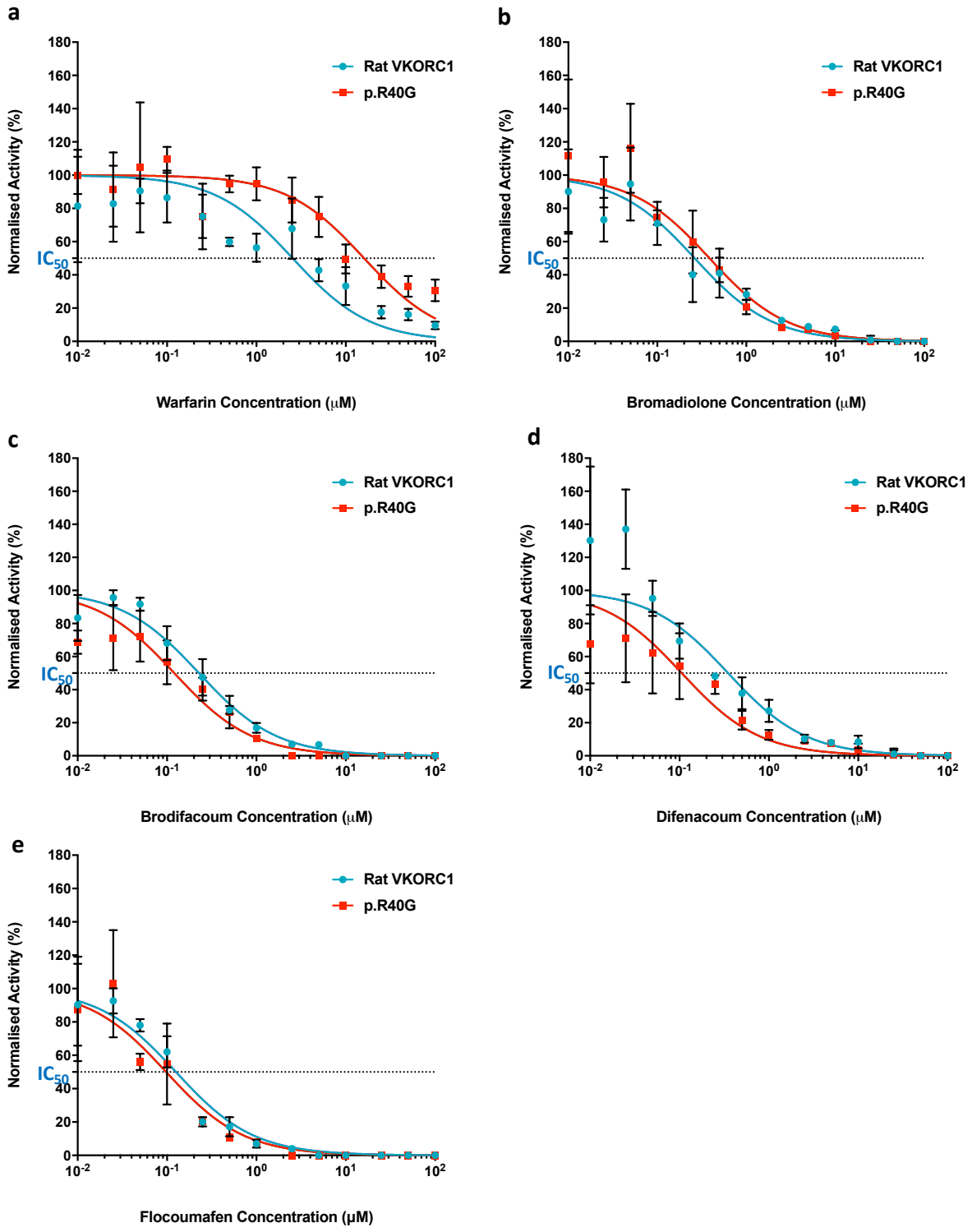


Figure 53: Comparison of anticoagulant dose-response curves for the wildtype rat VKORC1 and rat VKORC1 with p.R40G polymorphism expressed in *Sf9* cells. The IC_{50} is represented by the dotted line. Blue denotes wildtype rat VKORC1. Red denotes rat VKORC1 with p.R40G polymorphism. Experiments were performed in triplicate and values shown as mean and standard deviation. **a** Warfarin dose-response curves for wild type and p.R40G mutant rat VKORC1. **b** Bromadiolone dose-response curves for wild type and p.R40G mutant rat VKORC1. **c** Brodifacoum dose-response curves for wild type and p.R40G mutant rat VKORC1. **d** Difenacoum dose-response curves for wild type and p.R40G mutant rat VKORC1 (0.2 mg). **e** Flocoumafen dose-response curves for wild type and p.R40G mutant rat VKORC1.

	Warfarin (μM)	Bromadiolone (μM)	Brodifacoum (μM)	Difenacoum (μM)	Flocoumafen (μM)
WT	2.55 ± 0.11	0.26 ± 0.07	0.23 ± 0.04	0.35 ± 0.11	0.13 ± 0.65
p.R40G	16.05 ± 0.09	0.39 ± 0.09	0.12 ± 0.06	0.11 ± 0.08	0.10 ± 0.08
Ratio	6.3	1.5	1.9	3.2	1.3
P value	<0.0001	0.9614	0.9811	0.6668	>0.9999
Significant?	YES	NO	NO	NO	NO

Table 35: IC_{50} values derived from dose-response curves of different anticoagulants for wild type rat VKORC1 and rat VKORC1 with p.R40G polymorphism expressed in *Sf9* cells. Experiments were performed in triplicate and values shown as mean and standard deviation.

Figure 53 shows the bromadiolone dose-response curve for wild type rat VKORC1 and the p.R40G mutant. As with the warfarin dose-response curves, the p.R40G VKORC1 has a curve shift to the right compared to the wild type rat resulting in a ~1.5 fold increase in IC_{50} (Table 35). Bromadiolone is a derivative of warfarin and have a similar structure based on the 4-hydroxycoumarin. The p.R40G polymorphism appears to reduce binding of bromadiolone to VKORC1, showing a slight resistance to bromadiolone. In the previous preliminary results (Figure 53), the results showed that the inhibition by bromadiolone for the wild type rat VKORC1 and the p.R40G mutant was very similar across all of the concentrations tested resulting in no noticeable difference in sensitivity to bromadiolone (Table 35). However, when the bromadiolone dose-response curves were produced (Figure 53) and the IC_{50} values were derived (Table 35) for both wild type and the p.R40G variant it shows that the wild type rat VKORC1 is 1.5 fold more sensitive to bromadiolone compared with the p.R40G VKORC1 variant, although statistical analysis shows there is no statistical difference (Table 35).

Figure 53c show the brodifacoum dose-response curves for the wild type rat VKORC1 and the p.R40G mutant. When inhibited with brodifacoum, the dose-response curve for the p.R40G mutant shifts to the left in comparison to the wild type rat. This suggests that the p.R40G polymorphism increases the affinity for brodifacoum, causing sensitivity to brodifacoum. The p.R40G may thus aid the binding of brodifacoum. Although brodifacoum is derived from a 4-hydroxycoumarin, the structure of brodifacoum is different to both warfarin and bromadiolone (Section 1.6) due to the difference in side groups, therefore there may be difference in the docking and binding to VKORC1. The mutant may change the anticoagulant binding pocket and allow brodifacoum to bind more strongly than the native rat VKORC1.

There is a ~2 fold difference in IC_{50} values between the wild-type and the p.R40G mutant (Table 35).

Figure 53d show the difenacoum dose-response curves for the wild type rat VKORC1 and the p.R40G mutant. The difenacoum dose-response curves for the p.R40G mutant has the greatest shift to the left compared to the wild type rat. This suggests that the p.R40G polymorphism causes an increase in affinity of difenacoum, causing a sensitivity to difenacoum. Difenacoum is also a derivative of a 4-hydroxycoumarin and has the same basic structure as brodifacoum but without the bromine group on the side group. Difenacoum therefore appears to have a stronger binding to the p.R40G mutant than brodifacoum. This could be due to the lack of bromine in the compounds structure and the altered interaction with VKORC1.

This study provides an insight into the effects of flocoumafen on the wild type rat VKORC1 enzyme compared to other anticoagulant rodenticides and the effect on a novel *Rattus norvegicus* p.R40G polymorphism. Figure 53e shows the flocoumafen dose-response curves for the wild type rat VKORC1 and the p.R40G mutant. Of the five compounds tested, flocoumafen has a higher affinity for VKORC1 with an IC_{50} of 0.13 μM compared to all other anticoagulant rodenticides. The IC_{50} value for wild-type rat VKORC1 is 0.13 μM, whereas the IC_{50} value for the p.R40G mutant is 0.10 μM. There is therefore only a small difference between the wild type and the p.R40G mutant IC_{50} values, suggesting that the binding of flocoumafen is unaffected by the amino acid change at this position. This potency of flocoumafen for both the wild type and mutant VKORC1 enzymes could be due to the side group being very different to other SGARs in that is has a fluorine side group. This may bind differently to VKORC1 and cause a higher affinity to the VKORC1 binding pocket.

The p.R40G polymorphism is found in a different part of the VKORC1 protein compared to the most common anticoagulant resistance polymorphisms. Interestingly, the p.R40G polymorphism is also the most 'dramatic' amino acid change with a positive to a small uncharged amino acid change compared to other published anticoagulant resistant polymorphisms. For example, the p.L120Q polymorphism is a hydrophobic to a polar amino acid change. One of the more severe polymorphisms for anticoagulant resistance is the

p.Y139F polymorphism (Hodroge *et al.*, 2011) and both amino acids tyrosine and phenylalanine are both aromatic amino acids with similar physiochemical properties. It can also be noted that different resistance polymorphisms behave differently with different anticoagulants. As with the p.R40G polymorphism it is interesting that this polymorphism can generate resistance to warfarin but causes an increased sensitivity against other anticoagulant rodenticides such as difenacoum. This reflects a study by Hodroge *et al.* (2011) who showed that when inhibited with difenacoum the p.L120Q polymorphism is inhibited the least and the p.Y139S polymorphism is inhibited the most, whereas the opposite occurs when inhibited with chlorophacinone (Section 1.17). This suggests that there is no particular anticoagulant rodenticide that can be more potent than any other because depending on the polymorphism and how that changes the binding of the anticoagulant, this can vary depending on the amino acid change and location.

Chapter 4: Computational analysis of VKORC1 and VKORC1L1 to assess structure, function and evolutionary relationships

4.0 About this Chapter

Analysing the sequences of proteins using multiple sequence alignments allows for an inference of evolutionary history and identification of regions of conservation and the relationships between different species and between different proteins (Wang and Jiang, 1994; Daugelaite *et al.,* 2013). The focus of this chapter is on the evolutionary relationships of vertebrate VKORs. The vertebrate sequences of the VKOR family genes (VKORC1 and VKORC1L1) will be analysed separately by MSA and generation of consensus sequences (for the assessment of functional constraints). In addition, the amino acids involved in warfarin binding will be described. The VKORC1 and VKORC1L1 consensus sequences will be compared to assess the conserved residues in the VKOR family across all vertebrate classes. Finally, representatives of the key vertebrate classes will be chosen for cloning, recombinant expression, enzyme kinetics and inhibitor studies with common anticoagulant rodenticides.

The general phylogeny of the VKOR family of enzymes has been well characterised (Rost *et al.,* 2004; Goodstadt and Ponting, 2004; Robertson, 2004; Wan *et al.,* 2014; Bevans *et al.,* 2015; Lacombe and Ferron, 2018) (Section 1.15). However, these studies only used a relatively small number of vertebrate VKORC1/VKORC1L1 sequences to assess the structural and evolutionary relationships between VKORs in different species and between the two enzymes (Rost *et al.,* 2004; Goodstadt and Ponting, 2004; Robertson, 2004; Wan *et al.,* 2014; Bevans *et al.,* 2015; Lacombe and Ferron, 2018). Early studies by Rost *et al*. (2004) used multiple sequence alignments to align six VKORC1 and four VKORC1L1 sequences from only *Mus musculus* (house mouse)*, Rattus norvegicus* (brown rat) and *Homo sapiens* (human) VKORC1 and VKORC1L1 sequences as representative mammal sequences with *Xenopus laevis* (African clawed frog) and *Fugu rubripes* (Pufferfish) representing other vertebrate classes. Goodstadt and Ponting (2004) also used multiple sequence alignments to identify important residues in the VKOR family of enzymes. They used 37 VKORs with only the brown rat and human VKORC1 sequences representing vertebrate sequences. A study by Robertson (2004) provided phylogenetic analysis of 25 VKOR sequences, of these 7 were vertebrate VKORC1 and a further 7 were vertebrate VKORC1L1 sequences. Only 3 mammals, 1 bird, 1 amphibian and 2

fish VKORC1 and VKORC1L1 were selected in this study. A more recent study by Wan *et al.* (2014) constructed a phylogenetic tree consisting of 41 species including, plants algae, photosynthetic bacteria and vertebrates. Of these only 13 mammals and 2 fish VKORC1 sequences were compared. The following year Bevans *et al.* (2015) reconstructed a comprehensive phylogeny for the VKOR family of enzymes including 327 species of the major phyla of the Kingdoms of Life. However, of these only 15 vertebrate VKORC1 sequences were used (8 mammals, 1, bird, 2 amphibians, 4 fish) and 14 vertebrate VKORC1L1 sequences were used (6 mammals, 2 birds, 2 amphibians, 4 fish). Similarly, a study by Lacombe and Ferron (2018) only used very few vertebrate VKOR sequences with only 7 VKORC1 sequences (2 mammals, 1 bird, 1 reptile, 1 amphibian and 2 fish) and 7 VKORC1L1 (2 mammals, 1 bird, 1 reptile, 1 amphibian and 2 fish) sequences to conduct their analysis. Lacombe and Ferron (2018) are the only study to use a reptilian sequence in their analysis.

4.1 Computational Comparison of Vertebrate VKORC1 Amino Acid Sequences

In order to study the differences between the different species within vertebrate VKORC1 sequences multiple sequence alignments were performed using CLC Sequence Viewer. Protein sequences for VKORC1 were obtained from the NCBI database (See Appendix 6 – for accession numbers). Only full length sequences were used to generate the multiple sequence alignments. Full length VKORC1 sequences were identified as containing specific amino acid residues and a certain sequence length. Firstly, all sequences had to contain a methionine residue at the first amino acid position at the N terminus. This amino acid is encoded by the start codon and therefore is important for the beginning of vertebrate nuclear genome encoded protein sequences. At the C-terminus there should be two lysine residues at -3 and -5 positions, which is the endoplasmic reticulum retention signal found in the ER membrane bound VKOR (Jackson *et al.,* 1990). All vertebrate VKORC1 sequences found in this study contained the retention signal K-X-K-X-X at the C-terminus, suggesting that the VKORC1 enzyme is localized in the endoplasmic reticulum in all vertebrate species. The only exception is the *Gallus gallus* (chicken) VKORC1 sequence in which there is only a lysine at the -3 position. This sequence was included in the alignments as until recently the chicken was the only bird VKORC1 sequence found on the NCBI database. The chicken VKORC1 sequence is regarded as different to other vertebrate VKORC1 sequences. Robertson (2004) noted that

the chicken sequence is not present in the draft genome assembly and that the current VKORC1 sequence for chicken is built from two ESTs and a single whole gene shotgun trace (Robertson, 2004). This could be due to missing areas of bird genomes (Hillier *et al.,* 2004) or Yin *et al.* (2019) suggested that the reference sequence for the chicken genome was poor resulting in missing genes. Following from Robertson's observations, an assessment of the trace archives was carried out to try to identify the chicken VKORC1 sequence, however, it was difficult to identify regions of VKORC1 due to the quality of the trace sequences (Authors personal observation, data not shown). As the chicken sequence is used within other studies (Robertson, 2004; Bevans *et al*., 2015; Lacombe and Ferron, 2018) despite its difference to other VKORC1 sequences it was used in this study as well.

The most important amino acids that form part of the active site and characterise the VKOR enzyme family are C132 and C135 along with two other conserved cysteines C43 and C51 (Goodstadt and Ponting, 2004; Rost *et al.,* 2005). These four conserved cysteines were identified in all 135 vertebrate VKORC1 sequences in this study and are an important characteristic to define a full length VKORC1 sequence. Finally, a sequence length of above 160 amino acids for VKORC1 were accepted as full length sequences with the exception of birds which have a sequence length of 155-157 amino acids. All placental mammalian VKORC1 sequences contained 163 amino acids except for the Myodonta family (Rats, mice etc.) which are the only family to have a sequence length of 161 amino acids. The two amino acid deletion is at the -8 position from the C terminal end of VKORC1. Both the marsupial and monotreme VKORC1 sequences contain 169 amino acids, which could reflect the millions of years of evolution between the placental mammals and the marsupial and monotreme clades. The sequence length of VKORC1 varies throughout the non-mammalian classes. Birds have a sequence length of between 155-157 amino acids, whereas the length of the reptilian sequences is 168 amino acids except for the *Anolis carolinesis* (Green anole), which has 169 amino acids. The amphibian VKORC1 sequence has an amino acid length of 169. Fish VKORC1 sequences have a sequence length of 167 amino acids except for the species belonging to the Tetraodontiformes order which have a sequence length of 163 amino acids.

There are five main classes of vertebrates; Mammals, Birds, Reptiles, Amphibians and Fish (See Appendix 10 for phylogenetic tree for vertebrates). All non-mammalian VKORC1

sequences were aligned according to taxonomic class (Figures 54 – 66) and due to the large amount of sequences found for mammals the sequences were aligned according to taxonomic order (Figures 54 – 62).

All multiple sequence alignments were performed using CLC Sequence Viewer (Section 2.18). Each alignment contains a consensus sequence which is automatically generated by the CLC program and does not distinguish between fully conserved or partially conserved positions, whereas the sequence logo included with each alignment provides this information. The sequence logo is derived from the percentage of conservation at each amino acid position. The colours of the amino acids correspond to the physiochemical properties of the amino acids (See Appendix 8 for amino acid colour key).

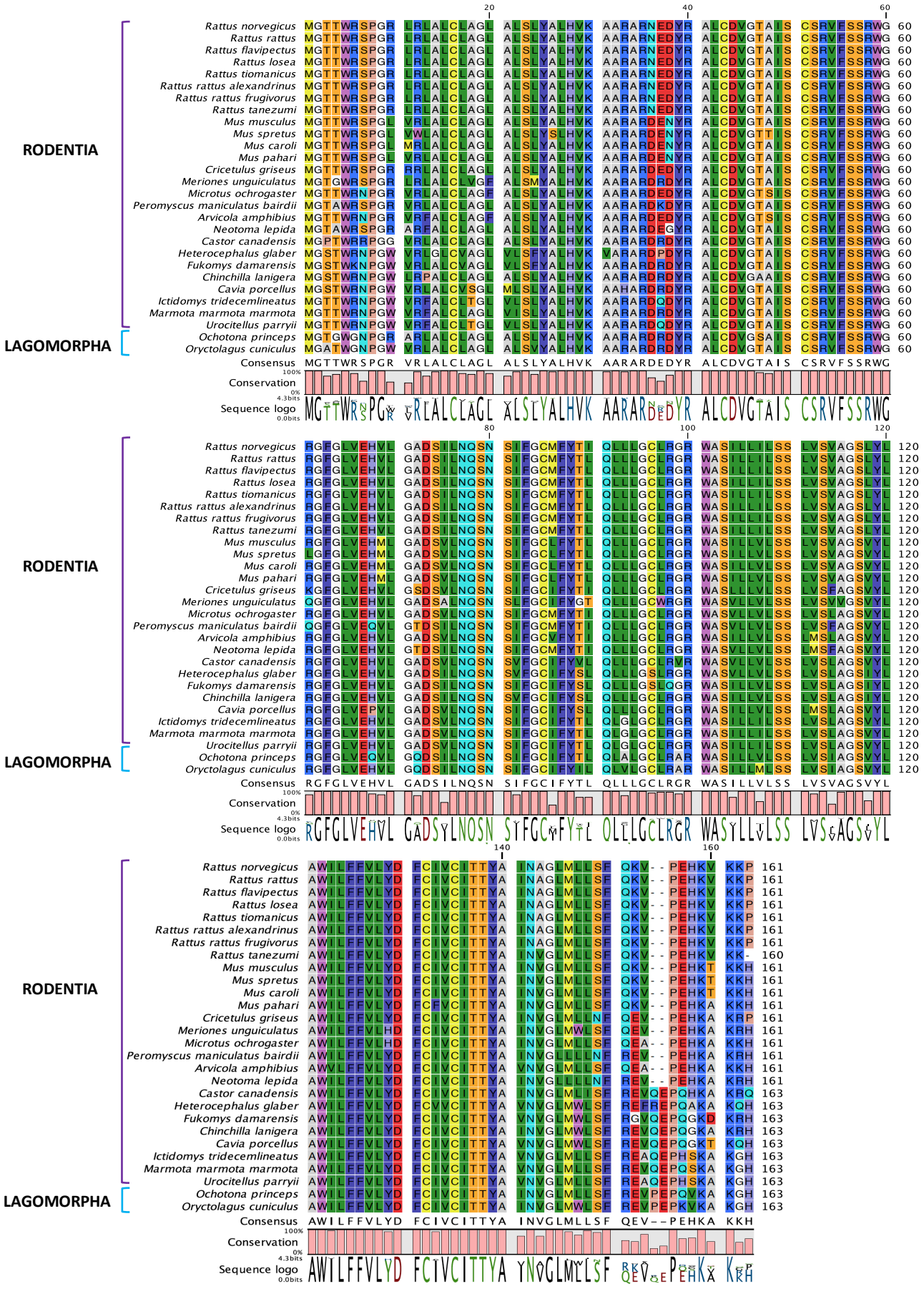


Figure 54: Multiple sequence alignment of Mammalian Rodentia and Lagomorpha VKORC1. Purple line denotes Rodentia sequences. Blue line denotes Lagomorpha sequences. Colours of amino acids are according to physiochemical properties, refer to Appendix 8.

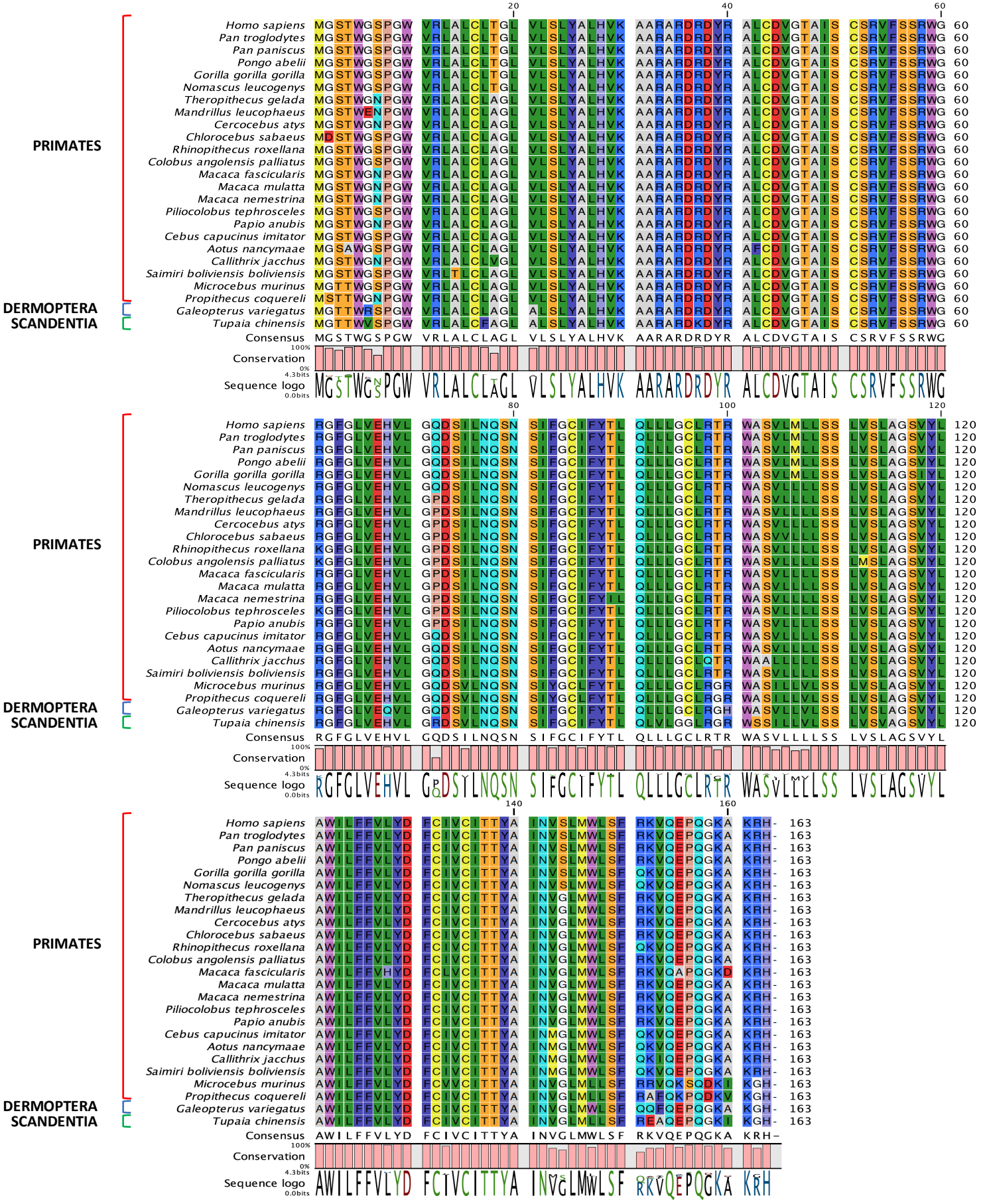


Figure 55: Multiple sequence alignment of Mammalian Primate, Dermoptera and Scandentia VKORC1. Red line denotes Primate sequences. Blue line denotes Dermoptera sequences. Green line denotes Scandentia sequences. Colours of amino acids are according to physiochemical properties, refer to Appendix 8.

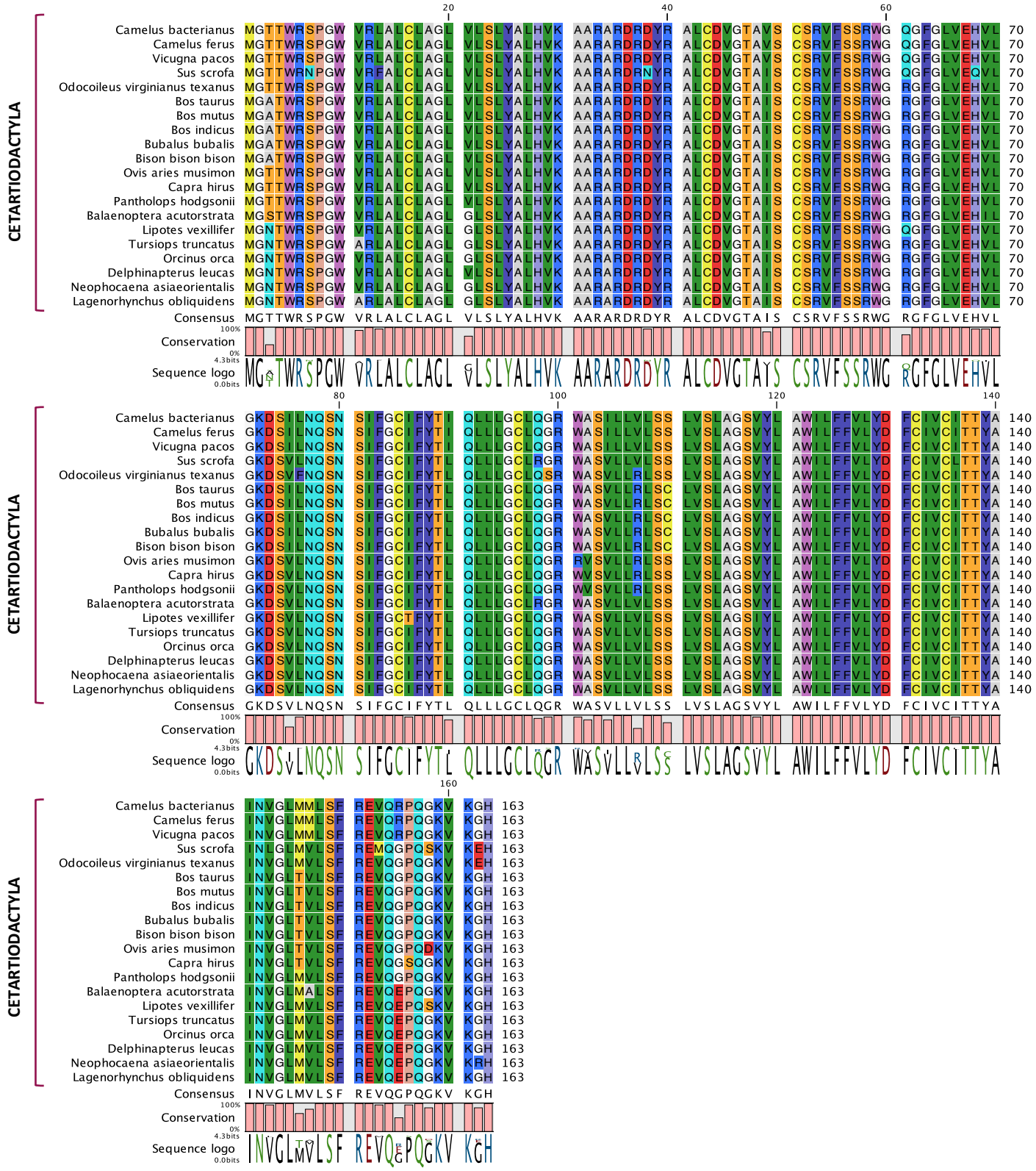


Figure 56: Multiple sequence alignment of Mammalian Cetartiodactyla VKORC1. Colours of amino acids are according to physiochemical properties, refer to Appendix 8.

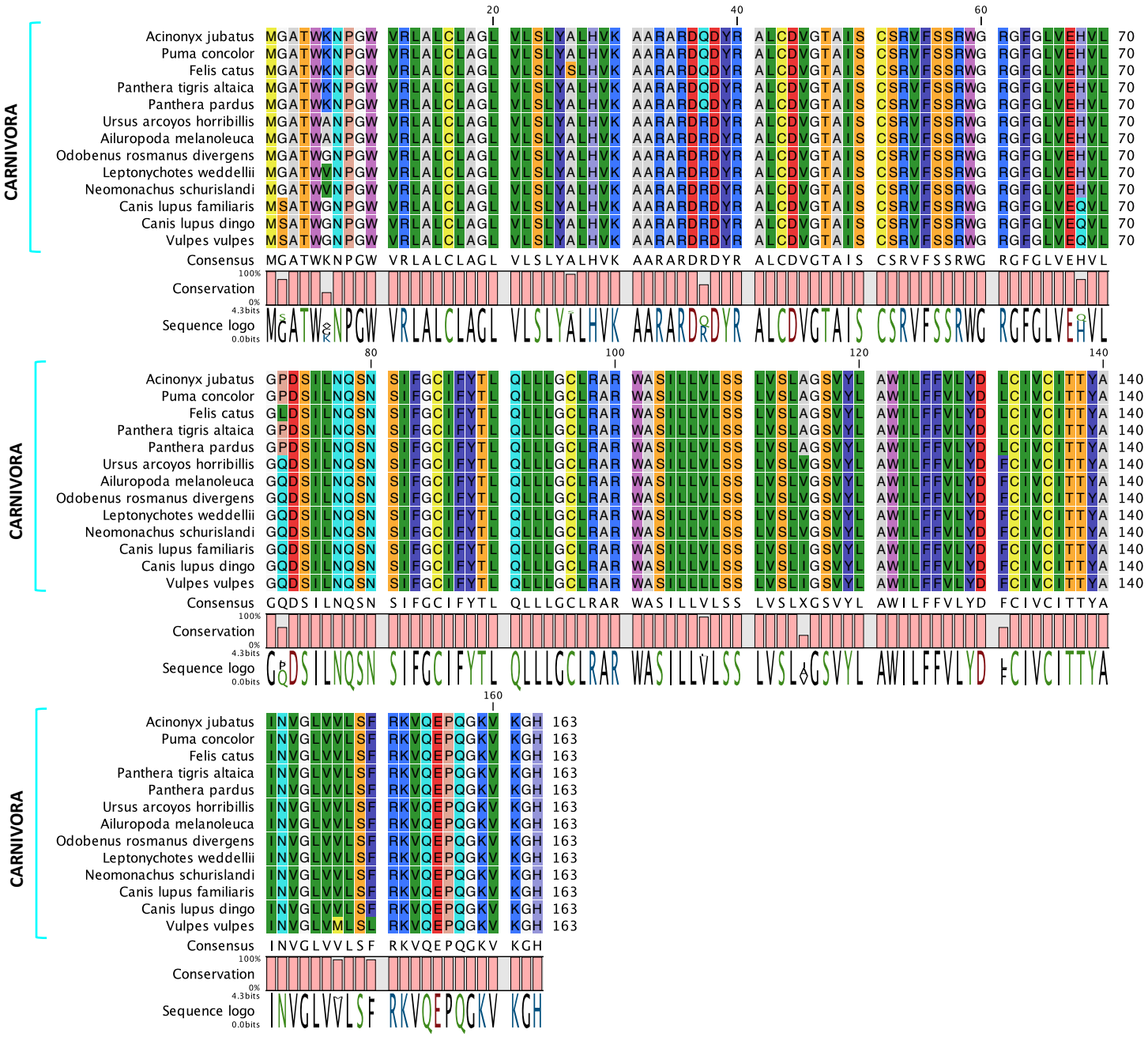


Figure 57: Multiple sequence alignment of Mammalian Carnivora VKORC1. Colours of amino acids are according to physiochemical properties, refer to Appendix 8.

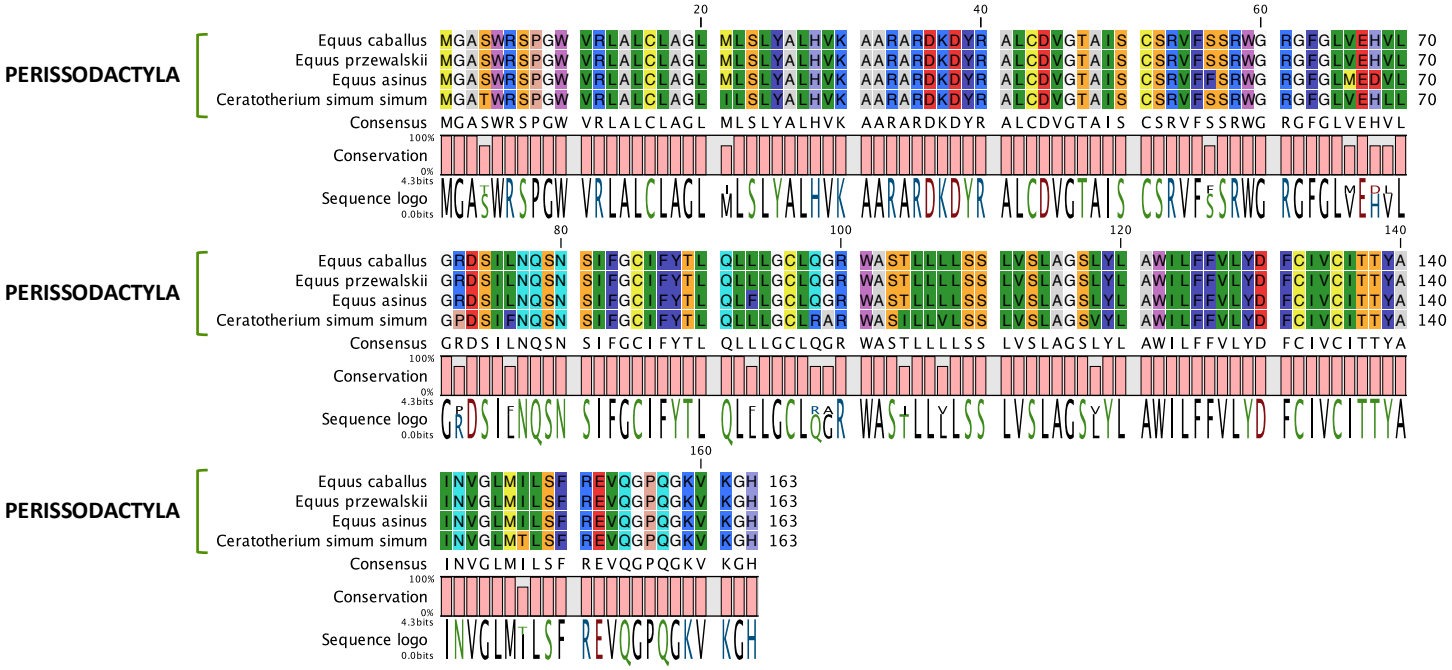


Figure 58: Multiple sequence alignment of Perissodactyla VKORC1. Colours of amino acids are according to physiochemical properties, refer to Appendix 8.

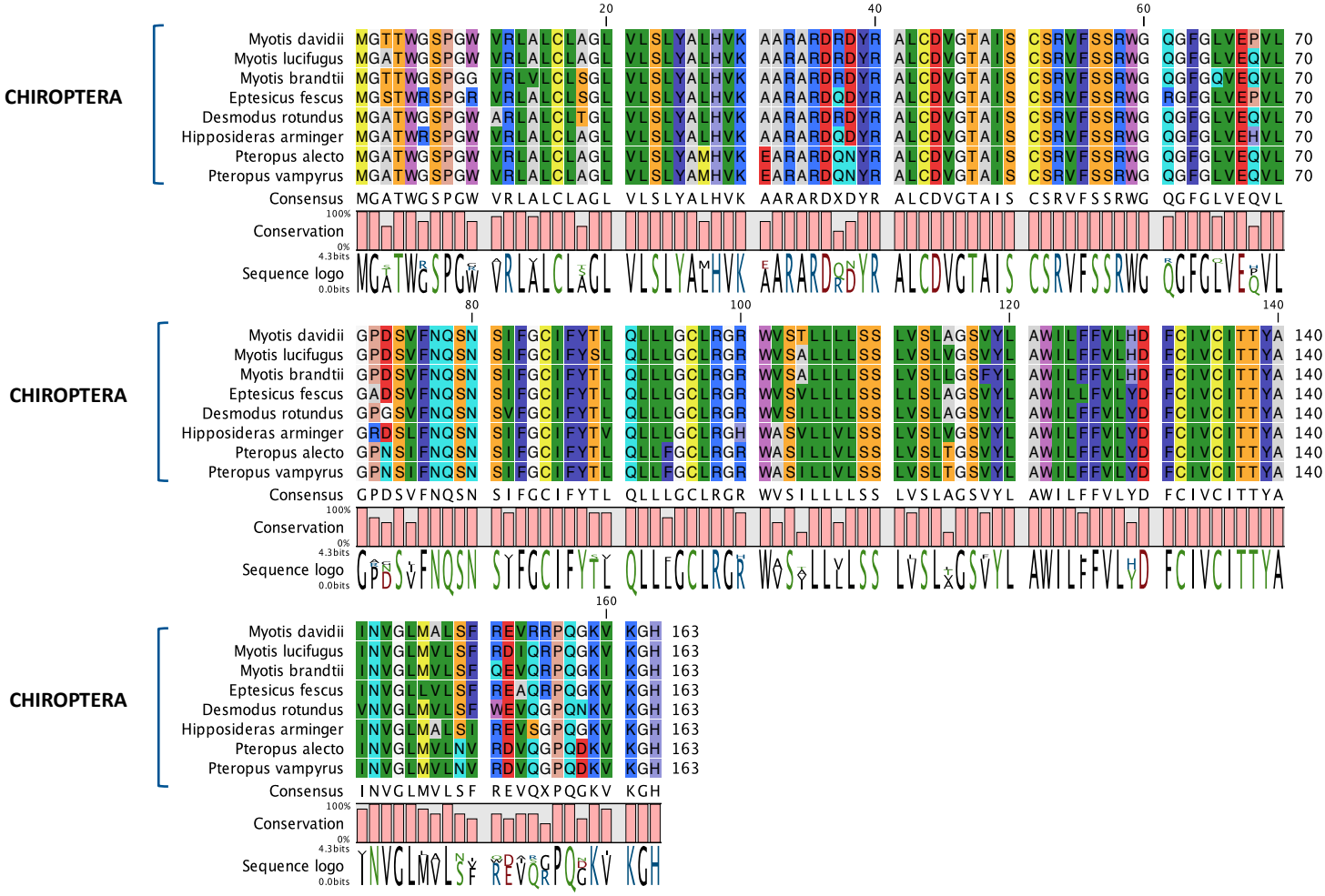


Figure 59: Multiple sequence alignment of Mammalian Chiroptera VKORC1. Colours of amino acids are according to physiochemical properties, refer to Appendix 8.

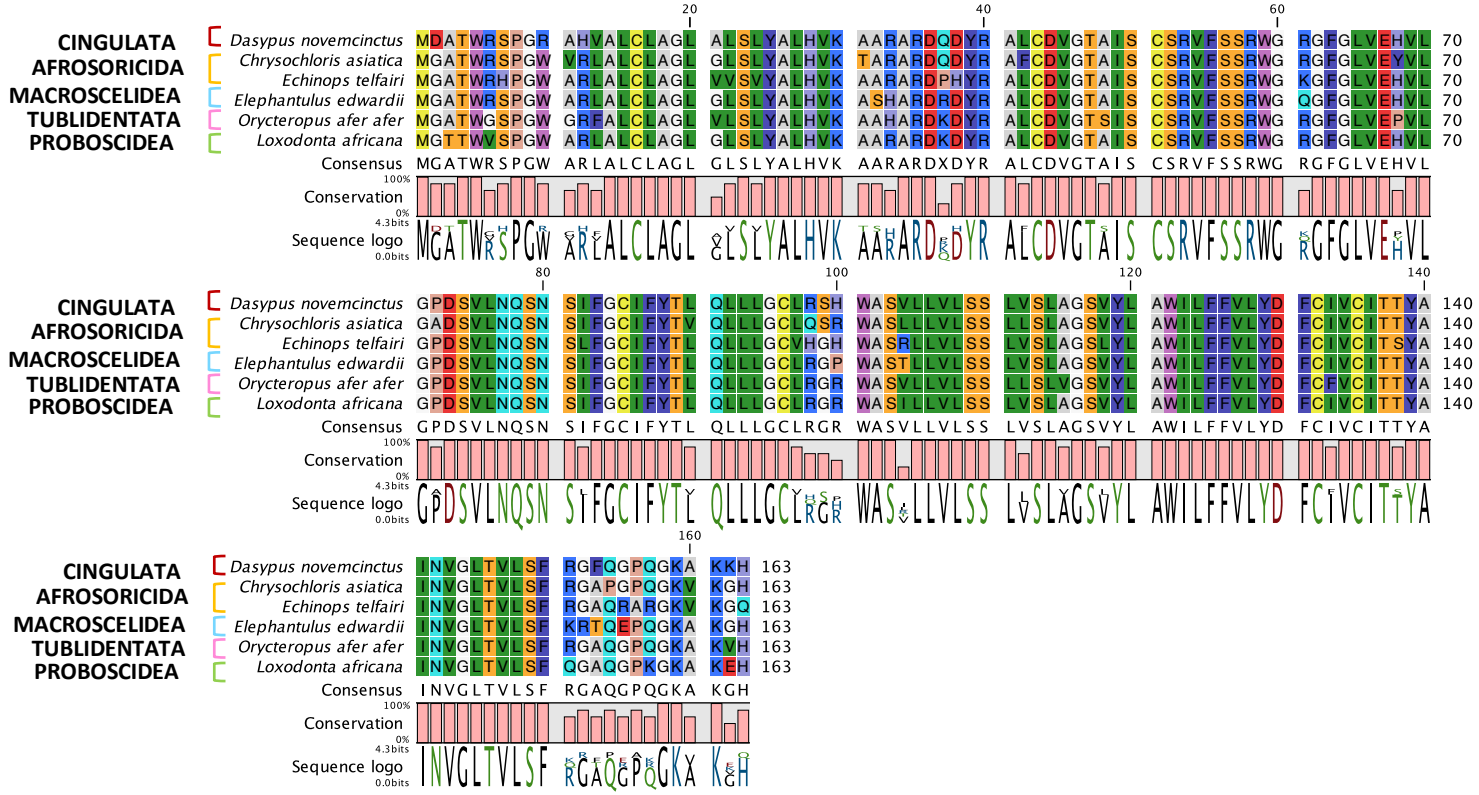


Figure 60: Multiple sequence alignment of Mammalian Cingulata, Afrosoricida, Macroscelidea, Tublidentata and Proboscidea VKORC1. Red line denotes Cingulata sequences. Yellow line denotes Afrosoricida sequences. Blue line denotes Macroscelidea sequences. Pink line denotes Tublidentata sequences. Green line denotes Proboscidea sequences. Colours of amino acids are according to physiochemical properties, refer to Appendix 8.

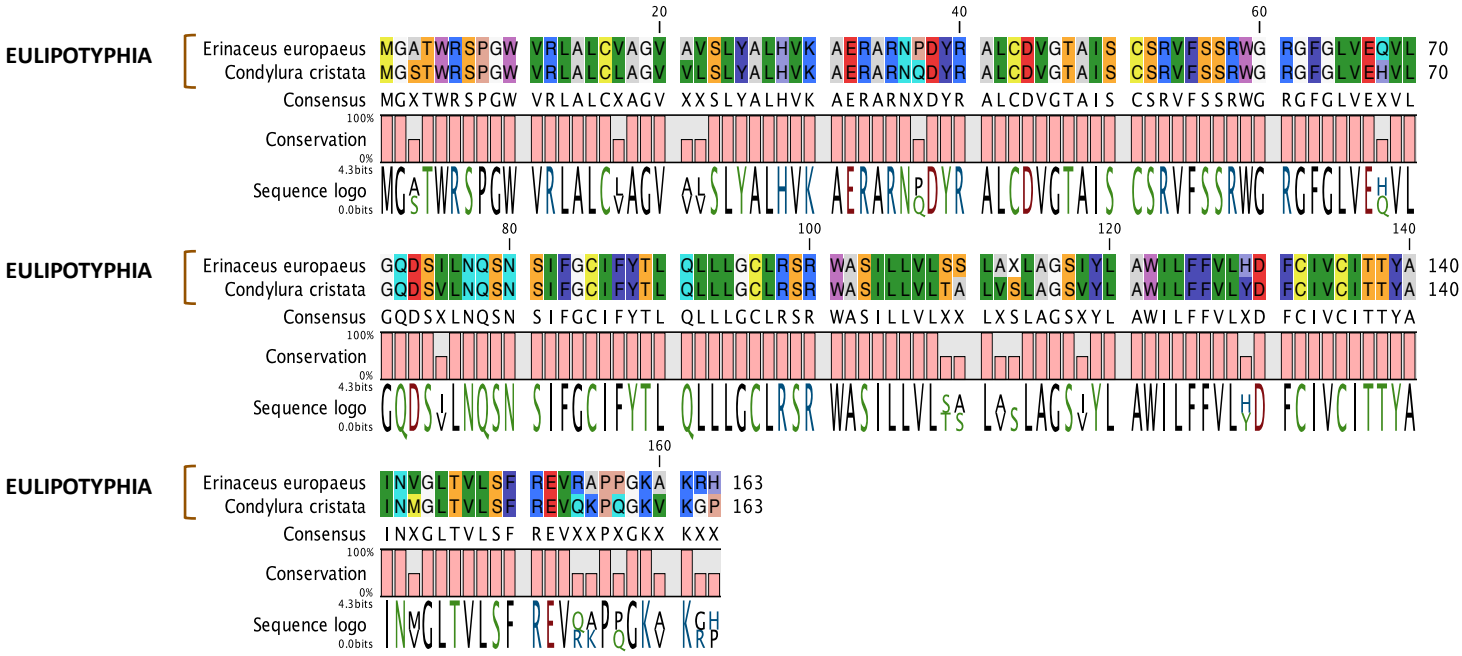


Figure 61: Multiple sequence alignment of Mammalian Eulipotyphia VKORC1. Colours of amino acids are according to physiochemical properties, refer to Appendix 8.

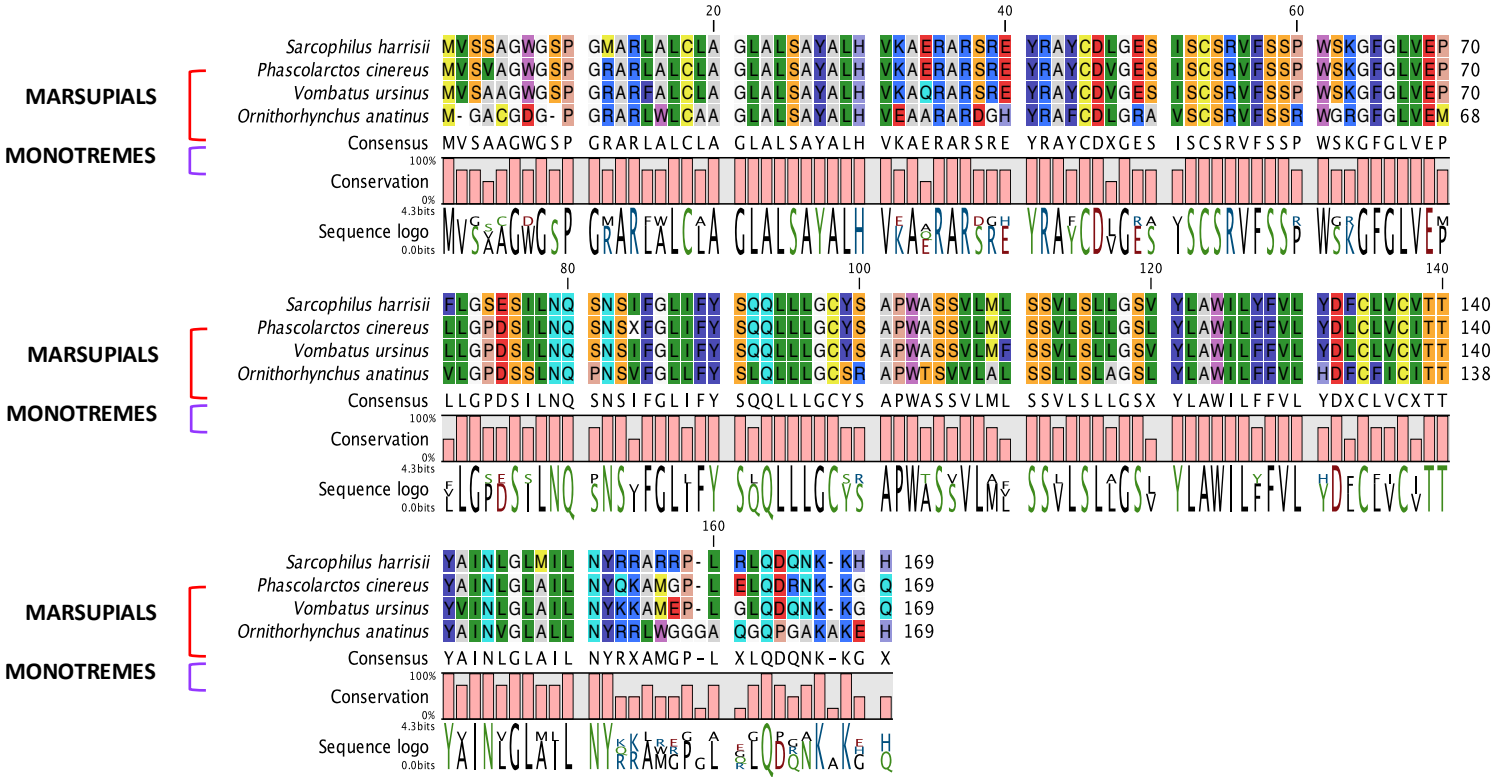


Figure 62: Multiple sequence alignment of Mammalian Marsupials and Monotreme VKORC1. Red line denotes Marsupial sequences. Purple line denotes Monotreme sequences. Colours of amino acids are according to physiochemical properties, refer to Appendix 8.

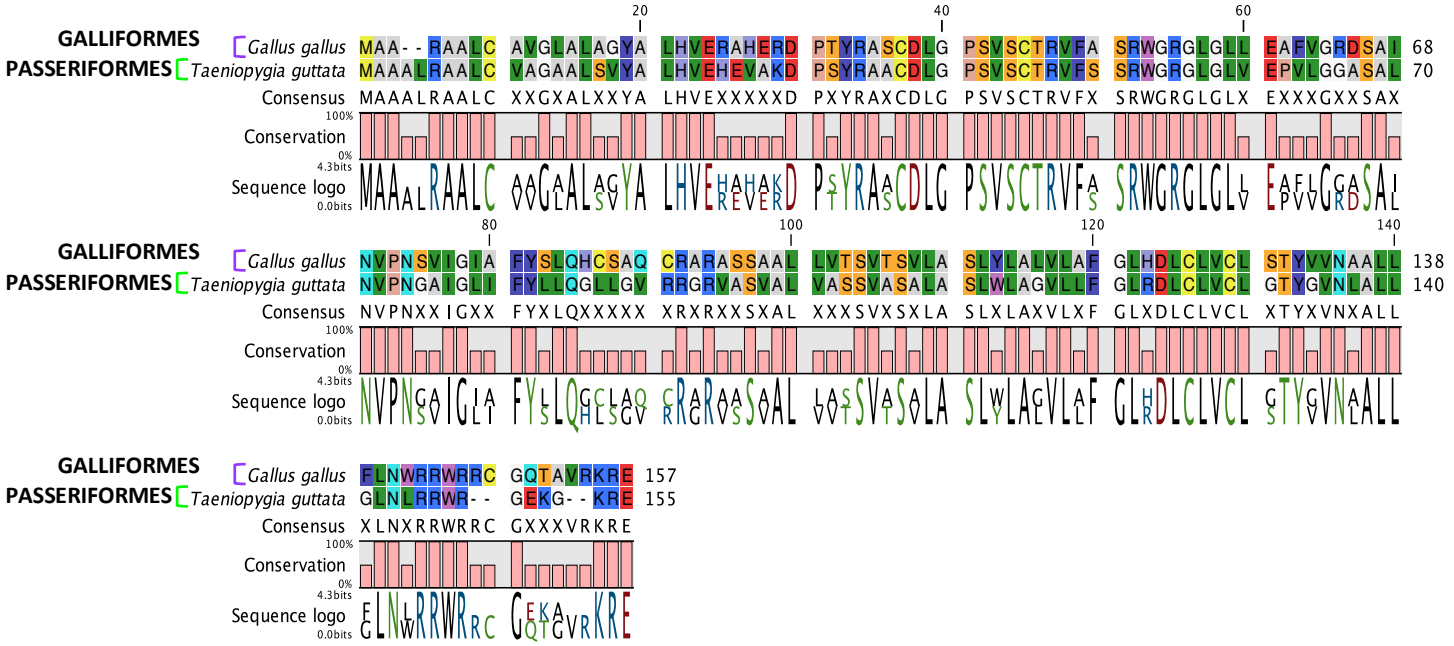


Figure 63: Multiple sequence alignment of Bird Galliformes and Passeriformes VKORC1. Purple line denotes Galliformes sequences. Green line denotes Passeriformes sequences. Colours of amino acids are according to physiochemical properties, refer to Appendix 8.

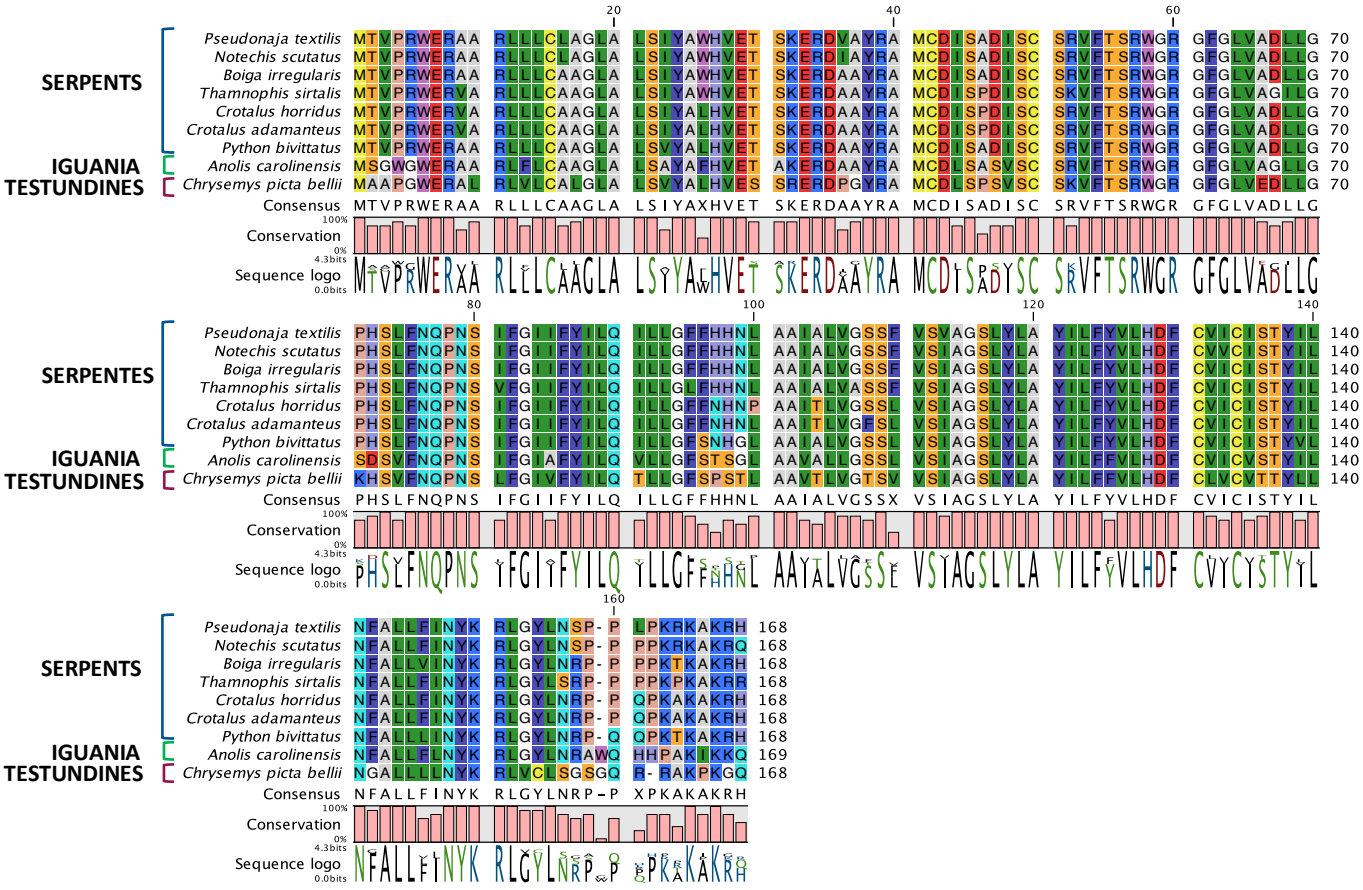


Figure 64: Multiple sequence alignment of Reptile Serpents, Iguania and Testundines VKORC1. Blue line denotes Serpents sequences. Green line denotes Iguania sequences. Pink line denotes Testundines sequences. Colours of amino acids are according to physiochemical properties, refer to Appendix 8.

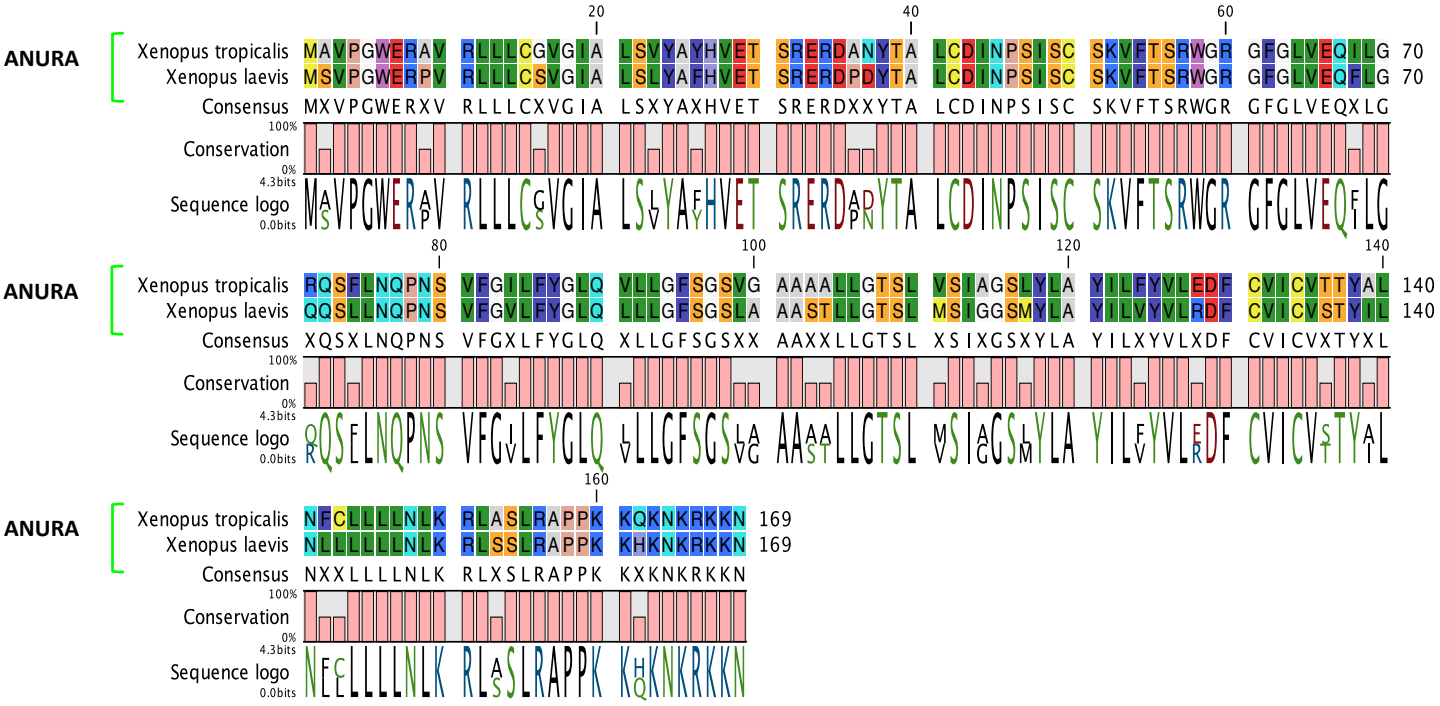


Figure 65: Multiple sequence alignment of Amphibian Anura VKORC1. Colours of amino acids are according to physiochemical properties, refer to Appendix 8.

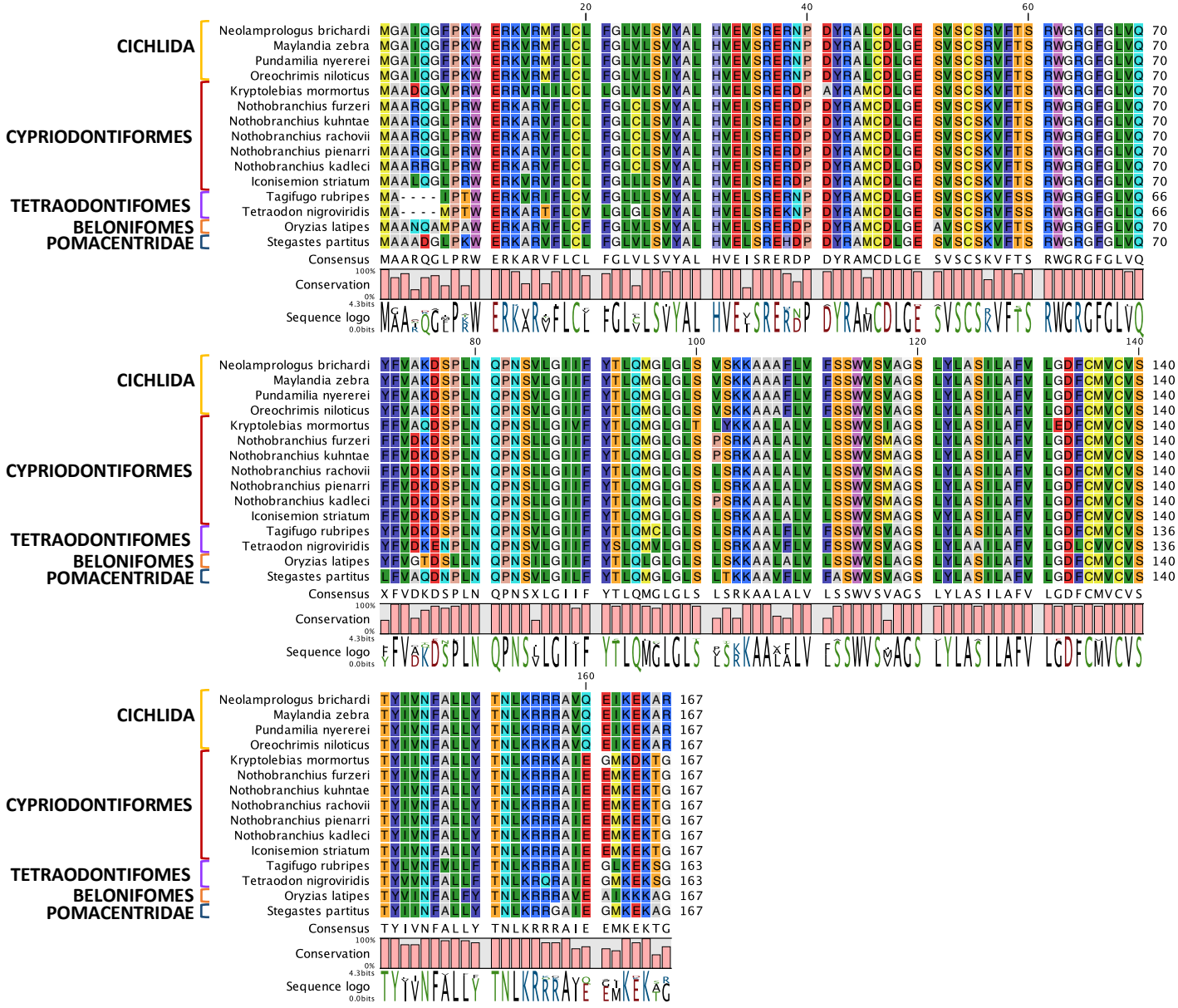


Figure 66: Multiple sequence alignment of Fish Cichlida, Cypriodontiformes, Tetraodontiformes Beloniformes and Pomcentridae VKORC1. Yellow line denotes Cichlida sequences. Red line denotes Cypriodontiformes sequences. Purple line denotes Tetraodontiformes sequences. Orange line denotes Beloniformes sequences. Blue line denotes Pomcentridae sequences. Colours of amino acids are according to physiochemical properties, refer to Appendix 8.

4.2 Analysis of VKORC1 Amino Acid Sequences in Mammals

By using multiple sequence alignments, the sequence identity was calculated within each taxonomic order (Table 36).

Taxonomic Order	Number of Sequences	Sequence Identity (%)	Evolutionary Time Span (My)	Figure Number
Rodentia	26	62	~ 70[a]	2
Lagomorpha	2	93	~ 2[b]	2
Primates	25	81	~ 32[c]	3
Dermoptera	1	-	-	3
Scandentia	1	-	-	3
Cetartiodactyla	20	82	~ 15[d]	4
Carnivora	13	94	~ 30[e]	5
Perissodactyla	4	91	~ 15[f]	6
Chiroptera	8	75	~ 8[g]	7
Afrosoricida	2	84	~ 10[h]	8
Macroscelida	1	-	-	8
Tublidentata	1	-	-	8
Proboscidea	1	-	-	8
Cingulata	1	-	-	8
Eulipotyphia	2	88	~ 10[i]	9
Marsupials	3	86	~ 30[j]	10
Monotremes	1	-	-	10
Mammalian Total:	112	36	~68	-

Table 36: Number of VKORC1 sequences found in each taxonomic order for Mammals with the sequence identity within the specific order and the evolutionary timespan between the different species. (a) Kumar and Hedges (1998); (b) Ge *et al.* (2013); (c) Pozzi *et al.* (2014); (d) Zurano *et al.* (2019); (e) Nyakatura and Bininda-Edmonds (2012); (f) Steiner and Ryder (2011); (g) Agnarsson *et al.* (2011); (h) Murphy *et al.* (2007); (i) He *et al.* (2017); (j) Haussler *et al.* (2009).

The sequence identity between all mammalian VKORC1 sequences is 36%. This suggests that just over a third of the VKORC1 protein is functionally constrained throughout mammalian

evolution around 68 millions of years and therefore may be essential for structure and function of the enzyme. The Rodentia order has the lowest sequence identity with 62% compared to other mammalian orders (Table 36). This is probably due to the large evolutionary timespan of ~70 millions of years between the rodent species found within this order. The Carnivora order has the highest sequence identity with 94% (Table 36) even with an evolutionary time span of ~30 million years suggesting high functional conservation and constraints in Carnivora VKORC1 sequences.

Throughout the mammalian VKORC1 sequences there are some amino acid changes that only occur within a specific taxonomic order or family. The Certartiodactyla order contains a few positions that are different to all other mammals. For example, within the Cetartiodactyla (Even-toed ungulates) order in the ruminant family which include cows, sheep etc. contain a positive arginine at position 107 whereas all other mammalian VKORC1 sequences contain a hydrophobic amino acid (valine/leucine/isoleucine) (Figure 56). This position is within the third transmembrane domain and therefore a positive amino acid at this position may change the helix-helix interactions. The Bovinae family which include the genus *Bos, Bison,* and *Bubalis*, contain a cysteine at position 110 whereas all other mammals contain a serine at this position with the exception of the *Condylura cristata* (Star-nosed mole) (Figure 56). Although this may be due to a sequencing error in the star-nosed mole. This is a change in physiochemical properties at this position and may result in a change in the structure or function of VKORC1 and potentially effect of anticoagulants on bovine VKORC1. The *Sus scrofa* (pig) sequence has a number of amino acid differences across its VKORC1 sequence which may be unique but there is also a possibility of poor sequence data.

By studying the multiple sequence alignments, it is possible to observe positions at which amino acid substitutions have occurred during evolution within the VKORC1 enzyme. An example of this is at position 146 which lies within TM4. All animals belonging to the Xenarthra and Afrotheria clades (Figure 60) and the Eulipotyphia order, the sister order to the even toed ungulates (Figure 60) contain a threonine at this position. From the multiple sequence alignment of the even toed ungulates (Figure 56) shows that only animals belonging to the ruminant family contain a threonine at this position and all other sequences contain a methionine, a hydrophobic residue at this position. Assessing this position throughout the

other mammalian orders show a hydrophobic residue suggesting that this change was retained in the rest of the clade containing the even-toed ungulates known as the Laurasiatheria clade and the sister clade Euarchontglires which contain humans (Haussler *et al.*, 2009). This amino acid change may change the affinity of substrate binding to VKORC1.

4.3 Analysis of VKORC1 Amino Acid Sequences in Non-Mammals

By using multiple sequence alignments, the sequence identity was calculated within each taxonomic class in non-mammals (Table 37).

Taxonomic Class	Number of Sequences	Evolutionary Time Span (My)	Sequence Identity (%)	Figure Number
Birds	2	~100[a]	63	11
Reptiles	9	~100[b]	61	12
Amphibians	2	~31[c]	85	13
Fish	15	~75[d]	63	14

Table 37: Number of VKORC1 sequences found in each taxonomic class for non-mammals with the sequence identity within each class. (a) Stapley *et al.* (2008); (b) Haussler *et al.* (2009); (c) Session *et al.* (2016); Betancur *et al.* (2013).

All non-mammalian classes have a higher sequence identity in comparison with mammalian VKORC1 (Table 36 and 37). Although the highest sequence identity is found between the amphibian VKORC1 sequences this could be expected especially as both sequences belong to the same genus (*Xenopus* – clawed frogs), so these VKORC1 sequences are not totally representative of all amphibians, but it still gives an insight into the amphibian VKORC1. The reptiles and fish VKORC1 proteins have a sequence identity of 61% and 63%, respectively. The VKORC1 sequences found for both classes span a vast evolutionary timescale of between 100 and 75 millions of years, respectively, therefore it is expected that there is a lower sequence identity between VKORC1 sequences.

Until recently there was only the *Gallus gallus* (chicken) VKORC1 sequence found on the NCBI database for birds, with the recent addition of the *Taeniopygia guttata* (Zebra finch) VKORC1 sequence to the NCBI database in August 2019 this allowed for a comparison between the two bird sequences (Figure 63). The sequence identity between the two sequences is 63%. The low conservation may be due to the two sequences belonging to two different orders

Galliformes (chicken) and Passeriformes (zebra finch) and are evolutionary diverse with an evolutionary timespan of 100 million years (Stapley *et al.,* 2008). Birds form part of the living members of the Archosauromorpha clade which is inclusive of the extinct dinosaurs. This diverse evolutionary history may explain the difference in VKORC1 sequences in birds. Although the addition of the zebra finch sequence allows for a better understanding of the bird VKORC1 sequence, there is a potential that these sequences are pseudogenes are not functional within the bird genome as no other bird genomes have VKORC1. Therefore, there is a possibility that another enzyme or system could be responsible for the blood clotting activation which could explain the difference seen within the sequence of bird VKORC1 and other vertebrate VKORC1 such as VKORC1L1. Searches on the NCBI database revealed that most bird genomes have a VKORC1L1 sequence and could be a candidate for the enzyme responsible for blood coagulation in birds. Birds are known to be naturally resistant to anticoagulant rodenticides, for example the LD_{50} in chicken for warfarin is >1000 mg/kg (Hagen and Radomski, 1953). Human and brown rat VKORC1L1 enzymes have been shown to be 50 and 30-fold more resistant respectively to warfarin than VKORC1. Therefore, this could also be evidence towards VKORC1L1 as a candidate for blood coagulation in birds rather than VKORC1.

Interestingly, although only one full length bird VKORC1 sequence (chicken) was identified with only partial sequences found (Nakayama *et al.,* 2020) prior to August 2019. Some studies have included incorrect bird sequences as VKORC1 when in fact they are of its paralogous enzyme VKORC1L1 (Wu *et al.,* 2018). For example, Wu *et al.* (2018) generated a multiple sequence alignment of a region of the large conserved loop and included the zebra finch "VKORC1" sequence, however, upon inspection by the author of this thesis the sequence is incorrect and is of zebra finch VKORC1L1. This is confirmed with the recent annotation of the VKORC1 sequence for zebra finch in August 2019 (Figure 63).

4.4 Percentage Identity Comparison of Vertebrate VKORC1

In order to assess the conservation between the different classes of vertebrate VKORC1 a percentage identity table was generated using the consensus sequences (Table 38).

	Mammal VKORC1	Bird VKORC1	Reptile VKORC1	Amphibian VKORC1	Fish VKORC1
Mammal VKORC1	100%	28%	29%	31%	30%
Bird VKORC1		100%	37%	41%	40%
Reptile VKORC1			100%	52%	43%
Amphibian VKORC1				100%	43%
Fish VKORC1					100%

Table 38: Percentage identity between the five different classes of vertebrate VKORC1.

The percentage identity between the different classes of vertebrate VKORC1 have a range from 28% to 52%. Mammalian VKORC1 sequences have the lowest percentage (28-31%) of conserved amino acids compared to all other classes of vertebrate VKORC1. Amphibian VKORC1 sequences have the highest similarity to other classes of vertebrate VKORC1, with the highest percentage similarity between reptile and amphibian at 52%. The percentage identity between the vertebrate VKORC1 sequences are generally <50% suggesting that only certain positions through the evolution of the protein are functionally constrained and there is a large amount of sequence variance throughout the evolution of VKORC1.

4.5 Comparison of the vertebrate VKORC1 sequences

4.5.1 Comparison of vertebrate VKORC1 sequences using an MSA

In order to compare VKORC1 sequences between each vertebrate class representative VKORC1 sequences were chosen and aligned (Figure 67). The alignment highlights conservation and the differences in amino acids found across the vertebrate VKORC1 sequences. Comparison between the classes shows marked differences between the vertebrate classes. Birds and amphibians VKORC1 sequences appear to be the most different compared to the mammals, reptile and fish VKORC1 sequences. This could be due to the millions of years of evolution between the different vertebrate classes. There are however regions that contain high conservation between all vertebrate species for example from position 49 (Isoleucine/Valine) to position 65 (Leucine) [XSCSRVFXSRWGXGXGL] which forms part of the large loop suggesting that this is essential for VKORC1 structure and function. There are also regions that show high conservation in mammals VKORC1 but differ in other vertebrate classes, such as position 30 (lysine) to position 35 (arginine) [KAARAR] which forms the beginning of the large loop. There are 41 positions in which there is 100% conservation

throughout all of the representative vertebrate species suggesting that these amino acids could be essential for the structure and function of vertebrate VKORC1. The alignment shows there is greater variation in the amino acid sequences between the different VKORC1 sequences at the N and C terminals. There are insertions at both the N and C terminals in non-mammalian VKORC1 sequences with the exception of mammals belonging to the Marsupial (*Phascolarctos cinereus* - Koala) and Monotreme (*Ornithorhynchus anatinus* - Duck-billed platypus) orders. One noticeable amino acid difference is shown within the *Bos taurus* (cow) sequence at position 107 where a positively charged arginine is found in a highly conserved hydrophobic position in all vertebrate VKORC1 sequences. This may have an effect on the helix-helix interactions due to its position in TM3.

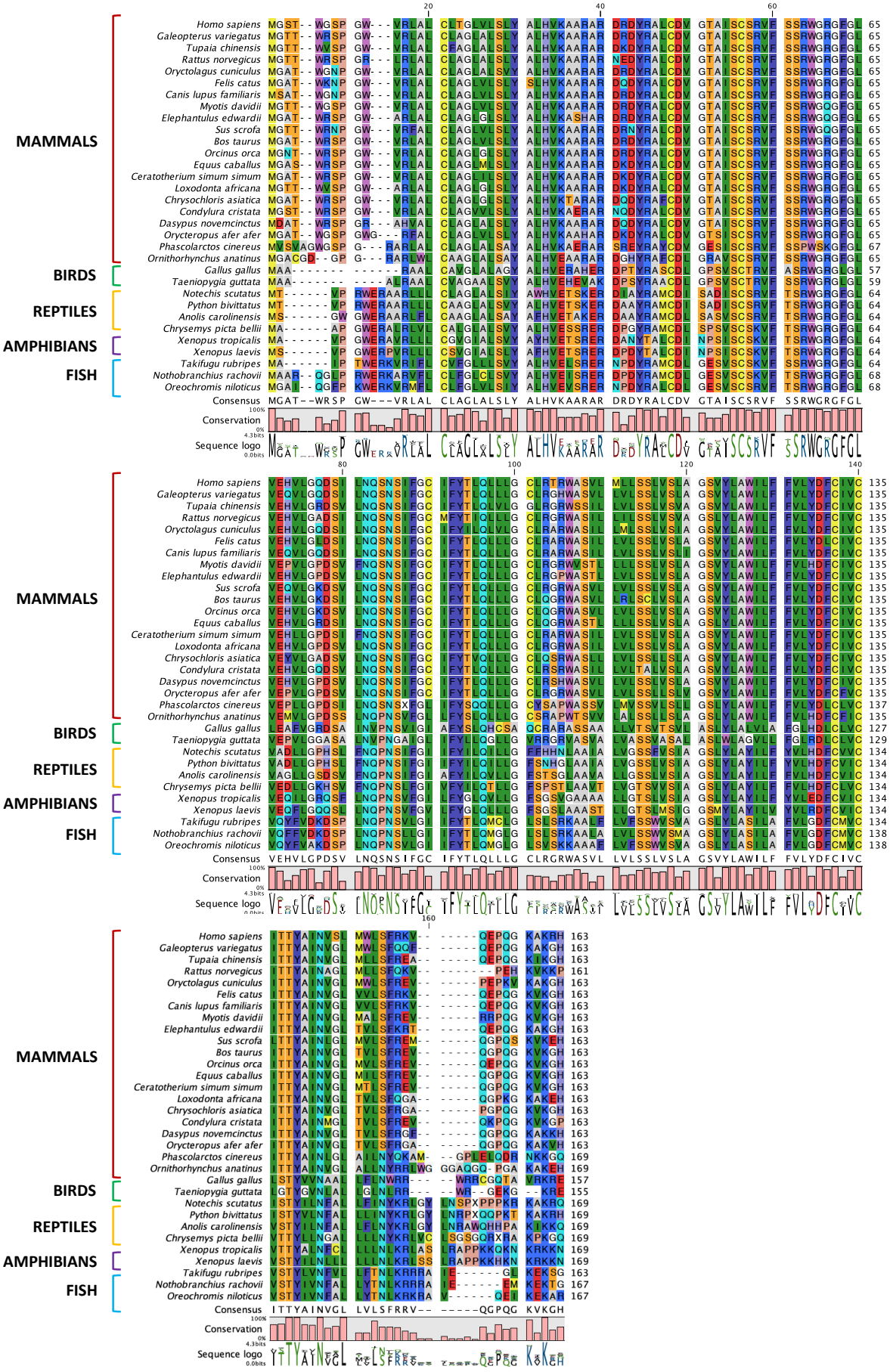


Figure 67: Multiple sequence alignment of representative vertebrate VKORC1 sequences. Red line denotes Mammalian sequences. Green line denotes bird sequences. Yellow line denotes reptile sequences. Purple line denotes amphibian sequences. Blue line denotes fish sequences. Colours of amino acids are according to physiochemical properties, refer to Appendix 8.

4.5.2 Consensus sequences for vertebrate VKORC1

To further compare the vertebrate VKORC1 sequences, consensus sequences were generated for each vertebrate class using the multiple sequence alignments (Figure 68) to observe conservation within and between the vertebrate classes. Although a consensus sequence is automatically generated by the CLC program for each alignment it does not distinguish between fully conserved or partially conserved positions whereas the sequence logo included with each alignment provides this information. The sequence logo is derived from the percentage of conservation at each amino acid position. Therefore, for the generated consensus sequences an amino acid position that was 100% conserved the single letter amino acid letter was used and for amino acid positions that were unconserved where one amino acid change or more was observed an 'X' was used. Consensus sequences allow a comparison of the amino acid sequences and allows the identification of conserved and common residues as well as specific amino acids to each vertebrate class.

From the consensus sequences created for the vertebrate classes for VKORC1 in Figure 66 shows amino acids that are conserved throughout vertebrate evolution such as the C_{132} XXC_{135} active site domain highlighted on Figure 68 with the red box, implying that these amino acids may have an important role in the structure and function of VKORC1. It also gives an indication of regions of the protein that are highly conserved, for example within the transmembrane domains. Mammalian VKORC1 sequence appear to have the greatest variation in the VKORC1 sequences compared to the other vertebrate classes (Figure 68). This could be due to the evolutionary timespan between the species used to generate the mammalian consensus VKORC1 sequence. At both N and C terminals in all vertebrate consensus sequences appears to have the most variation.

4.5.3 Using the Consensus sequences to assess functional constraint across vertebrate VKORC1

Figure 68 showed a protein sequence alignment of VKORC1 across the vertebrate classes. Conserved amino acids within a class are indicated with the single letter amino acid code. Variable positions within a class are shown with an X and the amino acids found at that position are shown in Figures 69-73.

The alignments reveal the functional conservation across the vertebrate classes. In general, the mammalian VKORC1 enzyme appears to have the least functional constraint, as 63% of positions are not 100% conserved and most positions have multiple amino acids found at these positions. Whereas, other vertebrate classes show a higher level of functional constraint, this may be due to the evolutionary time span between the species within these classes. Across all vertebrate classes, it appears that there is more variation at the N and C terminal ends compared to the rest of the protein sequences. These changes may be allowed within the enzyme as it may not affect the structure or function of the enzyme. The C terminal of the enzymes appear to have a high number of charged amino acids both positive and negative (Figures 69-73). This could be used as anchor for the protein in the endoplasmic reticulum membrane. The large loop between TM1 and TM2 found in all VKORC1 sequences appears to have the most amount of conservation and high functional constraint compared to the TM domains across all vertebrate classes.

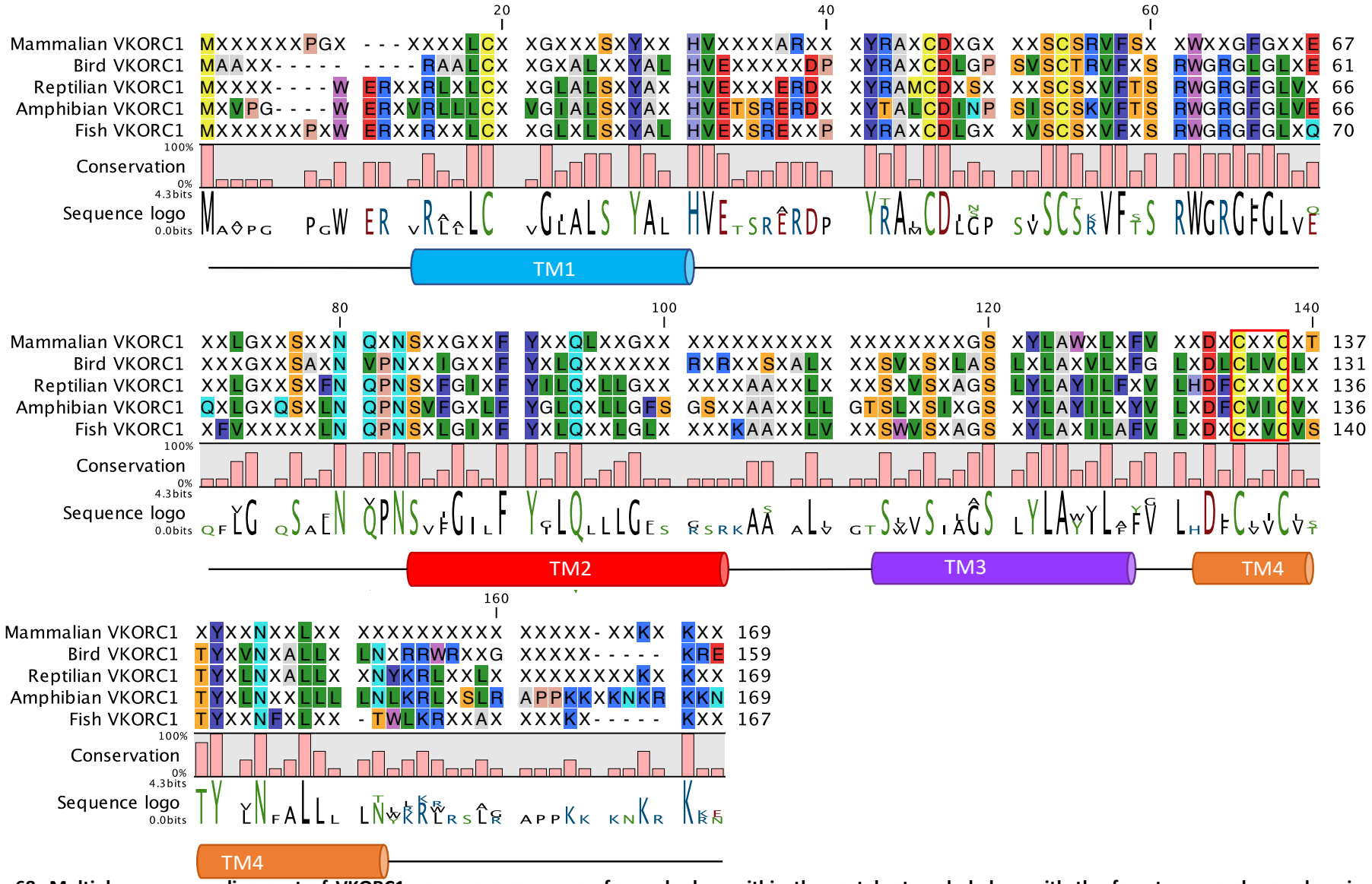


Figure 68: Multiple sequence alignment of VKORC1 consensus sequences for each class within the vertebrate subphylum with the four transmembrane domains highlighted. X denotes one or more amino acid differences. Red box denotes active site. Colours of amino acids are according to physiochemical properties refer to Appendix 8. The sequence logo indicates the sequence conservation of the amino acids.

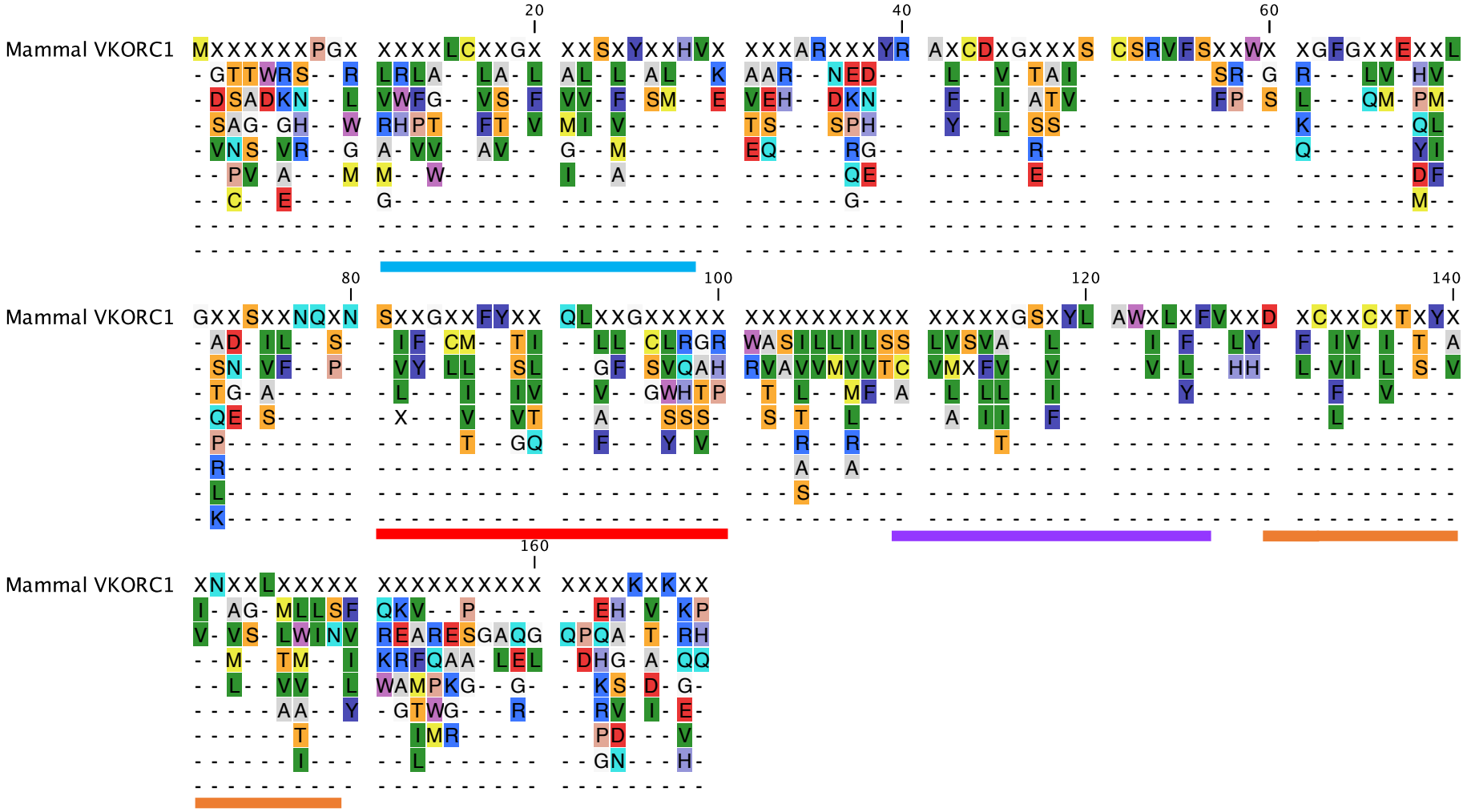


Figure 69: Multiple sequence alignment of the mammalian VKORC1 consensus sequence with the amino acid differences shown under the unconserved positions. X denotes one or more amino acid difference. Colours of amino acids are according to physiochemical properties refer to Appendix 8. Transmembrane domains are shown as coloured lines, TM1 – blue, TM2 – red, TM3 – purple and TM4 – orange.

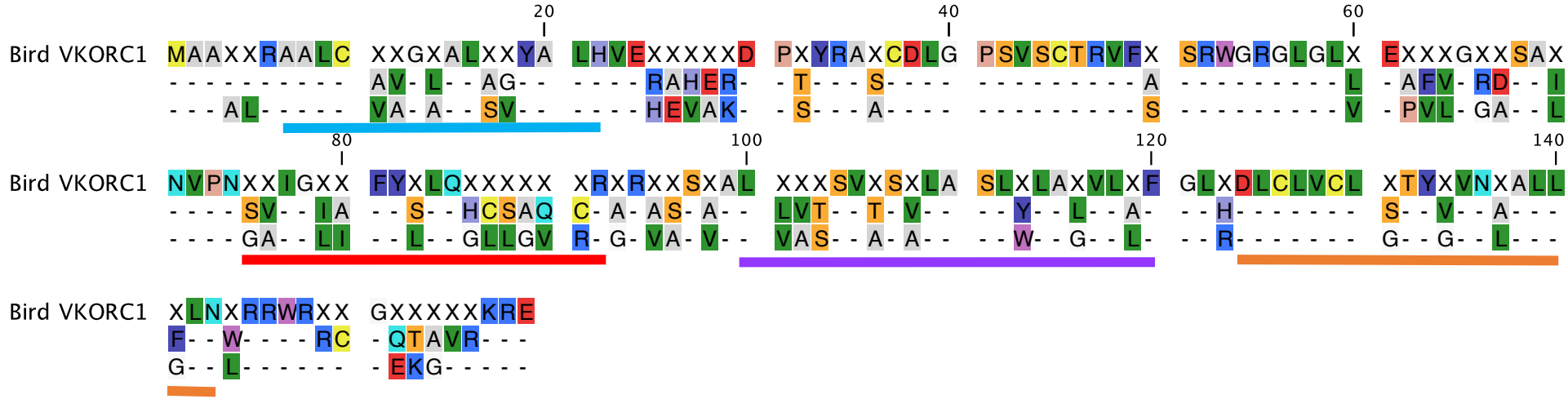


Figure 70: Multiple sequence alignment of the bird VKORC1 consensus sequence with the amino acid differences shown under the unconserved positions. X denotes one or more amino acid difference. Colours of amino acids are according to physiochemical properties refer to Appendix 8. Transmembrane domains are shown as coloured lines, TM1 – blue, TM2 – red, TM3 – purple and TM4 – orange.

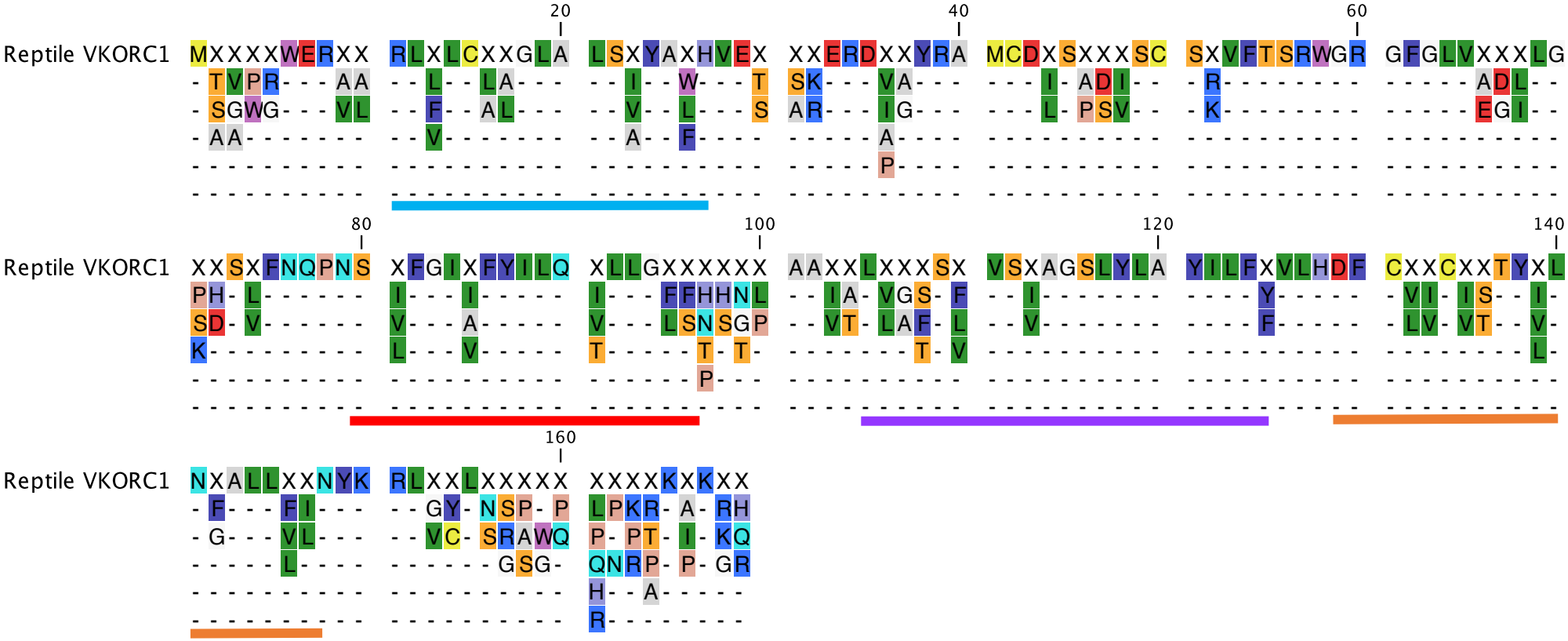


Figure 71: Multiple sequence alignment of the reptilian VKORC1 consensus sequence with the amino acid differences shown under the unconserved positions. X denotes one or more amino acid difference. Colours of amino acids are according to physiochemical properties refer to Appendix 8. Transmembrane domains are shown as coloured lines, TM1 – blue, TM2 – red, TM3 – purple and TM4 – orange.

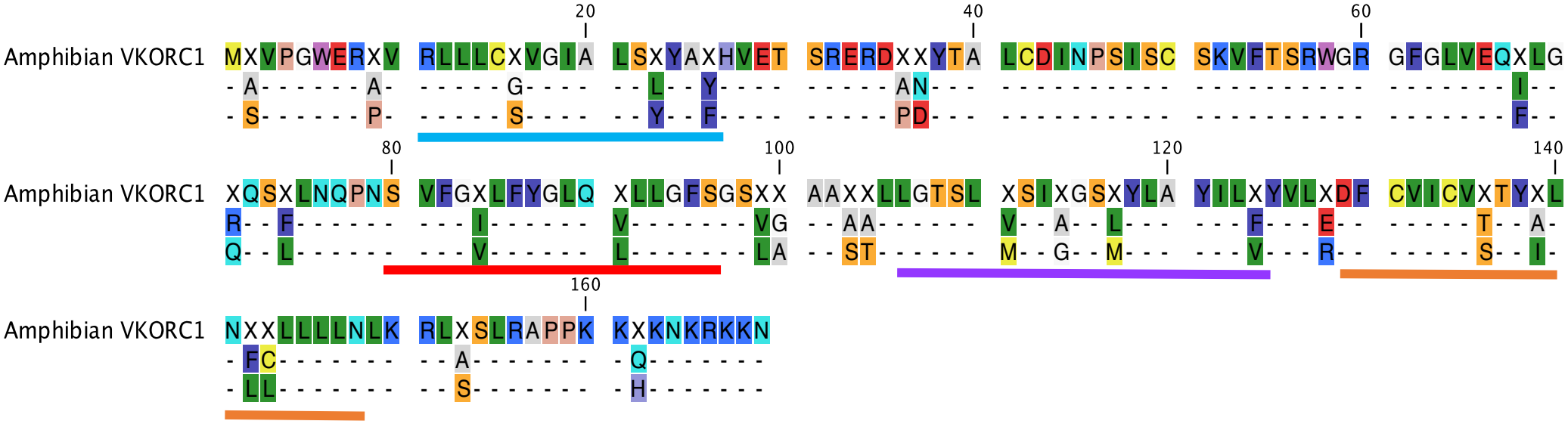


Figure 72: Multiple sequence alignment of the amphibian VKORC1 consensus sequence with the amino acid differences shown under the unconserved positions. X denotes one or more amino acid difference. Colours of amino acids are according to physiochemical properties refer to Appendix 8. Transmembrane domains are shown as coloured lines, TM1 – blue, TM2 – red, TM3 – purple and TM4 – orange.

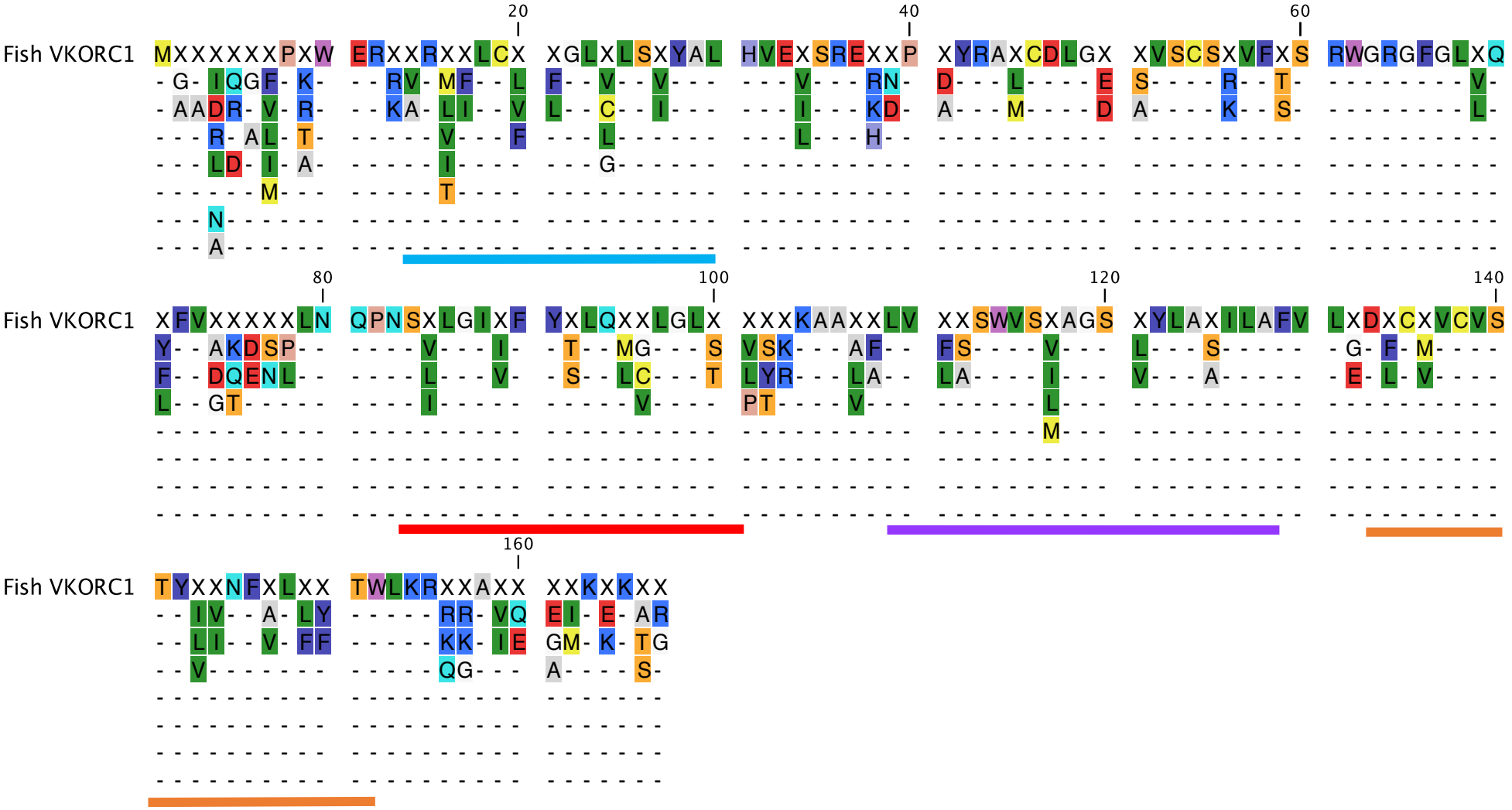


Figure 73: Multiple sequence alignment of the fish VKORC1 consensus sequences with the amino acid differences shown under the unconserved positions. X denotes one or more amino difference. Colours of amino acids are according to physiochemical properties refer to Appendix 8. Transmembrane domains are shown as coloured lines, TM1 – blue, TM2 – red, TM3 – purple and TM4 – orange.

4.6 Comparison of representative vertebrate VKORC1 sequences using Membrane topology and tertiary prediction modelling

Membrane topology and tertiary structure prediction can help to understand the structure of a protein. Both membrane topology and tertiary structure prediction has been used previously to predict the number of transmembrane domains contained within human VKORC1 (See Section 1.12). However, structure prediction has not been performed for species throughout the vertebrate classes. Preliminary structural models were performed for four mammalian VKORC1 sequences (*Homo* sapiens - Human, *Bos taurus* - Cow, *Vombatus ursinus* - Wombat, *Ornithorhynochus anatinus* - Duck-billed Platypus), one bird (*Gallus gallus* - chicken), one reptile (*Python bivittatus* - python), one amphibian (*Xenopus tropicalis* - Western clawed frog) and one fish (*Oreochromis niloticus* - Nile tilapia) using TMHMM for a membrane topology prediction model. For the membrane topology and tertiary prediction, models were created using SWISS-Model based on the original structure of the bacterial homologue *Synechococcus sp.* VKORC1 determined by x-ray crystallisation (PDB. 3KP9) (*Li et al.,* 2010) and then Chimera was used for visualisation of the models. Figure 74 and 75 show the prediction of the membrane topology and tertiary structures of four representative mammalian and four representative non-mammalian VKORC1 sequences.

From the TMHMM prediction, all mammalian VKORC1 structures contained 3 TM domains (Figure 74). Human VKORC1 contained the strongest 3 TM signals, whereas the other mammalian VKORC1 sequences have weaker signals in comparison. The TMHMM prediction for cow VKORC1 showed that the second TM domain is in a slightly different place in the enzyme in comparison to the other mammalian VKORC1 sequences. The TMHMM prediction in the chicken showed only two TM domains (Figure 75). This may be due to the differences seen within the primary sequences. Compared to the vertebrate VKORC1 sequences, the chicken appears to be missing the first transmembrane domain due to the lack of characteristic hydrophobic residues. Like mammalian VKORC1 sequences, the western clawed frog shows 3 TM domains (Figure 75). However, both python and Nile tilapia VKORC1 TMHMM prediction show 4TM models.

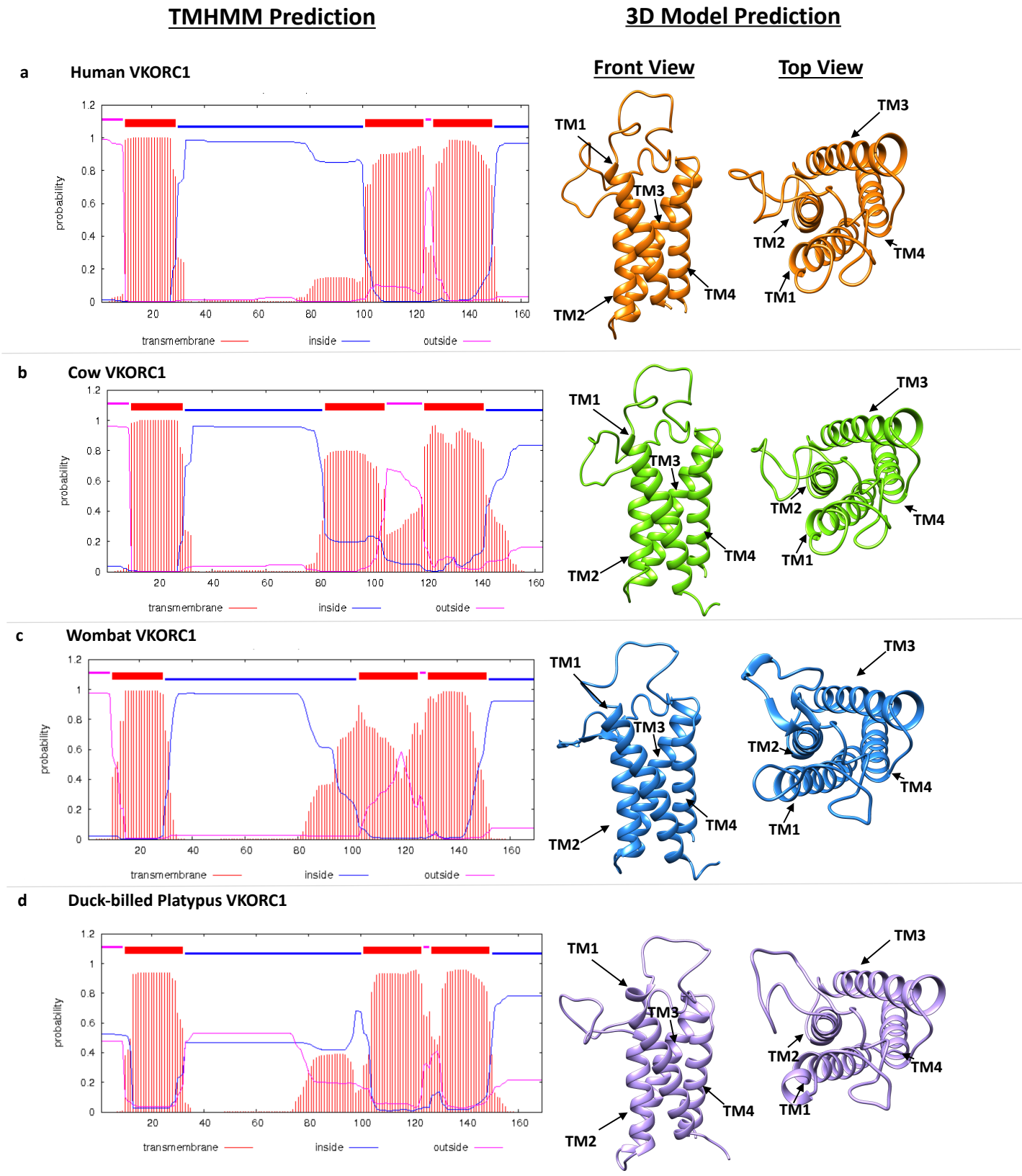


Figure 74: Membrane topology and tertiary structure prediction models for representative mammalian VKORC1 species; human, cow, wombat and duck-billed platypus. Each panel shows a TMHMM prediction graph and 3D model prediction using SWISS-Model and Chimera for a front and top view of the VKORC1 sequence with the transmembrane domains highlighted. a Human VKORC1. **b** Cow VKORC1. **c** Wombat VKORC1. **d** Duck-billed Platypus VKORC1.

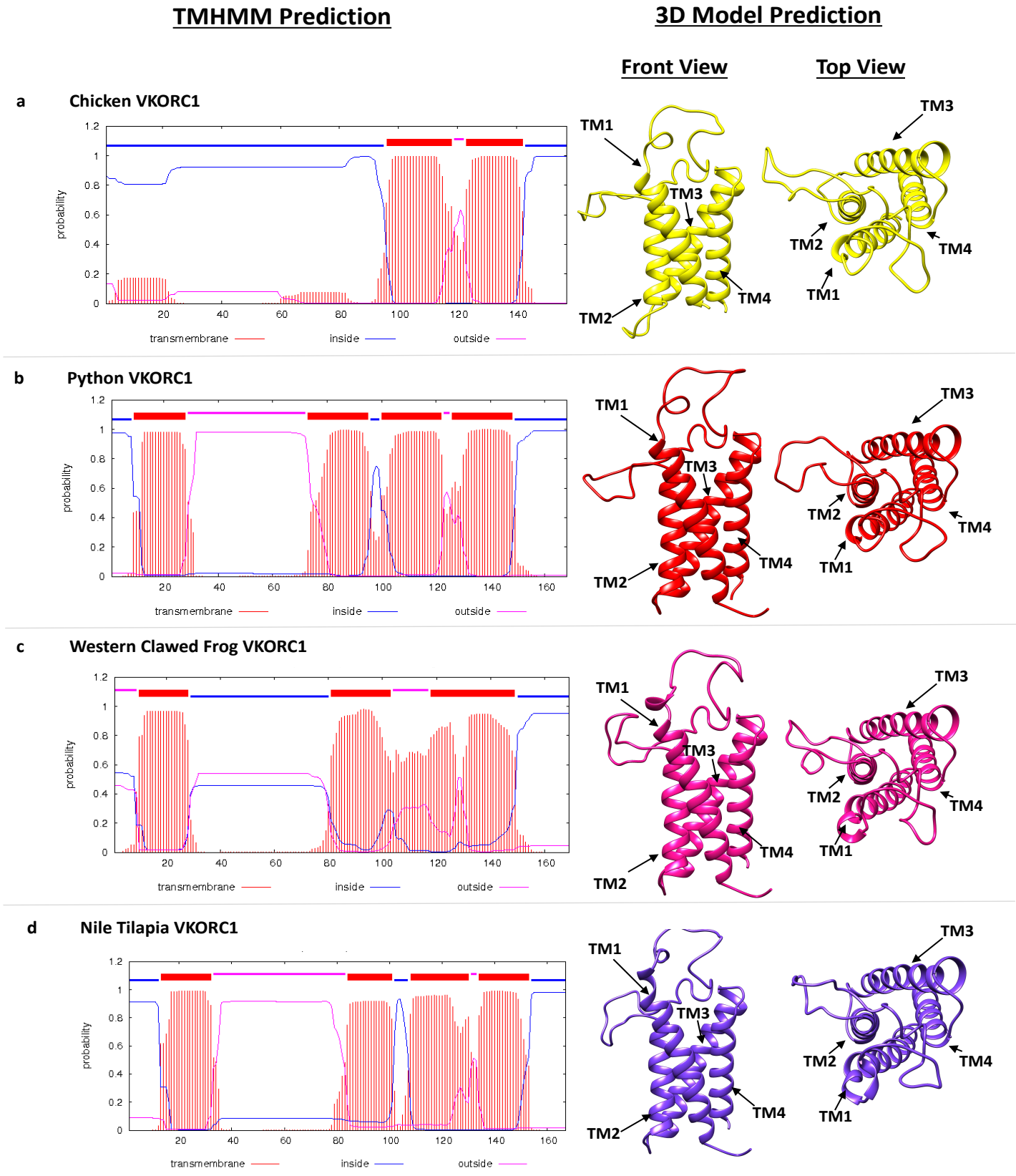


Figure 75: Membrane topology and tertiary structure prediction models for representative non-mammalian VKORC1 species; chicken, python, western clawed frog and Nile tilapia. Each panel shows a TMHMM prediction graph and 3D model prediction using SWISS-Model and Chimera for a front and top view of the VKORC1 sequence with the transmembrane domains highlighted. a Chicken VKORC1. **b** Python VKORC1. **c** Western clawed frog VKORC1. **d** Nile tilapia VKORC1.

The TMHMM prediction also gives an indication of the orientation of the protein. The human cow and wombat VKORC1 show that the N terminus is on the outside of the ER membrane and the C terminus is in the inside of the ER lumen, with the large loop. This is consistent with the 3 TM domain predictions by Tie *et al.* (2012) and Sinhadri *et al.* (2017) (See Section 1.12). However, the duck-billed platypus VKORC1 shows a difference in orientation although the 3 TM domains are the same as the other mammalian VKORC1. The signal is not as strong however, it shows that the N and C terminus are on the inside of the membrane and the large loop is on the outside of the ER membrane. The orientation is consistent with the 4 TM model described by Schulman *et al.* (2010) and Cao *et al.* (2016) (See Section 1.12). Of the non-mammalian VKORC1, the reptile, amphibian and fish VKORC1 has the same orientation as the duck-billed platypus, with only the amphibian VKORC1 with a weaker signal as seen for the duck-billed platypus. Although the chicken VKORC1 prediction only contains two TM domains the orientation shows the N and C terminus on the inside of the of the membrane.

From these results it suggests that there is a difference in the number of transmembrane domains found within the different vertebrate classes and in general there is a change from 4 TM domains to 3 TM throughout vertebrate evolution. There is also a difference in orientation with non-mammalian VKORC1 predictions showing the N and C terminus on the same side of the protein consistent with the 4 TM model described by Schulman *et al.* (2010) and Cao *et al.* (2016) (See Section 1.12). Interestingly, the duck-billed platypus contains the same orientation as non-mammals and there is a change in orientation in both marsupial and placental mammals. This change in orientation may have occurred during the evolution of mammals and changed within the extinct clade between the monotremes and the marsupials and placentals (Luo *et al.,* 2007).

The tertiary structure prediction models show a 4 TM domain structure for all representative vertebrate VKORC1 sequences (Figure 74 and 75). The prediction of the models was based on the original structure of the bacterial homologue *Synechococcus sp.* VKORC1 by Li *et al.* (2010). As this is the only defined structure for any VKORC1, all models based on this structure by Li *et al.* (2010) will bias towards a 4 TM prediction regardless of the secondary prediction. The large loop structure for all the vertebrate VKORC1 models show a difference suggesting that the binding of substrates or antagonists such as anticoagulants may have a different

effect on the enzymes. The wombat VKORC1 model has a major difference compared to all other VKORC1 models as there is a β-pleated sheet and a part helix found within the large loop structure.

4.7 Analysis of the previously reported roles of amino acids between the vertebrate classes for VKORC1

There are many amino acid positions identified in the literature that have roles in the structure, substrate binding (VK and VKE), warfarin binding and positions that are related to anticoagulant resistance in human, brown rat and house mouse (Section 1.16). The multiple sequence alignments created for VKORC1 (Figures 54-66) were used to examine conservation in different phyla regarding to different roles identified for VKORC1 (Tables 39-46). The percentage of an amino acid found at each position assessed was calculated for all vertebrate classes. The amino acid numbering used is according to the human VKORC1 sequence.

4.7.1 Analysis of Amino acids important in the structure and function of human and rat VKORC1 in other vertebrates

Amino acids can have different roles within a protein, some amino acids are involved in binding ligands and some are involved in stabilising the structure. Although it could be assumed that all vertebrate VKORC1 sequences catalyse the conversion of vitamin K epoxide to vitamin K and bind the same substrates, this may not be true as only human and brown rat VKORC1 enzymes have been scrutinized fully and may not be fully representative of all vertebrate sequences. Using the primary vertebrate VKORC1 sequences allows a prediction of this using the positions identified previously that are known for substrate binding, inhibitor binding and structure stabilisation.

There are many amino acids in VKORC1 which are important to maintain stability of VKORC1 (Table 39, 40 and 41). In general, most positions identified are conserved throughout vertebrate evolution, suggesting that vertebrate VKORC1 enzymes have the ability to catalyse the conversion of vitamin K epoxide to vitamin K.

Human Position	Previously Reported Role in VKORC1	Reference	Mammal VKORC1	Bird VKORC1	Reptile VKORC1	Amphibian VKORC1	Fish VKORC1
L15	Maintain a stable VKOR structure	Wu *et al.,* 2018	**L**	**L**	**L**	**L**	**L**
L22	Helps to hold TM1 and TM2 in VKORC1 together	Wu *et al.,* 2018	97% - L 2% - V 1% - I	**L**	**L**	**L**	**L**
L105	Helps to hold TM1 and TM2 in VKORC1 together	Wu *et al.,* 2018	99% - L 1% - V	**A**	67% - A 33% - T	50% - A 50% - T	54% - A 46% - F
L128	Maintain stable VKORC1 structure.	Wu *et al.,* 2018	99% - L 1% - H	**L**	**L**	**L**	**L**

Table 39: Amino acid positions with a previously reported role in the stability of VKORC1 with the percentage of amino acids found at each position for each vertebrate class. 100% is represented by bold single letter code. Amino acid numbering according to human VKORC1 sequence. Colours of amino acids are according to physiochemical properties, refer to Appendix 8.

Human Position	Previously Reported Role in VKORC1	Reference	Mammal VKORC1	Bird VKORC1	Reptile VKORC1	Amphibian VKORC1	Fish VKORC1
K30	Naphthoquinone head binding – VKE and VK	Czogalla *et al.,* 2017	99% - K 1% - E	**E**	**E**	**E**	**E**
F55	Naphthoquinone head binding – VKE and VK.	Czogalla *et al.,* 2017; Wu *et al.,* 2018	**F**	**F**	**F**	**F**	**F**
W59	Naphthoquinone head binding – VKE and VK.	Czogalla *et al.,* 2017	**W**	**W**	**W**	**W**	**W**
Q78	Naphthoquinone head binding – VK.	Czogalla *et al.,* 2017	**Q**	**V**	**Q**	**Q**	**Q**
N80	Naphthoquinone head binding – VK.	Czogalla *et al.,* 2017;	**N**	**N**	**N**	**N**	**N**
L120	Naphthoquinone head binding – VKE and VK.	Czogalla *et al.,* 2017;	**L**	**L**	**L**	**L**	**L**
I123	Naphthoquinone head binding – VK.	Czogalla *et al.,* 2017;	99% - I 1% - V	**V**	**I**	**I**	**I**
L124	Naphthoquinone head binding – VK.	Czogalla *et al.,* 2017;	**L**	**L**	**L**	**L**	**L**
L128	Naphthoquinone head binding – VKE and VK.	Czogalla *et al.,* 2017	99% - L 1% - H	**L**	**L**	**L**	**L**

Table 40: VKORC1 amino acid positions with a previously reported role of naphthoquinone head binding of vitamin K and vitamin K epoxide with the percentage of amino acids found at each position for each vertebrate class. 100% is represented by bold single letter code. Amino acid numbering according to human VKORC1 sequence. Colours of amino acids are according to physiochemical properties, refer to Appendix 8.

Human Position	Previously Reported Role in VKORC1	Reference	Mammal VKORC1	Bird VKORC1	Reptile VKORC1	Amphibian VKORC1	Fish VKORC1
F87	Isoprenoid chain binding	Czogalla *et al.*, 2017	**F**	**F**	**F**	**F**	**F**
Y88	Isoprenoid chain binding	Czogalla *et al.*, 2017;	**Y**	**Y**	**Y**	**Y**	**Y**
L90	Isoprenoid chain binding	Czogalla *et al.*, 2017	87% - L 8% - I 3% - Q 1% - V 1% - T	**L**	**L**	**L**	**L**
V112	Isoprenoid chain binding	Czogalla *et al.*, 2017	88% - V 4% - M 7% - L 1% - A	50% - T 50% - A	**V**	50% - V 50% - M	**V**
S113	Isoprenoid chain binding	Czogalla *et al.*, 2017	99% - S 1% - X	**S**	**S**	**S**	**S**

Table 41: VKORC1 amino acid positions with a previously reported role of isoprenoid chain binding of vitamin K and vitamin K epoxide with the percentage of amino acids found at each position for each vertebrate class. 100% is represented by bold single letter code. Amino acid numbering according to human VKORC1 sequence. Colours of amino acids are according to physiochemical properties, refer to Appendix 8.

A study by Wu *et al.* (2018) suggests that position L15 and L128 are essential for maintaining a stable VKORC1 structure and positions L22 and L105 help to hold TM1 and TM2 together in the 3TM model of VKORC1 (Table 39). From Table 39, L15 is completely conserved and L128 is completely conserved in all vertebrate classes except for one mammalian sequence (*Macaca fascicularis* – Long-tailed macaque) that contain a positive histidine at that position. Whilst this could be due to a sequencing error, if it is real this could cause some disruption in the stability of the VKORC1 structure due to the change in charge. L22 is conserved in all vertebrate VKORC1 except for 3% of mammalian VKORC1 sequences which contain either an isoleucine or valine (Isoleucine: *Marmota marmota marmota* – Alpine marmot; Valine: *Echinops telifari* – Lesser hedgehog tenrec, *Erinaceus europaeus* – European hedgehog). Due to the hydrophobic nature of isoleucine, valine and leucine, a change here would probably have little effect on the structure of VKORC1. Of all 4 positions that Wu *et al.* (2018) identified, L105 is the only position that is not highly conserved throughout vertebrate evolution. Although it can be noted that >50% of non-mammals have an alanine at this position suggesting that this amino acid may have a different role in non-mammals.

As well as structural stability within VKORC1, there are many amino acids identified that are responsible for the binding of substrates (Table 40). A study by Czogalla *et al.* (2017) used 3D modelling and molecular docking of vitamin K epoxide and vitamin K to identify the positions used for substrate binding. Table 40 shows the amino acids responsible for substrate binding and their conservation throughout vertebrate VKORC1 sequences. There are five amino acids that are required for the binding of the naphthoquinone head of both vitamin K epoxide and vitamin K. These are K30, F55, W59, L120 and L128. A further 4 amino acids, Q78, N80, I123 and L124 are required for the naphthoquinone head binding of vitamin K only. Of these, F55, W59, N80, L120 and L124 are completely conserved throughout vertebrate VKORC1 suggesting an essential role in the binding of vitamin K and vitamin K epoxide. In contrast, at position 30 the positively charged lysine residue is conserved in 99% of mammalian sequences with only one of the mammalian sequences (*Ornithorhynchus anatinus* – Duck-billed platypus) with a negatively charged glutamate residue. In all other vertebrate classes, a negatively charged glutamate residue is found. There is a potential that this amino acid evolved during mammalian evolution and changed between the monotreme and marsupial and placental clades, which may have an effect on the binding of the substrate due to the

charge difference at this position. Q78 is completely conserved in all vertebrates except for bird VKORC1 in which a valine is found at this position. This region of the VKORC1 protein is highly conserved and contains polar amino acids, therefore a change to a hydrophobic non-polar valine residue may affect the binding to the naphthoquinone head of vitamin K.

Table 41 shows positions F87, Y88, L90, V112 and S113 that are required for the isoprenoid chain binding for both vitamin K epoxide and vitamin K and their conservation throughout vertebrates. F87 and V112 are completely conserved throughout vertebrate VKORC1 sequences suggesting an essential role in isoprenoid chain binding. Both S113 and L90 are completely conserved in all non-mammalian sequences but not in mammalian VKORC1. At position 90 some mammals have a leucine, isoleucine or valine residue. Due to the hydrophobic nature of all three amino acids found in this position and their ability to be interchangeable, a substitution of these amino acids would probably not affect its function. The marsupials are the only species that contain a glutamine residue at position 90. This may have an effect on the binding of substrate due to the difference in physiochemical properties.

4.7.2 Amino Acids Involved in Warfarin Binding in human and rat VKORC1 in other vertebrate VKORC1s

Warfarin acts by binding to VKORC1 and inhibiting the conversion of vitamin K epoxide to vitamin K. Studies discussed in Section 1.17.5 show the biochemical effects of warfarin in liver microsomes in mammals other than the human and brown rat (e.g. sheep, cow and horse) and birds (e.g. chicken and ostrich) (Wilson *et al.,* 2003; Wantanabe *et al.,* 2010) suggesting that anticoagulants can bind to other mammals and birds. There are reports of anticoagulant rodenticides causing mortality in non-target animals (See Section 1.18). It is important to scrutinise the primary VKORC1 sequence of vertebrates predict whether other vertebrate VKORC1 enzymes have the ability to bind warfarin and be inhibited by rodenticides. There are a number of amino acid positions identified in the human and brown rat VKORC1 that are involved in warfarin binding (Table 42).

Human Position	Previously Reported Role in VKORC1	Reference	Mammal VKORC1	Bird VKORC1	Reptile VKORC1	Amphibian VKORC1	Fish VKORC1
Y25	Interact with Y139 to stabilise warfarin binding	Wu *et al.,* 2018	**Y**	**Y**	**Y**	**Y**	**Y**
A26	Interact with Y139 to stabilise warfarin binding.	Wu *et al.,* 2018;	99% - A 1% - S	**A**	**A**	**A**	**A**
R33	Charge stabilisation	Czogalla *et al.,* 2017	95% - R 5% - H	50% - H 50% - V	89% - K 11% - R	**R**	**R**
R40	Charge stabilisation	Czogalla *et al.,* 2017	**R**	**R**	**R**	**T**	**R**
R53	Charge stabilisation	Czogalla *et al.,* 2017	**R**	**R**	78% - R 22% - K	**K**	67% - K 33% - R
F55	Aromatic stacking – warfarin binding.	Wu *et al.,* 2018; Czogalla *et al.,* 2017	**F**	**F**	**F**	**F**	**F**
W59	Warfarin binding.	Czogalla *et al.,* 2017;	**W**	**W**	**W**	**W**	**W**
F63	Warfarin binding.	Wu *et al.,* 2018;	**F**	**L**	**F**	**F**	**F**
Y139	Warfarin binding site.	Wu *et al.,* 2018	**Y**	**Y**	**Y**	**Y**	**Y**

Table 42: VKORC1 amino acid positions with a previously reported role of warfarin binding of vitamin K and vitamin K epoxide with the percentage of amino acids found at each position for each vertebrate class. 100% is represented by bold single letter code. Amino acid numbering according to human VKORC1 sequence. Colours of amino acids are according to physiochemical properties, refer to Appendix 8.

A study by Wu *et al.* (2018) used molecular dynamics to determine the binding of warfarin in human VKORC1. All positions identified by Wu *et al.* (2018) are fully conserved throughout vertebrate evolution with the exception of positions 26 and 63. At position 26 an alanine residue is found in all non-mammalian VKORC1 sequences and 99% of mammalian sequences. Only two mammalian VKORC1 sequences (*Mus spretus* - Algerian mouse and *Felis catus* – cat) contain a serine residue at this position. This change in physiochemical properties may have an effect on the affinity of warfarin. At position 63 only bird VKORC1 sequences contain a different amino acid a leucine residue instead of a phenylalanine residue, which is a change in physiochemical properties from an aromatic side chain to an aliphatic side chain. This may therefore have an impact on the affinity of warfarin to bird VKORC1 enzymes.

Czogalla *et al.* (2017) identified that arginine residues (R33, R40, R53) in VKORC1 are shown to have charge stabilisation properties upon the binding of anionic warfarin. All three arginine residues are highly conserved. At position 33 the amino acids found at this position are largely positively charged amino acids such as lysine, arginine and histidine but a hydrophobic valine is found in one bird VKORC1 sequence (*Taeniopygia guttata* – Zebra finch). A change in physiochemical properties may affect the affinity of warfarin binding and the charge stability. R40 however, is completely conserved in all vertebrate VKORC1 but contains a threonine in amphibian VKORC1. A threonine change at this position may have not have an effect due its polar properties, however, it may not be as effective at stabilising the anionic warfarin. At position 53, the amino acids found at this position are largely positively charged amino acids such as lysine and arginine suggesting that charge stabilisation would occur due to the similar physiochemical properties of both residues.

4.7.3 Amino Acids that Cause Anticoagulant Resistance in human and rat VKORC1 in other vertebrates

SNPs that cause amino acid substitutions that give rise to resistance to anticoagulant rodenticides are known in human, rats and mice (Section 1.16). By looking at amino acids at these positions it can give an indication of the potential susceptibility to anticoagulants in vertebrate VKORC1 sequences.

4.7.3.1 Comparison of known human and rat VKORC1 SNPs to determine the susceptibility to anticoagulant rodenticides against vertebrate VKORC1 sequences

Tables 43-45 show the anticoagulant resistance polymorphisms in brown rat, human and house mouse with a comparison of amino acids found within each vertebrate class. Of the 32 positions identified that can cause anticoagulant resistance in the brown rat, human and house mouse there are nine that are present in warfarin sensitive human and rodent phenotypes that are fully conserved throughout vertebrate VKORC1 sequences (Table 43-45). These include; H28, V29, A41, V54, R58, W59, N77, L120 and Y139 (Table 43-45). Due to the strict conservation in all vertebrate VKORC1s it suggests that all vertebrates are potentially susceptible to anticoagulant rodenticides unless other amino acid changes occur which could cause anticoagulant resistance. There are four positions in which amino acids at these positions have similar physiochemical properties. These are: R35, V45, S52 and I123. For example, at position 35 only positively charged amino acids, lysine, arginine and histidine are found throughout vertebrate VKORC1 sequences. Due to the amino acids at these positions having similar physiochemical properties, it is likely that this would not change the affinity of warfarin or other anticoagulants and allow susceptibility to anticoagulants throughout vertebrates. Due to the high number of positions that infer susceptibility to anticoagulants in all vertebrates, it gives an explanation for the high number of reports of mortality of vertebrates by anticoagulant rodenticides.

In this study, multiple sequence alignments were also used to predict whether certain animals or orders contain amino acids which are associated with anticoagulant rodenticide resistance. From Table 43 there is 1% of mammals that contain a phenylalanine at position 56 and a methionine residue at position 66, both of these changes are found within the *Equus asinus* (donkey). Both of these amino acids are associated with anticoagulant resistance in humans and therefore, it suggests that the donkey may have natural anticoagulant resistance.

At position 68, a tyrosine residue that cause anticoagulant resistance in humans is found naturally in one mammal (*Chrysochloris asiatica* – Cape Golden Mole) and in 46% of fish VKORC1 sequences, there are seven species of fish which have a tyrosine at this position. Four of these fish belong to the Cichliformes (cichlids) order, two belong to the Tetradontidae (pufferfish) order and one fish belongs to the Beloniformes (medaka) order (Hughes *et al.,*

2018). These fish potentially acquired this amino acid through convergent evolution and potentially have a natural resistance to anticoagulant rodenticides. Similarly, at position 71, an alanine residue is found naturally in 40% of fish VKORC1 sequences and an alanine at this position is associated with natural resistance in humans. There are four fish that belong to the Cichliformes order, one fish that belongs to the Cyprinodontiformes order and one fish that belongs to the Pomacentridae family (Hughes *et al.,* 2018). Again, like the tyrosine at position 68 it is likely this amino acid was acquired through convergent evolution and potentially contain natural resistance to anticoagulant rodenticides.

There is also a potential for natural resistance to occur in the mammal *Macaca fascicularis* – Long-tailed macaque, which contains a positively charged histidine at position 128. A change to a polar (glutamine/serine) or positive residue (arginine) can cause anticoagulant resistance in humans, brown rats and mice. Therefore, it is possible that a change to a positively charged histidine that this may cause anticoagulant resistance in the long-tailed macaque

In 99% of non-mammalian VKORC1 sequences, a negative glutamate residue is found at position 34. This position when changed from an alanine to a proline causes anticoagulant resistance in humans. Therefore, there is an implied sensitivity to anticoagulants in 100% of mammals and the zebra finch but a potential natural resistance in non-mammals due to the negative glutamate change.

Human Position	Previously Reported Resistance Polymorphisms	Reference	Mammal VKORC1	Bird VKORC1	Reptile VKORC1	Amphibian VKORC1	Fish VKORC1
A26	A26T – *R. norvegicus*	Rost *et al.*, 2009	99% - A 1% - S	**A**	**A**	**A**	**A**
R33	R33P – *R. norvegicus*	Rost *et al.*, 2009	95% - R 5% - H	50% - H 50% - V	89% - K 11% - R	**R**	**R**
R35	R35P – *R. norvegicus*	Pelz *et al.*, 2005	**R**	50% - R 50% - K	**R**	**R**	88% - R 6% -K 6% - H
S56	S56P – *R. norvegicus*	Pelz *et al.*, 2005	99% - S 1% - F	50% - A 50% - S	**T**	**T**	87% - T 13% - S
F63	F63C – *R. norvegicus*	Rost *et al.*, 2009	**F**	**L**	**F**	**F**	**F**
S103	S103Y – *R. norvegicus*	Grandemange *et al.*, 2009	**S**	**S**	**A**	**A**	**A**
L120	L120Q – *R. norvegicus*	Pelz *et al.*, 2005;	**L**	**L**	**L**	**L**	**L**
I123	I123S – *R. norvegicus*		99% - I 1% - V	**V**	**I**	**I**	**I**
L128	L128Q/S – *R. norvegicus*	Pelz *et al.*, 2005	99% - L 1% - H	**L**	**L**	**L**	**L**
Y139	Y139C/F/S – *R. norvegicus*	Rost *et al.*, 2004; Pelz *et al.*, 2005	**Y**	**Y**	**Y**	**Y**	**Y**
A140	A140T – *R. norvegicus*	Ma *et al.*, 2018	99% - A 1% - V	50% - V 50% - G	78 % - I 11% - L 11% - V	50% - A 50% - I	81% - I 13% - V 6% - L

Table 43: Anticoagulant resistance polymorphisms in *Rattus norvegicus* with the percentage of amino acids found at each position for each vertebrate class. 100% is represented by bold single letter code. Amino acid numbering according to human VKORC1 sequence. Colours of amino acids are according to physiochemical properties, refer to Appendix 8.

Human Position	Previously Reported Resistance Polymorphisms	Reference	Mammal VKORC1	Bird VKORC1	Reptile VKORC1	Amphibian VKORC1	Fish VKORC1
A26	A26P/T – *H. sapiens*	Bodin *et al.*, 2008; Watzka *et al.*, 2011	99% - A 1% - S	**A**	**A**	**A**	**A**
L27	L27V – *H. sapiens*	Peoc'h *et al.*, 2009	98% - L 2% - M	**L**	44% - W 44% - L 12% - F	50% - Y 50% - F	**L**
H28	H28Q – *H. sapiens*	Watzka *et al.*, 2011	**H**	**H**	**H**	**H**	**H**
V29	V29L – *H. sapiens*	Rost *et al.*, 2004	**V**	**V**	**V**	**V**	**V**
A34	A34P – *H. sapiens*	Harrington *et al.*, 2011	**A**	50% - E 50% -A	**E**	**E**	**E**
D36	D36Y/G – *H. sapiens*	Watzka *et al.*, 2011	89% - D 8% - N 3% - S	**D**	**D**	**D**	60% - D 40% - N
A41	A41S – *H. sapiens*	Reider *et al.*, 2005	**A**	**A**	**A**	**A**	**A**
V45	V45A – *H. sapiens*	Rost *et al.*, 2004	97% - V 2% - L 1% - I	**L**	78% - I 22% - L	**I**	**L**
S52	S52L/W – *H. sapiens*	Watzka *et al.*, 2011; Schmeits *et al.*, 2010	**S**	**T**	**S**	**S**	**S**
V54	V54L – *H. sapiens*	Bodin *et al.*, 2008	**V**	**V**	**V**	**V**	**V**
S56	S56F – *H. sapiens*	Watzka *et al.*, 2011	99% - S 1% - F	50% - A 50% - S	**T**	**T**	87% - T 13% - S
R58	R58G – *H. sapiens*	Gryseels *et al.*, 2015.	97% - R 3% - P	**R**	**R**	**R**	**R**

Table 44: Anticoagulant resistance polymorphisms in *Homo sapiens* with the percentage of amino acids found at each position for each vertebrate class. 100% is represented by bold single letter code. Amino acid numbering according to human VKORC1 sequence. Colours of amino acids are according to physiochemical properties, refer to Appendix 8.

Human Position	Previously Reported Resistance Polymorphisms	Reference	Mammal VKORC1	Bird VKORC1	Reptile VKORC1	Amphibian VKORC1	Fish VKORC1
W59	W59R/L/C – *H. sapiens*	Watzka *et al.,* 2011	**W**	**W**	**W**	**W**	**W**
V66	V66M/G – *H. sapiens*	Watzka *et al.,* 2011	99% - V 1% - M	50% - L 50% - V	**V**	**V**	94% - V 6% - L
H68	H68Y – *H. sapiens*	Hodroge *et al.,* 2012	81% - H 10% - Q 6% - P 1% - Y 1% - D 1% - M	50% - A 50% - P	78% - D 22% - E	**Q**	48% - F 40% - Y 6% - L 6% - I
G71	G71A – *H. sapiens*	Watzka *et al.,* 2011	**G**	**G**	**G**	**G**	54% - D 40% - A 6% - G
N77	N77S/Y – *H. sapiens*	Watzka *et al.,* 2011	**N**	**N**	**N**	**N**	**N**
R98	R98W – *H. sapiens* (VKCFD2 polymorphism)	Rost *et al.,* 2004; Rost *et al.,* 2005	76% - R 20% - Q 3% - S 1% - H	**R**	45% - H 33% – N 11% – P 11% - T	**G**	54% - L 26% - V 20% - P
I123	I123N – *H. sapiens*	Watzka *et al.,* 2011	99% - I 1% - V	**V**	**I**	**I**	**I**
L128	L128R – *H. sapiens*	Pelz *et al.,* 2005	99% - L 1% - H	**L**	**L**	**L**	**L**
Y139	Y139H – *H. sapiens*	Wu *et al.,* 2018; Rost *et al.,* 2004; Pelz *et al.,* 2005; Watzka *et al.,* 2011	**Y**	**Y**	**Y**	**Y**	**Y**

Table 44 Continued: Anticoagulant resistance polymorphisms in *Homo sapiens* with the percentage of amino acids found at each position for each vertebrate class. 100% is represented by bold single letter code. Amino acid numbering according to human VKORC1 sequence. Colours of amino acids are according to physiochemical properties, refer to Appendix 8.

Human Position	Previously Reported Resistance Polymorphisms	Reference	Mammal VKORC1	Bird VKORC1	Reptile VKORC1	Amphibian VKORC1	Fish VKORC1
R12	R12T – *M. musculus*	Gryseels *et al.*, 2015	98% - R 1% - W 1% - H	**R**	**R**	**R**	**R**
A26	A26S – *M. musculus*	Rost *et al.*, 2009	99% - A 1% - S	**A**	**A**	**A**	**A**
R37	E37G – *M. musculus*	Gryseels *et al.*, 2015	66% - R 14% - E 11% - Q 5% - K 3% - P 1% - G	**P**	67% - A 11% - P 11% - V 11% - I	50% - A 50% - P	**P**
A48	A48T – *M. musculus*	Rost *et al.*, 2009	94% - A 5% - S 1% - T	**S**	78% - D 22% - S	**S**	94% - S 6% - A
R58	R58G – *M. musculus*	Rost *et al.*, 2004	97% - R 3% - P	**R**	**R**	**R**	**R**
W59	W59L – *M. musculus*	Song *et al.*, 2011	**W**	**W**	**W**	**W**	**W**
R61	R61L – *M. musculus*	Rost *et al.*, 2009	79% - R 11%- Q 9% - K 1% - L	**R**	**R**	**R**	**R**
L128	L128S – *M. musculus*	Pelz *et al.*, 2005	99% - L 1% - H	**L**	**L**	**L**	**L**
Y139	Y139C – *M. musculus*	Pelz *et al.*, 2005	**Y**	**Y**	**Y**	**Y**	**Y**

Table 45: Anticoagulant resistance polymorphisms in *Mus musculus* with the percentage of amino acids found at each position for each vertebrate class. 100% is represented by bold single letter code. Amino acid numbering according to human VKORC1 sequence. Colours of amino acids are according to physiochemical properties, refer to Appendix 8.

4.7.3.2 Comparison of natural resistance SNPs found in the Mus spretus VKORC1 sequence against vertebrate VKORC1 sequences

A previous study by Rost *et al.* (2009) reported house mice VKORC1 with four polymorphisms R12W, A26S, A48T and R61L and assessed the inhibition with warfarin of the individual polymorphisms on the house mouse VKORC1 enzyme. A26S, A48T and R61L caused a slight resistance to warfarin compared to the wild type (Section 1.16). The R12W caused an increased sensitivity to warfarin (Section 1.16). A study by Song *et al.* (2011) demonstrated that resistant phenotypes seen in the house mouse were in fact acquired by introgressive hybridization from the Algerian mouse (*Mus spretus*). Table 46 shows amino acid residues contained in house mouse and the Algerian mouse at the four positions with the percentage of amino acids found within each vertebrate class.

At position 12, an arginine is completely conserved throughout all vertebrate classes with only the Algerian mouse sequence showing a tryptophan at this position (Table 46). The tryptophan residue may change the conformation of VKORC1, which creates a stronger binding to VKORC1 by warfarin.

At position 26, 1% of mammalian sequences contained a serine whereas all other vertebrate VKORC1 sequences contained an alanine residue (Table 46). As well as the Algerian mouse sequence, a serine was found in the *Felis catus* (cat) sequence, suggesting that the cat VKORC1 sequence may have natural resistance to anticoagulants. Indeed, this is reflected in the LD_{50} values for the cat that show that the cat is in general more resistant to anticoagulant rodenticides in comparison to rat LD_{50} values (Section 1.6). Therefore, the change in this position may be responsible for the natural resistance seen in the cat. At position 48, the Algerian mouse is the only VKORC1 sequence which contains a polar threonine at this position, which is shown to cause some resistance to anticoagulant rodenticides (Rost *et al.,* 2009) suggesting a polar amino acid at this position may cause anticoagulant rodenticide resistance. Interestingly a serine which is a polar amino acid with similar physiochemical properties as threonine is found in 3% of mammals, all birds, 22% of reptiles, all amphibians and 94% of fish at this position, which may lead to inefficient binding of warfarin and therefore natural anticoagulant resistance in these vertebrate classes.

House Mouse Position	Algerian Mouse Position	Reference	Mammal VKORC1	Bird VKORC1	Reptile VKORC1	Amphibian VKORC1	Fish VKORC1
R12	W12	Song *et al.*, 2011	98% - R 1% - W 1% - H	**R**	**R**	**R**	**R**
A26	S26	Song *et al.*, 2011	99% - A 1% - S	**A**	**A**	**A**	**A**
A48	T48	Song *et al.*, 2011	94% - A 5% - S 1% - T	**S**	78% - D 22% - S	**S**	94% - S 6% - A
R61	L61	Song *et al.*, 2011	79% - R 11%- Q 9% - K 1% - L	**R**	**R**	**R**	**R**

Table 46: *Mus spretus* polymorphisms shown with the wild type house mouse and an assessment of the percentage of amino acids found at each position for each vertebrate class. 100% is represented by bold single letter code. Amino acid numbering according to human VKORC1 sequence. Colours of amino acids are according to physiochemical properties, refer to Appendix 8.

The final position R61 shows a positive/polar amino acid, mostly an arginine found at this position throughout vertebrate VKORC1 sequences and only the Algerian mouse contains a leucine at this position suggesting a hydrophobic amino acid at this position may cause anticoagulant rodenticide resistance.

4.8 Assessment of the conserved residues in VKORC1 between vertebrate classes

Amino acids that are completely conserved throughout different animal species are thought to have vital structural and functional roles within the enzyme. The consensus sequences derived for each vertebrate class for VKORC1 were used to assess the conservation of amino acids throughout all vertebrate sequences. A topology diagram was used to represent the positions of the conserved amino acids throughout vertebrate VKORC1 (Figure 76).

There are 35 amino acid positions that are completely conserved throughout vertebrate VKORC1 sequences and the 26 positions that have previously identified to play a role in VKORC1 are listed in Table 47. There are 9 novel conserved positions that have been identified in this study these are listed in Table 48 and the proposed function is suggested by reviewing previous researchers' models such as the topological model of the human VKORC1 as a model (Figure 76).

With regards to the new conserved amino acids found in this study, the tyrosine residue at position 39 is found in the large conserved loop found between TM1 and TM2 in VKORC1 (Table 48). This tyrosine could potentially have a role in warfarin binding due to its placement next to R40 which is found to have a role in warfarin binding (Czogalla *et al.,* 2017). Alternatively, it may be required for the structure of the large loop and interactions with substrates or anticoagulants. There are two glycine residues at positions 62 and 64 which are fully conserved in all vertebrate VKORC1 (Table 48). The glycine residues may have a role in the structure of the large loop and interactions with substrate or anticoagulants.

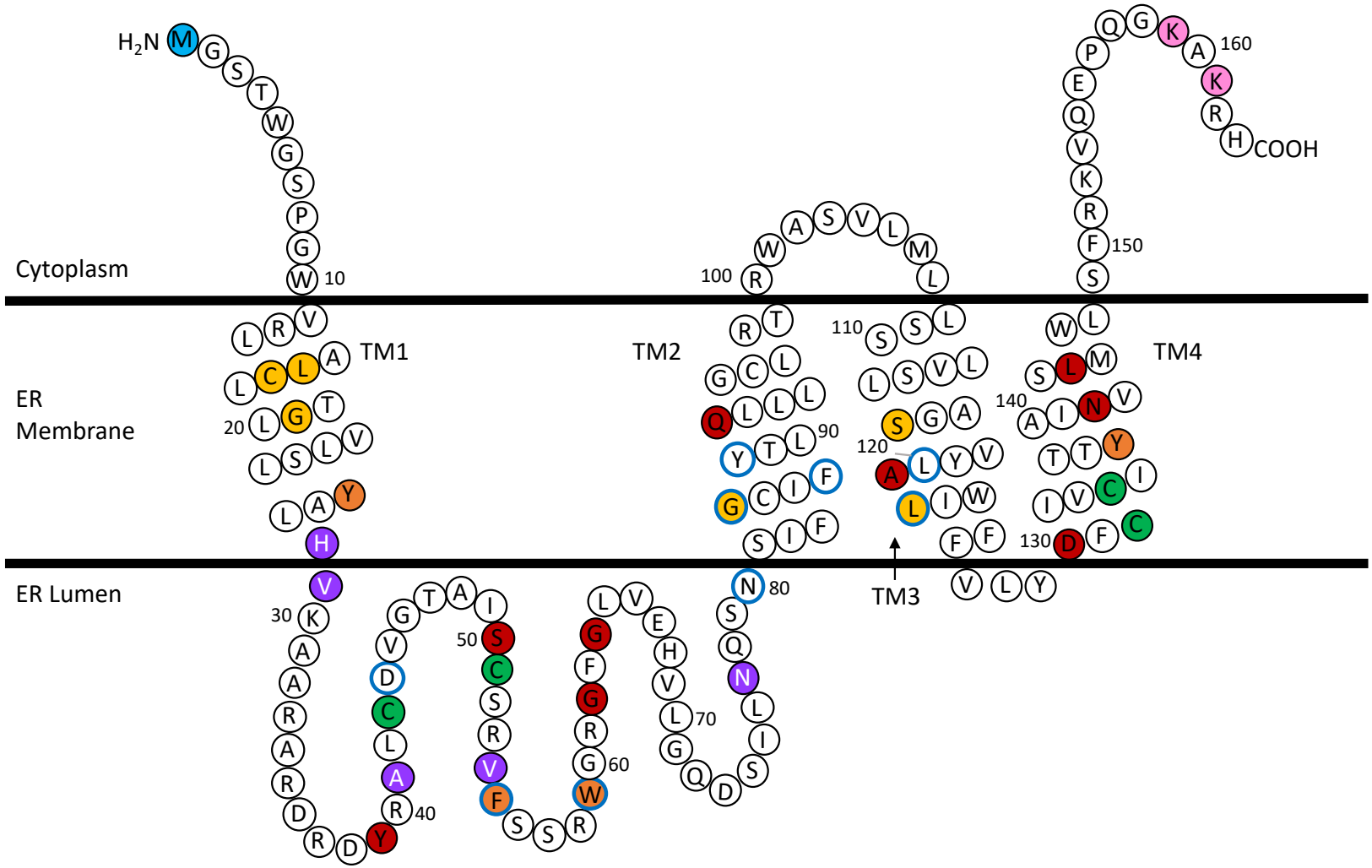


Figure 76: Topology diagram of human VKORC1 with the conserved residues throughout vertebrate VKORC1 sequences highlighted. Blue denotes the start codon. Yellow denotes structural amino acids for helix-helix interactions. Orange denotes warfarin binding amino acids. Purple denotes positions where human anticoagulant resistance polymorphisms are found. Blue outline denotes substrate binding amino acids. Pink denotes the ER retention signal. Red denotes conserved residues identified in this study. Green denotes conserved active site residues.

Conserved Position	**Role in VKORC1**	Reference
M1	Conserved start codon	
L15	Maintain Stable VKOR structure	Wu *et al.,* 2018
C16	Helix – helix interactions	Bevans *et al.,* 2015
G19	Helix – helix interactions	Bevans *et al.,* 2015
Y25	Interact with Y139 to stabilize warfarin binding	Wu *et al.,* 2018
H28	Warfarin resistance in humans (H28Q)	Watzka *et al.,* 2011
V29	Warfarin resistance in humans (V29L)	Rost *et al.,* 2004
A41	Warfarin resistance in humans (A41S)	Reider *et al.,* 2005; Tanaka *et al.,* 2012
C43	Involved in active site – conserved cysteine	Goodstadt and Ponting, 2004; Rost *et al.,* 2005
D44	Involved in substrate reduction/binding/specificity	Bevans *et al.,* 2015
C51	Involved in active site – conserved cysteine	Goodstadt and Ponting, 2004; Rost *et al.,* 2005
V54	Warfarin resistance in humans (V54L)	Bodin *et al.,* 2008
F55	Aromatic stacking – warfarin binding. Naphthoquinone head binding – VKE and VK.	Czogalla *et al.,* 2017; Wu *et al.,* 2018
W59	Naphthoquinone head binding – VKE and VK. Warfarin binding	Czogalla *et al.,* 2017; Wu *et al.,* 2018
N77	Warfarin resistance in humans (N77S/Y)	Watzka *et al.,* 2011
N80	Naphthoquinone head binding – VK. Involved in substrate reduction/binding/specificity	Czogalla *et al.,* 2017; Bevans *et al.,* 2015
G84	Helix – helix interactions Involved in substrate reduction/binding/specificity	Czogalla *et al.,* 2017; Bevans *et al.,* 2015
F87	Isoprenoid chain binding	Czogalla *et al.,* 2017
Y88	Isoprenoid chain binding	Czogalla *et al.,* 2017; Bevans *et al.,* 2015
S117	Helix – helix interactions	Bevans *et al.,* 2015
L120	Naphthoquinone head binding – VKE and VK. Involved in substrate reduction/binding/specificity	Czogalla *et al.,* 2017; Bevans *et al.,* 2015
L124	Naphthoquinone head binding – VKE and VK. Helix – helix interactions	Czogalla *et al.,* 2017; Bevans *et al.,* 2015
C132	Active site cysteine	Goodstadt and Ponting, 2004; Rost *et al.,* 2005
C135	Active site cysteine	Goodstadt and Ponting, 2004; Rost *et al.,* 2005
Y139	Warfarin binding site	Wu *et al.,* 2018; Rost *et al.,* 2004; Pelz *et al.,* 2005; Watzka *et al.,* 2011
K161	Part of the ER retention signal	Rost *et al.,* 2004
K161	Part of the ER retention signal	Rost *et al.,* 2004

Table 47: Conserved amino acid positions in all vertebrate VKORC1 sequences that have a previously identified role. Amino acid numbering according to human VKORC1 sequence.

Conserved Position	**Location/Role in VKORC1**	Reference
Y39	Potential involvement in warfarin binding and structure and interactions of the large loop	This study
S50	Potential involvement in the structure and interactions of the large loop	This study
G62	Potential involvement in the structure and interactions of the large loop	This study
G64	Potential involvement in the structure and interactions of the large loop	This study
Q91	Found in TM2 – potential involvement in helix-helix interactions and substrate binding	This study
A121	Found in TM3 – potential involvement in helix-helix interactions and substrate binding	This study
D130	Potential involvement in the structure of the linking loop between TM3 and TM4	This study
N142	Found in TM4 – potential involvement in helix-helix interactions and structure of VKORC1	This study
L145	Found in TM4 – potential involvement in helix-helix interactions and structure of VKORC1	This study

Table 48: Conserved amino acid positions in all vertebrate VKORC1 sequences found in this study with proposed role in VKORC1. Amino acid numbering according to human VKORC1 sequence.

At position 91 a conserved glutamine residue is found in TM2 towards the cytoplasmic side of the TM domain. Other residues identified in substrate binding reside near to this position and therefore Q91 may be involved in substrate binding or interactions but also may have a potential role in helix-helix interactions. With regards to A121 it is next to the important L120 residue which is responsible for substrate binding of vitamin K and vitamin K epoxide suggesting that this residue may also have substrate interactions and potential involvement in the helix interactions in VKORC1. Another conserved residue D130 is found in the small linking loop between TM3 and TM4 and may contribute to the structure of this loop joining the two transmembrane domains. Both N142 and L145 are part of TM4 with both side groups rotated into the substrate binding pocket (data not shown). This suggests that these amino acids may have a role in the binding of substrates and the interactions between other helices. Overall, the amino acids identified in this study are conserved over ~400 million years of vertebrate evolution. Interestingly, these amino acids have been previously unidentified by other research groups.

4.9 Computational Comparison of Vertebrate VKORC1L1 Amino Acid Sequences

In order to study the differences between the different species within vertebrate VKORC1L1 sequences multiple sequence alignments were performed using CLC Sequence Viewer. Protein sequences for VKORC1L1 were obtained from the NCBI database (See Appendix 6 – for accession numbers). Only full length sequences were used to generate the multiple sequence alignments. Full length VKORC1 sequences were identified as containing specific amino acid residues and a certain sequence length. Firstly, all sequences had to contain a methionine residue at the first amino acid position at the N terminus. This amino acid is encoded by the start codon and therefore is important for the beginning of vertebrate nuclear genome encoded protein sequences. Vertebrate VKORC1 sequences were identified by the ER retention signal at the C terminal (See Section 4.1), whereas this is not found at the C terminal of vertebrate VKORC1L1 sequences. Sinhadri *et al.* (2017) used immunofluorescence confocal imaging to show that the ER retention signal is important for ER localisation and the activity of VKORC1. However, they showed that there was more non-ER localization for VKORC1L1 suggesting a different localisation (Sinhadri *et al.* 2107). This could be a reason for the lack of ER retention signal in VKORC1L1 sequences.

Like for the VKORC1 sequences (Section 4.1), there are important amino acids that form the active site and characterise the VKOR enzyme family. These are C132 and C135 along with two other conserved cysteines C43 and C51 (Goodstadt and Ponting, 2004; Rost *et al.,* 2005). These four conserved cysteines were identified in all VKORC1L1 sequences in this study and are an important characteristic to define a full length VKORC1L1 sequence. Finally, a sequence length of above 170 amino acids for VKORC1L1 were accepted as full length sequences with the exception of some fish sequences which had sequence length of 186 amino acids. The 11 amino acid insertion is after the methionine starting residue at the N terminal. All mammalian VKORC1L1 sequences have a sequence length of 176 amino acids except for the marsupials, which have a sequence length of 175 amino acids. All avian and reptilian VKORC1L1 sequences have a sequence length of 176 amino acids, whereas all amphibian VKORC1L1 sequences have a sequence length of 175 amino acids. The fish VKORC1L1 sequences are the most varied with sequences ranging from 173 to 186 amino acids.

All non-mammalian VKORC1L1 sequences were aligned according to taxonomic class (Figures 77 – 88) and due to the large amount of sequences found for mammals and fish the sequences were aligned according to taxonomic order (Figures 77 – 82). All multiple sequence alignments were performed using CLC Sequence Viewer (Section 2.18). Each alignment contains a consensus sequence which is automatically generated by the CLC program and does not distinguish between fully conserved or partially conserved positions, whereas the sequence logo included with each alignment provides this information. The sequence logo is derived from the percentage of conservation at each amino acid position. The colours of the amino acids correspond to the physiochemical properties of the amino acids (See Appendix 8 for amino acid colour key).

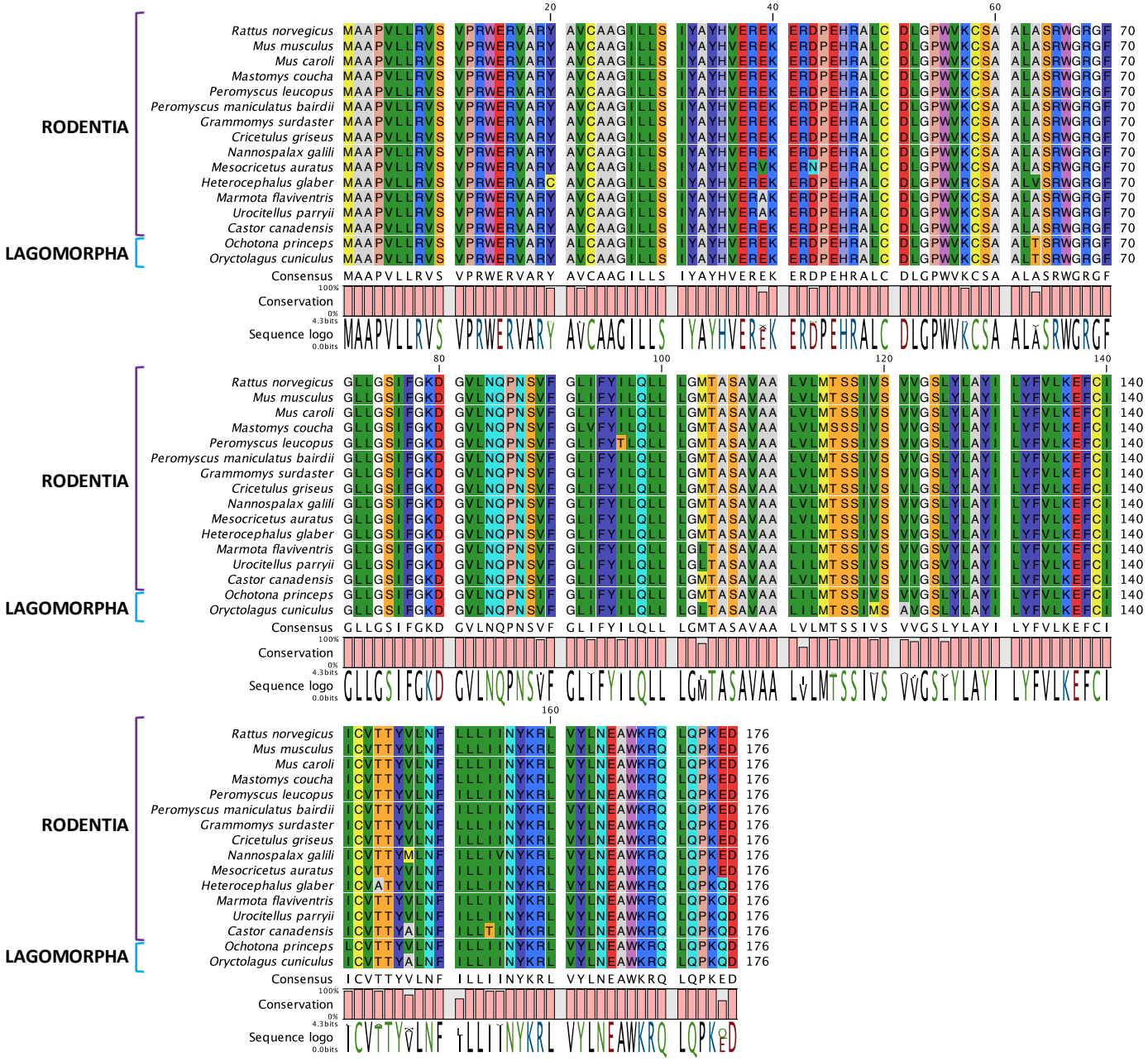


Figure 77: Multiple sequence alignment of Mammalian Rodentia and Lagomorpha VKORC1L1. Purple line denotes Rodentia sequences. Blue line denotes Lagomorpha sequences. Colours of amino acids are according to physiochemical properties, refer to Appendix 8.

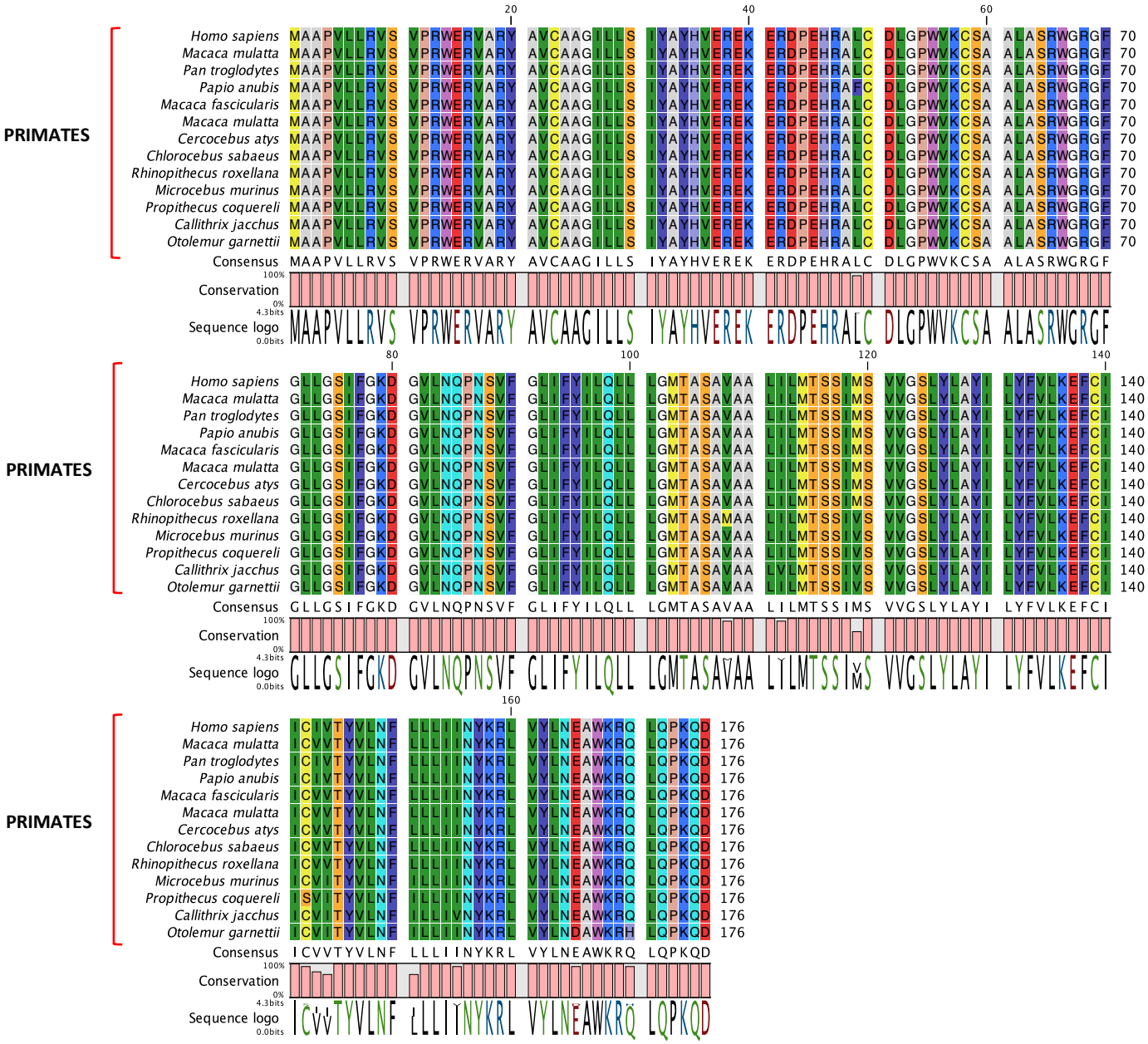


Figure 78: Multiple sequence alignment of Mammalian Primate VKORC1L1 sequences. Red line denotes Primate sequences. Colours of amino acids are according to physiochemical properties, refer to Appendix 8.

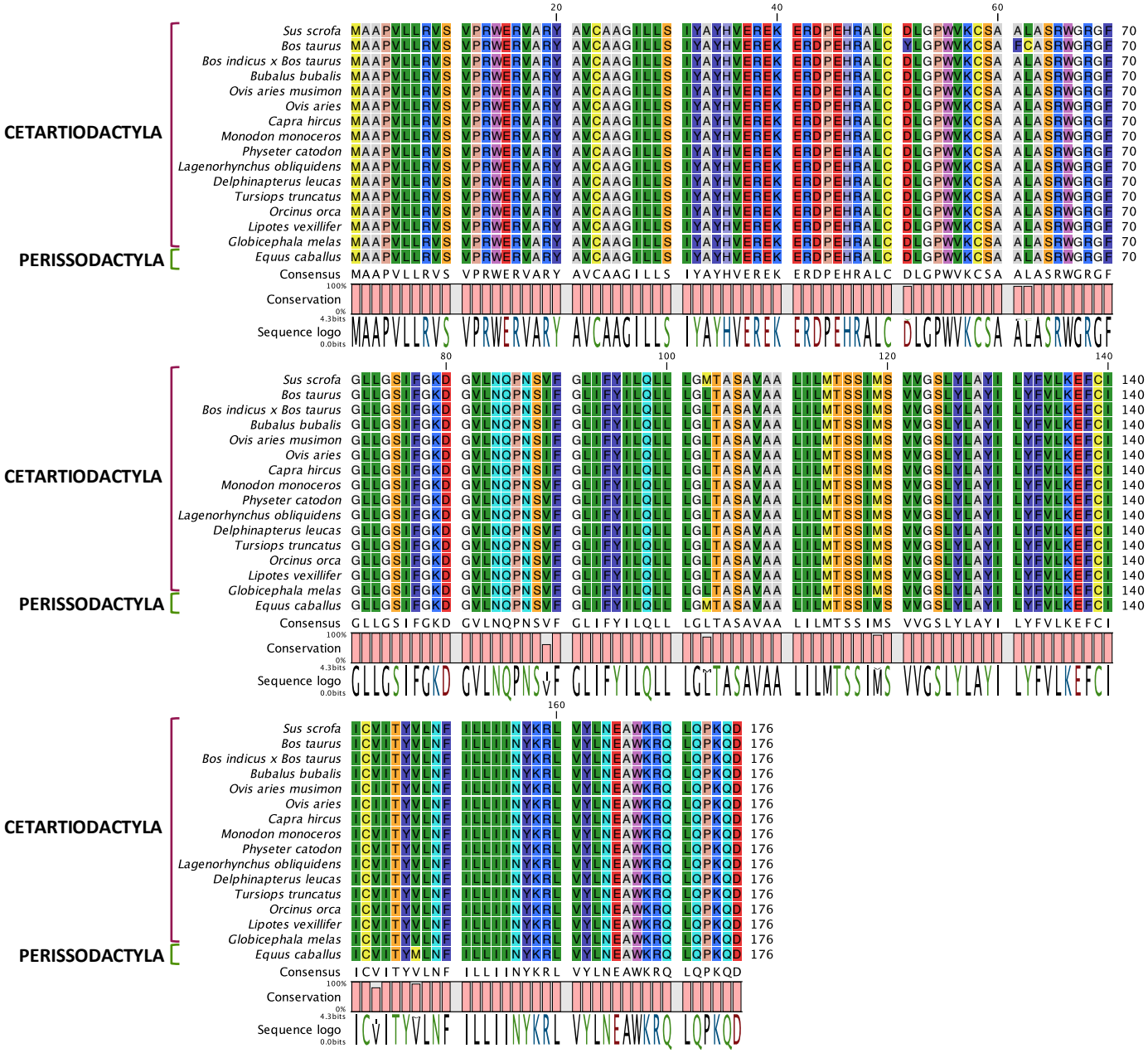


Figure 79: Multiple sequence alignment of Mammalian Cetartiodactyla and Perissodactyla VKORC1L1. Purple line denotes Cetartiodactyla sequences. Green line denotes Perissodactyla sequences. Colours of amino acids are according to physiochemical properties, refer to Appendix 8.

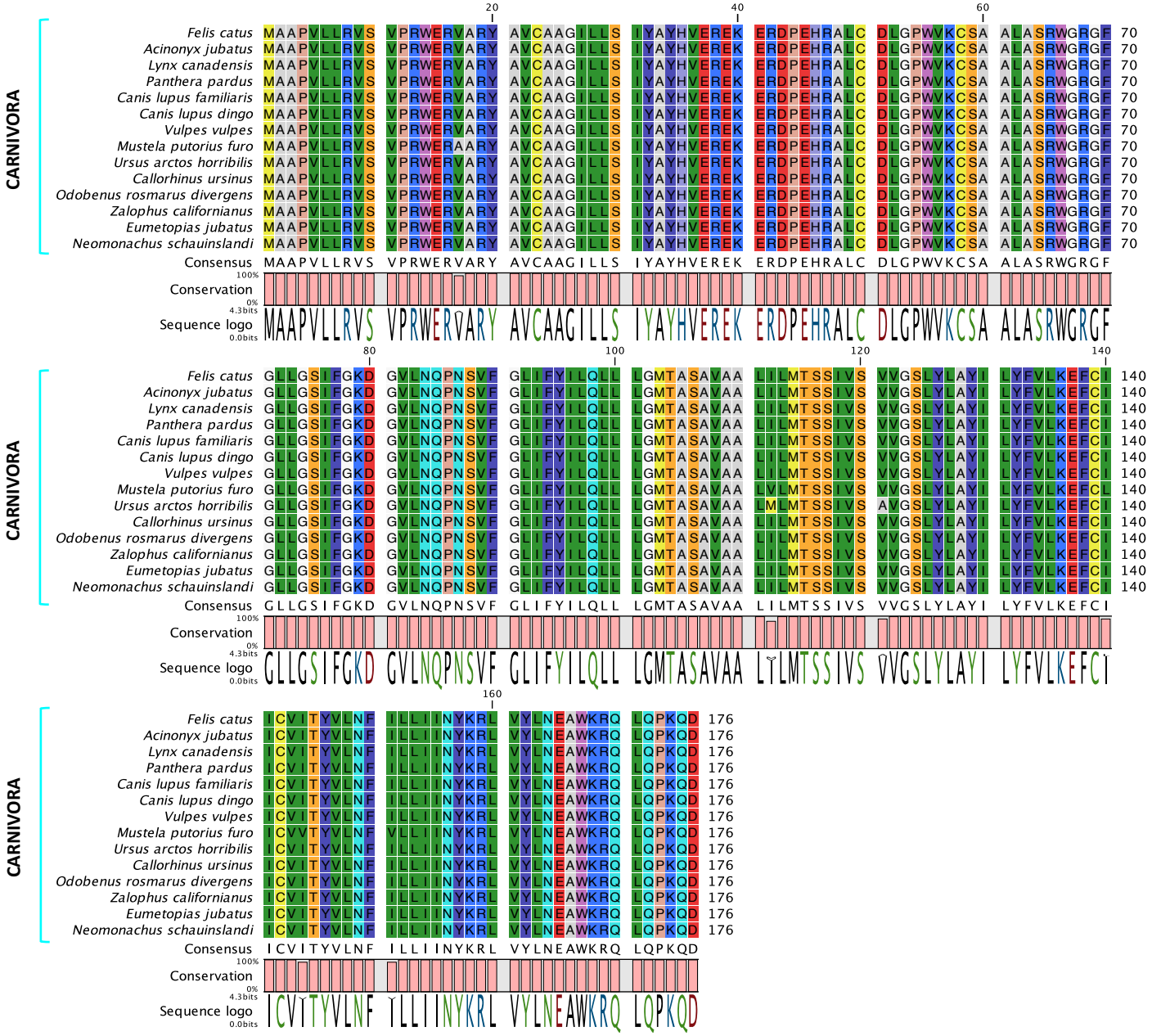


Figure 80: Multiple sequence alignment of Mammalian Carnivora VKORC1L1. Light blue line denotes Carnivora sequences. Colours of amino acids are according to physiochemical properties, refer to Appendix 8.

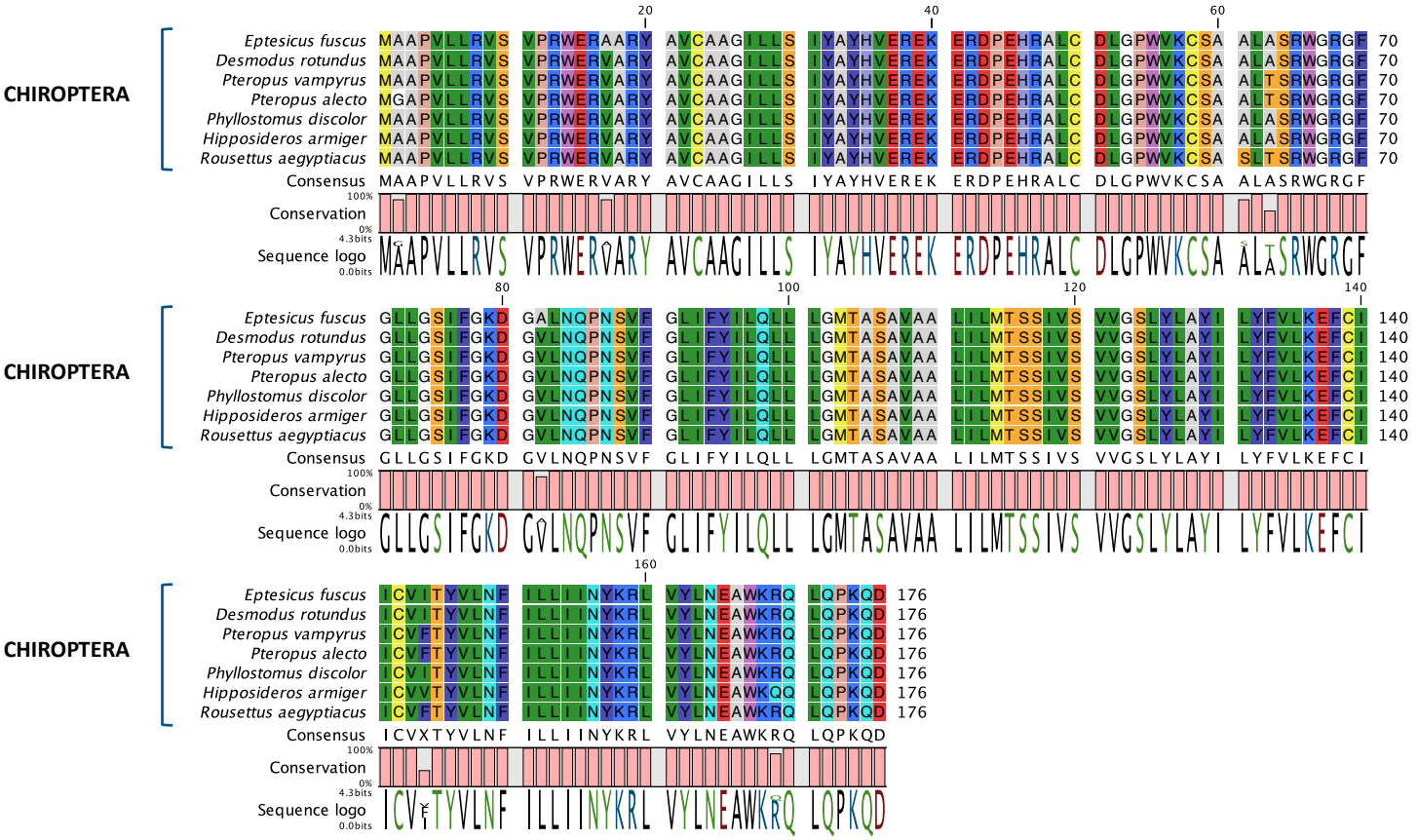


Figure 81: Multiple sequence alignment of Mammalian Chiroptera VKORC1L1. Blue denotes Chiroptera sequences. Colours of amino acids are according to physiochemical properties, refer to Appendix 8.

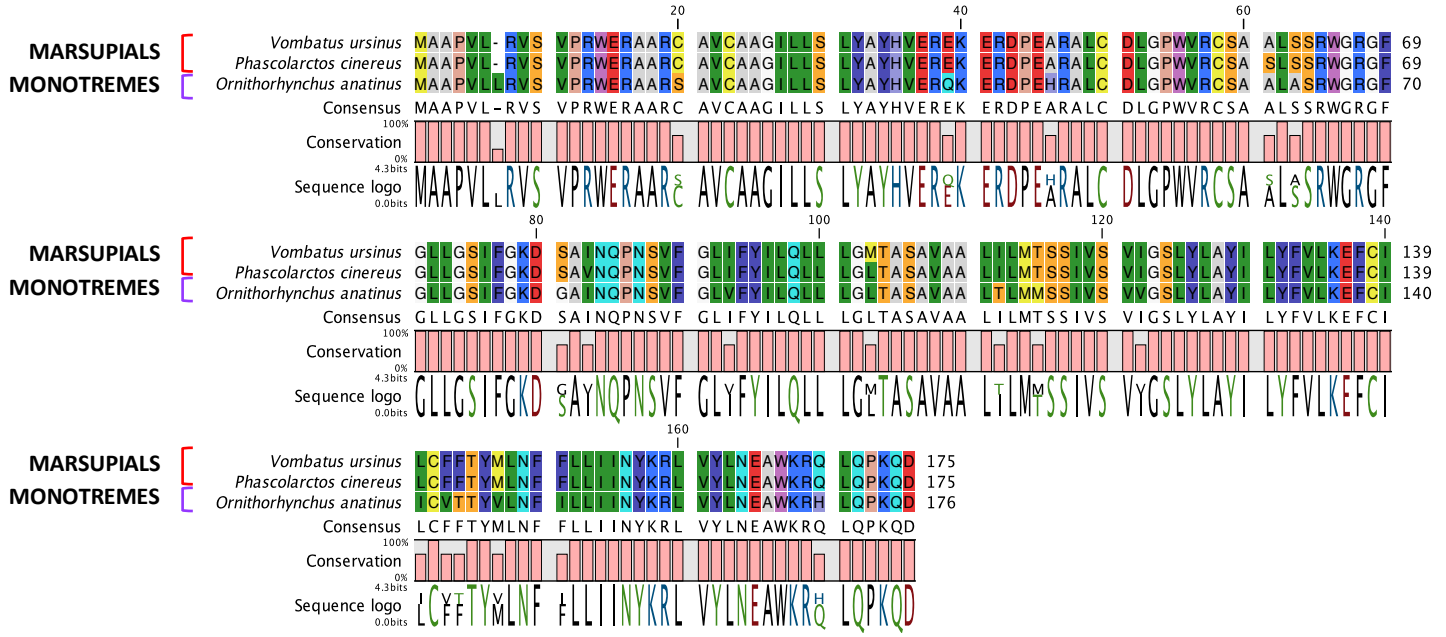


Figure 82: Multiple sequence alignment of Mammalian Marsupials and Monotreme VKORC1L1. Red line denotes Marsupial sequences. Purple line denotes Monotreme sequences Colours of amino acids are according to physiochemical properties, refer to Appendix 8.

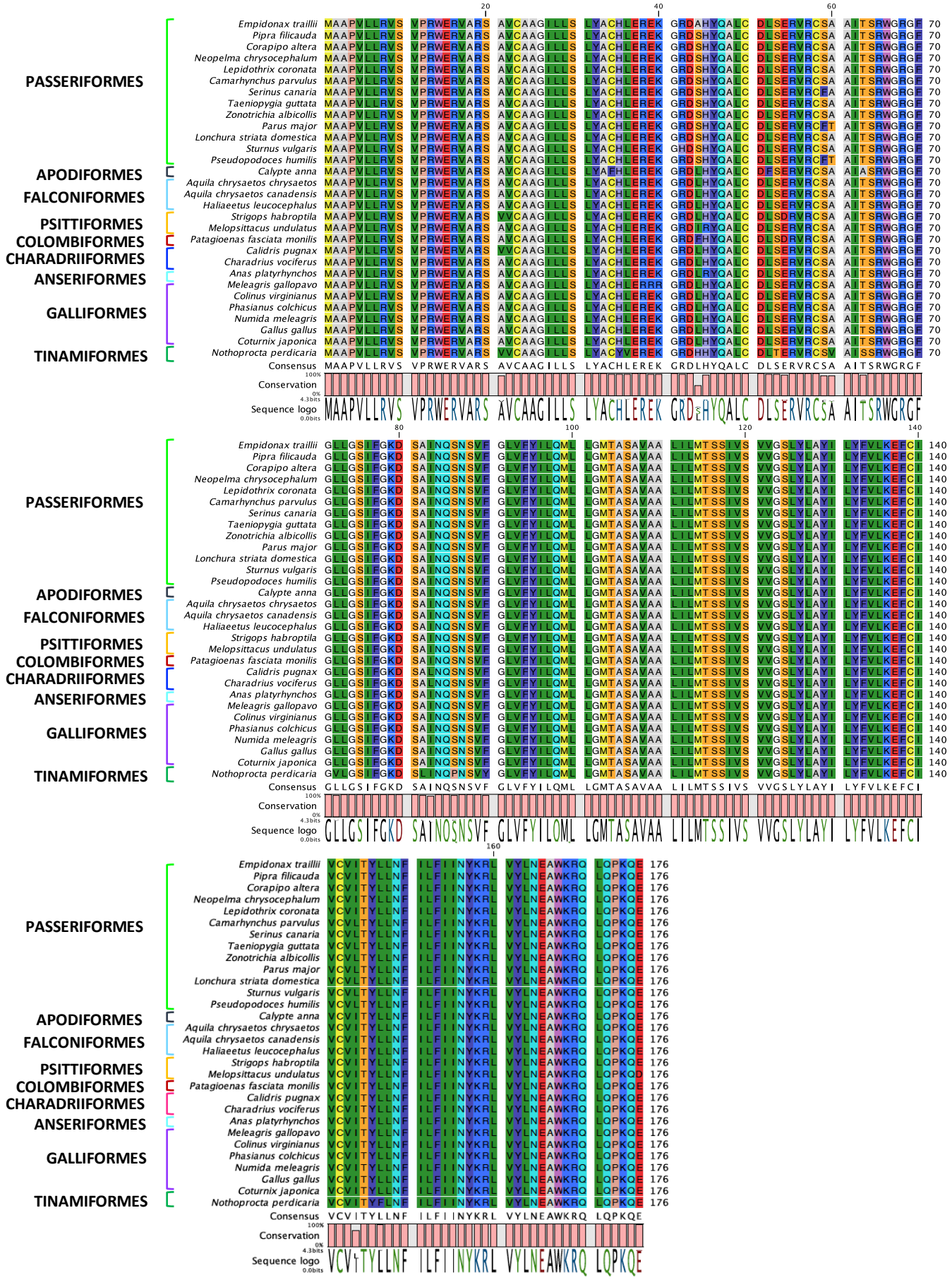


Figure 83: Multiple sequence alignment of Bird VKORC1L1 sequences. Light green line denotes Passeriformes sequences Grey line denotes Apodiformes. Light blue line denotes Falconiformes. Orange line denotes Psittiformes. Red line denotes Colombiformes. Pink line denotes Charadriifromes. Turquoise line denotes Anseriformes. Purple line denotes Galliformes sequences. Dark green line denotes Tinamiformes. Colours of amino acids are according to physiochemical properties, refer to Appendix 8.

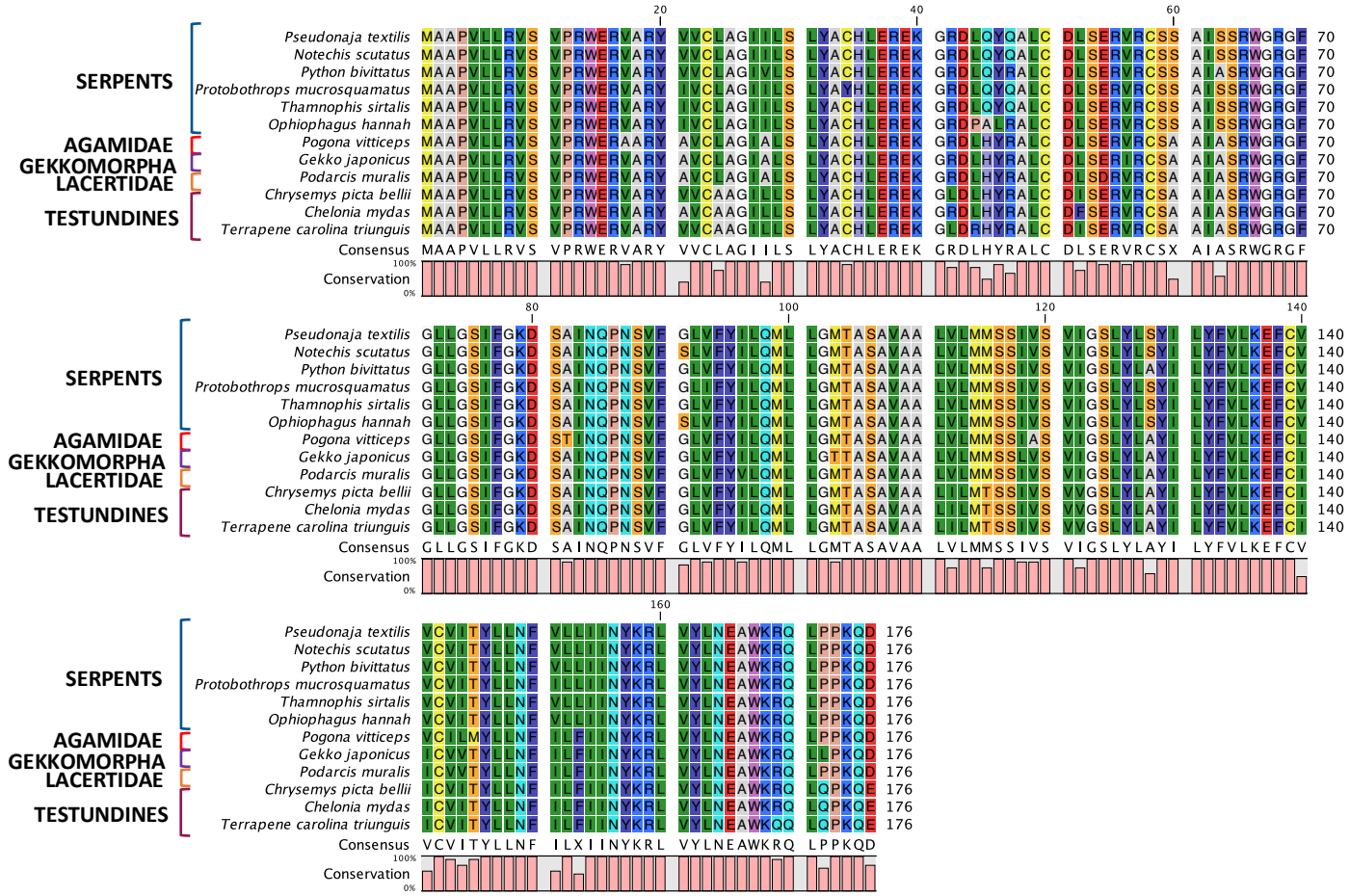


Figure 84: Multiple sequence alignment of Reptile VKORC1L1. Blue line denotes Serpents sequences. Pink line denotes Agamidae sequences. Purple line denotes Gekkomorpha sequences. Orange line denotes Lacertidae sequences. Pink line denotes Testundines sequences. Colours of amino acids are according to physiochemical properties, refer to Appendix X.

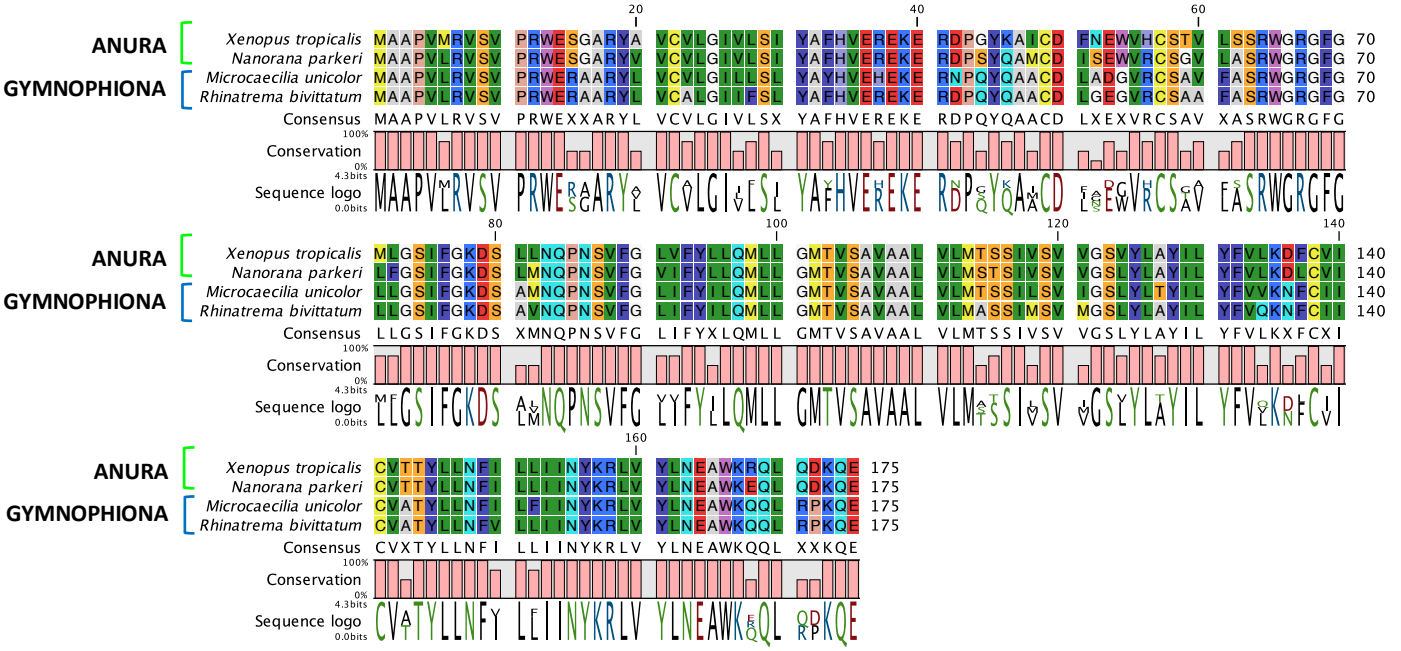


Figure 85: Multiple sequence alignment of Amphibian VKORC1L1 sequences. Green line denotes Anura sequences. Blue line denotes Gymnophiona sequences. Colours of amino acids are according to physiochemical properties, refer to Appendix 8.

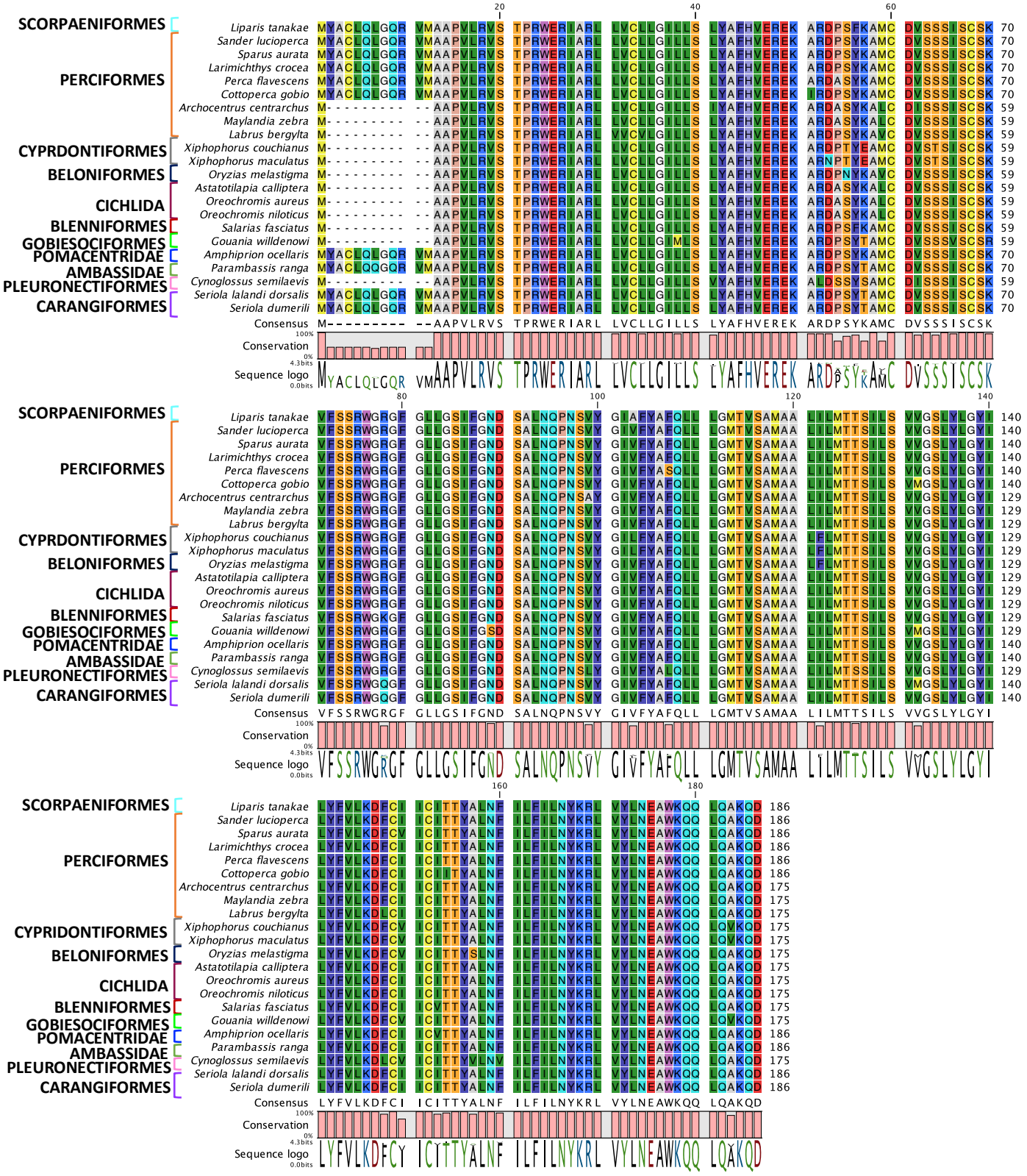


Figure 86: Multiple sequence alignment of Fish VKORC1L1 sequences. Turquoise line denotes Scoraeniformes. Orange line denotes Perciformes. Grey line denotes Cypridontiformes. Dark blue line denotes Beloniformes. Dark pink line denotes Cichlida. Red line denotes Blenniformes. Green line denotes Gobiesociformes. Blue line denotes Pomacentridae. Dark green line denotes Ambassidae. Light pink line denotes Pleuronectiformes. Purple denotes Carangiformes. Colours of amino acids are according to physiochemical properties, refer to Appendix 8.

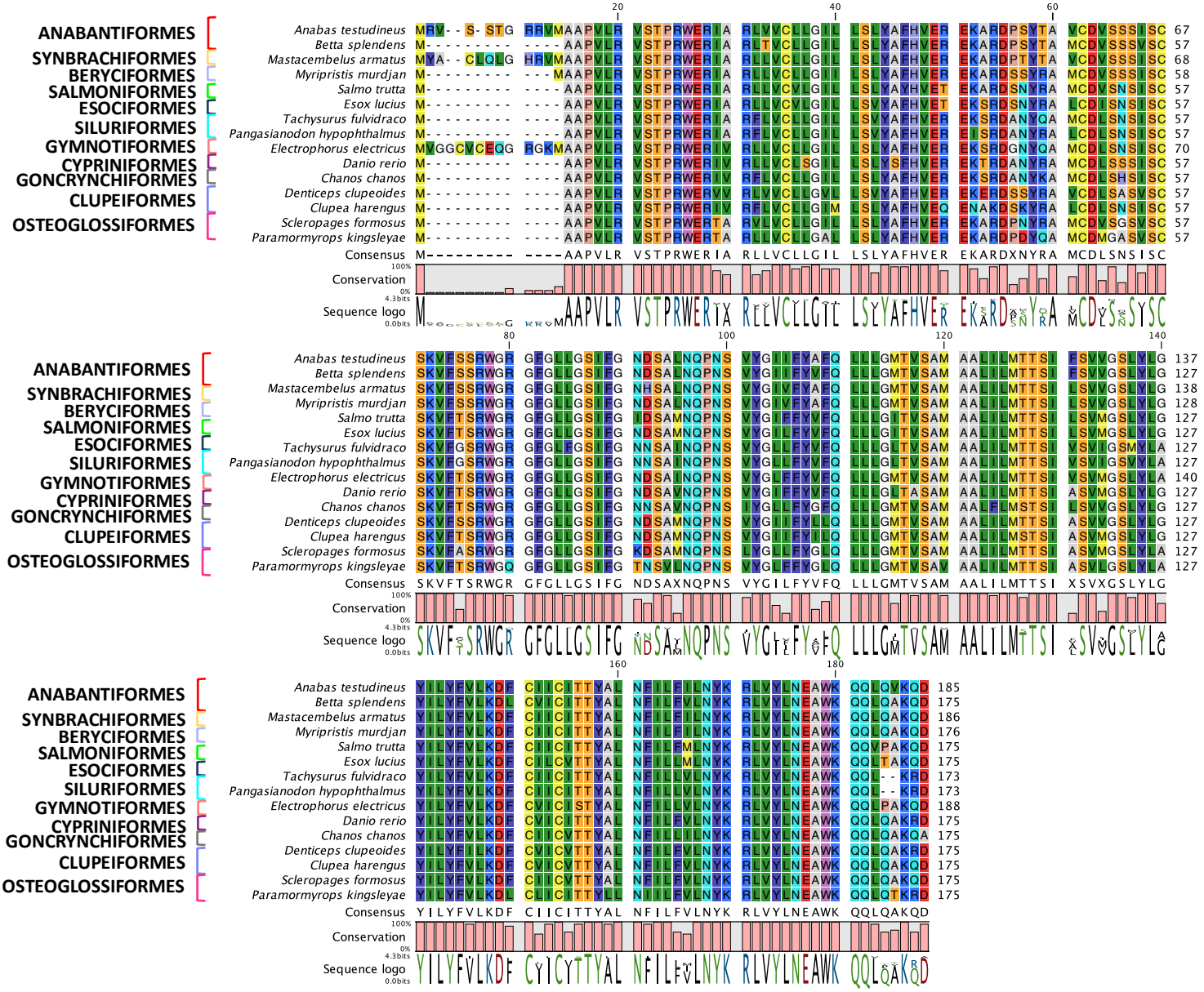


Figure 87: Multiple sequence alignment of Fish VKORC1L1 sequences. Red line denotes Anbantiformes. Yellow line denotes Synbranchiformes. Lilac line denotes Beryciformes. Green line denotes Salmoniformes. Dark blue line denotes Esociformes. Turquoise line denotes Siluriformes. Salmon pink line denotes Gymnotiformes. Dark pink line denotes Cypriniformes. Grey line denotes Goncrynchiformes. Purple line denotes Clupeiformes. Pink line denotes Osteoglossiformes. Colours of amino acids are according to physiochemical properties, refer to Appendix 8.

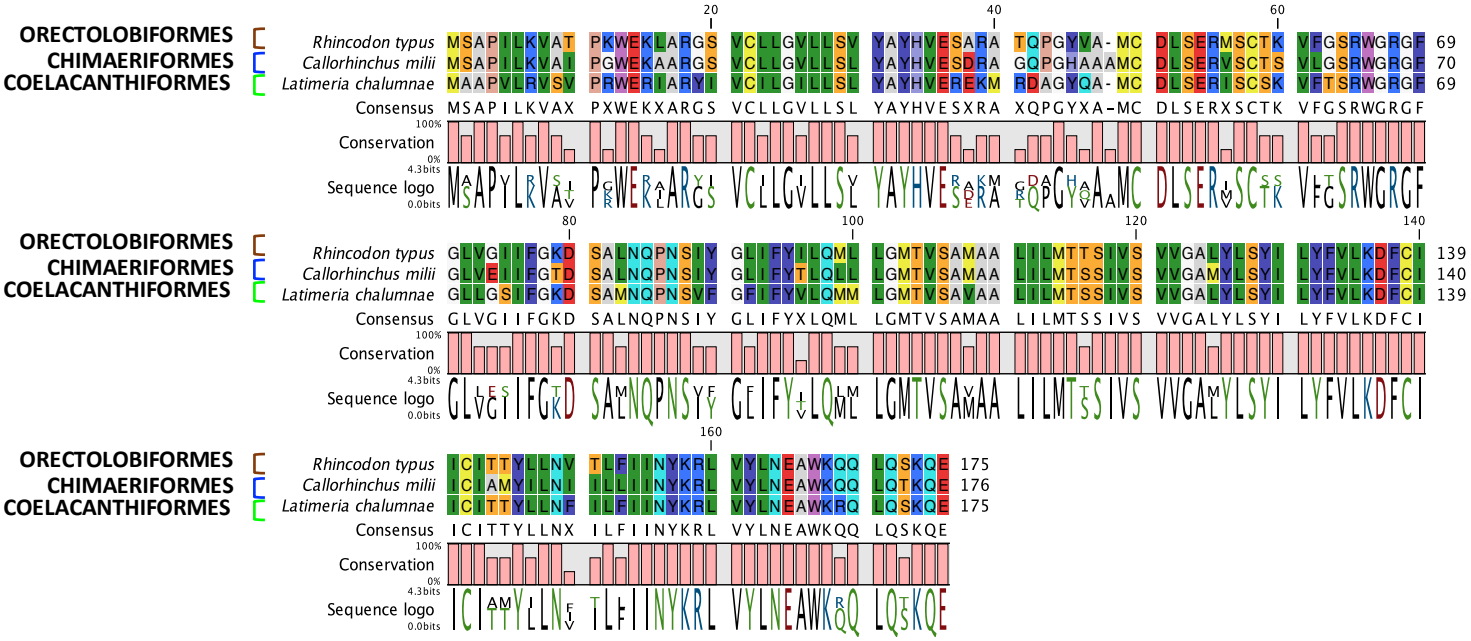


Figure 88: Multiple sequence alignment of Fish VKORC1L1 sequences. Brown line denotes Orectolobiformes. Blue line denotes Chimaeriformes. Green line denotes Coelacanthiformes. Colours of amino acids are according to physiochemical properties, refer to Appendix 8.

4.10 Analysis of VKORC1L1 Amino Acid Sequences in Mammals

By using multiple sequence alignments, the sequence identity was calculated within each taxonomic order (Table 49).

The mammalian VKORC1L1 sequences appear to be highly functionally constrained with an overall sequence identity between all mammalian VKORC1L1 sequences of 78% (Table 49). Compared to the paralogous enzyme VKORC1 (36%) (Section 4.2) in this study there is a ~2 fold difference between the sequence identity of the two enzymes. This suggests that VKORC1L1 has more functionally constrained amino acids compared to VKORC1 and amino acid changes in VKORC1L1 may have a greater impact on the function compared to VKORC1.

VKORC1L1 sequences belonging to the Rodentia order have the lowest sequence identity of 89%. This could be due to the large evolutionary timespan between the Rodentia sequences. Although there is an evolutionary timespan of around 30 million years, the Marsupials have the highest sequence identity with 98%.

Taxonomic Order	Number of Sequences	Sequence Identity (%)	Evolutionary Time Span (My)	Figure Number
Rodentia	14	89	~ 70[a]	2
Lagomorpha	2	96	~ 2[b]	2
Primates	13	93	~ 31.7[c]	3
Cetartiodactyla	15	96	~ 15[d]	4
Carnivora	14	96	~ 30e	5
Perissodactyla	1	-	-	6
Chiroptera	7	96	~ 8[f]	7
Marsupials	2	98	~ 30[g]	10
Monotremes	1	-	-	10
Mammalian Total:	69	78	~68	-

Table 49: Number of VKORC1L1 sequences found in each taxonomic order for Mammals with the sequence identity within the specific order and the evolutionary timespan between the different species. (a) Kumar and Hedges (1998); (b) Ge *et al.* (2013); (c) Pozzi *et al.* (2014); (d) Zurano *et al.* (2019); (e) Nyakatura and Bininda-Emonds (2012); (f) Agnarsson *et al.* (2011); (g) Haussler *et al.* 2009.

4.11 Analysis of VKORC1L1 Amino Acid Sequences in Non-Mammals

By using multiple sequence alignments, the sequence identity was calculated for each taxonomic class in non-mammals (Table 50).

Taxonomic Class	Number of Sequences	Evolutionary Time Span (My)	Sequence Identity (%)	Figure Number
Birds	30	~100[a, b]	86	11
Reptiles	12	~100[c]	79	12
Amphibians	4	~50[c]	73	13
Fish	49	~400[c,d]	49	14

Table 50: Number of VKORC1L1 sequences found in each taxonomic class for non-mammals with the sequence identity within each class. (a) Stapley *et al.* (2008); (b) Prum *et al.* (2015); (c) Haussler *et al.* (2009); (d) Betancur *et al.* (2013).

The bird VKORC1L1 sequences have the highest sequence identity at 86%, even with an evolutionary timespan of 100 My. This suggests that there is a high level of functional constraint across all the bird species. The fish VKORC1L1 sequences contain the lowest

sequence identity at 49%. The three main groups of fishes are represented within these alignments; ray-finned fish, lobe-finned fish and cartilaginous fishes which are evolutionary diverse groups with an evolutionary timespan of around 400 My.

4.12 Percentage Identity Comparison of Vertebrate VKORC1L1

In order to assess the conservation between the different classes of vertebrate VKORC1L1 a percentage identity table was generated using the consensus sequences (Table 51).

	Mammal VKORC1L1	Bird VKORC1L1	Reptile VKORC1L1	Amphibian VKORC1L1	Fish VKORC1L1
Mammal VKORC1L1	100%	66%	64%	60%	42%
Bird VKORC1L1		100%	72%	64%	44%
Reptile VKORC1L1			100%	63%	43%
Amphibian VKORC1L1				100%	43%
Fish VKORC1L1					100%

Table 51: Percentage identity between the five different classes of vertebrate VKORC1L1.

The percentage identity between the different classes of vertebrate VKORC1L1 have a range from 42% to 72%. The highest percentage similarity was between the reptilian VKORC1L1 sequences and the bird VKORC1L1 sequences with a percentage of 72%, which may be due to the evolutionary relationship between reptiles and birds as they both belong to the Sauropsida clade (Meyer and Zardoya, 2003). Whereas, the lowest sequence identity is between the mammalian VKORC1L1 sequences and the fish VKORC1L1 sequences with a percentage of 42%. This may be due to the vast evolutionary timespan of almost 300 My, suggesting that only amino acids with structural and functional roles may be conserved.

4.13 Comparison of the vertebrate VKORC1L1 sequences

4.13.1 Comparison of vertebrate VKORC1L1 sequences using an MSA

In order to compare across vertebrate VKORC1L1 sequences an alignment was created to compare representative VKORC1L1 sequences from each vertebrate class (Figure 89).

Across all representative vertebrate VKORC1L1 sequences, there is high conservation suggesting that VKORC1L1 is highly constrained across vertebrate evolution. The VKORC1L1 sequences within a class appear to be highly conserved but there are differences between the different vertebrate classes. For example, in general mammalian VKORC1L1 sequences are very similar with few amino acid changes but compared to other classes there are noticeable changes specifically at the beginning of the large loop. Across all the vertebrate VKORC1L1 sequences there appears to more variation N terminal of the protein and very conserved at the C terminal. This is different to the results obtained in Section 4.5 for VKORC1. Also, at the N terminal, the *Vombatus ursinus* (Wombat) and the representative amphibian fish species have an amino acid deletion at +7. There is also a base pair insertion at position 58 in the *Callorhinchus milii* (Australian ghostshark).

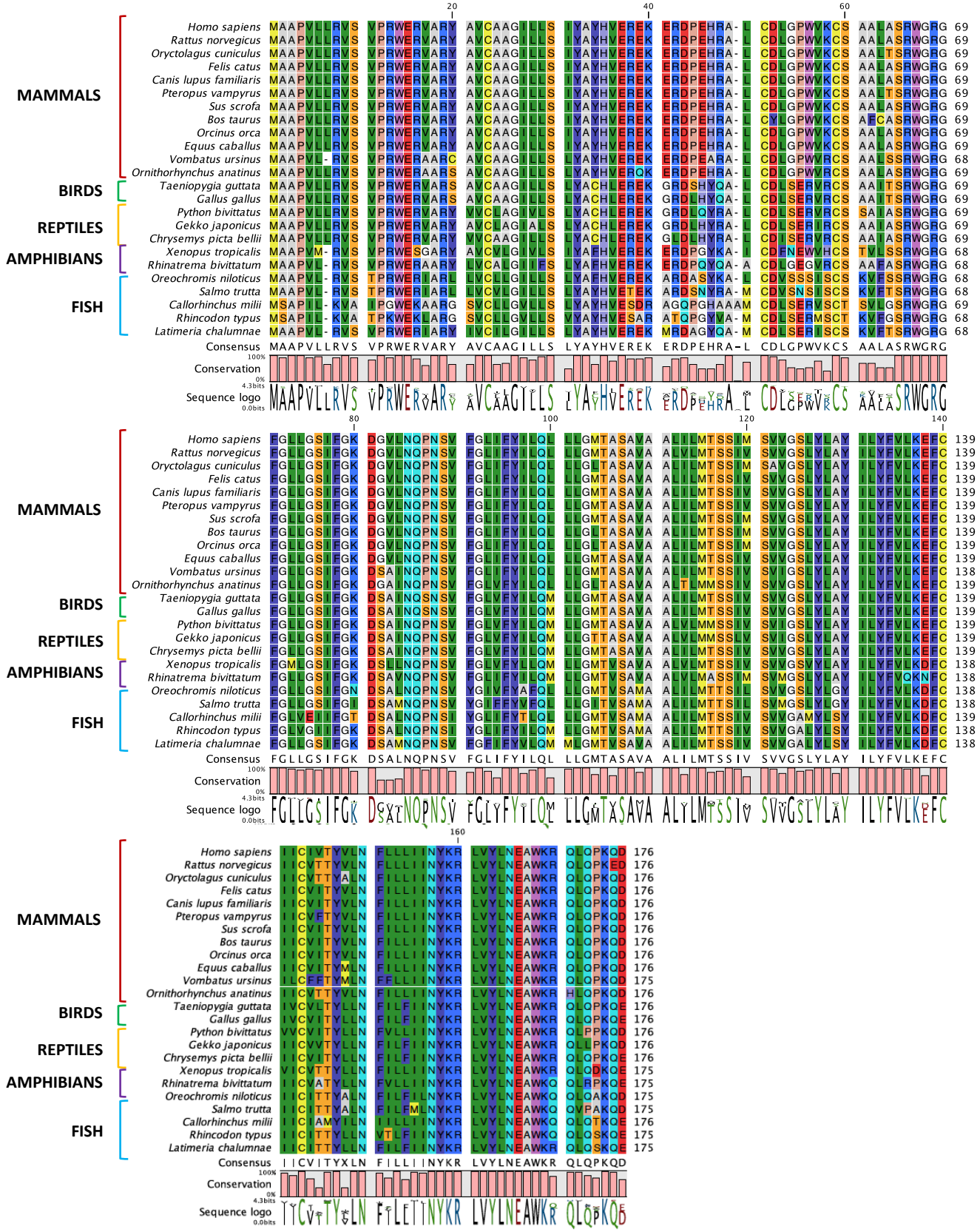


Figure 89: Multiple sequence alignment of representative vertebrate VKORC1L1 sequences. Red line denotes Mammalian sequences. Green line denotes bird sequences. Yellow line denotes reptile sequences. Purple line denotes amphibian sequences. Blue line denotes fish sequences. Colours of amino acids are according to physiochemical properties, refer to Appendix 8.

4.13.2 Consensus sequences for vertebrate VKORC1L1

The VKORC1L1 sequences were further compared by generating consensus sequences for each vertebrate class using multiple sequence alignments (Figure 90). The consensus sequences were created using the same method as the consensus sequences for VKORC1 in Section 4.5.

The VKORC1L1 consensus sequences highlight areas of the protein sequence where there is complete conservation throughout vertebrate evolution but also within a particular vertebrate class. In general, the conserved areas appear in the TM domains. Interestingly, there is one region of 13 amino acids that are fully conserved at the C terminal between positions 157 to 168 'NYKRLVYLNEAWK'. This is very different to the findings in Section 4.5 for VKORC1. VKORC1 appears to have the most variation at the C terminal compared to VKORC1L1.

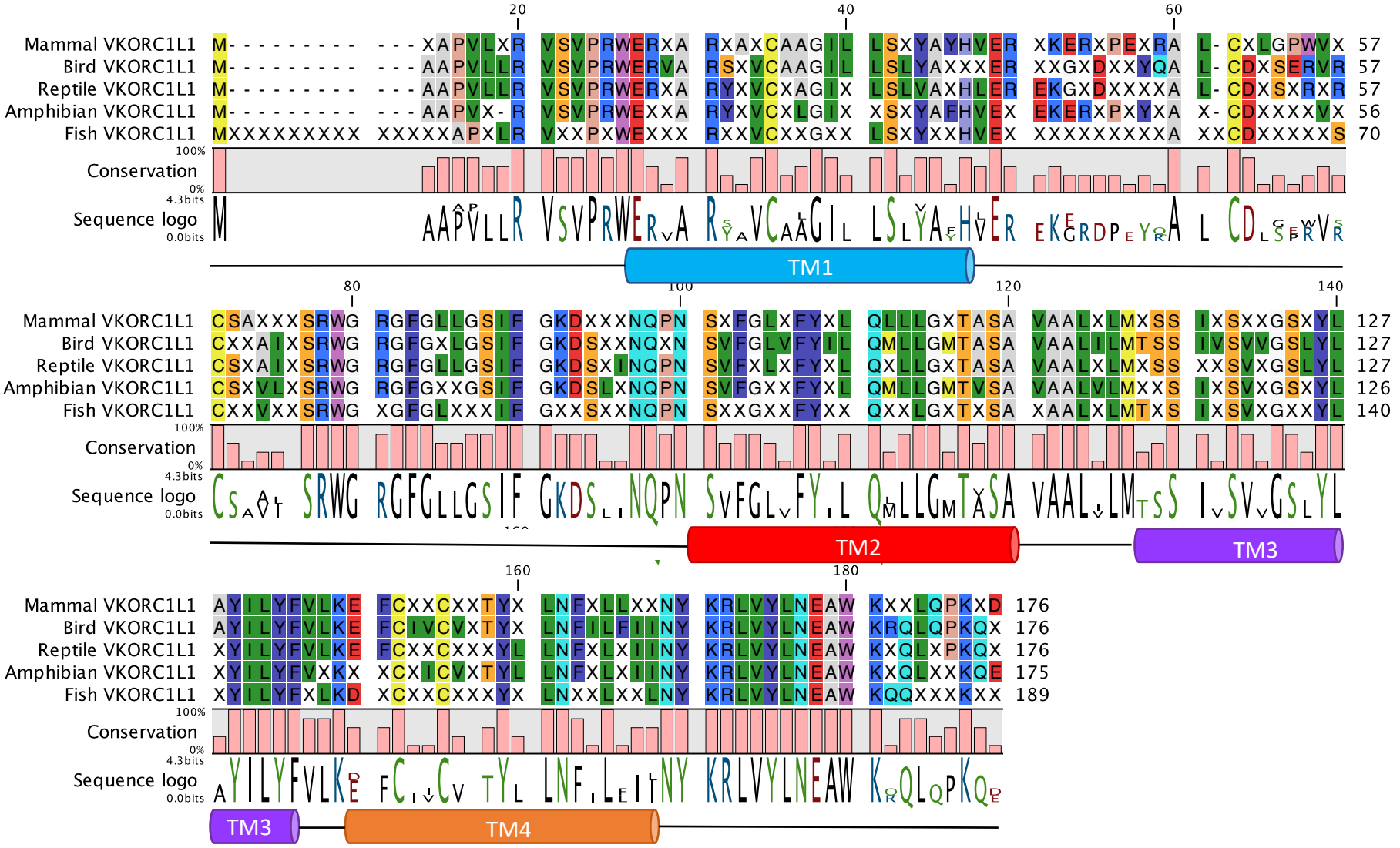


Figure 90: Multiple sequence alignment of VKORC1L1 consensus sequences for each class within the vertebrate subphylum with the four transmembrane domains highlighted. X denotes one or more amino acid differences. Blue arrows denoted 100% conserved amino acid positions. Red box denotes active site. Colours of amino acids are according to physiochemical properties refer to Appendix 8.

4.13.3 Using the Consensus sequences to assess functional constraint across vertebrate VKORC1L1

Due to the way the consensus sequences were constructed for the vertebrate VKORC1L1, an 'X' was used to denote amino acid positions where one or more amino acid change is observed, therefore concealing highly conserved regions or positions in which significant amino acid changes were found in a vertebrate class. Therefore, an alignment was made for each vertebrate class, whereby the amino acid residues found at positions denoted by an 'X' are shown (Figure 91-95).

The alignments reveal the functional constraint across the vertebrate classes. In general, amino acid changes are scattered throughout the vertebrate consensus sequences, with the majority of changes in the large loop and scattered throughout the TM domains. The bird VKORC1L1 sequences, however, show complete conservation in TM2 and TM3 compared to the other vertebrate classes. This suggests a high level of functional constraint over 100 My of evolution. Fish VKORC1L1 have lots of variation at the N terminus and after the first TM domain compared to other vertebrate classes. This may be due to the 400 My evolutionary timespan between the fish VKORC1L1 sequences. There appears to be more functional constraint in vertebrate VKORC1L1 sequences compared to the vertebrate VKORC1 consensus sequences analysed in Section 4.5. Analysis by Lacombe and Ferron (2018) suggest that VKORC1 is freer to diverge compared to its paralog VKORC1L1, these results are therefore consistent with these researchers results. Lacombe and Ferron (2018) only used 7 VKORC1 sequences (2 mammals, 1 bird, 1 reptile, 1 amphibian and 2 fish) and 7 VKORC1L1 (2 mammals, 1 bird, 1 reptile, 1 amphibian and 2 fish) sequences to conduct their analysis, which is not representative of all vertebrate VKORC1 and VKORC1L1 In comparison, the analysis carried out in this thesis used 112 mammals, 2 birds, 9 reptiles, 2 amphibians and 15 fish VKORC1 sequences and 69 mammals, 30 birds, 12 reptiles, 4 amphibians and 49 fish VKORC1L1 sequences.

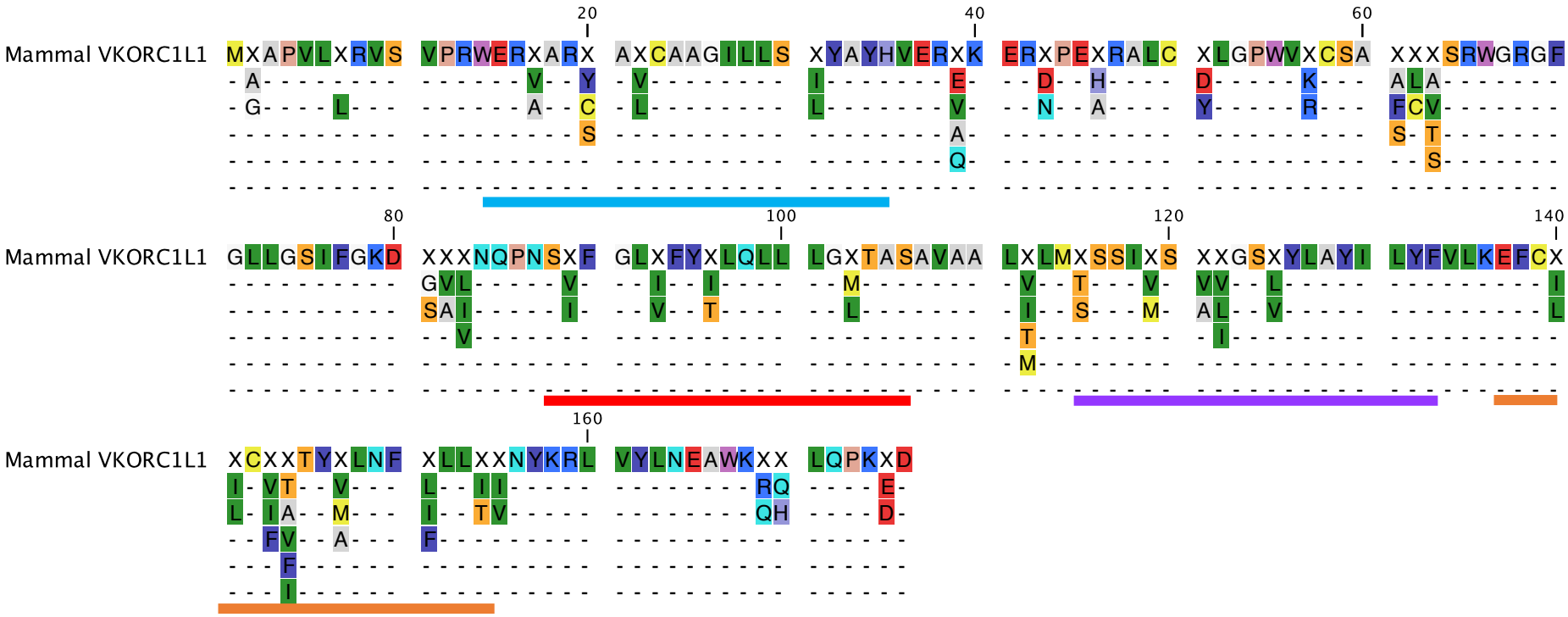


Figure 91: Multiple sequence alignment of the mammalian VKORC1L1 consensus sequence with the amino acid differences shown under the unconserved positions. X denotes one or more amino acid difference. Colours of amino acids are according to physiochemical properties refer to Appendix 8. Transmembrane domains are shown as coloured lines, TM1 – blue, TM2 – red, TM3 – purple and TM4 – orange.

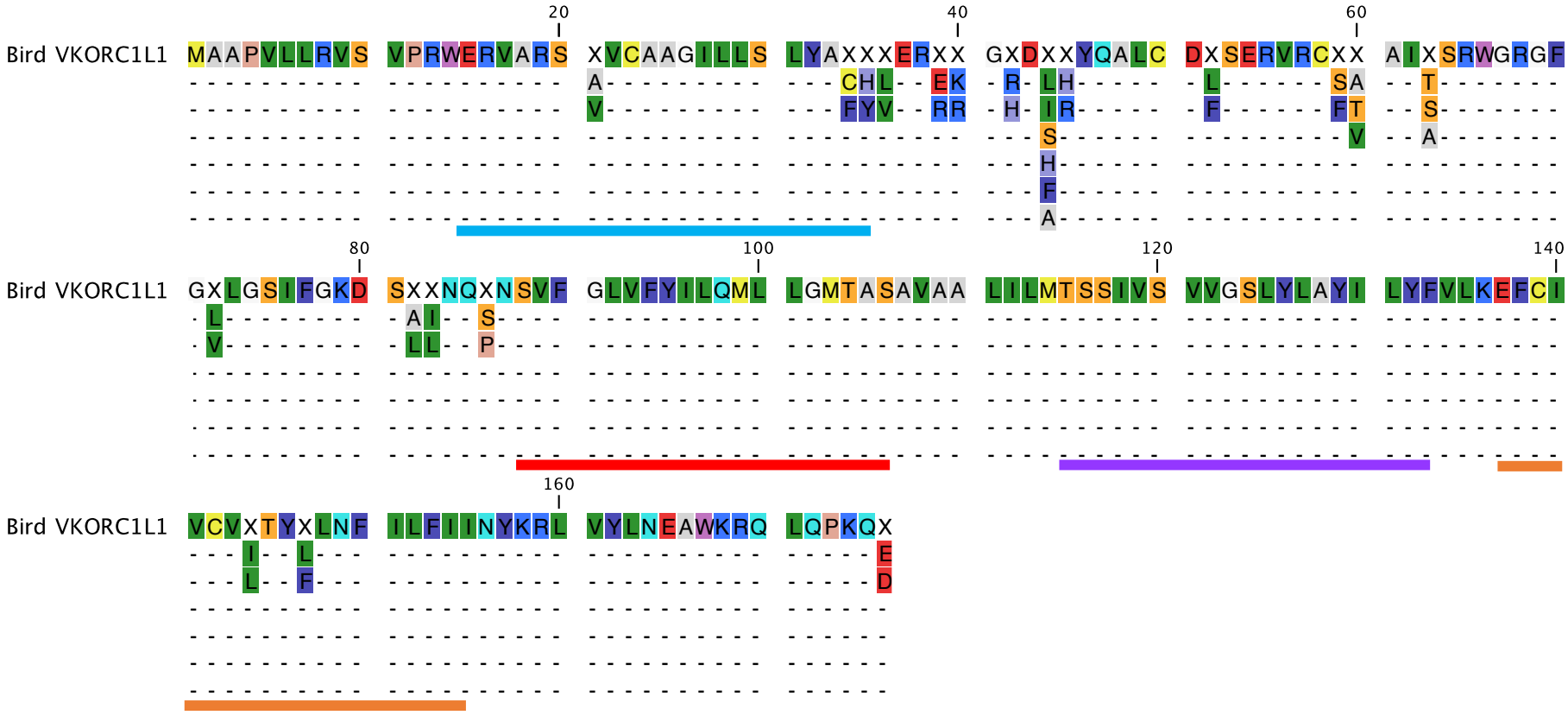


Figure 92: Multiple sequence alignment of the bird VKORC1L1 consensus sequence with the amino acid differences shown under the unconserved positions. X denotes one or more amino acid difference. Colours of amino acids are according to physiochemical properties refer to Appendix 8. Transmembrane domains are shown as coloured lines, TM1 – blue, TM2 – red, TM3 – purple and TM4 – orange.

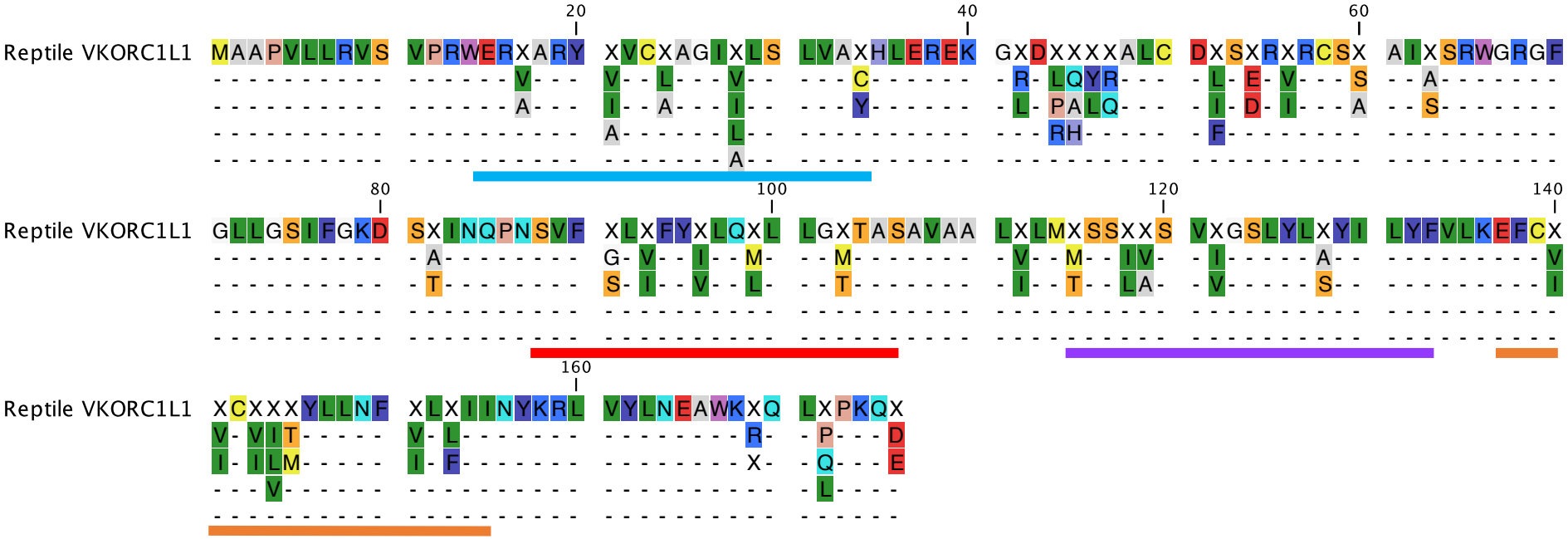


Figure 93: Multiple sequence alignment of the reptilian VKORC1L1 consensus sequence with the amino acid differences shown under the unconserved positions. X denotes one or more amino acid difference. Colours of amino acids are according to physiochemical properties refer to Appendix 8. Transmembrane domains are shown as coloured lines, TM1 – blue, TM2 – red, TM3 – purple and TM4 – orange.

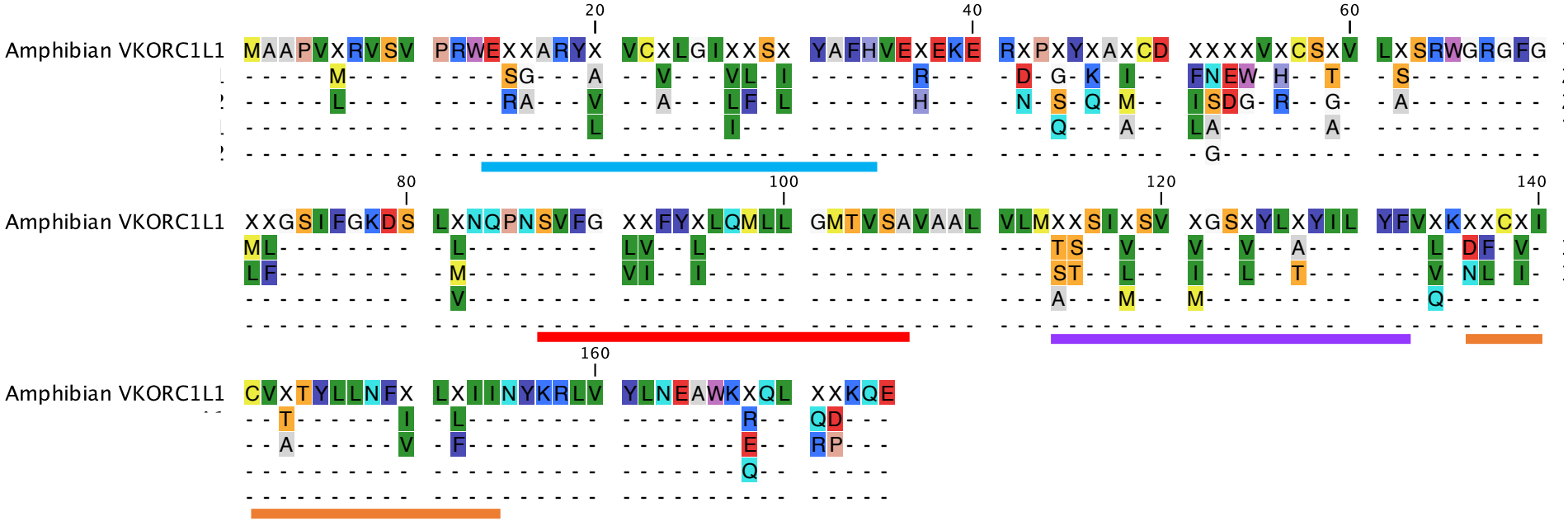


Figure 94: Multiple sequence alignment of the amphibian VKORC1L1 consensus sequence with the amino acid differences shown under the unconserved positions. X denotes one or more amino acid difference. Colours of amino acids are according to physiochemical properties refer to Appendix 8. Transmembrane domains are shown as coloured lines, TM1 – blue, TM2 – red, TM3 – purple and TM4 – orange.

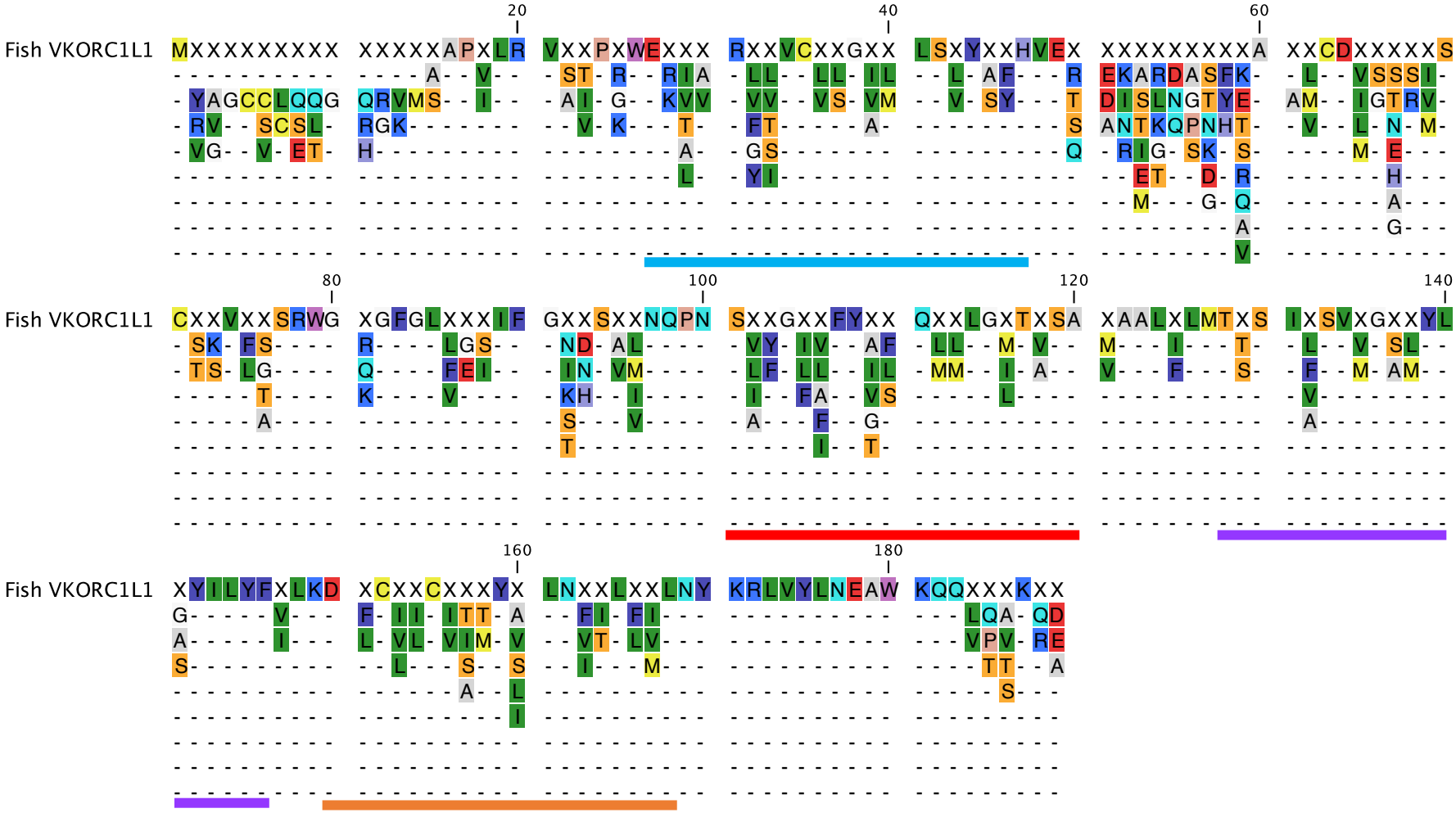


Figure 95: Multiple sequence alignment of the fish VKORC1L1 consensus sequences with the amino acid differences shown under the unconserved positions. X denotes one or more amino difference. Colours of amino acids are according to physiochemical properties refer to Appendix 8. Transmembrane domains are shown as coloured lines, TM1 – blue, TM2 – red, TM3 – purple and TM4 – orange.

4.14 Comparison of representative vertebrate VKORC1L1 using membrane topology and tertiary prediction modelling

Membrane topology and tertiary structure prediction can help to understand the structure of a protein. Currently only membrane topology and tertiary structure prediction has been used previously to predict the number of transmembrane domains contained within human VKORC1L1 (Westhofen *et al.,* 2011; Tie *et al.,* 2014; Lacombe and Ferron, 2018). However, like VKORC1, structure prediction has not been performed for species throughout the vertebrate classes. For both the membrane prediction and the 3D modelling, the same species and same prediction models were used to model VKORC1L1 as previously used for VKORC1 in this study (Section 4.6). Preliminary structural models were performed for four mammalian VKORC1L1 sequences (*Homo* sapiens - Human, *Bos taurus* - Cow, *Vombatus ursinus* - Wombat, *Ornithorhynochus anatinus* - Duck-billed Platypus), one bird (*Gallus gallus* - chicken), one reptile (*Python bivittatus* - python), one amphibian (*Xenopus tropicalis* - Western clawed frog) and one fish (*Oreochromis niloticus* - Nile tilapia). Similar to VKORC1, the 3D model for VKORC1L1 has not been previously solved and is proposed to be similar to the original structure of the bacterial homologue *Synechococcus sp.* VKORC1 determined by x-ray crystallisation (PDB. 3KP9) (*Li et al.,* 2010) and therefore the 3D models of VKORC1L1 in this study are based on this structure. Figure 96 and 97 show the prediction of the membrane topology and tertiary structures of four representative mammalian and four representative non-mammalian VKORC1L1 sequences.

From the TMHMM prediction there is a difference in the number of TM domains between the different species modelled from 2-4 TM domains (Figure 96 and 97). The human, wombat, platypus and chicken all have 2 TM domains, whereas the python and Nile tilapia have 3 TM domains. The cow and western clawed frog have 4 TM. A study by Tie *et al.* (2014) predicted the structure of VKORC1L1 by using a fluorescence protease protection assay in live mammalian cells. Tie *et al.* (2014) states that their model supports an even number of TM domains for VKORC1L1, either 2 or 4 TM domains with the N and C terminal in the cytoplasm but is most likely a 4 TM for human VKORC1L1.

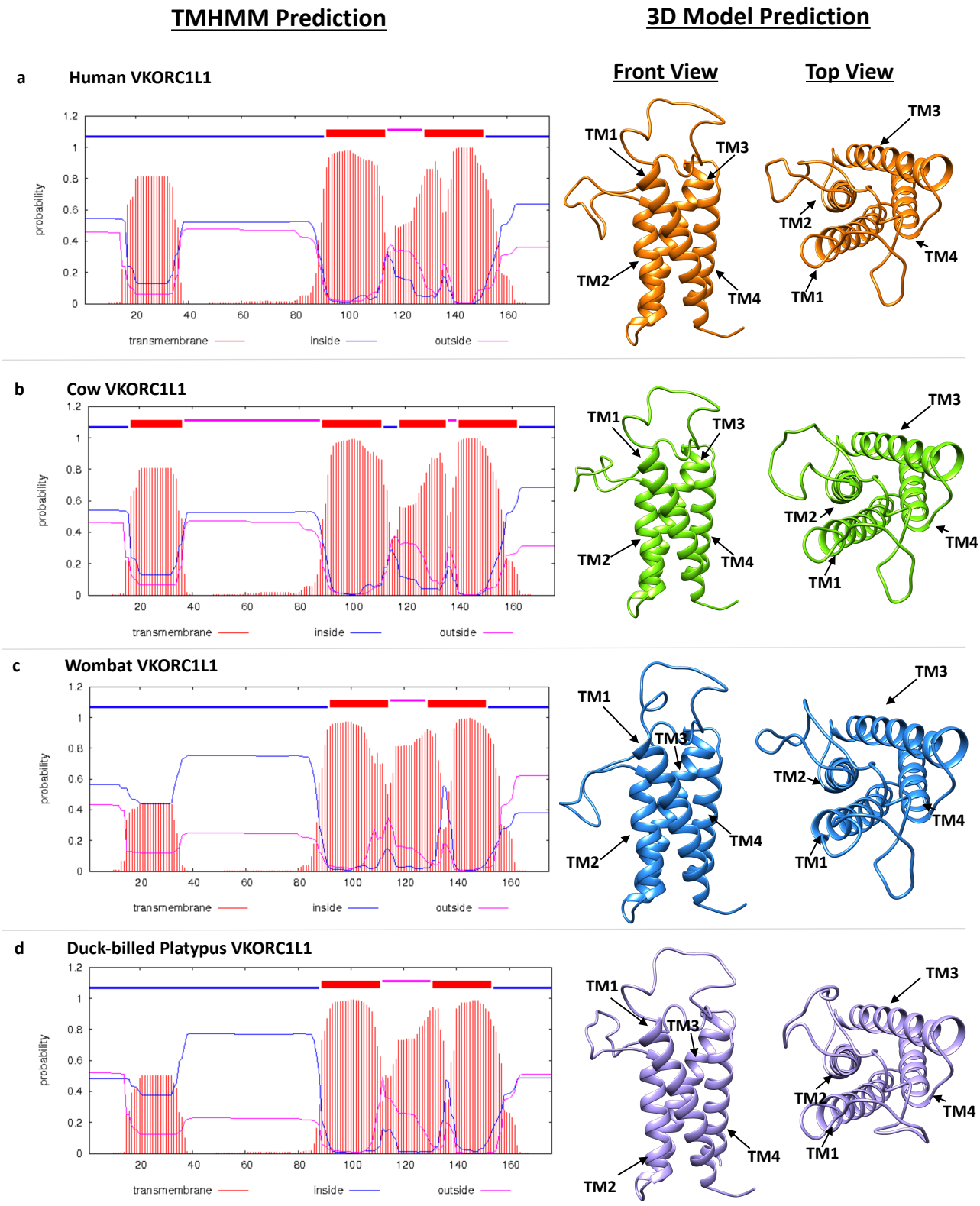


Figure 96: Membrane topology and tertiary structure prediction models for representative mammalian VKORC1L1 species; human, cow, wombat and duck-billed platypus. Each panel shows a TMHMM prediction graph and 3D model prediction using SWISS-Model and Chimera for a front and top view of the VKORC1 sequence with the transmembrane domains highlighted. a Human VKORC1L1. **b** Cow VKORC1L1. **c** Wombat VKORC1L1. **d** Duck-billed Platypus VKORC1L1.

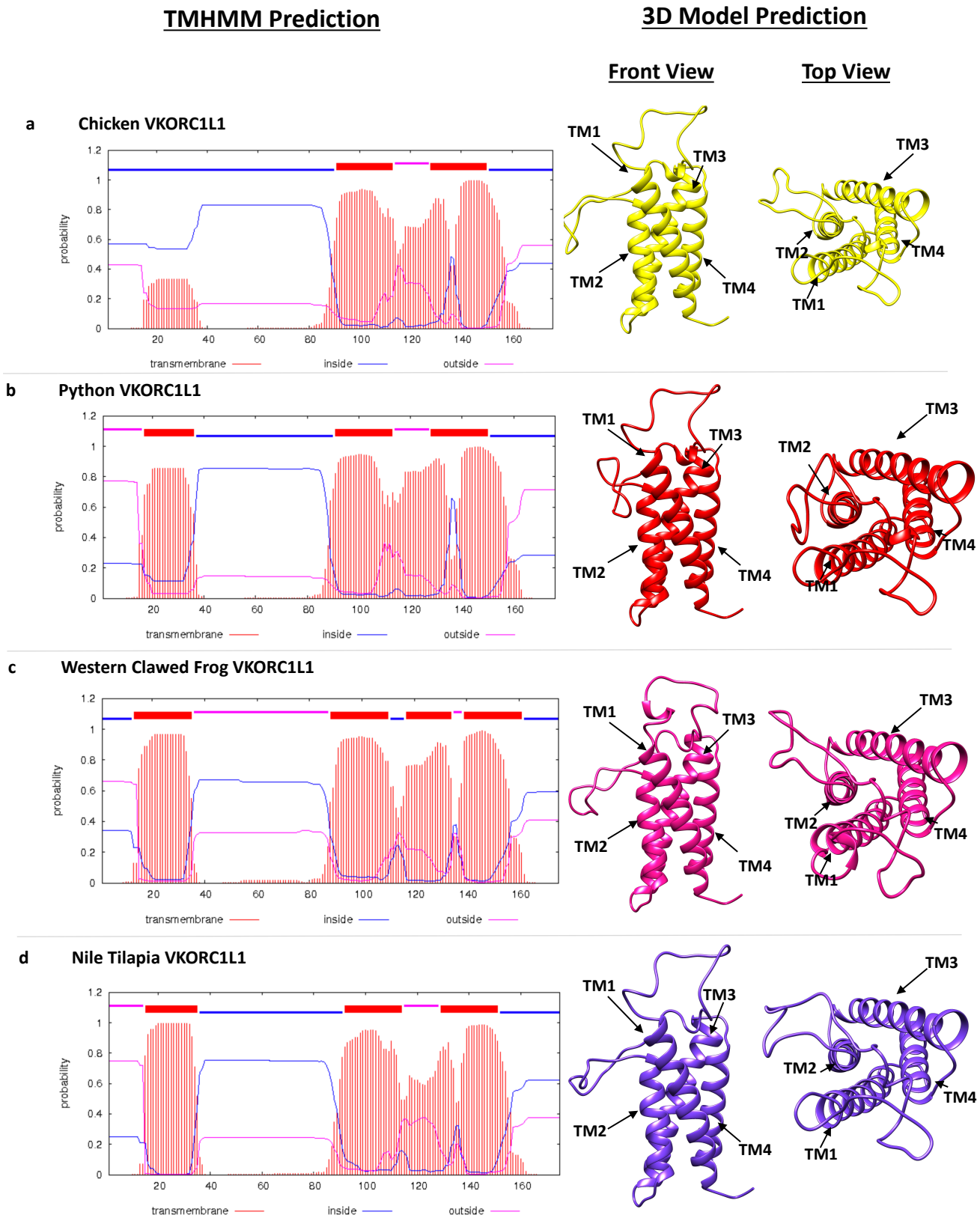


Figure 97: Membrane topology and tertiary structure prediction models for representative non-mammalian VKORC1L1 species; chicken, python, western clawed frog and Nile tilapia. Each panel shows a TMHMM prediction graph and 3D model prediction using SWISS-Model and Chimera for a front and top view of the VKORC1 sequence with the transmembrane domains highlighted. a Chicken VKORC1L1. **b** Python VKORC1L1. **c** Western clawed frog VKORC1L1. **d** Nile tilapia VKORC1L1.

The TMHMM prediction also gives an indication of the orientation of the protein. Like the number of TM domains predicted, the orientation of each species model is different, and the signals of the prediction are weak with a probability of less than 0.8. Tie *et al.* (2014) suggest that human VKORC1L1 has an orientation with the N and C terminal in the cytoplasm. The results from this study are consistent with Tie *et al.* (2014) in all VKORC1L1 sequences with an exception of the python and the Nile tilapia which have the N terminus in the ER lumen.

The tertiary structure prediction models show a 4 TM domain structure for all representative vertebrate VKORC1L1 sequences (Figure 96 and 97). The prediction of the models was based on the original structure of the bacterial homologue *Synechococcus sp.* VKORC1 by Li *et al.* (2010). As this is the only defined structure for any VKOR enzyme, all models based on this structure by Li *et al.* (2010) will bias towards a 4 TM prediction regardless of the secondary prediction. The large loop structure for all the vertebrate VKORC1L1 models show a difference suggesting that the binding of substrates or antagonists such as anticoagulants may have a different effect on the enzymes.

4.15 Analysis of the roles of amino acids between the vertebrate classes for VKORC1L1

There are many amino acid positions identified in the literature that have roles in the warfarin binding and that have been identified as conserved amino acids in all VKORC1L1. The multiple sequence alignments created for VKORC1L1 (Figures 77-88) were used to examine conservation in different phyla regarding to different roles identified for VKORC1L1 (Tables 52 and 53). The percentage of an amino acid found at each position assessed was calculated for all vertebrate classes. The amino acid numbering used is according to the human VKORC1L1 sequence.

4.15.1 Amino Acids Involved in Warfarin binding of human VKORC1L1 in other vertebrates

Czogalla *et al.* (2017) describe three arginine residues that have a role in warfarin binding with possible charge interactions with the anionic warfarin. VKORC1L1 has a different binding pocket to VKORC1 and therefore different arginine residues interact with warfarin (Czogalla *et al.,* 2017). These residues are: R38, R42 and R68 (Table 52). All 3 residues are highly conserved throughout vertebrate VKORC1L1 sequences. At position 38, an arginine residue is

100% conserved in mammal, bird and reptile VKORC1L1 sequences. In amphibian VKORC1L1 sequences, one sequence (*Microcacilia unicolor* – Caecillian) has a positively charged histidine residue, which possibly would not have an effect on the binding of warfarin due to the positively charged properties. 90% of fish VKORC1L1 sequences contain an arginine at this position with 8% containing a threonine residue or a serine residue and 2% containing a glutamine residue. There are differences in physiochemical properties with serine, threonine and glutamine having polar properties which may affect the affinity for anticoagulants. At position 42, there is only 100% conservation in mammals and amphibian VKORC1L1 sequences. There are 16% of reptiles with a hydrophobic leucine residue and in fish 2% of VKORC1L1 sequences have either a lysine, leucine, threonine or glycine residue. The difference in residues at these positions may affect the affinity of anticoagulants at this position causing anticoagulant resistance or sensitivity. Position 68 is the most highly conserved residue with 100% conservation in all vertebrate VKORC1L1 with the exception of fish VKORC1L1 sequences with contain a glutamine in 6% of sequences and a lysine in 2% of sequences.

4.15.2 Amino Acids Described as Conserved in VKORC1L1

A study by Schwarz *et al.* (2009) with only 12 vertebrate VKORC1L1 sequences reported 19 amino acid positions that were conserved and VKORC1L1-specific. The conservation of these positions was examined in this study and reported in Table 53. Of these reported positions there are 8 positions that are fully conserved throughout all vertebrate VKORC1L1 sequences. These are: E37, G74, I76, F77, T104, G123, I130, K158 and L160. Conservation in all these positions suggest that these are VKORC1L1 specific amino acids in agreement with Schwarz *et al.* (2009) and may have potential roles in structure and function of VKORC1L1. 11 of these positions identified by Schwarz *et al* (2009) were found to not be fully conserved in all VKORC1L1 sequences. As the Schwarz *et al*. (2009) study only included seven mammalian VKORC1L1 species, one species of amphibian and four fish VKORC1L1 sequences there was not enough scrutiny over all vertebrate VKORC1L1 sequences and this therefore caused biased and overestimation of number that were VKORC1L1 specific amino acids in their findings. Fish VKORC1L1 species have the least conservation amongst the amino acid positions identified by Schwarz *et al.* (2009), probably due to the millions of years of evolution between the fish species and between the other vertebrate classes.

Human Position	Previously Reported Role in VKORC1L1	Mammal VKORC1L1	Bird VKORC1L1	Reptile VKORC1L1	Amphibian VKORC1L1	Fish VKORC1L1
R38	Warfarin binding	**R**	**R**	**R**	75% - R 25% - H	90% - R 4% - T 4% - S 2% - Q
R42	Warfarin binding	**R**	97% - R 3% - H	84% - R 16% - L	**R**	92% - R 2% - L 2% - K 2% - G 2% - T
R68	Warfarin binding	**R**	**R**	**R**	**R**	92% - R 6% - Q 2% - K

Table 52: Amino acid positions with a previously reported role in warfarin binding of VKORC1L1 with the percentage of amino acids found at each position for each vertebrate class. 100% is represented by bold single letter code. Amino acid numbering according to human VKORC1L1 sequence. Colours of amino acids are according to physiochemical properties, refer to Appendix 8.

Human VKORC1L1 Position	Previously Reported Role in VKORC1L1	Mammal VKORC1L1	Bird VKORC1L1	Reptile VKORC1L1	Amphibian VKORC1L1	Fish VKORC1L1
E37	Conserved VKORC1L1- specific amino acid	**E**	**E**	**E**	**E**	**E**
E39	Conserved VKORC1L1- specific amino acid	95% - E 3% - A 1% - V 1% - Q	97% - E 3% - R	**E**	**E**	E 2% - D 2% - A
K40	Conserved VKORC1L1- specific amino acid	**K**	97% - K 3% - R	**K**	**K**	92%- K 4% - R 2% - N 2% - I
L73	Conserved VKORC1L1- specific amino acid	**L**	**L**	**L**	75% - L 25% - F	94% - L 4% - V 2% - F
G74	Conserved VKORC1L1- specific amino acid	**G**	**G**	**G**	**G**	98% - G 2% - E
S75	Conserved VKORC1L1- specific amino acid	**S**	**S**	**S**	**S**	96% - S 4% - I
I76	Conserved VKORC1L1- specific amino acid	**I**	**I**	**I**	**I**	**I**
F77	Conserved VKORC1L1- specific amino acid	**F**	**F**	**F**	**F**	**F**
T104	Conserved VKORC1L1- specific amino acid	**T**	**T**	**T**	**T**	**T**
A105	Conserved VKORC1L1- specific amino acid	**A**	**A**	**A**	**V**	98% - V 2% - A
V108	Conserved VKORC1L1- specific amino acid	99% - V 1% - M	**V**	**V**	**V**	96% - M 4% - V
T115	Conserved VKORC1L1- specific amino acid	98% - T 1% - S 1% - M	**T**	75% - M 25% - S	50% - T 25% - S 25% - A	96% - T 4% - S
S116	Conserved VKORC1L1- specific amino acid	**S**	**S**	**S**	75% - S 25% -T	94% - T 6% - S
M119	Conserved VKORC1L1- specific amino acid	66% - V 34% - M	**V**	92% - V 8% - A	50% - V 25% - V 25% - M	74% - L 12% - V 10% - A 4% - F
G123	Conserved VKORC1L1- specific amino acid	**G**	**G**	**G**	**G**	**G**
I130	Conserved VKORC1L1- specific amino acid	**I**	**I**	**I**	**I**	**I**

E137	Conserved VKORC1L1- specific amino acid	**E**	**E**	**E**	50% - D 50% - N	**D**
K158	Conserved VKORC1L1- specific amino acid	**K**	**K**	**K**	**K**	**K**
L160	Conserved VKORC1L1- specific amino acid	**L**	**L**	**L**	**L**	**L**

Table 53: Amino acid positions with a previously reported role of conservation of amino acid positions in VKORC1L1 with the percentage of amino acids found at each position for each vertebrate class. 100% is represented by bold single letter code. Amino acid numbering according to human VKORC1L1 sequence. Colours of amino acids are according to physiochemical properties, refer to Appendix 8.

4.16 Assessment of the conserved residues in VKORC1L1 between vertebrate classes

Amino acids that are completely conserved throughout different animal species are thought to have vital structural and functional roles within the enzyme. The consensus sequences derived for each vertebrate class for VKORC1L1 were used to assess the conservation of amino acids throughout all vertebrate sequences.

There are 71 amino acid positions that are completely conserved throughout vertebrate VKORC1L1 sequences and the 20 positions that have previously identified to play a role in VKORC1L1 or identified by Schwarz *et al.* (2009) as conserved in VKORC1L1 are listed in Table 54. There are 51 novel conserved positions that have been identified in this study these are listed in Table 55 to Table 57.

The conserved positions within vertebrate VKORC1L1 sequences suggest an important role in the structure and function of VKORC1L1. Compared to the paralogous enzyme VKORC1, which is only 36% conserved between vertebrate species there are almost 50% more conserved amino acids suggesting that vertebrate VKORC1L1 sequences are more functionally constrained that vertebrate VKORC1 sequences (Section 4.4). R8, V9, P12 and W14 are all conserved at the cytoplasmic N-terminal (Table 55). E15 and R19 are found in the first TM domain and therefore may have potential roles in helix-helix interactions and substrate binding as the conserved cysteines (C50 and C57) are involved in electron relay in VKORC1L1 are found in TM1 and therefore other amino acids surrounding the cysteines may be required for substrate binding (Table 56). A48, S64, R65, W66, G67, G69, F70 and G71 are found in the large loop connecting TM1 and TM2 (Table 57). These amino acids may be involved in the structure and interactions of substrate within the large loop. G78, N84, Q85, F94, Q98, L101 and G102 are found with the second TM domain (Table 56). These amino acids may have a potential role in the structural integrity of VKORC1L1 and a role in substrate binding. S106 and A107 are part of the linking loop between TM2 and TM3. Due to the small number of amino acids involved in the linking loop, it is likely that the two conserved amino acids are involved in the structure of the loop. A109, A110, L111, L113, M114, S117, S120, Y126, Y129, Y132 and F133 are all found in TM3 (Table 56).

Conserved Position	Role in VKORC1L1	Reference
M1	Conserved start codon	
C23	Helix-helix contacts	Bevans *et al.,* 2015
G26	Helix-helix contacts	Bevans *et al.,* 2015
S30	Helix-helix contacts	Bevans *et al.,* 2015
E37	Conserved VKORC1L1- specific amino acid	Schwarz *et al.,* 2009
C50	Active site cysteines	Tie *et al.,* 2014
C58	Active site cysteines	Tie *et al.,* 2014
I76	Conserved VKORC1L1- specific amino acid	Schwarz *et al.,* 2009
F77	Conserved VKORC1L1- specific amino acid	Schwarz *et al.,* 2009
N87	Involved in substrate reduction/binding/specificity	Bevans *et al.,* 2015
S88	Helix-helix contacts	Bevans *et al.,* 2015
Y95	Involved in substrate reduction/binding/specificity	Bevans *et al.,* 2015
T104	Conserved VKORC1L1- specific amino acid	Schwarz *et al.,* 2009
G123	Conserved VKORC1L1- specific amino acid	Schwarz *et al.,* 2009
L127	Involved in substrate reduction/binding/specificity	Bevans *et al.,* 2015
I130	Conserved VKORC1L1- specific amino acid	Schwarz *et al.,* 2009
L131	Helix-helix contacts	Bevans *et al.,* 2015
C139	Active site cysteines	Tie *et al.,* 2014
C142	Active site cysteines	Tie *et al.,* 2014
T145	Helix-helix contacts	Bevans *et al.,* 2015
K158	Conserved VKORC1L1- specific amino acid	Schwarz *et al.,* 2009
L160	Conserved VKORC1L1- specific amino acid	Schwarz *et al.,* 2009

Table 54: Conserved amino acid positions in all vertebrate VKORC1L1 sequences that have a previously identified role. Underlined residues denote active site cysteines. Amino acid numbering according to human VKORC1L1 sequence.

Conserved Position	Position in VKORC1L1	Reference
R8	Found at the cytoplasmic N-terminal	This Study
V9	Found at the cytoplasmic N-terminal	This Study
P12	Found at the cytoplasmic N-terminal	This Study
W14	Found at the cytoplasmic N-terminal	This Study
R159	Found at the cytoplasmic C-terminal	This Study
V161	Found at the cytoplasmic C-terminal	This Study
Y162	Found at the cytoplasmic C-terminal	This Study
L163	Found at the cytoplasmic C-terminal	This Study
N164	Found at the cytoplasmic C-terminal	This Study
E165	Found at the cytoplasmic C-terminal	This Study
A166	Found at the cytoplasmic C-terminal	This Study
W167	Found at the cytoplasmic C-terminal	This Study
K168	Found at the cytoplasmic C-terminal	This Study
K174	Found at the cytoplasmic C-terminal	This Study

Table 55: Conserved amino acid positions in all vertebrate VKORC1L1 sequences found at the N or C terminal in VKORC1L1 found in this study. Amino acid numbering according to human VKORC1L1 sequence.

Conserved Position	Position in VKORC1L1	Reference
E15	Found in TM1	This Study
R19	Found in TM1	This Study
G78	Found in TM2	This Study
N84	Found in TM2	This Study
Q85	Found in TM2	This Study
F94	Found in TM2	This Study
Q98	Found in TM2	This Study
L101	Found in TM2	This Study
G102	Found in TM2	This Study
A109	Found in TM3	This Study
A110	Found in TM3	This Study
L111	Found in TM3	This Study
L113	Found in TM3	This Study
M114	Found in TM3	This Study
S117	Found in TM3	This Study
S120	Found in TM3	This Study
Y126	Found in TM3	This Study
Y129	Found in TM3	This Study
Y132	Found in TM3	This Study
F133	Found in TM3	This Study
Y146	Found in TM4	This Study
L148	Found in TM4	This Study
N149	Found in TM4	This Study
L152	Found in TM4	This Study
N156	Found in TM4	This Study
Y157	Found in TM4	This Study

Table 56: Conserved amino acid positions with a potential involvement in helix-helix interactions and substrate binding in all vertebrate VKORC1L1 sequences found in this study. Amino acid numbering according to human VKORC1L1 sequence.

Conserved Position	Role in VKORC1L1	Reference
A48	Potential involvement in the structure and interactions of the large loop	This Study
S64	Potential involvement in the structure and interactions of the large loop	This Study
R65	Potential involvement in the structure and interactions of the large loop	This Study
W66	Potential involvement in the structure and interactions of the large loop	This Study
G67	Potential involvement in the structure and interactions of the large loop	This Study
G69	Potential involvement in the structure and interactions of the large loop	This Study
F70	Potential involvement in the structure and interactions of the large loop	This Study
G71	Potential involvement in the structure and interactions of the large loop	This Study
S106	Potential involvement in the structure of the linking loop between TM2 and TM3	This Study
A107	Potential involvement in the structure of the linking loop between TM2 and TM3	This Study
K136	Potential involvement in the structure of the linking loop between TM3 and TM4	This Study

Table 57: Conserved amino acid positions with a potential involvement in the structure and interactions of linking loops in all vertebrate VKORC1L1 sequences found in this study. Amino acid numbering according to human VKORC1L1 sequence.

These amino acids have potential roles in helix-helix interactions and the binding to the substrate. K136 is found in the linking loop between TM3 and TM4 and is likely to have a structural role due to the few amino acids that are part of the linking loop (Table 57). Y146, L148, N149, L152, N156 and Y157 are found in TM4 and are in the same TM domain as the active site cysteines (C139 and C142). Therefore, the roles that these amino acids may play are in substrate binding and reduction as well as structural helix-helix interactions. The remaining conserved amino acids are found in the cytoplasmic C-terminal of VKORC1L1. These include: R159, V161, Y162, L163, N164, E165, A166, W167, K168 and K174.

4.17 Analysis of the sequences between VKORC1 and VKORC1L1 vertebrates

After scrutiny of both vertebrate VKORC1 and VKORC1L1 enzymes independently, this section will analyse the similarities and differences between both enzymes. There are many differences and similarities observed between the two enzymes VKORC1 and VKORC1L1 in vertebrates. One of the main differences is the amino acid sequence length of the two enzymes. VKORC1 has a length of between 160-169 amino acids compared to VKORC1L1, which has a length of 173-186 amino acids.

4.17.1 Analysis of the Percentage Identity for the vertebrate classes for VKORC1 and VKORC1L1

In order to assess the identity between the different classes of vertebrate VKORC1 compared with vertebrate VKORC1L1 a percentage similarity table was constructed (Table 58).

	Mammal VKORC1L1	Bird VKORC1L1	Reptile VKORC1L1	Amphibian VKORC1L1	Fish VKORC1L1
Mammal VKORC1	25%	25%	23%	28%	29%
Bird VKORC1	36%	38%	34%	37%	33%
Reptile VKORC1	43%	44%	41%	44%	41%
Amphibians VKORC1	44%	45%	43%	48%	45%
Fish VKORC1	39%	38%	35%	40%	36%

Table 58: Percentage identity between the five different classes of vertebrate VKORC1 compared to vertebrate VKORC1L1.

The percentage identities between the different classes of vertebrate VKORC1 and VKORC1L1 have a range of 23% to 48%. Only 25% of amino acids are identical between mammalian VKORC1 and VKORC1L1 suggesting that there is high divergence between the two enzymes with only the essential amino acids for the VKOR family are conserved. The highest sequence identity is between amphibian VKORC1 and VKORC1L1 sequences at 48%. This suggests that the divergence of the two amphibian enzymes is lower compared to the other vertebrate classes. Fish VKOR enzymes have an identity of 36%. There is ~400 My between the fish species resulting in a low sequence identity. Both birds and reptiles have similar sequence identities of 38% and 41%, respectively. Bevans *et al.* (2015) suggest that vertebrate VKORC1 and VKORC1L1 arose from a gene duplication event during the divergence from invertebrates. Comparisons against vertebrate VKORC1 and vertebrate VKORC1L1 gives the impression that

throughout evolution the two enzymes have retained some similarities between their protein sequences but have lost at least 50% of protein similarity resulting in different functions. This could be due to the millions of years of evolution between the different vertebrate classes.

4.17.2 Analysis of the roles of amino acids in the VKOR family

Bevans *et al.* (2015) suggested that specific amino acids have specific roles in all VKOR family of enzymes including VKORC1 and VKORC1L1. They suggested that specific amino acids have potential roles of helix-helix interactions in VKOR enzymes (Table 59). These include: C16, G19, S23, A26 (on TM1); S81, G84 (on TM2); S117, L124, L128 (on TM3); and T138 (on TM4). C16, G19, S81, S117 and L124 are completely conserved in vertebrate VKORC1, suggesting that the structural roles are vital due to complete conservation throughout vertebrate evolution in both enzymes. There are 2 amino acid positions that are not completely conserved on TM1; these are S23 and A26. At position 23 the bird VKORC1 contains an alanine at this position. This may have an effect on helix-helix interactions due to a change from a polar amino acid to a small uncharged amino acid. At position 26, two mammalian VKORC1 sequences have a serine at this position (*Mus spretus* – Algerian mouse and *Felis catus* – Cat) and one fish VKORC1L1 sequence has a serine at this position (*Danio rerio* – Zebra fish). On TM4 there is only one position that has a role in helix-helix interactions, and this is T138. There is complete conservation in all vertebrate VKORC1 classes except for 1% found in mammalian VKORC1. The *Echinops telfairi* (Small Madagascan hedgehog) has a serine at this position. As serine and threonine can be interchangeable, there is probably no change in the role of this amino acid in this VKORC1 sequence. There are two reptile VKORC1L1 sequences that have an amino acid difference of a valine or a glutamine at position 138. It is likely that the valine would not have an effect on helix-helix interactions due to the similar hydrophobic properties whereas, a polar glutamine at this position may have an effect on the helix-helix interactions. Bevans *et al.* (2015) proposed that positions D44, N80, Y88, G95, L120 and L128 are involved in substrate binding, reduction or specificity (Table 60). From Table 60, D44, N80, Y88 and L120Q are fully conserved in all vertebrate VKOR sequences suggesting that these positions are fundamental for substrate binding. G95 is conserved in all vertebrate VKOR enzymes except for in bird VKORC1 which has an alanine at this position. Although both amino acids are small and uncharged, a change in a conserved glycine can have a drastic effect on the function of the protein.

Human Position	Mammal VKORC1	Bird VKORC1	Reptile VKORC1	Amphibian VKORC1	Fish VKORC1	Mammal VKORC1L1	Bird VKORC1L1	Reptile VKORC1L1	Amphibian VKORC1L1	Fish VKORC1L1
Conserved in TM1 – Putative helix-helix interactions										
C16	C	C	C	C	C	C	C	C	C	C
G19	G	G	G	G	G	G	G	G	G	G
S23	S	50% - S 50% - A	S	S	S	S	S	S	S	S
A26	99% - A 1% - S	A	A	A	A	A	A	A	A	98% - A 2% - S
Conserved in TM2 – Putative helix-helix interactions										
S81	S	S	S	S	S	S	S	S	S	S
G84	G	G	G	G	G	G	G	84% - G 16% - S	G	G
Conserved in TM3 – Putative helix-helix interactions										
S117	S	S	S	S	S	S	S	S	S	S
L124	L	L	L	L	L	L	L	L	L	L
L128	99% - L 1% - H	L	L	L	L	L	L	L	50% - L 25% - V 25% - Q	L
Conserved in TM4 – Putative helix-helix interactions										
T138	99% - T 1% - S	T	T	T	T	T	T	92% - T 8% - M	T	98% - T 2% - M

Table 59: Amino acid positions with a previously reported role by Bevans *et al.* (2015) of conserved amino acid positions TM domains leading to helix-helix interactions in VKOR with the percentage of amino acids found at each position for each vertebrate class. 100% is represented by bold single letter code. Amino acid numbering according to human VKORC1 sequence. Colours of amino acids are according to physiochemical properties, refer to Appendix 8.

Human Position	Mammal VKORC1	Bird VKORC1	Reptile VKORC1	Amphibian VKORC1	Fish VKORC1	Mammal VKORC1L1	Bird VKORC1L1	Reptile VKORC1L1	Amphibian VKORC1L1	Fish VKORC1L1
D44	**D**	**D**	**D**	**D**	**D**	**D**	**D**	**D**	**D**	**D**
N80	**N**	**N**	**N**	**N**	**N**	**N**	**N**	**N**	**N**	**N**
G84	**G**	**G**	**G**	**G**	**G**	**G**	**G**	84% - G 16% - S	**G**	**G**
Y88	**Y**	**Y**	**Y**	**Y**	**Y**	**Y**	**Y**	**Y**	**Y**	**Y**
G95	**G**	50% - G 50% - A	**G**	**G**	**G**	**G**	**G**	**G**	**G**	**G**
L120	**L**	**L**	**L**	**L**	**L**	**L**	**L**	**L**	**L**	**L**
L128	99% - L 1% - H	**L**	**L**	**L**	**L**	**L**	**L**	**L**	50% - L 25% - V 25% - Q	**L**

Table 60: Amino acid positions with a previously reported role by Bevans *et al.* (2015) of substrate interactions in VKOR with the percentage of amino acids found at each position for each vertebrate class. 100% is represented by bold single letter code. Amino acid numbering according to human VKORC1 sequence. Colours of amino acids are according to physiochemical properties, refer to Appendix 8.

As previously described L128 has a role in the stability of the VKORC1 structure (Section 4.7) but it also has another role in substrate binding in VKOR enzymes. As there are multiple roles assigned to this position, it suggests that it is important for both structure and function of VKOR enzymes and therefore is an explanation for the high conservation seen throughout vertebrate evolution.

4.17.3. Analysis of site-specific VKOR enzyme differences

A study by Schwarz *et al.* (2009) used a hidden Markov model to derive multiple sequence alignments for a small number of VKORC1 and VKORC1L1 sequences to analyse evolutionary and functional site-specific residues between the two VKOR enzymes. They identified positions that were VKORC1L1-specific and fish VKORC1-specific residues. The amino acid positions that were identified by Schwarz *et al.* (2009) were examined in this study (Table 61).

Position	Conserved Amino Acid in Mammalian VKORC1 sequences used by Schwarz *et al.* (2009)	Fish VKORC1-specific and VKORC1L1-specific residues identified by Schwarz *et al.* (2009)
30	**K**	**E**
79	**S**	**P**
82	**I**	**V**
103	**S**	**A**
143	**V**	**F**
150	**S**	**N**
152	**R**	**K**

Table 61: Amino acid positions identified by Schwarz *et al.* (2009) that are fish VKORC1-specific and VKORC1L1-specific. 100% is represented by bold single letter code. Amino acid numbering according to human VKORC1 sequence. Colours of amino acids are according to physiochemical properties, refer to Appendix 8.

Schwarz *et al.* (2009) used a small sample size of VKOR sequences (8 mammalian and 4 fish VKORC1 sequences and 7 mammalian, 1 bird, 1 amphibian and 4 fish VKORC1L1 sequences) which resulted in a data which does not represent all vertebrate classes for both enzymes and conclusions regarding fish VKORC1-specific and VKORC1L1-specific residues. Upon analysis of 135 VKORC1 and 164 VKORC1L1 sequences in this study, the conclusions made in this study are different when a large sample size is used.

Human Position	Mammal VKORC1	Bird VKORC1	Reptile VKORC1	Amphibian VKORC1	Fish VKORC1	Mammal VKORC1L1	Bird VKORC1L1	Reptile VKORC1L1	Amphibian VKORC1L1	Fish VKORC1L1
K30	99% - K 1% - E	**E**	**E**	**E**	**E**	**E**	**E**	**E**	**E**	**E**
S79	99% - S 1% - P	**P**	**P**	**P**	**P**	**P**	**S**	**P**	**P**	**P**
I82	94% - I 3% - V 1% - L	50% - V 50% - A	78% - I 11% - L 11% - V	**V**	48% - L 46% - V 6% - I	90% - V 10% - I	**V**	**V**	**V**	88% - V 6% - I 4% - L 2% - A
S103	99% - S 1% - A	**S**	**A**	**A**	**A**	**A**	**A**	**A**	**A**	**A**
V144	87% - V 6% - A 4% - M 3% - L	50% - A 50% - L	89% - F 11% - G	50% - F 50% - L	**F**	**F**	**F**	**F**	**F**	96% - F 4% – V 4% - I
S150	92% - S 8% - N	**N**	**N**	**N**	**N**	**N**	**N**	**N**	**N**	**N**
R152	74% - R 24% - Q 1% - K 1% - W	**R**	**K**	**K**	**K**	**K**	**K**	**K**	**K**	**K**

Table 62: Comparison of amino acid positions identified by Schwarz *et al.* (2009) that are fish VKORC1-specific and VKORC1L1-specific in all vertebrate classes. 100% is represented by bold single letter code. Amino acid numbering according to human VKORC1 sequence. Colours of amino acids are according to physiochemical properties, refer to Appendix 8.

The residues identified as fish VKORC1-specific and VKORC1L1-specific by Schwarz *et al.* (2009) are generally found across all vertebrate classes for both enzymes (Table 62). Although Schwarz *et al.* (2009) had representation for four out of five vertebrate classes for the VKORC1L1 sequences, there was not representation of all vertebrate classes for VKORC1 sequences and this therefore led to different conclusions regarding the fish-specific VKORC1, but also by choosing a small sample size there was not a representation of all species throughout all vertebrate classes which lead to biased conclusions. 99% of mammalian VKORC1 sequences have a lysine and serine at positions 30 and 79, respectively (Table 62). Interestingly, the *Ornithorhynchus anatinus* (Duck-billed platypus) has a glutamate and a proline at positions 30 and 79, respectively. The most dramatic change being the negative glutamate change to the positive arginine at position 30. These positions are 100% conserved in all remaining vertebrate VKORC1 sequences and all vertebrate VKORC1L1 sequences – with the exception of bird VKORC1L1 sequences at position 79 (Table 62). Between the evolution of modern mammals (placentals and marsupials) and the modern monotremes (e.g. duck billed platypus) there were a clade of extinct mammals. There is a possibility that the change occurred within this extinct clade of mammals and was retained in the mammalian VKORC1 sequences in placentals and marsupials.

4.17.4 Assessment of the conserved residues in VKOR between vertebrate classes

VKORC1 in general has a lower conservation of amino acids compared to VKORC1L1, which could be due to the different functional roles of the enzymes. To determine the conservation across the vertebrate VKORC1 and VKORC1L1 sequences an alignment was created using the consensus sequences (Figure 98). The conserved amino acids are listed in Table 63 with the previously reported roles (numbering according to human VKORC1).

There are 24 conserved positions throughout all 299 vertebrate VKOR enzymes analysed in this study (Figure 98 and Table 63). This suggests that these positions are likely to be essential for the structure and function of the VKOR family of enzymes. There are 6 positions found within this study that have not been previously reported. These are; G60, G62, G64, Q91, N142 and L145. G60, G62, and G64 are found in the large loop between TM1 and TM2. These amino acids potentially have a role in the structure of the loop and interactions of substrate

with the loop. Q91, N142 and L145 are found in TM domains and therefore may be responsible for helix-helix interactions and substrate binding in both VKORC1 and VKORC1L1.

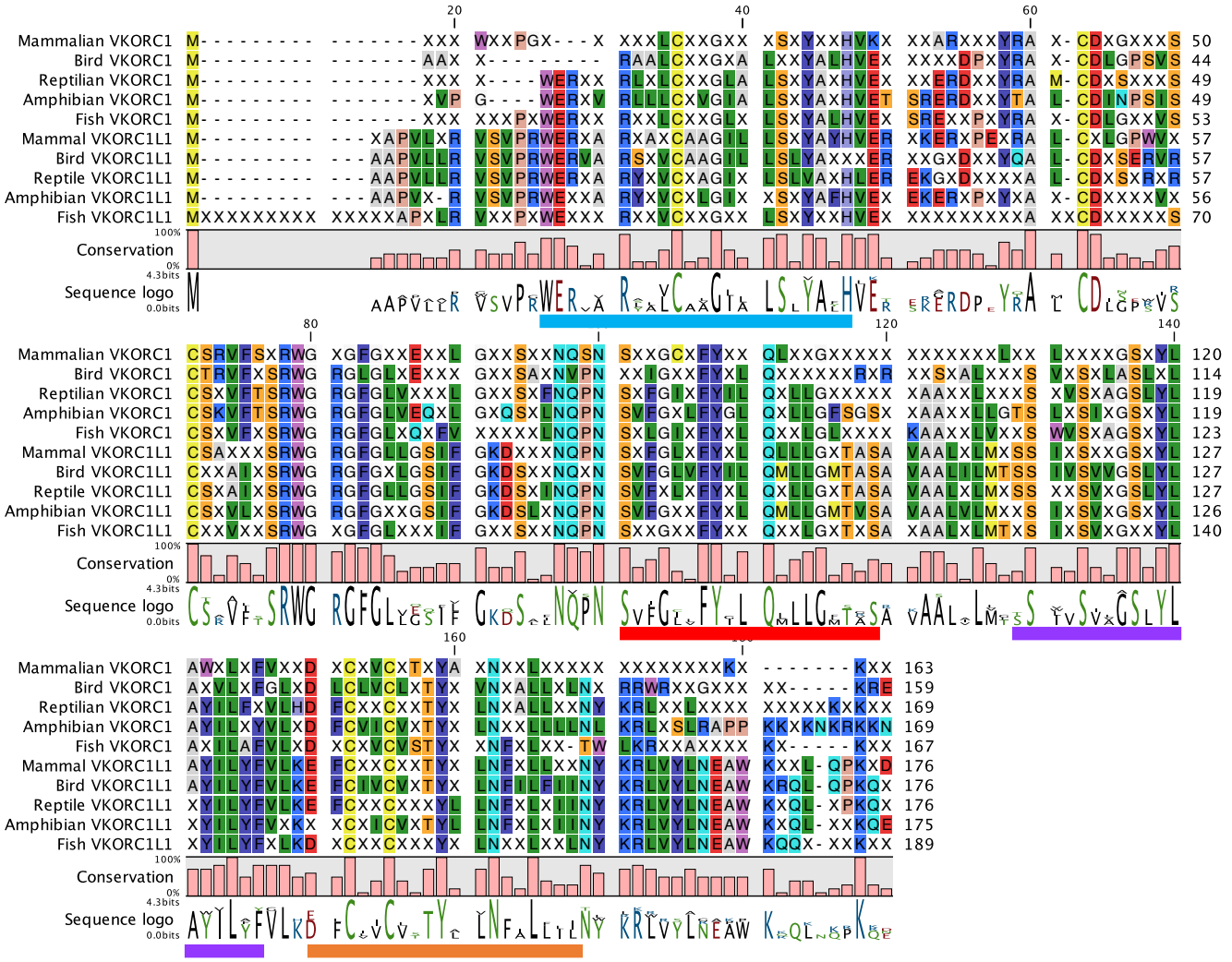


Figure 98: Multiple sequence alignment of VKOR consensus sequences for each class within the vertebrate subphylum with the four transmembrane domains highlighted. X denotes one or more amino acid differences. Colours of amino acids are according to physiochemical properties refer to Appendix 8.

Conserved Position	Role	Reference
M1	Conserved starting codon	
C16	Helix – helix interactions	Bevans *et al.,* 2015
G19	Helix – helix interactions	Bevans *et al.,* 2015
A41	Warfarin resistance in humans (A41S) and black rats (A41T/V)	Reider *et al.,* 2005; Tanaka *et al.,* 2012
C43	Involved in active site – conserved cysteine	Goodstadt and Ponting, 2004; Rost *et al.,* 2005
C51	Involved in active site – conserved cysteine	Goodstadt and Ponting, 2004; Rost *et al.,* 2005
R58	Warfarin resistance in humans (R58G) and mouse (R58G)	Rost *et al.,* 2004; Gryseels *et al.,* 2015.
W59	Naphthoquinone head binding – VKE and VK. Warfarin binding	Czogalla *et al.,* 2017; Song *et al.,* 2011; Watzka *et al.,* 2011; Wu *et al.,* 2018
G60	**Potential involvement in the structure and interactions of the large loop**	**This study**
G62	**Potential involvement in the structure and interactions of the large loop**	**This study**
G64	**Potential involvement in the structure and interactions of the large loop**	**This study**
N77	Warfarin resistance in humans (N77S/Y)	Watzka *et al.,* 2011
N80	Naphthoquinone head binding – VK. Involved in substrate reduction/binding/specificity	Czogalla *et al.,* 2017; Bevans *et al.,* 2015
F87	Isoprenoid chain binding	Czogalla *et al.,* 2017
Y88	Isoprenoid chain binding	Czogalla *et al.,* 2017; Bevans *et al.,* 2015
Q91	**Found in TM2 – potential involvement in helix-helix interactions and substrate binding**	**This study**
L120	Naphthoquinone head binding – VKE and VK. Involved in substrate reduction/binding/specificity	Czogalla *et al.,* 2017; Pelz *et al.,* 2005; Bevans *et al.,* 2015
L124	Naphthoquinone head binding – VKE and VK. Helix – helix interactions	Czogalla *et al.,* 2017; Bevans *et al.,* 2015
C132	Active site cysteine	Goodstadt and Ponting, 2004; Rost *et al.,* 2005
C135	Active site cysteine	Goodstadt and Ponting, 2004; Rost *et al.,* 2005
Y139	Warfarin binding site	Wu *et al.,* 2018; Rost *et al.,* 2004; Pelz *et al.,* 2005
N142	**Found in TM4 – potential involvement in helix-helix interactions and structure of VKORC1**	**This study**
L145	**Found in TM4 – potential involvement in helix-helix interactions and structure of VKORC1**	**This study**
K161	Part of the ER retention signal	Rost *et al.,* 2004

Table 63: Conserved amino acid positions between VKORC1 and VKORC1L1 throughout all classes of vertebrates. Underlined residues denote active site cysteines. Bold red denotes positions identified in this study. Blue denotes previously published amino acid positions with a role in VKORC1. Green denotes previously published amino acid positions with a role in all VKORs. Amino acid numbering according to human VKORC1 sequence.

4.18 Heterologous Expression of VKORC1 Constructs

Following the scrutiny of vertebrate VKORC1 and VKORC1L1 sequences (Section 4.1 – 4.17), four VKORC1 sequences were chosen for expression in the *Sf9* expression system with the intention to identify the effect of anticoagulant rodenticides and whether conclusions can be made about the differences in protein sequence. These were *Rattus norvegicus* (brown rat)*, Homo sapiens* (human)*, Bos taurus* (cow) and *Python bivittatus* (python) VKORC1. A multiple sequence alignment was generated to show the chosen sequences (Figure 99). A further alignment was generated show the chosen sequences aligned with VKORC1 sequences throughout the vertebrate classes (Figure 100).

The brown rat VKORC1 was chosen primarily as a control, as the effect of anticoagulant rodenticides has been intensively studied (e.g. Hodroge *et al.,* 2011; Matagrin *et al.,* 2013). The brown rat VKORC1 is also a good control as anticoagulant rodenticide polymorphisms have been found in this species and the effect of anticoagulant rodenticides has also been studied *in vitro* and *in vivo* (Section 1.7 and 1.17). In addition, from the sequence alignments (Figure 100) there are 10 amino acid differences between the brown rat sequence and the other sequences chosen, some of which are unique to the *Rattus* genus e.g. N36, M86 and P161.

The human VKORC1 sequence was chosen to assess the effect of anticoagulant rodenticides due primary and secondary poisoning of humans. At the beginning of the project the intention was to assess the effect of anticoagulant rodenticides on the human VKORC1 sequence as this was not known, however, during the project two papers were produced which highlighted these effects (Matagrin *et al.,* 2016; Czogalla *et al.,* 2018). Matagrin *et al.* (2016) assessed the effect on four anticoagulant rodenticides, warfarin, brodifacoum, difethialone and difenacoum on human VKORC1 using K_i values. Whereas, Czogalla *et al.* (2018) used IC_{50} to assess the effect of anticoagulants warfarin, bromadiolone and brodifacoum on human VKORC1. Although these papers give some indication of the effect of anticoagulant rodenticides on recombinant human VKORC1, flocoumafen was not tested so this was tested in addition to four other common rodenticides to provide a direct comparison. Human VKORC1 was also chosen as a model primate from the VKORC1 sequence alignments due to its amino acid sequence differences that are unique to primates in particular Hominids such

as R37, M106 and W147 (Section 4.1). Both human and brown rat VKORC1 sequences are highly studied and therefore are good control sequences to use for comparison with other VKORC1 sequences chosen that have not been previously studied.

The cow VKORC1 sequence was chosen for *in vitro* scrutiny as a model even-toed ungulate for a number of reasons. Firstly, the cow is a domesticated farm animal and is susceptible to non-target poisoning from anticoagulant rodenticides (WIIS, 2009). There are reports of non-target poisoning from second generation anticoagulant rodenticides in the cow and other even-toed farm animals such as the pig and sheep (WIIS, 2010; Dolgormaa, 2004). Currently only one study has biochemically characterised the effect of FGAR warfarin on cow liver microsomes (Louvet *et al.,* 2015). No other more potentially potent anticoagulant rodenticides have been tested against the cow VKORC1, which is important to examine due to the increased use of SGARs on farms. The cow was also chosen as a representative of this group of domesticated even toed ungulates, due to the scrutiny of the VKORC1 sequence in Section 4.1 which contains amino acid differences specific to bovines that are interesting to investigate, including R107, C110 and E152 (Section 4.3).

In other vertebrate classes it could be assumed the function of VKORC1 remains the same however, as no non-mammalian VKORC1 sequence has been characterised biochemically. Although it would have been ideal to pick a bird VKORC1 sequence due to the large number of journal papers on the secondary poisoning by SGARs, the only full length sequence was the chicken VKORC1 and due to the vastly difference sequence this sequence was not chosen. A reptile VKORC1 was therefore chosen based on the evolutionary history of reptiles and having amino acid residues that have been retained in reptile evolution from fish and amphibians and also residues that have evolved in reptiles that have been retained in birds and mammals. Reptiles have also been reported to having exposure to anticoagulant rodenticides and in some cases causing mortality. Reptilian sequences appear to be an amalgamation of all vertebrate VKORC1 sequences. Some amino acid positions of interest are; E30, S44 and P79. Python VKORC1 was chosen as it is part of the clade Sauropsida which is inclusive of reptiles and birds.

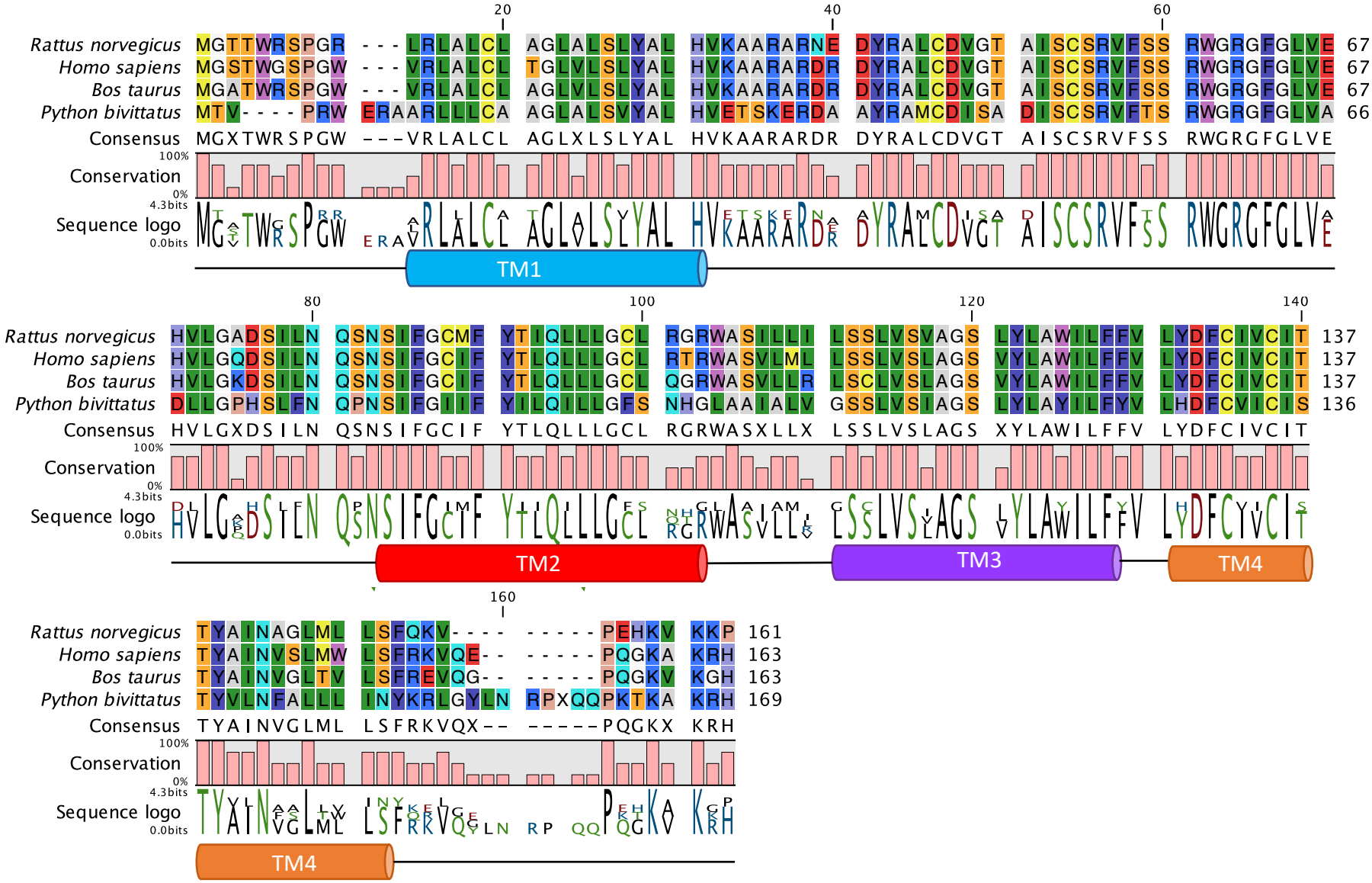


Figure 99: Multiple sequence alignment of the four chosen VKORC1 sequences, brown rat, human, cow and python with the four transmembrane domains highlighted. Colours of amino acids are according to physiochemical properties, refer to Appendix 8.

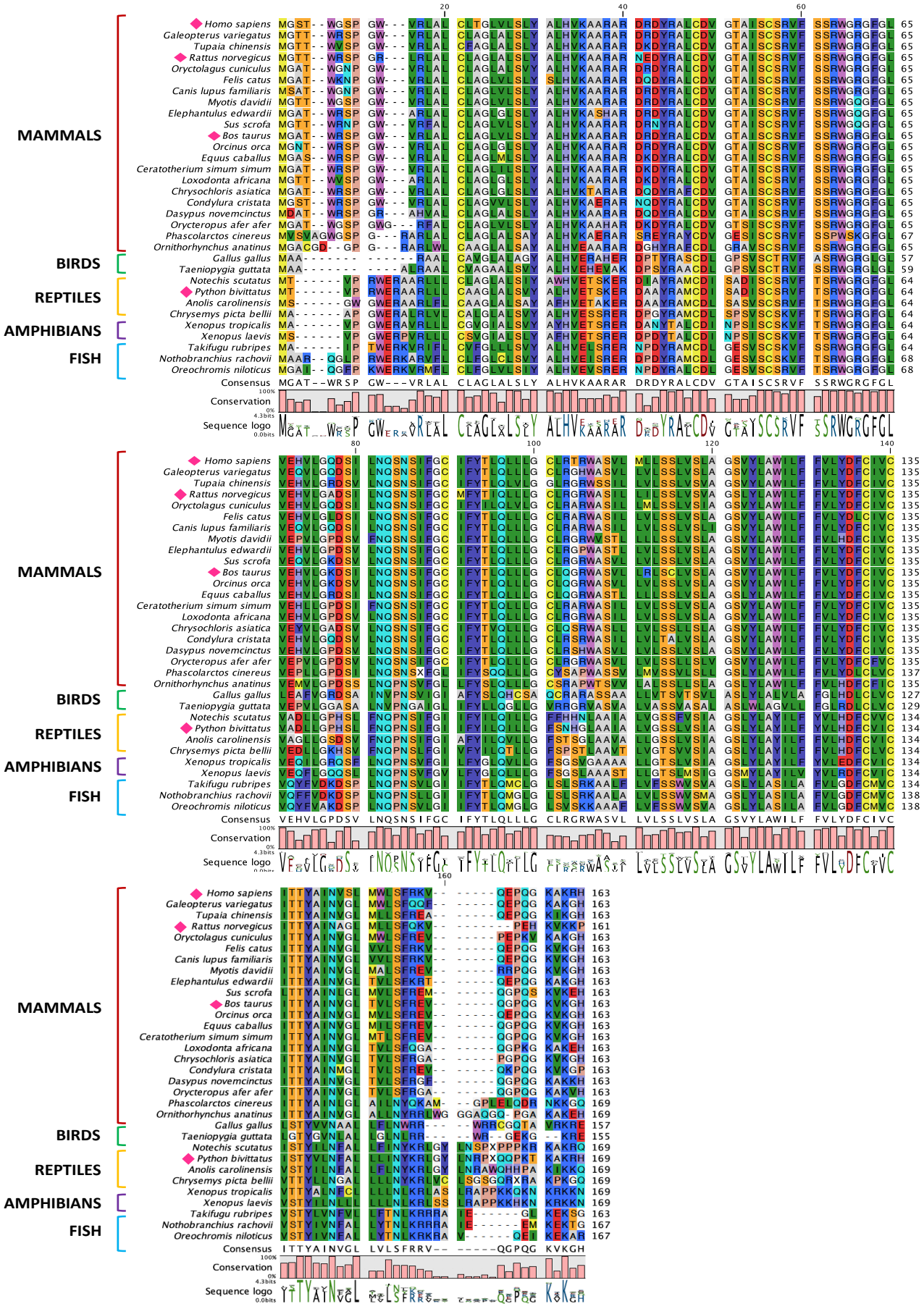


Figure 100: Multiple sequence alignment of representative vertebrate VKORC1 sequences. Red line denotes Mammalian sequences. Green line denotes bird sequences. Yellow line denotes reptile sequences. Purple line denotes amphibian sequences. Blue line denotes fish sequences. Colours of amino acids are according to physiochemical properties, refer to Appendix 8. Pink diamonds denote the chosen VKORC1 constructs.

4.19 Structural Modelling of Chosen VKORC1 Constructs

Preliminary structural models were performed for the chosen VKORC1 sequences, *Rattus norvegicus* – brown rat, *Homo* sapiens - Human, *Bos taurus* - Cow, *Python bivittatus* – python using SWISS-Model based on the original structure of the bacterial homologue *Synechococcus sp,* which has a sequence identity of ~24% sequence identity with human VKORC1 (Li *et al.,* 2010). VKORC1 determined by x-ray crystallisation (PDB. 3KP9) (*Li et al.,* 2010) and then Chimera was used for visualisation of the models. Figure 101 and 102 show the prediction of the tertiary structures of four chosen VKORC1 sequences from the front and the top, respectively.

All structural models were based on the solved 4TM domain structure of the bacterial homologue *Synechococcus* sp. VKORC1 by Li *et al.* (2010) (Figure 101 and 102). As the modelling of the VKORC1 structures were based on the bacterial homologue VKORC1 the models show 4 TM domains for all VKORC1 constructs chosen with one large loop between TM1 and TM2 (Figure 101). The cow VKORC1 appears to have a shorter TM2 alpha helix with two amino acids less compared to the other VKORC1 structures. The orientation of the large loop is different in all the VKORC1 structures (Figure 102) and may affect the binding affinity of substrate and anticoagulant rodenticides. The positioning of the conserved large loop in human and cow VKORC1 appears to be very similar. This may be due to only one amino acid difference a glutamine to a lysine change between the human and cow VKORC1 sequence at position 72. The difference in physiochemical properties, however, may have had an effect on the structure of the loop. The rat VKORC1 has a very different loop structure compared to human and cow VKORC1s. This may be caused by the difference at position 72 where both human and cow VKORC1 have a polar amino acid whereas, the rat has an alanine at this position. In addition, the python loop structure is different to the mammalian loop structures and this may be caused by the many amino acid differences between reptiles and mammals in the loop structure (Figure 102). One of the main differences is the charge difference at the beginning of the large loop (Figure 101 and 102).

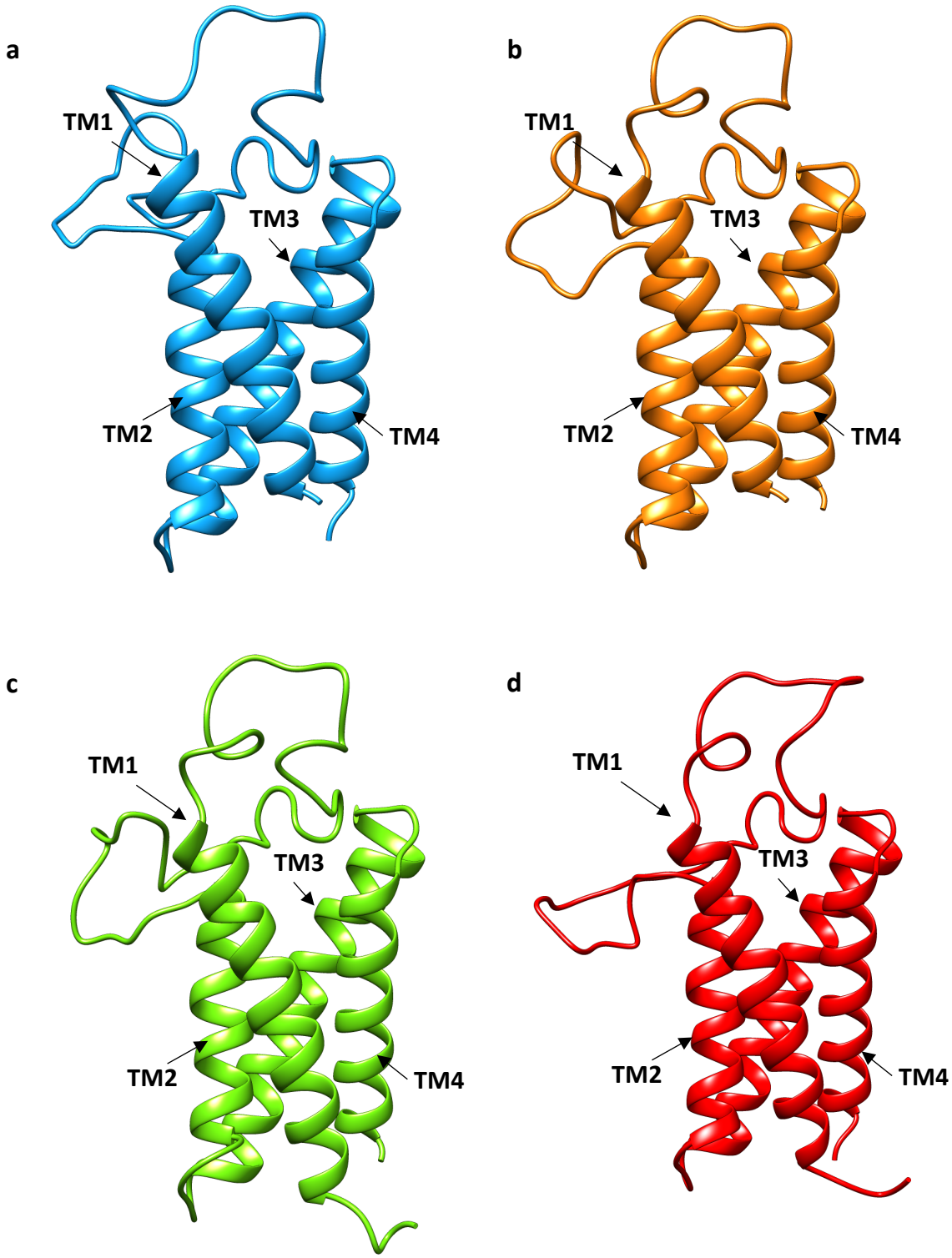


Figure 101: Structural modelling diagrams of rat, human, cow and python VKORC1 based on the VKORC1 structure defined by (Li *et al.,* 2010). a Brown rat VKORC1. **b** Human VKORC1. **c** Cow VKORC1. **d** Python VKORC1.

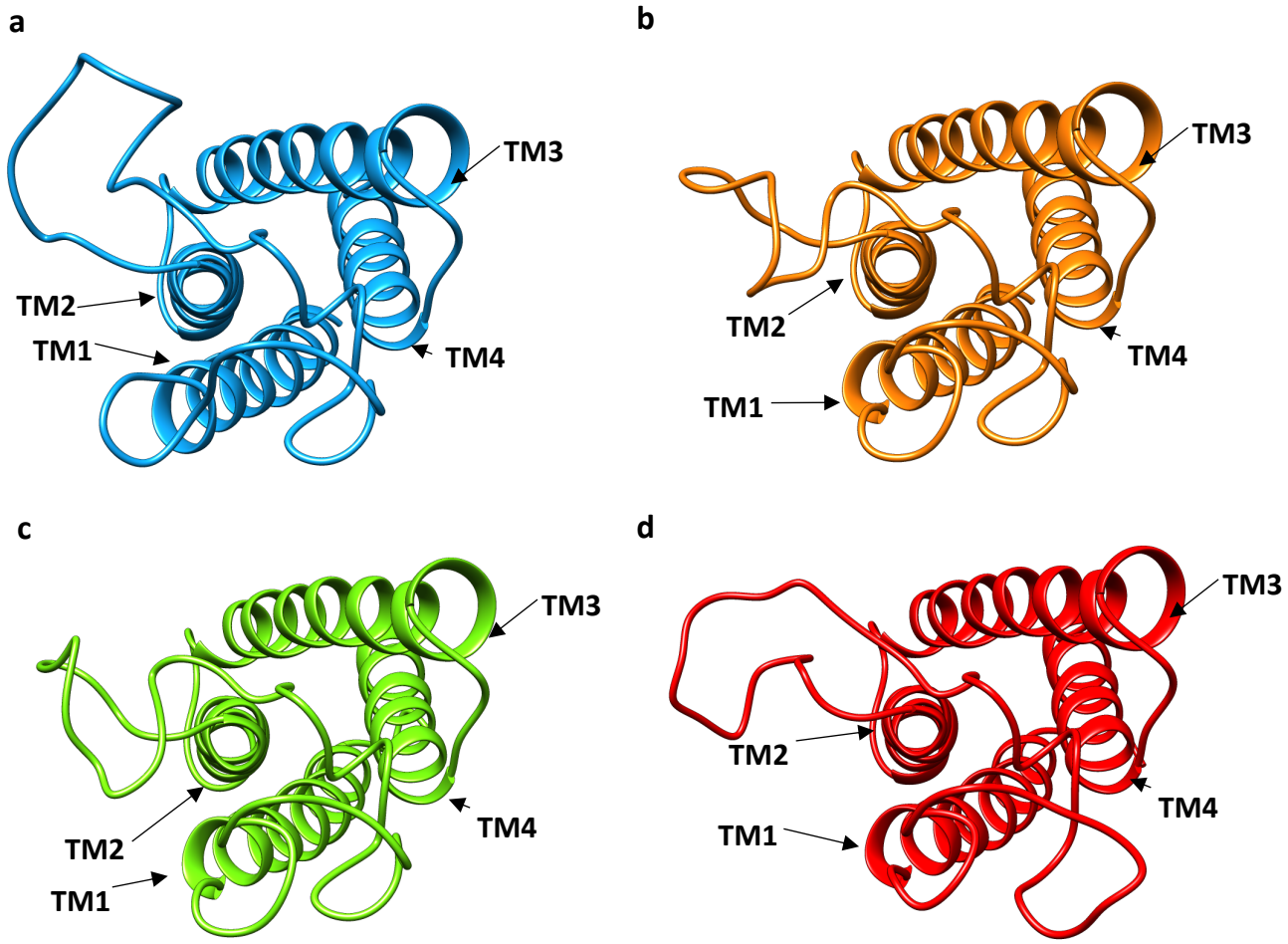


Figure 102: Structural diagrams of rat, human, cow and python VKORC1 from above, based on the VKORC1 structure defined by *Li et al.* (2010). a Brown rat VKORC1. **b** Human VKORC1. **c** Cow VKORC1. **d** Python VKORC1.

4.20 Expression of Recombinant VKORC1 Constructs

Due to high levels of expression, VKORC1 has been expressed using the baculovirus expression system in a number of studies (Li *et al.,* 2004; Chu *et al.,* 2006; Jin *et al.,* 2007; Rishavy *et al.,* 2011). In order to facilitate the characterisation of the effect of anticoagulant rodenticides on the human, rat, cow and python VKORC1, recombinant DNA constructs were generated and expressed in the baculovirus expression system. Brown rat VKORC1-pFB-LIC-Bse, Human VKORC1-pFB-LIC-Bse, python VKORC1-pFB-LIC-Bse and Cow VKORC1-pFB-LIC-Bse constructs were generated following the methods by Savitsky *et al.* (2010) with modifications

stated in Section 2.6. The recombinant rat, human, python and cow VKORC1 constructs were expressed in *Sf9* cells. Example cell micrographs of VKORC1 constructs expressed in *Sf9* cells were shown and described in Section 3.4. After expression of the recombinant VKORC1 constructs in the *Sf9* cells, microsomes were isolated from the suspension culture preparations of infected *Sf9* cells and used in the VKORC1 HPLC assay. HPLC chromatograms are shown for 30 minute incubations with 50 μM vitamin K epoxide for microsomes isolated from the untransfected Sf9 and rat, human, cow and python VKORC1 expressed in *Sf9* cells (Figure 103).

Figure 103 shows that rat, human, cow and python VKORC1 expressed in *Sf9* cells had active VKORC1 protein. The untransfected cells have no background VKORC1 activity due to no detectable vitamin K peak after 30 minutes. Li *et al.* (2004) describe that insect cells have no measurable VKORC1 activity, which is consistent with these results. Unfortunately, the activity of the python VKORC1 was not enough to conduct K_m or IC_{50} results but did show that it expressed successfully. This shows that using multiple sequence alignments to predict substrate binding in reptilian VKORC1 (Section 4.1) is a good prediction model and that python VKORC1 catalyses the same reaction as mammalian VKORC1 enzymes.

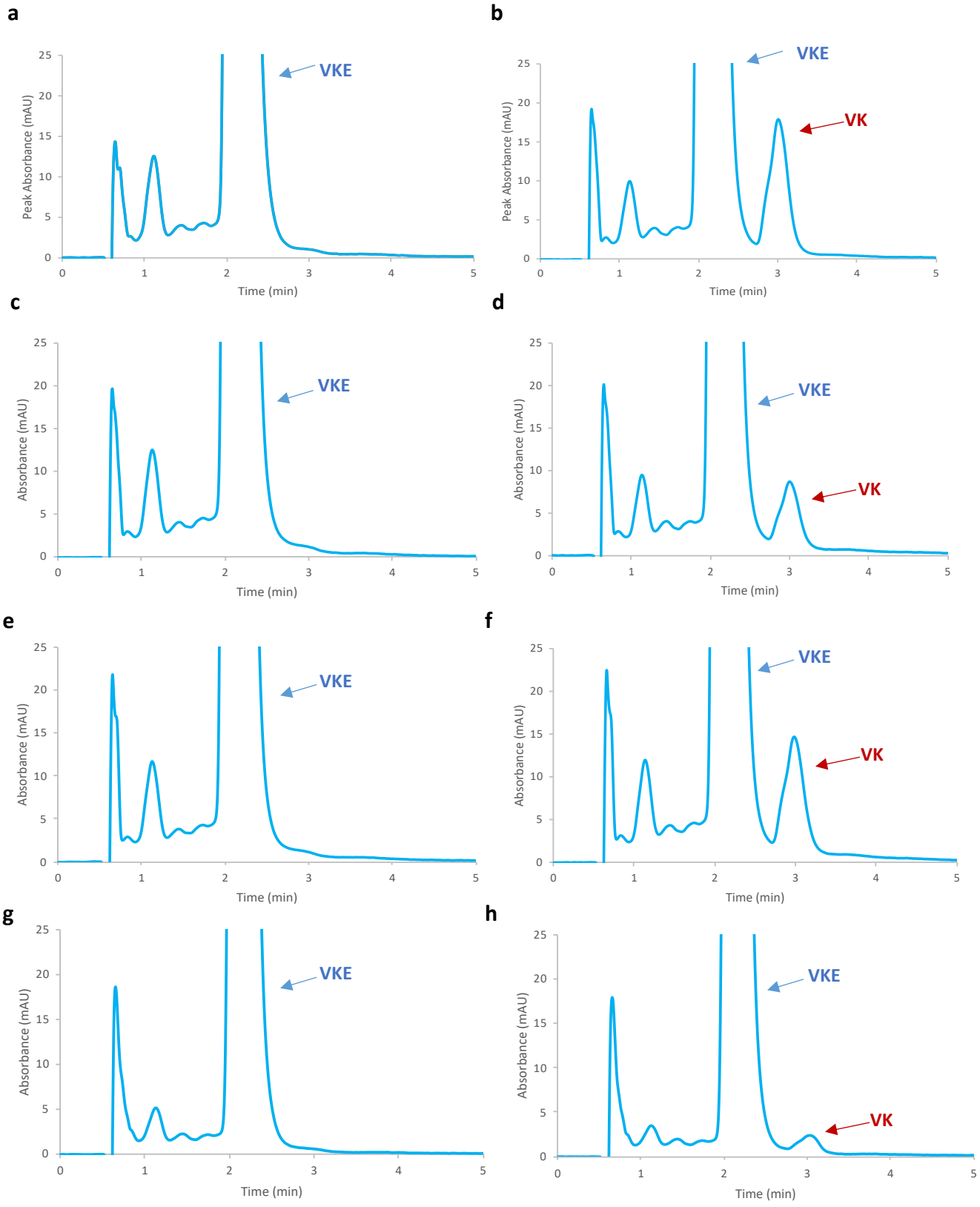


Figure 103: HPLC chromatograms showing the vitamin K production from recombinant rat, human, cow and python VKORC1 expressed in *Sf9* insect cells at 0 and 30 minute incubations at 50 µM VKE. a, c, e and g 0 minute incubations of rat, human cow and python VKORC1 respectively**. b, d, f and h** 30 minute incubations of rat, human cow and python VKORC1 respectively.

4.21 Enzyme Kinetics of Recombinant VKORC1 Constructs

To compare the kinetic properties for rat, human and cow VKORC1, the affinity constant, K_m was determined for vitamin K epoxide substrate using a range of VKE concentrations (Figure 104). The K_m and V_{max} values for rat, human and cow VKORC1 are listed in Table 64.

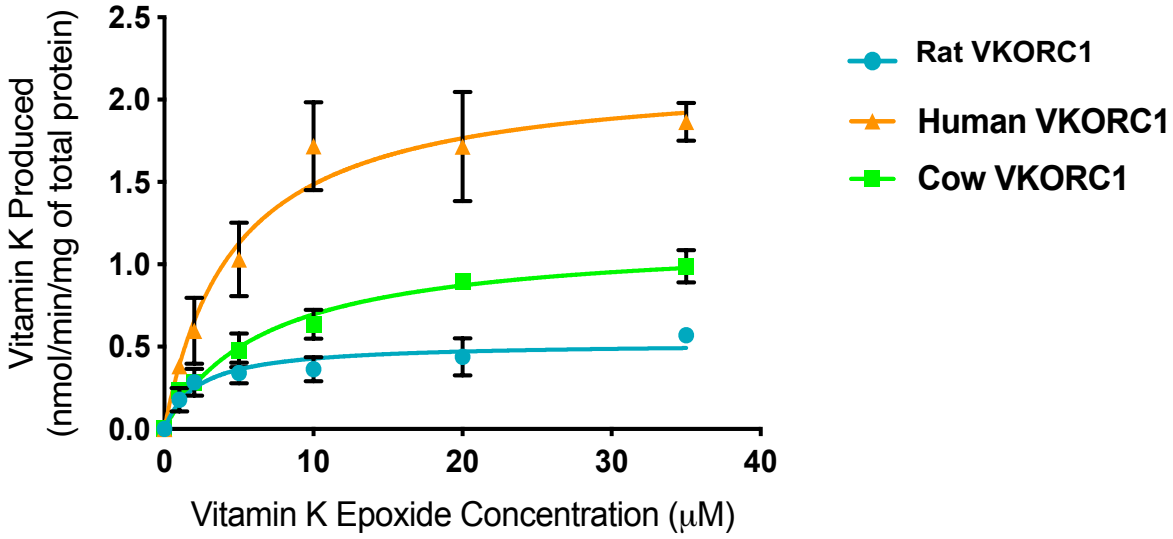


Figure 104: Kinetic analysis of rat, human and cow VKORC1 expressed in *Sf9* cells. Experiments were performed in triplicate and values shown as mean and standard deviation.

	K_m (μM)	V_{max} (nmol min^{-1} mg^{-1})
Rat	2.23 ± 0.67	0.52 ± 0.038
Human	4.65 ± 1.01	2.18 ± 0.14
Cow	6.77 ± 1.09	1.17 ± 0.064

Table 64: K_m and V_{max} values derived from Michaelis-Menten graphs of rat, human and cow VKORC1 expressed in *Sf9* cells. Experiments were performed in triplicate and values shown as mean and standard deviation.

The graphs for all recombinant VKORC1 constructs followed Michaelis-Menten kinetics and followed a rectangular hyperbola shape (Figure 104). There is a difference in affinity for the substrate vitamin K epoxide between the rat, human and cow VKORC1. Rat VKORC1 appears to have a stronger affinity with a K_m of 2.23 ± 0.67 μM, in comparison to both the human VKORC1 (K_m = 4.65 ± 1.01 μM) and cow VKORC1 (K_m = 6.77 ± 1.09 μM). The cow VKORC1 has the highest K_m suggesting a lower affinity with vitamin K epoxide. There is a ~2-fold difference

in Km between the rat and human K_m and a ~3-fold difference between rat and cow K_m. The difference in K_m values between the three species could be due to the differences in amino acid sequences and their interactions with the substrate, vitamin K epoxide. Rat, human and cow VKORC1 have 13, 5 and 4 positions respectively that are different to the other two sequences and 5 positions in which there is a different amino acid found in each of the three VKORC1 sequences (Figure 99). There are 3 amino acid differences, M86, V114 and L118, in the rat VKORC1 sequence that are different from the other species which are close to previously reported amino acids with roles of substrate binding. These differences may account for the lower K_m seen in the rat VKORC1 sequence. The cow VKORC1 sequence has the least number of amino acid differences compared against the human and rat VKORC1 sequences. However, at position 98 the cow VKORC1 sequence contains a glutamine at this position, whereas an arginine is found in both rat and human sequences. In humans if this amino acid position is mutated from an arginine residue to a tryptophan residue it causes vitamin K clotting factor deficiency type 2 (VKCFD2). A study by Rost *et al.* (2005) used site directed mutagenesis to mutate the R98 to amino acids with different properties and tested the VKORC1 activity, of which one was a glutamine residue also found in the cow VKORC1 sequence. They showed that a glutamine residue retained around 50% of the VKORC1 activity compared with the control and concluded that a positive amino acid may be essential for efficient substrate binding or protein folding. Therefore, a change in this position to a glutamine residue may cause inefficient substrate binding and may explain the higher K_m values seen in this study for cow VKORC1. Robinson (2005) states that the same enzyme but in different species can have vast differences in their K_m values. Also, from the 3D structural modelling in Figure 101 the large loop structure is similar in both cow and human which may explain similar K_m values and low affinity compared to the rat VKORC1 which has a different loop structure.

Currently, this is the only study that used VKORC1 expressed in *Sf9* cells to assess the enzyme kinetics. Table 65 compares the K_m values of this study with previously published K_m. Previously published studies used liver microsomes and VKORC1s expressed in mammalian HEK-293 cells and *Pichia pastoris* to assess the enzyme kinetics of VKORC1 (e.g. Wilson *et al.,* 2003; Hammed *et al.,* 2013; Hodroge *et al.,* 2011). Due to the differences in the expression system used and experimental design (e.g. DTT driven assays; FIX-indirect assays) could

account for the differences in the K_m values reported in this study compared to published results. The differences in microsomal membrane composition of the different expression systems could also account for differences seen in K_m values. Interestingly, a study by Wilson *et al.* (2003) determined the K_m values for VKORC1 in different species including rat, human and cow using liver microsomes. The values obtained by Wilson *et al.* (2003) are the closest values for K_m compared to the current study. Results obtained from Hodroge *et al.* (2011) and Hodroge *et al.* (2012) for rat and human VKORC1, respectively, have a 2.75-fold difference between their results for the recombinant human and rat VKORC1 expressed in yeast cells. The results from this study show a consistency with results from both studies by Hodroge and colleagues with a ~2-fold difference between human and rat VKORC1. However, the difference between the Hodroge *et al.* (2011) and Hodroge *et al.* (2012) studies and this study could be due to the difference membrane environment in the different expression systems used. Both studies by Hodroge and colleagues used a *Pichia* expression system (Hodroge *et al.,* 2011; Hodroge *et al.,* 2012). As this study is the first study to determine the enzyme kinetics for recombinantly expressed cow VKORC1 no comparison could be made for the cow enzyme in another expression system.

Table 65 compares the V_{max} values of this study with previously published V_{max} values. Previously published studies used liver microsomes to assess the V_{max} in rat, human and cow VKORC1 (Wilson *et al.,* 2003; Wantanabe *et al.,* 2010). For rat, human and cow VKORC1 are 64, 24 and 54 fold difference respectively between this study compared to the study by Wilson *et al.* (2003). Whereas, the values for V_{max} obtained in this study for rat VKORC1 are consistent with the results obtained by Wantanabe *et al.* (2010).

Species	Expression System	Km (μM)	Vmax (nmol min^{-1} mg^{-1})	Study
Rat	Liver Microsomes	0.60 ± 0.03		Hildebrandt *et al.,* 1984
		57.7 ± 12.5		Lasseur *et al.,* 2005
		8.40 ± 0.90		Hodroge *et al.,* 2011
		4.25 ± 0.40	33.5 ± 1.0	Wilson *et al.,* 2003
		176.1 ± 14.2	0.51 ± 0.0315	Wantanabe *et al.,* 2010
				Louvet *et al.,* 2015
				Gebauer, 2007
	HEK-239 cells	19.6 ± 1.6		Hammed *et al.,* 2013
	Pichia pastoris	15.9 ± 4.5		Goulois *et al.,* 2015
		7.2 ± 2.5		Matagrin *et al.,* 2013
		7.2 ± 2.5		Hodroge *et al.,* 2011
	***Sf9* cells**	**2.23 ± 0.67**	**0.52 ± 0.038**	**Current Study**
Human	Liver Microsomes	8		Wallin and Martin, 1985
		3.09	53.1	Wilson *et al.,* 2003
	HEK-239 cells	21.5 ± 4.2		Hammed *et al.,* 2013
		1.88 ± 0.13		Westhofen *et al.,* 2011
				Czogalla *et al.,* 2018
				Tie *et al.,* 2011
				Tie *et al.,* 2013
				Fregin *et al.,* 2013
				Haque *et al.,* 2014
	Pichia pastoris	1.20		Krettler *et al.,* 2015
				Matagrin *et al.,* 2014
		1.24		Bevans *et al.,* 2013
		19.8		Hodroge *et al.,* 2012
		21.5 ± 4.2		Matagrin *et al.,* 2016
	***Sf9* cells**	**4.65 ± 1.01**	**2.18 ± 0.14**	**Current Study**
Cow	Liver Microsomes	6.46 ± 0.77	64.0 ± 5.9	Wilson *et al.,* 2003
				Louvet *et al.,* 2015
	***Sf9* cells**	**6.77 ± 1.09**	**1.17 ± 0.064**	**Current Study**

Table 65: Comparison of published kinetic VKORC1 data with vitamin K epoxide substrate with the current study.

4.22 Effect of anticoagulant rodenticides on VKORC1

There has been a significant use of different coumarin and indandione anticoagulant rodenticides over a 60 year period due to the increase in anticoagulant resistance seen in rodents and the increase of populations of rodents in general (Section 1.16). With the increase in use of anticoagulants, effects on non-target animals, including humans and the environment have been reported (Health and Safety Executive, 2012). There are many reports of both primary and secondary poisoning in humans, through misuse for example, with the lacing of anticoagulants in illicit drugs and accidental consumption (Spahr *et al.,* 2007). Non-target animals such as farm animals are at a higher risk of non-target poisoning with reports of fatalities due to anticoagulants in cows, sheep and pigs (WIIS, 2009; WIIS, 2010; Dolgormaa, 2004). To determine the toxic effects of anticoagulants in animal species an estimation is made using LD_{50} which uses live animals to establish the concentration at which 50% of the tested population of animals are killed. In order to test and predict the effects of anticoagulant rodenticides on different species without using live animals a cell culture based system was used. In this study using recombinant VKORC1 from rat, human and cow this conforms to the Three R's of animal welfare by replacing the use of live animals (Russel and Burch, 1959).

Dose-response curves were produced for the rat, human and cow VKORC1 for five anticoagulant rodenticides; warfarin, bromadiolone, brodifacoum, difenacoum and flocoumafen (Figure 105) and IC_{50} values were derived from the dose response curves (Table 66). Table 67 shows the statistical values from the 2-way ANOVA for the conditions tested from Figure 105. Figure 105a shows the comparison of rat, human and cow VKORC1 warfarin dose-response curves. The warfarin IC_{50} values for recombinantly expressed rat VKORC1 was 2.55 μM and is consistent with the IC_{50} results obtained by Gebauer (2007) with rat liver microsomes (Table 66). Although the use of liver microsomes gives a good indication of the effect of anticoagulants, recombinant expression has advantages due to the characterisation of one enzyme only. In rat liver microsomes both VKORC1 and VKORC1L1 are found and both enzymes have the ability to convert vitamin K epoxide to vitamin K (Westhofen *et al.,* 2011) and can be subjected to inhibition by anticoagulants (Matagrin *et al.,* 2016).

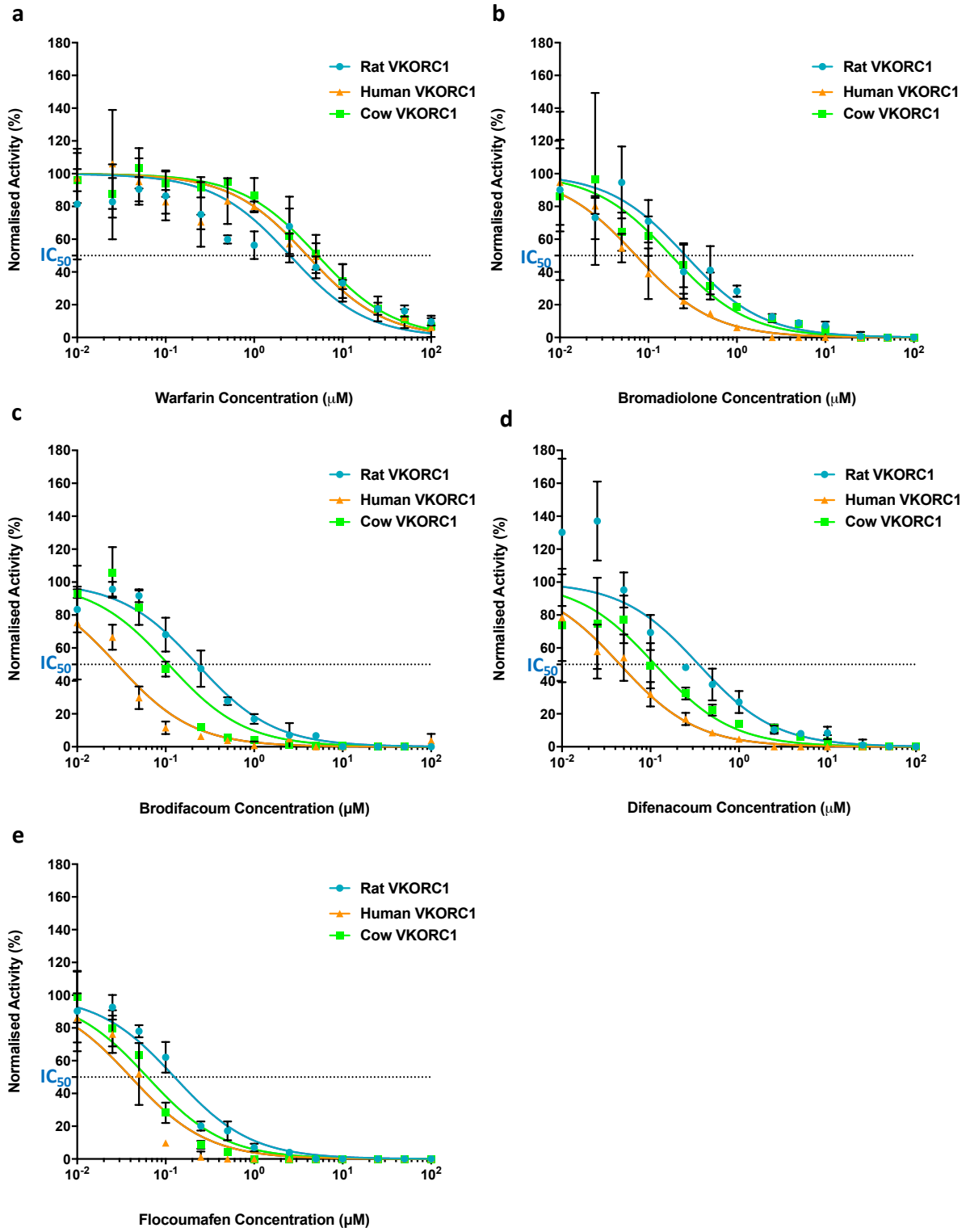


Figure 105: Comparison of anticoagulant dose-response curves for the rat, human and cow VKORC1 expressed in *Sf9* cells. The IC_{50} is represented by the dotted line. Blue denotes rat VKORC1. Orange denotes human VKORC1. Green denotes cow VKORC1. Experiments were performed in triplicate and values shown as mean and standard deviation. **a** Warfarin dose-response curves for rat, human and cow VKORC1. **b** Bromadiolone dose-response curves for rat, human and cow VKORC1. **c** Brodifacoum dose-response curves for rat, human and cow VKORC1. **d** Difenacoum dose-response curves for rat, human and cow VKORC1. **e** Flocoumafen dose-response curves for rat, human and cow VKORC1.

	Warfarin (μM)	Bromadiolone (μM)	Brodifacoum (μM)	Difenacoum (μM)	Flocoumafen (μM)
Rat	2.55 ± 0.11	0.26 ± 0.07	0.23 ± 0.04	0.35 ± 0.11	0.13 ± 0.65
Human	3.98 ± 0.07	0.073 ± 0.04	0.028 ± 0.06	0.045 ± 0.05	0.040 ± 0.06
Cow	5.21 ± 0.05	0.18 ± 0.10	0.11 ± 0.06	0.10 ± 0.07	0.062 ± 0.05

Table 66: IC_{50} values derived from dose-response curves of different anticoagulants for rat, humans and cow VKORC1 expressed in *Sf9* cells. Experiments were performed in triplicate and values shown as mean and standard deviation.

Variable	P value	Significant?
Warfarin:		
Rat VKORC1 vs. Human VKORC1	<0.0001	Yes****
Rat VKORC1 vs. Cow VKORC1	<0.0001	Yes****
Human VKORC1 vs. Cow VKORC1	<0.0001	Yes****
Bromadiolone:		
Rat VKORC1 vs. Human VKORC1	0.9747	No
Rat VKORC1 vs. Cow VKORC1	>0.9999	No
Human VKORC1 vs. Cow VKORC1	>0.9999	No
Brodifacoum:		
Rat VKORC1 vs. Human VKORC1	0.9524	No
Rat VKORC1 vs. Cow VKORC1	0.9998	No
Human VKORC1 vs. Cow VKORC1	>0.9999	No
Difenacoum:		
Rat VKORC1 vs. Human VKORC1	0.5270	No
Rat VKORC1 vs. Cow VKORC1	0.8025	No
Human VKORC1 vs. Cow VKORC1	>0.9999	No
Flocoumafen:		
Rat VKORC1 vs. Human VKORC1	>0.9999	No
Rat VKORC1 vs. Cow VKORC1	>0.9999	No
Human VKORC1 vs. Cow VKORC1	>0.9999	No

Table 67: 2 way ANOVA results showing the P values and significance of each anticoagulant compared to each VKORC1 construct.

Other studies that use recombinantly expressed VKORC1 use K_i values to characterise the effects of anticoagulants on rat VKORC1 instead of IC_{50} values (e.g. Hodroge *et al.,* 2011). The published warfarin IC_{50} results for human VKORC1 have between a 40 and 2000-fold difference depending on the study (Table 68). This could be due to the difference in experimental methods. Czogalla *et al.* (2018) uses an indirect cell culture-based FIX-assay to determine the warfarin dose-response curves for VKORC1. These differences in methods can

have an effect on the results between different studies. Also, different cells were used in the expression systems were used to determine IC_{50} for human VKORC1, in comparison to this study. The warfarin IC_{50} values for recombinantly expressed cow VKORC1 was 5.21 μM. Louvet *et al.* (2015) studied the effects of warfarin on domestic animals, including the cow which reported a K_i of 2.5 μM. Louvet *et al.* (2015) is the only study to produce inhibition data for cow VKORC1 (Table 67).

The hierarchy of sensitivity to anticoagulant rodenticides to rat VKORC1 from most to least is as follows: flocoumafen > brodifacoum > bromadiolone > difenacoum. A study by Damin-Pernik *et al.* (2016) reported K_i values for flocoumafen, brodifacoum, bromadiolone and difenacoum cis- and trans-isomers in rat liver microsomes. This gave the general hierarchy of sensitivity to anticoagulant rodenticides from most to least is as follows: difenacoum > brodifacoum > bromadiolone > flocoumafen. The differences seen in the study by Damin-Pernik *et al.* (2016) and the results shown in Table 69 for this study may be due to the individual testing of the isomers and as in general each current SGAR is a mixture of both isomers. This may affect the affinity of the different anticoagulants to recombinant rat VKORC1. Also, Damin-Pernik *et al.* (2016) used rat liver microsomes which is gives a good indication of the effect of anticoagulants but both VKORC1 and VKORC1L1 are present. However, the difference in membrane composition between *Sf9* cells and rat liver microsomes may contribute the binding of anticoagulants. When comparing the LD_{50} results for the four SGARs for rat (Section 1.6) the results in this study have a similar hierarchy. This is from most to least as follows: flocoumafen > bromadiolone > brodifacoum > difenacoum. With the similar general trend seen between the LD_{50} values and the results from this study this suggests that the *Sf9* recombinant expressed VKORC1 cell culture based system for testing and predicting the effect of anticoagulants rodenticides can be used as a good prediction model.

Species	Expression System	Ki (μM) (Warfarin)	IC50 (μM) (Warfarin)	Study
Brown Rat	Liver Microsomes	0.72 ± 0.06		Lasseur *et al.,* 2005
		0.72 ± 0.01		Hodroge *et al.,* 2011
			0.07 ± 0.01	Wilson *et al.,* 2003
		0.280		Wantanabe *et al.,* 2010
		0.5 ± 0.1		Louvet *et al.,* 2015
			2.2	Gebauer, 2007
	HEK-239 cells	0.6 ± 0.04		Hammed *et al.,* 2013
	Pichia pastoris	0.32 ± 0.07		Goulois *et al.,* 2015
		0.50 ± 0.05		Hodroge *et al.,* 2011
	***Sf9* cells**		**2.55 ± 0.11**	**Current Study**
Human	Liver Microsomes		0.18	Wilson *et al.,* 2003
	HEK-239 cells	1.8 ± 0.2		Hammed *et al.,* 2013
			0.0019	Czogalla *et al.,* 2018
			0.1	Tie *et al.,* 2011
			<0.05	Tie *et al.,* 2013
			0.025	Fregin *et al.,* 2013
			0.125	Haque *et al.,* 2014
	Pichia pastoris	1.65		Matagrin *et al.,* 2014
		2.481		Bevans *et al.,* 2013
		1.65 ± 0.79		Hodroge *et al.,* 2012
		1.65 ± 0.79		Matagrin *et al.,* 2016
	***Sf9* cells**		**3.98 ± 0.07**	**Current Study**
Cow	Liver Microsomes	2.5 ± 0.4		Louvet *et al.,* 2015
	***Sf9* cells**		**5.21 ± 0.05**	**Current Study**

Table 68: Comparison of published warfarin inhibition data for VKORC1 with the data from the current study.

Species	Expression System	Ki (μM) (Bromadiolone)	IC50 (μM) (Bromadiolone)	Ki (μM) (Brodifacoum)	IC50 (μM) (Brodifacoum)	Ki (μM) (Difenacoum)	IC50 (μM) (Difenacoum)	Ki (μM) (Flocoumafen)	IC50 (μM) (Flocoumafen)	Study
Brown Rat	Liver Microsomes	0.031 ± 0.002 (cis) 0.026 ± 0.002 (trans)		0.018 ± 0.002 (cis) 0.022 ± 0.001 (trans)		0.017 ± 0.001 (cis) 0.021 ± 0.002 (trans)		0.047 ± 0.002 (cis) 0.055 ± 0.005 (trans)		Damin-Pernik *et al.*, 2016 Damin-Pernik *et al.*, 2016
	Pichia pastoris	0.07 ± 0.01		0.03 ± 0.01		0.03 ± 0.01				Hodroge *et al.*, 2011
	Sf9		**0.26 ± 0.07**		**0.23 ± 0.04**		**0.35 ± 0.11**		**0.13 ± 0.65**	**Current Study**
Human	HEK-293 cells			0.15		0.12				Matagrin *et al.*, 2016
			0.0016		0.0005					Czogalla *et al.*, 2018
	Sf9		**0.073 ± 0.04**		**0.028 ± 0.06**		**0.045 ± 0.05**		**0.040 ± 0.06**	**Current Study**
Cow	***Sf9***		**0.18 ± 0.10**		**0.11 ± 0.06**		**0.10 ± 0.06**		**0.062 ± 0.05**	**Current Study**

Table 69: Comparison of published second generation anticoagulant rodenticide inhibition data for the current study.

The hierarchy of sensitivity to anticoagulant rodenticides to human VKORC1 from most to least is as follows: brodifacoum > flocoumafen > difenacoum > bromadiolone. The published bromadiolone and brodifacoum IC_{50} results for human VKORC1 have a 50 and 60-fold difference compared to the results obtained in this study (Table 69). However, Czogalla *et al.* (2018) used an indirect cell culture-based FIX-assay to determine the dose-response curves for human VKORC1. The differences in methods can have a large effect on the results between different studies. Also, the expression system used is different and this could contribute to the difference seen between the two studies. Although, there are differences in the values obtained, the trend is the same, human VKORC1 is less sensitive to bromadiolone and more sensitive to brodifacoum. This is the first study to test the effect of inhibition by flocoumafen on human VKORC1 (Table 69). This is also the first study to characterise the effects of second generation anticoagulant rodenticides on cow VKORC1. The hierarchy of sensitivity to anticoagulant rodenticides to cow VKORC1 from most to least is as follows: flocoumafen > difenacoum > brodifacoum > bromadiolone.

The IC_{50} values allows a comparison of anticoagulant sensitivity between different species. Relative anticoagulant sensitivity between the three VKORC1s from most to least is as follows: human > cow > rat. From the results obtained in Figure 105, rat VKORC1 is more sensitive to warfarin than both human and cow VKORC1. Amino acid differences in the human and cow VKORC1 sequences may allow for a weaker affinity for warfarin and natural resistance in comparison to the rat VKORC1. From Table 65, there is a statistical difference between the warfarin IC_{50} values for human and cow. This may be due to the 16 amino acid differences seen between human and cow VKORC1, which causes the cow VKORC1 to be more resistant to warfarin than human VKORC1. However, when subjected to SGARs, the rat VKORC1 is the least sensitive compared to both human and cow. There is a significant difference between rat and human VKORC1 when subjected to bromadiolone, brodifacoum and difenacoum, with the human VKORC1 as the most sensitive. The human and cow VKORC1 have no significant difference when subjected to any second generation anticoagulant rodenticide, suggesting that both enzymes have similar affinity for these anticoagulants.

Chapter 5: General Discussion and Future Work

5.0 About this Chapter

This chapter summarises the findings of this study and also highlight the future work for this project.

The study is a comprehensive analysis of VKORC1 mutation-derived anticoagulant resistance in rat populations in the UK and parts of Sweden. It summarises the geographic spread of previously known and novel, VKORC1 mutations that were experimentally determined from fresh samples of rodent populations and undertakes a phylogeography analysis of these samples.

In addition, extensive sequence alignment studies were undertaken to predict the effect of anticoagulant rodenticides on the VKORC1 proteins of many species (including target species and many non-target animals). An *in vitro* biochemical system was developed to assess the activity of anticoagulant rodenticides on native and mutant VKORC1 proteins and it was shown that this can be used to predict the toxicity of these agents on non-target organisms by recombinant expression of the corresponding VKORC1 protein.

Together, these studies form a way to assess the extent of rodenticide resistance of rat populations in a given geography, to make recommendations of the most effective rodenticides to use for controlling the specific population and also for assessing the possible local environmental impact of rodenticide application use.

5.1 Anticoagulant Resistance in Rattus norvegicus in the UK and Sweden

Rattus norvegicus (brown rats) are amongst the top 15 rodent pests in the world, and have a large impact on agriculture, ecosystems, forestry and public health (Capizzi *et al.,* 2014). To control rodent pests, a variety of pest control measures are used, the most successful of which involves removing the animal, usually by killing it (Tobin and Fall, 2006; Smith and Meyer, 2015). Of all the pest control measures, the most effective and most widely used are

anticoagulant rodenticides. After the introduction of first generation anticoagulant rodenticides (FGARs) in the 1950's, anticoagulant resistance was reported in brown rats in Scotland (Boyle, 1960). In order to overcome the anticoagulant resistance in brown rats, second generation anticoagulant rodenticides (SGARs) were developed (Hadler and Shadbolt, 1975; Dubock and Kaukeinen, 1978; Meehan, 1978; Lechevin and Poche, 1988; Lund, 1988). However, shortly after their introduction, reports emerged of anticoagulant resistance to SGARs (Greaves *et al.,* 1982, Gill *et al.,* 1994). Following the identification of the VKORC1 gene in 2004 (Rost *et al.,* 2004; Li *et al.,* 2004) single nucleotide polymorphisms (SNP) were identified in VKORC1 in brown rats that were shown to be the molecular basis of anticoagulant resistance (e.g. Rost *et al.*, 2004; Pelz *et al.*, 2005).

In the UK, there are eight reported anticoagulant resistant polymorphisms; p.A26T, p.R33P, p.F63C, p.L120Q, p.L128Q, p.Y139C, p.Y139F and p.Y139S (Pelz *et al.*, 2015; Rost *et al.,* 2009; Prescott *et al.,* 2011; Haniza *et al.,* 2015). The UK is the most diverse for anticoagulant resistance polymorphisms in the brown rat. Previous studies on anticoagulant resistance in brown rats in the UK do not, however, highlight the current status of anticoagulant rodenticides due to small sample size and the use of frozen samples collected between 1990-2000 (Pelz *et al.,* 2005; Rost *et al.,* 2009; Haniza *et al.,* 2015). Although in the study by Prescott *et al.* (2011) collected a greater number of samples compared to other studies, all samples were collected from one farm and only representative of one population of brown rats. At present there has been no study of genetic resistance in Swedish rodents.

Therefore, an aim of this study was to identify the current frequency and distribution of VKORC1 resistance polymorphisms in wild *Rattus norvegicus* from UK and Sweden by sequencing the VKORC1 gene. The results showed that there were 69% of anticoagulant resistance polymorphisms found in brown rats in 21 counties in the UK, with four of the previously reported anticoagulant resistance polymorphisms identified; p.L120Q, p.L128Q, p.Y139C and p.Y139S. In Sweden, only 14% of the brown rats tested had anticoagulant resistance polymorphisms with only p.L128Q and p.Y139C polymorphism identified.

With over two thirds of the wild brown rats tested from 21 counties in the UK that contain anticoagulant resistance polymorphisms, this presents potential problems for rodent pest

control. One solution may be to use more 'potent' next generation anticoagulants, however, legislation in Europe states that compounds such as brodifacoum and flocoumafen are not permitted for outdoor use in Europe (Heath and Safety Executive, 2012). Greaves *et al.* (1994) suggested using higher bait concentrations of anticoagulant rodenticides, which may be more effective. However, an issue with increased rodenticide concentrations is the effect of poisoning of non-target animals and the increased amount of toxic compounds released into the environment.

Therefore, other pest control methods may have to be considered in areas with reported resistance. This may include methods such as mechanical trapping, habitat modification, fertility treatments or non-anticoagulant rodenticides. However, there are limitations to these methods. Mechanical trapping can be effective with small rodent populations but less effective with larger infestations (Buckle, 2011). Trapping is not very cost effective in terms of the number of traps required to eliminate a population of rats and also in terms of manual labour as traps will need to be visited daily (Buckle, 2011). Habitat modification could be considered as a measure to reduce rat populations and should be considered as part of rat eradication programmes but modifying certain habitats may have impact on other species (Lambert *et al.,* 2008). Fertility treatments can be effective in lowering the general population of rats over a long period of time but are not very effective for immediate action. Non-anticoagulant rodenticides could be considered; however, these compounds have an immediate effect on the rodents upon consumption of the bait. The sudden onset of symptoms deters rodents from consuming more bait (Hadler and Buckle, 1992). Therefore, pre-baiting with non-toxic bait is required to combat this 'bait shyness', which is very time consuming (Hyngstrom and Virchow, 1992). These compounds have no specificity to pest animals and high doses are required and sub-lethal doses could have long-lasting effects in the animals leading to non-target poisoning (Berny *et al.,* 2014; Hadler and Buckle, 1992).

As part of the current study, a novel VKORC1 p.R40G polymorphism was identified in one UK brown rat sample and in one Swedish brown rat sample. A baculovirus expression system was used to successfully express wild type rat VKORC1 and the p.R40G VKORC1 variant. To test the effect of anticoagulant rodenticides on the wild type rat VKORC1 and the novel p.R40G VKORC1 variant dose-response curves were produced with five anticoagulant rodenticides;

warfarin, bromadiolone, brodifacoum, difenacoum and flocoumafen and IC_{50} values were derived. The novel p.R40G variant was found to be resistant to warfarin but sensitive to the other rodenticides tested, in particular difenacoum. It is interesting to note that the p.R40G polymorphism can generate resistance to one anticoagulant but increased sensitivity to another. This type of effect was also shown in a study by Hodroge *et al.* (2011). Hodroge *et al.* (2011) compared two FGARs, warfarin and chlorophacinone with four SGARs, bromadiolone, difenacoum, brodifacoum and difethialone but depending on the anticoagulant tested against the specific polymorphisms the sensitivity differed (Section 1.16). Therefore, in order to control resistant populations of brown rats it may be necessary to employ polymorphism-specific anticoagulant rodenticide targeting, which may help to eliminate resistant populations and would ensure that rodenticides that are not effective against the local population are used, reducing the risk of secondary poisoning and also reducing the potential environmental impact. This study will enable pest controllers to have an indication of where resistance occurs in the country and which specific polymorphisms occur in a population.

Due to the limitations in all rodent pest control methods discussed, it is more than likely that anticoagulant rodenticides will remain an integral part of pest control but it could be advisable to incorporate a variety of pest control measures as well as polymorphism-specific anticoagulant rodenticide targeting, when dealing with the eradication of a population of rats.

To determine if the p.R40G polymorphism affected the enzyme kinetics of rat VKORC1, the affinity constant, K_m was determined for the vitamin K epoxide substrate for wild type and p.R40G mutant VKORC1. The wild-type rat VKORC1 has a K_m of 2.23 ± 0.67 μM, whereas the p.R40G mutant had a K_m of 5.58 ± 1.36 μM. Studies have shown that brown rats with anticoagulant resistance polymorphisms are inefficient at recycling vitamin K (Matagrin *et al.,* 2013), which can lead to retarded growth (Smith *et al.* 1991) and vascular calcification (Kohn *et al.,* 2008). This can be reflected in this study as there is a 2.5-fold increase of the K_m of the p.R40G VKORC1 variant compared to the wild-type rat VKORC1.

5.2 Mitochondrial D loop analysis and the relationship of anticoagulant resistance polymorphisms.

With regards to the research on the phylogeography of brown rats, studies by Song *et al.* (2014) used mitochondrial DNA sequencing of rats to map mtDNA variants worldwide although no UK rat and only one Swedish rat sample were included. The study also looked at relationships of French and German rodenticide resistance rats and the mtDNA genotypes (Song *et al.,* 2014). The only study that has assessed the geographical population structure of rats in the UK was by Haniza *et al.* (2015) and used a partial mtDNA D-loop sequence of 333 bp to identify haplotypes in populations of *Rattus norvegicus* in the UK. The samples used were frozen tissue samples from the years 1990-2000 from the CSL, York, which does not provide a current population structure for wild brown rats in the UK. In the current study, an aim was to identify mitochondrial D-loop haplotypes in *Rattus norvegicus* from UK and Sweden and assess the relationship between these haplotypes and anticoagulant resistant populations.

The mitochondrial D loop was successfully sequenced in 110 UK and 16 Swedish brown rats. In the UK brown rats, the D1, D5 and D12 haplotypes were the main haplotypes found and 11 novel haplotypes were identified which are exclusive to UK brown rats. In Swedish brown rats, four haplotypes were identified; D1, D5, D6 and D12 with one novel haplotype identified which was exclusive to Swedish brown rats.

The D1 haplotypes found in the UK and Sweden share haplotypes with rat populations in France, Germany, Society Islands and Tubuai Islands (Song *et al.,* 2014). The D5 haplotypes found in the UK and Sweden share haplotypes with rat populations in France, Germany, Sweden, Japan, Egypt and Society Islands (Song *et al.,* 2014). Haplotype sharing amongst rat populations with D1 and D5 haplotypes may have occurred via world trading routes. The D6 haplotype found in Sweden share the haplotype with German rat populations. The D12 haplotype was identified in one sample from Denmark in the study by Song *et al.* (2014). Although it is now known that brown rats originated from Southwest China, the brown rat was mistakenly called the Norway Rat (*Rattus norvegicus*) by John Berkenhout in 1769

(Berkenhout, 1769). It is assumed that Berkenhout named the Norway rat because he believed that the brown rat arrived in England from Norwegian lumber ships. However, it is more likely the brown rats arrived from Denmark as the brown rats had not settled in Norway at that time (Sullivan, 2012). This may be reflected in the results from this study as the D12 haplotype is the most common haplotype in the UK.

The relationship between the mitochondrial D loop haplotypes and anticoagulant rodenticide resistant polymorphisms was assessed and it was found that some anticoagulant resistant polymorphisms appear to be associated with specific haplotypes. >50% of brown rats that contain a p.L128Q polymorphism are found in the D1 haplotype. ~50% of brown rat samples including those associated with the haplotype have a p.L120Q polymorphism associated with the D5 haplotype and ~50% of brown rat samples that are wild type are found associated with the D12 haplotype. The p.Y139S polymorphism is only found within the D1 haplotype. It also can be noted that the p.Y139C polymorphism that Song *et al.* (2014) suggested was associated with the D1 haplotype was not identified within the D1 haplotype in this study but in the D5 and D12 haplotype.

5.3 Prediction of the susceptibility of vertebrate VKORC1s to anticoagulant rodenticides

The increased number of anticoagulant resistance in the UK and around the world has resulted in an increased usage of anticoagulant rodenticides in an attempt to control populations of rodent pests (Vyas, 2017). This has resulted in a high number of reports of poisoning in non-target animals, humans and the environment. In general, exposure to anticoagulant rodenticides can arise due to accidental, intentional or the misuse of rodenticides. Unfortunately, the public have limited knowledge about the toxicity of anticoagulant rodenticides in humans and other species and therefore, misuse anticoagulant rodenticides (Lin *et al.,* 2018). A review of the literature performed in this study revealed that 6805 vertebrate animals were poisoned by anticoagulant rodenticides over >25 years, which included 156 species spanning all vertebrate classes. Of these, 70% are bird species, with 25% of cases that are mammalian species and 5% of animals that belong to the amphibian, reptile and fish classes (Section 1.18 and Appendices 1-4).

In this study, it was an important aim to use multiple sequence alignments as a prediction model for the susceptibility of vertebrate VKORC1s to anticoagulant rodenticides by assessing known human and rat SNP VKORC1 positions. First, amino acid sequences were assessed to determine whether vertebrate VKORC1s had the ability to bind anticoagulants such as warfarin. The results revealed that there was high conservation across the positions assessed, suggesting that all vertebrate VKORC1 proteins have the ability to bind warfarin. Then, amino acids were assessed for the susceptibility to anticoagulant rodenticides by assessing known anticoagulant resistance positions in human and rat VKORC1s. This revealed that in general all vertebrates may have a sensitivity due to the conservation of warfarin sensitive phenotypes found in rat and human VKORC1s. Further analysis revealed that certain animals may contain natural resistance. In general, non-mammalian and non-avian species contained sequence polymorphisms consistent with resistance phenotypes, which may explain why only 5% of reported poisonings were found in these vertebrate classes.

Traditionally, to determine the toxic effects of anticoagulants in animal species an estimation is made using LD_{50} which uses live animals to establish the concentration at which 50% of the tested population of animals are killed (Godfrey, 1986). This method is unethical and not practical. Therefore, to predict the toxicity of anticoagulant rodenticides on different species a cell-culture based system was used, which conforms to the Three R's of animal welfare by replacing the use of live animals (Russel and Burch, 1959). Four representative VKORC1 sequences (*Rattus norvegicus* - brown rat*, Homo sapiens* - human*, Bos taurus* - cow and *Python bivittatus* - python) were chosen for heterologous expression in the baculovirus expression system. All four were successfully expressed and were active when subjected to the VKORC1 HPLC assay. A reptilian VKORC1 sequence has not been recombinantly expressed before this study and was shown to be successful in the production of vitamin K as a result of VKORC1 activity. Unfortunately, due to the low activity produced by the python VKORC1, this construct was not used further in enzyme kinetic and inhibition studies. To test the effect of anticoagulant rodenticides on human, cow and rat VKORC1, dose-response curves were produced with five anticoagulant rodenticides; warfarin, bromadiolone, brodifacoum, difenacoum and flocoumafen and IC_{50} values were derived. From the results, the hierarchy of sensitivity to anticoagulant rodenticides to rat VKORC1 from most to least is as follows:

flocoumafen > brodifacoum > bromadiolone > difenacoum > warfarin. When comparing the LD_{50} results for the five anticoagulant rodenticides for rat (Section 1.6), the results in this study have a similar hierarchy: flocoumafen > bromadiolone > brodifacoum > difenacoum > warfarin. With the similar general trend seen between the LD_{50} values and the results from this study this suggests that the *Sf9* recombinant expressed VKORC1 cell culture based system for testing and predicting the effect of anticoagulants rodenticides can be used as a good prediction model. Therefore, the results showed that the hierarchy in human VKORC1 which from most to least is as follows: brodifacoum > flocoumafen > difenacoum > bromadiolone > warfarin. The hierarchy of sensitivity to anticoagulant rodenticides to cow VKORC1 from most to least is as follows: flocoumafen > difenacoum > brodifacoum > bromadiolone > warfarin.

Comparisons of the relative sensitivity to warfarin between the three VKORC1s from most to least is as follows: rat > human > cow. From the results in this study, it shows that cow VKORC1 is more resistant to warfarin than human or rat VKORC1, as the cow had a warfarin IC_{50} value of 5.21 μM compared the human and rat VKORC1 which had IC_{50} values of 3.98 μM and 2.55 μM, respectively based on 2-way ANOVA results ($P<0.0001$) (Table 67). The difference between cow and rat VKORC1 is reflected in the study by Louvet *et al.* (2015) which shows that the cow has the higher K_i value at 2.3 μM compared to the rat which has a K_i value of 0.5 μM (Section 1, Figure 20). Differences seen in the inhibition characteristics may be due to differences in the conserved loop structure within cow and rat VKORC1 (Figure 101 and 102), which may cause the differences in the affinity for warfarin. There are 3 amino acid differences found in the conserved loop structure, with another 23 amino acid differences within the whole protein, which may cause the differences seen in the sensitivity for warfarin. The IC_{50} data in this study reflects the LD_{50} data for the cow and rat that show the same relationship. Papworth (1958) reported a natural resistance to warfarin in cows compared to the rat (McGirr and Papworth, 1953; Papworth, 1958) and estimated the warfarin LD_{50} value of 200 mg/kg for the cow and 1 mg/kg for the rat. Clearly the 2-fold IC_{50} difference cannot account for the 200-fold estimated LD_{50} difference. However, Papworth suggest that this resistance could be due to the ruminant type of digestion in cattle (Papworth, 1958). In general, a 15 day treatment of two rats with a body weight of 250 g would require 1.5 kg of made up bait (Health and Safety Executive, 2011). Taking into account the body weight of the

cow, it is improbable that accidental consumption of warfarin would be fatal. For example, a calf weighing approximately 159 kg would require 32 g of warfarin per day, meaning 640 kg of made-up bait would need to be consumed (Papworth, 1958). The maximum amount of bait for use for rats should not exceed 1.5 kg (Health and Safety Executive, 2011). However, Crowell *et al.* (2013) showed that anticoagulants such as diphacinone have hepatic persistence for over 100 days after given a single dose of 1.5 mg/kg and suggest that diphacinone is metabolised and distributed differently within the cow. This could have implications for secondary poisoning of humans in the food production industry if there is accidental exposure of anticoagulant rodenticides to cattle.

As well as the first generation rodenticide warfarin, the relative sensitivity to the second generation anticoagulant rodenticides (bromadiolone, brodifacoum, difenacoum and flocoumafen) were also tested, to compare the human, rat and cow VKORC1s. The hierarchy of sensitivity for all second generation anticoagulant rodenticides tested between the three VKORC1s from most to least is as follows: human > cow > rat, indicating that although the compounds were developed as potent rodenticides, the rat is the least sensitive species tested. This may help to explain the high number of non-target species reported with primary and secondary poisoning due to second generation anticoagulant rodenticides (Section 1.18).

As seen with the anticoagulant rodenticide polymorphisms discussed in Section 5.1, different anticoagulant rodenticides have a different toxicity on different species VKORC1, suggesting that anticoagulant rodenticides have different potencies depending on the animals VKORC1. This may be due to the differences in VKORC1 protein sequence. It also suggests that a change to the VKORC1 sequence may have an effect in the binding of anticoagulants but also in substrate binding. This can be reflected in the K_m values determined in this study for human, rat and cow VKORC1. Rat VKORC1 has a K_m value of 2.23 ± 0.67 μM, in comparison to both the human VKORC1 (K_m = 4.65 ± 1.01 μM) and cow VKORC1 (K_m = 6.77 ± 1.09 μM). These differences may be due to the small size of VKORC1 with ~163 aa (Rost *et al.,* 2004) and any change is more likely to have an effect. It can be noted that over a third of the amino acids in VKORC1 have been associated with the 3D structure, substrate binding, warfarin binding, and anticoagulant resistance in humans and rat VKORC1. For example, between human, rat and cow VKORC1 there is 81% sequence identity and the K_m and inhibition results show

differences between these species. Also, by looking at the sequences between human, rat and cow VKORC1 it is possible to have an indication of additional positions that may be important in substrate and anticoagulant binding due to the differences seen experimentally. For example, there are 3 amino acid differences, M86, V114 and L118, in the rat VKORC1 sequence that are different from the other species which are close to previously reported amino acids with roles of substrate binding. These differences may account for the lower K_m seen in the rat VKORC1 sequence. This study provides an ethical method to test the toxicity of anticoagulant rodenticides on non-target organisms.

5.4 Computational Analysis of VKORC1 and VKORC1L1 to assess the structural, functional and evolutionary relationships

The general overall phylogeny of the VKOR family of enzymes has been well characterized in terms of phylogenetic trees and relationships of VKORs (Rost *et al.,* 2004; Goodstadt and Ponting, 2004; Robertson, 2004; Wan *et al.,* 2014; Bevans *et al.,* 2015; Lacombe and Ferron, 2018). With respect to amino acid sequence comparisons these studies have however only used a relatively small number of vertebrate VKORC1 and VKORC1L1 sequences to assess the structural, functional and evolutionary relationships between VKORs in different species and between the two enzymes. In this study multiple sequence alignments were used to determine the structural, functional and evolutionary relationships between the 135 vertebrate VKORC1 sequences and 164 VKORC1L1 sequences by assessing known positions in human and rat VKORC1. The results revealed that vertebrate VKORs have the ability to bind vitamin K and vitamin K epoxide due to the high conservation at the known amino acids for substrate binding. The structural relationship between representative VKORC1 and VKORC1L1s was assessed using membrane topology prediction and 3D modelling. The predicted membrane topology suggests that vertebrate VKOR sequences range between 2 to 4 TM domains. In general, there appears to be a change from 4 TM domains to 3 TM throughout vertebrate VKORC1 evolution. There is also a difference in orientation with non-mammalian VKORC1 predictions showing the N and C terminus on the same side of the protein consistent with the 4 TM model described by Schulman *et al.* (2010) and Cao *et al.* (2016). In vertebrate VKORC1L1, the number of TM domains predicted and the orientation of

each species model is different but supports the findings of Tie *et al.* (2014) which suggested that their model supports an even number of TM domains for VKORC1L1. Assessing the 3D structures showed that the large loop structure for all the vertebrate VKOR models show a difference suggesting that the binding of substrates or antagonists such as anticoagulants may have a different effect on the enzymes.

By using conservation as a tool to assess functional constraint, it was found that there are 35 amino acid positions that are 100% conserved throughout all 164 vertebrate VKORC1 sequences. Of these, 9 amino acid positions are previously unidentified. Assessment of the vertebrate VKORC1L1 sequences 71 amino acid positions are 100% conserved throughout all 135 vertebrate VKORC1L1 sequences with 51 positions previously unidentified. Analysis by Lacombe and Ferron (2018) suggest that VKORC1 is freer to diverge compared to its paralog VKORC1L1, these results are therefore consistent with these researchers results. The conservation between vertebrate VKORC1 and VKORC1L1 sequences were also assessed and it was found that there are 24 conserved positions throughout all 299 vertebrate VKOR enzymes with 6 previously unidentified. This suggests a potential importance in all vertebrate VKORs which have remained integral to the structure and function of both enzymes throughout their evolution.

5.4 Future Work

i. Although this study provides the current status of the frequency and distribution of anticoagulant resistant polymorphisms, there are still areas that are uncharacterised. In order for pest controllers to employ alternative methods or specific anticoagulants it would be beneficial to undertake DNA sequencing of VKORC1 in wild brown rats in these uncharacterised areas. This will provide a further understanding of the full extent of anticoagulant resistance in the UK and Sweden.

ii. This study identified the mitochondrial D-loop haplotypes in wild *Rattus norvegicus* from UK and Sweden. However, there are other mitochondrial DNA markers to assess population structure. Song *et al.* (2014) used cytochrome b as well as the D-loop to

assess the phylogeography of brown rats. Currently, there is no study that identifies the cytochrome b haplotypes in UK brown rats. Therefore, it would be of interest to use DNA sequencing to determine the cytochrome b haplotypes of the UK and Swedish wild brown rat populations.

iii. This study provides a cell-culture based method to test the toxicity of anticoagulant rodenticides on non-target species without the necessity of using live animals. It would be beneficial to use this method to test other non-target animals to assess the potential toxicity of anticoagulant rodenticides. For example, domestic and wild mammals and birds would be the key organisms that should be tested in this system due to the high number of reports of fatalities in these species due to anticoagulant rodenticides.

iv. This study used multiple sequence alignments to predict the structural, functional and evolutionary relationships. It would be of interest to test the predictions determined in this study *in vitro* using the cell culture based system. For example, to express a bird, amphibian and fish VKORC1 as well as one VKORC1L1 from each vertebrate class.

v. This study also predicted areas of conservation within vertebrate VKOR protein sequences that are evolutionarily constrained. Currently, these newly identified conserved positions have a proposed role but it would be interesting to use site directed mutagenesis to alter these positions to reveal if these specific amino acids have essential function in vertebrate VKORs.

References

Adam, R. D. (1991) 'The biology of Giardia spp'. *Microbiology Review,* 55,(40), pp. 706-732.

Agnarsson, I., Zambrana-Torrelio, C. M., Flores-Saldana, N. P. and May-Collado, L. J. (2011) 'A time-calibrated species-level phylogeny of bats (Chiroptera, Mammalia)'. *PLOS Currents,* 3: RRN1212.

Aguilar, P.V., Greene, I.P., Coffey, L.L., Medina, G., Moncayo, A.C., Anishchenko, M., Ludwig, G.V., Turell, M.J., O'Guinn, M.L., Lee, J., Tesh, R.B., Watts, D.M., Russell, K.L., Hice, C., yanoviak, S., Morrison, A.C., Klein, T.A., Dohm, D.J., guzman, H., Travassos de Rosa, A.P.A., Guevara, C., Kochel, T., Olson, J., cabezas, C. and Weaver, S.C. (2004) 'Endemic Venezuelan Equine Encephalitis in Northern Peru'. *Emerging Infectious Diseases,* 10, (5), pp.880-888.

Albert, C. A., Wilson, L. K., Mineau, P., Trudeau, S. and Elliott, J. E. (2010) 'Anticoagulant rodenticides in three owl species from Western Canada, 1988-2003'. *Archives of Environmental Contamination and Toxicology,* 58, (2), pp.451-459.

Almeida, A., Corrigan, R. and Sarno, R. (2013) 'The Economic Impact of Commensal Rodents on Small Businesses in Manhattan's Chinatown: trends and possible causes'. *Suburban Sustainability,* 1, (1), pp.1-15.

Anton, A. L. Cerzo-Manchado, J. J., Padilla, J., Perez-Andreu, V., Corral, J., Vincente, V., Roldan, V. and Gonzalez-Conejero, R. (2013) 'Novel associations of VKORC1 variants with higher acenocoumarol requirements'. *PLOS:ONE, 8:e64469.*

Babcock, J., Hartman, K., Pedersen, A., Murphy, M. and Alving, B. (1993) 'Rodenticide-induced coagulopathy in a young child. A case of Munchausen syndrome by proxy'. Journal of Pediatric Hematology/ Oncology, 15, (1), pp.68-70.

Baert, K., Stuyck, J., Breyne, P., Maes, D. and Casaer, L. (2012) 'Distribution of anticoagulant resistance in the brown rat in Belgium'. *Belgium Journal of Zoology,* 142, (1) pp.39-48.

Basset, D., Girou, C., Nozais, I. P., D'Hermies, F., Hoang, C., Gordon, R. and D'Alessandro, A. (1998) 'Neotropical echinococcosis in Suriname: *Echinococcus oligarthrus* in the orbit and *Echinococcus vogeli* in the abdomen'. *American Journal of Tropical Medicine Hygiene,* 59, (5), pp.787-790.

Basra, G., Berman, M.A., and Blanton, L.S. (2012) 'Murine typhus: An important consideration for the nonspecific febrile illness'. *Case Reports in Medicine,* 2012: 134601.

Bell, R. G. and Matschiner, J. (1972) 'Warfarin and the inhibition of vitamin K activity by an oxide metabolite'. *Nature,* 237, pp.32-33.

Bell, R. G., Sadowski, J. A. and Matschiner, J. T. (1972) 'Mechanism of action of warfarin. Warfarin and metabolism of vitamin K1'. *Biochemistry,* 11, (10), pp.1959-1961.

Bentley, E. W. (1972) 'A review of anticoagulant rodenticides in current use'. *Bulletin of the World Health Organisation,* 47, (3), pp.275-280.

Berkenhout, J. (1769) *Outlines of the natural history of Great Britain and Ireland, containing a systematic arrangement and concise description of all the animals, vegetables and fossils which have hitherto been discovered in these kingdoms.* London: Oxford University.

Berny, P., Esther, A., Jacob, J., and Prescott, C. (2014) *Risk mitigation measures for anticoagulant rodenticides as biocidal products.* Luxembourg: European Union.

Berny, P. J., Buronfosse, T., Buronfosse, F., Lamarque, F. and Lorgue, G. (1997) 'Field evidence of secondary poisoning of foxes (*Vulpes vulpes*) and buzzards (*Buteo buteo*) by bromadiolone, a 4 year survey', *Chemosphere,* 35, (8), pp.1817-1829.

Betancur -R, R., Broughton, R. E., Wiley, E. O., Carpenter, K., López, J. A., Li, C., Holcroft, N. I., Arcila, D., Sanciangco, M., Cureton II, J. C., Zhang, F., Buser, T., Campbell, M. A., Ballesteros, J. A., Roa-Varon, A., Willis, S., Borden, W. C., Rowley, T., Reneau, P. C., Hough, D. J., Lu, G., Grande, T., Arratia, G. and Ortí, G. (2013) 'The Tree of Life and a New Classification of Bony Fishes'. *PLOS Currents,* 18, (5).

Bettink, K. (2015) *Control and eradication of Black rats (Rattus rattus) on Penguin Island, Western Australia, December 2012 - December 2014.* Perth: Western Australia.

Bevans, C.G., Krettler, C., Reinhart, C., Watzka, M. and Oldenburg, J. (2015) 'Phylogeny of the vitamin K 2,3-epoxide reductase (VKOR) family and evolutionary relationship to the Disulfide Bond Formation Protein B (DsbB) family'. *Nutrients,* 7, (8), pp.6224-6249.

Bharti, A. R., Nally, J. E., Ricaldi, J. N., Matthias, M. A., Diaz, M. M., Lovett, M. A., Levett, P. N., Gilman, R. H., Willig M. R., Gotuzzo, E. and Vinetz, J. M. (2003) 'Leptospirosis: a zoonotic disease of global importance'. *The Lancet Infectious Diseases,* 3, (12), pp.757-771.

Blus, L. J., Henny, C. J. and Grove, R. A. (1985) 'Effects of pelletised anticoagulant rodenticides on California quail'. *Journals of Wildlife Diseases,* 21, (4), pp.391-395. Available at: http://dx.doi.org/10.7589/0090-3558-21.4.391 [Accessed: 16 November 2019].

Bodin, L., Perdu, J., Diry, M., Horellou, M. H. and Loriot, M. A. (2008) 'Multiple genetic alterations in vitamin K epoxide reductase complex subunit 1 gene (VKORC1) can explain the high dose requirements during oral anticoagulant in humans'. *Journal of Thrombosis and Haemostasis,* 6, (8), pp.1436-1439.

Boettcher, S., Wacker, A., Moerike, K., Kopp, H. G., Jaschonek, K., Grobosch, T., Kanz, L. and Salih, H.R. (2011) 'Acquired coagulopathy caused by intoxication with the superwarfarin-type anticoagulant rodenticide flocoumafen'. *European Journal of Haematology,* 86, (2), pp.173-175.

Boyle, M. (1960) 'A case of apparent resistance of *Rattus norvegicus* (Berkenhout) to anticoagulant poisons'. *Nature,* 188, p.519.

Breitschwerdt, E. B. and Kordick, D. L. (2000) 'Bartonella infection in animals: carriership, reservoir potential, pathogenicity and zoonotic potential for human infection', *Clinical microbiological Review,* 13, (3), pp.428-438.

Brown, K. P. (1997) 'Impact of brodifacoum poisoning operations on South Islands robins *Petroica australis australis* in a New Zealand *Nothofagus* forest'. *Bird Conservation International,* 7, (4), pp.399-407.

Brown, T. A. (2007) *Genomes 3.* Oxford: Garland Science Publishing.

Buckle, A. (2011) 'Anticoagulant resistance in the United Kingdom and a new guideline for the management of resistance infestations of Norway rats (*Rattus norvegicus* Berk)' *Pest Management Science,* 69, (3), pp. 334-341.

Bull, J. O. (1976) 'Laboratory and field investigations with difenacoum, a promising new rodenticides'. *Proceedings of the 7th Vertebrate Pest Conference,* 5.

Buscaglia, C. A. and Di Noia, J. M. (2003) '*Trypanosoma cruzi* clonal diversity and the epidemiology of Chagas' disease'. *Microbes and Infection,* 5, (5), pp.419-427.

Campbell, H. A. and Link, K. P. (1941) 'Studies on the hemorrhagic sweet clover disease: IV. The isolation and crystallization of the hemorrhagic agent', *Journal of Biological Chemistry,* 138, pp.21-33.

Campbell, H. A., Roberts, W. L., Smith, W. K. and Link, K. P. (1940) 'Studies on the hemorrhagic sweet clover disease: I. The preparation of hemorrhagic concentrates'. *Journal of Biological Chemistry,* 136, pp.47-55.

Cao, Z., van Lith, M., Mitchel, L. J., Pringle, M. A., Inaba, K. and Bulleid, N. J. (2016) 'The membrane topology of vitamin K epoxide reductase is conserved between human isoforms and the bacterial enzyme'. *Biochemical Journal,* 473, (7), pp.851-858.

Capizzi, D., Bertolino, S. and Mortelliti, A. (2014) 'Rating the rat: global patterns and research priorities in impacts and management of rodent pests'. *Mammal Review,* 44, (2), pp.148-162.

Carleton, M. D. and Musser, G. G. (2005) *Order Rodentia. In:* Wilson D.E. and Reeder, D.M. eds. *Mammalian species of the world: a taxonomic and geographic reference.* Baltimore: John Hopkins University Press.

Carlisle, T. L. and Suttie, J. W. (1980) 'Vitamin K dependent carboxylase: subcellular location of the carboxylase and enzymes involved in vitamin K metabolism in rat liver'. *Biochemistry,* 19, (6), pp.1161-1167.

Chen, X., Jin, D. Y. Stafford, D. W. and Tie, J. K (2018) 'Evaluation of oral anticoagulants with vitamin K epoxide reductase in its native milieu'. *Blood,* 132, (18), pp.1974-1984.

Childs, J. E., Glass, G. E., Korch, G. W., Ksiazek, T. G. and Leduc, J. W. (1992) 'Lymphocytic Choriomeningitis Virus Infection and House Mouse (*Mus Musculus*) Distribution in Urban Baltimore'. *American Journal of Tropical Medicine and Hygiene,* 47, (1), pp.27-34.

Childs, J. E., Glass, G. E., Ksiazek, T. G., Rossi, C. A., Oro, J. G. and Leduc J. W. (1991) 'Human-Rodent Contact and Infection with Lymphocytic Choriomeningitis and Seoul Viruses in an Inner-City Population', *American Journal of Tropical Medicine and Hygiene,* 44, (2), pp.117-121.

Christensen, T., Lassen, P. and Elmeros, M. (2012) 'High exposure rates of anticoagulant rodenticides in predatory bird species in intensively managed in Denmark'. *Archives of Environmental Contamination and Toxicology,* 63, pp.437-444.

Chu, P. H., Huang, T. Y., Williams, J., and Stafford, D. W. (2006) 'Purified vitamin K epoxide reductase alone is sufficient for conversion of vitamin K epoxide to vitamin K and vitamin K to vitamin KH2'. *PNAS*, 103, (51), pp.19308-19313.

Chua, J. D. and Friedenberg, W. R. (1998) 'Superwarfarin poisoning'. *Archives of Internal Medicine*, 158, (17), pp.1929-1932.

Comer, J. A. Diaz, T., Vlahov, D., Monterroso, E. and Childs, J. E. (2001) 'Evidence of rodent-associated Bartonella and Rickettsia infections among intravenous drug users from Central and East Harlem, New York City'. *American Journal of Tropical Medicine Hygiene,* 65, (6), pp.855-860.

Comer, J. A., Paddock, C. D. and Childs, J. E. (2001) 'Urban zoonoses caused by Bartonella, Coxiella, Ehrlichia and Rickettsia Species'. *Vector Borne and Zoonotic Diseases,* 1, (2), pp.91-118.

Contreras-Gómez, A., Sánchez-Mirón, A., García-Camacho, F., Molina-Grima, E. and Chisti, Y. (2014) 'Protein production using the baculovirus-insect cell expression system'. *Biotechnology Progress,* 30, (1), pp.1-18.

Cowan, P. E., Gleeson, D. M., Howitt, R. L. J., Ramón-Laca, A., Esther, A. and Pelz, H. J. (2016) 'Vkorc1 sequencing suggests anticoagulant resistance in rats in New Zealand'. *Pest Management Science,* 73, (1), pp.262-266.

Crowell, M., Eason, C., Hix, S., Broome, K., Fairweather, A., Moltchanova, E., Ross, J. and Murphy, E. (2013) 'First generation anticoagulant rodenticide persistence in large mammals and implications for wildlife management'. *New Zealand Journal of Zoology,* 40 (3), pp.205-216.

Cwiklinski, K., O'Neill, S.M., Donnelly, S. and Dalton, J.P. (2016) 'A prospective view of animal and human Fasciolosis'. *Parasite Immunology,* 38, (9), pp.558-568.

Czogalla, K.J., Biswas, A., Höning, K., Hornung, V., Liphardt, K., Watzka, M. and Oldenburg, J. (2017) 'Warfarin and vitamin K compete for binding to Phe55 in human VKOR'. *Nature Structural and Molecular Biology,* 24, (1) pp.77-85.

Czogalla, K. J., Biswas, A., Rost, S., Watzka, M. and Oldenburg, J. (2014) 'The Arg98Trp mutation in human VKOC1 causing VKCFD2 disrupts a di-arginine-based ER retention motif'. *Blood,* 124, (8), pp.1354-1362.

Czogalla, K. J., Biswas, A., Wendeln, A. C., Westhofen, P., Miiller, C. R., Watzka, M. and Oldenburg, J. (2013) 'Human VKORC1 mutations cause variable degrees of 4-hydroxycoumarin resistance and affect putative warfarin binding interfaces'. *Blood,* 122, (15), pp.2743-2750.

Czogalla, K.J., Liphardt, K., Höning, K., Horning, V., Biswas, A., Watzka, M. and Oldenburg, J. (2018) 'VKORC1 and VKORC1L1 have distinctly different oral anticoagulant dose-response characteristics and binding sites', *Blood Advances,* 2, (6), pp.691-702.

D'Alessio, M., Wang, T., Swift, C. E., Shanmungam, M.S. and Ray, C. (2018) 'A Tier-I leaching risk assessment of three anticoagulant compounds in the forested areas of Hawaii', *Science of the Total Environment*, 630, pp.889-902.

D'Ambrosio, R. L., D'Andrea, G., Cafolla, A., Faillace, F. and Margaglione, M. (2007) 'A new vitamin K epoxide reductase complex subunit-1 (VKORC1) mutation in a patient with decreased stability of CYP2C9'. *Journal of Thrombosis and Haemostasis,* 5, pp.191-193.

Dam, H. (1935) 'The antihaemorrhagic vitamin of the chick'. *Biochemical Journal,* 29, (6) pp.1273-1285.

Dam, H. and Schønheyder, F. (1934) 'A deficiency disease in chicks resembling scurvy'. *Biochemical Journal,* 28, (4) pp.1355-1359.

Damin,-Pernik, M., Espana, B., Lefebvre, S., Fourel, I., Caruel, H., Benoit, E. and Lattard, V. (2016) 'Management of rodent populations by anticoagulant rodenticides: Towards third-generation anticoagulant rodenticides'. *Drug Metabolism Disposition,* 45, (2), pp.160-165.

Daugelaite, J., O'Driscoll, A. and Sleator, R. D. (2013) 'An Overview of Multiple Sequence Alignments and Cloud Computing Bioinformatics'. *ISRN Biomathematics,* 2013, pp.337 – 348.

Dehhaghi, M., Panahi, H. K. S., Holmes, E. C., Hudson, B. J., Schloeffel, R. and Guillemin, G.J. (2019) 'Human Tick-borne disease in Australia'. *Frontiers in Cellular and Infection Microbiology*, 9 (3).

Demma, L. J., McQuiston, J. H., Nicholson, W. L., Murphy, S.M., Marumoto, P., Sengebaul-Kingzio, J. M., Kuartei, S., Durand, A. M. and Swerdlow, D. L. (2006) 'Scrub typhus, Republic of Palau'. *Emerging Infectious Diseases,* 12 (2), pp.290-295.

Dennis, G. C. and Gartell, B. D. (2015) 'Non-Target Mortality of New Zealand Lesser Short-Tailed Bats (*Mystacina tuberculata)* Caused by Diphacinone'. *Journal of Wildlife Diseases,* 51, (1), pp.177-186.

Despommier, D. (2003) 'Toxcariasis: Clinical aspects, epidemiology, medical ecology and molecular aspects'. *Clinical Microbiology Reviews,* 16, (2), pp.265-272.

Díaz, J.C., Song, Y., Moore, A., Borchert, J.N. and Kohn, M.H. (2010) 'Analysis of vkorc1 polymorphisms in Norway rats using the roof rat as outgroup'. *BMC Genetics,* 11, (43), pp.1-11.

Dodsworth, E. (1961) 'Mice are spreading despite poisons such as warfarin'. *Municipal Engineering London,* 3746, 1668.

Doisy, E.A., Birkley, S.B., Thayer, S.A. and McKee, R.W. (1940) 'Vitamin K'. *Science*, 91, (2351) pp.58-62.

Dolbeer, R. A., Holler, N. R., and Hawthorne, D. W. (1994) 'Identification and Assessment of Wildlife Damage: an Overview', *The Handbook: Prevention and Control of Wildlife Damage,* 2.

Dolgormaa, L. (2004) 'Toxic issues in Mongolia'. *World Wildlife Fund,* p.6.

Dowding, C. V., Shore, R. F., Worgan, A., Baker. P. J. and Stephen Harris (2010) 'Accumulation of anticoagulant rodenticides in a non-target insectivore, the European hedgehog (*Erinaceus europaeus*)'. *Environmental Pollution,* 158, (1), pp.161-166.

Dowding, J. E., Lovegrove, T. G., Ritchie, J., Kast, S. N. and Puckett, M. (2006) 'Mortality of northern New Zealand dotterels (*Charadrius obscurus aquilonius)* following an aerial poisoning operation'. *Notornis*, 53, pp.235-239.

Dowding, J. E., Murphy, E. C. and Veitch, C. R. (1999) 'Brodifacoum residues in target and non-target species following an aerial poisoning operation on Motuihe Island, Hauraki Gulf, New Zealand'. *New Zealand Journal of Ecology,* 23, (2), pp.207-214.

Drummond, D. C. and Wilson, E. J. (1968) 'Laboratory investigations of resistance to warfarin of *Rattus norvegicus Berk.* in Montgomeryshire and Shropshire', Association of Applied Biologists*,* 61, pp.303-312.

Dubock, A. C. and Kaukeinen, D. E. (1978) 'Brodifacoum (TALON^{TM} Rodenticide), a novel concept', *Proceedings of the 8th Vertebrate Pest Conference*. 16.

Dworkin, M.S., Schwan, T.G., Anderson, D.E. and Borchardt, S.M. (2008) 'Tick-Borne Relapsing Fever'. *Infectious Disease Clinics of North America,* 22, (3).

Ebbert, S. and Burek-Huntingon, K. (2010) 'Anticoagulant Residual Concentration and Poisoning in Birds Following a Large-Scale Aerial Application of 25 ppm Brodifacoum Bait for Rat Eradication on Rat Island, Alaska'. *Proceedings of the Vertebrate Pest Conference,* 24, (24), pp.153-160.

Elliot, S.P. (2007) 'Rat bite fever and *Streptobacillus moniliformis*'. *Clinical Microbiology Reviews,* 20, (1), pp.13-22.

Elliot, J.E., Hindmarch, S., Albert, C.A., Emery, J., Mineau, P. and Maisonneuve, F. (2014) 'Exposure pathways of anticoagulant rodenticides to nontarget wildlife'. *Environmental Monitoring and Assessment.* 186, (2), pp.895-906.

Elmeros, M., Christensen, T. K. and Lassen, P. (2011) 'Concentrations of anticoagulant rodenticides in stoats *Mustela erminea* and weasels, *Mustela nivalis* from Denmark'. *Science of the Total Environment,* 409, (12), pp.2373–2378.

Elston, D. M. (2005) 'Rickettsial skin disease: uncommon presentations'. *Clinics in Dermatology,* 23, (6), pp.541-544.

Empson, R. A. and Miskelly, C. M. (1999) 'The risks, costs and benefits of using brodifacoum to eradicate rats from Kapiti Islands, New Zealand'. *New Zealand Journals of Ecology,* 23, (2), pp.241-254.

Enserink, M. (2000) 'Emerging Diseases: New Arenavirus Blamed for Recent Deaths in California'. *Science,* 289, (5481), pp.842-843.

Erickson, W. and Urban, D. (2004) *Potential risks of nine rodenticides to birds and non-target mammals: a comparative approach.* Washington DC: United States Environmental Protection Agency.

Esmon, C.T., Sadowski, J.A and Suttie, J.W. (1975) 'A new carboxylation reaction. The vitamin K-dependent incorporation of $H^{14}CO_3^-$ into prothrombin'. *Journal of Biological Chemistry,* 250, (12) pp.4744-4748.

Feng, A. Y. T. and Himsworth, C. G. (2014) 'The secret life of the city rat: a review of the ecology of urban Norway and black rats (*Rattus norvegicus and Rattus rattus)'. Urban Ecosystems,* 17, (1), pp.149–162.

Fernandes, B. J., Cooper, J. D., Cullen, J. B., Freeman, R. S., Ritchie, A. C., Scott, A. A. and Stuart, P. F. (1976) 'Systemic infection with Alaria americana (Trematoda)'. *Canadian Medical Association Journal,* 115, (11), pp.1111-1114.

Fisher, P., Griffiths, R., Speedy, C. and Broom, K. (2011) *Environmental monitoring for brodifacoum residues after aerial application of baits for rodent eradication.* In: Veitch, C. R., Clout, M. N. and Towns, D. R. (Eds.), Island Invasives: Eradication and Management. IUCN, Gland, Switzerland, pp.300-304.

Fomenko, D. E. and Gladyshev, V. N. (2003) 'Identity and functions of CxxC-derived motifs'. *Biochemistry,* 42, pp.11214-11225.

Forbes, A. E., Zochowski, W. J., Dubrey, S. W. and Sivaprkasam, V. (2012) 'Leptospirosis and Weil's disease in the UK'. *An International Journal of Medicine,* 105, (12), pp.1151 – 1162.

Fourhier-Chambrilion, C., Berny, P. J., Coiffier, O., Barbedienne, P., Dassé, B., Delas, G., Galineau, H., Mazet, A., Pouzenc, P., Rosoux, R. and Fournier, P. (2004) 'Evidence of secondary poisoning for free-ranging riparian mustelids by anticoagulant rodenticides in France: Implications for conservation of European mink (*Mustela lutreola*)'. *Journal of Wildlife Diseases,* 40, (4), pp.688-695.

Franklin, A. B., Carlson, P. C., Rex, A., Rockweit, J. T., Garza, D., Culhane, E., Volker, S. F., Dusek, R. J., Shearn-Bochsler, V. I., Gabriel, M. W. and Horak, K. E. (2018) 'Grass is not always greener: rodenticide exposure of a threatened species near marijuana growing operations'. *BMC Research Notes*, 11, (94), pp.1-7.

Fregin, A., Czogalla, K.J., Gansler, J., Rost, S., Taverna, M., Watzka, M., Bevans, C.G., Müller, C.R. and Oldenburg, J. (2013) 'A new cell culture-based assay quantifies vitamin K 2,3-epoxide reductase complex subunit 1 function and reveals warfarin resistance phenotypes not shown by the dithiothreitol-driven VKOR assay'. *Journal of Thrombosis and Haemostasis,* 11, (5), pp.872-880.

Fregin, A., Rost, S., Wolz, W., Krebsova, A., Müller, C.R. and Oldenburg, J. (2002) 'Homozygosity mapping of a second gene locus for hereditary combined deficiency of vitamin K-dependent clotting factors to the centromeric region of chromosome 16'. *Blood*, 100, (9), pp.3229-3232.

Friedl, A., Heinzer, I. and Fankhauser, H. (2005) 'Tularemia after a dormouse bite in Switzerland'. *European Journal of Clinical Microbiology & Infectious Diseases,* 24, (5), pp.352-354.

Fritz, C. L. and Glaser, C. A. (1998) 'Ehrlichiosis'. *Infectious Disease Clinics of North America,* 12, (1), pp.123-136.

Gavin, P. J., Kazacos, K. R. and Shulman, S. T. (2005) 'Baylisascariasis'. *Clinical Microbiology Review,* 18, (4), pp.703-718.

Ge, D., Wen, Z., Xia, L., Zhang, Z., Erbajeva, M., Huang, C. and Yang, Q. (2013) 'Evolutionary History of Lagomorphs in Response to Global Environmental Change'. *PLOS:ONE,* 8, (4), pp.1-15.

Gebauer, M. (2007) 'Synthesis and structure – activity relationships of novel warfarin derivatives'. *Bio-organic and Medicinal Chemistry,* 15, (6), pp.2414-2420.

Gehlawat, P., Gehlawat, V.K., Singh, P. and Gupta, R. (2015) 'Munchausen syndrome by proxy: an alarming face of child abuse'. *Indian Journal of Psychological Medicine,* 37, (1), pp.90-92.

Gill, J. E., Kerins, G. M., Langton, S. D. and MacNicoll, A. D. (1994) 'Blood-clotting response test for bromadiolone resistance in Norway Rats'. *Journal of Wildlife Management,* 58, (3), pp.454 – 461.

Gillespie, J. J., Ammerman, N. C., Beier-Sexton, M., Sobral, B.S. and Azad, A. F. (2008) 'Louse- and flea-borne rickettsioses: biological and genomic analyses'. *Vetinary Research,* 40 (2).

Godfrey, M.E.R. (1986) 'An evaluation of the acute oral toxicity of brodifacoum to birds'. *Proceedings of the Twelfth Vertebrate Pest Conference,* 27.

Gómez-Canela, C., Barata, C. and Lacorte, S. (2014) 'Occurrence, elimination and risk of anticoagulant rodenticides and drugs during wastewater treatment'. *Environmental Science and Pollution Research,* 21, pp.7194-7203.

Goodstadt, L. and Ponting, C.P. (2004) 'Vitamin K epoxide reductase: homology, active site and catalytic mechanism'. *Trends in Biochemical Sciences,* 29, (6) pp.289-292.

Goulois, J., Chapuzet, A., Lambert, V., Chatron, N., Tchertanov, L., Legros, L., Benoît E. and Lattard, V. (2016) 'Evidence of a target resistance to antivitamin K rodenticides in the roof rat *Rattus rattus*: identification and characterisation of a novel Y25F mutation in the Vkorc1 gene'. *Pest Management Science,* 72, (3) pp.544-550.

Grandemange, A., Lasseur, R., Longin-Sauvageon, C., Benoit, E. and Berny, P. (2010) 'Distribution of VKORC1 single nucleotide polymorphisms in wild *Rattus norvegicus* in France'. *Pest Management Science,* 66, (3), pp.270-276.

Greaves, J. H. and Ayres, P. (1969) 'Linkages between genes for coat colour and resistance to warfarin in *Rattus norvegicus*'. *Nature,* 244, (5216), pp.284-285.

Greaves, J. H. and Ayres, P. (1973) 'Warfarin resistance and vitamin K requirement in the rat'. *Laboratory Animals,* 7, pp.141-148.

Greaves, J. H. and Rennison, B. D. (1973) 'Population aspects of warfarin resistance in the brown rat, *Rattus norvegicus*'. *Mammals Reviews*, 3, (2), pp.27-29.

Greaves, J. H., Shepherd, D. S. and Quy, R. (1982) 'Field trials of second-generation anticoagulants against difenacoum – resistant Norway rat populations'. *Journal of Hygiene,* 89, (2), pp.295-301.

Gruber, K. (2016) 'Rodent meat- a sustainable way to feed the world?'. *EMBO reports,* 17, (5), pp.630-633.

Gryseels, S., Leirs, H., Makundi, R. and Goüy de Bellocq, J. (2015) 'Polymorphism in the vkorc1 gene of Natal Multimammate Mice, *Mastomys natalensis*, in Tanzania'. *Journal of Heredity,* 106, (5), pp.637-643.

Guitart, R., Croubels, S., Caloni, F., Sachana, M., Davanzo, F., Vandenbroucke, V. and Berny, P. (2010) 'Animal poisoning in Europe. Part 1: from livestock and poultry'. *Veterinary Journal,* 183, (3), pp.249-254.

Hadler, M.R. and Buckle, A.P. (1992) 'Forty five years of anticoagulant rodenticides – past, present and future trends'. *Proceedings of the Fifteenth Vertebrate Pest Conference,* 36.

Hadler, M.R. and Shadbolt, R.S. (1975) 'Novel 4-hydroxycoumarin anticoagulants active against resistant rats'. *Nature,* 253, pp.275-277.

Hagen, E.C. and Radomski, J.L. (1953) 'The toxicity of 3-(acetonylbenzyl)-4-hydroxy-coumarin (warfarin) to laboratory animals'. *Journal of American Pharmacological Association,* 42, pp.379-382.

Halonen, S.K. and Weiss, L.M. (2013) 'Toxoplasmosis'. *Handbook of Clinical Neurology,* 114, pp.125-145.

Hammed, A., Matagrin, B., Spohn, G., Prouillac, C., Benoit, E and Lattard, V. (2013) 'VKORC1L1, an enzyme rescuing the vitamin K 2, 3-epoxide reductase activity in some extrahepatic tissues during anticoagulation therapy'. *Journal of Biological Chemistry,* 288, (40) pp.28733-28743.

Haniza, M. Z. H., Adams, S., Jones, E. P., MacNicoll, A., Mallon E. B., Smith, R. H. and Lambert, M. S. (2015) 'Large-scale structure of brown rat (*Rattus norvegicus*) populations in England: Effects on rodenticide resistance'. *Journal of Life and Environmental Sciences,* 3:e1458.

Harrington, D. J., Siddiq, S., Allford, S. L., Shearer, M. J. and Mumford, A. D. (2011) 'More on: endoplasmic reticulum loop VKORC1 substitutions cause warfarin resistance but do not diminish gamma-carboxylation of the vitamin K-dependent coagulation factors'. *Journal of Thrombosis and Haemostasis,* 9, (5), pp.109-118.

Hatahet, F., Blazyk, J.L., Martineau, E., Mandela, E., Zhao, Y., Campbell, R.E., Beckwith, J. and Boyd, D. (2015) 'Altered *Escherichia coli* membrane protein assembly machinery allows proper membrane assembly of eukaryotic protein vitamin K epoxide reductase'. *PNAS,* 112, (49) pp.15182-15189.

Haussler, D., O'Brien, S. J., Ryder, O. A., Barker, F. K., Clamp, M., Crawford, A. J., Hanner, R., Hanotte, O., Johnson, W. E., McGuire, J. A., Miller, W., Murphy, R. W., Murphy, W. J., Sheldon, F. H., Sinervo, B., Venkatesh, B., Wiley, E. O., Allendorf, F. W., Amato, G., Baker, C. S., Bauer, A., Beja-Pereira, A., Bermingham, E., Bernardi, G., Bonvicino, C. R., Brenner, S., Burke, T., Cracraft, J., Diekhans, M., Edwards, S., Ericson, P. G., Estes, J., Fjelsda, J., Flesness, N., Gamble, T., Gaubert, P., Graphodatsky, A. S., Marshall Graves, J. A., Green, E. D., Green, R. E.,

Hackett, S., Hebert, P., Helgen, K. M., Joseph, L., Kessing, B., Kingsley, D. M., Lewin, H. A., Luikart, G., Martelli, P., Moreira, M. A., Nguyen, N., Ortí, G., Pike, B. L., Rawson, D. M., Schuster, S. C., Seuánez, H. N., Shaffer, H. B., Springer, M. S., Stuart, J. M., Sumner, J., Teeling, E., Vrijenhoek, R. C., Ward, R. D., Warren, W. C., Wayne, R., Williams, T. M., Wolfe, N. D. and Zhang, Y. P. (2009) 'Genome 10K: a proposal to obtain whole-genome sequence for 10,000 vertebrate species'. *Journal of Heredity,* 100, (6), pp. 659-674.

He, K., Shinohara, A., Helgen, K. M., Springer, M. S., Jiang, X. L. and Campbell K. L. (2017) 'Talpid Mole Phylogeny Unites Shrew Moles and Illuminates Overlooked Cryptic Species Diversity'. *Molecular Biology and Evolution,* 34, (1), pp.78-87.

Health and Safety Executive (2011) *Human health risk mitigation measures for anticoagulant rodenticide baits. Draft proposals for BPR product authorization in the UK.* [online] Available at: https://www.hse.gov.uk/Biocides/eu-bpr/human-health-risk-mitigation.pdf. [Accessed 8 March 2019].

Health and Safety Executive (2012) *Consideration of the environmental risk from the use of brodifacoum, flocoumafen, difethialone, difenacoum and bromadiolone.* [online] Available at: www.hse.gov.uk/biocides/downloads/er-sgar.pdf. [Accessed 8 March 2019].

Helgeland, L. (1980) 'The action of vitamin K and coumarin anticoagulants'. *Biochemical Education,* 8, pp.66-69.

Hepburn, N. C. (2000) 'Cutaneous leishmaniasis.' *Clinical and Experimental Dermatology,* 25, (5), pp.363-370.

Hernandez-Moreno, D., de la Casa-Resino, A., Lopez-Beceiro, A., Fidalgo, L.E., Soler, F. and Perez-Lopez, M. (2013) 'Secondary poisoning of non-target animals in an Ornithological Zoo in Galicia (NW Spain) with anticoagulant rodenticides: a case report'. *Veterinarni Medicina,* 58, (10), pp.553-559.

Heymann, W. R. (1996) 'Rickettsialpox', *Clinics in Dermatology,* 14, (3), pp.279-282.

Hildebrandt, E. F., Preusch, P. C., Patterson, J. L. and Suttie, J. W. (1984) 'Solubilization and characterization of vitamin K epoxide reductase from normal and warfarin resistant rat liver microsomes'. *Archives of Biochemistry and Biophysics,* 228, (2), pp.480-492.

Hillier, L., Miller, W., Birney, E., Warren, W., Hardison, R. C., Ponting, C. P., Bork, P., Burt, D. W., Groenen, M. A. M., Delany, M. E. and Dodgson, J. B. (2004) 'Sequence and comparative analysis of the chicken genome provide unique perspective on vertebrate evolution', *Nature,* 432, pp.695-716.

Hodroge, A., Longin-Sauvageon, C., Fourel, I., Benoit, E. and Lattard, V. (2011) 'Biochemical characterization of spontaneous mutants of rat VKORC1 involved in the resistance to antivitamin K anticoagulants'. *Archives of Biochemistry and Biophysics*, 515, pp.14-20.

Hodroge, A., Matagrin, B., Moreau, C., Fourel, I., Hammed, A., Benoit, E. and Lattard, V. (2012) 'VKORC1 mutations detected in patients resistant to vitamin K antagonists are not all associated with a resistant VKOR activity'. *Journal of Thrombosis and Haemostasis,* 10, (12), pp.2535-2543.

Hoffman, S. L. (1980) 'Plague in the United States: the "Black Death" is still alive'. *Annals of Emergency Medicine,* 9, (6), pp.319-322.

Howald, G., Donlan, C. J., Faulkner, K. R., Ortega, S., Gellerman, H., Croll, D. A. and Tershy, B. R. (2009) 'Eradication of black rats *Rattus rattus* from Anacapa Island', *Oryx,* 44, (1), pp.30-40. Available at: https://training.fws.gov/resources/course-resources/pesticides/IPM/Howaldetal2010_Oryx.pdf [Accessed: 11 November 2019].

Howald, G., Donlan, C.J., Galván, J.P., Russel, J.C., Parkes, J., Samaniego, A., Wang, Y., Veitch, D., Genovesi, P., Pascal, M., Saunders, A. and Tershy, B. (2007) 'Invasive rodent eradication on islands'. *Conversation Biology,* 21, (5), pp.1258-1268.

Howald, G.R., Mineau, P., Elliott, J.E. and Cheng, K.M. (1999) 'Brodifacoum poisoning of avian scavengers during rat control on a seabird colony'. *Ecotoxicology,* 8, pp.431-447.

Huang, B.H., Feng, Z.Y., Yue, L.F., Yao, D.D., Gao, Z.H., Wang, D.W. and Lui, X.H. (2011) 'Warfarin resistance test and polymorphism screening in the VKORC1 gene in *Rattus flavipectus*'. *Journal of Pest Science,* 84, (1), pp.87-92.

Huebner, C.F., Karjala, S.A., Sullivan, W.R. and Link, K.P. (1944) 'Studies on 4-hydroxycoumarins. VI. Glucosides of 4-hydroxycoumarins'. *Journal of the American Chemical Society,* 66, (6), pp.906-909.

Huebner, C.F., Sullivan, W.R., Stahmann, M.A. and Link, K.P. (1943) 'Studies on 4-hydroxycoumarins. III. Dehydration of the aldehyde condensation products'. *Journal of the American Chemical Society,* 65, (12) pp.2292-2296.

Hughes, L. C., Ortí, G., Huang, Y., Sun, Y., Baldwin, C. C., Thompson, A. W., Arcila, D., Betancur-R, R., Li, C., Becker, L., Bellora, N., Zhao, Z., Li, X., Wang, M., Fang, C., Xie, B., Zhou, Z., Huang, H., Chen, S., Venkatesh, B. and Shi, Q. (2018) 'Comprehensive phylogeny of ray-finned fishes (*Actinopterygii)* based on transcriptomic and genomic data'. *PNAS,* 115, (24), pp.6249-6254.

Hygnstrom, S.E. and Virchow, D.R. (1992) 'G92-1106 Controlling rats'. *Historical Materials from University of Nebraska – Lincoln Extension,* 1512.

Iacucci, A., Colangelo, P., Gamberi, V., Mori, E., Capizzi, D, Baert, K., Esther, A., Leirs, H., Petit, T., Ribas Salvador, A., Aloise, G., Annesi, F. and Castiglia, R. (2018) 'VKORC1 mutation in European populations of *Rattus norvegicus* with first data for Italy and the report of a new amino acid substitution'. *Italian Journal of Mammalogy,* 29, (1) pp. 95-99.

Ikawa, M., Stahmann, M.A. and Link, K.P. (1944) 'Studies on 4-hydroxycoumarins. V. The condensation of α,β-unsaturated ketones with 4-hydroxycoumarins'. *Journal of the American Chemical Society,* 66, (6) pp.902-906.

Iralu, J., Bai, Y., Crook, L., Tempest, B., Simpson, G., McKenzie, T. and Foster, K. (2006) 'Rodent-associated Bartonella febrile illness, Southwestern United States'. *Emerging Infectious Diseases Journal,* 12, (7), pp.1081-1086.

Ishizuka, M., Okajima, F., Tanikawa, T., Min, H., Tanaka, K.D., Sakamoto, K.Q. and Fujita, S. (2007) 'Elevated warfarin metabolism in warfarin-resistant roof rats (*Rattus rattus*) in Tokyo'. *Drug Metabolism and Disposition,* 35, (1), pp.62-66.

Ishizuka, M., Tanikawa, T., Tanaka, K.D., Heewon, M., Okajima, F., Sakamoto, K.Q. and Fujita, S. (2008) 'Pesticide resistance in wild mammals – mechanisms of anticoagulant resistance in wild rodents'. *Journal of Toxicological Sciences,* 33, (3), pp.283-291.

Jackson, M.R., Nilsson, T. and Peterson, P.A. (1990) 'Identification of a consensus motif for retention of transmembrane proteins in the endoplasmic reticulum'. *The EMBO Journal,* 9, (10), pp.3153-3162.

Jaenecke, F., Friedrich-Epler, B., Parthier, C. and Stubbs, M.T. (2015) 'Membrane composition influences the activity of *in vitro* refolded human vitamin K epoxide reductase'. *Biochemistry,* 54, pp.6454-6461.

Jin, C., Qin, D., Pan, W., Wang, W., Zhang, Y, Deng, C. and Zheng, J. (2008) 'Micromammals of the gigantopithecus fauna from Sahne Cave, Chongzuo, Guangxi'. *Quaternary Sciences,* 28, pp.1129-1137.

Jin, D. Y., Tie, J. K. and Stafford, D. W. (2007) 'The conversion of vitamin K epoxide to vitamin K quinone and vitamin K quinone to vitamin K hydroquinone uses the same active site cysteines'. *Biochemistry,* 46, pp.7279-7283.

King, N. and Tran, M. (2015) 'Long-acting anticoagulant rodenticide (superwarfarin) poisoning: a review of its historical development, epidemiology and clinical management'. *Transfusion Medicine Reviews,* 29, (4), pp.250-258.

Kinnunen, P. M., Palva, A., Vaheri, A. and Vapalahti, O. (2013) 'Epidemiology and host spectrum of Borna disease virus infections'. *Journal of General Virology,* 94, pp.247-262.

Kohn, M. H. and Pelz, H. J. (1999) 'Genomic assignment of the warfarin resistance locus, *Rw*, in the rat'. *Mammalian Genome,* 10, (7), pp.696-698.

Kohn, M.H. and Pelz, H.J. (2000) 'A gene-anchored map position of the rat warfarin-resistance locus, *Rw*, and its orthologs in mice and humans'. *Blood,* 96, (5), pp.1996-1998.

Kohn, M.H., Price, R.E. and Pelz, H.J. (2008) 'A cardiovascular phenotype in warfarin-resistant Vkorc1 mutant rats'. *Artery Research,* 2, (4), pp.138-147.

Koivisto, E., Santangeli, A., Koivisto, P., Korkolainen, T., Vuorisalo, T., Hanski, I.K., Loivamaa, I., and Koivisto, S. (2018) 'The prevalence and correlates of anticoagulant rodenticide exposure in non-target predators and scavengers in Finland'. *Science of the Total Environment,* 642, pp.701-707.

Krettler, C., Bevans, C.G., Reinhart, C., Watzka, M. and Oldenburg, J. (2015) 'Tris(3-hydroxypropyl)phosphine is superior to dithiothreitol for *in vitro* assessment of vitamin K 2,3-epoxide reductase activity'. *Analytical Biochemistry,* 474, pp.89-94.

Kumar, S. and Hedges, S. B. (1998) 'A molecular timescale for vertebrate evolution'. *Nature,* 392, pp.917–920.

La Rosa, F.G., Clarke, S.H. and Lefkowitz, J.B. (1997) 'Brodifacoum intoxication with marijuana smoking'. *Archives of Pathology and Laboratory Medicine,* 121, (1), pp.67-69.

Laakso, S., Suomalainen, K., and Koivisto, S. (2010) *Literature review on resides of anticoagulant rodenticides in non-target animals.* Copenhagen: Nordic Council of Ministers.

Lacombe, J. and Ferron, M. (2018) 'VKORC1L1, an enzyme mediating the effects of vitamin K in liver and extra hepatic tissues'. *Nutrients,* 10, (8), e:970.

Ladoukakis, E.D. and Zouros, E. (2017) 'Evolution and inheritance of animal mitochondrial DNA: rules and exceptions'. *Journal of Biological Research,* 24, (2).

Lambert, M. S., Quy, R. J., Smith, R. H. and Cowan, D. P. (2008) 'The effect of habitat management on home-range size and survival of rural Norway rat populations'. *Journal of Applied Ecology,* 45, (6), pp.1753-1761.

Lambert, O., Pouliquen, H., Larhantec, M., Thorin, C. and L'Hostis, M. (2007) 'Exposure of raptors and waterbirds to anticoagulant rodenticides (difenacoum, bromadiolone, coumatetralyl, coumafen, brodifacoum): Epidemiological survey in Loire Atlantique (France)', *Bulletin of Environmental Contamination and Toxicology,* 79, (1), pp.91-94.

Langford, K. H., Reid, M. and Thomas, V. K. (2013) 'The occurrence of second generation anticoagulant rodenticides in non-target raptor species in Norway', *Science of Total Environment,* 450 – 451, pp.205-208.

Lasseur, R., Grandemange, A., Longin-Sauvageon, C., Berny, P. and Benoit, E. (2006) 'Heterogeneity of the coumarin anticoagulant targeted vitamin K epoxide system. Study of the kinetic parameters in susceptible and resistant mice (*Mus musculas domesticus*)'. *Journal of Biochemical and Molecular Toxicology,* 20, (5), pp.221-229.

Lasseur, R., Longin-sauvageon, C., Videmann, B., Billeret, M., Berny, P. and Benoit, E. (2005) 'Warfarin Resistance in a French strain of rats'. *Journal of Biological and Molecular Toxicology,* 19, (6), pp.379-385.

Lechevin, J.C. and Poché, R.M. (1988) 'Activity of LM 2219 (Difethialone), a new anticoagulant rodenticide, in commensal rodents'. *Proceedings of the Thirteenth Vertebrate Pest Conference.* 13.

Lefebvre, S., Fourel, I., Queffélec, S., Vodovar, D., Mégarbane, B., Benoit, E., Siguret, V. and Lattard, V. (2017) *Poisoning by anticoagulant rodenticides in humans and animals: Causes and consequences*. *In:* Malangu, N. *Poisoning: From specific toxic agents to novel rapid and simplified techniques for analysis.* IntechOpen. Available at: http://www.interopen.com/books/poisoning-from-specific-toxic-agents-to-a-novel-rapid-and-simplified-techniques-for-analysis/poisoning-by-humans-causes-and-consequences. [Accessed at: 8 March 2019].

Leirs, H. (2003) *Management of rodents in crops: The pied piper and his orchestra.* In: Singleton, G. R., Hinds, L. A., Krebs, C. J. and Spratt, D. M. (Eds). *Rats, mice and people: Rodent biology and management.* Canberra, Australia. ACIAR. pp. 183-190.

Leitch, G.J. and He, Q. (2011) 'Cryptosporidiosis-an overview'. *Journal of Biomedical Research,* 25, (1), pp.1-16.

Levin, H., Nichols, W. L., Massung, R. F., Sumner, J. W. and Fish, D. (2002) 'Comparison of the Reservoir Competence of Medium-sized Mammals and *Peromyscus leucopus* for *Anaplasma phagocytophilum* in Connecticut'. *Vector-Borne and Zoonotic Diseases,* 2, (3), pp.125-136.

Li, T., Chang, C.Y., Jin, D.Y., Lin, P.J., Khvorova, A. and Stafford, D.W. (2004) 'Identification of the gene for vitamin K epoxide reductase'. *Nature,* 427, pp.537-541.

Li, W., Schulman, S., Dutton, R.J., Boyd, D., Beckwith, J. and Rapoport, T.A. (2010) 'Structure of a bacterial homologue of vitamin K epoxide reductase'. *Nature,* 463, pp.507-512.

Li, T., Yang, C. T., Jin, D. and Stafford, D. W (2000) 'Identification of a Drosophila vitamin K-dependent γ– glutamyl carboxylase'. *Journal of Biological Chemistry,* 275, pp.18291-18296.

Lin, C., Yen, T., Juang, Y., Lee, C. and Lee, S. (2018) 'Distinct psychopathology of patients who attempted suicide with rodenticide in Taiwan: a comparative study with patients of suicide with paraquat'. *Psychology Research and Behaviour Management,* 11, pp.323-328.

Liu, J., Xiong, K., Ye, X., Zhang, J., Yang, Y. and Ji, L. (2015) 'Toxicity and bioaccumulation of bromadiolone to earthworm *Eisenia fetida*'. *Chemosphere,* 135, pp.250-256.

Lohr, M.T. (2018) 'Anticoagulant rodenticide exposure in an Australian predatory bird increases with proximity to developed habitat'. *Science of the Total Environment,* 643, pp.134-144.

Lohr, T. and Davis, R. A. (2018) 'Anticoagulant rodenticide use, non-target impacts and regulation: A case study from Australia', *Science of the Total Environment,* 634, pp.1372-1384.

Lorenz, H., Hailey, D.W., Wunder, C. and Lippincott-Schwartz, J. (2006) 'The fluorescence protease protection (FPP) assay to determine protein localization and membrane topology'. *Nature Protocols,* 1, (1), pp.276-279.

Louvet, M.S., Gault, G., Lefebvre, S., Popowycz, F., Boulven, M., Besse, S., Benoit, E., Lattard, V. and Grancher, D. (2015) 'Comparative inhibitory effect of prenylated coumarins, ferulenol and ferprenin, contained in the 'poisonous chemotype' of *Ferula communis* on mammal liver microsomal VKORC1 activity'. *Phytochemistry,* 118, pp.124-130.

Lund, M. (1988) 'Flocoumafen – a new anticoagulant rodenticide'. *Proceedings of the Thirteenth Vertebrate Pest Conference,* 12.

Lund, M. (2015) Commensal Rats. *In:* Buckle, A.P. and Smith, R.H. *Rodent pests and their control.* Oxfordshire: CAB International.

Luo, Z. X. (2007) 'Transformation and diversification in early mammal evolution', *Nature,* 450, pp.1011–1019.
Ma, X., Wang, D., Li, N., Liu, L., Tian, L., Luo, C., Cong, L., Feng, Z., Liu, X.H. and Song, Y. (2018) 'Low warfarin resistance frequency in Norway rats in two cities in China after 30 years of usage of anticoagulant rodenticides'. *Pest Management Science,* 74, (11), pp.2555-2560.

MacNicoll, A. D. (1985) 'A comparison of warfarin resistance and liver microsomal vitamin K epoxide reductase activity in rats'. *Biochemica et Biophysica acta,* 840, (1), pp.13-20.

Mack, D.O., Suen, E.T., Girardot, J.M., Miller, J.A., Delaney, R. and Johnson, B.C. (1976) 'Soluble enzyme system for vitamin K-dependent carboxylation'. *Journal of Biological Chemistry,* 251, (11), pp.3269-3276.

Marie, C. and Petri, W.A. (2013) 'Amoebic dysentery'. *BMJ Clinical Evidence,* 2013.

Markussen, M.D., Heiberg, A.C., Fredholm, M. and Kristensen, M. (2008) 'Identification of cytochrome P450 differentiated expression related to developmental stages in bromadiolone resistance in rats (*Rattus norvegicus*)'. *Pesticide Biochemistry and Physiology,* 91, pp.147-152.

Marquez, A., Khalil, R. A., Fourel, I., Ovarbury, T., Pinot, A., Rosine, A., Thalmensi, G., Jaffory, G, Kodjo, A., Benoit, E. and Lattard, V. (2019) 'Resistance to anticoagulant rodenticides in Martinique could lead to inefficient rodent control in a context of endemic leptospirosis'. *Scientific Reports,* 9, (1), e.13491.

Matagrin, B., Hammed, A., Michaux, A., Hodroge, A., Benoit, E. and Lattard, V. (2016) 'Identification of key functional residues in the active site of vitamin K epoxide reductase-like protein (VKORC1L1)'. *Biochemistry and Molecular Biology Journal,* 2, (3).

Matagrin, B., Hodroge, A., Montagut-Romans, A., Andru, J., Fourel, I., Besse, S., Benoit, E. and Lattard, V. (2013) 'New insights into the catalytic mechanisms of vitamin K epoxide reductase (VKORC1) – The catalytic properties of the explain the biological cost associated to mutations'. FEBS, 3, (1), pp.144-150.

Matschiner, J.T., Bell, R.G., Amelotti, J.M. and Knauer, T.E. (1970) 'Isolation and characterization of a new metabolite of phylloquinone in the rat'. *Biochimica et Biophysica acta,* 201, (2), pp.309-315.

Matschiner, J. T., Zimmerman, A. and Bell R. G. (1974) 'The influence of warfarin on vitamin K epoxide reductase'. *Thrombosis et diathesis haemorrhagica,* 57, pp.45-52.

Maurin, M. and Raoult, D. (1999) 'Q fever'. Clinical Microbiology Reviews, 12, (4), pp.518-553.

Mayol, J., Mayol, M., Domenech, O., Oliver, J., McMinn, M. and Rodríguez, A. (2012) Aerial Broadcast of Rodenticide on the Island of Sa Dragonera (Balearic Islands, Spain). A promising Rodent Eradication Experience on a Mediterranean island. In: Genovesi, P. and Scalera, R. Aliens: The Invasive Species Bulletin. Rome, Italy: ISPRA, 32, 29–32.

McClelland, P. J. (2002) 'Eradication of Pacificrats (Rattus exulans) from Whenua Hou Nature Reserve (Codfish Island), Putauhinu and Rarotoka Islands, New Zealand'. In Veitch, C.R., Clout, M.N. (Eds.), 'Turning the tide: the eradication of invasive species', *Proceedings of the International Conference On Eradication of Island Invasives Occasional Paper of the IUCN Species Survival Commission*, 27. IUCN SSS Invasive Species Specialist Group, Gland, Switzerland, pp.173–181 Available at: https://portals.iucn.org/library/efiles/documents/SSC-OP-028.pdf#page=179 [Accessed 11 November 2019].

McClelland, P. J. (2011). *Campbell Island–pushing the boundaries of rat eradications*. In Veitch, C. R., Clout, M. N., Towns, D. R. (eds.), .Island Invasives: Eradication and Management. Gland, Switzerland, IUCN, pp 204–207. http://www.issg.org/pdf/publications/Island_Invasives/pdfHQprint/2McClellandC.pdf. [Accessed: 11 November, 2019].

McCurdy, W. (1988) 'An attempted homicide using d-CON rat poison'. *Journal of Analytical Toxicology,* 12, (1) pp.51-52.

McDonald, R. A., Harris, S., Turnbull, G., Brown, p. and Fletcher, M. (1998) 'Anticoagulant rodenticides in stoats (*Mustela erminea*) and weasels (*Mustela nivalis*) in England', *Environmental Pollution,* 103, (1), pp.17-23.

McGirr, J. L. and Papworth, D. S. (1953) 'Toxic hazards of the newer insecticides and herbicides'. *Veterinary Record,* 65, pp.857-862.

Meehan, A.P. (1978) 'Rodenticidal activity of bromadiolone – a new anticoagulant'. *Proceedings of the 8th Vertebrate Pest Conference*. 31.

Meerburg, B.G., Singleton, G.R. and Kijlstra, A. (2009) 'Rodent-borne diseases and their risks for public health'. *Critical Reviews in Microbiology,* 35, (3) pp.221-270.

Meersburg, B.G., van Gent-Pelzer, M.P., Schoelitsz, B. and van der Lee, T.A.J. (2014) 'Distribution of anticoagulant rodenticide resistance in *Rattus norvegicus* in the Netherlands according to Vkorc1 mutations'. *Pest Management Science,* 70, (11), pp.1761-1766.

Merton, D., Climo, G., Laboudallon, V., Robert, S. and Mander, C. (2002) *Alien mammal eradication and quarantine on inhabited islands in the Seychelles. In:* Veitch, C.R. and Clout, M.N. (eds) *Turning the tide: the eradication of invasive species.* Cambridge: Occasional Paper of the IUCN Species Survival Commission, No27.

Meyer, A. and Zardoya, R. (2003) 'Recent Advances in the (molecular) phylogeny of Vertebrates', *Annual Review of Ecology, Evolution and Systematics,* 34, pp.311–338.

Miller, M. J. (1940) 'Plague: History and Epidemiology'. *Journal of Comparative Medicines,* 4, (7), pp.183–193.

Mooney, J., Lynch, M.R., Prescott, C.V., Clegg, T., Loughlin, M., Hannon, B., Moore, C. and Faulkner, R. (2018) 'VKORC1 sequence variants associated with resistance to anticoagulant rodenticides in Irish populations of *Rattus norvegicus* and *Mus musculus domesticus*'. *Scientific Reports,* 8, 4535.

Morgan, D. R., Wright, G. R., Ogilvie, S.C., Pierce, R. and Thomson, P. (1996) 'Assessment of the environmental impact of brodifacoum during rodent eradication operations in New Zealand', *Proceedings of the Seventeenth Vertebrate Pest Conference 1996,* 38, pp.213-218.

Mostafa, M. H., Sheweita, S. A. and O'Connor, P. J. (1999) 'Relationship between Schistosomiasis and Bladder Cancer'. *Clinical Microbiology Reviews,* 12, (1), pp.97-111.

Mowat, D. (1891) 'Suicide from rat poison'. *Lancet,* 138, pp.1387-1388.

Müller, E., Keller, A., Fregin, A., Müller, C.W. and Rost, S. (2014) 'Confirmation of warfarin resistance of naturally occurring VKORC1 variants by co-expression with coagulation factor IX and *in silico* protein modelling'. *BMC Genetics,* 15.

Murphy, E. C., Clapperton, B. K., Bradfield, M. F. and Speed, H. J. (1998) 'Brodifacoum residues in target and non-target animals following large-scale poisons operations in New Zealand podocarp-hardwood forests'. *New Zealand Journals of Zoology,* 25, (4), pp.307-314.

Murphy, W. J., Pringle, T. H., Crider, T. A., Springer, M. S. and Miller, W. (2007) 'Using genomic data to unravel the root of the placental mammal phylogeny', *Genome Research,* 17, pp.413–421.

Myszka, D.G. and Swenson, R.P. (1991) 'Synthesis of the photoaffinity probe 3-(p-azidobenzyl)-4-hydroxycoumarin and identification of the dicoumarol binding site in rat liver NAD(P)H:quinone reductase (EC 1.6.99.2)'. *Journal of Biological Chemistry,* 266, (8) pp.4789-4797.

Nakayama, S. M. M., Morita, A., Ikenaka, Y., kawai, Y. K., Wantanabe, K. P., Ishii, C., Mizukawa, H., Yohannes, Y. B., Saito, K., Wantanabe, Y., Ito, M., Ohsawa, N. and Ishizuka, M. (2020) 'Avian interspecific differences in VKOR activity and inhibition: Insights from amino acid sequence and MRNA expression ratio of VKORC1 and VKORC1L1'. *Comparative Biochemistry and Physiology,* Part C, 228, e.108635.

National Research Council Committee on Diet and Health (1989) 'Fat soluble vitamins in diet and health: implications for reducing chronic disease risk'. *National Academies Press,* Washington DC.

Nelsestuen, G.L. and Suttie J.W. (1972) 'Mode of action of vitamin K. Calcium binding properties of bovine prothrombin'. *Biochemistry,* 11, (26) pp.4961-4964.

Nelsestuen, G.L. and Suttie, J.W. (1973) 'The mode of action of vitamin K. Isolation of a peptide containing the vitamin K-dependent portion of prothrombin'. *PNAS,* 70, (12) pp.3366-3370.

Nelsestuen, G.L., Zytkovicz, T.H. and Howard, J.B. (1974) 'The mode of action of vitamin K identification of γ-carboxyglutamic acid as a component of prothrombin'. *Journal of Biological Chemistry,* 249, (19) pp.6347-6350.

Newton, I. (1979) *Population ecology of raptors.* London: Poyster.

Nyakatura, K. and Bininsa-Emonds, O. R. P. (2012) 'Updating the evolutionary history of Carnivora (Mammalia): a new species-level supertree complete with divergence time estimates'. *BMC Biology,* 10, (12).

O'Reilly, R.A., Pool, J.G. and Aggeler, P.M. (1968) 'Hereditary resistance to coumarin anticoagulant drugs in man and rat'. *Annals of the New York Academy of Sciences,* 151, (1), pp.913-931.

Ogilvie, S.C., Pierce, R.J., Wright, G.R.G., Booth, L.H. and Eason, C.T. (1997) 'Brodifacoum residue analysis in water, soil, invertebrates and birds after rat eradication on Lady Alice Island'. *New Zealand Journal of Ecology,* 21, (2) pp.195-197.

Okello, A.L., and Thomas, L.F. (2017) 'Human taeniasis: current insights into prevention and management strategies in endemic countries'. *Risk Management and Healthcare Policy,* 10, pp.107-116.

Oldenburg, J., von Brederlow, B., Fregin, A., Rost, S., Wolz, W., Eberl, W., Eber, S., Lenz, E., Schwaab, R., Brackmann, H. H., Effenberger, W., Harbrecht, U., Schurgers, L. J., Vermeer, C. and Müller, C. R. (2000) 'Congenital deficiency of vitamin K dependent coagulation factors in two families presents as a genetic defect of the vitamin K-epoxide-reductase-complex'. *Thrombosis and Haemostasis,* 84, (6), pp.937-941.

Oppel, S., Lavers, J.L., Bond, A.L. and Harrison, G. (2016) 'Reducing the primary exposure risk to Henderson Crakes (*Zapornia atra*) during aerial broadcast eradication by selecting appropriate bait colour'. *Wildlife Research,* 43, (4), pp.298-303.

Osman, A. and Hannestad, U. (2008) 'A possible ethanol-catalyzed rearrangement of vitamin K_1 detected by gas chromatography/mass spectrometry'. *Rapid Communications in Mass Spectrometry,* 22, (23) pp.3861-3866.

Özdemir, Z.N., Sahin, U., Merter, M., Gündüz, M., Atesagaoglu, B. and Beksaç, M (2016) 'A case of superwarfarin poisoning due to repetitive occupational dermal rodenticide exposure in a worker'. *Turkish Journal of Haemotology,* 33, (3) pp.251-253.

Palmer, R.B., Alakija, P., de Baca, J.E. and Nolte, K.B. (1999) 'Fatal brodifacoum rodenticide poisoning: Autopsy and Toxicologic Findings'. *Journal of Forensic Sciences,* 44, (4) pp.851-855.

Panigrahi, B., Jones, B.C. and Rowe, S.P. (2018) 'Brodifacoum-contaminated synthetic marijuana: clinical and radiologic manifestations of a public health outbreak causing life-threatening coagulopathy'. *Emergency radiology,* 25, pp.715-718.

Papworth, D. S. (1958) 'A review of the dangers of warfarin poisoning to animals other than rodents'. *Royal Society of Health Journal,* 78 (1), pp.52-60.

Patillon, B., Luisi, P., Blanché, H., Patin, E., Cann, H. M., Gēnin, E. and Sabbagh, A. (2012) 'Positive selection in the chromosome 16 VKORC1 genomic region has contributed to the variability in humans'. *PLOS: ONE,* 7, (12), e.53049.

Pelz, H.J., Rost, S., Hünerberg, M., Fregin, A., Heiberg, A.C., Baert, K., MacNicoll, A.D., Prescott, C.V., Walker, A.S., Oldenberg, J. and Müller, C.R. (2005) 'The genetic basis of resistance to anticoagulants in rodents'. *Genetics,* 170, (4) pp.1839-1847.

Peoc'h, K., Pruvot, S., Gourmel, C., dit Sollier, C. B. and Drouet, L. (2009) 'A new VKORC1 mutation leading to an isolated resistance to fluindione'. *British Journal of Haematology,* 145, (6), pp.841-843.

Perry, R. D. and Fetherston, J. D. (1997) '*Yersinia pestis*-etiologic agent of plague', *Clinical Microbiology Reviews,* 10(1), p.35.

Pitt, W.C., Berentsen, A.R., Shiels, A.B., Volker, S.F., Eisemann, J.D., Wegmann, A.S. and Howald, G.R. (2015) 'Non-target species mortality and the measurement of brodifacoum rodenticide residues after a rat (*Rattus rattus*) eradication on Palmyra Atoll, tropical pacific'. *Biological Conservation,* 185, pp.36-46.

Pitt, W.C., Higashi, M. and Primus, T.M. (2011) 'The effect of cooking on diphacinone residues related to human consumption of feral pigs'. *Food and Chemical Toxicology,* 49, (9), pp.2030-2034.

Plank, R. and Dean, D. (2000) 'Overview of epidemiology, microbiology and pathogenesis of Leptospira spp in humans'. *Microbes and infection,* 2, (10), pp.1265-1276.

Pool, J.G., O'Reilly, R.A., Schneiderman, L. and Alexander, M. (1968) 'Warfarin resistance in the rat'. *American Journal of Physiology,* 215, (3), pp.627-631.

Pozzi, L., Hodgson, J. A., Burrell, A. S., Sterner, K. N., Raaum, R. L., Disotell, T. R. (2014) 'Primate phylogenetic relationships and divergence dates inferred from complete mitochondrial genomes', *Molecular Phylogenetics and Evolution,* 75, pp.165–183.

Pozzi, N. and Di Cera, E. (2014) 'Prothrombin structure: unanticipated features and opportunities'. *Expert Review Proteomics,* 11, (6) pp.653-655.

Prakash, J., Das, R.C., Srivastava, K., Patra, P., Khan, S.A. and Shashikumar, R. (2014) 'Munchausen syndrome: Playing sick or sick player'. *Industrial Psychiatry Journal,* 23, (1), pp.68-70.

Prescott, C.V., Buckle, A.P., Gibbings, J.G., Allan, N.W. and Stuart, A.M. (2011) 'Anticoagulant resistance in Norway Rats (*Rattus norvegicus* Berk.) in Kent – a VKORC1 single nucleotide polymorphism, tyrosine 139 phenylalanine, new to the UK'. *International Journal of Pest Management,* 57, (1), pp.61-65.

Primus, T., Wright, G. and Fisher, P. (2005) 'Accidental discharge of brodifacoum baits in a tidal marine environment'. *Bulletin of Environmental Contamination and Technology,* 74, pp.913-919.

Proulex, G. (2010) 'Field Evidence of Non-Target and Secondary Poisoning by Strychnine and Chlorophacinone Used to Control Richardson's Ground Squirrels in Southwest Saskatchewan', *Proceedings 9th Conservation and Endangered Species Conference,* pp.128-134.

Prum, R.O., Berv, J.S., Dornburg, A., Field, D.J., Townsend, J.P., Lemmon, E.M. and Lemmon, A.R. (2015) 'A comprehensive phylogeny of birds (Aves) using targeted next-generation DNA sequencing'. *Nature,* 526, pp.569-573.

Raber, M. N. (1990) *Coagulation Tests.* In: Walker, H. K., Hall, W. D., Hurst, J. W. (Eds.), The History, Physical, and Laboratory Examinations. Butterworths, Boston.

Raoult, D. and Roux, V. (1999) 'The body louse as a vector of reemerging Human Diseases', *Clinical Infectious Diseases,* 29(4), pp.888-911.

Randolph, S., Miklisová, D., Lysy, J., Roger, D. J. and Labuda, M. (1999) 'Incidence from coincidence patterns of tick infestations on rodents facilitate transmission of tick-borne encephalitis virus'. *Parasitology,* 118 (2), pp.177-186.

Rattner, B.A. and Nicholas, M.F. (2018) *Anticoagulant rodenticide toxicity to non-wildlife under controlled exposure conditions.* USDA National Wildlife Research Centre – Staff Publications. 2103.

Reece, R. L., Scott, P. C., Forsyth, J. A., Gould, J. A. and Barr, D. A. (1985) ' Toxicity episodes involving agricultural chemicals and other substances in birds in Victoria, Australia', *The Veterinary Record,* 16, pp.525-527.

Rieder, M. J., Reiner, A. P., Gage, B. F., Nickerson, D. A., Eby, C. S., McLeod, H. L., Pharm, D., Blough, D. K., Thummel, K. E., Veenstra, D. L., Pharm, D. and Rettie, A. E. (2005) 'Effect of VKORC1 Haplotypes on Transcriptional Regulation and Warfarin Dose', *New England Journal of Medicine,* 352, (22), pp.2285 – 2293.

Riley, S.P.D., Bromley, C., Poppenga, R.H., Uzal, F.A., Whited, L. and Sauvajot, R.M. (2007) 'Anticoagulant exposure and notoedric mange in bobcats and mountain lions in urban Southern California'. *Journal of Wildlife Management,* 71, pp.1874-1884.

Rishavy, M. A., Usubalieva, A., Hallgren, K. W. and Berkner, K. L. (2011) 'Novel insight into the mechanism of the vitamin K oxidoreductase (VKOR): Electron relay through Cys43 and Cys51 reduces VKOR to allow vitamin K reduction and facilitation of vitamin K-dependent protein carboxylation'. *The Journal of Biological Chemistry*, 286, (9) pp.7267-7278.

Robertson, H. A., Colbourne, R. M., Graham, P. J., Miller, P. J. and Pierce, R. J. (1999) 'Survival of Brown Kiwi (*Apteryx Mantelli)* Exposed to brodifacoum poison in Northland, New Zealand'. *New Zealand Journal of Ecology,* 23, (2), pp.225-231.

Robertson, H.M. (2004) 'Genes encoding vitamin-K epoxide reductase are present in Drosophila and trypanosomatid protists'. *Genetics,* 168, (2), pp.1077-1080.

Robinson, P. K. (2005) 'Enzymes: principles and biotechnological applications?', *Essays in Biochemistry,* 59, pp.1-41.

Roderick, L.M. (1931) 'A problem in the coagulation of the blood. Sweet clover disease of cattle'. *Animal Journal of Physiology*, 96, (2) pp. 413-425.

Rost, S., Fregin, A., Hünerberg, M., Bevans, C.G., Müller, C.R. and Oldenburg, L. (2005) 'Site-directed mutagenesis of coumarin-type anticoagulant-sensitive VKORC1: evidence that highly conserved amino acids define structural requirements for enzymatic activity by warfarin'. *Thrombosis and Haemostasis,* 94, (4), pp.780-786.

Rost, S., Fregin, A., Ivaskevicius, V., Conzelmann, E., Hörtnagel, K., Pelz, H.J., Lappegard, K., Seifried, E., Scharrer, I., Tuddenham, E.G., Müller, C.R., Strom, T.M. and Oldenburg, J. (2004) 'Mutations in VKORC1 cause warfarin resistance and multiple coagulation factor deficiency type 2'. *Nature,* 427, pp.537-541.

Rost, S., Pelz, H.J., Menzel, S., MacNicoll, A.D., León, V., Song, K.J., Jäkel, T., Oldenburg, J. and Müller, C.R. (2009) 'Novel mutations in the VKORC1 gene of wild rats and mice – a response to 50 years of selection pressure by warfarin?'. *BMC Genetics,* 10.

Ruder, M. G., Poppenga, R. H., Bryan II, J. A., Bain, M., Pitman, J. and Keel, M. K. (2011) 'Intoxication of Nontarget Wildlife with Rodenticides in Northwestern Kansas', *Journal of Wildlife Diseases,* 47, (1), pp.212–216.

Rueda, D., Campbell, K.J., Fisher, P., Cunninghame, F. and Ponder, J.B. (2016) 'Biologically significant residual persistence of brodifacoum in reptiles following invasive rodent eradication, Galapagos Islands, Ecuador'. *Conservation Evidence,* 13, p.38.

Ruiz-Suárez, N., Henríquez-Hernández, L.A., Valerón, P.F., Boada, L.D., Zumbado, M.,Camacho, M., Almeida-González, M. and Luzardo, O.P. (2014) 'Assessment of anticoagulant rodenticide exposure in six raptor species from the Canary Islands (Spain)', *Science of the Total Environment,* 485–486, pp.371–376.

Runge, M., Von Keyserlingk, M., Braune, S., Freise, J., Eiler, T., Plenge-Bönig, A., Becker, D., Pelz, H. J., Esther, A., Rost, S. and Müller, C. R. (2011) 'Distribution and frequency of VKORC1 sequence variants conferring resistance to anticoagulants in *Mus musculus*', *8th European Vertebrate Pest Management Conference.*

Russell, W. M. S. and Burch, R. L. (1959) *The principles of humane experimental technique.* Wheathampstead: UK, Universities federation for Animal Welfare.

Rutkevich, L.A. and Williams, D.B. (2012) 'Vitamin K epoxide reductase contributes to protein disulfide formation and redox homeostasis within the endoplasmic reticulum'. *Molecular Biology of the Cell,* 23, (11) pp.2017-2027.

Sánchez-Barbudo, I.S., Camarero, P.R. and Mateo, R. (2012) 'Primary and secondary poisoning by anticoagulant rodenticides of non-target animals in Spain'. *Science of the Total Environment,* 420, pp.280-288.

Savitsky, P., Bray, J., Cooper, C. D., Marsden, B. D., Mahajan, P., Burgess-Brown, N. A. and Gileadi, O. (2010) 'High-throughput productions of human proteins for crystallization: the SGC experience'. *Journal of Structural Biology,* 172, (1), pp.3-13.

Schmeits. P. C. J., Hermans, M. H. A., van Geest-Daalderop, J. H. G., Poodt, J., de Sauvage Nolting, P. R. W. and Conemans, J. M. H. (2009) 'VKORC1 mutations in patients with partial resistance to phenprocoumon'. *British Journal of Haematology,* 148, pp.948-963.

Schmitt, N., Saville, J. M., Greenway, J. A., Stovell, P. L. Friis, L. and Hole, L. (1978) 'Sylvatic trichinosis in British Columbia: potential threat to human health from an independent cycle'. *Public Health Report,* 93, (2), pp.189-193.

Schulman, S., Wang, B., Li, W. and Rapoport, T.A. (2010) 'Vitamin K epoxide reductase prefers ER membrane-anchored thioredoxin-like redox partners'. *Proceedings of the National Academy of Sciences,* 107, (34), pp.15027-15032.

Schwartz, R., Seibel, P. N., Rahmann, S., Schoen, C., Huenerberg, m., Müller-Reible, C., Dandekar, T., Karchin, R., Schultz, J., Müller, T. (2009) 'Detecting species-site dependencies in large multiple sequence alignments'. *Nucleic Acids Research,* 37, (18), pp.5959-5968.

Schwind, V. (2016) *Viral Hemorrhagic Fever Attack: Flaviviruses* In: Ciottone. G.R. *Ciottone's Disaster Medicine.* 2nd ed. Elsevier.

Scott, S. A., Edelmann, L., Kornreich, R. and Desnick, R. J. (2008) 'Warfarin pharmacogenetics: CYP2C9 and VKORC1 genotypes predict different sensitivity and resistance frequencies in the Ashkenazi and Sephardi Jewish populations'. *American Journal of Human Genetics,* 82, (2), pp.495-500.

Session, A. M., Uno, Y., Kwon, T., Chapman, J. A., Toyoda, A., Takahashi, S., Fukui, A., Hikosaka, A., Suzuki, A., Kondo, M., van Heeringen, S. J., Quigley, I., Heinz, S., Ogino, H., Ochi, H., Hellsten, U., Lyons, J. B., Simakov, O., Putnam, N., Stites, J., Kuroki, Y., Tanaka, T., Michiue, T., Watanabe, M., Bogdanovic, O., Lister, R., Georgiou, G., Paranjpe, S. S., van Kruijsbergen, I., Shu, S., Carlson, J., Kinoshita, T., Ohta, Y., Mawaribuchi, S., Jenkins, J., Grimwood, J., Schmutz, J., Mitros, T., Mozaffari, S. V., Suzuki, Y., Haramoto, Y., Yamamoto, T. S., Takagi, C., Heald, R., Miller, K., Haudenschild, C., Kitzman, J., Nakayama, T., Izutsu, Y., Robert, J., Fortriede, J., Burns, K., Lotay, V., Karimi, K., Yasuoka, Y., Dichmann, D. S., Flajnik, M. F., Houston, D. W., Shendure, J., DuPasquier, L., Vize, P. D., Zorn, A. M., Ito, M., Marcotte, E., Wallingford, J., Ito, Y., Asashima, M., Ueno, N., Matsuda, Y., Veenstra, G. J., Fujiyama, A., Harland, R. M., Taira, M. and Rokhsar, D. (2016) 'Genome evolution in the allotetraploid frog *Xenopus laevis'. Nature,* 558, pp.336-343.

Shah, D.V. and Suttie, J.W. (1971) 'Mechanism of Action of Vitamin K: Evidence for the conversion of a precursor protein to prothrombin in the rat'. *Proceedings of the National Academy of Sciences of the United States of America,* 68, (7), pp.1653-1657.

Shah, S. Z., Jabbar, B., Ahmed, N., Rehman, A., Nasir, H., Nadeem, S., Jabbar, I., Rahman, Z. and Azam, S. (2018) 'Epidemiology, pathogenesis, and control of tick-borne disease – Kyasanur Forest disease: Current status and future directions'. *Front Cell Infect Microbiology,* 8, 149.

Shahin, M. H. A., Cavallari, L. H., Perera, M. A., Khalifa, S. I., Misher, A., Langaee, T., Patel, S., Perry, K., Meltzer, D. O., McLeod, H. L. and Johnson, J. A. (2013) 'VKORC1 Asp36Tyr geographic distribution and its impact on warfarin dose requirements in Egyptians'. *Journal of Thrombosis and Haemostasis,* 109, (6), pp.1045-1050.

Sheafor, S.E and Couto, C.G. (1999) 'Anticoagulant rodenticide toxicity in 21 dogs'. *Journal of the American Animal Hospital Association,* 35, (1), pp.38-46.

Shearer, M.J. and Newman, P. (2008) 'Metabolism and cell biology of vitamin K'. *Thrombosis and Haemostasis*, 100, pp.530-547.

Shimshoni, J.A., Soback, S., Cuneah, O., Shlosberg, A. and Britzi, M. (2013) 'New validated multiresidue analysis of six 4-hydroxycoumarin anticoagulant rodenticides in hen eggs'. *Journal of Veterinary Diagnostic Investigation,* 25, (6), pp.736-743.

Shipley, L. C., Taylor, S.T., Grimsley, C., Shoffer, K. and Goldstein, J. (2018) 'Rats! Hantavirus: A case report of a suspected case in Eastern Tennessee'. *The Permanente Journal,* 22.

Shivaprasad, H. L. and Galey, F. (2001) 'Diphacinone and zinc phosphide toxicity in a flock of Peafowl'. *Avian Pathology,* 30, (6), pp.599-603.

Shoop, W. L. (1994) 'Vertical transmission in the Trematoda'. *Journal of the Helminthological Society of Washington,* 61, (2), pp.153-161.

Shore, R. F., Birks, J. D. S., Afsar, A., Wienburg, C. L. and Kitchener, A. C. (2003) 'Spatial and temporal analysis of second-generation anticoagulant rodenticide residues in polecats (*Mustela putorius*) from throughout their range in Britain, 1992-1999'. *Environmental Pollution,* 122, (2), pp.183-193.

Silverman, R. B., and Nandi, D. L. (1988) 'Reduced thioredoxin: A possible physiological cofactor for vitamin k epoxide reductase. Further support for an active site disulfide'. *Biochemical and Biophysical Research Communications,* 155, (3), pp.1247–1254.

Silverman, R.B. (1981) 'Chemical model studies for the mechanism of vitamin K epoxide reductase'. *Journal of American Chemical Society,* 103, pp.5939-5941.

Singleton, G.R. (2003) 'Impacts of Rodents on Rice Production in Asia'. Laos Baños: International Rice Research Institute.

Singleton, G.R., Belmain, S.R., Brown, P.R. and Hardy, B. (2010) *Rodent Outbreaks: Ecology and Impacts.* Los Baños: International Rice Research Institute.

Sinhadri, B.C.S., Jin, D.Y., Stafford, D.W., Tie, J.K. (2017) 'Vitamin K epoxide reductase and its paralogous enzyme have different structures and functions'. *Scientific Reports,* 7:17632, pp.1-12.

Smith, P. K., Krohn, R. I., Hermanson, A. K., Mallia, F. H., Gartner, M. D., Provenzano, E. K., Fujimoto, N. M., Goeke, B. J.,OLson, D. C. and Klenk, D. C. (1985) 'Measurement of protein using bicinchoninic acid'. *Analytic Biochemistry,* 150, (1), pp.76-85.

Smith, R.H. and Meyer, A.P. (2015) *Rodent control methods: non-chemical and non-lethal chemical, with special reference to food stores. In:* Buckle, A.P. and Smith, R.H. *Rodent pests and their control.* Oxfordshire: CAB International.

Smith, P., Townsend, M. G. and Smith, R. H. (1991) 'A cost of resistance in the brown rat? Reduced growth rate in warfarin – resistant lines'. *Functional Ecology,* 5, (3), pp.441-447.

Smolinske, S.C., Scherger, D.L, Kearns, P.S., Wruk, K.M, Kulig, K.W. and Rumack, B.H. (1989) 'Superwarfarin, poisoning in children: a prospective study'. *Pediatrics,* 84, (3), pp.490-494.

Song, Y., Endepols, S., Klemann, N., Richter, D., Matuschka, F.R., Shih, C.H., Nachman, M.W. and Kohn, M.H. (2011) 'Adaptive introgression of anticoagulant rodent poison resistance by hybridization between old world mice'. *Current Biology,* 21, (15), pp.1296-1301.

Song, Y., Lan, Z. and Kohn, M.H. (2014) 'Mitochondrial DNA phylogeography of the Norway rat'. *PLOS ONE,* 9, (2).

Soute, B. A. M., Groenen-van Dooren, M. M. C. L., Holmgren, A., Lundström, L. and Vermeer, C. (1992) 'Stimulation of the dithiol-dependent reductases in the vitamin K cycle by the thioredoxin system. Strong synergistic effects with protein disulphide-isomerase', *Biochemical Journal,* 281(1), pp.255–259.

Spahr, J.E., Maul, J.S. and Rodgers, G.M. (2007) 'Superwarfarin poisoning: a report of two cases and review of the literature'. *American Journal of Hematology,* 82, (7), pp.656-660.

Spratt, D. M. (2005) 'Australian ecosystems, capricious food chains and parasitic consequences for people'. *International Journal for parasitology,* 35, (7), pp.717-724.

Spurr, E.B., Maitland, M.J., Taylor, G.E., Wright, G.R.G., Radford, C.D. and Brown, L.E. (2005) 'Resistance of brodifacoum and other anticoagulant pesticides in target and non-target species, Nelson Lakes National Park, New Zealand'. *New Zealand Journal of Zoology,* 32, (4), pp.237-249.

Stafford, D.W. (2005) 'The vitamin K cycle'. *Journal of Thrombosis and Haemostasis,* 3, (8), pp.1873-1878.

Stahmann, M.A., Graf, L.H., Huebner, C.F., Roseman, S. and Link, K.P. (1944) 'Studies on 4-hydroxycoumarins. IV. Esters of the 4-hydroxycoumarins'. *Journal of the American Chemical Society,* 66, (6) pp. 900-902.

Stahmann, M.A., Huebner, C.F. and Link, K.P. (1941) 'Studies on the hemorrhagic sweet clover disease: V. Identification and synthesis of the hemorrhagic agent'. *Journal of Biological Chemistry,* 138, pp.513-527.

Stahmann, M.A., Wolff, I., and Link, K.P. (1943) 'Studies on 4-hydroxycoumarins. I. The synthesis of 4-hydroxycoumarins'. *Journal of the American Chemical Society,* 65, (12), pp.2285-2287.

Stansley, W., Cummings, M., Vudathala, D. and Murphy, L. A. (2014) 'Anticoagulants Rodenticides in Red-Tailed Hawks, *Buteo jamaicensis*, and Great Horned Owls, *Bubo virginianus,* from New Jersey, USA, 2008-2010', *Bulletin of Environmental Contamination and Toxicology,* 92, pp.6-9.

Stapley, J., Birkhead, T. R., Burke, T. and Slate, J. (2008) 'A Linkage Map of the Zebrafinch *Taeniopygia guttata* Provides New Insights into Avian Genome Evolution'. *Genetics*, 179, (1), pp.651–667.

Steiner, C. C. and Ryder, O. A. (2011) 'Molecular phylogeny and evolution of the Perissodactyla'. *Journal of the Linnean Society,* 163, (4), pp.1289–1303.

Stenseth, N. C., Leirs, H., Skonhoft, A., Davis, S. A., Pech, R. P., Andreassen, H. P., Singleton, G. R., Lima, M., Machang'u, R. S., Makundi, R. H., Zhang, Z., Brown, P. R., Shi, D. and Wan, X. (2003) 'Mice, rats, and people: the bio-economics of agricultural rodent pests'. *Frontiers in Ecology and the Environment,* 1, (7), pp.367–375.

Stephenson, B. M., Minot, E. O. and Armstrong, D. P. (1999) 'Fate of moreporks (*Ninox Novaeseelandiae)* during a pest control operation on Mokoia Island, Lake Rotorua, North Island, New Zealand'. *New Zealand Journal of Ecology,* 23, (2), pp.233-240.

Stone, W.B., Okoniewski, J.C. and Stedelin, J.R. (1999) 'Poisoning of wildlife with anticoagulant rodenticides in New York'. *Journal of Wildlife Diseases,* 35, pp.187-193.

Sullivan, R. (2012) *Rats: A year with New York's Most Unwanted Inhabitants.* London: Granta Books.

Sullivan, W.R., Huebner, C.F., Stahmann, M.A. and Link, K.P. (1943) 'Studies on 4-hydroxycoumarins. II. The condensation of aldehydes with 4-hydrocoumarins'. *Journal of the American Chemical Society,* 65, (12), pp.2288-2291.

Sun, Y. B., Xiong, Z. J., Xiang, X. Y., Liu, S. P., Zhou, W. W., Tu, X. L., Zhong, L., Wang, L., Wu, D. D., Zhang, B. L., Zhu, C. L., Yang, M. M., Chen, H. M., Li, F., Zhou, L., Feng, S. H., Huang, C., Zhang, G. J., Irwin, D., Hillis, D. M., Murphy, R. W., Yang, H., M., Che, J., Wang, J. and Zhang, Y. P. (2015) 'Whole-genome sequence of the Tibetan frog Nanorana *parkeri* and the comparative evolution of tetrapod genomes'. *PNAS,* 112, (11), pp.E1257–E1262.

Suttie, J.W. and Booth, S.L. (2011) 'Vitamin K'. *Advances in Nutrition,* 2, (5), pp.440-441.

Tanaka, K.D., Kawai, Y.K., Ikenaka, Y., Harunari, T., Tanikawa, T., Fujita, S. and Ishizuka, M. (2013) 'A novel mutation in VKORC1 and its effect on enzymatic activity in Japanese warfarin-resistant rats'. *Journal of Veterinary Medical Science,* 75, (2), pp.135-139.

Tanaka, K.D., Kawai, Y.K., Ikenaka, Y., Harvnari, T., Tanikawa, T., Ando., S., Min, H., Okajima, F., Fujita, S. and Ishizuka, M. (2012) 'The genetic mechanisms of warfarin resistance in *Rattus rattus* found in the wild in Japan'. *Pesticide Biochemistry and Physiology,* 103, (2), pp.144-151.

Taylor, M.J., Sharp, E.A., Watson, J.E., Melton, L.M. and Giela, A. (2009) 'A report of investigations in Scotland'. *Science and Advice for Scottish Agriculture, Edinburgh.* [Accessed: 10 May 2019 http://www.sasa.gov.uk/animal-poisoning-reports]

Thibault, J. C. and Meyer, J. Y. (2001) 'Contemporary extinctions and population declines of the monarchs (*Pomarea spp.)* in French Polynesia, South Pacific'. *Oryx,* 35, (1), pp.73-80.

Thierry-Palmer, M. (1984) 'Synthesis of vitamin K epoxide. An undergraduate biochemistry experiment'. *Journal of Chemical Education,* 61, (2), pp.179-180.

Thomas, P. J., Mineau, P., Shore, R. F., Champoux, L., Martin, L. K., Wilson, L. K., Fitzgerald, G., and Elliott, J. E. (2011) 'Second generation anticoagulant rodenticides in predatory birds: Probabilistic characterisation of toxic liver concentrations and implications for predatory bird populations in Canada'. *Environment International,* 37, (5), pp.914-920.

Thorsen, M. J., Shorten. R., Lucking, R. and Lucking, V. (2000) 'Norway rats (*Rattus norvegicus*) on Frégate Island, Seychelles: the invasion; subsequent eradication attempts and implications for the island's fauna', *Biological Conservation,* 96, (2), pp.133-138.

Tie, J.K., Jin, D.Y. and Stafford, D. W. (2012) 'Human vitamin K epoxide reductase and its bacterial homologue have different membrane topologies and reaction mechanisms'. *Journal of Biological Chemistry*, 287, (41), pp.33945-33955.

Tie, J. K., Jin, D. Y. and Stafford, D. W. (2014) 'Conserved loop cysteines of vitamin K epoxide reductase complex subunit 1-like 1 (VKORC1L1) are involved in its active site regeneration.' *Journal of Biological Chemistry,* 289, (13), pp.9396-9407.

Tobin, M.E. and Fall, M.W. (2006) Pest Control: Rodents. *In:* Developed under the Auspices of the UNESCO. *Encyclopedia of Life Support Systems,* Oxford: Eolss Publishers.

Torr, N. (2002*) Eradication of the rabbits and mice from subantarctic Enderby and Rose Islands.* In Veitch, C. R., Clout, M. N. (Eds.) *Turning the tide: the eradication of invasive species. Proceedings of the International Conference on Eradication of Island Invasives Occasional Paper of the IUCN Species Survival Commission,* 27 IUCN SSS Invasive Species Specialist Group, Gland, Switzerland. pp.319-328.

Towns, D., McFadden, I. and Lovegrove, T. (1993) 'Offshore Islands Co-operative Conservation Project with ICI Crop Care Division: Phase One (Stanley Island)', *Science & Research Internal Report,* 138, pp.1-23.

Towns, D.R., McFadden, I. and Lovegrove, T. (1993) 'Offshore Islands co-Operative Conservation Project with ICI Crop Care Division: Phase One (Stanley Island) Science & Research Internal Report No. 138', Department of Conservation, Wellington, New Zealand, p. 24. Available at: http://www.doc.govt.nz/Documents/science-and-technical/SRIR138.pdf [Accessed April 8, 2019].

Tudge, C. (2000) *The Variety of Life – a survey and a celebration of all the creatures that have ever lived.* Oxford: Oxford University Press.

Üstün-Aytekin, Ö., Gürhan, I. D., Ohura, K., Imai, T. and Öngen, G. (2014) 'Monitoring of the effects of transfection with baculovirus on Sf9 cell line and expression of human dipeptidyl peptidase IV', *Cytotechnology,* 66, pp.159–168.

Vannier, E., Gewurz, B.E. and Krause, P.J. (2008) 'Human Babesiosis'. *Infectious Disease Clinics of North America,* 22, (3), pp.469-488.

Veitch, C. R. (2002a) *Eradication of Pacific rats (Rattus exulans) Tiritiri Matangi Island, Hauraki Gulf, New Zealand.* In: Veitch, C.R., Clout, M.N. (Eds.), 'Turning the tide: the eradication of invasive species', *Proceedings of the International Conference On Eradication of Island Invasives Occasional Paper of the IUCN Species Survival Commission*, 27 IUCN SSS Invasive Species Specialist Group, Gland, Switzerland, pp.360–364

Veitch, C. R. and Clout, M. N. (2002) 'Turning the Tide: The Eradication of Invasive Species', *Proceedings of the International Conference on Eradication of Island Invasives,* 27, pp.1-414.

Veitch, C.R., (2002b) 'Eradication of Norway rats (Rattus norvegicus) and house mouse (*Mus musculus*) from Motuihe Island, New Zealand'. In: Veitch, C.R., Clout, M.N. (Eds.), 'Turning the tide: the eradication of invasive species', *Proceedings of the International Conference On Eradication of Island Invasives Occasional Paper of the IUCN Species Survival Commission*, 27. IUCN SSS Invasive Species Specialist Group, Gland, Switzerland, pp. 353–356 Available at: //portals.iucn.org/library/efiles/documents/SSC-OP-028.pdf#page=359 [Accessed: 23 March, 2019].

Voordouw, M.J., Lachish, S. and Dolan, M. C. (2015) 'The Lyme disease pathogen has no effect on the survival of its rodent reservoir host'. *PLOS ONE,* 10 (2).

von Heijne, G. (1989) 'Control of topology and mode of assembly of a polytopic membrane protein by positively charged residues'. *Nature,* 341, pp.456-458.

Vudathala, D., Cummings, M. and Murphy, L. (2010) 'Analysis of multiple anticoagulant rodenticides in animal blood and liver tissue using principles of QuEChERS method'. *Journal of AnalyticalToxicology,* 34, (5), pp.273-279.

Vyas, N. B. (2013) 'Untested pesticide mitigation requirements: ecological, agricultural, and legal implications'. *Drake Journal of Agricultural Law,* 18, (2), pp.335-3348. Available at: http://students.law.drake.edu/agLawJournal/docs/agVol18No2-Vyas.pdf (Accessed: 11 November 2019).

Vyas, N.B. (2017) 'Rodenticide incidents of exposure and adverse effects on non-raptor birds'. *Science of Total Environment,* 609, pp.68-76.

Wajih, N., Hutson, S. M. and Wallin, R. (2007) 'Disulfide-dependent Protein Folding Is Linked to Operation of the Vitamin K Cycle in the Endoplasmic Reticulum: A Protein Disulfide Isomerase-VKORC1 Redox Enzyme Complex Appears to be Responsible for Vitamin K1, 2,3-Epoxide Reduction'. *The Journal of Biological Chemistry,* 282, (4), pp.2626–2635.

Wajih, N., Sane, D.C., Hutson, S.M. and Wallin, R. (2005) 'Engineering of a recombinant vitamin K-dependent gamma-carboxylation system with enhanced gamma-carboxyglutamic acid forming capacity: evidence for a functional CXXC redox center in the system'. *Journal of Biological Chemistry,* 280, (11) pp.10540-10547.

Walker, L. A., Shore, R. F., Turk, A., Pereira, M. G. and Best, J. (2008) 'The Predatory Bird Monitoring Scheme: Identifying Chemical Risks to Top Predators in Britain'. *Ambio,* 37, (6), pp.466-471.

Walker, L.A., Chaplow, J.S., Moeckel, C., Pereira, M.G., Potter, E.D. and Shore, R.F. (2015) *Anticoagulant rodenticides in sparrowhawks: a predatory bird monitoring scheme (PBMS).* Lancashire, UK: Centre for Ecology and Hydrology.

Wallin, R. and Martin, L.F. (1985) 'Vitamin K-dependent carboxylation and vitamin K metabolism in liver'. *Journal of Clinical Investigation,* 76, (5), pp.1879-1884.

Wallin, R., Hutson, S.M., Cain, D., Sweatt, A. and Sane, D.C. (2001) 'A molecular mechanism for genetic warfarin resistance in the rat'. *The FASEB Journal,* 15, pp.2542-2544.

Walther, B., Karl, T.P., Booth, S.L. and Boyaval, P. (2013) 'Menaquinones, Bacteria and the food supply: The relevance of dairy and fermented food products to vitamin K requirements'. *Advances In Nutrition,* 4, (4) pp.463-473.

Wan, C. M., Yang, X. J., Du, J. J., Lu, Y., Yu, Z. B., Feng, V. G. and Wang, X. Y. (2014) 'Identification and characterization of SLVKOR, a disulfide bond formation protein from *Solanum lycopersicum* and bioinformatic analysis of plant VKORS'. *Biochemistry,* 79, (5), pp.440-449.

Wang, D., Chen, H., Momary, K. M., Cavallari, L. H., Johnson, J. A. and Sadée, W. (2008) 'Regulatory polymorphism in vitamin K epoxide reductase complex subunit 1 (VKRC1) affects gene expression and warfarin dose requirement'. *Blood,* 112, (4), pp.1013-1021.

Wang, L. and Jiang, T. (1994) 'On the Complexity of Multiple Sequence Alignment'. *Journal of Computing Biology,* 1, (4), pp.337–348.

Wantanabe, K.P., Saengtienchai, A., Tanaka, K.D., Ikenaka, Y. and Ishizuka, M. (2010) 'Comparison of warfarin sensitivity between rat and bird species'. *Comp. Biochem. Physiol. C. Toxixol. Pharmacol.*, 152, (1) pp.114-119.

Wardrop, D. and Keeling, D. (2008) 'The story of the discovery of heparin and warfarin'. *British Journal of Haematology,* 141, pp.757-763.

Watzka, M., Geisen, C., Bevans, C. G., Sittinger, K., Spohn, G., Rost, S., Seifried, E., Müller, C. R. and Oldenburg, J. (2011) 'Thirteen novel VKORC1 mutations associated with oral anticoagulant resistance: insights into improved patient diagnosis and treatment'. *Journal of Thrombosis and Haemostasis,* 9, (1), pp.109-118.

Weir, S.M., Yu, S., Talent, L.G., Maul, J.D., Anderson, T.A. and Salice, C.J. (2015) 'Improving reptile ecological risk assessment: oral and dermal toxicity of pesticides to a common lizard species (*Sceloporus occidentalis*)'. *Environmental Toxicology and Chemistry,* 34, (8), pp.1778-1786.

Welc-Faleciak, R., Paziewska, A., Bajer, A. and Behnke, J. M. (2008) 'Bartonella spp Infection in Rodents from Different Habitats in the Mazury Lake District, Northeast Poland'. *Vector-Borne and Zoonotic Diseases*, 8, (4), pp.467-474

West, B.D., Preis, S., Schroeder, C.H. and Link, K.P. (1961) 'Studies on the 4-hydroxycoumarins. XVII. The reduction and absolute configuration of warfarin'. *Journal of the American Chemical Society,* 83, pp.2676-2679.

Westhofen, P., Watzka, M., Marinova, M., Hass, M., Kirfel, G., Müller, J., Bevans, C.G., Müller, C.R. and Oldenburg, J. (2011) 'Human vitamin K 2,3-epoxide reductase complex subunit 1-like 1 (VKORC1L1) mediates vitamin K-dependent intracellular antioxidant function'. *Journal of Biological Chemistry,* 286, (17), pp.15085-15094.

Whitlon, D.S., Sadowski, J.A. and Suttie, J.W. (1978) 'Mechanism of coumarin action: significance of vitamin K epoxide reductase inhibition'. *Biochemistry,* 17, (8), pp.1371-1377.

Wildlife Incident Investigation Scheme (1998) *Pesticide poisoning of animals in 1998.* Available at: https://www.hse.gov.uk/pesticides/resources/W/WIIS_1998.pdf [Accessed 17 March 2019].

Wildlife Incident Investigation Scheme (2008) *Pesticide poisoning of animals in 2008.* Available at: https://www.sasa.gov.uk/document-library/animal-poisoning-report-2008 [Accessed 17 March 2019].

Wildlife Incident Investigation Scheme (2009) *Pesticide poisoning of animals in 2009.* Available at: https://www.sasa.gov.uk/document-library/pesticide-poisoning-animals-2009 [Accessed 17 March 2019].

Wildlife Incident Investigation Scheme (2010) *Pesticide poisoning of animals in 2010.* Available at: https://www.sasa.gov.uk/document-library/pesticide-poisoning-animals-2010 [Accessed 17 March 2019].

Wildlife Incident Investigation Scheme (2011) *Pesticide poisoning of animals in 2011.* Available at: https://www.sasa.gov.uk/document-library/pesticide-poisoning-animals-2011 [Accessed 17 March 2019].

Wildlife Incident Investigation Scheme (2012) *Pesticide poisoning of animals in 2012.* Available at: https://www.sasa.gov.uk/animal-poisoning-reports [Accessed 26 March 2019].

Wildlife Incident Investigation Scheme (2013) *Pesticide poisoning of animals in 2013.* Available at: https://www.sasa.gov.uk/animal-poisoning-reports [Accessed 26 March 2019].

Wildlife Incident Investigation Scheme (2014) *Pesticide poisoning of animals in 2014.* Available at: https://www.sasa.gov.uk/animal-poisoning-reports [Accessed 26March 2019]

Wildlife Incident Investigation Scheme (2015) *Pesticide poisoning of animals in 2015.* Available at: https://www.sasa.gov.uk/animal-poisoning-reports [Accessed 26 March 2019].

Wildlife Incident Investigation Scheme (2016) *Pesticide poisoning of animals in 2016.* Available at: https://www.sasa.gov.uk/animal-poisoning-reports [Accessed 26 March 2019].

Wildlife Incident Investigation Scheme (2017) *Pesticide poisoning of animals in 2017.* Available at: https://www.sasa.gov.uk/animal-poisoning-reports [Accessed 17 March 2019].

Wildlife Incident Investigation Scheme (2018) *Pesticide poisoning of animals in 2018.* Available at: https://www.sasa.gov.uk/animal-poisoning-reports [Accessed 17 March 2019].

Willingham, A.K. and Matschiner, J.T. (1974) 'Changes in phylloquinone epoxidase activity related to prothrombin synthesis and microsomal clotting activity in the rat'. *Biochemical Journal,* 140, (3), pp.435-441.

Wilms, E. B., Touw, D. J., Conemans, J. M., Veldkamp, R. and Hermans, M. (2008) 'A new VKORC1 allelic variant - p.Trp59Arg - in a patient with partial resistance to acenocoumarol and phenprocoumon'. *Journal of Thrombosis and Haemostasis,* 6, (7), pp.1224-1226.

Wilson, C. R., Sauer, J. M., Carlson, G. P., Wallin, R., Ward, M. P., and Hooser, S. B. (2003) 'Species comparison and vitamin K1, 2-3-epoxide reductase activity in vitro: Kinetics and warfarin inhibition'. *Toxicology,* 189, (3), pp.191-198.

Witmer, G.W., Pitt, W.C. and Howald, G. (2014) 'Invasive rodent ecology, impacts and management with an emphasis on the United States'. *Proceedings of the 26th Vertebrate Pest Conference,* pp.15-20.

Wolfs, T. F. W., Wagenaar, J. A., Niesters, H. G. M. and Osterhaus, A. D. M. E. (2002) 'Rat-to-Human Transmission of Cowpox Infection'. *Emerging Infectious Diseases Journal,* 8, (12), p.1495-1496.

Wu, S., Chen, X., Jin, D. Y., Stafford, D. W., Pederson, L. G. and Tie, J. K. (2018) 'Warfarin and vitamin K epoxide reductase: A molecular accounting for deserved inhibition'. *Blood,* 132, (6), pp.647-657.

Wu, S., Tie, J.K., Stafford, D.W. and Pedersen, L.G. (2014) 'Membrane topology for human vitamin K epoxide reductase'. *Journal of Thrombosis and Haemostasis,* 12, (1), pp.112-114.

Wu, S.M., Morris, D.P. and Stafford, D.W. (1991) 'Identification and purification to near homogeneity of the vitamin K-dependent carboxylase'. *PNAS,* 88, (6), pp.2236-2240.

Wu, X. and Wang, Y. (2012) 'Fossil materials and migrations of *Mus musculus* and *Rattus norvegicus*'. *Research of China's Frontier Archeology,* 1, pp.1-9.

Yamada, J., Kuramoto, T. and Serikawa, T. (1994) 'A rat genetic linkage map and comparative maps for mouse or human homologous rat genes'. *Mammalian Genomes,* 5, (2), pp.63-83.

Yan, H., Zhu, L., Zhou, X., Shen, M. and Xiang, M. (2016) 'Anticoagulant rodenticide intoxication in east China: a three-year analysis'. *Forensic Sciences Research,* 1, (1), pp.22-27.

Yin, Z. T., Zhu, F., Lin, F. B., Jia, T., Wang, Z., Sun, D. T., Li, G. S., Zhang, C. L., Smith, J., Yang, N. and Hou, Z. C. (2019) 'Revisiting avian 'missing' genes from de novo assembled transcripts'. *BMC Genetics,* 20, (4).

Zhang, Y. Z., Zou, Y., Fu, Z. F. and Plyvsnin, A. (2010) 'Hantavirus infections in humans and animals in China'. *Emerging Infectious Diseases,* 16 (8), pp.1195-1203.

Zhou, P., Chen, N., Zeng, R-L., Lin, R-Q. and Zhu, X-Q. (2008) 'Food-borne parasitic zoonoses in China: perspective for control'. *Trends in Parasitology,* 24, (9), pp.190-196.

Zurano, J. P., Magalhães, F. M., Asato, A. E., Silva, G., Bidau, C. J., Mesquita, D. O. and Costa, G. C. (2019) 'Cetartiodactyla: Updating a time-calibrated molecular phylogeny', *Molecular Phylogenetics and Evolution,* 133, pp.,256 – 262.

Appendix 1: Review of Literature for Non-targeted anticoagulant rodenticide poisoning in Non-raptor birds

Scientific Name	Common Name	Rodenticide	No of Animals Poisoned	Incident Type	Residues/ Physical Symptoms	Location	Reference
Apteryx mantelli	North Island Brown Kiwi	Brodifacoum	2	Mortality	Physical Symptoms	New Zealand	Fisher et al., 2011
Apteryx mantelli	North Island Brown Kiwi	Brodifacoum	5	Mortality	Residues	New Zealand	Robertson et al., 1999
Apteryx owenii	Little Spotted Kiwi	Brodifacoum	2	Mortality	Residues	New Zealand	Empson and Miskelly, 1999
Chen canagica	Emperor Goose	Brodifacoum	1	Exposure	Residues	United States	Ebbert and Burek-Huntington, 2010
Chen rossii	Ross's Goose	Warfarin	1	Mortality	Residues	United Kingdom	WIIS, 1998
Anserini spp.	Goose spp.	Brodifacoum, Difenacoum	1	Exposure	Physical Symptoms	Scotland	WIIS, 2005
Anserini spp.	Goose spp.	Brodifacoum	2	Mortality	N/A	United States	Erickson and Urban, 2004
Cygnus Cygnus	Whooper Swan	Bromadiolone	3	Mortality	N/A	Mongolia	in Dolgormaa, 2004
Cygnus	Swan spp.	Bromadiolone	1	Mortality	Residues	France	Berny et al., 1997
Tadorna ferruginea	Ruddy Shelduck	Bromadiolone	3	Mortality	N/A	Mongolia	in Dolgormaa, 2004
Tadorna variegata	Paradise Shelduck	Brodifacoum	4	Mortality	Residues	New Zealand	Dowding et al., 1999
Tadorna variegata	Paradise Shelduck	Brodifacoum	1	Mortality	Physical Symptoms	New Zealand	Veitch and Clout, 2002
Anas platyrhynchos domesticus	Khaki Campbell Duck	Bromadiolone	1	Mortality	Physical Symptoms	United Kingdom	WIIS, 2015
Notiomystis cincta	Mallard	Brodifacoum	2	Mortality	Residues	New Zealand	Dowding et al., 1999
Anas platyrhynchos	Mallard	Brodifacoum	1	Mortality	N/A	New Zealand	McClelland, 2011
Anas platyrhynchos	Mallard	Bromadiolone	1	Mortality	Residues	France	Berny et al., 1997
Anas platyrhynchos	Mallard	Chlorophacinone	3	Mortality	Residues	Spain	Sánchez-Barbudo et al., 2012
Anas platyrhynchos	Mallard	Bromadiolone	1	Mortality	Residues	France	Lambert et al., 2007
Anas superciliosa	Pacific black duck	Brodifacoum	1	Mortality	Residues	New Zealand	Dowding et al., 1999
Anas acuta	Northern Pintail	Brodifacoum	2	Exposure	Residues	United States	Pitt et al., 2015

Anas aucklandica	Auckland Islands Teal	Brodifacoum	4	Mortality	Residues	New Zealand	Torr, 2002
Anas aucklandica	Auckland Islands Teal	Brodifacoum	1	Mortality	Physical Symptoms	New Zealand	Veitch and Clout, 2002
Histrionicus histrionicus	Harlequin Duck	Brodifacoum	1	Mortality	Suspected	United States	Ebbert and Burek-Huntington, 2010
Mergus merganser	Goosander	Bromadiolone	1	Mortality	Residues	United Kingdom	WIIS, 2016
Callipepla californica	California Quail	Chlorophacinone	1	Exposure	Residues	United States	Blus et al., 1985
Pavo cristatus	Indian Peafowl	Bromadiolone	3	Mortality	Physical Symptoms	Australia	Reece et al., 1985
Alectoris rufa	Red-legged Partridge	Flocoumafen	1	Mortality	Residues	Spain	Sánchez-Barbudo et al., 2012
Gallus gallus domesticus	Chicken	Brodifacoum	1	Mortality	Residues	United States	WIIS, 1998
Gallus gallus domesticus	Chicken	Brodifacoum, Difenacoum	1	Mortality	Physical Symptoms	United Kingdom	WIIS, 2017
Gallus gallus domesticus	Chicken	Difethialone	1	Mortality	Physical Symptoms	United Kingdom	WIIS, 2016
Phasianus colchicus	Ring-necked Pheasant	Bromadiolone, Difenacoum	1	Mortality	Physical Symptoms	United Kingdom	WIIS, 1998
Tetrao tetrix	Black Grouse	Brodifacoum, Difenacoum	2	Mortality	Physical Symptoms	Spain	Hernandez-Moreno et al., 2013
Meleagris gallopavo	Wild Turkey	Chlorophacinone	48	Mortality	Physical Symptoms	United States	Ruder et al., 2011
Meleagris gallopavo	Wild Turkey	Chlorophacinone	5	Mortality	Residues	United States	Erickson and Urban, 2004
Eudyptula minor	Little Penguin	Brodifacoum	3	Exposure	Residues	New Zealand	Fisher et al., 2011
Fulmarus glacialis	Northern Fulmar	Brodifacoum	1	Exposure	Residues	United States	Ebbert and Burek-Huntington, 2010
Phalacrocorax pelagicus	Pelagic Cormorant	Brodifacoum	1	Exposure	Residues	United States	Ebbert and Burek-Huntington, 2011
Ardea cinerea	Gray Heron	Brodifacoum, Difenacoum	1	Mortality	Residues	United Kingdom	WIIS, 2010
Ardea cinerea	Gray Heron	Bromadiolone	1	Mortality	Physical Symptoms	France	Berny et al., 1997
Ardea cinerea	Gray Heron	Bromadiolone	1	Mortality	Residues	Spain	Sánchez-Barbudo et al., 2012
Ardea herodias	Great Blue Heron	Bromadiolone	1	Mortality	Residues	United States	Erickson and Urban, 2004
Ardeidae spp.	Heron spp.	Brodifacoum, Difenacoum	1	Mortality	Residues	Scotland	WIIS, 2012
Bubulcus ibis	Cattle Egret	Brodifacoum	5	Mortality	Residues	Seychelles	Merton et al., 2002

Gallirallus australis	Weka	Brodifacoum	1	Exposure	Residues	New Zealand	Spurr et al., 2005
Gallirallus australis	Weka	Brodifacoum	1	Mortality	Residues	New Zealand	Stephenson et al., 1999
Aramides cajaneus	Gray-cowled Wood-Rail	Brodifacoum, Difenacoum	2	Mortality	Physical Symptoms	Spain	Hernandez-Moreno et al., 2013
Zapornia atra	Henderson Island Crake	Brodifacoum	21	Mortality	Both	United Kingdom	in Oppel et al., 2016
Zapornia tabuensis	Spottless Crake	Brodifacoum	1	Mortality	Residues	New Zealand	Veitch and Clout, 2002
Porphyrio porphyrio	Western Swamphen	Bromadiolone	1	Mortality	Physical Symptoms	Australia	in Reece et al., 1985
Porphyrio melanotus	Australasian Swamphen	Brodifacoum	9	Mortality	Residues	New Zealand	Dowding et al., 1999
Porphyrio melanotus	Australasian Swamphen	Brodifacoum	5	Mortality	Residues	New Zealand	Fisher et al., 2011
Porphyrio melanotus	Australasian Swamphen	Brodifacoum	4	Mortality	Physical Symptoms	New Zealand	Veitch and Clout, 2002
Gallinula chloropus	Eurasian Moorhen	Warfarin	1	Mortality	Physical Symptoms	United Kingdom	WIIS, 1998
Fulica atra	Eurasian Coot	Brodifacoum, Bromadiolone	3	Mortality	Residues	France	Lambert et al., 2007
Anthropoides virgo	Demoiselle Crane	Bromadiolone	149	Mortality	N/A	Mongolia	in Dolgormaa, 2004
Himantopus himantopus	Pied Stilt	Brodifacoum	3	Mortality	Residues	New Zealand	Dowding et al., 2006
Pluvialis fulva	Pacific Golden-Plover	Brodifacoum	4	Mortality	Residues	United States	Pitt et al., 2015
Vanellus spinosus	Spur-winged Plover	Brodifacoum	1	Mortality	Residues	New Zealand	Dowding et al., 2006
Charadrius obscurus	Red-breasted Dotterel	Brodifacoum	4	Mortality	Residues	New Zealand	Dowding et al., 2006
Numenius phaeopus	Whimbrel	Brodifacoum	2	Mortality	Residues	Seychelles	Merton et al., 2002
Numenius tahitiensis	Bristle-thighed Curlew	Brodifacoum	10	Mortality	Residues	United States	Pitt et al., 2015
Arenaria interpres	Ruddy Turnstone	Brodifacoum	72	Mortality	Residues	Seychelles	Merton et al., 2002
Arenaria interpres	Ruddy Turnstone	Brodifacoum	4	Mortality	Residues	United States	Pitt et al., 2015
Calidris ptilocnemis	Rock Sandpiper	Brodifacoum	2	Exposure	Residues	United States	Ebbert and Burek-Huntington, 2010
Tringa incana	Wandering Tattler	Brodifacoum	2	Mortality	Residues	United States	Pitt et al., 2015
Stercorarius antarcticus	Brown Skua	Brodifacoum	40	Mortality	Residues	New Zealand	Torr, 2002
Chroicocephalus bulleri	Black-billed Gull	Brodifacoum	1	Mortality	Residues	New Zealand	Spurr et al., 2005

Chroicocephalus bulleri and Chroicocephalus scopulinus	Black-billed and Red-billed Gull	Brodifacoum	10	Mortality	N/A	New Zealand	McClelland, 2011
Larus occidentalis	Western Gull	Brodifacoum	2	Mortality	Both	United States	Howald et al., 2009
Larus argentatus	Herring Gull	Bromadiolone	152	Mortality	N/A	Mongolia	in Dolgormaa, 2004
Larus argentatus	Herring Gull	Bromadiolone	1	Mortality	Residues	United Kingdom	WIIS, 2013
Larus michahellis	Yellow-legged Gull	Brodifacoum	273	Mortality	Residues	Spain	Mayol et al., 2012
Larus fuscus	Lesser Black-backed Gull	Bromadiolone	3	Mortality	Residues	Spain	Sánchez-Barbudo et al., 2012
Larus glaucescens	Glaucous-winged Gull	Brodifacoum	24	Mortality	Physical Symptoms	United States	Ebbert and Burek-Huntington, 2010
Larus dominicanus	Kelp Gull	Brodifacoum	9	Mortality	Residues	New Zealand	Dowding et al., 1999
Larus	Gull sp.	Bromadiolone	1	Mortality	Residues	United Kingdom	WIIS, 2015
Larus canus	Common Gull	Bromadiolone, Difenacoum	1	Mortality	Residues	United Kingdom	WIIS, 2016
Larus canus	Common Gull	Bromadiolone	1	Mortality	Residues	United Kingdom	WIIS, 2013
Columba livia	Rock Pigeon	Chlorophacinone	64	Mortality	Residues	Spain	Sánchez-Barbudo et al., 2012
Columba livia	Rock Pigeon	Brodifacoum, Diphacinone	2	Mortality	Residues	United States	Erickson and Urban, 2004
Columba palumbus	Common Wood-Pigeon	Brodifacoum, Bromadiolone	1	Exposure	Residues	United Kingdom	WIIS, 2010
Streptopelia decaocto	Eurasian Collared-Dove	Bromadiolone	1	Mortality	Residues	Spain	Sánchez-Barbudo et al., 2012
Streptopelia picturata	Madagascar Turtle-Dove	Brodifacoum	320	Mortality	Residues	Seychelles	Merton et al., 2002
Geopelia striata	Zebra Dove	Brodifacoum	545	Mortality	Residues	Seychelles	Merton et al., 2002
Columba livia domestica	Domestic Pigeon	Bromadiolone	2	Mortality	Physical Symptoms	Scotland	WIIS, 2005
Columba livia domestica	Domestic Pigeon	Chlorophacinone	3	Mortality	Residues	France	Berny et al., 1997
Zenaida macroura	Mourning Dove	Bromadiolone	1	Mortality	Residues	United States	Erickson and Urban, 2004
Clamator glandarius	Great Spotted Cuckoo	Chlorophacinone	1	Exposure	Residues	Spain	Sánchez-Barbudo et al., 2012
Nestor notabilis	Kea	Brodifacoum	1	Exposure	Physical Symptoms	New Zealand	Spurr et al., 2005
Nestor meridionalis	New Zealand Kaka	Brodifacoum	4	Mortality	Physical Symptoms	New Zealand	Empson and Miskelly, 1999

Nestor meridionalis	New Zealand Kaka	Brodifacoum	2	Mortality	Residues	New Zealand	Spurr et al., 2005
Alcedines	Kingfisher	Brodifacoum	1	Mortality	Suspected	New Zealand	Towns et al., 1993
Cyanoramphus novaezelandiae	Red-crowned Parakeet	Brodifacoum	1	Mortality	Residues	New Zealand	Ogilvie et al., 1997
Cyanoramphus novaezelandiae	Red-crowned Parakeet	Brodifacoum	1	Mortality	Physical Symptoms	New Zealand	Veitch and Clout, 2002
Cyanoramphus novaezelandiae	Kankariki	Brodifacoum	2	Mortality	Residues	New Zealand	Fisher et al., 2011
Prosthemadera novaeseelandiae	Tui	Brodifacoum	2	Mortality	Both	New Zealand	McClelland, 2002
Philesturnus rufusater	North Island Saddleback	Brodifacoum	1	Mortality	Residues	New Zealand	Stephenson et al., 1999
Philesturnus rufusater	North Island Saddleback	Brodifacoum	1	Mortality	Both	New Zealand	Veitch and Clout, 2002
Philesturnus rufusater	North Island Saddleback	Brodifacoum	9	Mortality	Residues	New Zealand	Towns et al., 1993
Notiomystis cincta	Stitchbird	Brodifacoum	1	Mortality	Residues	New Zealand	Stephenson et al., 1999
Notiomystis cincta	Stitchbird	Brodifacoum	2	Mortality	Residues	New Zealand	Murphy et al., 1999
Gymnorhina tibicen	Australian Magpie	Brodifacoum	2	Mortality	Residues	New Zealand	Dowding et al., 1999
Pica pica	Eurasian Magpie	Bromadiolone	1	Exposure	Residues	United Kingdom	WIIS, 2009
Pica pica	Eurasian Magpie	Brodifacoum, Difenacoum	2	Mortality	Residues	Finland	Koivisto et al., 2018
Corvus dauuricus	Daurian Jackdaw	Bromadiolone	20	Mortality	N/A	Mongolia	in Dolgormaa, 2004
Corvus brachyrhynchos	American Crow	Brodifacoum	1	Mortality	Physical Symptoms	United States	Stone et al., 1999
Corvus brachyrhynchos	American Crow	Brodifacoum	13	Mortality	Residues	United States	in Erickson and Urban, 2004
Corvus caurinus	Northwestern Crow	Brodifacoum	2	Exposure	Residues	Canada	Howald et al., 1999
Corvus corone	Carrion Crow	Brodifacoum, Difenacoum	4	Mortality	Residues	Finland	Koivisto et al., 2018
Corvus	Crow spp.	Bromadiolone, Difenacoum	1	Mortality	Residues	United Kingdom	WIIS, 2014
Corvus	Crow spp.	Bromadiolone	1	Mortality	Residues	United Kingdom	WIIS, 2010
Corvus	Crow spp.	Brodifacoum	4	Mortality	Residues	United States	Erickson and Urban, 2004
Corvus ossifragus	Fish Crow	Bromadiolone	1	Mortality	Residues	United States	Erickson and Urban, 2004
Corvus corax	Common Raven	Brodifacoum	13	Mortality	Both	Canada	Howald et al., 1999

Corvus corax	Common Raven	Brodifacoum	1	Mortality	Residues	United States	Erickson and Urban, 2004
Corvus corax	Common Raven	Brodifacoum	1	Mortality	Residues	United States	Howald et al., 2009
Corvus corax	Common Raven	Brodifacoum	1	Mortality	Physical Symptoms	United States	Stone et al., 1999
Corvus corax	Common Raven	Bromadiolone, Difenacoum	2	Mortality	Residues	United Kingdom	WIIS, 2013
Corvus mellori	Little Raven	Bromadiolone	1	Mortality	Residues	Australia	Reece et al., 1985
Petroica australis	New Zealand Robin	Brodifacoum	1	Mortality	Residues	New Zealand	Spurr et al., 2005
Melanocorypha calandra	Calandra Lark	Chlorophacinone	2	Mortality	Residues	Spain	Sánchez-Barbudo et al., 2012
Zosterops lateralis	Silver-Eye	Brodifacoum	1	Mortality	Residues	New Zealand	Brown, 1997
Zosterops lateralis	Silver-Eye	Brodifacoum	1	Mortality	Residues	New Zealand	Spurr et al., 2005
Copsychus sechellarum	Seychelles Magpie-Robin	Brodifacoum	1	Mortality	Residues	Seychelles	Thorsen et al., 2000
Turdus merula	Eurasian Blackbird	Brodifacoum	2	Mortality	Residues	New Zealand	Dowding et al., 1999
Turdus merula	Eurasian Blackbird	Brodifacoum	5	Mortality	Suspected	New Zealand	Towns et al., 1993
Turdus merula	Eurasian Blackbird	Brodifacoum	1	Mortality	Residues	New Zealand	Brown, 1997
Turdus merula	Eurasian Blackbird	Brodifacoum	1	Mortality	Physical Symptoms	New Zealand	McClelland, 2002
Turdus merula	Eurasian Blackbird	Brodifacoum	10	Mortality	Both	New Zealand	Torr, 2002
Turdus merula	Eurasian Blackbird	Brodifacoum	3	Mortality	Residues	New Zealand	Fisher et al., 2011
Turdus philomelos	Song Thrush	Brodifacoum	1	Mortality	Physical Symptoms	New Zealand	McClelland, 2002
Acridotheres tristis	Common Myna	Brodifacoum	3	Mortality	Residues	New Zealand	Dowding et al., 1999
Acridotheres tristis	Common Myna	Brodifacoum	175	Mortality	Residues	Seychelles	Merton et al., 2002
Sturnus vulgaris	European Starling	Bromadiolone	1	Mortality	Residues	Spain	Sánchez-Barbudo et al., 2012
Bombycilla garrulus	Bohemian Waxwing	Difenacoum	1	Mortality	Physical Symptoms	United Kingdom	WIIS, 2010
Calcarius lapponicus	Lapland Longspur	Brodifacoum	2	Mortality	Physical Symptoms	United States	Ebbert and Burek-Huntington, 2010
Oreothlypis celata	Orange-crowned Warbler	Brodifacoum	1	Mortality	Residues	United States	Howald et al., 2009
Passerella iliaca	Fox Sparrow	Brodifacoum	3	Mortality	Residues	United States	Howald et al., 2009
Zonotrichia leucophrys	White-crowned Sparrow	Brodifacoum	29	Mortality	Both	United States	Howald et al., 2009
Zonotrichia atricapilla	Golden-crowned Sparrow	Brodifacoum	6	Mortality	Both	United States	Howald et al., 2009

Melospiza melodia	Song Sparrow	Brodifacoum	1	Mortality	Residues	Canada	Elliott et al., 2014
Melospiza melodia	Song Sparrow	Brodifacoum	3	Mortality	Both	United States	Howald et al., 2009
Prunella modularis	Hedgesparrow	Brodifacoum	1	Mortality	Suspected	New Zealand	Towns et al., 1993
Pipilo maculatus	Spotted Towhee	Brodifacoum	1	Mortality	Residues	United States	Howald et al., 2009
Sturnella neglecta	Western Meadowlark	Brodifacoum	6	Mortality	Both	United States	Howald et al., 2009
Sturnella neglecta	Western Meadowlark	Chlorophacinone	1	Mortality	Both	United States	Vyas et al., 2013
Fringilla coelebs	Chaffinch	Brodifacoum	2	Mortality	Residues	New Zealand	Brown, 1997
Fringilla coelebs	Chaffinch	Brodifacoum	3	Mortality	Residues	New Zealand	Dowding et al., 1999
Fringilla coelebs	Chaffinch	Brodifacoum	1	Mortality	Residues	New Zealand	Stephenson et al., 1999
Fringilla coelebs	Chaffinch	Brodifacoum	1	Mortality	Physical Symptoms	New Zealand	Veitch and Clout, 2002
Fringilla coelebs	Chaffinch	Brodifacoum	3	Mortality	Suspected	New Zealand	Towns et al., 1993
Leucosticte tephrocotis	Gray-crowned Rosy-Finch	Brodifacoum	2	Mortality	Physical Symptoms	United States	Ebbert and Burek-Huntington, 2010
Haemorhous mexicanus	House Finch	Brodifacoum	2	Mortality	Both	United States	Howald et al., 2009
Acanthis flammea	Common Redpoll	Brodifacoum	10	Mortality	N/A	New Zealand	McClelland, 2011
Passer domesticus	House Sparrow	Brodifacoum	2	Mortality	Suspected	New Zealand	Towns et al., 1993
Foudia madagascariensis	Red Fody	Brodifacoum	250	Mortality	Residues	Seychelles	Merton et al., 2002
Foudia sechellarum	Seychelles Fody	Brodifacoum	25	Mortality	Residues	Seychelles	Merton et al., 2002
Plectrophenax nivalis	Snow Bunting	Brodifacoum	2	Mortality	Suspected	United States	Ebbert and Burek-Huntington, 2010

Appendix 2: Review of Literature for Non-targeted anticoagulant rodenticide poisoning in raptor birds

Scientific Name	Common Name	Rodenticide	No of Animals Poisoned	Incident Type	Residues/ Physical Symptoms	Location	Reference
Ninox novaeseelandiae	Morepork	Brodifacoum	14	Mortality	Residues	New Zealand	Fisher et al., 2011
Ninox novaeseelandiae	Morepork	Brodifacoum	1	Mortality	Physical Symptoms	New Zealand	Empson and Miskelly, 1999
Ninox novaeseelandiae	Morepork	Brodifacoum	1	Mortality	Physical Symptoms	New Zealand	McClelland, 2002
Ninox novaeseelandiae	Morepork	Brodifacoum	2	Mortality	Residues	New Zealand	Spurr et al., 2005
Ninox novaeseelandiae	Morepork	Brodifacoum	12	Mortality	Residues	New Zealand	Stephenson et al., 1999
Ninox novaeseelandiae	Morepork	Brodifacoum	1	Mortality	Residues	New Zealand	Ogilvie et al., 1997
Ninox novaeseelandiae	Morepork	Brodifacoum	1	Mortality	Suspected	New Zealand	Towns et al., 1993
Ninox novaeseelandiae	Morepork	Brodifacoum	1	Mortality	Residues	New Zealand	Murphy et al., 1998
Aquila sp.	Eagle	Chlorophacinone	1	Mortality	Residues	France	Berny et al., 1997
Haliaeetus leucocephalus	Bald Eagle	Brodifacoum	18	Mortality	Physical Symptoms	United States	Ebbert and Burek-Huntington, 2010
Haliaeetus leucocephalus	Bald Eagle	Multiple Rodenticides	3	Mortality	Both	United States	Erickson and Urban, 2004
Haliaeetus leucocephalus	Bald Eagle	Warfarin	1	Mortality	Physical Symptoms	United States	Stone et al., 1999
Haliaeetus leucocephalus	Bald Eagle	Brodifacoum	23	Mortality	Residues	Canada	Howald et al., 1999
Aquila chrysaetos	Golden Eagle	Multiple Rodenticides	1	Mortality	Residues	Scotland	WIIS, 2012
Aquila chrysaetos	Golden Eagle	Multiple Rodenticides	2	Mortality	Residues	United Kingdom	WIIS, 2015
Aquila chrysaetos	Golden Eagle	Multiple Rodenticides	3	Mortality	Residues	United Kingdom	WIIS, 2018
Aquila chrysaetos	Golden Eagle	Difenacoum	2	Mortality	Residues	United Kingdom	WIIS, 2014
Aquila chrysaetos	Golden Eagle	Brodifacoum	2	Mortality	Residues	United Kingdom	WIIS, 2013
Aquila chrysaetos	Golden Eagle	Bromadiolone	1	Mortality	Residues	United Kingdom	WIIS, 2011

Aquila chrysaetos	Golden Eagle	Difenacoum	1	Mortality	Residues	United Kingdom	WIIS, 2009
Aquila chrysaetos	Golden Eagle	Flocoumafen	1	Mortality	Residues	Spain	Sánchez-Barbudo et al., 2012
Aquila chrysaetos	Golden Eagle	Brodifacoum	13	Mortality	Residues	United States	Erickson and Urban, 2004
Aquila chrysaetos	Golden Eagle	Brodifacoum	1	Mortality	Physical Symptoms	United States	Stone et al., 1999
Aquila chrysaetos	Golden Eagle	Multiple Rodenticides	2	Mortality	Residues	Norway	Langford et al., 2013
Haliaeetus	Sea Eagle	Bromadiolone	1	Mortality	Residues	Scotland	WIIS, 2012
Haliaeetus albicilla	White-tailed eagle	Bromadiolone	1	Mortality	Residues	Scotland	WIIS, 2005
Haliaeetus albicilla	White-tailed eagle	Multiple Rodenticides	1	Mortality	Residues	United Kingdom	WIIS, 2014
Haliaeetus albicilla	White-tailed eagle	Bromadiolone	1	Mortality	Residues	United Kingdom	WIIS, 2013
Haliaeetus albicilla	White-tailed eagle	Multiple Rodenticides	3	Mortality	Residues	United Kingdom	WIIS, 2011
Haliaeetus albicilla	White-tailed eagle	Bromadiolone	1	Mortality	Residues	United Kingdom	WIIS, 2009
Circaetus gallicus	Short-tailed Snake-Eagle	Multiple Rodenticides	1	Mortality	Residues	Spain	Sánchez-Barbudo et al., 2012
Aquila adalberti	Spanish Imperial Eagle	Difenacoum	1	Mortality	Residues	Spain	Sánchez-Barbudo et al., 2012
Falco peregrinus	Peregrine Falcon	Brodifacoum	1	Mortality	Physical Symptoms	United States	Ebbert and Burek-Huntington, 2010
Falco peregrinus	Peregrine Falcon	Multiple Rodenticides	1	Mortality	Residues	Scotland	WIIS, 2012
Falco peregrinus	Peregrine Falcon	Bromadiolone	1	Mortality	Residues	United Kingdom	WIIS, 2015
Falco peregrinus	Peregrine Falcon	Multiple Rodenticides	2	Mortality	Residues	United Kingdom	WIIS, 2018
Falco peregrinus	Peregrine Falcon	Bromadiolone	1	Mortality	Residues	United Kingdom	WIIS, 2016
Falco peregrinus	Peregrine Falcon	Multiple Rodenticides	2	Mortality	Residues	United Kingdom	WIIS, 2014
Falco peregrinus	Peregrine Falcon	Multiple Rodenticides	2	Mortality	Residues	United Kingdom	WIIS, 2011
Falco peregrinus	Peregrine Falcon	Bromadiolone	1	Mortality	Residues	United Kingdom	WIIS, 2010
Falco peregrinus	Peregrine Falcon	Multiple Rodenticides	1	Mortality	Residues	United Kingdom	WIIS, 2009
Falco peregrinus	Peregrine Falcon	Warfarin	1	Mortality	Residues	United States	Erickson and Urban, 2004
Falco peregrinus	Peregrine Falcon	Warfarin	1	Mortality	Both	United States	Stone et al., 1999
Falco peregrinus	Peregrine Falcon	Multiple Rodenticides	16	Mortality	Residues	Spain	Ruiz-Suārez et al., 2014
Falco cherrug	Saker Falcon	Bromadiolone	2	Mortality	N/A	Mongolia	in Dolgormaa, 2004

Milvus milvus	Red Kite	Multiple Rodenticides	2	Mortality	Both	United Kingdom	WIIS, 1998
Milvus milvus	Red Kite	Multiple Rodenticides	6	Mortality	Both	Scotland	WIIS, 2005
Milvus milvus	Red Kite	Multiple Rodenticides	8	Both	Both	Scotland	WIIS, 2012
Milvus milvus	Red Kite	Multiple Rodenticides	2	Mortality	Both	United Kingdom	WIIS, 2015
Milvus milvus	Red Kite	Multiple Rodenticides	1	Mortality	Both	United Kingdom	WIIS, 2018
Milvus milvus	Red Kite	Multiple Rodenticides	2	Mortality	Residues	United Kingdom	WIIS, 2017
Milvus milvus	Red Kite	Multiple Rodenticides	5	Mortality	Residues	United Kingdom	WIIS, 2016
Milvus milvus	Red Kite	Multiple Rodenticides	2	Mortality	Residues	United Kingdom	WIIS, 2014
Milvus milvus	Red Kite	Multiple Rodenticides	5	Mortality	Residues	United Kingdom	WIIS, 2013
Milvus milvus	Red Kite	Multiple Rodenticides	7	Mortality	Both	United Kingdom	WIIS, 2011
Milvus milvus	Red Kite	Multiple Rodenticides	9	Mortality	Both	United Kingdom	WIIS, 2010
Milvus milvus	Red Kite	Multiple Rodenticides	3	Mortality	Residues	United Kingdom	WIIS, 2009
Milvus milvus	Red Kite	Difenacoum	2	Mortality	Residues	United Kingdom	WIIS, 2008
Milvus milvus	Red Kite	Multiple Rodenticides	7	Mortality	Residues	Spain	Sánchez-Barbudo et al., 2012
Milvus milvus	Red Kite	Multiple Rodenticides	3	Mortality	Residues	Denmark	Christensen et al., 2012
Milvus milvus	Red Kite	Multiple Rodenticides	17	Mortality	Residues	United Kingdom	Walker et al., 2013
Milvus milvus	Red Kite	Multiple Rodenticides	23	Mortality	Residues	United Kingdom	Walker et al. , 2008
Milvus migrans	Black Kite	Bromadiolone	2	Mortality	N/A	Mongolia	in Dolgormaa, 2004
Milvus migrans	Black Kite	Bromadiolone	5	Mortality	Residues	France	Berny et al., 1997
Milvus migrans	Black Kite	Brodifacoum	3	Mortality	Residues	Spain	Sánchez-Barbudo et al., 2012
Buteo buteo	Buzzard	Difenacoum	1	Mortality	Residues	United Kingdom	WIIS, 1998
Buteo buteo	Buzzard	Bromadiolone	15	Mortality	Physical Symptoms	France	Berny et al., 1997
Buteo buteo	Buzzard	Chlorophacinone	6	Mortality	Physical Symptoms	France	Berny et al., 1997
Buteo buteo	Buzzard	Multiple Rodenticides	18	Mortality	Residues	Scotland	WIIS, 2012
Buteo buteo	Buzzard	Multiple Rodenticides	22	Mortality	Residues	Scotland	WIIS, 2005
Buteo buteo	Buzzard	Multiple Rodenticides	35	Mortality	Both	United Kingdom	WIIS, 2015
Buteo buteo	Buzzard	Multiple Rodenticides	11	Mortality	Both	United Kingdom	WIIS, 2018
Buteo buteo	Buzzard	Multiple Rodenticides	17	Mortality	Both	United Kingdom	WIIS, 2017
Buteo buteo	Buzzard	Multiple Rodenticides	35	Mortality	Residues	United Kingdom	WIIS, 2016
Buteo buteo	Buzzard	Multiple Rodenticides	20	Mortality	Residues	United Kingdom	WIIS, 2014

Buteo buteo	Buzzard	Multiple Rodenticides	38	Mortality	Both	United Kingdom	WIIS, 2013
Buteo buteo	Buzzard	Multiple Rodenticides	20	Mortality	Both	United Kingdom	WIIS, 2011
Buteo buteo	Buzzard	Multiple Rodenticides	36	Mortality	Both	United Kingdom	WIIS, 2010
Buteo buteo	Buzzard	Multiple Rodenticides	19	Mortality	Residues	United Kingdom	WIIS, 2009
Buteo buteo	Buzzard	Multiple Rodenticides	27	Mortality	Both	United Kingdom	WIIS, 2008
Buteo buteo	Buzzard	Multiple Rodenticides	5	Mortality	Residues	Spain	Sánchez-Barbudo et al., 2012
Buteo buteo	Buzzard	Multiple Rodenticides	10	Mortality	Residues	France	Lambert et al., 2007
Buteo buteo	Buzzard	Multiple Rodenticides	133	Mortality	Residues	Denmark	Christensen et al., 2012
Buteo buteo	Buzzard	Multiple Rodenticides	36	Mortality	Residues	Spain	López-Perea et al., 2015
Buteo buteo	Buzzard	Multiple Rodenticides	9	Mortality	Residues	Spain	Ruiz-Suārez et al., 2014
Buteo hemilasius	Upland Buzzard	Bromadiolone	2	Mortality	N/A	Mongolia	in Dolgormaa, 2004
Buteo lagopus	Rough-legged Buzzard	Multiple Rodenticides	26	Mortality	Residues	Denmark	Christensen et al., 2012
Strix aluco	Tawny Owl	Flocoumafen	1	Mortality	Residues	United Kingdom	WIIS, 1998
Strix aluco	Tawny Owl	Multiple Rodenticides	2	Mortality	Residues	Scotland	WIIS, 2005
Strix aluco	Tawny Owl	Bromadiolone	1	Mortality	Residues	Scotland	WIIS, 2012
Strix aluco	Tawny Owl	Multiple Rodenticides	5	Mortality	Residues	United Kingdom	WIIS, 2015
Strix aluco	Tawny Owl	Brodifacoum	1	Mortality	Residues	United Kingdom	WIIS, 2018
Strix aluco	Tawny Owl	Multiple Rodenticides	2	Mortality	Residues	United Kingdom	WIIS, 2017
Strix aluco	Tawny Owl	Brodifacoum	1	Mortality	Residues	United Kingdom	WIIS, 2016
Strix aluco	Tawny Owl	Multiple Rodenticides	2	Mortality	Residues	United Kingdom	WIIS, 2014
Strix aluco	Tawny Owl	Bromadiolone	1	Mortality	Residues	United Kingdom	WIIS, 2013
Strix aluco	Tawny Owl	Multiple Rodenticides	3	Mortality	Residues	United Kingdom	WIIS, 2011
Strix aluco	Tawny Owl	Bromadiolone	1	Mortality	Residues	United Kingdom	WIIS, 2010
Strix aluco	Tawny Owl	Multiple Rodenticides	2	Mortality	Residues	United Kingdom	WIIS, 2009
Strix aluco	Tawny Owl	Bromadiolone	1	Mortality	Residues	United Kingdom	WIIS, 2008
Strix aluco	Tawny Owl	Bromadiolone	2	Mortality	Residues	France	Lambert et al., 2007
Strix aluco	Tawny Owl	Multiple Rodenticides	41	Mortality	Residues	Denmark	Christensen et al., 2012
Strix aluco	Tawny Owl	Multiple Rodenticides	21	Mortality	Residues	Spain	López-Perea et al., 2015
Strix aluco	Tawny Owl	Multiple Rodenticides	9	Mortality	Residues	Finland	Koivisto et al., 2018
Falco tinnunculus	Kestrel	Multiple Rodenticides	1	Mortality	Residues	Scotland	WIIS, 2005

Falco tinnunculus	Kestrel	Multiple Rodenticides	2	Mortality	Residues	United Kingdom	WIIS, 2015
Falco tinnunculus	Kestrel	Bromadiolone	1	Mortality	Residues	United Kingdom	WIIS, 2018
Falco tinnunculus	Kestrel	Multiple Rodenticides	2	Mortality	Residues	United Kingdom	WIIS, 2017
Falco tinnunculus	Kestrel	Bromadiolone	1	Mortality	Residues	United Kingdom	WIIS, 2016
Falco tinnunculus	Kestrel	Multiple Rodenticides	2	Mortality	Residues	United Kingdom	WIIS, 2014
Falco tinnunculus	Kestrel	Bromadiolone	1	Mortality	Residues	United Kingdom	WIIS, 2011
Falco tinnunculus	Kestrel	Multiple Rodenticides	1	Mortality	Residues	United Kingdom	WIIS, 2010
Falco tinnunculus	Kestrel	Multiple Rodenticides	2	Mortality	Both	United Kingdom	WIIS, 2008
Falco tinnunculus	Kestrel	Multiple Rodenticides	3	Mortality	Residues	France	Lambert et al., 2007
Falco tinnunculus	Kestrel	Multiple Rodenticides	59	Mortality	Residues	Denmark	Christensen et al., 2012
Falco tinnunculus	Kestrel	Multiple Rodenticides	21	Mortality	Residues	Spain	Ruiz-Suārez et al., 2014
Falco tinnunculus	Kestrel	Multiple Rodenticides	20	Mortality	Residues	United Kingdom	Walker et al., 2013
Falco sparverius	American Kestrel	Bromadiolone	1	Mortality	Residues	United States	Erickson and Urban, 2004
Falco sparverius	American Kestrel	Brodifacoum	1	Mortality	Residues	United States	Howald et al., 2009
Tyto alba	Barn Owl	Multiple Rodenticides	2	Mortality	Both	Scotland	WIIS, 2005
Tyto alba	Barn Owl	Chlorophacinone	1	Mortality	Residues	France	Berny et al., 1997
Tyto alba	Barn Owl	Multiple Rodenticides	2	Mortality	Both	United Kingdom	WIIS, 2015
Tyto alba	Barn Owl	Multiple Rodenticides	1	Mortality	Residues	United Kingdom	WIIS, 2018
Tyto alba	Barn Owl	Multiple Rodenticides	1	Mortality	Residues	United Kingdom	WIIS, 2017
Tyto alba	Barn Owl	Multiple Rodenticides	1	Mortality	Residues	United Kingdom	WIIS, 2016
Tyto alba	Barn Owl	Bromadiolone	1	Mortality	Residues	United Kingdom	WIIS, 2011
Tyto alba	Barn Owl	Multiple Rodenticides	4	Mortality	Both	United Kingdom	WIIS, 2010
Tyto alba	Barn Owl	Difenacoum	1	Mortality	Residues	United Kingdom	WIIS, 2009
Tyto alba	Barn Owl	Multiple Rodenticides	3	Mortality	Residues	United Kingdom	WIIS, 2008
Tyto alba	Barn Owl	Multiple Rodenticides	3	Mortality	Residues	Spain	Sánchez-Barbudo et al., 2012
Tyto alba	Barn Owl	Multiple Rodenticides	8	Mortality	Residues	United States	Erickson and Urban, 2004
Tyto alba	Barn Owl	Multiple Rodenticides	7	Mortality	Residues	France	Lambert et al., 2007
Tyto alba	Barn Owl	Brodifacoum	1	Mortality	Residues	United States	Howald et al., 2009
Tyto alba	Barn Owl	Multiple Rodenticides	75	Mortality	Residues	Denmark	Christensen et al., 2012
Tyto alba	Barn Owl	Multiple Rodenticides	28	Mortality	Residues	Spain	López-Perea et al., 2015
Tyto alba	Barn Owl	Multiple Rodenticides	21	Mortality	Residues	Spain	Ruiz-Suārez et al., 2014

Tyto alba	Barn Owl	Multiple Rodenticides	49	Mortality	Residues	United Kingdom	Walker et al., 2013
Tyto alba	Barn Owl	Multiple Rodenticides	49	Mortality	Both	Canada	Albert et al., 2010
Asio otus	Long-eared Owl	Difenacoum	1	Mortality	Residues	United Kingdom	WIIS, 2018
Asio otus	Long-eared Owl	Bromadiolone	1	Mortality	Residues	United Kingdom	WIIS, 2013
Asio otus	Long-eared Owl	Brodifacoum	1	Mortality	Residues	United States	Erickson and Urban, 2004
Asio otus	Long-eared Owl	Multiple Rodenticides	36	Mortality	Residues	Denmark	Christensen et al., 2012
Asio otus	Long-eared Owl	Multiple Rodenticides	7	Mortality	Residues	Spain	López-Perea et al., 2015
Asio otus	Long-eared Owl	Multiple Rodenticides	23	Mortality	Residues	Spain	Ruiz-Suārez et al., 2014
Athene noctua	Little Owl	Difenacoum	1	Mortality	Residues	Spain	Sánchez-Barbudo et al., 2012
Athene noctua	Little Owl	Multiple Rodenticides	9	Mortality	Residues	Denmark	Christensen et al., 2012
Athene noctua	Little Owl	Multiple Rodenticides	5	Mortality	Residues	Spain	López-Perea et al., 2015
Bubo virginianus	Great Horned Owl	Multiple Rodenticides	51	Mortality	Both	United States	Erickson and Urban, 2004
Bubo virginianus	Great Horned Owl	Multiple Rodenticides	13	Mortality	Physical Symptoms	United States	Stone et al., 1999
Bubo virginianus	Great Horned Owl	Multiple Rodenticides	43	Mortality	Both	Canada	Albert et al., 2010
Bubo virginianus	Great Horned Owl	Multiple Rodenticides	123	Mortality	Residues	Canada	Thomas et al., 2011
Bubo virginianus	Great Horned Owl	Multiple Rodenticides	22	Mortality	Residues	United States	Stansley et al., 2014
Megascops asio	Eastern Screech Owl	Multiple Rodenticides	9	Mortality	Residues	United States	Erickson and Urban, 2004
Megascops asio	Eastern Screech Owl	Brodifacoum	2	Mortality	Physical Symptoms	United States	Stone et al., 1999
Strix occidentalis caurina	Northern Spotted Owl	Brodifacoum	2	Mortality	Residues	United States	Erickson and Urban, 2004
Strix occidentalis caurina	Northern Spotted Owl	Brodifacoum	1	Mortality	Residues	United States	Franklin et al., 2018
Aegolius acadicus	Northern Saw-whet Owl	Bromadiolone	1	Mortality	Residues	United States	Erickson and Urban, 2004
Strix varia	Barred Owl	Diphacinone	1	Mortality	Residues	United States	Erickson and Urban, 2004
Strix varia	Barred Owl	Multiple Rodenticides	23	Mortality	Both	Canada	Albert et al., 2010
Bubo scandiacus	Snowy Owl	Diphacinone	1	Mortality	Residues	United States	Erickson and Urban, 2004
Bubo scandiacus	Snowy Owl	Diphacinone	1	Mortality	Physical Symptoms	United States	Stone et al., 1999
Athene cunicularia	Burrowing Owl	Brodifacoum	2	Mortality	Residues	United States	Howald et al., 2009
Bubo bubo	Eurasian Eagle Owl	Multiple Rodenticides	4	Mortality	Residues	Spain	Sánchez-Barbudo et al., 2012

Bubo bubo	Eagle Owl	Multiple Rodenticides	10	Mortality	Residues	Denmark	Christensen et al., 2012
Bubo bubo	Eagle Owl	Multiple Rodenticides	14	Mortality	Residues	Spain	López-Perea et al., 2015
Bubo bubo	Eagle Owl	Multiple Rodenticides	5	Mortality	Residues	Norway	Langford et al., 2013
Bubo bubo	Eagle Owl	Multiple Rodenticides	17	Mortality	Residues	Finland	Koivisto et al., 2018
Asio flammeus	Short-eared Owl	Multiple Rodenticides	5	Mortality	Residues	Denmark	Christensen et al., 2012
Otus	Scops Owl	Multiple Rodenticides	16	Mortality	Residues	Spain	López-Perea et al., 2015
Circus pygargus	Harrier	Bromadiolone	1	Mortality	Residues	France	Berny et al., 1997
Circus approximans	Australian Harrier	Brodifacoum	2	Mortality	Residues	New Zealand	Dowding et al., 1999
Circus approximans	Australian Harrier	Brodifacoum	1	Mortality	Residues	New Zealand	Fisher et al., 2011
Circus cyaneus	Hen Harrier	Multiple Rodenticides	1	Mortality	Residues	United Kingdom	WIIS, 2018
Circus aeruginosus	Marsh Harrier	Difenacoum	1	Mortality	Residues	United Kingdom	WIIS, 2016
Circus aeruginosus	Marsh Harrier	Multiple Rodenticides	3	Mortality	Residues	Denmark	Christensen et al., 2012
Accipiter nisus	Sparrowhawk	Multiple Rodenticides	1	Mortality	Residues	Scotland	WIIS, 2012
Accipiter nisus	Sparrowhawk	Multiple Rodenticides	2	Mortality	Residues	Scotland	WIIS, 2005
Accipiter nisus	Sparrowhawk	Multiple Rodenticides	7	Mortality	Both	United Kingdom	WIIS, 2015
Accipiter nisus	Sparrowhawk	Difenacoum	3	Mortality	Residues	United Kingdom	WIIS, 2018
Accipiter nisus	Sparrowhawk	Bromadiolone	1	Mortality	Residues	United Kingdom	WIIS, 2017
Accipiter nisus	Sparrowhawk	Bromadiolone	10	Mortality	Residues	United Kingdom	WIIS, 2016
Accipiter nisus	Sparrowhawk	Multiple Rodenticides	4	Mortality	Residues	United Kingdom	WIIS, 2014
Accipiter nisus	Sparrowhawk	Multiple Rodenticides	6	Mortality	Residues	United Kingdom	WIIS, 2011
Accipiter nisus	Sparrowhawk	Multiple Rodenticides	9	Mortality	Residues	United Kingdom	WIIS, 2010
Accipiter nisus	Sparrowhawk	Multiple Rodenticides	3	Mortality	Residues	United Kingdom	WIIS, 2008
Accipiter nisus	Sparrowhawk	Multiple Rodenticides	94	Mortality	Residues	United Kingdom	Walker et al., 2015
Accipiter nisus	Sparrowhawk	Multiple Rodenticides	14	Mortality	Residues	Spain	Ruiz-Suārez et al., 2014
Parabuteo unicinctus	Harris Hawk	Multiple Rodenticides	1	Mortality	Residues	United Kingdom	WIIS, 2015
Accipiter	Goshawk sp.	Multiple Rodenticides	1	Mortality	Residues	United Kingdom	WIIS, 2016
Accipiter	Goshawk sp.	Multiple Rodenticides	2	Mortality	Residues	Finland	Koivisto et al., 2018
Accipiter gentilis	Northern Gooshawk	Brodifacoum	1	Mortality	Residues	Spain	Sánchez-Barbudo et al., 2012
Buteo jamaicensis	Red-tailed Hawk	Multiple Rodenticides	49	Mortality	Both	United States	Erickson and Urban, 2004
Buteo jamaicensis	Red-tailed Hawk	Brodifacoum	1	Mortality	Residues	United States	Howald et al., 2009
Buteo jamaicensis	Red-tailed Hawk	Multiple Rodenticides	101	Mortality	Residues	United States	Stansley et al., 2014

Buteo jamaicensis	Red-tailed Hawk	Multiple Rodenticides	58	Mortality	Residues	Canada	Thomas et al., 2011
Buteo lineatus	Red-shouldered Hawk	Multiple Rodenticides	5	Mortality	Residues	United States	Erickson and Urban, 2004
Buteo lineatus	Red-shouldered Hawk	Brodifacoum	7	Mortality	Physical Symptoms	United States	Stone et al., 1999
Accipiter cooperii	Cooper's Hawk	Brodifacoum	8	Mortality	Residues	United States	Erickson and Urban, 2004
Accipiter striatus	Sharp-shinned Hawk	Brodifacoum	2	Mortality	Residues	United States	Erickson and Urban, 2004
Buteo swainschi	Swainson's Hawk	Chlorophacinone	1	Mortality	Suspected	Canada	Proulx, 2010
Pandion haliaetus	Osprey	Difenacoum	1	Mortality	Residues	United Kingdom	WIIS, 2008
Ninox boobook	Boobook	Multiple Rodenticides	52	Mortality	Residues	New Zealand	Lohr, 2018
Gypaetus barbatus	Beared Vulture	Bromadiolone	1	Mortality	Residues	Spain	Sánchez-Barbudo et al., 2012
Coragyps atratus	Black Vulture	Brodifacoum	1	Mortality	Residues	United States	Erickson and Urban, 2004
Cathartes aura	Turkey Vulture	Multiple Rodenticides	2	Mortality	Residues	United States	Erickson and Urban, 2004
Gyps fulvus	Eurasian Griffon	Multiple Rodenticides	3	Mortality	Residues	Spain	Sánchez-Barbudo et al., 2012

Appendix 3: Review of Literature for Non-targeted anticoagulant rodenticide poisoning in mammals

Scientific Name	Common Name	Rodenticide	No of Animals Poisoned	Incident Type	Residues/ Physical Symptoms	Location	Reference
Sciurus carolinensi	Grey Squirrel	Multiple Rodenticides	1	Mortality	Residues	United Kingdom	WIIS, 1998
Sciurus carolinensi	Grey Squirrel	Multiple Rodenticides	1	Mortality	Physical Symptoms	Scotland	WIIS, 2005
Sciurus carolinensi	Grey Squirrel	Multiple Rodenticides	60	Mortality	Residues	United States	Erickson and Urban, 2004
Sciurus carolinensi	Grey Squirrel	Multiple Rodenticides	8	Mortality	Physical Symptoms	United States	Stone et al., 1999
Sciurus niger	Fox Squirrel	Brodifacoum	8	Mortality	Residues	United States	Erickson and Urban, 2004
Tamias striatus	Eastern Chipmunck	Brodifacoum	4	Mortality	Residues	United States	Erickson and Urban, 2004
Tamias striatus	Eastern Chipmunck	Brodifacoum	1	Mortality	Physical Symptoms	United States	Stone et al., 1999
Canus familiaris	Dog	Multiple Rodenticides	8	Mortality	Residues	United Kingdom	WIIS, 1998
Canus familiaris	Dog	Bromadiolone	9	Exposure	Residues	Scotland	WIIS, 2005
Canus familiaris	Dog	Multiple Rodenticides	6	Both	Both	Scotland	WIIS, 2012
Canus familiaris	Dog	Multiple Rodenticides	2 (2)	Mortality	Both	United Kingdom	WIIS, 2015
Canus familiaris	Dog	Multiple Rodenticides	2 (1)	Mortality	Both	United Kingdom	WIIS, 2018
Canus familiaris	Dog	Bromadiolone	2 (2)	Mortality	Both	United Kingdom	WIIS, 2017
Canus familiaris	Dog	Multiple Rodenticides	2 (3)	Mortality	Both	United Kingdom	WIIS, 2016
Canus familiaris	Dog	Multiple Rodenticides	2	Mortality	Residues	United Kingdom	WIIS, 2014
Canus familiaris	Dog	Multiple Rodenticides	2	Both	Residues	United Kingdom	WIIS, 2013
Canus familiaris	Dog	Brodifacoum	1(1)	Both	Both	United Kingdom	WIIS, 2011
Canus familiaris	Dog	Multiple Rodenticides	4 (2)	Mortality	Both	United Kingdom	WIIS, 2010
Canus familiaris	Dog	Multiple Rodenticides	3 (2)	Mortality	Both	United Kingdom	WIIS, 2009
Canus familiaris	Dog	Multiple Rodenticides	4 (1)	Mortality	Both	United Kingdom	WIIS, 2008
Canus familiaris	Dog	Multiple Rodenticides	4	Mortality	Residues	Spain	Sánchez-Barbudo et al., 2012
Felis catus	Cat	Multiple Rodenticides	3	Mortality	Residues	United Kingdom	WIIS, 1998
Felis catus	Cat	Chlorophacinone	1	Mortality	Residues	Scotland	WIIS, 2005
Felis catus	Cat	Multiple Rodenticides	4	Mortality	Residues	United Kingdom	WIIS, 2018
Felis catus	Cat	Coumatetryl	1(1)	Mortality	Both	United Kingdom	WIIS, 2016

Felis catus	Cat	Multiple Rodenticides	3	Mortality	Residues	United Kingdom	WIIS, 2014
Felis catus	Cat	Bromadiolone	1(1)	Mortality	Both	United Kingdom	WIIS, 2013
Felis catus	Cat	Bromadiolone	1	Mortality	Residues	United Kingdom	WIIS, 2010
Felis catus	Cat	Multiple Rodenticides	2	Mortality	Residues	United Kingdom	WIIS, 2009
Felis catus	Cat	Multiple Rodenticides	3	Mortality	Residues	Spain	Sánchez-Barbudo et al., 2012
Felis catus	Cat	Brodifacoum	8	Mortality	Residues	Seychelles	Merton et al., 2002
Felis catus	Cat	Brodifacoum	45	Mortality	Residues	New Zealand	Spurr et al., 2005
Felis catus	Cat	Brodifacoum	2	Mortality	Residues	New Zealand	Murphy et al., 1998
Felis catus	Cat	Multiple Rodenticides	4	Mortality	Residues	Finland	Koivisto et al., 2018
Felis manul	Manular Cat	Bromadiolone	2	Mortality	N/A	Mongolia	in Dolgormaa, 2004
Meles meles	Badger	Bromadiolone	5	Mortality	Physical Symptoms	United Kingdom	WIIS, 1998
Meles meles	Badger	Multiple Rodenticides	1	Mortality	Physical Symptoms	Scotland	WIIS, 2005
Meles meles	Badger	Bromadiolone	1	Mortality	Residues	France	Berny et al., 1997
Meles meles	Badger	Multiple Rodenticides	1	Mortality	Residues	Scotland	WIIS, 2012
Meles meles	Badger	Multiple Rodenticides	1	Mortality	Residues	United Kingdom	WIIS, 2018
Meles meles	Badger	Multiple Rodenticides	2	Mortality	Residues	United Kingdom	WIIS, 2017
Meles meles	Badger	Multiple Rodenticides	2 (1)	Mortality	Both	United Kingdom	WIIS, 2016
Meles meles	Badger	Bromadiolone	1	Mortality	Residues	United Kingdom	WIIS, 2014
Meles meles	Badger	Bromadiolone	1	Mortality	Physical Symptoms	United Kingdom	WIIS, 2013
Meles meles	Badger	Bromadiolone	1	Mortality	Residues	United Kingdom	WIIS, 2009
Meles meles	Badger	Multiple Rodenticides	3	Mortality	Residues	Finland	Koivisto et al., 2018
Vulpes vulpes	Red Fox	Multiple Rodenticides	2	Mortality	Physical Symptoms	United Kingdom	WIIS, 1998
Vulpes vulpes	Red Fox	Multiple Rodenticides	19	Mortality	Both	Scotland	WIIS, 2005
Vulpes vulpes	Red Fox	Multiple Rodenticides	29	Mortality	Physical Symptoms	France	Berny et al., 1997
Vulpes vulpes	Red Fox	Chlorophacinone	7	Mortality	Physical Symptoms	France	Berny et al., 1997
Vulpes vulpes	Red Fox	Multiple Rodenticides	8	Mortality	Residues	Scotland	WIIS, 2012
Vulpes vulpes	Red Fox	Multiple Rodenticides	6 (1)	Mortality	Both	United Kingdom	WIIS, 2015
Vulpes vulpes	Red Fox	Multiple Rodenticides	4	Mortality	Residues	United Kingdom	WIIS, 2018
Vulpes vulpes	Red Fox	Multiple Rodenticides	20	Mortality	Residues	United Kingdom	WIIS, 2017
Vulpes vulpes	Red Fox	Multiple Rodenticides	4 (1)	Mortality	Both	United Kingdom	WIIS, 2016
Vulpes vulpes	Red Fox	Bromadiolone	1	Mortality	Residues	United Kingdom	WIIS, 2014

Vulpes vulpes	Red Fox	Multiple Rodenticides	15	Mortality	Residues	United Kingdom	WIIS, 2013
Vulpes vulpes	Red Fox	Multiple Rodenticides	24 (10)	Mortality	Both	United Kingdom	WIIS, 2011
Vulpes vulpes	Red Fox	Multiple Rodenticides	2	Mortality	Physical Symptoms	United Kingdom	WIIS, 2010
Vulpes vulpes	Red Fox	Multiple Rodenticides	12	Mortality	Residues	Spain	Sánchez-Barbudo et al., 2012
Vulpes vulpes	Red Fox	Brodifacoum	5	Mortality	Residues	United States	Erickson and Urban, 2004
Vulpes vulpes	Red Fox	Brodifacoum	2	Mortality	Physical Symptoms	United States	Stone et al., 1999
Vulpes vulpes	Red Fox	Multiple Rodenticides	28	Mortality	Residues	Finland	Koivisto et al., 2018
Vulpes corsac	Corsac Fox	Bromadiolone	2	Mortality	N/A	Mongolia	in Dolgormaa, 2004
Vulpes macrotis (JUST KIT FOX)	San joaquin Kit Fox	Multiple Rodenticides	34	Mortality	Residues	United States	Erickson and Urban, 2004
Urocyon cinereoargenteus	Grey fox	Brodifacoum	3	Mortality	Residues	United States	Erickson and Urban, 2004
Lutra lutra	Otter	Multiple Rodenticides	3	Mortality	Both	Scotland	WIIS, 2005
Lutra lutra	Otter	Bromadiolone	1	Mortality	Residues	Scotland	WIIS, 2012
Lutra lutra	Otter	Bromadiolone	1	Mortality	Residues	United Kingdom	WIIS, 2015
Lutra lutra	Otter	Multiple Rodenticides	1	Mortality	Residues	United Kingdom	WIIS, 2013
Lutra lutra	Otter	Bromadiolone	1	Mortality	Residues	United Kingdom	WIIS, 2011
Lutra lutra	Otter	Flocoumafen	1	Mortality	Residues	Spain	Sánchez-Barbudo et al., 2012
Lutra lutra	Otter	Multiple Rodenticides	2	Mortality	Residues	United Kingdom	WIIS, 2009
Lutra lutra	Otter	Multiple Rodenticides	3	Mortality	Residues	France	Fournier-Chambrilion et al., 2004
Lutra lutra	Otter	Multiple Rodenticides	4	Mortality	Residues	Finland	Koivisto et al., 2018
Ovis aries	Sheep	Bromadiolone	3	Mortality	N/A	Mongolia	in Dolgormaa, 2004
Lepus capensis	Hare	Multiple Rodenticides	14	Mortality	Residues	France	Berny et al., 1997
Lepus granetensis	Iberian Hare	Multiple Rodenticides	8	Mortality	Residues	Spain	Sánchez-Barbudo et al., 2012
Oryctolagus cuniculus (EUROPEAN)	Rabbit	Multiple Rodenticides	10	Mortality	Residues	France	Berny et al., 1997
Oryctolagus cuniculus (EUROPEAN)	Rabbit	Multiple Rodenticides	1	Mortality	Physical Symptoms	United Kingdom	WIIS, 2010
Sylvilagus	Cottontail Rabbit	Diphacinone	1	Mortality	Physical Symptoms	United States	Erickson and Urban, 2004
Lepus townsendii	White-tailed Jackrabbit	Chlorophacinone	1	Mortality	Physical Symptoms	Canada	Proulx, 2010

Sus scrofa	Pig	Multiple Rodenticides	6	Mortality	Residues	France	Berny et al., 1997
Sus scrofa	Pig	Multiple Rodenticides	1	Exposure	Residues	United Kingdom	WIIS, 2010
Sus scrofa	Pig	Brodifacoum	5	Mortality	Residues	New Zealand	Murphy et al., 1998
Bos taurus	Cow	Difenacoum	1	Mortality	Residues	United Kingdom	WIIS, 2009
Capreolus sp.	Roe Deer	Bromadiolone	2	Mortality	Residues	France	Berny et al., 1997
Martes foina	Stone Marten	Bromadiolone	2	Mortality	Physical Symptoms	France	Berny et al., 1997
Martes foina	Stone Marten	Multiple Rodenticides	11	Mortality	Residues	Spain	Sánchez-Barbudo et al., 2012
Martes martes (EUROPRAN)	Pine Marten	Bromadiolone	2	Mortality	Residues	Scotland	WIIS, 2012
Martes martes (EUROPRAN)	Pine Marten	Multiple Rodenticides	1	Mortality	Residues	United Kingdom	WIIS, 2017
Martes martes (EUROPRAN)	Pine Marten	Bromadiolone	1	Mortality	Residues	United Kingdom	WIIS, 2016
Martes martes (EUROPRAN)	Pine Marten	Multiple Rodenticides	16	Mortality	Residues	Finland	Koivisto et al., 2018
Lynx lynx	Lynx	Bromadiolone	1	Mortality	Residues	France	Berny et al., 1997
Lynx rufus	Bobcat	Multiple Rodenticides	16	Mortality	Residues	United States	Erickson and Urban, 2004
Lynx rufus	Bobcat	Multiple Rodenticides	34(1)	Mortality	Both	United States	Riley et al., 2007
Erinaceus europeaus	Hedgehog	Difenacoum	2	Mortality	Residues	Scotland	WIIS, 2005
Erinaceus europeaus	Hedgehog	Difenacoum	1	Mortality	Residues	United Kingdom	WIIS, 2018
Erinaceus europeaus	Hedgehog	Bromadiolone	1	Mortality	Residues	United Kingdom	WIIS, 2016
Erinaceus europeaus	Hedgehog	Multiple Rodenticides	2	Mortality	Residues	Spain	Sánchez-Barbudo et al., 2012
Erinaceus europeaus	Hedgehog	Brodifacoum	37	Mortality	Residues	New Zealand	Spurr et al., 2005
Erinaceus europeaus	Hedgehog	Multiple Rodenticides	2	Mortality	Residues	Spain	López-Perea et al., 2015
Erinaceus europeaus	Hedgehog	Multiple Rodenticides	107	Mortality	Residues	United Kingdom	Dowding et al., 2010
Atelerix algirus	Algerian Hedgehog	Multiple Rodenticides	61	Mortality	Residues	Spain	López-Perea et al., 2015
Mephitis mephitis	Skunk	Bromadiolone	3	Mortality	Physical Symptoms	United States	Stone et al., 1999
Mephitis mephitis	Striped Skunk	Multiple Rodenticides	5	Mortality	Residues	United States	Erickson and Urban, 2004
Puma concolor	Mountain Lion	Multiple Rodenticides	2	Mortality	Residues	United States	Erickson and Urban, 2004
Puma concolor	Mountain Lion	Multiple Rodenticides	4	Mortality	Both	United States	Riley et al., 2007
Mustela nivalis	Weasel	Brodifacoum	1	Mortality	Residues	Spain	Sánchez-Barbudo et al., 2012

Mustela nivalis	Weasel	Chlorophacinone	1	Mortality	Residues	United Kingdom	WIIS, 2014
Mustela nivalis	Weasel	Difenacoum	1	Mortality	Residues	United Kingdom	WIIS, 2013
Mustela nivalis	Weasel	Brodifacoum	47	Mortality	Residues	New Zealand	Spurr et al., 2005
Mustela nivalis	Weasel	Chlorophacinone	1	Mortality	Physical Symptoms	Canada	Proulx, 2010
Mustela nivalis	Weasel	Brodifacoum	10	Mortality	Residues	New Zealand	Murphy et al., 1998
Mustela nivalis	Weasel	Multiple Rodenticides	3	Mortality	Residues	England	McDonald et al., 1998
Mustela nivalis	Weasel	Multiple Rodenticides	66	Mortality	Residues	Denmark	Elmeros et al., 2011
Mustela nivalis	Weasel	Multiple Rodenticides	10	Mortality	Residues	Finland	Koivisto et al., 2018
Mustela frenata	Long-tailed Weasel	Brodifacoum	1	Mortality	Residues	United States	Erickson and Urban, 2004
Mustela frenata	Long-tailed Weasel	Chlorophacinone	3	Mortality	Physical Symptoms	Canada	Proulx, 2010
Mustela erminea	Stoat	Brodifacoum	120	Mortality	Residues	New Zealand	Spurr et al., 2005
Mustela erminea	Stoat	Brodifacoum	31	Mortality	Residues	New Zealand	Murphy et al., 1998
Mustela erminea	Stoat	Multiple Rodenticides	9	Mortality	Residues	England	McDonald et al., 1998
Mustela erminea	Stoat	Multiple Rodenticides	59	Mortality	Residues	Denmark	Elmeros et al., 2011
Mustela erminea	Stoat	Multiple Rodenticides	5	Mortality	Residues	Finland	Koivisto et al., 2018
Mustela putorius	Polecat	Multiple Rodenticides	1	Mortality	Residues	United Kingdom	WIIS, 2014
Mustela putorius	Polecat	Multiple Rodenticides	49	Mortality	Residues	England	Shore et al., 2003
Mustela putorius	Polecat	Bromadiolone	5	Mortality	Residues	France	Fournier-Chambrilion et al., 2004
Mustela putorius furo	Ferret	Brodifacoum	8	Mortality	Residues	New Zealand	Spurr et al., 2005
Mustela putorius furo	Ferret	Brodifacoum	9	Mortality	Residues	New Zealand	Murphy et al., 1998
Mustela lutreola	European Mink	Bromadiolone	1	Mortality	Residues	France	Fournier-Chambrilion et al., 2004
Mustela vision	American Mink	Multiple Rodenticides	7	Mortality	Residues	France	Fournier-Chambrilion et al., 2004
Procyon lotor	Racoon	Bromadiolone	2	Mortality	Residues	Spain	Sánchez-Barbudo et al., 2012
Procyon lotor	Racoon	Multiple Rodenticides	1	Mortality	Physical Symptoms	United States	Ruder et al., 2011
Procyon lotor	Racoon	Multiple Rodenticides	13	Mortality	Residues	United States	Erickson and Urban, 2004
Procyon lotor	Racoon	Brodifacoum	6	Mortality	Physical Symptoms	United States	Stone et al., 1999
Nyctereutes procyonoides	Racoon Dog	Multiple Rodenticides	88	Mortality	Residues	Finland	Koivisto et al., 2018
Odocoileus virginianus	White-tailed Deer	Multiple Rodenticides	7	Mortality	Residues	United States	Erickson and Urban, 2004

Odocoileus virginianus	White-tailed Deer	Multiple Rodenticides	7	Mortality	Physical Symptoms	United States	Stone et al., 1999
Mystacina tuberculata	NZ Lesser Short-tailed Bats	Diphacinone	118	Both	Both	New Zealand	Dennis et al., 2015
Didelphis virginiana	Opossum	Multiple Rodenticides	3	Mortality	Residues	United States	Erickson and Urban, 2004
Didelphis virginiana	Opossum	Brodifacoum	2	Mortality	Physical Symptoms	United States	Stone et al., 1999
Didelphimorphia	Possom	Brodifacoum	7	Mortality	Residues	New Zealand	Spurr et al., 2005
Rattus norvegicus	Brown Rat	Multiple Rodenticides	1	Mortality	Physical Symptoms	United Kingdom	WIIS, 2014
Rattus norvegicus	Brown Rat	Brodifacoum	21	Mortality	Residues	United States	Pitt et al., 2015
Rattus norvegicus	Brown Rat	Multiple Rodenticides	6	Mortality	Residues	Canada	Elliot et al., 2014
Rattus norvegicus	Brown Rat	Multiple Rodenticides	5	Mortality	Residues	Finland	Koivisto et al., 2018
Rattus rattus	Black Rat	Brodifacoum	84	Mortality	Residues	New Zealand	Spurr et al., 2005
Mus musculus	House Mouse	Brodifacoum	31	Mortality	Residues	New Zealand	Spurr et al., 2006
Dipodomys heermanni	Heermann's Kangaroo Rat	Diphacinone	1	Mortality	Residues	United States	Erickson and Urban, 2004
Peromyscus maniculatus	Deer Mouse	Chlorophacinone	2	Mortality	Physical Symptoms	Canada	Proulx, 2010
	Vole	Multiple Rodenticides	1	Mortality	Residues	Canada	Elliot et al., 2014
Genetta genetta	Common Genet	Multiple Rodenticides	2	Mortality	Residues	Spain	Sánchez-Barbudo et al., 2012
Taxidea taxus	American badger	Chlorophacinone	1	Mortality	Both	United States	Ruder et al., 2011
Taxidea taxus	American badger	Chlorophacinone	1	Mortality	Physical Symptoms	Canada	Proulx, 2010
Canis latrans	Coyote	Multiple Rodenticides	33	Mortality	Both	United States	Erickson and Urban, 2004

Appendix 4: Review of Literature for Non-targeted anticoagulant rodenticide poisoning in other vertebrates

Scientific Name	Common Name	Rodenticide	No of Animals Poisoned	Incident Type	Location	Reference
			Amphibians			
Apoda	Caecilian	N/A	1	Mortality	Seychelles	Thorsen et al., 2000
			Reptiles			
Egernia kingii	King's Skink	Brodifacoum	1	Mortality	Australia	Bettink, 2015
Hemorrhois hippocrepis	Horseshoe Whip Snake	Flocoumafen	1	Mortality	Spain	Sánchez-Barbudo et al., 2012
Microlophus duncanensis	Lava Lizard	Brodifacoum	270	Exposure	Ecuador	Rueda et al., 2016
Hemidactylus frenatus	Gecko	Brodifacoum	11	Mortality	United States	Pitt et al., 2015
Chelonia mydas	Green Sea Turtle	Brodifacoum	1	Mortality	United States	Pitt et al., 2015
Geochelone giantea	Aldabran Giant Tortoise	Brodifacoum	3	Mortality	Seychelles	Merton et al., 2002
			Fish			
Abudefduf sordidus	Black Spotted Sergant Fish	Brodifacoum	7	Mortality	United States	Pitt et al., 2015
Mugilidae	Mullet Fish	Brodifacoum	24	Mortality	United States	Pitt et al., 2015
Tetraodontidae spp.	Puffer Fish	Brodifacoum	1	Mortality	United States	Pitt et al., 2015
Peprilus triacanthus	Butterfish	Brodifacoum	1	Mortality	New Zealand	Primus et al., 2005

Appendix 5: Review of Literature for Non-targeted anticoagulant rodenticide poisoning in invertebrates

Scientific Name	Common Name	Rodenticide	No of Animals Poisoned	Incident Type	Residues/ Physical Symptoms	Location	Reference
N/A	Cockroach	Brodifacoum	14	Mortality	Residues	United States	Pitt *et al.,* 2015
Formicidae	Ant sp.	Brodifacoum	15	Mortality	Residues	United States	Pitt *et al.,* 2015
N/A	Snail sp.	Brodifacoum, Difenacoum	N/A	Exposure	Residues	Spain	Hernandez-Moreno *et al.,* 2013
Rhaphidophoridae	Cave Weta	Brodifacoum	1	Mortality	Residues	New Zealand	Ogilvie *et al.,* 1997
N/A	Slug	Brodifacoum	1	Mortality	Residues	New Zealand	Morgan *et al.,* 1996
N/A	Slug	Brodifacoum	1	Mortality	Residues	Canada	Elliot *et al.,* 2014
Dermesres spp.	Carrion Beetle	Diphacinone	1	Mortality	Residues	Canada	Elliot *et al.,* 2014
Asteroidea	Starfish	Brodifacoum	1	Mortality	Residues	New Zealand	Primus *et al.,* 2005
N/A	Crayfish	Brodifacoum	13	Mortality	Residues	New Zealand	Primus *et al.,* 2005
N/A	Crab	Brodifacoum	1	Mortality	Residues	New Zealand	Primus *et al.,* 2005
Mytilus edulis	Mussels	Brodifacoum	N/A	Mortality	Residues	New Zealand	Primus *et al.,* 2005
N/A	Limpet Tissue	Brodifacoum	N/A	Mortality	Residues	New Zealand	Primus *et al.,* 2005
Lumbricina	Earthworm	Bromadiolone	N/A	Mortality	Residues	China	Liu *et al.,* 2015
Uca tetragonon	Fiddler Crab	Brodifacoum	7	Mortality	Residues	United States	Pitt *et al.,* 2015
Coenobita perlatus	Hermit Crab	Brodifacoum	17	Mortality	Residues	United States	Pitt *et al.,* 2015
Cardisoma spp.	Land Crab	Brodifacoum	7	Mortality	Residues	United States	Pitt *et al.,* 2015

Appendix 6: VKORC1 and VKORC1L1 Accession Numbers

Scientific Name	Common Name	VKORC1 Accession Number	VKORC1L1 Accession Number
	Mammals		
Rattus norvegicus	Brown rat	AAR82917	NP_976083
Rattus rattus	Black rat	BAM22603	
Rattus flavipectus	Yellow-breasted rat	ACO94163	
Rattus losea	Lesser ricefield rat	ABK27271	
Rattus tiomanicus	Malaysian field rat	AFK30344	
Rattus rattus alexandrinus	Roof rat	ADI56528	
Rattus rattus frugivorous	White bellied rat	ADI56530	
Rattus tanezumi	Asian house rat	AFK30348	
Mus musculus	House mouse	AAH31732	AAI38133
Mus spretus	Algerian mouse	ADN94694	
Mus caroli	Ryukyu mouse	XP_021023197	XP_021019518
Mus pahari	Gairdner's shrewmouse	XP_021069312	
Cricetulus griseus	Chinese hamster	EGW03244	XP_007628061
Meriones unguiculatus	Mongolian gerbil	XP_021517691	
Microtus ochrogaster	Prairie vole	XP_005351379	
Peromyscus maniculatus bairdii	Deer mouse	XP_006977082	XP_006971420
Arvicola amphibius	European water vole	ACS31824	
Neotoma lepida	Desert woodrat	OBS63438	
Castor canadensis	North American Beaver	JAV40678	JAV40820
Heterocephalus glaber	Naked mole-rat	EHB14287	XP_004840037
Fukomys damarensis	Damara mole-rat	KFO36327	
Chinchilla lanigera	Long-tailed chinchilla	XP_005405357	
Cavia porcellus	Guinea pig	XP_003477938	
Ictidomys tridecemlineatus	Thirteen-lined ground squirrel	XP_005323937	
Marmota marmota marmota	Alpine Marmot	XP_015346828	
Urocitellus parryii	Arctic ground squirrel	XP_026256196	XP_026256191
Mastomys coucha	Southern multimammate mouse		XP_031193958
Peromyscus leucopus	White-footed mouse		XP_028726000
Grammomys surdaster	African woodland thicket rate		XP_028622069
Nannospalax galili	Spalax		XP_008837376
Mesocricetus auratus	Golden hamster		XP_005080393
Marmota flaviventris	Yellow-bellied marmot		XP_027804445
Ochotona princeps	American pika	XP_004586876	XP_004599459
Oryctolagus cuniculus	European rabbit	XP_002721799	XP_008247878
Homo sapiens	Human	AAH02911	AAH27734
Pan troglodytes	Chimpanzee	JAA14858	JAA37129
Pan paniscus	Bonobo	XP_003807542	
Pongo abelii	Sumatran orangutan	XP_002826416	

Gorilla gorilla gorilla	Western lowland gorilla	XP_018867958	
Nomascus leucogenys	Northern white-cheeked gibbon	XP_003280502	
Theropithecus gelada	Gelada	XP_025226308	
Mandrillus leucophaeus	Drill	XP_011837904	
Cercocebus atys	Sooty mangabey	XP_011945174	XP_011931739
Chlorocebus sabaeus	Green monkey	XP_007988685	XP_008016437
Rhinopithecus roxellana	Golden snub-nosed monkey	XP_010360555	XP_030788999
Colobus angolensis palliatus	Angola colobus	XP_011789012	
Macaca fascicularis	Crab-eating macaque	EHH60338	XP_005549500
Macaca mulatta	Rhesus macaque	EHH31612	AFJ71318
Macaca nemestrina	Southern pig-tailed macaque	XP_011741749	
Piliocolobus tephrosceles	Ugandan red colobus	XP_026311203	
Papio anubis	Olive baboon	XP_003916841	XP_003895978
Cebus capucinus imitator	Panamanian white-faced capuchin	XP_017371000	
Aotus nancymaae	Nancy Ma's night monkey	XP_012325399	
Callithrix jacchus	Common marmoset	XP_017834364	JAB36524
Saimiri boliviensis boliviensis	Black-capped squirrel monkey	XP_003930102	
Microcebus murinus	Gray mouse lemur	XP_012619617	XP_012619550
Propithecus coquereli	Coquerel's sifaka	XP_012515728	XP_012495803
Otolemur garnettii	Northern greater galago		XP_003794266
Galeopterus variegatus	Sunda flying lemur	XP_008592488	
Tupaia chinensis	Chinese treeshrew	ELW66329	
Camelus bacterianus	Camel	XP_010970725	
Camelus ferus	Wild Bactrian camel	EQB77946	
Vicugna pacos	Alpaca	XP_006201383	
Sus scrofa	Wild boar	XP_003124521	JAA53638
Odocoileus virginianus texanus	White-tailed deer	XP_ 003124521	
Bos taurus	Cow	AAT85856	DAA15317
Bos mutus	Wild yak	ELR62800	
Bos indicus	Zebu	XP_019843320	XP_02383637
Bubalus Bubalis	Water buffalo	XP_006070471	XP_025130971
Bison bison bison	Bison	XP_010835658	
Ovis aries musimon	European Sheep	XP_012021572	XP_012023722
Capra hircus	Goat	XP_017895520	XP_017895826
Pantholops hodgsonii	Tibetan antelope	XP_005960047	
Balaenoptera acutorostrata	Minke whale	XP_007186507	
Lipotes vexillifer	Dolphin	XP_007186507	XP_007452717
Tursiops truncatus	Common bottlenose dolphin	XP_004323791	XP_019777497
Orcinus orca	Killer whale	XP_004268762	XP_004268794
Delphinapterus leucas	Beluga whale	XP_022443935	XP_022443875
Neophocaena asiaeorientalis	Narrow-ridged finless porpoise	XP_024600180	
Lagenorhynchus obliquidens	Pacific white-sided dolphin	XP_026982126	XP_026982044

Ovis aries	Sheep		XP_027817737
Monodon monoceros	Narwhal		XP_029076442
Physeter catodon	Sperm whale		XP_023989670
Globicephala melas	Long-finned pilot whale		XP_030727760
Acinonyx jubatus	Cheetah	XP_014932399	XP_026897632
Puma concolor	Cougar	XP_025776136	
Felis catus	Cat	XP_003998687	XP_023101986
Panthera tigris altaica	Siberian tiger	XP_007092238	
Panthera pardus	Leopard	XP_019291910	XP_019277303
Ursus arctos horribilis	Grizzly bear	XP_026371649	XP_026371699
Ailuropoda melanoleuca	Giant panda	XP_002924800	
Odobenus rosmarus divergens	Pacific Walrus	XP_004397307	XP_004405478
Leptonychotes weddellii	Weddell seal	XP_006729912	
Neomonachus schaurislandi	Hawaiian monk seal	XP_021556278	XP_021555992
Canis lupus familiaris	Dog	XP_005621301	XP_848485
Canis lupus dingo	Dingo	XP_025271714	XP_025281503
Vulpes vulpes	Red fox	XP_025867002	XP_025873271
Lynx canadensis	Canadian lynx		XP_030156193
Mustela putorius furo	Ferret		XP_012916453
Callorhinus ursinus	Northern fur seal		XP_025720368
Zalophus californianus	Californian sea lion		XP_027468807
Eumetopias jubatus	Steller sea lion		XP_027965787
Equus caballus	Horse	XP_001500839	XP_023511313
Equus przewalskii	Przewalski's horse	XP_008512546	
Equus asinus	Donkey	XP_014697847	
Ceratotherium simum simum	Southern white rhinoceros	XP_004439516	
Myotis davidii	Vesper bat	XP_006774132	
Myotis lucifugus	Little brown bat	XP_006106095	
Myotis brandtii	Brandt's bat	EPQ11028	
Eptesicus fuscus	Big brown bat	XP_008151015	XP_008139739
Desmodus rotundus	Common vampire bat	XP_024416183	JAA45309
Hipposideros armiger	Great roundleaf bat	XP_019484120	XP_019488610
Pteropus alecto	Black flying fox	XP_06914219	XP_015450164
Pteropus vampyrus	Large flying fox	XP_011376902	XP_011365294
Phyllostomus discolor	Pale spear-nosed bat		XP_028367064
Rousettus aegyptiacus	Egyptian fruit bat		XP_015994031
Dasypus novemcinctus	Nine-banded armadillo	XP_004479467	
Chrysochloris asiatica	Cape golden mole	XP_006871987	
Echinops telfairi	Lesser hedgehog tenrec	XP_004706072	
Elephantulus edwardii	Cape elephant shrew	XP_006896564	
Orycteropus afer afer	Aardvark	XP_007948458	
Loxodonta africana	African bush elephant	XP_010596839	
Erinaceus europaeus	European hedgehog	XP_007530098	
Condylura cristata	Star-nosed mole	XP_004692020	
Sarcophilus harrisii	Tasmanian devil	XP_003775312	
Phascolarctos cinereus	Koala	XP_020864278	XP_020862671
Vombatus ursinus	Common wombat	XP_027730631	XP_027717705
Ornithorhynchus anatinus	Platypus	XP_028913552	XP_028938278
	Birds		
Empidonax traillii	Willow flycatcher		XP_027745856
Pipra filicauda	Wire-tailed manakin		XP_027581749

Corapipo altera	White-ruffed manakin		XP_027522627
Neopelma Chrysocephalum	Saffron-crested Tyrant-manakin		XP_027546554
Lepidothrix coronata	Blue-crowned manakin		XP_017688031
Camarhynchus parvulus	Small tree finch		XP_030818425
Serinus canaria	Atlantic canary		XP_009092958
Taeniopygia guttata	Zebra finch	XP_030142038	XP_002196290
Zonotrichia albicollis	White-throated sparrow		XP_014129461
Parus major	Great tit		XP_015501836
Lonchura striata domestica	Bengalese finch		OWK59947
Sturnus vulgaris	Common starling		XP_014732015
Pseudopodoces humilis	Ground tit		XP_005525873
Calypte anna	Anna's hummingbird		XP_030318151
Aquila chrysaetos chrysaetos	Golden eagle		XP_029884040
Aquila chrysaetos canadensis	American golden eagle		XP_011579937
Haliaeetus leucocephalus	Bald eagle		XP_010571880
Strigops habroptila	Kakapo		XP_030328751
Melopsittacus undulatus	Budgerigar		XP_005154383
Patagioenas fasciata monilis	Band-tailed pigeon		OPJ78686
Calidris pugnax	Ruff		XP_014808599
Charadrius vociferus			KGL933390
Anas platyrhynchos	Mallard		XP_027328071
Meleagris gallopavo	Wild turkey		XP_03211783
Colinus virginianus	Northern Bobwhite		OXB57514
Phasianus colchicus	Common pheasant		XP_031447623
Numida meleagris	Helmeted guineafowl		XP_021271667
Gallus gallus	Chicken	NP_996530	NP_001001328
Coturnix japonica	Japanese quail		XP_015735979
Nothoprocta perdicaria	Chilean tinamou		XP_025892723
	Reptiles		
Pseudonaja textilis	Eastern brown snake	XP_026576913	XP_026564415
Notechis scutatus	Tiger snake	XP_026539294	XP_026527486
Boiga irregularis	Brown tree snake	JAG65918	
Thamnophis sirtalis	Common garter snake	XP_013917568	XP_013915383
Crotalus horridus	Timber rattlesnake	JAA95021	
Crotalus adamanteus	Eastern diamondback rattlesnake	JAI0602	
Python bivittatus	Burmese python	XP_007437611	XP_007429740
Protobothrops mucrosquamatus	Brown spotted pit viper		XP_015671024
Ophiophagus hannah	King cobra		ETE72926
Anolis carolinensis	Carolina anole	XP_003223943	
Chrysemys picta bellii	Painted turtle	XP_005279429	XP_005283481
Chelonia mydas	Green sea turtle		XP_027687308
Terrapene Carolina triunguis	Three-toed box turtle		XP_024060728
Pogona vitticeps	Central bearded dragon		XP_020659613
Gekko japonicus	Schlegel's Japanese gecko		XP_015269142

Podarcis muralis	Wall lizard		XP_028564642
	Amphibians		
Xenopus tropicalis	Western clawed frog	AAH76993	CAJ81550
Xenopus laevis	African clawed frog	AAH77384	
Nanorana parkeri	High Himalaya frog		XP_018426521
Microcaecilia unicolor			XP_030041779
Rhinatrema bivittatum	Two-lined caecilians		XP_029468158
	Fish		
Liparis tanakae	Tanaka's snailfish		TMM64994
Sander lucioperca	Zander		XP_031166590
Sparus aurata	Gilt-head bream		XP_030293932
Larimichthys crocea	Large yellow croaker		XP_010741415
Perca flavescens	Yellow perch		XP_028451421
Cottoperca gobio	Thornfish		XP_029304130
Archocentrus centrarchus	Green fin cichlid		XP_030602333
Maylandia zebra	Zebra mbuna	XP_004575900	XP_004557496
Labrus bergylta	Ballan wrasse		XP_020505596
Xiphophorus couchianus	Monterrey platyfish		XP_027886306
Xiphophorus maculatus	Southern platyfish		XP_005815601
Kryptolebias marmoratus	Mangrove killifish	XP_017274069	
Nothobranchius furzeri	Turquoise killifish	SBP45555	
Nothobranchius kuhntae	Beira killifish	SBQ91109	
Nothobranchius rachovii	Bluefin notho	SBR76995	
Nothobranchius pienarri	Ranchow's Nothobranch	SBR53719	
Nothobranchius kadleci		SBP84395	
Iconisemion striatum		SBP20640	
Takifugo rubripes	Japanese pufferfish or Tiger pufferfish or torafugo pufferfish	NP_001027838	
Tetraodon nigroviridis	Spotted green pufferfish	CAG07588	
Oryzias melastigma	Medaka		XP_024121477
Oryzias latipes	Japanese rice fish	XP_004080362	
Stegastes partitus		XP_008281492	
Neolamprologus brichardi	Princess of burundi	XP_006805785	
Pundamilia nyererei	Nyerere's Victoria Cichlid	XP_00573138	
Oreochromis Niloticus	Nile tilapia	XP_003438529	XP_019209926
Astatotilapia calliptera	Eastern river bream		XP_026037773
Oreochromis aureus	Blue tilapia		XP_031600814
Salarias fasciatus	Jewelled blenny		XP_029956299
Gouania willdenowi	Blunt-snouted Clingfish		XP_028323151
Amphiprion Ocellaris	Ocellaris clownfish		XP_023132274
Parambassis ranga	Indian glassy fish		XP_028277249
Cynoglossus semilaevis			XP_008330607
Seriola lalandi dorsalis	California yellowtail		XP_023273974
Seriola dumerili	Greater yellowtail		XP_022601461
Anabas testudineus	Climbing perch		XP_026228448
Betta splendens	Siamese fighting fish		XP_029028746

Mastacembelus armatus	Marbled spiny eel	XP_026185206
Myripristis murdjan	Soldierfish	XP_029924555
Salmo trutta	Sea trout	XP_029546166
Esox lucius	Northern pike	XP_010865864
Tachysurus fulvidraco	Yellowhead catfish or Korean bullhead	XP_026993575
Pangasianodon hypophthalmus	Iridescent shark	XP_026777943
Electrophorus electricus	Electric eel	XP_026866066
Danio rerio	Zebrafish	NP_001018524
Chanos Chanos	Milkfish	XP_030648325
Denticeps clupeoides	Denticle herring	XP_028838380
Clupea harengus	Atlantic herring	XP_012678234
Scleropages formosus	Asian arowana	XP_018586621
Paramormyrops kingsleyae	Old Calabar mormyrid	XP_023688727
Rhincodon typus	Whale shark	XP_020384061
Callorhinchus milii	Australian ghost shark	XP_007894765
Latimeria chalumnae	West Indian Ocean Coelacanth	XP_005987585

Appendix 7: DNA Sequences of Novel D-loop Haplotypes found in the UK and Sweden

>OS7–DLF **D26_ZH**

TATATTGTACATTAAATTATTTTCCCCAAGCATATAAGCATGTAATATATATCTAATGATTTAGGACATACATTTAAACTCAA
CTATAAATTTACAACAACATGTCTATTCTCAAATACATTAAGATAATGCTTATTAGACATATCTGTGTTATTAGACATACACC
ATTAAGTCATAAACCTTTCTCTTCCATATGACTATCCCTGTCCCCAATTGGTCTCTATTTCTACCATCCTCCGTGAAATCAAC
AACCCGCCCACTCGTCCCCCTCTTCTCGCTCCGGGCCCATTCGTCCTGGGGGGTGACTATACTGAAACTTTACCAGGCATCTGG
TTCTTACTTCAGGGCCATCAATTGGTTCATCGTCCATACGTTCCCCTTAAATAAGACATCTCGATGGTAACGGGTCTAATCAG
CCCATGATCAACATAACTGTGGTGATATACATTTGGTATTTTTTAATTTTCGGATGCCTTCCTCAACATAGCCGTCAAGGCAT
GAAGGCCAGCACAAAGTCCTGTGGAACCTTTTAGTTAAGGGTCATTTATCCTCATAGACAAAGCTCGAAAGGCTATTTTATTC
ATGTTTGTAAGACATAAATATTTATAAATACTGAAAAATCTGTC

>WW3–DLF **D27_ZH**

TATATTGTACATTAAATTATTTTCCCCAAGCATATAAGCATGTAATATATATCTAATGATTTAGGACATACATTTAAACTCAA
CTATAAATTTACAACAACATGTCTATTCTCAAATACATTAAGATAATGCTTATTAGACATATCTGTGTTATTAGACATACACC
ATTAAGTCATAAACCTTTCTCTTCCATATGACTATCCCTGTCCCCAATTGGTCTCTATTTCTACCATCCTCCGTGAAATCAAC
AACCCGCCCACTCGTCCCCCTCTTCTCGCTCCGGGCCCATTCGTCCTGGGGGGTGACTATACTGAAACTTTACCAGGCATCTGG
TTCTTACTTCAGGGCCATCAATTGGCTCATCGTCCATACGTTCCCCTTAAATAAGACATCTCGATGGTAACGGGTCTAATCAG
CCCATGATCAACATAACTGTGGTGATATACATTTGGTATTTTTTAATTTTCGGATGCCTTCCTCAACATAGCCGTCAAGGCAT
GAAGGTCAGCACAAAGTCCTGTGGAACCTTTTAGTTAAGGGTCATTTATCCTCATAGACAAAGCTCGAAAGGCTATTTTATTC
ATGTTTGTAAGACATAAATATTTATAAATACTGAAAAATCTGTC

>OL2–DLF **D28_ZH**

TATATCGTACATTAAATTATTTTCCCCAAGCATATAAGCATGTAATATATATCTAATGATTTAGGACATACATTTAAACTCAA
CTATAAATTCACAACAACATGTCTACTCTCAAATACATTAAGATAATGCTTATTAGACATATCTGTGTTATTAGACATACACC
ATTAAGTCATAAACCTTTCTCTTCCATATGACTATCCCTGTCCCCAATTGGTCTCTATTTCTACCATCCTCCGTGAAATCAAC
AACCCGCCCACTCGTCCCCCTCTTCTCGCTCCGGGCCCATTCGTCCTGGGGGGTGACTATACTGAAACTTTACCAGGCATCTGG
TTCTTACTTCAGGGCCATCAATTGGTTCATCGTCCATACGTTCCCCTTAAATAAGACATCTCGATGGCAACGGGTCTAATCAG
CCCATGATCAACATAACTGTGGTGATATACATTTGGTATTTTTTAATTTTCGGATGCCTTCCTCAACATAGCCGTCAAGGCAT
GAAGGTCAGCACAAAGTCCTGTGGAACCTTTTAGTTAAGGGTCATTTATCCTCATAGACAAAGCTCGAAAGACTATTTTATTC
ATGTTTGTAAGACATAAATATTTATAAATACTGAAAAATCTGTC

>OL1–DLF **D29_ZH**

TATATCGTACATTAAATTATTTTCCCCAAGCATATAAGCATGTAATATATATCTAATGATTTAGGACATACATTTAAACTCAA
CTATAAATTCACAACAACATGTCTACTCTCAAATACATTAAGATAATGCTTATTAGACATATCTGTGTTATTAGACATACACC
ATTAAGTCATAAACCTTTCTCTTCCATATGACTATCCCTGTCCCCAATTGGTCTCTATTTCTACCATCCTCCGTGAAATCAAC
AACCCGCCCACTCGTCCCCCTCTTCTCGCTCCGGGCCCATTCGTCCTGGGGGGTGACTATACTGAAACTTTACCAGGCATCTGG
TTCTTACTTCAGGGCCATCAATTGGTTCATCGTCCATACGTTCCCCTTAAATAAGACATCTCGATGGTAACGGGTCTAATCAG
CCCATGATCAACATAACTGTGGTGATATACATTTGGTATTTTTTAATTTTCGGATGCCTTCCTCAACATAGCCGTCAAGGCAT
GAAGGTCAGCACAAAGTCCTGTGGAACCTTTTAGTTAAGGGTCATTTATCCTCATAGACAAAGCTCGAAAGACTATTTTATTC
ATGTTTGTAAGACATAAATATTTATAAATACTGAACAATCTGTC

>NR06-DLF **D30_ZH**

TATATCGTACATTAAATTATTTTCCCCAAGCATATAAGCATGTAATATATATCTAATGATTTAGGACATACATTTAAACTCAA
CTATAAATTCACAACAACATGTCTACTCTCAAATACATTAAGATAATGCTTATTAGACATATCTGTGTTATTAGACATACACC
ATTAAGTCATAAACCTTTCTCTTCCATATGACTATCCCTGTCCCCAATTGGTCTCTATTTCTACCATCCTCCGTGAAATCAAC
AACCCGCCCACTCCTCCCCCTCTTCTCCCTCCGGGCCCATTCGTCCTGGGGGGTGACTATACTGAAACTTTACCAGGCATCTGG
TTCTTACTTCAGGGCCATCAATTGGTTCATCGTCCATACGTTCCCCTTAAATAAGACATCTCGATGGTAACGGGTCTAATCAG
CCCATGATCAACATAACTGTGGTGATATACATTTGGTATTTTTTAATTTTCGGATGCCTTCCTCAACATAGCCGTCAAGGCAT
GAAGGTCAGCACAAAGTCCTGTGGAACCTTTTAGTTAAGGGTCATTTATCCTCATAGACAAAGCTCGAAAGACTATTTTATTC
ATGTTTGTAAGACATAAATATTTATAAATACTGAAAAATCTGTC

>WW10-DLF **D31_ZH**

TATATCGTACATTAAATTATTTTCCCCAAGCATATAAGCATGTAATATATATTTAATGATTTAGGACATACATTTAAACTCAA
CTATAAATTCATAACAACATGTCTATTCTCAAATACATTAAAATAATGCTTATTAGACATATCTGTGTTATTAGACATGCACC
ATTAAGTCATAAACCTTTCTCTTCCATATGACTATCCCTGTCCCCAATTGGTCTCTATTTCTACCATCCTCCGTGAAATCAAC
AACCCGCCCACTCGTCCCCCTCTTCTCGCTCCGGGCCCATTCGTCCTGGGGGGTGACTATACTGAAACTTTACCAGGCATCTGG
TTCTTACTTCAGGGCCATCAATTGGTTTATCGTCCATACGTTCCCCTTAAATAAGACATCTCGATGGTAACGGGTCTAATCAG
CCCATGATCAACATAACTGTGGTGATATACATTTGGTATTTTTTAATTTTCGGATGCCTTCCTCAACATAGCCGTCAAGGCAT
GAAGGTCAGCACAAAGTCCTGTGGAACCTTTTAGTTAAGGGTCATTTATCCTCATAGACAAAGCTCGAAAGACTATTTTATTC
ATGTTTGTAAGACATAAATATTTATAAATACTGAAAAATCTGTC

>KN01-DLF **D32_ZH**

TATATCGTACATTAAATTATTTTCCCCAAGCATATAAGCATGTAATATATATTTAATGATTTAGGACATACATTTAAACTCAA
CTATAAATTCATAACAACATGTCTATTCTCGAATACATTAAAATAATGCTTATTAGACATATCTGTGTTATTAGACATGCACC
ATTAAGTCATAAACCTTTCTCTTCCATATGACTATCCCTGTCCCCAATTGGTCTCTATTTCTACCATCCTCCGTGAAATCAAC
AACCCGCCCACTCGTCCCCCTCTTCTCGCTCCGGGCCCATTCGTCCTGGGGGGTGACTATACTGAAACTTTACCAGGCATCTGG
TTCTTACTTCAGGGCCATCAATTGGTTTATCGTCCATACGTTCCCCTTAAATAAGACATCTCGATGGTAACGGGTCTAATCAG
CCCATGATCAACATAACTGTGGTGATATACATTTGGTATTTTTTAATTTTCGGATGCCTTCCTCAACATAGCCGTCAAGGCAT
GAAGGTCAGCACAAAGTCCTGTGGAACCTTTTAGTTAAGGGTCATTTATCCTCATAGACAAAGCTCGAAAGGCTATTTTATTC
ATGTTTGTAAGACATAAATATTTATAAATACTGAAAAATCTGTC

>CB07-DLF **D33_ZH**

TATATCGTACATTAAATTATTTTCCCCAAGCATATAAGCATGTAATATATATTTAATGATTTAGGACATACATTTAAACTCAA
CTATAAATTCATAACAACATGTCTATTCTCGAATACATTAAAATAATGCTCATTAGACATATCTGTGTTATTAGACATGCACC
ATTAAGTCATAAACCTTTCTCTTCCATATGACTATCCCTGTCCCCAATTGGTCTCTATTTCTACCATCCTCCGTGAAATCAAC
AACCCGCCCACTCGTCCCCCTCTTCTCGCTCCGGGCCCATTCGTCCTGGGGGGTGACTATACTGAAACTTTACCAGGCATCTGG
TTCTTACTTCAGGGCCATCAATTGGTTTATCGTCCATACGTTCCCCTTAAATAAGACATCTCGATGGTAACGGGTCTAATCAG
CCCATGATCAACATAACTGTGGTGATATACATTTGGTATTTTTTAATTTTCGGATGCCTTCCTCAACATAGCCGTCAAGGCAT
GAAGGTCAGCACAAAGTCCTGTGGAACCTTTTAGTTAAGGGTCATTTATCCTCATAGACAAAGCTCGAAAGACTATTTTATTC
ATGTTTGTAAGACATAAATATTTATAAATACTGAAAAATCTGTC

>BD01-DLF **D34_ZH**

TATATCGTACATTAAATTATTTTCCCCAAGCATATAAGCATGTAATATATATTTAATGATTTAGGACATACATTTAAACTCAA
CTATAAATTCATAACAACATGTCTATTCTCGAATACATTAAAATAATGCTTATTAGACATATCTGTGTTATTAGACATACACC
ATTAAGTCATAAACCTTTCTCTTCCATATGACTATCCCTGTCCCCAATTGGTCTCTATTTCTACCATCCTCCGTGAAATCAAC
AACCCGCCCACTCGTCCCCCTCTTCTCGCTCCGGGCCCATTCGTCCTGGGGGTGACTATACTGAAACTTTACCAGGCATCTGG
TTCTTACTTCAGGGCCATCAATTGGTTTATCGTCCATACGTTCCCCTTAAATAAGACATCTCGATGGTAACGGGTCTAATCAG
CCCATGATCAACATAACTGTGGTGATATACATTTGGTATTTTTTAATTTTCGGATGCCTTCCTCAACATAGCCGTCAAGGCAT
GAAGGTCAGCACAAAGTCCTGTGGAACCTTTTAGTTAAGGGTCATTTATCCTCATAGACAAAGCTCGAAAGACTATTTTATTC
ATGTTTGTAAGACATAAATATTTATAAATACTGAAAAATCTGTC

>NW1-DLF **D35_ZH**

TATATCGTACATTAAATTATTTTCCCCAAGCATATAAGCATGTAATATATATTTAATGATTTAGGACATACATTTAAACTCAA
CTATAAATTCATAACAACATGTCTATTCTCGAATACATTAAAATAATGCTTATTAGACATATCTGTGTTATTAGACATGCACC
ATTAAGTCATAAACCTTTCTCTTCCATATGACTATCCCTGTCCCCAATTGGTCTCTATTTCTACCATCCTCCGTGAAATCAAC
AACCCGCCCACTCGTCCCCCTCTTCTCGCTCCGGGCCCATTCGTCCTGGGGGTGACTATACTGAAACTTTACCACGCATCTGG
TTCTTACTTCAGGGCCATCAATTGGTTTATCGTCCATACGTTCCCCTTAAATAAGACATCTCGATGGTAACGGGTCTAATCAG
CCCATGATCAACATAACTGTGGTGATATACATTTGGTATTTTTTAATTTTCGGATGCCTTCCTCAACATAGCCGTCAAGGCAT
GAAGGTCAGCACAAAGTCCTGTGGAACCTTTTAGTTAAGGGTCATTTATCCTCATAGACAAAGCTCGAAAGACTATTTTATTC
ATGTTTGTAAGACATAAATATTTATAAATACTGAAAAATCTGTC

>HU6-DLF **D36_ZH**

TATATCGTACATTAAATTATTTTCCCCAAGCATATAAGCATGTAATATATATTTAATGATTTAGGACATACATTTAAACTCAA
CTATAAATTCATAACAACATATCTATTCTCGAATACATTAAAATAATGCTTATTAGACATATCTGTGTTATTAGACATGCACC
ATTAAGTCATAAACCTTTCTCTTCCATATGACTATCCCTGTCCCCAATTGGTCTCTATTTCTACCATCCTCCGTGAAATCAAC
AACCCGCCCACTCGTCCCCCTCTTCTCGCTCCGGGCCCATTCGTCCTGGGGGTGACTATACTGAAACTTTACCAGGCATCTGG
TTCTTACTTCAGGGCCATCAATTGGTTTATCGTCCATACGTTCCCCTTAAATAAGACATCTCGATGGTAACGGGTCTAATCAG
CCCATGATCAACATAACTGTGGTGATATACATTTGGTATTTTTTAATTTTCGGATGCCTTCCTCAACATAGCCGTCAAGGCAT
GAAGGTCAGCACAAAGTCCTGTGGAACCTTTTAGTTAAGGGTCATTTATCCTCATAGACAAAGCTCGAAAGACTATTTTATTC
ATGTTTGTAAGACATAAATATTTATAAATACTGAAAAATCTGTC

>801-DLF **D37_ZH**

TATATCGTACATTAAATTATTTTCCCCAAGCATATAAGCATGTAATATATATTTAATGATTTAGGACATACATTTAAACTCAA
CTATAAATTCATAACAACATGTCTATTCTCGAATACATTAAAATAATGCTTATTAGACATATCTGTGTTATTAGACATGCACC
ATTAAGTCATAAACCTTTCTCTTCCATATGACTATCCCTGTCCCCAATTGGTCTCTATTTCTACCATCCTCCGTGAAATCAAC
AACCCGCCCACTCGTCCCCCTCTTCTCGCTCCGGGCCCATTCGTCCTGGGGGTGACTATACTGAAACTTTACCAGGCATCTGG
TTCTTACTTCAGGGCCATCAATTGGTTTATCGTCCATACGTTCCCCTTAAATAAGACATCTCGATGGTAACGGGTCTAATCAG
CCCATGATCAACATAACTGTGGTGATATACATTTGGTATTTTTTAATTTTCGGATGCCTTCCTCAACATAGCCGTCAAGGCAT
GAAGGTCAGCACAAAGTCCTGTGGAACCTTTTAGTTAAGGGTCATTTATCCTCATAGATAAAGCTCGAAAGACTATTTTATTC
ATGTTTGTAAGACATAAATATTTATAAATACTGAAAAATCTGTC

Appendix 8: Key for Amino Acid Colours According to Physiochemical Properties

Key for the amino acid colours according to physiochemical properties for use in multiple sequence alignments and tables in which amino acids are compared.

Small Uncharged: **Alanine, A; Glycine, G**

Hydrophobic: **Isoleucine, I; Leucine, L; Valine, V**

Serine Containing: **Cysteine, C; Methionine, M**

Polar: **Asparagine, N; Glutamine, Q; Serine, S; Threonine, T**

Aromatic: **Phenylalanine, F; Tyrosine, Y**

Positively Charged: **Arginine, R; Histidine, H; Lysine, K**

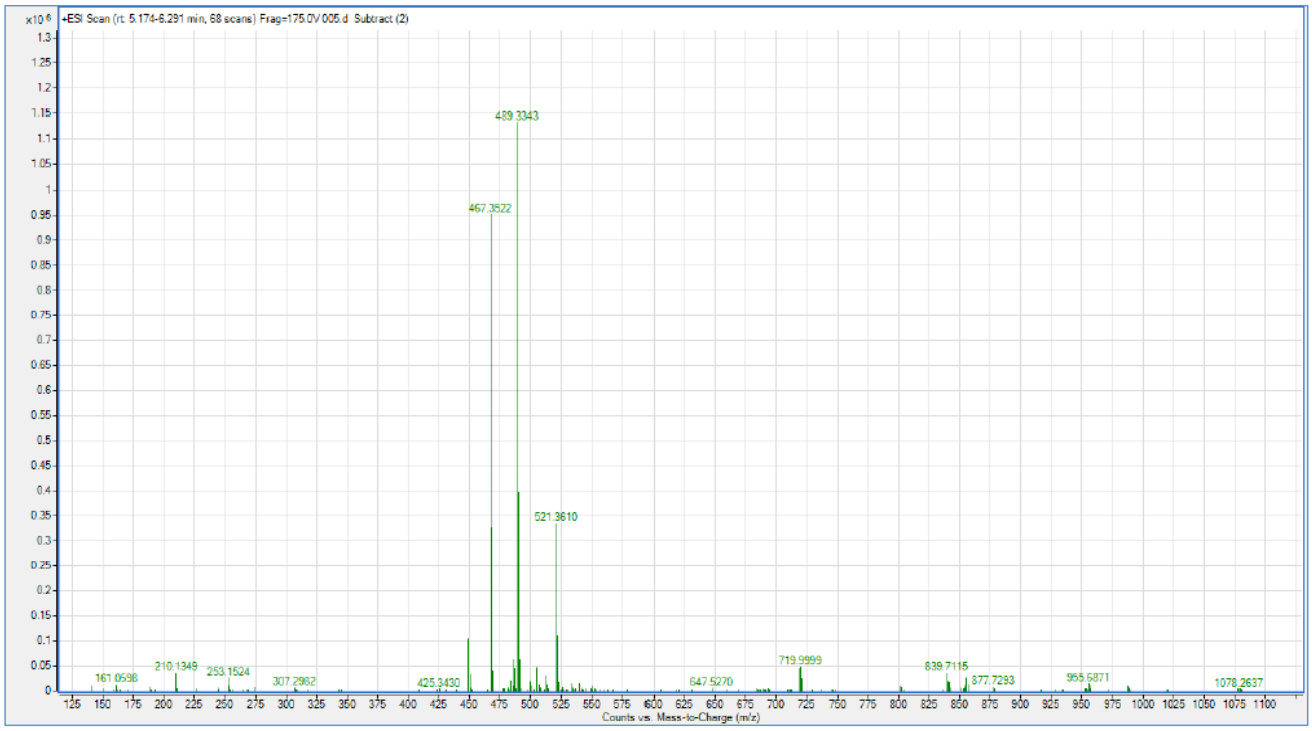
Negatively Charged: **Aspartate, D; Glutamate, E**

Other: **Proline, P; Tryptophan, W**

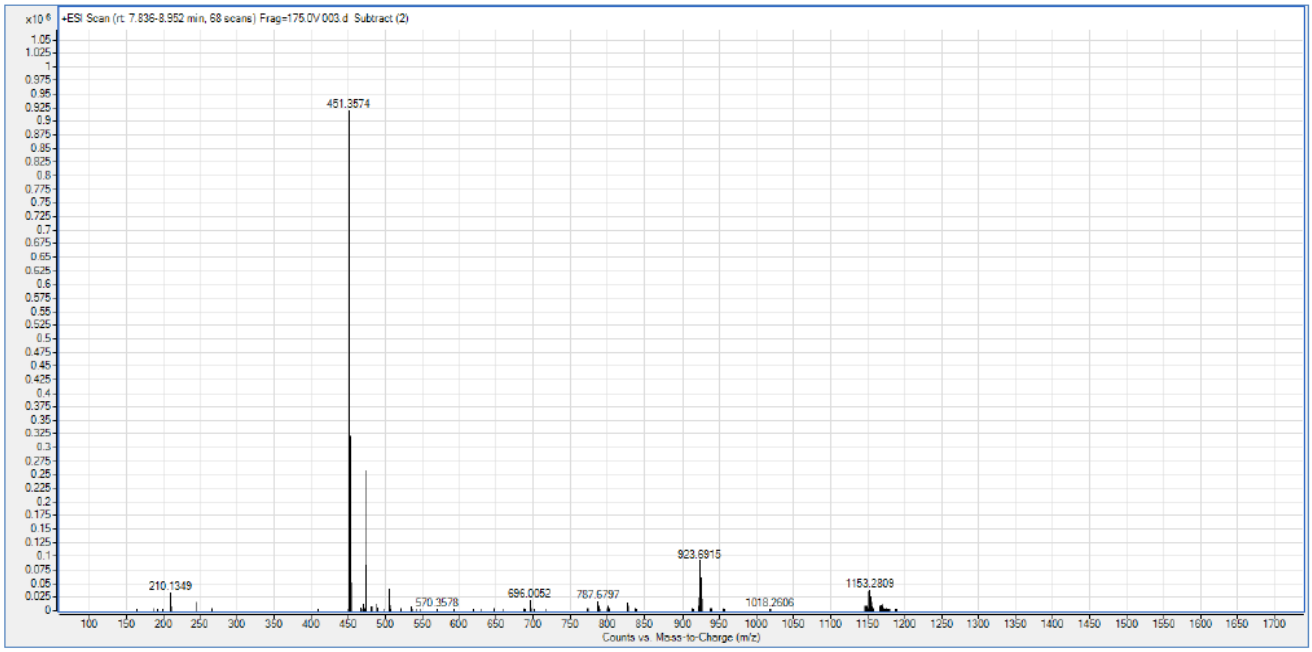
Appendix 9: Mass Spectra of Vitamin K epoxide and Vitamin K

Mass spectra of K>O and VK. a Mass spectra of K>O. **b** Mass spectra of VK.

a



b



Appendix 10: Phylogenetic Tree of Vertebrates

Phylogenetic tree of vertebrate evolution based on Meyer and Zardoya, 2003.

